

RADIOISOTOPES AND THE AGE OF THE EARTH

A YOUNG-EARTH CREATIONIST
RESEARCH INITIATIVE

Edited by: Larry Vardiman
Andrew A. Snelling
Eugene F. Chaffin

First Printing 2000

**Radioisotopes and the Age of the Earth
A Young-Earth Creationist Research Initiative**

Copyright © 2000

Institute for Creation Research
PO Box 2667
El Cajon, California 92021

and

Creation Research Society
PO Box 8263
St. Joseph, Missouri 64508

Cover Design by Janell Robertson

Library of Congress Cataloging in Publication Data
Catalog Card Number: 00 134175
ISBN 0-932766-62-5

ALL RIGHTS RESERVED

No portion of this book may be used in any form without written permission of the publishers, with the exception of brief excerpts in magazine articles, reviews, etc.

Printed in the United States of America

Prologue

John D. Morris, Ph.D.*

Contrary to the claims of some, creationists are not anti-science, nor are they afraid of scientific data. While no generalization can characterize all individuals who believe in Creation any more than one statement can describe all who believe in evolution, all knowledgeable, scientifically-minded creationists fully welcome new scientific data. Every scientist worthy of the name should always be willing to adjust his thinking as new data come in, continually striving for a more complete understanding of reality.

Remember, creationists and evolutionists have exactly the same data. Reality is the same for both. Perception of that reality and interpretation of that data can, however, be remarkably different for the two, depending on the individual's perspective, or assumptions, world-view or even bias.

Philosophers of science have rightly noted that bias plays an important role in designing of experiments, assigning the worth of an individual observation, and interpreting the meaning of results. They are correct in insisting that "there is no such thing as a value-free fact." Presuppositions or bias often play the definitive role in every decision-making process, especially when important questions are being considered. Philosophers have also rightly observed that scientists are some of the most bias-driven folks one can ever meet, most notably when it comes to the world-view issue of Creation/evolution.

Scientists who hold the Creation view quickly admit that they approach science with a bias, but all too often evolution advocates deny their bias, claiming an objectivity which does not and cannot exist. To be sure, most research scientists today hold to evolution and an extremely old earth, and use that perspective as the framework within which to interpret all data. Often these basic tenets dominate their thinking as an

* *President, Institute for Creation Research, Santee, California*

unexpressed backdrop—seldom acknowledged and never questioned. Other views are ignored, denied or ridiculed. Legislation and official guidelines often forbid alternative views, and peer pressure to conform can be intense. Creation thinking is the most prominent “banned” view, even though the majority of Americans agree with it, and a rapidly growing number of scientists embrace it.

Keep in mind that both Creation and evolution (specifically large-scale macroevolution) are views of history, neither occurring today, as far as we can observe. Obviously, the historical sciences are not in the same category as the empirical sciences like chemistry or physics or the applied sciences like engineering or medicine. Even the disciplines of geology and biology primarily concern themselves with the nature and operation of things in the observed present. Only the subsets of historical geology and evolutionary biology deal with theories of the unobserved past. Many creationist professionals occupy positions in these non-historical disciplines.

Since neither creationists nor evolutionists can go back in time and observe past events, neither can rightly claim their view of origins to be scientifically proven. Thus both are on equal scientific footing. Honesty demands modesty regarding such claims. The issue can only be addressed scientifically by comparing which of the competing views handles the data better, and which is better able to make predictions of new experimental and observational results. In that regard, I contend that the Creation/young-earth bias is superior to the evolution/old-earth bias.

Briefly, the Creation model of earth history based on Scripture includes the recent Creation of all things, at the conclusion of which all things were deemed to be “very good” (Genesis 1:31) from God’s perspective. Creation came under God’s curse due to Adam’s rebellion (Genesis 3: 19–24), no longer as good as before. Soon the world was remolded by the global Flood in the days of Noah. We reside and do our scientific study in a once ideal world, created perfect by a wise and omnipotent God, but now cursed and flooded. To a creationist, these great worldwide events constitute true history, and must form the basis for any historical reconstruction. This is our “bias,” and we claim it is a better bias than the old-earth bias, and we offer it as an alternative for your

consideration.

Furthermore, the majority bias of evolution and old earth has frequently led to destructive consequences in society and individual lives. By viewing God as unnecessary, or at best, long ago and far away, many have been led into degrading philosophies and hurtful practices. The Creation world-view, on the other hand, rightly applied, promotes a high view of human life, stewardship over Creation, and accountability for choices and actions, both to God and fellow man.

This book deals with the issue of radioisotope dating, thought by many to represent unassailable proof of millions and billions of years of earth history. However, most are unaware that it often yields contradictory, internally inconsistent results. Different methods often disagree with each other. Rocks of known, historical origins, frequently date to great age. What is wrong? Is there a better way to date rocks? Does the old-earth bias hinder good science? Does the Creation model handle the data better?

It has always been easy to critique radioisotope dating, for it simply does not work very well. Based on the knowledge that certain atoms (for example, ^{238}U) are unstable, and decay into other atoms (^{206}Pb) over time, the amounts of parent and daughter isotopes are measured, as is the rate of decay. Thus, at least in theory, the age of the rock can be calculated as the length of time necessary for decay of the parent into the amount of daughter present. But this straightforward concept has proven unreliable. Creationists have rightly pointed out that the method is based on three unprovable and questionable assumptions which may be the root cause of this failure.

Assumptions of Radioisotope Dating

1. That the rate of decay has been constant throughout time.
2. That the isotope abundances in the specimen dated have not been altered during its history by addition or removal of either parent or daughter.
3. That when the rock first formed it contained a known amount of daughter material.

Up to now, creationist critiques of radioisotope dating methods have focused on assumption numbers two and three, and rightly so. Numerous examples of contamination can be cited and mechanisms are well known. Examination of historically dated lava flows has revealed that unexpectedly high levels of daughter products are frequently present. But now, due to recent discoveries, several hints have surfaced calling assumption number one into question as well. We may be witnessing the demise of a failed theory. Creationists desire to replace it with something better.

At the invitation of the Institute for Creation Research (ICR), several scientists (all faculty or adjunct faculty at ICR) have banded together to investigate this issue. Sponsored jointly by ICR and the Creation Research Society (CRS), the group has chosen the acronym RATE, (for **R**adioisotopes and the **A**ge of **T**he **E**arth). Each scientist is a true professional in his field, with research and publications in radioisotope dating. In addition, each scientist is a mature, Bible-believing Christian, committed to young-earth Creation. Each is strongly sensitive to scientific observation, willing to modify specific views, as demanded by the data.

There were differing positions around the table at the first meeting, but the scientists recognized that they were together marching into uncharted territory, learning as they marched, gleaning wisdom from each other. The one inviolate perspective was that Scripture, rightly interpreted, will always agree with science (not necessarily all the claims of scientists). Being intensely interested, but only somewhat knowledgeable in this field, I was allowed to attend the meetings, and was asked to summarize the flavor of the meetings in this prologue.

Right from the start each scientist declared his complete faith in Scripture. While secular scientists bristle at the notion of melding science with the scriptural world-view, they do much the same thing with their naturalistic, materialistic world-view. The RATE scientists insisted on starting with Scripture and building their understanding of science on that foundation.

They discussed God's creative activity during Creation week, and noted how often various processes were used. Verbs like "moved," "divided,"

“gathered,” “made,” and “formed” imply that creative processes were not always instantaneous, but that some took at least a finite amount of time to be accomplished. During Creation week, these processes were not strictly the same as analogous processes today. For instance, gravity must have been in operation, but when the waters of Day 2 drained off the rising continents on Day 3, they were able to move faster and farther than waters can be moved today. Modern natural laws, operating at rates we recognize today were evidently not fully instituted until Creation was completed on Day 6, and God rested from His creative acts, but even these laws were altered at the time of the Curse on all of Creation (Genesis 3:19–24, Romans 8:20–22). But then what happened during the Flood? It is as if we cannot clearly see all the way back to Creation. Several curtains have been drawn between then and now. We must try to understand Creation as best we can, responding to all the evidence we have, including both scriptural and scientific data, but the scientists around that table fully understand that the task calls for their very best work. We must study the results of past processes, some of which are not occurring at all now, and others which were operating at rates, scales and intensities far different from similar processes today, and infer unobserved, past events.

The four meetings over these past three years have not been a conference, although papers and research results were presented. This is a working group, a research consortium. They are occupied with clarifying issues, thinking together, and blazing new trails toward the goal of replacing a wrong idea with one that works better.

Each meeting opens and closes with prayer, asking the Creator Himself for wisdom in “thinking outside the box.” Each one desires to “think God’s thoughts after Him,” and to give Him glory for His mighty acts. The Bible tells us that “iron sharpens iron,” and we’ve seen that happen over and over again. The synergy of a room full of brilliant minds is something to behold. To them, even when the problems seem daunting, there must be an answer, and this answer must come within the framework of Biblical history.

Questions have been asked, and projects proposed which would never have been investigated by old-earth advocates. And preliminary results are beginning to come in which suggest they’re on the right track. Could

it be that the noticeable weaknesses of standard thinking linger because mainstream scientists are stuck on the wrong track?

From the meetings have come position papers, statements of current knowledge, documentation of the failure of standard theory, estimates of the amount of past decay and hints of accelerated decay rates. They appear in the first portion of this book. Detailed research proposals appear in the appendix. Some projects are not intuitively obvious but are crucial in this stage of the investigation. Others will follow and even more are needed. Of course, other qualified researchers and access to research labs are needed as well. One research project has even been granted to a Hebrew language scholar to make sure the RATE group stays on course.

The RATE committee has come a long way, but now the work begins in earnest. This research, however, is expensive and time-consuming, and you may consider this document an invitation to help fund it with designated, tax-deductible gifts. Designated gifts should come through ICR as facilitator, but all will be applied directly to RATE. Of course, the investigators must also be upheld with prayer for wisdom, protection, and success.

Here's my prediction. As God's Word is honored and the specially trained scientists continue to do their work in submission to the Biblical world-view, answers will begin to come which will thrill Christians and change science. It may take a few more years, but standard, old-earth thinking based on radioisotope decay will begin to crumble. Time is running out on the theory of evolution. To God be the glory!

Acknowledgments

The members of the RATE group thank the Institute for Creation Research (ICR) and the Creation Research Society (CRS) for publishing this book. We recognize that statements the RATE group makes or conclusions it reaches may not necessarily represent the positions or viewpoints of ICR or CRS. We also thank Laurel Hemmings, for the excellent word processing she did on this book.

We thank the technical reviewers who read the early manuscripts and made comments to the authors. Most reviewers are young-earth creationists, but several do not agree with some of the positions or conclusions reached by the authors. However, all were gracious in offering their comments to make this book the best technical resource possible. The following scientists helped in the review process: Dr. Gerald Aardsma, Lodi, Illinois; Mr. Mark Armitage, Azusa Pacific University, Azusa, California; Dr. David R. Boylan, Dean of the College of Engineering (retired), Iowa State University, Ames, Iowa, currently Professor of Science, Faith Bible College and Theological Seminary, Ankeny, Iowa; Dr. Ben Clausen, Geoscience Research Institute, Loma Linda, California; Dr. Paul Giem, Loma Linda University, Loma Linda, California; Dr. Larry Helmick, Cedarville College, Cedarville, Ohio; Dr. J. C. Keister, 3M Corporation, Minneapolis, Minnesota; Dr. Ron Mathis, Ramona, California; Dr. Theodore Rybka, Reno, Nevada; Dr. Ker Thomson, Oklahoma Baptist University (retired), Dayton, Tennessee; Dr. Erich A. Von Fange, Dean of Concordia Lutheran College (retired), Ann Arbor, Michigan; Dr. Keith Wanser, California State University at Fullerton, Fullerton, California; Dr. Clyde Webster, Geoscience Research Institute, Loma Linda, California; Dr. Kurt P. Wise, Bryan College, Dayton, Tennessee; and Dr. Paul A. Zimmerman, former President of Concordia College, Seward, Nebraska, Concordia University, River Forest, Illinois, and Concordia College, Ann Arbor, Michigan.

Finally, the RATE group thanks the many donors who have contributed to the research efforts on which we are about to embark. This book was

published using some of those funds. Over the next five years we hope to answer some of the questions which have been raised in this book. At a minimum, we hope to advance our understanding about the age of the earth and possibly resolve the apparent dilemma regarding radioisotopes. We request your continued prayers on our behalf.

List of Tables

Table	Title	Page
Introduction		
1	High priority RATE experiments	16
2	Lower priority RATE experiments	17
Radioisotope Dating Review		
1	Radioactive isotopes commonly used in radioisotope dating	30
Distribution of Radioactive Isotopes in the Earth		
1	Classification of the elements	55
2	Estimated chemical composition for the bulk silicate earth	70
Geochemical Processes in the Mantle and the Crust		
1	Examples from the literature of recent or young volcanic rocks	128
2	Patterns of discordance between U-Th-Pb “ages”	173
3	Model Nd “ages” calculated for CHUR and depleted mantle	229
4	The isotopic character of crust and mantle reservoirs	240
Theoretical Mechanisms of Accelerated Radioactive Decay		
1	Alternative fission track producers	319
Accelerated Nuclear Decay: A Viable Hypothesis?		
1	Biblical evidence for a young world	338
2	Scientific evidence for a young world	339
3	Helium retention in Jemez zircons	346
Radiohalos		
1	Comparison of sizes of ^4He induced coloration bands	388
2	Half-lives and energies of the α -particles emitted by radioisotopes	396
3	Frequency of halo sizes in a Madagascan biotite	402
4	A list of localities from which polonium halos have been reported	442
5	Geology of localities of reported polonium halos	444

List of Figures

Figure	Title	Page
Radioisotope Dating Review		
1	The decay scheme for ^{238}U or Neptunium Series.	33
2	The decay scheme for ^{235}U or Actinium Series.	34
3	Thorium or ^{232}Th Series.	35
4	A typical isochron graph.	41
Distribution of Radioisotopes in the Earth		
1	Cross-sectional view through the earth.	52
2	Concentrations of selected trace and major elements.	60
3	Ratios of element abundances.	62
4	Sections of Bencubbin meteorite and chondrite fragment.	64
5	Variation diagrams using refractory lithophile element ratios.	68
6	Plot of the abundances of elements in the pyrolite model.	72
7	Proportion of the element budget of the bulk silicate earth.	75
8	Surface heat flow versus radiogenic heat production rate.	81
Mineral Isochron Method Applied as a Test of the Assumptions of Radioisotope Dating		
1	The assumptions and methods of isochron dating.	100
2	Lead-lead isochron plot of five meteorites used by Patterson.	102
3	Samarium-neodymium whole-rock isochron ages for the Lewisian Metamorphic Complex.	110
4	Lead-lead and Samarium-neodymium mineral isochron ages for one amphibolite rock from the Lewisian Metamorphic Complex.	111
5	Lead-lead linear array plot for fifteen chondritic meteorites.	114
6	Rubidium-strontium linear array plot for 23 chondritic meteorites.	115
Geochemical Processes in the Mantle and Crust		
1	Excess content of radiogenic ^{40}Ar ($^{40}\text{Ar}^*$) and apparent age as functions of distance inwards from the rim of a basalt pillow.	132
2	K-Ar "model ages" of the Cardenas Basalt, eastern Grand Canyon.	134
3	Schematic model of the pathways by which atmospheric, crustal, and mantle-derived noble gases enter magmas.	143
4	Apparent age versus distance profile across adjacent biotite grains.	145

List of Figures

Figure	Title	Page
5	^{40}Ar - ^{39}Ar “age” spectra for plagioclases.	147
6	Mantle-crust domains and the distribution of mafic magmas.	150
7	Plot of apparent mineral “ages” against outward distance.	155
8	$^{40}\text{Ar}^*$ versus ^{40}K for the Middle Proterozoic Cardenas Basalt of the eastern Grand Canyon.	157
9	Whole-rock plus mineral isochron diagrams for Granite Mountains.	162
10	Concordia diagram for samples of the granite of Lankin Dome.	164
11	Changes in $^{206}\text{Pb}/^{238}\text{U}$ and $^{207}\text{Pb}/^{206}\text{Pb}$ “ages” and in concentrations of U, Th, and ^{206}Pb in zircons.	167
12	SHRIMP analytical results for baddeleyite.	170
13	Pb-Pb “isochron” diagram defined by ocean island basalts.	180
14	Plot of initial Pb isotope ratios for Tertiary igneous rocks.	183
15	Plot of $^{207}\text{Pb}/^{206}\text{Pb}$ versus $^{204}\text{Pb}/^{206}\text{Pb}$ in soils from Koongarra.	185
16	Epsilon (ϵ) values of Nd and Sr of granitic rocks and xenoliths.	195
17	Hyperbolic Sr-Nd isotopic array for Lachlan Fold Belt rocks.	197
18	Rb-Sr model “ages” of Holocene glauconite pellets.	207
19	Isotopic evolution of Nd in a chondritic uniform reservoir (CHUR).	223
20	The evolution of $^{143}\text{Nd}/^{144}\text{Nd}$ in the mantle.	226
21	The evolution of $^{143}\text{Nd}/^{144}\text{Nd}$ for depleted mantle and crust.	231
22	Map of the USA, showing the Nd “model age” provinces.	233
23	Estimated area of North American crustal basement.	236
24	$^{143}\text{Nd}/^{144}\text{Nd}$ versus $^{87}\text{Sr}/^{86}\text{Sr}$ isotope correlation diagram.	242
25	$^{143}\text{Nd}/^{144}\text{Nd}$ versus $^{87}\text{Sr}/^{86}\text{Sr}$ (ϵ_{Nd} versus ϵ_{Sr}) correlation diagram.	243
26	$^{208}\text{Pb}/^{204}\text{Pb}$ versus $^{206}\text{Pb}/^{204}\text{Pb}$ isotope correlation diagram.	244
27	$^{87}\text{Sr}/^{86}\text{Sr}$ versus $^{206}\text{Pb}/^{204}\text{Pb}$ isotope correlation diagram.	245
28	Cartoon diagram showing crust and mantle reservoirs.	247
29	The “evolution” of Sr isotopes with time.	252
30	The evolution of $^{87}\text{Sr}/^{86}\text{Sr}$ with time in the crust and mantle.	254
31	The evolution of $^{143}\text{Nd}/^{144}\text{Nd}$ isotopes with time.	255
32	The evolution of Pb isotopes with time.	256
33	$^{143}\text{Nd}/^{144}\text{Nd}$ versus $^{87}\text{Sr}/^{86}\text{Sr}$ correlation diagram.	259

List of Figures

Figure	Title	Page
34	Change in $^{87}\text{Sr}/^{86}\text{Sr}$ with stratigraphic height in the Bushveld intrusion, South Africa.	261
35	Lead isotope evolution curves for the crust, mantle, and orogene.	265
36	Reservoirs and fluxes of the transport balance model.	269
37	Cartoon of stratified mantle convection.	270
38	Alternative paradigm of whole mantle convection.	271
Theoretical Mechanisms of Accelerated Radioactive Decay		
1	The ion-explosion spike model of fission track formation.	314
2	A graph of α -decay half-life versus spontaneous fission half-life.	317
Accelerated Nuclear Decay: A Viable Hypothesis?		
1	Mature ^{238}U radiohalo with all eight rings produced by α -particles.	335
2	Possible history of nuclear decay rates.	341
3	Published radioisotope ages related to their geologic stratum.	342
4	Lava flows deposited during the year of the Genesis Flood.	343
5	Zircons in a Precambrian granitic formation retain radiogenic He.	345
6	Helium diffuses very rapidly out of bare zircons.	347
7	Predictions of experiments on He diffusion through biotite.	348
8	Some α -particles have energy to surmount "coulomb barrier".	358
9	The α -decay half-life of ^{226}Ra .	361
10	The "vacuum" of quantum field theory.	368
Radiohalos		
1	Sunburst effect of α -damage trails.	382
2	Part of the chart of the nuclides showing the Th- and U-series.	385
3	Schematic drawing of a ^{238}U halo and a ^{232}Th halo.	386
4	Composite drawings of ^{218}Po , ^{238}U , ^{214}Po , and ^{210}Po halos.	408
5	Schematic drawings of ^{232}Th and ^{212}Bi - ^{212}Po halos.	439

Contents

Chapter	Subject	Author	Page
	Prologue	John D. Morris	iii
	Acknowledgments		ix
	List of Tables		xii
	List of Figures		xiii
1	Introduction	Larry Vardiman	1
2	Radioisotope Dating Review	Don DeYoung	27
3	Distribution of Radioactive Isotopes in the Earth	John R. Baumgardner	49
4	Mineral Isochron Method Applied as a Test of the Assumptions of Radioisotope Dating	Steven A. Austin	95
5	Geochemical Processes in the Mantle and Crust	Andrew A. Snelling	123
6	Theoretical Mechanisms of Accelerated Radioactive Decay	Eugene F. Chaffin	305
7	Accelerated Nuclear Decay: A Viable Hypothesis?	D. Russell Humphreys	333
8	Radiohalos	Andrew A. Snelling	381
	Glossary		469
	Appendix		561
	Index		629

Chapter 1

Introduction

Larry Vardiman, Ph.D.*

Abstract. One of the most significant challenges to young-earth creationism is the perception that radioisotope dating methods have established that the earth and universe are billions of years old. A group of young-earth researchers called RATE (**R**adioisotopes and the **A**ge of **T**he **E**arth) have banded together to investigate the basis of these claims and offer an alternative young-earth explanation. It is believed by the RATE group that processes other than radioactive decay over long periods of time may better explain the presence of secondary decay products. This introduction discusses the deliberations of the four meetings held by this group of scientists to date and their projected plans for research on this problem. It further outlines some of the details for the research projects, time lines, and costs and summarizes the contents of the remainder of this report.

1. The Age Issue

The conventional scientific view expressed today is that the earth is about 4.6 billion years old and the universe between 10 and 20 billion years old. These estimates are based primarily on the abundances of parent and daughter radioisotopes and the implications of stellar and cosmological models. Yet, a literal interpretation of Scripture and much scientific evidence indicates that the Creation of the earth, the solar system, and the universe occurred a few thousand years ago.

One of the principal driving forces which has traditionally driven estimates of an old age for the earth is the necessity for long periods of time for evolution. Even before radioactivity was discovered in the 1890s,

* *Administrative Vice President and Astrogeophysics Department Chairman,
Institute for Creation Research, Santee, California*

estimates of the age of the earth were growing longer and longer as the complex nature of life became more evident. It has never been demonstrated that the evolution of life from inorganic chemicals has occurred or that life has evolved from simple life forms to the complex ones we see today. Evidence for the evolution of life is fragmentary or missing at best, and illogical and improbable at worst. However, even if life could somehow have evolved, it would take much longer than billions of years for the process to occur.

Some Christians have questioned the young-earth interpretation and some have now abandoned the clear statements of Scripture about the age of the earth. They believe that the evidence for an old earth is so compelling that they must accommodate some form of long ages and even evolution with the Bible. Two traditional methods of accommodation have been to hypothesize either a long period of time between Genesis 1:1 and 1:2 (the Gap Theory) or that the days of Creation were long periods of time (the Day-Age Theory). A popular form of accommodation today is called Progressive Creationism in which God supernaturally guided the process attributed to evolution by intervening in the process at critical steps along the way. All of these attempts to harmonize science and the Bible have serious flaws, however.

No matter which form of accommodation is used, the effect is to degrade the reliability and authority of Scripture. Even the statements of Christ are viewed by many as not coming from the triune God but containing error because of Christ's limited knowledge of science. Carl Sagan (now deceased) once asked me, "How can you seriously believe the pronouncements of a band of ignorant shepherds who lived several thousand years before the discoveries of the 20th century?" I responded that because God inspired the very words of Scripture, many of the statements in the Bible reveal information which not even the writers may have understood. Because of prevalent attitudes such as those of Carl Sagan, I believe it is time that the age of the earth be addressed more thoroughly and the specific question of radioactive decay be explained in a young-earth timeframe. Only then will some Christians be able to accept statements from Scripture about the age of the earth and miraculous events such as Creation, the Flood, and the Incarnation.

Young-earth creationists are not convinced that long periods of time have occurred since the origin of the earth and the universe. In defending a young-earth position, they typically point to questionable assumptions in dating schemes. For example, in radioisotope dating, when a parent isotope decays into a daughter isotope, the concentration of the daughter isotope in existence at the initial time will affect the estimate of time since the process started. Creationists sometimes question the conventional assumption that the amount of daughter product is small at the initial time. Isochron dating attempts to correct for this, but the technique itself apparently has problems. Also frequently questioned by creationists are the assumptions that the quantities of the parent and daughter isotopes were not affected by other non-radioactive processes and that the rate of decay from parent to daughter was constant during the period of the decay process. Attempts are made by most researchers to justify each of these three assumptions, but ultimately no one can be certain if the conditions were met, particularly over long periods of time.

For many years, creationists have been satisfied to criticize age estimates based on radioisotope methods because of this unjustified dependence upon these assumptions. However, it has now become evident that even when the weaknesses of these assumptions are pointed out, many people are still convinced of the legitimacy of the estimated long periods of time. Even Christians who wish to believe in a literal, recent creation seem to be overwhelmed by the argument that the earth and universe are old. It is clear that the age issue must be readdressed and an attempt made to discover an explanation for the abundances of radioactive elements within a young-earth timeframe.

It appears that much larger quantities of nuclear decay have occurred in most nuclear processes than would be expected for a few thousand years of radioactivity at the currently observed rates. If this large amount of nuclear decay occurred, when did it occur and what caused it? Is it scientifically feasible for the rates of decay of radioisotopes to be accelerated? What are the implications of accelerated rates of decay on radioactive materials? Where did all the heat go? What about life on the earth during the accelerated decay?

It is hypothesized by the RATE group (**R**adioisotopes and the **A**ge of

The Earth) that at some time in the past much higher rates of radioisotope decay may have occurred, leading to the production of large quantities of daughter products in a short period of time. It has been suggested that these increased decay rates may have been part of the rock-forming process on the early earth and/or one of the results of God's judgment upon man following the Creation, that is, the Curse or during the Flood.

The amount of decay products which should exist, given the conventional old-earth model, differs from that expected by the young-earth creationist model, in most cases, by over five orders of magnitude (that is, 100,000 times). The RATE group believes this large difference may make it possible to validate a true model of earth history. For example, the expected rate of escape of helium ($^4\text{He}^*$) from minerals in rocks which have undergone a large degree of nuclear decay only a few thousand years ago would seem to indicate that much of the decay-produced He should still be trapped in the rocks. The observation of minimal He in the rocks would support the old-earth model, but abundant He still in the rocks would validate the young-earth model. This difference should be capable of confirmation in the laboratory. The exciting part of this effort is that the evolution model would be on the defensive if abundant He is confirmed. Initial observations indicate that a vast amount of He has been produced by radioactive decay but most has been retained in the rocks.

Before proceeding to discuss the particulars of the meetings of the RATE group and research plans for exploring alternative young-earth explanations for radioactive decay, a few words should be said about a traditional view of Creation by young-earth creationists—that of *fiat* Creation with little or no subsequent process. Although the RATE group is studying geophysical and geochemical processes which have produced radioactive daughter products, halos, fission tracks, and residual heat, we are not yet fully convinced that these features are not part of the *fiat* Creation in the beginning. It is conceivable that these geophysical and geochemical evidences for “process” could have been part of the first

* Elements have been abbreviated in this book using the standard symbols. See the inside front cover for a list of names, symbols, and atomic weights. See the inside back cover for a periodic table. The superscripted number in front of a symbol indicates the atomic weight.

day of Creation.

It is the position of the RATE group that the Creator formed the earth *ex nihilo* (from nothing) a few thousand years ago. We also believe it is possible that the ratios of parent and daughter elements were created the same, or nearly the same as they are observed today in that instantaneous creative process. However, both Scriptures and scientific evidence seem to say that a significant process was involved in the Creation of the earth.

For example, the Scriptures say that during the first three days of Creation a sequence of events was orchestrated by God which was not instantaneous, but occurred at an extremely high rate, and would be considered catastrophic today. Mass, space, and time were created; the primordial earth was formed in a matrix of “waters”; the waters were separated to form the heaven; and the waters were further separated to form the dry land and the seas. This all occurred in three literal 24-hour days, according to the Scriptures. The scientific evidence also seems to indicate that major upheavals in the earth have occurred in the past. It is likely that overturning of the earth’s crust, mantle, and core has mixed reservoirs of molten elements and rearranged their contents. These catastrophic processes could have been incidental to or directly associated with periods of high rates of radioactive decay.

The RATE group suspects that large amounts of radioactive decay occurred during the first three days of Creation as part of the supernatural Creation process. The jury is still out and, until we complete our research phase, this concept is only hypothetical. The presence of supernatural “process” during Creation is essential to our approach, however.

The implications of “process” during Creation are much deeper than at first might be thought. If a radioactive “decay” process occurred rapidly during Creation and continued more slowly thereafter, how is it possible for God to say at the end of the sixth day, “*And God saw every thing that He had made, and, behold, it was very good*” (Genesis 1:31)? The assumption when saying this, of course, is that radioactive decay is inherently “bad”. The RATE group does not have an adequate response to this criticism yet. We will need to address this theological issue further as we conduct our research over the next few years.

Scripture also talks of at least two other major events which occurred after Creation, the Judgment in the Garden of Eden and the Flood. Creation, the Judgment, and the Flood were all supernatural events and it would seem appropriate to at least consider that an original distribution of elements could have been mixed and radioactive processes speeded up during one or any of them.

Within the RATE group there are several concepts for solving the age-of-the-earth problem. Initially, we attempted to narrow our approach from several hypotheses to only one. However, we decided by the time this book was published that we would be better served to pursue multiple hypotheses. We are beginning to suspect that the final explanation may involve a combination of at least two of them, accelerated decay and mixing. Not all RATE members are in agreement with one another or with this pluralistic approach. However, all members are able to work together, peaceably critique each other's work, and function as a team. Most of these different views may be resolved by the end of the research effort.

The key to research of this type is to allow God's revelation to be our primary guide when exploring new data. Our unified premise is that observation and theory should always be subservient to a proper understanding of the Word of God. But, this being said, we should never be afraid to search out new data and develop new theories. Of course, it is vital that we interpret the Word of God correctly. None of these issues are easy and are fraught with many pitfalls. A major safeguard in this endeavor is submission to the Holy Spirit as He illumines our minds and guides our efforts.

2. The First RATE Meeting

For several years Dr. Robert Armstrong, a Board member for the Institute for Creation Research (ICR), had been suggesting that radioisotopes and the age of the earth was a major problem which needed significant research attention. On July 5, 1997 a group of six active young-earth creationist researchers agreed to meet together and address this issue. They met in San Diego, California and each presented a

position paper on the topic of radioactive decay and the age of the earth. It was recognized by the group that radioisotopes and the age of the earth were significant problems which must be addressed if young-earth creationism was to continue to have a significant impact on the issue of origins both within and outside the Christian community.

The six members of the research group were Dr. Steve Austin, Dr. John Baumgardner, Dr. Eugene Chaffin, Dr. Don DeYoung, Dr. Russell Humphreys, and Dr. Andrew Snelling. Dr. Larry Vardiman served as moderator. Dr. Henry M. Morris, Dr. John Morris, and Dr. Kenneth Cumming attended as observers. Three members of the research team have training and expertise in physics and three in geology or geophysics. Dr. Chaffin agreed to function as the chair for the physics sub-group and Dr. Andrew Snelling agreed to serve as chair for the geology/geophysics sub-group. It was agreed that the group would adopt the acronym RATE for **R**adioisotopes and the **A**ge of **T**he **E**arth and would conduct annual meetings to exchange data, findings, and plans. The group also agreed to publish its findings.

The RATE group decided that the principal tentative approach to this research effort for the first year would be to explore accelerated rates of decay of radioisotopes during one or more of the Creation, Fall, and Flood events. Several sources of data suggest that significant quantities of radioactive decay have occurred in the history of the earth and cosmos. The conventional old-earth model assumes that this decay has occurred over billions of years rather than in concentrated episodes over short periods of time. Research may be able to distinguish reasons for the difference in these models.

Part of the group believed that the evidence was sufficiently strong to justify an all-out effort on accelerated decay, immediately. Another part of the group was sympathetic to this approach, but preferred to gather more data before committing to only one direction. It was anticipated that these data and other avenues of research could be evaluated sufficiently by the year 2000 to make an informed decision on the approach for the next stage of the effort.

Whether accelerated decay would be the final approach followed or not, the geochemical/geophysical evidence in the rocks must be

consistent with whatever theory is proposed. In other words, the distribution of parent and daughter elements in the stratigraphic record must occur in a manner which would validate the theory, and any deviations should be explained by geological/geochemical processes. For example, if accelerated decay occurred only during the Flood, then strata which were laid down before the Flood should show different ratios of radioisotopes and daughter products than strata laid down during or following the Flood. Because there are still major differences of opinion about the location of Flood boundaries, this is expected to be difficult. In fact, a study of the distribution of parent and daughter elements relative to the Flood may go a long way toward helping define the boundaries of Flood strata. Radioisotope data from the Moon or Mars may add additional insights.

One major obstacle to accelerated decay is an explanation for the disposal of the great quantities of heat which would be generated by radioactive decay over short periods of time. For example, if most of the radioactive decay implied by fission tracks or quantities of daughter products occurred over the year of the Flood, the amount of heat generated may have been sufficient to vaporize all the waters of the oceans and melt portions of the earth's crust, given present conditions.

A second obstacle to accelerated decay is the ability of life to cope with the great quantities of ionizing radiation that would have been generated by accelerated decay over short periods of time. This is particularly so with respect to ^{40}K in animal and human bodies. For example, Noah and his family and the animals would likely have been subjected to deadly concentrations of radiation during their stay on the ark if accelerated rates of decay occurred during the Flood. Although the water beneath the ark would have probably protected him from radiation from the earth below, if Noah had similar concentrations of K in his body as we do today, radioactive decay from within his body would have been very destructive.

A third obstacle is the theological difficulties with the notion of "decay" prior to the Fall. If accelerated decay is believed to have occurred during days 1 and 2 of the Creation week before there was any life on the earth, this would seem to be inconsistent with the perfect world God created

before the sin of Adam and Eve. Yet, if accelerated decay occurred after days 1 and 2, it would likely have damaged or destroyed life as we know it unless there were other extenuating circumstances.

At least one theory of cosmology has been proposed by a member of the RATE group which would compensate for this large amount of heat and possibly even result in net volumetric cooling in places. It has been suggested by others that animals and plants did not contain significant concentrations of ^{40}K until after the Flood when the crust of the earth was disrupted. This would permit accelerated decay during the Flood without Noah and the animals being affected by it. Such theories seem to ultimately depend upon supernatural intervention at the time of Creation, Fall, and the Flood. God's intervention is explicitly stated in Scripture (II Peter 3: 5–7). Although these concepts have not been adequately explored at this time, they could well result in an alternative explanation to many processes in the earth and cosmos. The group is strongly committed to exploring various ways in which data for large quantities of radioactive decay can be explained within a young-earth timeframe. In this effort the RATE group is committed to a literal interpretation of the Bible which honors God as Creator and Sustainer of this world.

Interaction among the researchers helped focus on the primary research needs with each contributing to the thinking of the whole. The theorists in the group listed several sets of data needed from the experimentalists to verify or disprove their theories. The experimentalists listed several concepts and processes which needed to be explored by the theorists to explain existing data. Both theorists and experimentalists plan to expand their lists to help the others in their research.

It was agreed among the RATE group that the focus of RATE research would be primarily on long-age isotopes and their use as geochronometers. This is due to the importance they play in the origin of the universe and solar system. Carbon-14 dating is a field unto itself and concerns archeological and other more-recent events. Although separating long and short-age isotopes is a somewhat artificial distinction, the group felt that by narrowing the problem somewhat a greater likelihood of success was possible. For similar reasons the study of

geochronometers other than those which involved radioactive processes would also not be considered.

A general principle commonly used in science was discussed and agreed upon for application to our research, that of Occam's razor. This is the approach to truth that says the simplest, most elegant explanation for an observed phenomenon which appeals to the fewest miracles is considered to be the most-likely solution. This principle is based on the concept that God designs systems to operate in accordance with efficiency, order, and beauty. Use of this principle by the RATE group does not imply that we eliminate the occurrence of miracles, but rather, we minimize the number of miracles and attempt to relate them to supernatural events specifically mentioned in the Scriptures.

3. The Second RATE Meeting

On May 20–21, 1998 a second RATE conference met in San Diego, California. The same six research scientists with specialized training in geology, geophysics, astrophysics, and physics who formed the original group met to report on research completed over the past year. Dr. John Morris, President of ICR and Dr. Kenneth Cumming, Academic Dean of the ICR Graduate School attended as observers. Dr. Larry Vardiman of ICR chaired the meeting. The Institute for Creation Research (ICR), Answers in Genesis (AiG), and the Creation Research Society (CRS) jointly sponsored this conference.

Dr. Steven Austin, Professor of Geology at ICR, led off the conference with a paper entitled, "Continuing Research on Isochron Dating Methods Applied to Grand Canyon Rocks." He presented plots of the ratios of various radionuclides usually interpreted as "isochron ages" from over 40 rock samples collected from Grand Canyon Pleistocene and Precambrian layers. These samples were analyzed using Pb-Pb, Sm-Nd, Rb-Sr, and K-Ar methods. Attention was focused on daughter products Pb, Nd, Sr, and Ar in whole-rock and mineral concentrates. The various linear array plots could be interpreted as "isochrons" from the different dating methods. However, discordant "ages" resulted, even for mineral concentrates from the same rock. Although the discordant

isochron “ages” are the normal pattern, the discordance seems to differ in a predictable fashion. Alpha-decay methods generally seem to give older “ages” than β -decay methods. He suggested that more measurements and analyses, especially mineral isochrons, might help identify the cause of the observed trends.

Dr. Andrew Snelling, Associate Professor of Geology at ICR (formerly with Answers in Genesis), continued the geological emphasis with a paper entitled, “Solving the Long-Age Isotope Dating Problem: Geology and Geochemistry.” He reported on the K-Ar analyses of recent (less than 50 years old) lava flows at Mt. Ngauruhoe, New Zealand which produced model ages as high as 3.5 million years. He presented the view that the large age is due to excessive concentrations of Ar in the samples which render problematic the use of K-Ar and Ar-Ar as methods for dating rocks. It is not possible to distinguish the primordial Ar incorporated as a rock formed from that produced later by nuclear decay. Dr. Snelling demonstrated that Ar is infiltrating the crust of the earth from reservoirs in the mantle over various space and time scales. Additionally, the Sm-Nd, Rb-Sr, and U-Th-Pb dating methods also rely on assumptions about the initial starting conditions in the earth’s mantle. Various hypothetical models for different compositional domains in the mantle are utilized by geochemists to explain the measured isotope ratios in crustal rocks, in some instances without resorting to age interpretations. Dr. Snelling indicated that he intended to pursue this explanation in addition to accelerated decay.

Dr. John Baumgardner, geophysicist at the Los Alamos National Laboratories, offered a paper entitled, “The Distribution of Radioactive Elements in the Earth and Implications Relative to the History of Nuclear Decay.” He presented data for the concentration of radioactive elements and corresponding heat production for different geological materials and their distribution relative to the earth’s surface. The data showed that the most radioactive rocks are strongly concentrated toward the earth’s surface, particularly in the continental crust. Dr. Baumgardner emphasized the curious fact that the flow of heat out of bodies of continental igneous rocks is strongly correlated, at an outcrop-to-outcrop level, with the amount of radioactivity measured in the rocks exposed at

the surface. This suggests the current surface heat flow is dominated by the radioactive heat generation that has occurred in the recent past in the rock near the surface. Such a pattern of heat flow is consistent with an episode of accelerated nuclear decay just a few thousand years ago in connection with the Genesis Flood that abruptly raised the temperature in these rocks and caused the subsequent total heat flow to be dominated by a near surface contribution. The amount of decay associated with such a decay episode seems to be strongly constrained by the concentrations of radioactive elements in these rocks to, at most, only a few million years' worth at present rates.

Dr. Donald DeYoung, currently President of the Creation Research Society and Professor of Physics at Grace College in Indiana, in response to a request to begin writing chapters for the Status Report to be published by the RATE group in the year 2000, presented a paper entitled, "Radiometric Dating Review." In this paper he discussed the procedures and assumptions of seven of the more popular dating methods used for rocks, including Sm-Nd, Re-Os, U-Pb, Th-Pb, Rb-Sr, K-Ar, and Ar-Ar. He stressed that all of these methods make three main assumptions. In all cases it is assumed in conventional age dating that the nuclear decay rate or half-life has always remained constant, that the isotopic composition of rock samples has not been changed by fractionation over time, and that rock samples have been closed systems over time with no migration of parent or daughter elements into or out of the rocks. Dr. DeYoung then explored briefly the magnitude of accelerated decay necessary to explain all of the daughter products typically found in rocks.

Dr. Eugene Chaffin, recently editor of the *Creation Research Society Quarterly* and Professor of Physics at Bob Jones University, led off a series of three physics presentations. He presented a paper entitled, "A Study of the Variation in the Neutron Resonance and Effective Capture Cross Section of Samarium for the Oklo Natural Reactor." The Oklo natural reactor is an accumulation of fissionable ^{238}U (uranium) in a sandstone layer in Africa which apparently was active during earth history. This natural reactor has produced fission products which could provide clues about higher decay rates in the past. By looking at residual daughter elements Dr. Chaffin has attempted to show that the natural

reactor would be consistent with a young earth, not one which is billions of years old. If an accelerated decay event occurred, the concern is that the ore in the Oklo natural reactor would not be present in the measured amounts. In this presentation, Dr. Chaffin called into question the treatment of the calculated cross section of the Sm isotopes which act as “poisons” in the reactor to slow down the process. He suggested that several variables in the calculation of nuclear cross section could change by orders of magnitude under conditions of an accelerated decay rate.

Dr. D. Russell Humphreys, a physicist at Sandia National Laboratories, presented a paper entitled, “Helium Diffusion in Granite.” Dr. Humphreys offered both experimental and theoretical data to support his hypothesis that the concentration of radiogenic ^4He generated by α -decay is too high in certain minerals in granite if the earth is billions of years old. The diffusion rate of ^4He through granite should have permitted most of the ^4He to have already “leaked” into the atmosphere. However, if an accelerated decay event occurred only a few thousand years ago, the measured concentrations of ^4He would be consistent with the calculated diffusion rate. Helium-4 is produced by radioactive decay of ^{238}U and ^{232}Th within zircon crystals embedded in biotite crystals in granite. Although the diffusion rate of a similar gas, ^{40}Ar , has been measured in biotite, no results for ^4He diffusion have been reported in the literature. The predictions of diffusion rates between the two age models differ by five orders of magnitude. Dr. Humphreys suggested that a high-priority experiment for the RATE project should be a well-designed and executed laboratory experiment on the diffusion rate of He through biotite.

Dr. Keith Wanser, Professor of Physics at California State University Fullerton, and guest at this meeting was invited to present a paper to the RATE group entitled, “Non-Exponential Decay of Quantum Mechanical Systems Due to Tunneling.” Although Dr. Wanser is not part of the steering committee for the RATE project, he was invited to participate on the first day of presentations because of the possible significance of his research to the effort. The RATE group plans to include other researchers in the formal presentations from time to time, on an invited basis, as appropriate research and opportunities occur. Dr. Wanser’s presentation dealt with the rigorous quantum theory of time dependent

tunneling, which produces non-exponential time dependence in nuclear decay rates. The difficulty in making these calculations is finding analytical methods which will allow computation of the decay probability over an extreme range of time scales (at least 37 orders of magnitude). He found an analytical solution for the Green's function which reduces the time dependence of the decay probability to the evaluation of a single integral. For the α -decay problem, he plans to investigate Sm first, which has the longest half-life (2.1×10^{15} years) and the lowest α -particle energy (1.83 MeV) of any α -emitter. As such, it is expected to exhibit the greatest non-exponential decay effects at short times.

The RATE group met for a second day to discuss plans for additional research and publication of the Status Report in 2000. About a dozen theoretical and experimental research projects were identified for consideration. The RATE group decided to write research proposals during the following year so that individuals and foundations could be approached for funding. Additional researchers would be solicited in the various areas of expertise needed to work directly with the RATE scientists. A Status Report and a Research Plan were expected to be published in the summer of 2000. Following release of this report the RATE group plans to conduct research on this project for a period of five years and report on the progress in a final report in the year 2005.

4. The Third RATE Meeting

The RATE group met again on June 3–4, 1999 in Albuquerque, New Mexico to receive the first draft of its Status Report on radioisotope dating and establish priorities on research projects. Dr. Larry Vardiman facilitated the meeting and offered to serve as editor of the upcoming report. Drs. Steve Austin, John Baumgardner, Eugene Chaffin, Don DeYoung, Russell Humphreys, and Andrew Snelling contributed draft chapters to the book and suggested research projects for the five-year research program. Dr. John Morris, President of ICR, and Dr. David Boylan, a member of the ICR technical advisory board, attended as observers by invitation.

The RATE group continued its plans for publishing a report in the

year 2000. Drafts of each of the chapters for this book were reviewed during the Fall of 1999 and a second draft was received for final editing in the Spring of 2000. After a final review by the authors the book release was planned for the Fall of 2000. The purpose of the report is to provide a benchmark on radioisotope dating and lay out a five-year plan for research. Part of the report is a five-year plan for research to explain the apparent disparity between conventional and Biblical dates.

At the Albuquerque meeting a full day was devoted to the discussion of suggested research projects. Ten research projects were offered by the RATE group which were designed to resolve various issues or answer questions about how nuclear decay has occurred. The basic question which is to be addressed in most of the research projects is how to explain the evidence for large amounts of daughter products.

It appears that much larger quantities of nuclear decay may have occurred than would be expected for a few thousand years of radioactivity at the currently observed rate. The evidence for this concern stems from:

- the presence of daughter isotopes along the entire decay chain in proximity to parent isotopes,
- visible scars (halos) from α -decay,
- the presence of α -particles themselves (He nuclei) still within the rock where they were apparently formed by nuclear decay,
- visible tracks from decay by fission,
- residual heat produced by nuclear decay in proximity to high U concentrations.

Of the ten research projects suggested to the RATE group, five were selected for their value in addressing some of the more important questions in distinguishing the Creation and evolution models. These five projects will be emphasized in fundraising and rapid accomplishment. Although all ten projects will contribute to the solution of the radioisotope dating problem, it was decided that priority should be given to the five projects shown in Table 1 to advance the solution rapidly during the first few years of the research phase. If some of the first five projects are completed quickly or sufficient amounts of funding and expertise are received to address all ten, then the group will advance the timetable to address the others as well. Donors had contributed about

Table 1. High priority RATE experiments.

Experiment	Description	Expected Results	Cost	Time
He diffusion	Determine He diffusion rates through biotites under various temperature conditions.	Acquisition of data on which to base a claim that the amount of He in rocks today should not be so high if it was produced by nuclear decay over millions of years. If the He was produced within the most recent thousands of years, it would be expected to still remain in the rocks as observed.	\$100,000	2 years
Isochron Discordance	Construct 5-point mineral and whole-rock isochrons on selected gabbros formed during the Flood.	Increase evidence for discordance among isotopic dating methods using isochrons for mineral components of Flood-related rocks. Based on the consistency of the discordance from these specimens and others, infer the processes which led to the distribution of isotopes.	\$50,000	2 years
Nuclear Decay Theory	Conduct a literature search for evidence and models of accelerated nuclear decay and adapt to a creationist worldview if appropriate. Complete studies on α and β decay.	Increase evidence that nuclear decay can vary radically in response to changes in cosmological "constants" and environmental effects. Associate other likely effects with Biblical statements and observational data.	\$30,000	2 years
Radiohalos	Determine the geological distribution of Po halos, their proximity to concentrations of U and the relationship to different halo types.	Resolve the question if Po halos are special evidence for created rocks only or could they also occur in Flood rocks. This effort may also allow inferences about the process of radioisotope decay and halo formation.	\$50,000	5 years
Fission Tracks	Estimate nuclear decay rates during the Flood using the fission track method. Select an initial sample from a tuff bed in the Muav Formation of Grand Canyon.	Fission track estimates of nuclear decay rates are thought to be absolute following rock formation and do not inherit prior evidence of decay. It is important to know if decay rates were accelerated during the Flood.	\$50,000	2 years

\$50,000 toward the RATE effort by June of 1999. At least another \$450,000 in donations was anticipated to be needed over the five years of the project to complete the entire research plan.

Estimated costs and timetables are approximate. Since it is recognized that establishment of laboratories to specifically conduct this type of work would be extremely expensive, and the results would tend to be disbelieved by critics, it is the intent of the RATE group to contract most of the studies to commercial, university, or government laboratories with oversight by members of the RATE group. Analysis, interpretation, and reporting of the results would be conducted by a principal RATE investigator(s). Cost and time estimates will need refinement after contract negotiations with selected laboratories have been completed.

In addition to the five high-priority projects, eight other projects considered valuable by the RATE group were shown in Table 2. Only the project name and cost and time estimates were given because of space constraints. Of these projects only the first two related directly to the difference in decay rates and time between the Creation and evolution

Table 2. Lower priority RATE experiments.

Experiment	Cost	Time
Uranium (U)/Thorium (Th) Halos	\$50,000	4 years
Case Studies in Rock Dating	\$100,000	5 years
Biblical Word Studies	\$10,000	2 years
Pu in Oklo Reactor	\$25,000	1 year
Allende Meteorite Origin	\$25,000	1 year
Diffusion of Ar in Biotite	\$40,000	2 years
Origin of Chemical Elements	\$30,000	2 years
Cosmology and Nuclear Decay	\$100,000	5 years

models. Potential donors were offered a complete description of all thirteen research projects in a booklet entitled, "Research proposals for RATE."

5. The Fourth RATE Meeting

The RATE group met in San Diego on June 5–6, 2000 for its fourth annual meeting to complete the final draft of its new book, "Radioisotopes and the Age of the Earth: A Young-Earth Creationist Research Initiative." Each of the seven members of the RATE group wrote one or more chapters in the book and all chapters were reviewed by technical specialists. The fourth RATE meeting permitted a final review of all chapters by the authors.

Numerous changes were suggested to make the book more readable and to emphasize issues which needed to be addressed in the research over the next five years. These editorial changes were added during June and July and the book was printed in September. The hardbound book contains a complete glossary and about 700 pages of discussion on Radioisotope Dating, Radioactive Isotopes in the Earth, the Mineral Isochron Method, Geochemical Processes, Accelerated Radioactive Decay, and Radiohalos. It is expected to become a major source document for both the creationist and evolutionist communities.

The last afternoon of the meeting was spent discussing research findings and plans. Total donations of about \$135,000 were allocated to the research projects at the January meeting of the executive committee of RATE and the expenditures made by June 2000 were reviewed. Three laboratories were located at which the He diffusion experiment of He in biotite could be conducted. It was hoped that an agreement could be finalized with one of the labs by the end of 2000 to conduct the experiment under contract. This experiment was identified as the highest priority experiment in RATE and was designed to confirm the calculated diffusion rate of He in the mineral biotite found in many granites. If the diffusion rate can be measured and agrees with the calculated rate, this experiment would show that He concentrations found in granite are far too high if the earth is 4.6 billion years old. On the other hand, if the

calculated diffusion rate is correct, the observed He concentration is about right for a young earth.

Several other research projects had begun, including the study of theoretical mechanisms for accelerated radioactive decay and the search for Po halos in granites. It was discovered during the discussions on the research that the RATE group needs to put more emphasis on meteorites. The primary method used to estimate the age of the earth comes from radioisotopic analysis of chondritic meteorites. If a large amount of accelerated decay and mixing have affected the earth, how do meteorites fit into this story? Do they reveal information about accelerated decay with no mixing processes? The RATE group decided to procure chondritic meteorite material and conduct its own laboratory analyses.

It was realized by Dr. John Baumgardner during his review of Dr. Snelling's chapter on radiohalos that there was an apparent absence of fully-formed U halos in Phanerozoic rocks (ones containing fossils) reported in the research literature. This was significant because there should be abundant fully-formed U halos in granites during the period when life has been present on earth if the evolutionary timescale is true. If life has been present on the earth for over millions of years, U would have had plenty of time to form complete U halos. If such halos are not present, then the earth must be much younger than the evolutionary model predicts. Given this result, one of the models on which the RATE group is working, the accelerated decay model, seemed to imply that a large amount of radioactive decay may have occurred during the first 2–3 days of Creation with a much smaller amount occurring later, possibly during the Genesis Flood. Another model suggested that primordial daughter products like Pb, Sr, He, and Ar were mixed together with parent elements like U, Rb, and K during catastrophic processes of Creation and the Flood. Both the accelerated decay model and the mixing model are beginning to show real promise in explaining why there seems to be an apparent conflict between the age of the earth stated in Scripture and simplistic calculations based on measurements of radioisotope concentrations. It is too early to reach any conclusions, but both these models were beginning to show encouraging results.

6. Research Proposals for RATE

Beginning in late July, 1999 a booklet containing 13 research proposals was distributed to interested donors. Three research proposals were added to the set of ten which the RATE group had considered at the Third RATE meeting in Albuquerque. The total estimated cost for all 13 research proposals was about \$500,000, including labor costs. As monies come into the RATE project they will be identified by designated research project and the principal investigator. When sufficient monies are received the principal investigator will be authorized to proceed with his research up to a certain spending level. Undesignated funds will be distributed to the high priority projects first. Progress reports will be published annually following the RATE meetings.

7. Allocation of Resources

On January 7–8, 2000 an executive committee of the RATE group met to allocate monies which were donated to RATE. Approximately \$145,000 was donated by the end of 1999 for research and publications. Of these funds \$50,000 was allocated to the He diffusion research project, \$20,000 to publishing expenses for the Status Report, \$15,000 for operating expenses, and \$60,000 distributed over most of the remaining research efforts.

8. Initial Report

It was intended that this initial report entitled, *Radioisotopes and the Age of the Earth: A Young-Earth Creationist Initiative*, be published in 2000. It contains eight chapters, a glossary, and an appendix. The titles, authors, and a short summary of each technical chapter follow:

Radioisotope Dating Review—Don DeYoung, Ph.D.

In Chapter 2, Dr. DeYoung reviews the limitations and assumptions of nine radioisotope dating methods. He critiques their applications and results. The concept of accelerated decay is also briefly explored.

Distribution of Radioactive Isotopes in the Earth—John R. Baumgardner, Ph.D.

In Chapter 3, Dr. Baumgardner reviews the evidence that the earth has experienced a vast amount of chemical differentiation during its history. Such differentiation involved processes that extracted the entire continental crust from the underlying mantle and concentrated into it a large fraction of the mantle's incompatible elements, including the major heat-producing radioactive elements. Dr. Baumgardner concludes that God employed extremely rapid processes to fashion the earth during the early part of Creation Week that left a genuine record in the Archean rocks, including mature ^{238}U halos. He also describes surface heat flow measurements from crustal rocks that argue for an episode of accelerated nuclear decay associated with the Genesis Flood.

Mineral Isochron Method Applied as a Test of the Assumptions of Radioisotope Dating—Steven A. Austin, Ph.D.

In Chapter 4, Dr. Austin reviews four categories of isochron discordance which can be recognized within the published literature on geochronology. The most extraordinary category of discordance (called “category four discordance”) occurs where the individual mineral isochron ages greatly exceed the whole-rock isochron ages for a cogenetic suite of rocks. Lead-lead (Pb-Pb) mineral isochron ages for individual chondritic meteorites usually significantly exceed the associated Pb-Pb, Rb-Sr, and Ar-Ar whole-rock isochron ages for the class of meteorite from which they are derived. Such discordances are not easily explained in the conventional framework of assumptions in geochronology.

Geochemical Processes in the Mantle and Crust—Andrew A. Snelling, Ph.D.

In Chapter 5, Dr. Snelling reviews the radioisotopic systems used for rock “dating” and shows that each has its own peculiarities, but there are difficulties common to them all which raise questions as to their suitability as geochronometers. These problems are evident on all observational scales, even within mineral grains, and are often severe

enough to raise doubts about all attempts at radioisotope dating. Modern mantle-derived oceanic volcanics consistently have radioisotopic signatures that yield excessively old “ages” and has led to their use to identify geochemical reservoirs in the mantle. Such geochemical “fingerprinting” has demonstrated that mixing of mantle and crustal sources produces crustal rocks which retain those radioisotopic signatures. Alternately, radioisotopic “ages” might have been produced as an artifact of systematic mixing of mantle and crustal sources endowed with fundamental geochemical signatures from the origin of the earth.

Theoretical Mechanisms of Accelerated Radioactive Decay—Eugene F. Chaffin, Ph.D.

In Chapter 6, Dr. Chaffin examines physical mechanisms for accelerated decay as well as possible explanations for fission track data in terms of short-lived, fissioning nuclides. He attempts to rid any assumptions of uniformitarian philosophy from his discussion and formulate views which are not hampered by anti-Biblical biases.

Accelerated Nuclear Decay: A Viable Hypothesis?—D. Russell Humphreys, Ph.D.

In Chapter 7, Dr. Humphreys reviews geoscience and nuclear data which strongly imply that “billions of years” worth of nuclear decay took place within thousands of real, earth years. He proposes that since Creation, one or more episodes occurred when nuclear decay rates were billions of times greater than today’s rates. Dr. Humphreys outlines the scientific and Biblical evidence for accelerated nuclear decay, investigates theoretical ways God may have chosen to cause the acceleration, reviews some problems with this hypothesis, and offers preliminary scientific predictions to test it.

Radiohalos—Andrew A. Snelling, Ph.D

In Chapter 8, Dr. Snelling reviews all types of radiohalos. He confirms their radioactive origin and probable constant radioactive decay rates. Most attention and controversy has surrounded the Po halos, because isotopic analyses of the radiocenters indicates the Po isotopes responsible

for the halos were “parentless” (that is, no traces of their precursors are found). Debate has centered on whether the Po halos are secondary, due to fluid transport of Ra, Rn and/or Po isotopes along fractures, defects, and cleavage planes, or primordial, due to the fleeting existence of ^{218}Po (half-life of 3 minutes) and ^{214}Po (half-life of 164 microseconds) thus suggesting fiat Creation of the Po isotopes in place with the host minerals and rocks. Polonium halos are not just in Precambrian and granitic rocks; some hosts intrude Phanerozoic fossil-bearing (Flood-related) strata. However, the apparent absence of α -recoil tracks and the uniform background distribution of fission tracks are consistent with the primordial hypothesis.

Glossary

Appendix (The RATE Research Program)

9. Purpose of the Initial Report

By publishing this report before the research phase is begun the RATE group is staking a claim. The RATE group hopes that the research conducted during the next five years will result in a new confidence in the age of the earth as stated in the Bible. But, the problem has not been solved yet. Expectations stated before the fact have more credibility. They are known as *a priori* statements. They lend structure and direction to the effort. Since the financial support for the effort will come from donors, such statements made beforehand also tell contributors what they can expect from their gifts.

It is expected that knowledge, outlooks, conclusions, and research approaches will change as the project proceeds. Documentation of these changes will be most important at the beginning and end of the five years of research. Another purpose of this book is its use as a primary source for anyone interested in working on issues related to radioisotope dating and the age of the earth. The Initial and Final Reports are expected to be stocked by many libraries as a resource for new creationist research, and as an example of quality creationist research.

10. Final Report

A final report is planned to be published in 2005 by the RATE group reporting on the findings and conclusions of the 5-year research effort. Hopefully, each of the six RATE principal investigators will be able to contribute to the final report and demonstrate a significant advancement in the young-earth creationist position. If the RATE project is successful in describing a physical process by which daughter isotopes were formed in a young-earth, Biblical timeframe and consistent evidence is found to justify the conclusions, the final report should become an extremely important document, not only to creationists, but also to Christians of all persuasions and the scientific community as a whole. If RATE is unable to solve the problem fully, but advance the knowledge in this area, the final report will still be an important resource for others who may wish to continue where RATE left off. In either case, it will be important to document the results of this study to justify the investment that donors will expect.

11. David and Goliath

Several times throughout the initiation and development of the RATE project, prayer and devotionals during annual meetings have compared the difficulty of this effort to David's challenge when he faced Goliath. In both cases, the obstacle seemed insurmountable and the consequences of failure seemed deadly. Failure to achieve success on this problem might bring embarrassment to the creationist cause and delay the development of a new generation of young Christians. Yet, David as our example, not only faced literal death, but potential enslavement of his entire country. His father and mother, his brothers and sisters, and his family and friends would all be subject to cruel treatment by the Philistines if he failed. The success of the entire battle depended upon the bravery of a teenage boy who had never been tested in battle and was probably less than half the size of his adversary.

What presumption! What arrogance! Yet, David was not depending on his own strength, he was depending upon God's. Before David killed

Goliath in the valley of Elah he said to the Philistine:

“Thou comest to me with a sword, and with a spear, and with a shield: but I come to thee in the name of the LORD of hosts, the God of the armies of Israel, whom thou hast defied. This day will the LORD deliver thee into mine hand; and I will smite thee, and take thine head from thee; and I will give the carcasses of the host of the Philistines this day unto the fowls of the air, and to the wild beasts of the earth; that all the earth may know that there is a God in Israel. And all this assembly shall know that the LORD saveth not with sword and spear: for the battle is the LORD’s, and he will give you into our hands.”

I Samuel 17: 45–47

As we face the issues of the age-of-the-earth battle, I’m sure many of us feel about as tall as David before Goliath. The problem seems too big! What if we fail? It’s at these times we must exercise our faith and look to David as our example. May we not stand in our own strength, but in the strength of the LORD. Jehovah Jireh—the LORD will provide.

Chapter 2

Radioisotope Dating Review

Don DeYoung, Ph.D.*

Abstract. For a century, radioisotope dating has been widely used as a research tool. Its development is part of the fascinating story of nuclear discovery. Over the years there have been extensions of the dating method to include many new isotopes. The limitations and assumptions of the dating method also have been realized, but these are often under-emphasized. Nine dating isotopes are reviewed in this chapter. Their applications and results are critiqued. The concept of accelerated decay is also briefly explored.

1. Introduction

This chapter reviews the major radioisotope dating methods used today for rock samples. The strengths and weaknesses of each approach are outlined briefly. The treatment is not exhaustive, since lengthy books have been written on these isotope methods. However, one distinction offered here is a radioisotope description which is not unduly enamored with the method itself. Too often, radioisotope dating is presented as an infallible proof of ancient earth history. As the only experimental method which gives an absolute date to a geologic sample, the dating results may be trusted too completely. Very precise isotope detection is indeed possible in the range of parts per billion and even parts per trillion. The correct interpretation of this atomic abundance data, however, may be something entirely different than sample age.

Several specialized radioisotope dating methods are not described here, including potassium-calcium (K-Ca), lanthanum-barium (La-Ba), and lanthanum-cerium (La-Ce) isotopes. These specialized dating methods are not widely used thus far and have limited application. The chapter

* *Professor of Physics, Grace College, Winona Lake, Indiana*

concludes with a discussion of an alternative to conventional nuclear decay, accelerated decay. Since nuclear physics is now one century old, perhaps it is time to evaluate its assumptions. Alternatives to the standard model of nuclear decay presented here remain theoretical and speculative. However, such new insights may greatly increase our nuclear understanding.

2. Background

Radioactivity was first studied during the early decades of the 1900s. Ernest Rutherford, Frederick Soddy, and Henri Becquerel described nuclear decay in 1901–1902. Using compounds of radioactive uranium (U) and thorium (Th), they discovered the concept of *half-life*. This is the characteristic time for 50% of a radioactive species to decay. Letting an arrow represent *half-life*, an initial amount of nuclear material (N) shows a geometric or exponential decay, with time,

$$N \rightarrow \frac{N}{2} \rightarrow \frac{N}{4} \rightarrow \frac{N}{8} \rightarrow N \left(\frac{1}{2} \right)^n \quad (1)$$

where n is the number of half-lives that have elapsed. The rate of decay dN/dt is found experimentally to be directly proportional to the number of radioisotope atoms remaining,

$$\frac{dN}{dt} = -\lambda N \quad (2)$$

If we begin at t_0 with N_0 radioactive atoms, the number remaining at a later time t is found by mathematically integrating equation (2),

$$N = N_0 e^{-\lambda t} \quad (3)$$

where λ is the decay constant for the particular radioactive material. Further, the half-life $t_{1/2}$ is given by

$$t_{1/2} = \frac{\ln 2}{\lambda} \quad (4)$$

The historical progress in nuclear understanding is illustrated by several important dates of discovery:

- 1895 Wilhelm Roentgen (1845–1923) discovers x-rays.
- 1898 Pierre and Marie Curie coin the term *radioactivity*.
- 1899 Electrons first described by J. J. Thompson (1856–1940).
- 1911 Ernest Rutherford (1871–1937) describes the compact nature of the atomic nucleus.
- 1914 The proton is discovered by Rutherford.
- 1932 Neutrons are discovered by James Chadwick (1891–1974).

Rutherford and colleagues developed the initial radioisotope dating methods around 1905. Geochronology continues to be developed and refined today.

3. Particular Radioactive Isotopes

3.1 Samarium-Neodymium (Sm-Nd)

These two elements are part of the *lanthanide* series in the periodic table. The 15 lanthanides all have physical properties similar to the silvery-white metal lanthanum (La). They are also called *rare earth* elements, based on earlier, incorrect thinking that these elements occurred only rarely in nature.

Radioactive Sm decays to neodymium (Nd) by α -emission,



In the decay reactions shown in this chapter, the neutrinos, antineutrinos, and energy amounts are not listed. Superscripts shown are the isotopic atomic weights or masses of atoms. This value is the total number of protons and neutrons in the atom's nucleus. The subscript values are the atomic numbers. Atomic number measures the total number of protons in the atom's nucleus. The atomic number also represents an atom's total electrons. The Sm half-life is 106 billion years, more than twice that of the other common radioisotopes which are listed in Table 1. Both ${}^{147}\text{Sm}$ and ${}^{143}\text{Nd}$ isotopes occur in parts-per-million amounts in nearly

Table 1. Radioactive isotopes commonly used in radioisotope dating. Daughter isotopes and approximate parent half-lives are listed, along with materials commonly dated.

Radioisotope Methods			
Parent Isotope	Daughter Isotope	Half-life (billions of years)	Materials Commonly Dated
^{14}C	^{14}N	.000005730 (5730 years)	Wood, plant remains, bone, shells, glacial ice.
^{40}K	^{40}Ar ^{40}Ca	1.25	Muscovite Biotite Hornblende Whole volcanic rock
^{87}Rb	^{87}Sr	48.8	Muscovite Biotite Potassium feldspar Whole igneous or metamorphic rock
^{147}Sm	^{143}Nd	106	Metamorphic rocks Ancient basalt Achondrite meteorites
^{176}Lu	^{176}Hf	.35	Apatite Garnet Monazite
^{187}Re	^{187}Os	43	Molybdenite ore deposits Metallic meteorites
^{232}Th	^{208}Pb	14.1	Zircon
^{235}U	^{207}Pb	0.704	Uraninite
^{238}U	^{206}Pb	4.47	Pitchblende

all rocks and minerals, including silicates, phosphates, and carbonates. Since the 1980s these small quantities have been measurable by mass spectrometry in rock samples and applied to age determinations.

There usually is little difference in Sm and Nd concentrations in rocks since they are chemically similar elements with minimal fractionation.

As a result the ratio of natural Sm to Nd in samples varies by only about 0.1 to 0.5, with a slight excess of Nd. Initial ^{143}Nd amounts are present in all samples so the isochron method is typically applied to sample dating, based on the stable isotope ^{144}Nd . This method is discussed later in the chapter. Neodymium-144 itself is the end product of the decay of ^{144}Ce .

The Sm-Nd method is thought to offer two advantages in age studies. First, selective atomic migration during heating or metamorphism can effectively rule out other radioisotope methods. However, such metamorphism is not expected to affect Sm-Nd ratios greatly because of their atomic similarities. Second, along with resistance to metamorphic change, the long half-life of ^{147}Sm is thought to be useful for very old samples. Hence Sm-Nd has found widespread application in dating stony meteorites, lunar rocks, and Precambrian lavas. The method is thought to give reliable ages regardless of sample erosion, metamorphism, and even remelting [*Dickin*, 1995, p. 86].

3.2 Rhenium-Osmium (Re-Os)

This dating method is mainly applied to iron meteorites and ore deposits. The decay process involves electron β -emission,



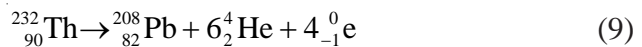
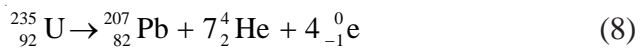
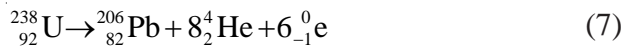
with a half-life of about 43 billion years. The abundance of Re and Os in common silicate minerals is less than one part per billion, ruling out widespread radioisotope application. However, in iron meteorites the abundance is sometimes a thousand times greater. As a metal, Re also tends to concentrate in copper sulfide minerals.

The isochron method has been applied to Re-Os to determine initial ^{187}Os in samples. The stable isotope ^{186}Os is used for this calibration. One basic problem with the Re-Os technique for dating ores is the nature of hydrothermal deposits. By definition these minerals involve widescale migration and exchange of atoms. As expected, ore measurements of Re-Os give a wide range of sample ages.

The isotope ^{187}Os has played an interesting part in theories of dinosaur extinction. In particular, the possible impact of a large (10 km diameter) asteroid has become a popular explanation for the demise of the dinosaurs. This collision event is usually dated at 65 million years ago, ending the Mesozoic era. A clay layer found at the Cretaceous-Tertiary boundary has a high concentration of Ir, perhaps of extraterrestrial origin. This layer also reveals a small ratio of $^{187}\text{Os}/^{186}\text{Os}$, as compared with crustal rocks. It is further known that nonmetallic meteorites typically contain less ^{187}Os than terrestrial rocks, presumably due to radiogenic ^{187}Os accumulation during earth history. Therefore the amount of ^{187}Os in the clay layer is taken as further evidence for a meteorite origin. Of course there are many unknowns in this data, such as mixing and fractionation within the clay layer. There is also a possible volcanic origin for the Cretaceous-Tertiary boundary clay layer instead of an impact event. The earth has definitely been bombarded with meteorites throughout Biblical history. In the creation model, however, the extinction of the dinosaurs can be better related to climatic changes and to the Genesis Flood itself.

3.3 Uranium/Thorium-Lead (U/Th-Pb)

The isotopes ^{238}U , ^{235}U , and ^{232}Th all decay eventually to distinct, stable isotopes of lead (Pb). The word *eventually* is used because there are many intermediate radioactive isotopes formed before the element Pb is reached. These complex decays series release several α -particles, or He nuclei, and also electrons. The final daughter Pb isotope in each case is stable:



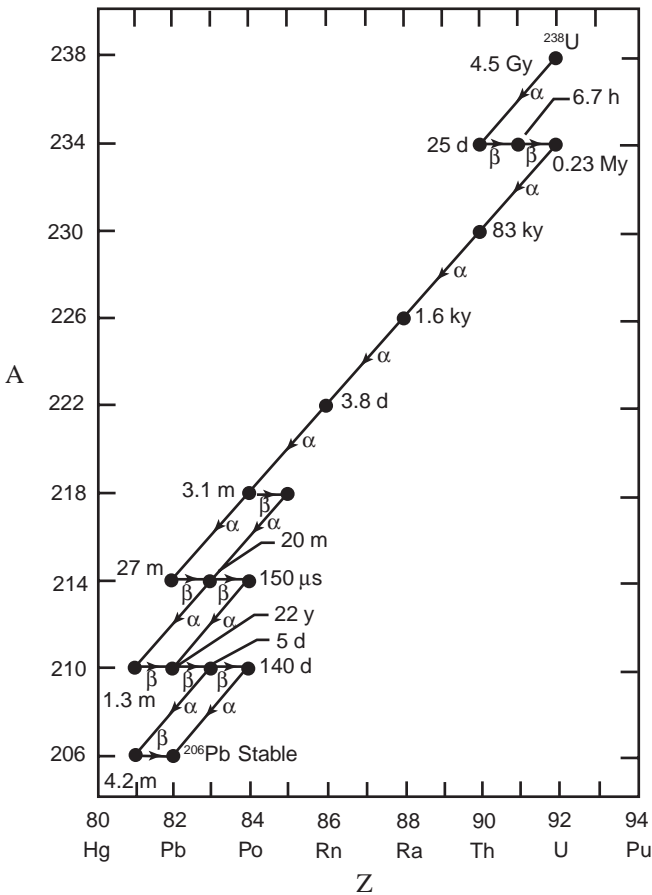


Figure 1. The decay scheme for ^{238}U or Neptunium Series. The symbols are α (alpha-decay); β (beta-emission); s, ms, μs (seconds, millisecon, microsecond); m (minutes); h (hours); d (days); y, ky, My, Gy (years, kiloyears, megayears, billions of years); A (atomic mass or weight); Z (atomic number). [Adapted from *Rohlf*, 1994.]

Total half-lives for these decays are respectively 4.47, 0.704, and 14.1 billion years. Figures 1–3 picture the decay schemes. Uranium and Th are chemically similar elements. They occur in parts per million amounts in many common rocks such as granite, but are more abundant in certain minerals like zircon (ZrSiO_4) and uraninite (UO_2), which has a variety

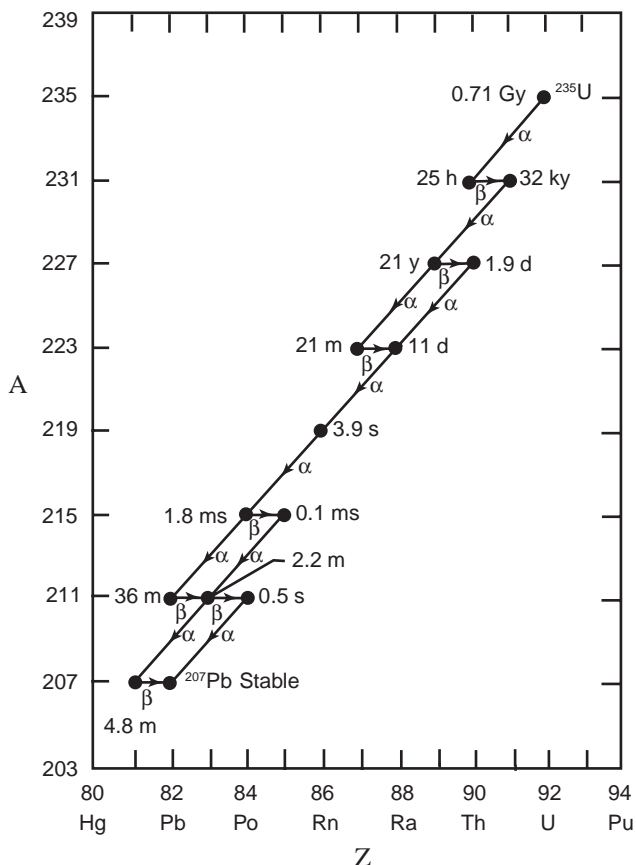


Figure 2. The decay schemes for the ^{235}U or Actinium Series. See Figure 1 caption for abbreviations. [Adapted from *Rohlf*, 1994.]

called pitchblende. The radioactive isotopes ^{238}U and ^{232}Th are generally thought responsible for about 90% of the earth's internal heat production.

The three ratios $^{238}\text{U}/^{206}\text{Pb}$, $^{235}\text{U}/^{207}\text{Pb}$, and $^{232}\text{Th}/^{208}\text{Pb}$ are separately obtained for a rock sample, then compared as an internal cross-check. The results often do not agree. Lead is a mobile element and readily migrates out of a sample if heat is experienced. Assuming that the three Pb isotopes are equally depleted from a particular sample, this loss is accounted for by basing sample dates on the $^{207}\text{Pb}/^{206}\text{Pb}$ ratio. Lead isochrons are also used to determine initial Pb in samples.

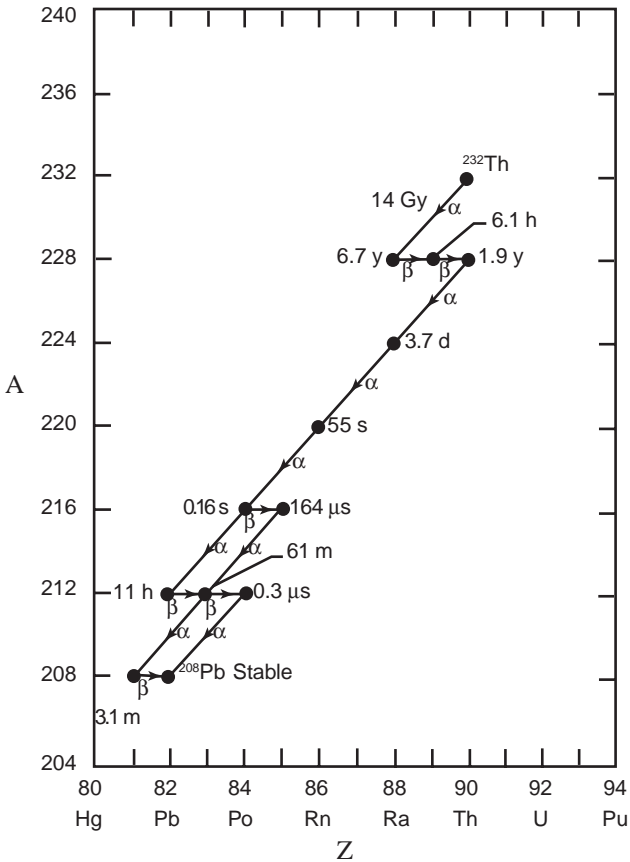


Figure 3. Thorium or ^{232}Th Series. See Figure 1 caption for abbreviations. [Adapted from *Rohlf*, 1994.]

3.4 Rubidium-Strontium (Rb-Sr)

Rubidium occurs in the same column of the periodic table as K and Na, having a single unpaired outer electron. Because of this chemical similarity, Rb appears as a trace element at K and Na sites in many common minerals. These include micas, potassium feldspar, and clay. Strontium is likewise chemically similar to Ca, and often occurs as an impurity at Ca lattice sites. The result is that the Rb-Sr clock is widely used in radioisotope dating. Rubidium decays by β -emission with a half-

life of 48.8 billion years,



Isochron techniques are essential in Rb-Sr dating because of initial Sr in rock samples.

Because of the long half-life, the Rb-Sr method is commonly applied to the oldest rock samples from earth and space. It is usually assumed that radiogenic Sr remains chemically bound in such rocks over long time periods. Many rocks contain more than one distinct mineral with Rb and Sr. In these cases a cross-check is possible for the calculated rock age. When separate mineral ages agree for a rock sample, they are said to be *concordant*. In practice, discordance of dates is the more common result. This frequent shortcoming of radioisotope dating is usually blamed on the migration of radiogenic ${}^{87}\text{Sr}$ atoms either into or out of the minerals. In such cases the “whole-rock isochron method” may be used. This approach averages the various calculated mineral dates to arrive at an age for the rock.

The Rb-Sr method is often applied to metamorphic rocks such as gneiss and slate which have experienced extreme heat and pressure. However, even modest heating of 100°C to 200°C is known to greatly effect the movement of Rb and Sr atoms in minerals, and thus control the derived sample age. There are mathematical attempts to account for such atomic migration, but uncertainties remain.

As a general rule radioisotope dating is limited to igneous rocks. These form from magma, and are therefore thought to be new rocks with their “internal clocks” reset. That is, radiogenic daughter products begin to accumulate at this time. However, the Rb-Sr method also has been applied to sedimentary rocks. These rocks, limestones, shale, and conglomerate, as examples, are made of pre-existing rock debris. It is thought that such age data will be an average of the original rock materials. However, several problems cast doubt on sedimentary rock dating results. Shale, in particular, may have a large variation in Sr content due to mineral inclusions [Dickin, 1995, p. 54]. Other sedimentary samples are known to be open systems, since Sr atomic migration commonly occurs. Because

of these and other problems, sedimentary rock dating remains of doubtful value.

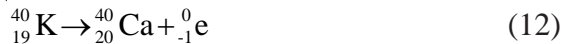
3.5 Potassium-Argon (K-Ar)

For three reasons, K-Ar remains the most popular rock dating method. *First*, Ar is an inert gas which quickly escapes from molten material or heated rocks. Therefore, an initial presence of the daughter product ^{40}Ar is believed to be less of a problem than with the other radioisotope methods. *Second*, K is the seventh most abundant element in the earth's crust (2.6% by weight), and therefore is very common in rocks and minerals. *Third*, the half-life of ^{40}K leads to easily measurable quantities of K and Ar on a uniformitarian timescale.

Potassium decays to Ar by electron capture with a half-life of 1.25 billion years,



Actually just 11% of ^{40}K decays this way, the majority converting to ^{40}Ca by electron emission.



However, this latter reaction is of little value for dating because of the widespread prevalence of ^{40}Ca in nature.

A rock sample is dated by measuring its accumulated ^{40}Ar . The gaseous nature of Ar is a hindrance as well as a help to this method. Since inert Ar is not chemically bound to other atoms, it may leak in or out of a sample over time. Argon-40 also has an abundance of 1.29% of the earth's atmosphere, so this isotope is present virtually everywhere within and above the earth. There are efforts to account for atmospheric Ar by subtracting out this component from sample data. It is usually further assumed that atmospheric Ar isotope ratios have been constant over geologic time. Geochronologist Brent Dalrymple has downplayed the problems of Ar movement. He promotes the illustration that ^{40}Ar atoms

are trapped within mineral crystals like “a bird in a cage,” unable to either enter or leave the crystal matrix [*Dalrymple*, 1991, p. 91]. However, at temperatures of only 150°C to 550°C, depending on the mineral, Ar atoms have been found to easily migrate through the sample [*Plummer and McGeary*, 1996, p. 170]. Potassium feldspar is not suitable for K-Ar dating precisely because of major Ar loss at low temperatures [*Faure*, 1986, p. 70].

The popular “bird in a cage” picture of Ar itself is also open to question. The atomic radius of argon is 1.9 Å (angstroms) (1.9×10^{-10} m), on the same order as the dimensions of typical crystal lattice spacings. At elevated temperatures, lattice expansion and atom vibrations can readily allow movement of unbonded atoms, as has been observed. In addition, a crystal lattice containing radioactive K experiences many lattice defects over time. These openings will also permit passage of Ar atoms either in or out of samples.

Potassium is especially abundant in mica, feldspar, amphibole, and clay minerals. This has led to use of the K-Ar method for samples as “young” as 6000 years [*Dalrymple*, 1991, p. 93].

3.6 Lutetium-Hafnium (Lu-Hf)

Lutetium-hafnium dating has had limited application since its beginning, around 1970. Lutetium-176 is widely dispersed as a trace element in most rocks, usually at less than one part per million. Lutetium-176 has a half-life of about 35 million years, decaying by electron emission.



The combination of low parent abundance and long half-life makes analytical measurements difficult. There is some evidence that Lu/Hf ratios are elevated for igneous and metamorphic rocks of the continental crust. Thus, these isotopes eventually may aid the study of crustal history.

3.7 Argon-Argon (Ar-Ar)

This dating method was first described in the 1960s. It is an alternate method of K-Ar dating. An unknown rock sample is placed within a nuclear reactor and exposed to a high flux of fast neutrons (n). A certain number of stable ^{39}K atoms in the sample are converted to ^{39}Ar , each with the emission of a proton (p),



The ratio of $^{40}\text{Ar}/^{39}\text{Ar}$ in the irradiated sample is then precisely measured by mass spectrometry. The number of ^{39}Ar atoms, formed from ^{39}K , is assumed to be proportional to the sample's original ^{40}K content. Thus the $^{40}\text{Ar}/^{39}\text{Ar}$ ratio of an irradiated sample, upon proper calibration, is assumed to give the sample age. Argon-39 has a half-life of 265 years and does not occur naturally.

The touted advantages of Ar-Ar dating over K-Ar are several. Only one isotopic ratio measurement is needed instead of separate ^{40}K and ^{40}Ar determinations. This avoids problems of sample inhomogeneity. In this way Ar-Ar is especially useful for small specimens, including lunar rocks and meteorites. Also, the $^{40}\text{Ar}/^{39}\text{Ar}$ ratio can be progressively measured as a sample is heated. This provides chemical information on possible changes within rock samples that may have been heated in the past within the earth.

Several complications with Ar-Ar dating are similar to those in the K-Ar method. For example, atmospheric Ar in the sample must be accounted for. Also, neutron bombardment of a sample produces several other Ar isotopes. These additional nuclear reactions are poorly understood, and must be accounted for.

4. Isochrons

A fundamental problem in radioisotope dating is determining the amount of initial daughter isotopes in a mineral sample. Such isotopes have not accumulated gradually over time within the sample, but are

already present when the sample cools.

The isochron method was first suggested by geologist Nicolaysen in 1961. As an example, we will consider the isochron method for Rb-Sr dating. The technique begins with the selection of a group or *suite* of mineral samples from a larger rock. Several rocks from the same source can also be used. These particular samples should satisfy several conditions.

- Specimens are of the same age.
- They had the same initial $^{87}\text{Sr}/^{86}\text{Sr}$ ratios.
- Samples have remained as closed systems since their formation.
- Minerals have a wide range of Rb/Sr ratios.

To derive the isochron equation, let the original amounts of isotopes in a sample be designated as $^{87}\text{Rb}_0$, $^{86}\text{Sr}_0$, and $^{87}\text{Sr}_0$. Amounts existing at the present time are written here without subscripts. As ^{87}Rb decays into radiogenic ^{87}Sr , its decay formula can be written as

$$^{87}\text{Rb} = ^{87}\text{Rb}_0 e^{-\lambda t} \quad (15)$$

also

$$^{87}\text{Rb}_0 = ^{87}\text{Rb} + ^{87}\text{Sr}_{\text{radiogenic}} \quad (16)$$

and

$$^{87}\text{Sr}_{\text{radiogenic}} = ^{87}\text{Sr} - ^{87}\text{Sr}_0 \quad (17)$$

Substituting back,

$$^{87}\text{Rb} = \left(^{87}\text{Rb} + ^{87}\text{Sr} - ^{87}\text{Sr}_0 \right) e^{-\lambda t} \quad (18)$$

Now divide through by ^{86}Sr , a stable, nonradiogenic isotope which is also present in samples,

$$\frac{^{87}\text{Rb}}{^{86}\text{Sr}} = \left(\frac{^{87}\text{Rb}}{^{86}\text{Sr}} + \frac{^{87}\text{Sr}}{^{86}\text{Sr}} - \frac{^{87}\text{Sr}_0}{^{86}\text{Sr}} \right) e^{-\lambda t} \quad (19)$$

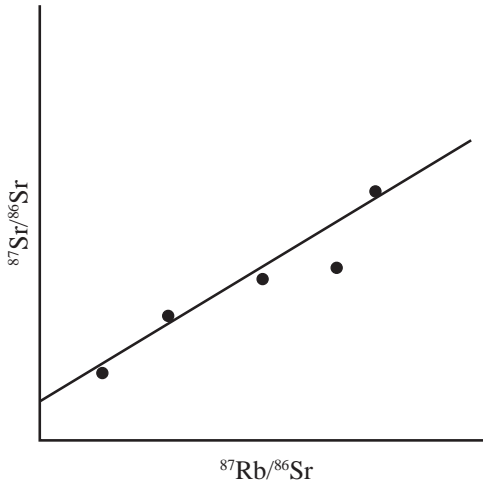


Figure 4. A typical isochron graph.

Rearranging, the equation can be written as

$$\frac{^{87}\text{Sr}}{^{86}\text{Sr}} = (e^{\lambda t} - 1) \frac{^{87}\text{Rb}}{^{86}\text{Sr}} + \frac{^{87}\text{Sr}_0}{^{86}\text{Sr}} \quad (20)$$

The term on the left represents ^{87}Sr that has accumulated over time. The first term on the right represents the ^{87}Rb that has accumulated, and the second term stands for initial $^{87}\text{Sr}_0/^{86}\text{Sr}$ amounts, assumed to be the same for all samples. The $^{87}\text{Sr}/^{86}\text{Sr}$ and $^{87}\text{Rb}/^{86}\text{Sr}$ ratios are precisely determined for each sample. The results are then graphed as shown in Figure 4. In general, the vertical axis plots ratios of daughter isotopes/nonradiogenic isotopes, and the horizontal axis is the ratio between parent isotopes/nonradiogenic isotopes. Note that the preceding equation is just the slope-intercept form of a straight line,

$$y = mx + b \quad (21)$$

The slope of the line (m) gives the rock age,

$$m = e^{\lambda t} - 1 \quad (22)$$

$$t = \frac{1}{\lambda} \ln (m + 1) \quad (23)$$

As shown by the equation, the slope of the line increases with sample age. The straight line graph also is taken as evidence that the initial assumptions were valid. The resulting age is called the “whole-rock” isochron age. The word *isochron* itself means “same age,” referring to the plotted line.

The vertical intercept (*b*) of the isochron line gives the initial daughter composition of the mineral samples. A rigorous statistical analysis is typically done to determine accurately the slope and intercept values [York, 1969; Jones, 1979]. When some data points do not fall on the straight line, they are assumed to come from contaminated samples.

The isochron method is often assumed to solve completely the problem of initial daughter isotopes in samples. However, reality is never quite this simple. Consider three problems:

- In K-Ar dating, isochrons are based on the initial $^{40}\text{Ar}/^{36}\text{Ar}$ ratio of samples, assumed to be constant. This is the intercept of the isochron graph. But this ratio can range widely in samples because of variable atmospheric contamination.
- It is also found that the initial $^{87}\text{Sr}/^{86}\text{Sr}$ ratio is not always a constant for related samples. In fact, this ratio can vary directly with $^{87}\text{Rb}/^{86}\text{Sr}$. In this case a straight line still results, but its slope does not give a valid age.
- Suppose two material components with different $^{87}\text{Rb}/^{86}\text{Sr}$ and $^{87}\text{Sr}/^{86}\text{Sr}$ ratios are *mixed* together in mineral samples. The resulting isochron line still can be straight, but have nothing to do with sample age. In fact, such lines even may have a downward slope, implying a negative sample age. Such mixing lines are called fictitious or pseudoisochrons [Austin, 1994, p. 127].

5. Accelerated Decay

Radioisotope dating assumes that the decay of nuclei has been predictable and uniform over a vast timescale. The half-lives of radioactive parent atoms are taken as constants. Particular half-lives indeed show little variation today since the nucleus is well-shielded from the external atomic environment [DeYoung, 1976]. However, the

creationist view allows for a possible large-scale change in radioactive decay during a limited period of time in the past. Accelerated decay may have been a supernaturally-directed part of Creation, the Curse of Genesis 3, or possibly a part of the Genesis Flood catastrophe. At whatever point in history this accelerated decay may have occurred, it would invalidate all traditional radioisotope ages from that time forward.

As an example, consider the basic formula for sample age (t), used in the Rb-Sr method, obtained by substituting equation (20) into (23),

$$t = \frac{1}{\lambda} \ln \left\{ \frac{{}^{86}\text{Sr}}{{}^{87}\text{Rb}} \left[\left(\frac{{}^{87}\text{Sr}}{{}^{86}\text{Sr}} \right)_p - \left(\frac{{}^{87}\text{Sr}}{{}^{86}\text{Sr}} \right)_o \right] + 1 \right\} \quad (24)$$

where $\lambda = {}^{87}\text{Rb}$ decay constant
 $p =$ Present-day ratio
 $o =$ Initial ratio

Now suppose that for some short period Δt in history the decay of ${}^{87}\text{Rb}$ was greatly increased. This would require a new temporary decay constant λ' much greater than the conventional λ . The sample age relationship would then be modified by the addition of a term giving a new age t' ,

$$t' = t - \frac{\lambda' \Delta t}{\lambda} \quad (25)$$

Suppose that Δt is one year, the time during which nuclear decay is greatly increased. Further, using round numbers, suppose that the traditional sample age t is one billion years, and the true age t' is only 1000 years. To a good approximation then,

$$\begin{aligned} \lambda' &= \frac{\lambda t}{\Delta t} \\ &= 10^9 \lambda \end{aligned} \quad (26)$$

For ${}^{87}\text{Rb}$,

$$\lambda = \frac{1.42 \times 10^{-11}}{\text{year}} \quad (27)$$

This gives

$$\lambda' = \frac{1.42 \times 10^{-2}}{\text{year}} \quad (28)$$

and the temporary half-life during accelerated decay is reduced from 48.8 billion years to only 48.8 years, a billion times less.

Could such an event have occurred? Would the resulting excessive heat completely melt the earth? Would accelerated decay have left an identifiable signature in the rocks? Such are the questions addressed in this book.

6. Conclusion

This ends our short excursion into isotope dating methods and geochronology. There are several other dating methods, such as potassium-calcium (K-Ca) isotopes, for particular applications. This chapter also has not considered ^{14}C dating, applied exclusively to organic samples.

Three major weaknesses of radioisotope dating are apparent from this study. Each involves a major assumption for the isotopes. The *first* assumption is that of a constant nuclear decay rate or half-life in the past. From all evidence, half-lives are indeed quite constant today and largely independent of changes in the chemical environment. However, this book proposes that decay rates were temporarily and dramatically accelerated at some time in the past. This acceleration may or may not have a natural explanation. The postulated temporary change gave rise to a large, rapid accumulation of daughter products, but not to a large timescale.

Second, it is assumed that the isotope composition of rock samples has not been changed by *fractionation* over time. This term refers to a separation of isotopes based on their weights, due to various chemical interactions. Fractionation of K isotopes [Faure, 1986, p. 68] has been

observed, as well as with many other isotopes [DeYoung, 1974]. The conclusion is that current isotope ratios may have been quite different in the past, thus invalidating published rock ages. Fractionation is a relatively new area of chemical studies and we still have much to learn about this type of isotopic separation.

Third, it is often assumed that rock samples have been closed systems over eons of time. This idea simply must be challenged. One message of modern science is that no part of nature is completely isolated. Over time, parent or daughter atoms may move into or out of rocks. Therefore, radioisotope data often may be describing atom migration rather than sample age. Radioisotope dating has not proved with absolute confidence that the earth is old.

References

- Austin, S., *Grand Canyon: Monument to Catastrophe*, Institute for Creation Research, Santee, California, 1994.
- Dalrymple, G. B., *The Age of the Earth*, Stanford University Press, Stanford, California, 1991.
- DeYoung, D. B., Geochemistry of the stable isotopes, *Creation Research Society Quarterly*, 11, 32–36, 1974.
- DeYoung, D. B., The precision of nuclear decay rates, *Creation Research Society Quarterly*, 12, 38–41, 1976.
- Dickin, A., *Radiogenic Isotope Geology*, Cambridge University Press, New York, 1995.
- Faure, G., *Principles of Isotope Geology*, John Wiley and Sons, New York, 1986.
- Jones, T. A., Fitting straight lines when both variables are subject to errors, *Mathematical Geology*, 11, 1–25, 1979.
- Plummer, C. C., and D. McGearry, *Physical Geology*, Wm. C. Brown Publishers, New York, 1996.
- Rohlf, J. W., *Modern Physics from α to Z^0* , John Wiley and Sons, Inc., New York, 1994.
- York, D., Least squares fitting of a straight line with correlated errors, *Earth and Planetary Sciences Letters*, 5, 320–324, 1969.

Bibliography

- Aardsma, G. E., Radiocarbon, dendrochronology, and the date of the Flood, in *Proceedings of the Second International Conference on Creationism*, vol. 2, edited by R. E. Walsh and C. L. Brooks, Creation Science Fellowship, Pittsburgh, Pennsylvania, pp. 1–10, 1990.
- Barnes, T. G., Earth's young magnetic age: an answer to Dalrymple, *Creation Research Society Quarterly*, 21, 109–113, 1984.
- Barnes, T. G., Earth's young magnetic age confirmed, *Creation Research Society Quarterly*, 23, 30–33, 1986.
- Brown, R. H., Radiometric dating from the perspective of Biblical chronology, in *Proceedings of the First International Conference on Creationism*, vol. 2, edited by R. E. Walsh, C. L. Brooks and R. S. Crowell, Creation Science Fellowship, Pittsburgh, Pennsylvania, pp. 31–58, 1986.
- Chaffin, E. F., A young earth?—a survey of dating methods. *Creation Research Society Quarterly*, 24, 109–117, 1987.
- Cook, M. A., How and when “Pangaea” ruptured and the continents shifted, in *Proceedings of the First International Conference on Creationism*, vol. 2, edited by R. E. Walsh, C. L. Brooks and R. S. Crowell, Creation Science Fellowship, Pittsburgh, Pennsylvania, pp. 69–88, 1986.
- Cook, M. A., Nonequilibrium radiocarbon dating substantiated, in *Proceedings of the First International Conference on Creationism*, vol. 2, edited by R. E. Walsh, C. L. Brooks and R. S. Crowell, Creation Science Fellowship, Pittsburgh, Pennsylvania, pp. 59–68, 1986.
- Dalrymple, G. B., and M. A. Lanphere, *Potassium-Argon Dating*, W. H. Freeman and Company, San Francisco, 1969.
- Helmick, L. S., and D. P. Baumann, A demonstration of the mixing model to account for Rb-Sr isochrons, *Creation Research Society Quarterly*, 26, 20–23, 1989.
- Johns, W. H., Egypt and carbon-14 dating, *Creation Research Society Quarterly*, 23, 37, 1986.
- Kofahl, R. E., One error of Dalrymple corrected, *Creation Research Society Quarterly*, 21, 114–115, 1984.
- Oard, M. J., Ice Ages: the mystery solved? Part II: The manipulation of deep-sea cores, *Creation Research Society Quarterly*, 21, 125–137, 1984.
- Overn, W. M., and Arndts, R. T., Radiometric dating—an unconvincing art, in *Proceedings of the First International Conference on Creationism*, vol. 2, edited by R. E. Walsh, C. L. Brooks and R. S. Crowell, Creation Science

- Fellowship, Pittsburgh, Pennsylvania, pp 167–174, 1986.
- Overn, W. M., The truth about radiometric dating, in *Proceedings of the First International Conference on Creationism*, vol. 2, edited by R. E. Walsh, C. L. Brooks and R. S. Crowell, Creation Science Fellowship, Pittsburgh, Pennsylvania, pp. 101–104, 1986.
- Peterson, E. H., Prehistory and the Tower of Babel, *Creation Research Society Quarterly*, 19, 87–90, 1982.
- Stewart, R., *The Illustrated Almanac of Historical Facts*, Prentice Hall, New York, pp. 138, 155, 166, 184, 194, 196, 239, 255, 1992.
- Vaninger, S. F., Archaeology and the antiquity of ancient civilization: a conflict with Biblical chronology?—Part II. *Creation Research Society Quarterly*, 22, 64–67, 1985.
- Von Fange, E., Are there two potassium/argon (K/Ar) dating systems?, in *Proceedings of the Second International Conference on Creationism*, vol. 2, edited by R. E. Walsh and C. L. Brooks, Creation Science Fellowship, Pittsburgh, Pennsylvania, pp. 79–84, 1990.
- Wise, K. P., The way geologists date!, in *Proceedings of the First International Conference on Creationism*, vol. 1, edited by R. E. Walsh, C. L. Brooks and R. S. Crowell, Creation Science Fellowship, pp. 135–140, 1986.
- Woodmorappe, J., A reply to G. Brent Dalrymple, *Creation Research Society Quarterly*, 21, 184–186, 1985.

Chapter 3

Distribution of Radioactive Isotopes in the Earth

John R. Baumgardner, Ph.D.*

Abstract. The plate tectonics revolution of the 1960s brought to the geochemistry community, given the implied convective stirring taking place within the earth's mantle, the awareness that magmatic rocks from the seafloor and from ocean islands represent an important chemical probe into the earth's deeper interior. Detailed analysis of such rocks, especially their trace element compositions, over the last three and a half decades has revealed a great wealth of insight concerning the composition and probable history of our planet. In particular, it has revealed that Earth seems to be made from the same recipe of higher melting temperature elements as observed in the Sun as well as in most meteorites. Moreover, there seems to be a strong case that the earth has undergone significant chemical differentiation during its history. This differentiation includes segregation of much of the planet's iron to the center to form the core. The chemical data also strongly suggest the continental crust has been extracted via partial melting processes from the remaining silicate mantle. These processes also appear to have extracted and concentrated into the continental crust a large fraction of the mantle's incompatible elements, including the major heat producing radioactive elements. This chapter seeks to review the work that has led to the present understanding of the earth's basic chemical makeup, and in particular how the radioactive isotopes are distributed. It is this author's opinion that because most of these analyses deal with present-day rocks from the present-day earth without a major reliance on large extrapolations, many of the inferences are likely correct. The strong implication is that indeed God used chemical differentiation processes during the early part of Creation week to fashion the earth. A section near the end of the chapter shows that a long-standing uniformitarian enigma as to why there is such a strong local correlation between surface heat flow and the concentration of radioactive elements in

* *Theoretical Division, Los Alamos National Laboratories, Los Alamos, New Mexico*

surface rocks appears to be explainable in terms of an episode of accelerated nuclear decay during or shortly after the Genesis Flood.

1. Introduction

One of the many ways the earth is so special is that approximately 40% of its surface is covered with a rock layer known as continental crust. This layer is on average about 35 km thick and has notably lower density, about 2700 kg/m^3 versus 3300 kg/m^3 , compared with the rock beneath it. Its lower density arises because of a higher abundance of minerals such as quartz and plagioclase that contain less Fe and Mg than the rocks below. Due to a principle known as isostasy (which says that rock columns above a depth of about 100 km all tend to have the same weight), the continental surface is about four kilometers higher on average than the ocean bottom that covers the rest of the planet. These special crustal rocks also contain a much higher concentration, by a factor of about 100, of the so-called incompatible elements, including U, Th and K. Studies of the settings in which rocks melt and magmas are generated today inside the earth suggest that continental crust is the product of partial melting of less differentiated rock and that water plays an important role in the process. The special role of water may account for the fact that no other planetary body in the solar system seems to have this type of rock. The earth's continental crust not only provides an expansive habitat above sea level for the land animals and plants, but its rocks naturally and readily weather to provide a rich soil to support this amazing diversity of living organisms.

How did this prominent aspect of the earth's structure come about? Did God simply speak it and it instantly appeared that way, or did He speak and a process unfolded, albeit rapidly, that yielded this result? The chemical makeup of the earth's rocks seems to be telling a story that God used a process. Understanding as well as is possible today the processes God employed to fashion our planet for the special purposes He intended seems to be a crucial step in obtaining the insight needed to unravel the history of radioactive decay in the earth, and therewith provide an informed and credible critique of uniformitarian radioisotopic dating

claims. We shall therefore seek to provide an overview of the effort, mostly by geochemists, over the past 40 years to collect and analyze igneous rocks from a wide variety of geological settings for clues concerning the processes that operated in the earth's past to yield such features as its continental crust and metallic core. Studies of the isotopic and trace element compositions, in particular, have yielded important information concerning our planet's chemical history. The first part of this chapter will attempt to summarize the results of this enterprise.

2. Seismology and Earth Structure

Before we address the geochemical observations that bear directly on the distribution of radioactive elements in the earth, it will be useful to survey some of the early observations that helped elucidate the large-scale structure of the earth itself. Most of our knowledge about the physical structure of our planet has come from seismology—the study of how elastic waves, mainly those produced by earthquakes, propagate through the earth. Since the propagation speed of these elastic waves depends on the type of material as well as on its temperature and pressure, studying how these waves propagate within the planet can reveal a great deal about the earth's internal composition, structure, and thermodynamic state.

Very early in the history of these investigations seismologists identified a basic division of the earth into an outer shell about 2900 km thick with rock-like properties, known as the mantle, and an inner spherical region with much different properties as shown in Figure 1. In particular, the inner region displayed a much higher compressional wave speed. An early guess was that this inner region was an Fe/Ni core with a composition similar to that of iron meteorites. These early seismic studies also revealed the fact that shear waves did not propagate from the rock-like part of the earth into the core. Since liquids do not support shear waves, the case seemed strong that the core was in the liquid state and therefore very hot. Further study showed the core is actually divided into two major regions, an outer liquid layer with a thickness of about 2300 km and a solid spherical inner region with a radius of about

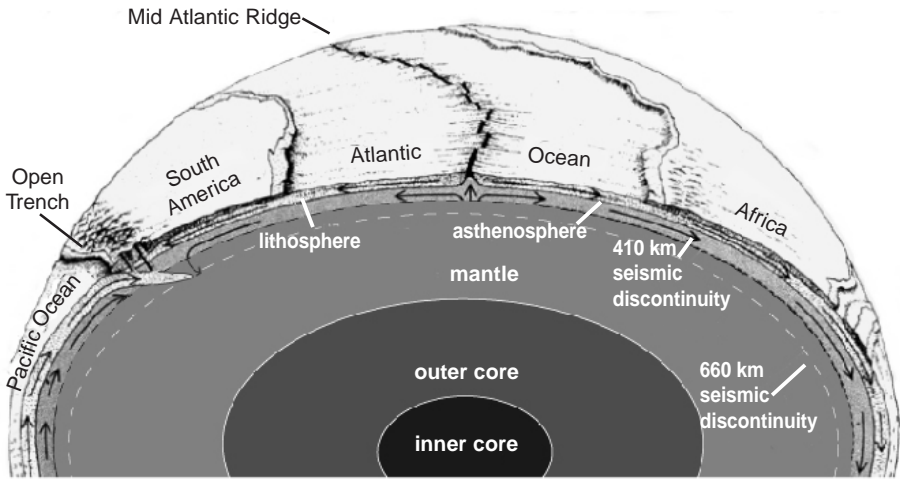


Figure 1. Cross-sectional view through the earth. The two major divisions of the planet are its mantle, made of silicate rock, and its core, comprised mostly of Fe. Portions of the surface covered with a low-density layer of continental crust represent the continents. Lithospheric plates at the surface, which include the crust and part of the upper mantle, move laterally over the asthenosphere. The asthenosphere is hot and also weak, probably because of the presence of water within its constituent minerals. Oceanic lithosphere, lacking the layer of continental crust, is chemically similar on average to the underlying mantle. Because oceanic lithosphere is substantially cooler, its density is higher, and it therefore has an ability to sink into the mantle below. The sliding of an oceanic plate into the mantle is known as subduction, as shown here beneath South America. As two plates pull apart at a mid-ocean ridge, material from the asthenosphere rises to fill the gap, and some of this material melts to produce basaltic lava to form new oceanic crust on the ocean floor. The continental regions do not participate in the subduction process because of the buoyancy of the continental crust. These are the main elements of the view of the earth's dynamics known as plate tectonics. Catastrophic plate tectonics [Austin *et al.*, 1994; Baumgardner, 1994a, 1994b] argues that these dynamics unfolded in a catastrophic manner only a few thousand years ago to cause Noah's Flood described in Genesis and produced most of the geological record above the point where fossils of multi-celled organisms suddenly appear.

1200 km. Subsequent laboratory experiments on materials at high pressures and temperatures, some using shock techniques to reach conditions approaching those in the core, have confirmed that the properties of the core inferred from seismology do indeed match closely the properties of Fe, including its density and seismic velocity, at these conditions.

In a similar manner seismology, early in its history was able to identify distinct regions in the outer rock-like, or silicate, portion of the earth based on their distinctive seismic velocity characteristics. The four regions so identified were the crust, the upper mantle, the transition zone, and the lower mantle. A jump in seismic velocity, or a seismic discontinuity, separates each layer from the next. These jumps are interpreted to represent abrupt changes in composition and/or mineralogy. Based on rock samples readily collected at the earth's surface, the discontinuity between the crust and upper mantle, the so-called Mohorovicic discontinuity, is known to be compositional in nature. There is an abrupt change from lighter crustal rock to denser mantle rock with a distinctly different chemical composition.

The two other discontinuities, at 410 and 660 km depth, are almost certainly due to changes in mineral phase because of increasing hydrostatic pressure with depth. Based on laboratory experiments at suitable pressures and temperatures, it has been determined that the mineral olivine, $(\text{Fe,Mg})_2\text{SiO}_4$, which is abundant in samples from the upper mantle, transforms at pressures corresponding to about 410 km depth to a denser spinel structure. At pressures corresponding to about 660 km depth, such material undergoes a further transition to an even denser perovskite structure. The picture is in reality more complex because there are other minerals present in upper mantle rock such as pyroxene and garnet. These also undergo changes in phase as the pressure increases, especially in the depth range between 410 and 660 km. This is reflected in the relatively high rate of change with depth in density and seismic velocity observed seismically through this depth range.

This basic picture of the earth's radial structure, derived from seismic observations, was in place 60 years ago [*Jeffreys and Bullen, 1940*] and has actually changed very little since that time [for example, *Dziewonski*

and Anderson, 1981]. However, major advances in seismological hardware and analysis techniques since the mid-1980s have made possible what is called seismic tomography that is now providing ever more detailed images of the earth's three-dimensional internal structure [Grand *et al.*, 1997].

3. Geochemistry and Processes of Chemical Fractionation

Although seismology has provided a wealth of information regarding our planet's internal structural features, the actual chemical composition is also of immense interest. Over the last 40 years the field of geochemistry has generated a huge base of information concerning the earth's chemical makeup. As geochemists in the 1960s and 1970s began to collect and analyze rocks from the ocean floor and from ocean island volcanoes, and to compare these analyses with those of rocks from the continental crust, a clear set of patterns emerged. First, it became clear that typical continental crustal rocks were extremely enriched in the so-called incompatible elements. The term "incompatible" in this context applies to elements whose large ionic size and/or charge preclude them from fitting readily within the lattice structure of the dominant higher melting temperature silicate minerals. On the other hand, evidence was compelling that the mantle source rocks for mid-ocean ridge basalt (MORB) were significantly and systematically depleted in these elements. This class of elements includes the large-ion lithophile elements like K, Rb, Cs, U, Th, Sr, and Ba; rare earth elements (REE) like La, Ce, Nd, Sm, and Lu; and the high field strength elements with high ionic charge such as Nb, Ta, Hf, and Ti. Note that all the major radioactive heat producing elements (U, Th, and K) are in this incompatible category. Most of the radioactive elements used as isotopic tracers and for dating purposes (for example, Sm, Rb, Lu, K, U, and Th) are in this category as well. Table 1 provides a classification of the elements with respect to their affinities for the different chemical environments of the earth.

As geophysicists and geochemists engaged in exploring the mechanical and chemical processes occurring at the mid-ocean ridges and subduction

zones, a strong case emerged that the continental crust was the product of chemical fractionation of the rock that comprises at least the upper third, and perhaps even more, of the earth's mantle. Studies over the last 35 years have yielded considerable insight into these fractionation processes by which incompatible- and silica-rich, and Fe- and Mg-poor continental crust is extracted from mantle rock. The several stages involve specifically the formation, alteration, subduction, and re-assimilation

Table 1. Classification of the elements. The volatility categories are here defined in terms of a temperature T_c at which 50% condensation occurs for a pressure of 10 Pa (10^{-4} atm). Refractory elements refer to those having a T_c exceeding 1400 K; transitional elements, a T_c between 1250 and 1400 K; moderately volatile elements, a T_c between 800 and 1250 K; and highly volatile elements, a T_c less than 800 K. At high pressures elements denoted with a superscript + may develop siderophile characteristics and thus have a tendency to partition into the earth's core [after *McDonough and Sun, 1995*].

Lithophile elements

Refractory:	Be, Al, Ca, Sc, Ti, V ⁺ , Sr, Y, Zr, Nb, Ba, REE, Hf, Ta, Th, U
Transitional:	Mg, Si, Cr ⁺
Moderately volatile:	Li, B, Na, K, Mn ⁺ , Rb, Cs ⁺
Highly volatile:	F, Cl, Br, I, Zn

Siderophile elements

Refractory:	Mo, Ru, Rh, W, Re, Os, Ir, Pt
Transitional:	Fe, Co, Ni, Pd
Moderately volatile:	P, Cu, Ga, Ge, As, Ag, Sb, Au
Highly volatile:	Tl, Bi

Chalcophile elements

Highly volatile:	S, Se, Cd, In, Sn, Te, Hg, Pb
------------------	-------------------------------

Atmosphere elements

Highly volatile:	H, He, C, N, O, Ne, Ar, Kr, Xe
------------------	--------------------------------

of oceanic lithosphere. Since this topic has such a significant bearing on the distribution of radioactive elements in the earth as a whole, I will provide a moderately detailed summary.

In what we can assume as the beginning stage of a larger process, hot mantle rock ascends passively beneath an oceanic ridge as the tectonic plates diverge and migrate away from the actively spreading ridge (see Figure 1). Because the melting temperature of silicate minerals decreases with decreasing pressure, this hot rising rock below the ridge typically undergoes partial melting as it reaches shallow depths where the hydrostatic pressure becomes small (a process also referred to as decompression melting). Mantle rock, of course, is comprised of a mixture of minerals, each of which has its own melting temperature. When the temperature of the bulk rock exceeds the melting temperature of a specific mineral component, that component begins to melt. This process of partial melting, then, is a process that preferentially extracts the lowest melting temperature components, such as quartz (SiO_2) and plagioclase ($\text{CaAl}_2\text{Si}_2\text{O}_8$).

These low melting temperature minerals were also the last ones to form as the rock had earlier cooled and crystallized from a higher temperature state. These, therefore, are the minerals that tend to have the highest concentrations of incompatible elements—elements which because of their large ionic size and/or charge do not conveniently fit within the lattice structure of the dominant higher melting point mineral phases that comprise the bulk of the rock. Partial melting therefore preferentially extracts the incompatible elements. This melted material derived from upper mantle rock has a basaltic composition and a very low viscosity. Even for a few percent of partial melting, such melt because of its buoyancy is able to percolate through the residual solid and preferentially rise to the surface where it then solidifies to form new oceanic crust. Because this basaltic rock is formed at a mid-ocean ridge, it is commonly called mid-ocean ridge basalt (MORB). The typical thickness of the layer is about 6 km. This magma extraction process leads to a two-layer structure for oceanic lithosphere—an upper layer of solidified basaltic magma and a lower layer comprised of the complementary residual solid. The uppermost part of the lower layer is

strongly depleted in low-melting-temperature minerals and grades into rock where no partial melting has occurred at a depth of about 50 km. It is estimated that about 20 km³ of new basaltic crust per year is presently formed by this process along the earth's 60,000 km of mid-ocean ridges [*Hofmann, 1997*].

The next stage in this larger fractionation process involves chemical alteration of the freshly emplaced oceanic crust by seawater via vigorous hydrothermal circulation near the spreading ridge where temperatures are high. Cooling produces volumetric contraction that leads to formation of fractures and allows seawater to penetrate to fine spatial scales and significant depths. This hydrothermal activity is effective in extracting Pb from the basaltic crust and precipitating it in metalliferous sulfide deposits. As the lithosphere migrates away from the ridge it is eventually covered by a blanket of sediment that tends to reduce the hydrothermal flow. Recent studies, however, suggest that significant hydrothermal flow occurs far away from mid-ocean ridges and that the sediment blanket is less effective in restricting such flow than once believed [*Stein and Stein, 1994*].

Another major stage of chemical differentiation occurs as oceanic lithosphere plunges back into the mantle at a subduction zone. Although most of the sediment gets scraped away by the overriding plate, some of it, along with some water, is carried down into the mantle on the top surface of the subducting lithospheric slab. At a depth of about 125 km, temperatures become sufficiently high for melting to occur. Again, the phases with the lowest melting temperatures begin to melt first. However, in this environment significant water tends to be present, and water has a potent effect on reducing the melting temperatures. Moreover, this second stage of partial melting acts predominantly on material that has already undergone significant chemical differentiation through partial melting as well as hydrothermal alteration at a mid-ocean ridge. The partial melting again scavenges incompatible elements, as well as the Pb in hydrothermal sediments, and yields a magma that is even more silica-rich. The resulting volcanism, known as convergent margin volcanism, is the primary way new continental crust is formed in the contemporary world. The estimated crustal production rate from this

type of volcanism on earth today is about $1 \text{ km}^3/\text{yr}$ [Hofmann, 1997].

The cold, dense layered oceanic lithosphere, with some fraction of its incompatible elements and lightest mineral phases stripped from its basaltic layer, sinks back into the mantle. However, the exact fate of this subducted oceanic lithosphere, and in particular its basaltic crustal layer, is still poorly known and is a topic vigorously debated in the earth science community. A key issue is the fact that, at a depth of about 60 km, basalt with a density of about 2900 kg/m^3 transforms to a rock type known as eclogite with a density of about 3400 kg/m^3 , which is denser than the surrounding mantle rock. Except for a depth range from about 650 to 750 km, the basaltic mineral assemblage appears to be denser than the mineral assemblage estimated for the bulk mantle [Irfune and Ringwood, 1993] all the way down to the core-mantle boundary.

The crucial question is whether this relatively thin but dense basaltic crustal layer can mechanically delaminate from the rest of the lithospheric slab before the slab as a whole gets re-assimilated into the mantle. If this does occur, then it is possible for a layer of mostly basaltic composition to exist just above 650 km depth and/or at the very bottom of the mantle. If such a layer or layers exist, they could be a significant repository of incompatible (including radioactive) elements, since this basaltic material still retains much of its original inventory. Since 3D seismic tomography methods are now able to image lithospheric slabs that clearly penetrate through the 660 km seismic discontinuity into the lower mantle [Grand *et al.*, 1997] it seems likely that much if not most of this basaltic layer penetrates the barrier between 650 and 750 km and arrives in the lower mantle. What its fate is after this remains somewhat uncertain at this point. In particular it is uncertain just how much basaltic crust through earth history may have delaminated to preserve its identity as a distinct layer at the base of the mantle.

This multi-stage process just described that produces silica-rich continental crust from mantle rock is believed responsible for extracting most of the incompatible elements from at least a third, and probably half, of the earth's mantle and placing them into the reservoir of the earth's continental crust. The reservoir of mantle rock mostly depleted of its incompatible elements (which from geochemical observations is

also the source of the mid-ocean ridge basalt, or MORB), has come to be known in the geochemical community as the depleted MORB mantle (DMM). Physically, this DMM reservoir is generally understood to include the entire upper mantle and transition zone, and possibly a significant fraction of the lower mantle as well.

4. Composition of the Deeper Mantle: Clues from Ocean Island Volcanism

A class of volcanic rocks at the earth's surface does seem to offer some constraints on the fate of the oceanic crust. So-called hotspot, or ocean island basalt (OIB), volcanism appears to represent expression of hot plume-like upwellings from rather deep within the mantle that are relatively enriched in incompatible elements. Since the late 1970s the combined use of several isotope tracers applied to such OIB rocks has identified three distinct source regions in the mantle, in addition to presumably shallower DMM. These three OIB source regions have been designated HIMU, EM I, and EM II [Zindler and Hart, 1986]. HIMU is characterized by a high $^{206}\text{Pb}/^{204}\text{Pb}$ ratio that is diagnostic of a high U/Pb ratio ($\mu = ^{238}\text{U}/^{204}\text{Pb}$; hence the designation, HIMU). The two "enriched mantle" (EM) sources are distinguished by a high $^{207}\text{Pb}/^{204}\text{Pb}$ ratio for a given $^{206}\text{Pb}/^{204}\text{Pb}$ ratio, relative to MORB. EM I has relatively low $^{206}\text{Pb}/^{204}\text{Pb}$ and $^{87}\text{Sr}/^{86}\text{Sr}$ ratios compared to EM II. EM II has intermediate $^{206}\text{Pb}/^{204}\text{Pb}$ and high $^{87}\text{Sr}/^{86}\text{Sr}$ ratios [Hart, 1988; Carlson, 1994]. These three regions can also be distinguished by trace element ratios [Weaver, 1991]. Figure 2 provides a comparison of the concentrations of selected trace and major elements for HIMU and EM I basalts with typical MORB and continental crust.

Trace element and radioisotope characteristics of HIMU basalts have led to the conclusion that HIMU represents ancient basaltic oceanic crust subducted and imperfectly mixed into the mantle [Hofmann and White, 1982; Hofmann et al., 1986; Hauri and Hart, 1993]. This suggests that at least some of the basaltic oceanic crust retains its identity as it penetrates deep within the lower mantle. EM I and EM II on the other hand appear to have a component of recycled sediment in their

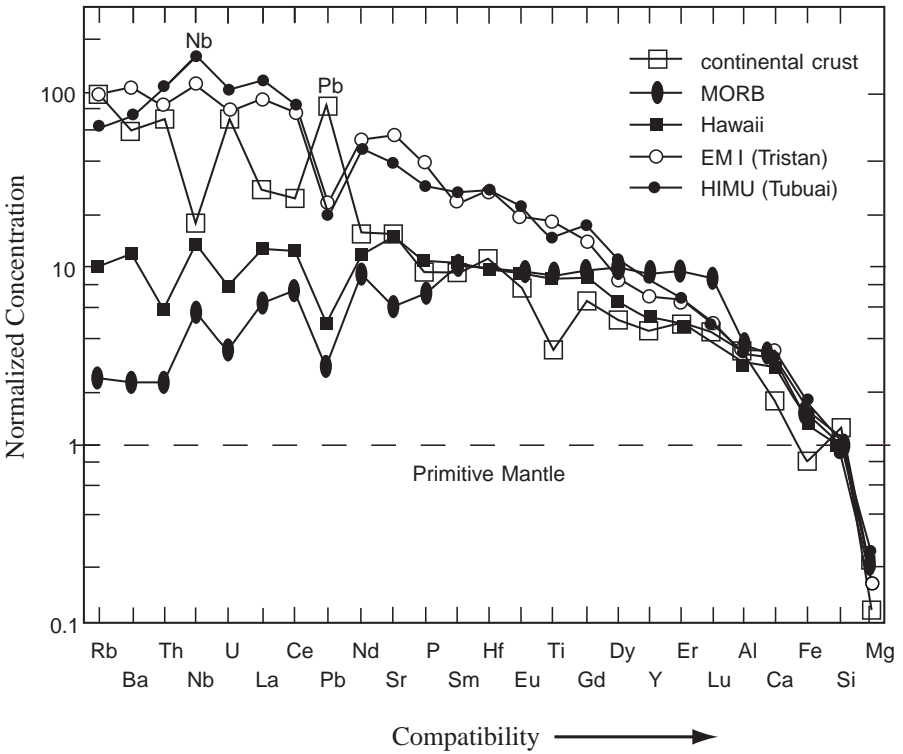


Figure 2. Concentrations of selected trace and major elements, arranged in order of decreasing incompatibility and normalized to estimated primitive mantle values for average continental crust, average MORB, and three types of OIB: average Mauna Loa, Hawaii, average Tristan da Cunha, South Atlantic (representing EM I), and Tubuai, South Pacific (representing HIMU). The patterns for MORB and the ocean island basalts differ by their different enrichments in incompatible elements, but they are similar with respect to their positive Nb and negative Pb anomalies. The continental crust has opposite Nb and Pb anomalies [after *Hofmann, 1997*].

composition [*Hofmann and White, 1982; Zindler and Hart, 1986; Chauvel et al., 1992*]. This suggests not only preservation and isolation of basaltic oceanic crust in the lower mantle, but oceanic crust together with subducted sediments in substantial quantities. It is important to point out that many ocean island basalts appear to be mixtures from two or more of these three source end members. The picture emerging not

only from these isotopic and trace element studies of OIB, but also from detailed seismic investigations of the lowermost part of the mantle, is that this region of the earth is very heterogeneous and has a complex history.

Since the early 1990s there has been interest in the possibility of a significant common component in mantle plumes that produce OIB. *Hart et al.* [1992] found that almost all the isotopic variation in the OIB data can be captured in terms of just three isotope ratios. This reinforced previous conclusions that mantle plumes can be modeled as mixtures of just a few components. However, as these authors plotted the data in a tertiary diagram, they observed that the distributions of composition for different volcanic islands converged on a common composition they called FOZO (for “focus zone”). FOZO basalt has an isotopic composition similar to that of MORB, except that its Pb is more radiogenic than MORB. It also displays a high $^3\text{He}/^4\text{He}$ ratio. *Hart et al.* [1992] argued that FOZO represents a significant portion of the lowermost mantle and plumes emerging from the core-mantle boundary viscously entrain this material. Several recent efforts have attempted to work out the mantle dynamics that might allow such a layer to persist in the lower part of the mantle without losing its identity through mixing [*Kellogg et al.*, 1999].

5. Toward Estimating the Earth’s Overall Composition: Data from Meteorites and the Sun

Vital to a serious interpretation of these geochemical data in terms of earth history is an estimate of the total inventory of the various elements that comprise the earth as a whole. The two approaches most often applied include use of meteorite compositions and the relative abundance of elements in the Sun, as estimated by spectroscopic analysis of the photosphere and corona, as well as measurement of solar wind and solar energetic particles [*Anders and Grevesse*, 1989]. These two approaches give strikingly similar elemental abundances as illustrated in Figure 3. Well-determined elemental abundances agree individually to within about $\pm 10\%$ on average over an absolute range of about eight orders of

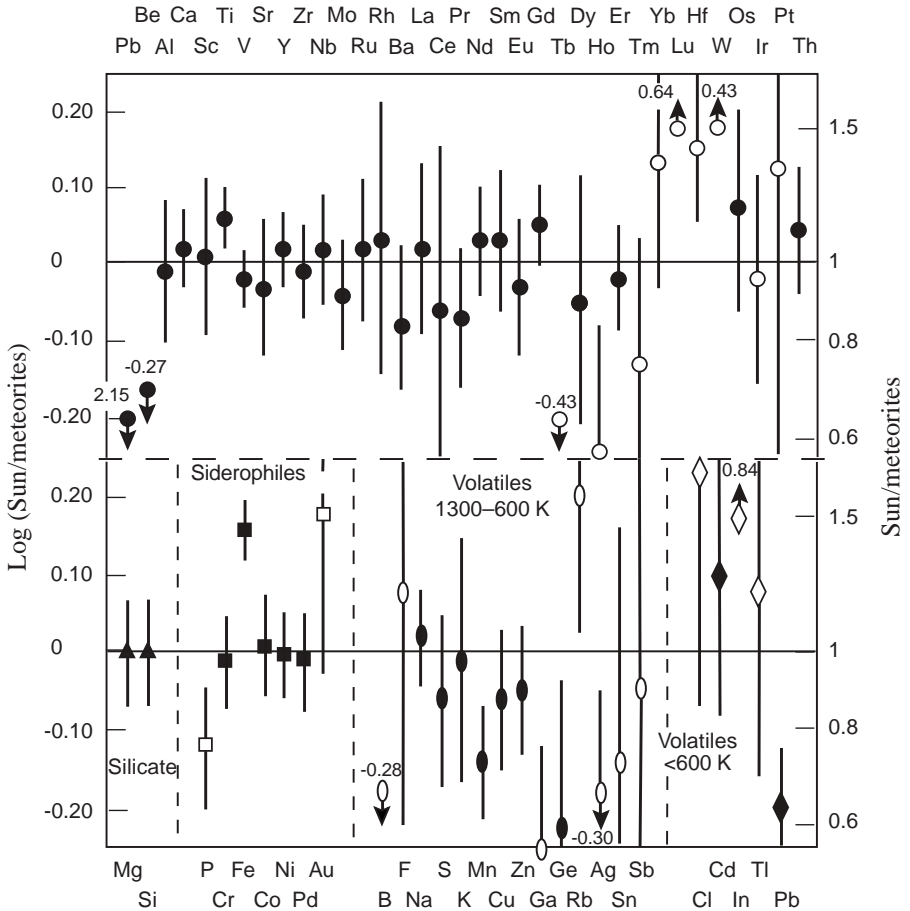


Figure 3. Ratios of element abundances as measured in the Sun's photosphere versus in meteorites. The ratios are strikingly close to unity across the five major cosmochemical groups, except for elements involved with thermonuclear reactions (Li, Be), elements poorly determined in the photosphere (open symbols), and five problematic cases (Fe, Mn, Ge, Pb, and W) [after *Anders and Grevesse, 1989*].

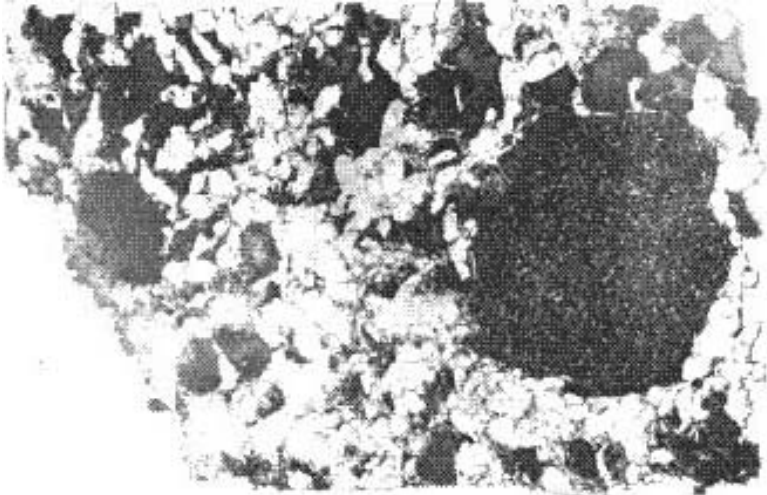
magnitude. Significant differences between the Sun and meteorites exist only for Fe, Mn, Ge, Pb, and W [see *Anders and Grevesse, 1989*, for their explanation].

This high level of agreement between solar and meteoritic abundances relies, however, on a careful selection of the meteoritic material. In particular, only a special class of meteorite is used for the determinations, namely, CI carbonaceous chondrites. There are only five specimens of such material, and of these five specimens only three have compositional data reliable enough to make accurate determinations [*McDonough and Sun, 1995*].

Meteorites are usually grouped in four main classes: chondrites, achondrites, stony-irons, and irons [*Stacey, 1992*]. Chondrites are the most common type of meteorite and represent more than 90% of observed falls. Because iron meteorites are generally larger, the mass of meteoritic material in space is probably less than 90% chondritic, however. The characteristic feature of chondrites is the presence of chondrules, which are small glassy spherules of silicate typically about 1 mm in diameter as shown in Figure 4. These chondrules appear to have been dust-like particles that melted and then rapidly cooled to acquire their glassy character and roughly spherical shapes prior to being incorporated into larger coherent bodies. Achondrites are much less common than chondrites and are similar to many terrestrial rocks. They are crystalline silicates, for the most part with no metallic phase present. Chondrules are also generally absent in these objects. Iron meteorites are mostly metallic Fe, with about 10% Ni in solid solution. Stony-irons are about halfway between achondrites and irons.

An important subclass of chondrites is the carbonaceous chondrites. These have several percent C and substantial amounts of volatiles, especially water, which implies these objects have never been strongly heated. These meteorites are relatively few in number and also small in size. Their rarity and small size is likely due to their extreme friability and consequent inability to survive passage through the atmosphere. Carbonaceous chondrites are divided into three types. Types II and III are more like ordinary chondrites. Type I carbonaceous chondrites (designated CI) are nearly homogeneous, especially rich in volatiles, comprised of fine particles, but without chondrules (despite their name). Most workers in the community have come to the conclusion these objects represent the best-preserved samples of the primitive dust material

(a)



(b)

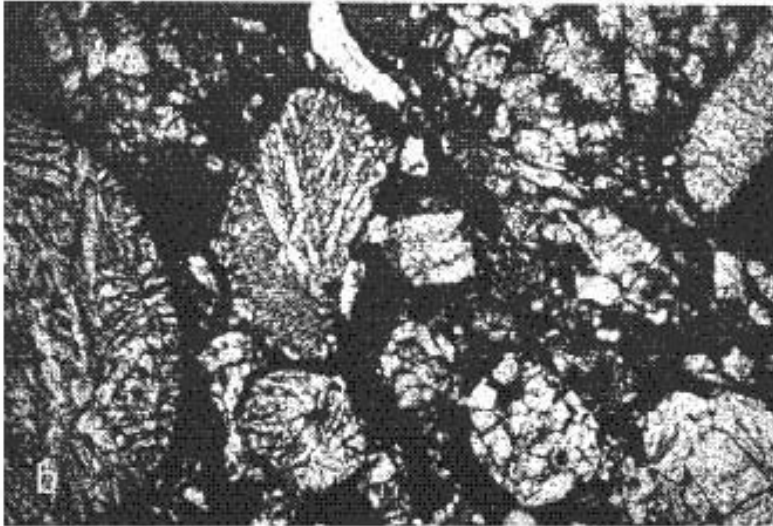


Figure 4. (a) Polished section of the Bencubbin meteorite. The bulk of the meteorite has a well-developed crystalline (achondritic) structure, but a large chondritic inclusion appears as the dark area on the right-hand side of the photograph. On the left-hand side is a carbonaceous chondritic inclusion. (b) Enlarged section of the ordinary chondrite fragment, showing the structure of the chondritic spherules, just apparent in (a) [photographs by *J. F. Lovering*, after *Stacey*, 1992].

out of which they believe the solar system was formed. The detailed analyses of three of these small CI carbonaceous chondrites today provide the reference meteoritic element abundances for entire the solar system [Anders and Grevesse, 1989]. It is noteworthy that their composition indeed so closely matches the solar data. Of course, they are lacking the majority of the most volatile elements such as H, He, C, N, O, Ne, and Ar observed in the Sun.

The meteorite and solar data provide a reference composition to which the earth's estimated major-element, as well as minor- and trace-element, inventory can be compared. The melting properties of upper mantle rocks yield important information on how various elements are segregated into the melt, as we have seen, and provide a basis for interpreting the likely melting and differentiation histories of various rock samples that can be collected at the earth's surface. Many investigators have worked many years to attempt to integrate all these various sources of information together in an effort to assemble a consistent model of the earth's overall composition.

6. Estimating the Earth's Major and Minor Element Composition

Although we believe we have physical samples from each of the three primary layers of the mantle, the upper mantle offers by far the most material for detailed analysis. Upper mantle samples are brought to the surface in three primary ways: as magmas, as xenolith fragments in magmas, and through tectonic processes that physically emplace massifs or slabs of mantle rock (known as ophiolites when derived from the ocean floor) at the surface. Samples from the transition zone and lower mantle are available only as tiny inclusions in diamonds and poly-mineralic fragments in kimberlites.

Samples from the upper mantle display a mineralogy dominated by the minerals olivine, orthopyroxene, clinopyroxene, and garnet, with an overall major element composition known as pyrolite [Ringwood, 1975]. In regard to the lower mantle, the composition of some mineral inclusions

in diamonds, apparently formed at lower mantle pressures, suggests these inclusions were in equilibrium with rock similar in composition to that of the upper mantle [*Kesson and Fitz Gerald, 1991*]. Seismic evidence for lithospheric slabs penetrating the 660 km seismic discontinuity suggests considerable mass transfer between upper and lower mantle, which also implies the bulk composition of upper and lower mantle may be similar. Although there is still considerable debate concerning this issue, the evidence in this author's opinion favors a nearly uniform major element composition throughout the mantle except for its bottommost 100–200 km, known as the seismic D" layer.

In regard to the core, we have no physical samples. It is generally assumed, however, the core is dominantly a Fe-Ni mixture similar to that observed in iron meteorites. The seismically derived density for the outer core is actually a bit lower than that of such an Fe-Ni alloy. This has led to the conclusion by most investigators that from 5% to 15% of a low-atomic-weight element (or elements) is present in the outer core. Possible candidate elements include O, Si, S, C, and H, but there are few constraints available to limit the identity further.

7. Composition of the Silicate Earth

Many geochemists have applied radioisotope and trace element data from mantle-derived samples, combined with solar system abundance data from meteorites and solar spectroscopy, to obtain more detailed estimates for the silicate part of the earth. Two general classes of models have been advanced over the past 40 years. The first is *Ringwood's* [1966] pyrolite model based largely on the complementary melt-residuum relationship between basalts and peridotite source rocks. *Ringwood* [1966] found that the refractory (high melting temperature) lithophile element composition of his pyrolite model was in remarkably close agreement with the composition of CI carbonaceous chondrites. Other workers since that time have used similar methods, also based on upper mantle samples and melting relationships, and have obtained models for overall mantle composition remarkably similar to *Ringwood's* original model [for example, *Sun, 1982; Waenke et al., 1984; Palme and*

Nickel, 1985; Hart and Zindler, 1986; McDonough and Sun, 1995]. The main criticism of these models has been that they are based almost exclusively on upper mantle data, and therefore may not correctly capture the chemistry of the lower mantle.

The second class of models is known as the CI chondritic type. These models simply assume the earth has a bulk refractory element composition equal to that of CI chondrites (but depleted in volatile elements such as K and Rb). The difficulty with this approach is that relative to CI chondrites, the upper mantle's major element values for Mg and Si are noticeably (some tens of percent) lower than observed in CI chondrites. For such models to be consistent, the missing Mg and Si must be in the lower mantle, but this implies the upper and lower mantles are chemically distinct with respect to their major element compositions. The evidence for significant mass exchange between upper and lower mantle, however, seems to argue against such a major chemical difference.

McDonough and Sun [1995] argue that while a CI chondritic model is a good starting point from a historical perspective, a better approach is to allow the vast number of samples from the mantle itself to be the basis for determining the mantle's actual composition. They use a large suite of 160 peridotite samples, about half from xenoliths and the other half from massifs, as the basis for estimating the concentrations of 76 of the elements in an updated pyrolite model for the silicate part of the earth. Their suite was selected to eliminate samples that had experienced excessive loss of a basaltic component and/or been modified significantly by secondary enrichment processes.

By measuring and comparing large numbers of element ratios in these 160 samples, these authors come to a number of conclusions. First, they conclude none of the samples represents pristine mantle. In some samples the composition indicates a melt component has been extracted, while in others it suggests a limited degree of secondary melt enrichment has occurred. Nevertheless, major-, minor- and trace-element ratios display amazingly tight and consistent trends when plotted against one another for the vast majority of the samples. In particular, the data from these peridotites define coherent trends in ratio-ratio plots that pass through

uniquely defined chondritic values for the refractory lithophile element ratios, as illustrated in Figure 5.

This in the view of *McDonough and Sun* [1995] is strong evidence these peridotites originally possessed chondritic relative proportions of the refractory lithophile elements (e.g., Al, Ca, Ti, Nb, Ba, REE, Hf, Th,

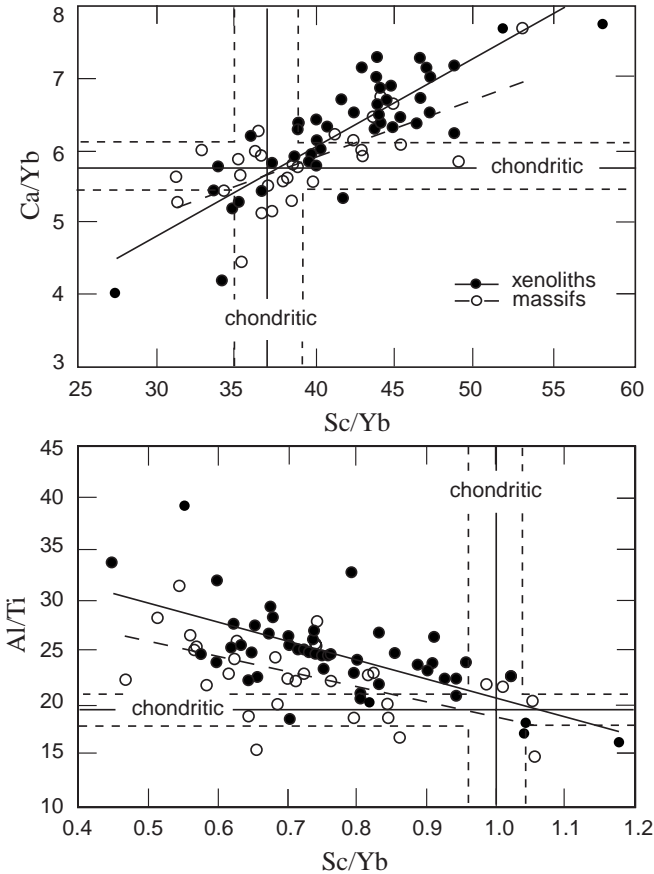


Figure 5. Variation diagrams using refractory lithophile element ratios for peridotite massifs (open circles) and peridotite xenoliths (dots). The chondritic values are given as a range (between fine dashed lines) and best estimate (fine solid line). Linear regressions are given for peridotite massifs (dashed line) and peridotite xenoliths (solid line) [after *McDonough and Sun*, 1995].

U). It is consistent with the proposition that the silicate earth has chondritic relative abundances of these elements, as previous less detailed studies had suggested. Using the absolute abundances for Al, Ca, and Ti inferred from these peridotite samples, with the assumption that the refractory lithophile elements all have chondritic abundance in the earth, the authors are able to provide absolute abundances for all 28 of these refractory lithophile elements as displayed in Table 2. Their estimates of the accuracies for these abundances are all within $\pm 20\%$, and most are within $\pm 10\%$.

Further, the authors use the measured trends for Si, Mg, and Fe versus ratios of the refractory lithophile elements in these samples to obtain the absolute abundances for these major elements in the silicate earth. In terms of their oxides, these values are 45.0% for SiO_2 , 37.8% for MgO , and 8.05% FeO . The accuracy they estimate for these numbers is $\pm 10\%$. They note, however, the Mg/Si ratio they find for the earth is 20–40% higher than what is observed for the various types of chondrites. They acknowledge they have no explanation for such a difference in major element chemistry.

The authors conclude, based on the relatively smooth refractory lithophile element depletion patterns (depletion is due to modest melt fractionation) they observe in these samples, together with experimental mineral/melt partition coefficient data for lower mantle mineral phases, that these upper mantle peridotites have not experienced any high pressure fractionation involving such lower mantle phases. This argues that these peridotites are not residues from a global mantle melting event, nor the crystallized melt products from such an event.

McDonough and Sun [1995] apply their general method of using measured elemental values for their suite of 160 peridotite samples, together with careful geochemically based adjustments to account for the extraction of melt and/or secondary melt enrichment, to obtain estimates for many of the other 47 elements they list in their Table 5, reproduced here as Table 2. They emphasize that elements not in the category of refractory lithophile elements (or transitional lithophiles, such as Si and Mg) are noticeably too strongly depleted in the silicate earth relative to their chondritic abundances. This they argue is largely a

Element	Chondritic	BSE	Ratio	±	Element	Chondritic	BSE	Ratio	±
Li (ppm)	1.5	1.6	0.39	30	Pd	550	3.9	0.0026	80
Be	0.025	0.068	1.00	20	Ag	200	8	0.015	F3
B	0.9	0.30	0.12	F2	Cd	710	40	0.021	30
C	35000	120	0.0013	F2	In	80	11	0.050	40
N	3180	2.0	0.0002	F2	Sn	1650	130	0.029	30
F	60	25	0.15	F2	Sb	140	5.5	0.014	50
Na	5100	2670	0.19	15	Tc	2330	12	0.002	F2
Mg (%)	9.65	22.8	0.86	10	I	450	10	0.008	F3
Al (%)	0.860	2.35	1.00	10	Cs	190	21	0.040	40
Si (%)	10.65	21.0	0.72	10	Ba	2410	6600	1.00	10
P	1080	90	0.030	15	La	237	648	1.00	10
S	54000	250	0.0017	20	Ce	613	1675	1.00	10
Cl	680	17	0.009	F2	Pr	92.8	254	1.00	10
K	550	240	0.16	20	Nd	457	1250	1.00	10
Ca (%)	0.925	2.53	1.00	10	Sm	148	406	1.00	10
Sc	5.92	16.2	1.00	10	Eu	56.3	154	1.00	10
Ti	440	1205	1.00	10	Gd	199	544	1.00	10
V	56	82	0.53	15	Tb	36.1	99	1.00	10
Cr	2650	2625	0.36	15	Dy	246	674	1.00	10
Mn	1920	1045	0.20	10	Ho	54.6	149	1.00	10
Fe (%)	18.1	6.26	0.13	10	Er	160	438	1.00	10
Co	500	105	0.077	10	Tm	24.7	68	1.00	10
Ni	10500	1960	0.068	10	Yb	161	441	1.00	10
Cu	120	30	0.091	15	Lu	24.6	67.5	1.00	10
Zn	310	55	0.065	15	Hf	103	283	1.00	10
Ga	9.2	4.0	0.16	10	Ta	13.6	37	1.00	15
Ge	31	1.1	0.013	15	W	93	29	0.11	F2
As	1.85	0.05	0.010	F2	Re	40	0.28	0.0026	30
Se	21	0.0750	0.0013	70	Os	490	3.4	0.0026	30
Br	3.57	0.0500	0.005	F2	Ir	455	3.2	0.0026	30
Rb	2.30	0.6000	0.095	30	Pt	1010	7.1	0.0026	30
Sr	7.25	19.9	1.00	10	Au	140	1.0	0.0026	F2
Y	1.57	4.30	1.00	10	Hg	300	10	0.012	F4
Zr	3.82	10.5	1.00	10	Tl	140	3.5	0.0095	40
Nb (ppb)	240	658	1.00	15	Pb	2470	150	0.022	20
Mo	900	50	0.020	40	Bi	110	2.5	0.0086	30
Ru	710	5.0	0.0026	30	Th	29	79.5	1.00	15
Rh	130	0.9	0.0026	40	U	7.4	20.3	1.00	20

Table 2 (opposite). Estimated chemical composition for the bulk silicate earth (BSE) from the pyrolite model of *McDonough and Sun* [1995]. Concentrations for elements from Li to Zr are in ppm and from Nb to U are in ppb, except for Mg, Al, Si, Ca, and Fe which are in wt%. The ratio of the BSE to chondritic abundance is based upon measured values for Al, Ca, and Ti in peridotites normalized to 2.74 times the CI chondrite abundance. (The factor of 2.74 reflects the fact that the peridotite samples, and hence the silicate earth, lack most of the volatiles and siderophiles present in CI chondrites.) The \pm column is a subjective estimate of the uncertainty. Uncertainties are expressed in % or in terms of a factor F (for example, F2 means uncertainty of a factor of 2).

consequence of two main processes: (1) the loss of volatile elements because of a postulated high temperature environment in which the earth originally was assembled, and (2) in the case of the siderophile elements, the subsequent formation of the earth's core. They show that lithophile elements with moderate to high volatility (low condensation temperature) tend to be depleted in a manner strikingly related to their volatility. They further observe that the siderophile elements (those that readily dissolve in molten Fe) are also strongly depleted relative to their chondritic abundances, and when such elements have moderate to high volatility, they tend to be even more strongly depleted. These trends are indicated in Figure 6. They also note the almost perfectly chondritic relative abundances of the siderophile Pt group elements that they speculate is due to the addition of a small amount of chondritic material to the earth after the core had formed.

They interpret these trends in terms of the manner they believe the earth was formed via gravitational collapse of a rotating interstellar cloud of dust and gas, coalescing of planetesimals, and subsequent collisions of these planetesimals to form planets. They propose at earlier stages of this process, due to the Earth's proximity to the Sun, the material from which the Earth formed was dominated by refractory elements and contained little of the moderately volatile and volatile components that existed in the cooler regions more distant from the Sun. In addition, they interpret the strong depletion of siderophile elements to argue for a core formation event in which 80–90% of the Fe, plus large fractions of the siderophile elements, were extracted from the rest of the material

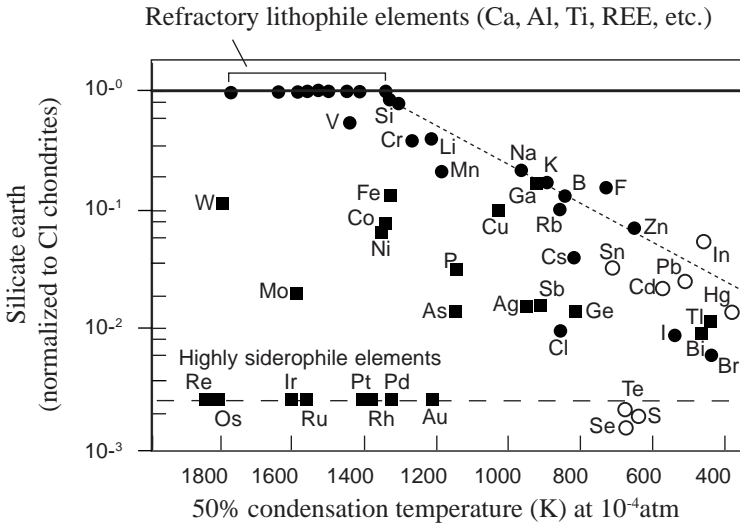


Figure 6. Plot of the abundances of elements in the pyrolite model for the silicate earth of *McDonough and Sun* [1995], normalized to CI chondrite abundances, versus 50% condensation temperature at 10^{-4} atm. Filled circles denote lithophile elements, filled squares denote siderophile elements, and open circles denote chalcophile elements. Note the chondritic abundance pattern of the refractory lithophile elements, the increasing degree of depletion with increasing volatility for the moderately volatile lithophile elements, the generally moderate to strong depletion of the siderophile elements, and the chondritic relative abundance of the highly siderophile elements. The dotted line represents *McDonough and Sun's* [1995] Early Stage Volatility Trend, while the dashed line represents the amount of chondritic material these authors suggest was added to the earth after core formation.

comprising the proto-earth and were sequestered into the core. These authors also postulate a late stage accretion event involving the addition of about 0.3% by mass of a body with chondritic composition to provide the observed amounts of Pt group elements, as well as Se, Te, S, and C. This latter material would then have to be thoroughly mixed throughout the mantle to yield the abundance patterns measured in the upper mantle peridotites.

Finally, by evaluating the constancy of ratios for various pairs of lithophile and siderophile elements (for example, P/Nd, Ti/P, Ba/W)—

ratios which should be markedly different for the core and the mantle—*McDonough and Sun* [1995] sought to evaluate the degree of core-mantle interaction over the earth's history. They found these ratios were nearly constant for peridotites and basalts with a wide range of radioisotope ages, and conclude there has been negligible exchange between core and mantle since the most ancient peridotite rocks crystallized.

8. Abundance of Radioactive Elements in the Earth as Supplied by Current Geochemical Models

Essentially all models for the composition of the earth proposed by the geochemistry community over the past 40 years, including the pyrolite model summarized above, conclude the relative abundances of all the refractory lithophile elements for the silicate earth match closely the abundances observed in the CI carbonaceous chondrites. In the case of the radioactive elements U and Th, the absolute numbers estimated for the silicate earth are 20 ppb for U and 80 ppb for Th. These have changed little over the last 25 years. The current uncertainties are $\pm 20\%$ and $\pm 15\%$, respectively [*McDonough and Sun*, 1995]. Samarium and Lu are also refractory lithophile elements with abundances of 406 ppb and 68 ppb, with $\pm 10\%$ uncertainties, respectively, estimated in this same manner.

In regard to K and Rb, which are moderately volatile lithophile elements, their abundances for the silicate earth are based on K/U ($\sim 10^4$), K/Rb (~ 400), Rb/Sr (~ 0.03) and Ba/Rb (~ 11) ratios as measured in crustal and mantle-derived rocks, together with Sr, Nd, and Hf isotope systematics [*McDonough et al.*, 1992]. The continental crust and depleted MORB mantle (DMM) have similar K/U and Ba/Rb ratios, which suggests these ratios are preserved during crust-mantle differentiation processes. Thus, given estimates for the absolute abundances of Ba and U, estimates for absolute abundances for K and Rb can be obtained. These numbers are 240 ppm $\pm 20\%$ for K and 0.60 ppm $\pm 30\%$ for Rb [*McDonough and Sun*, 1995].

The decay of ^{187}Re to ^{187}Os has recently become useful in isotopic analysis in several geochemical contexts. Rhenium is a highly siderophile

element, so most of it presumably resides with Fe in the earth's core. From studies of basalts and peridotites, however, investigators have concluded that the Pt group elements (Ru, Rh, Pd, Os, Ir, Pt) plus Re and Au display a strongly coherent chondritic relative abundance pattern, but at a ratio of about 0.003 to that of Mg for the earth. They speculate this abundance pattern is the result of a late stage accretion (after core formation) of a veneer (<1% by mass) of chondritic material onto the earth that was then thoroughly mixed into the mantle by convective processes. The value estimated for Re is 40 ppb with $\pm 30\%$ uncertainty [McDonough and Sun, 1995].

From these estimates for the abundances of U, Th, and K, together with the present-day heat generation rates per unit mass for each of these elements [Stacey, 1992], one obtains a mean heat generation rate for the silicate earth of 4.9×10^{-12} W/kg.

Given that we have reasonably well-constrained estimates for the abundances of the radioactive elements for the earth as a whole, what about their spatial distribution?

9. Distribution of Radioactive Elements in the Earth's Continental Crust and Mantle

As we have seen already, processes that create continental crust remove incompatible elements from the mantle. By measuring the composition of crustal rocks it is possible to estimate what fraction of the mantle's incompatible elements actually reside in the continental crust. Although the upper crust (roughly the upper 10 km) is reasonably accessible to direct sampling and analysis, the deeper portions of the continental crust are relatively inaccessible. The deepest hole ever drilled, for example, reached a depth of only 12 km. Our knowledge of the composition of the lower crust (below about 20 km depths) is based primarily on outcrops of a few terrains that have been uplifted and exposed at the surface by tectonic processes, as well as from rock fragments (xenoliths) that have been stripped from conduit walls deep in the continental crust as rapidly rising volcanic magma rose through such conduits and carried them to the earth's surface. There appears to be considerable spatial heterogeneity

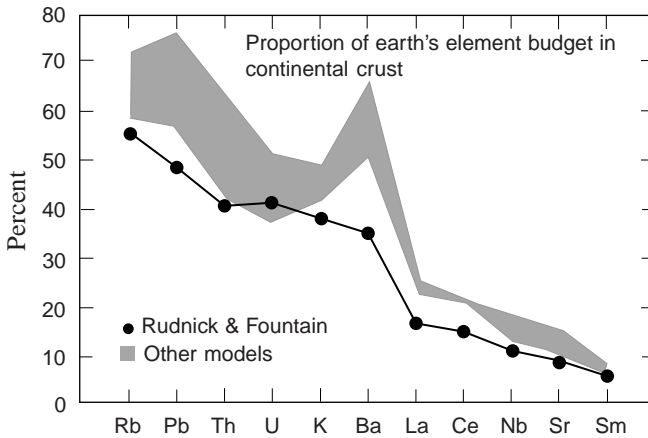


Figure 7. Proportion of the element budget of the bulk silicate earth contained within the continental crust as estimated by *Rudnick and Fountain* [1995]. The shaded region is the range of model compositions of *Weaver and Tarney* [1984], *Shaw et al.* [1986], and *Wedepohl* [1994] [after *Rudnick and Fountain*, 1995].

in the structural features as well as composition of the continental crust, so refraction seismology data have been used to attempt to arrive at plausible lateral averages over this heterogeneity.

In a review paper *Rudnick and Fountain* [1995] describe the procedures used to obtain such global averages of crustal composition. These authors estimate approximately 40% of the earth's U, Th, and K resides in the continental crust as shown in Figure 7. They present evidence that the lower crust has an average composition resembling a primitive mantle-derived basalt, but with a significantly greater incompatible element content relative to typical oceanic crust. The lower crustal xenoliths, for example, suggest there is 10 to 30 times as much K. These authors estimate the amount of heat generated by the radioactive elements, averaged over depth and over different age and tectonic provinces, is 0.93 mW/m^3 , or $332 \times 10^{-12} \text{ W/kg}$. The corresponding surface heat flow, averaged over all age and tectonic provinces, is 37 mW/m^2 . This is close to the estimated average observed continental heat flow, which implies very little of the surface heat flow on average is derived from the mantle via thermal conduction through the crust. In fact, it seems these authors

may even have been influenced to make somewhat conservative estimates of the crustal radioactivity by giving more weight to mafic xenoliths than to composition data from outcrops so that the resulting averaged surface heat flow would not exceed the observed value.

If 40%, or perhaps even more, of the total inventory of heat producing elements resides in the continental crust, how is the remainder distributed within the earth's silicate mantle? Typical upper mantle peridotites display an amount of radioactive components corresponding to a heat production rate of about 1.5×10^{-12} W/kg [Stacey, 1992], or about 30% of the mean value of 4.9×10^{-12} W/kg for the bulk silicate earth given earlier in this chapter. A depleted MORB mantle (DMM) reservoir 70% depleted of its primary heat producing elements U, Th, and K represents 57% ($= 0.40/0.70$) of the total mantle mass when 40% of the total heat producing inventory is in the continental crust, provided none of these depleted constituents are elsewhere in the mantle. Similarly, when 50% of the mantle's total heat producing inventory is in the continental crust, the DMM represents 71% ($= 0.50/0.70$) of the total mantle mass. In the first case 57% of the total inventory resides in the DMM and continental crust together, while in the second case, 71% is accounted for in these two reservoirs.

In regard to the remaining 30–40% of the earth's heat producing inventory, Hofmann [1997] argues at least some volume of subducted basaltic ocean crust must reside at the base of the mantle to serve as the source material for plumes (particularly the HIMU and EM II type plumes) that yield OIB enriched in heat producing elements. Hofmann [1997] points out at the present time there is about 20 times the amount of ocean crust being formed (about $20 \text{ km}^3/\text{yr}$) as there is continental crust (about $1 \text{ km}^3/\text{yr}$), and if such a ratio is even approximately valid for the past, then a huge amount of basalt has been created and recycled into the mantle. Just how much of this material is actually present at the base of the mantle is not strongly constrained at this point. However, a zone with anomalous seismic properties, known as the D" layer and corresponding to the bottom 100–200 km of the mantle, has been known for many decades.

A layer at the base of the mantle 150 km in thickness represents about

3% of the mass of the silicate earth. If this layer is predominately subducted ocean crust with a typical MORB heat production rate of 27×10^{-12} W/kg [Stacey, 1992], then 18% of the total silicate earth heat production inventory resides in this layer. Such a layer 200 km thick would contribute 24% of the total inventory. Within the uncertainties of the estimates being used here it is therefore possible to account for the entire budget of heat producing elements in terms of just three reservoirs: the continental crust, a layer at the base of the mantle 150–200 km thick comprised mostly of subducted oceanic crust, and the remainder of the mantle with a DMM composition. However, the radiogenic heat production in HIMU, EM I, and EM II material is typically a factor of ten higher than typical MORB [Hofmann, 1997; also see Figure 2]. A layer just a few tens of kilometers thick with this level of heat production could readily account for the remaining inventory, with the rest of the lower mantle having a DMM composition.

For some time in the geochemistry community, and more recently in the seismology and geodynamics communities [for example, *van der Hilst and Karason, 1999; Kellogg et al., 1999*], there has been support for the idea of a fourth reservoir of largely undepleted material in the lower mantle. Advocates of this possibility point to the prevalence of non-radiogenic noble gases, such as ^3He , ^{20}Ne , and ^{36}Ar , in plume magmas, presumably from deep within the lower mantle. Because of the increase in viscosity with pressure, material in the deeper part of the lower mantle behaves sluggishly relative to the rest of the mantle. Therefore some amount of primitive material, advocates argue, may have escaped being cycled to the earth's surface and having its incompatible elements, including rare gas volatiles, extracted by partial melting.

It is this author's opinion, however, that the seismological evidence suggesting a distinct reservoir of remarkably hot material (presumably because of its high level of radiogenic heat production) in the lower mantle, but with an intrinsic density high enough to keep it negatively buoyant, is more plausibly explained by this material being simply ancient subducted oceanic crust as discussed above. The recent seismological data suggest, however, its volume may exceed that of the D'' region by as much as a factor of three. If such a volume of basaltic

material is actually present, there is no difficulty with the remainder of the lower mantle having a DMM composition. The source of the non-radiogenic noble gases in this case would be meteorite material that settled on the ancient seafloor, became mechanically associated with the oceanic crust, and upon subduction formed a dense and radioactive layer rich in non-radiogenic noble gases at the base of the mantle.

10. Robustness of Current Geochemical Models

From a creationist perspective, just how robust are current geochemical models for the earth's chemical composition and associated conjectures about the earth's origin and history? For example, a key issue is: how strong is the evidence that the earth's major chemical/structural divisions, that is, its crust, mantle, and core, are the result of chemical differentiation processes? This is a crucial issue because the extraction of the core from an initially undifferentiated earth is not a trivial process that occurs in a few hours time according to the physical laws we currently observe. Likewise, the chemical segregation of the continental crust via partial melting of mantle rock assisted by the presence of water also seems to require much more than a few hours time in the framework of presently observed physical laws. So an extremely important question is: just how solid is the case that such processes actually occurred in earth history?

First, it seems to this author that basic features of the geochemical data, such as the complementary abundances of incompatible elements between the continental crust and the depleted MORB mantle, as well as the complementary abundances of siderophile elements between the core and the mantle, argue forcefully that a significant amount of chemical differentiation has indeed occurred during earth's history. In other words, I am persuaded the geochemical data do strongly favor the conclusion the continental crust is the result of partial melting/differentiation processes through which much if not most of the rock material of the mantle has been cycled. In the framework of a literal understanding of Genesis 1, this implies to me God simply employed special means to accomplish these changes—methods outside the physics we observe today. That this conclusion is the correct one is at least

suggested by the passage in II Peter 3 in which the apostle is refuting the view that God never intervenes in this world and points to formation of the earth as one time God intervened in a special way.

To summarize the observations and conclusions given above which I believe are reliable, let me begin by affirming the present day earth structure as deduced by seismology as firm and trustworthy. In regard to the major element composition and mineralogy of the main structural divisions of the earth—inferences drawn from seismology, rock samples from the top few hundred kilometers of the earth, and mineral physics experiments—I believe the current models are generally robust and unlikely to change in any significant way. In other words, I believe the major element compositions and mineralogies inferred for the core, the mantle, and the crust are essentially correct. In my assessment, the main uncertainties lie at the level of detail, such as the identity of the light alloying element in the outer core and the nature of the complexity of the zone just above the core-mantle boundary. I further believe the processes involved in generating ocean crust, as well as the more silicic magmas corresponding to continental crustal rocks, are reasonably well understood at a basic level and correct.

In regard to the broadly held conclusion that the refractory incompatible element inventory of the earth matches closely the solar abundance pattern as well as that of CI carbonaceous chondrites, I believe the chemical evidence is definitely suggestive this is so. Of course, the tantalizing implication is that the whole solar system was formed from material of more or less uniform trace element composition. I have no real problem with that possibility, but I regard the naturalistic mechanisms commonly proposed by which this may have happened to be speculative.

Concerning the spatial distribution of the radioactive elements in the earth, I believe the conclusions based on direct measurements of rock composition, which include crustal rocks and samples from the upper mantle, are reliable and robust. Conclusions about the distributions of such elements in the lower mantle that rely on more tenuous assumptions and less observational data are much less certain in my opinion. This is also the outlook to the mainstream community. A final observation relating to the robustness of these conclusions is that most of them depend

hardly at all on the validity of radioisotopic dating methods or even on the age of the earth. Most of these conclusions are derived from direct observations and measurements of the present-day Earth, the present-day Sun, and in some cases present-day meteorites.

11. Correlation Between Surface Heat Flow and the Radioactivity of Surface Rocks

There is, however, a set of observations relating to the distribution of radioactive elements that has been somewhat of a puzzle to the earth science community for more than 30 years. This is the surprising correlation, on an outcrop to outcrop level, of the measured surface heat flow and the measured radioactivity of surface continental igneous rocks. This correlation was first reported by *Roy et al.* [1968] based on combined radioactivity and heat flow measurements from plutonic rocks at 38 localities in three different tectonic provinces in the United States. Since that time it has been confirmed by many other investigators. *Roy et al.* [1968] found that in each tectonic province the heat flow Q in W/m^2 and the heat production H in W/m^3 are related by a simple linear equation of the form $Q = Q_0 + DH$, where Q_0 is a constant for the given tectonic province and D has units of depth with values on the order of 10 km as shown in Figure 8. The authors interpreted this relationship to indicate that the observed local variability was due to variable heat sources in the upper 10 km of the continental crust, and that contributions from below that depth were relatively uniform in a spatial sense within each tectonic province.

Lachenbruch [1970] showed that several distributions of radioactive heat production versus depth could give the linear relationship documented by *Roy et al.* [1968], including a uniform distribution to depth D , a distribution decreasing linearly to a depth of $2D$, and an exponentially decreasing distribution with an e-folding depth D . He showed, however, that only a distribution for which heat production decreases in an exponential manner with depth could account for the observations in the presence of differential erosion. Such a relationship has $H(z) = H(0)e^{-z/D}$ for depths z between zero and some maximum depth

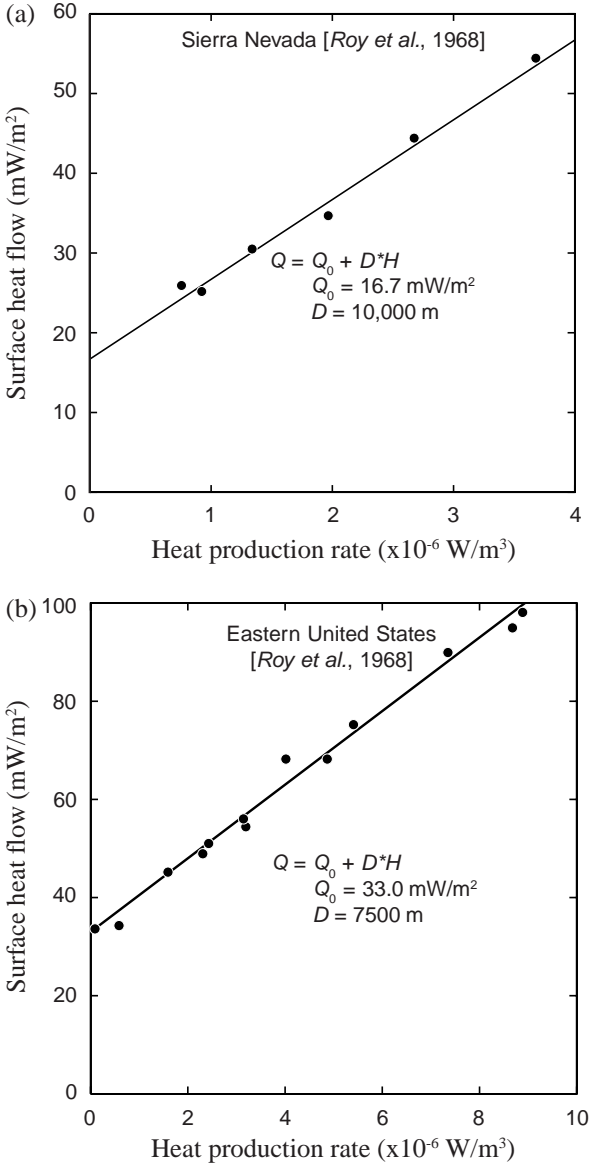


Figure 8. Measured surface heat flow versus measured radiogenic heat production rate for plutonic rock bodies in (a) Sierra Nevada mountains and (b) New England and Central Stable Region of North America [after Roy et al., 1968].

z^* . *Lachenbruch* [1970] assumed z^* to be the depth at which the heat flow is uniform throughout the region, and he showed it should be on the order of three times the scale depth D or more. Although *Lachenbruch's* analysis generally quelled the discussion regarding how the simple relationship between Q and H should be interpreted, the nagging question of just why Q should vary so precisely with H for plutonic bodies merely kilometers apart was never truly answered.

This issue has become even more of a puzzle during the past 15 years with the drilling of several deep holes into the continental crust, including the 12 km deep Kola project in Russia and the 9 km deep KTB project in Germany. In none of these deep boreholes was there observed the exponential decrease in the heat production as forecast by *Lachenbruch* [1970]. Instead, the heat production was observed simply to correspond to the rock type. In a discussion of the heat production observed in the German deep borehole *Clauser et al.* [1997] state,

None of the published data from boreholes penetrating deeply into the crystalline crust show clear evidence for a systematic variation of heat production with depth, neither linear nor exponential. Instead, heat production at Cajon Pass, United States [*Sass et al.*, 1992], Kola, Russia [*Arshavskaya et al.*, 1987], Siljan, Sweden [*Balling et al.*, 1990], and Urach, Germany [*Haenel and Zoth*, 1982] rather follows lithology [that is, rock type].

Similarly, *Pribnow and Winter* [1997] state,

Similar to investigations in other metamorphic regions [for example, *Kremenetsky et al.*, 1989; *Ashwal et al.*, 1987], the heat production profile to 9.1 km at KTB vitiates any hope of finding simple, general and systematic models for the vertical distribution of [heat production] $A(z)$ in the upper crystalline continental crust.

But the lack of a systematic vertical variation in radiogenic heat production means such systematic variation then cannot be the explanation for the correlation between surface heat flow and radioactivity in surface rocks.

A relatively simple answer, however, is available in the creationist framework. The crux of the answer is that a modest pulse of nuclear decay during the Genesis Flood has caused the near surface radioactive heat production to dominate the surface heat flow. The unlikely requirement in the uniformitarian explanation that a vertical column of

rock ten or more kilometers in height display throughout a level of radioactivity closely correlated with the surface rock is no longer needed. In the alternative explanation the characteristic depth D is actually not a physical depth at all, but instead a measure of the amplitude of the nuclear decay pulse and the thermal diffusivity of the rock. Because this result has never before been published, I will provide a reasonably detailed development.

The approach to the analysis is to employ the well-known solution for the cooling of an infinite half-space with an initially uniform internal temperature. The temperature of the half-space surface remains fixed. This solution is applicable to the problem at hand, provided the distribution of heat producing elements is reasonably uniform through a sufficient depth of rock. This depth corresponds to the distance heat can diffuse during the time interval of interest and is equal to $(4\kappa t)^{1/2}$, where κ is the thermal diffusivity and t is the time. The thermal diffusivity κ of granite is about $1.35 \times 10^6 \text{ m}^2/\text{s}$ [Stacey, 1992]. For an elapsed time of 5000 years ($1.5 \times 10^8 \text{ s}$) the diffusion depth is 900 m. The assumption that the radioactive heat producing elements are uniform through a layer 900 m thick in most continental granite bodies is not that unreasonable. Certainly it is more plausible than the requirement in the uniformitarian explanation that a strong vertical correlation exists over depths of 10 km or more.

Suppose by way of hypothesis a brief episode of accelerated nuclear decay occurred 5000 years ago in earth history. Such an episode of nuclear decay would raise the temperature of all materials containing radioactive elements, including the earth's crustal rock. The amount of the temperature jump would be directly related to the concentration of the heat producing elements present. Let the resulting temperature rise be denoted by T_1 . The component of surface heat flow out of such a body of rock due to this temperature rise corresponds to the solution of the infinite half-space problem, provided the distribution of heat producing elements is reasonably uniform over a sufficient depth as described above. This component of heat flow which we can denote as Q_1 simply adds to the pre-existing heat flow Q_0 due to the pre-existing thermal gradient.

The infinite half-space problem with an initial uniform internal temperature T_1 relative to its boundary has a surface flux Q_1 given by the expression [see *Carslaw and Jaeger*, 1959]

$$Q_1(t) = \left(\frac{\kappa}{\pi t} \right)^{1/2} \rho C_p T_1 \quad (1)$$

where κ is the thermal diffusivity, t is time, ρ is density, and C_p is the specific heat. The temperature rise T_1 due to the burst of accelerated nuclear decay can be expressed as

$$T_1 = \frac{E}{\rho C_p} \quad (2)$$

where E represents the energy per unit volume released in the accelerated decay episode. We can express E as the product of the present-day heat production rate H per unit volume and a time interval τ . The time interval τ can be viewed as how long it would take nuclear decay at present-day rates to generate the amount of heat released in the decay episode. Using the new variables we can rewrite (1) as

$$Q_1(t) = \left[\left(\frac{\kappa}{\pi t} \right)^{1/2} \tau \right] H \quad (3)$$

We note the quantity $(\kappa / \pi t)^{1/2} \tau$ has dimensions of length and displays the same relationship to H as does the parameter D in the expression for heat flow versus heat production discovered by *Roy et al.* [1968]. If we use D to denote this quantity, that is,

$$D = \left(\frac{\kappa}{\pi t} \right)^{1/2} \tau \quad (4)$$

we recover the identical relationship for the observed heat flow Q in terms of the measured radioactive heat production H , namely,

$$Q = Q_0 + DH . \quad (5)$$

Roy et al. [1968] found that when they plotted heat flow versus heat production, the slope D of the resulting straight-line relationship had values for the different tectonic provinces on the order of 10 km. We can use this information to get an estimate for τ and thus for the amount of accelerated nuclear decay. Solving equation (4) for τ we have

$$\tau = \frac{D}{(\kappa/\pi t)^{1/2}} . \quad (6)$$

When we use a value for κ of $1.35 \times 10^{-6} \text{ m}^2/\text{s}$ characteristic of granite, 5000 years for t , and 10 km for D , we obtain a value for τ of 190,000 years. This means that an episode of accelerated nuclear decay 5000 years ago representing 190,000 years worth of decay at presently observed rates can account for the observations.

It is of further interest to calculate the temperature rise associated with such an episode of accelerated decay. Using values typical of granite for ρ of 2670 kg/m^3 and for C_p of 830 J kg K^{-1} [*Stacey*, 1992], we obtain a temperature rise, given by $H\tau/\rho C_p$, of 5.5 K for $H = 2 \times 10^{-6} \text{ W/m}^3$ and 22 K for $H = 8 \times 10^{-6} \text{ W/m}^3$. These values for H span those measured for most granites. The amplitude of temperature rise associated with the hypothesized decay episode is therefore modest and reasonable.

To summarize this section we find that an episode of accelerated nuclear decay about 5000 years ago near the end of the Genesis Flood, with an amplitude corresponding to about 200,000 years of nuclear decay at presently measured rates, can account for the surprising observation that the heat flow from continental granite bodies correlates extremely well with the heat production rate measured in rocks from surface outcrops of these rock units. The temperature rise associated with such a hypothesized episode is on the order of 25 K or less. The main assumption on which this analysis depends is that the variation in the heat production rate H be relatively uniform to a depth of about 1000 m.

This is much more reasonable than the requirement in the uniformitarian explanation that the radioactivity content observed at the surface be correlated with that below to depths of 10 km or more.

Finally, I note Humphreys in Chapter 7 argues in the context of a model involving the stretching of the fabric of space itself that accelerated decay may be accompanied by volumetric cooling. As Humphreys explains, this mechanism for accelerated decay affects the electronic structure of matter in only minor ways (such as lowering temperature) and therefore is benign to most of chemistry and biology. If this conjecture regarding volumetric cooling can be confirmed, then the estimate for heat release I obtained in the above analysis corresponds instead to the *net* energy increase per unit volume resulting from the *combination* of heat production due to nuclear decay and heat loss due to volume cooling. In such a case our value of 200,000 years for the amount of accelerated decay implied by the field observations becomes a lower bound, applicable only if the accompanying volume cooling is negligibly small relative to the heat release from nuclear decay. At this point, however, I view this potential explanation of the correlation of surface heat flow with the radioactivity of surface crystalline rocks merely as one clue that God has acted in ways that has caused nuclear decay rates not to be invariant over cosmological history.

12. Discussion

How do the inferences concerning the structure, chemical composition, and differentiation history of the earth relate to the main theme of this report, namely, radioisotope dating? First of all, the amount of processing of mantle rock required to extract the continental crust together with its huge store of incompatible elements is staggering. Such processing appears to require cycling of a large fraction of the mantle's silicate rock via rapid thermal convection to very near the earth's surface where two stages of partial melting plus the interaction with water could take place. Did God use such an intricate process to fashion the earth before He created life upon it? In my opinion the chemical evidence is strongly

suggestive that, in fact, He did.

Moreover, did a significant amount of nuclear decay accompany this chemical differentiation process, as the large radioisotope ages of Archean and Proterozoic rocks indicate and the occurrence of mature ^{238}U radiohalos in these rocks indeed seem to require? Again, I believe the evidence is compelling that the answer to this question is yes. The amount of convective circulation in the mantle involved with the extraction of the continental crust implies a vast amount of heat extraction from the planet's interior. This convective circulation, of course, provides the means for removal of the heat from nuclear decay. And there is further abundant evidence for high temperatures in the earth during its earliest history as seen, for example, in high temperature Archean magmas known as komatiites.

But how does this fit into the Biblical framework? To me God must have completed this portion of earth history by some point during day 3 according to the text of Genesis 1. This means in my opinion the processes of nuclear transmutation, mantle convection, magma generation and cooling, together with a spectrum of tectonic and geological processes must have unfolded at rates many orders of magnitude faster than we observe today. Of course, God could have created the earth together with its diverse forms of life instantly. But even the Genesis text indicates process was involved. For example, we read concerning day 3, "Then God said, 'Let the waters below the heavens be gathered together into one place, and let the dry land appear', and it was so." This suggests dramatic geological change that unfolded in a brief span of time. As with many Biblical texts, this one seems to represent a profound understatement of the action that actually occurred.

Because the history of nuclear decay is such a central concern to this project, let me be so bold as to lay out my own tentative model based on the data I currently have available. I stress this is my own model and other members of the RATE group may not necessarily agree. First, I propose that on the order of 4.5 billion years' worth of nuclear decay at present rates unfolded rapidly in the earth before the end of day 3. This may at first seem astonishing, but if very little nuclear decay has occurred since God created the plants and animals, as I will attempt to justify

below, it is consistent with the concordant 4.5 billion year radioisotope ages for meteorites and up to 4 billion year radioisotope ages for terrestrial Archean rocks that will be discussed in Chapter 4.

Indeed I do believe there is evidence suggesting very little nuclear decay has taken place since God first created plant life on day 3. In support of this surprising possibility I appeal to ^{238}U radiohalos. The key observation is their apparent absence in Phanerozoic crystalline rocks. As described in Chapters 7 and 8, there is sufficient ^{238}U in zircons in most granite to produce mature radiohalos in 100 million years or less with present rates of nuclear decay. Zircons are so common in granite that if 540 million years or more of time has really elapsed since multi-celled life appeared on earth, then Phanerozoic granites corresponding to this time interval ought to contain abundant examples of mature ^{238}U radiohalos. Their apparent absence, if it can be rigorously confirmed, would argue that dramatically less nuclear decay has actually taken place since multi-celled life first appeared.

The only Phanerozoic ^{238}U radiohalos clearly documented in the scientific literature of which I am aware are those reported by *Gentry et al.* [1976] in coalified wood of Triassic/Jurassic age from the Colorado Plateau and of Devonian age from the Chattanooga shale near Nashville, Tennessee. These halos are all embryonic in their stage of development, and they owe even this degree of development to large total amounts of U in their radiocenters. *Gentry et al.* [1976] measured the $^{238}\text{U}/^{206}\text{Pb}$ ratios in several of the halo radiocenters using highly sensitive ion microprobe mass spectrometer techniques and obtained surprisingly large values that suggest little nuclear decay has occurred since these halos formed. The $^{238}\text{U}/^{206}\text{Pb}$ ratio *Gentry et al.* [1976] considered most reliable for the Triassic/Jurassic halos, for example, was 27,300. This ratio corresponds to an age of 240,000 years assuming constant decay rates at presently observed values.

Since radiohalos provide a tangible, visible, physical record of nuclear decay, I believe a well-documented case for the lack of mature ^{238}U halos in Phanerozoic samples would call into question the results of methods that rely on whole rock, or even mineral, isotope ratios for such material. My working hypothesis, influenced to be sure by the radiohalo data, is

that the standard isotope ratio methods are particularly vulnerable to inheritance of parent/daughter correlations, and that the large ages commonly obtained for Phanerozoic samples is mostly a consequence of such inheritance. To validate or reject this hypothesis, to me, ought to represent a major thrust for our RATE initiative for the next five years.

Finally, let me try to tie together the overall chronology picture. The model I am proposing has the events of Genesis 1 unfolding less than 10,000 years ago and culminating in an earth teeming with a spectacular diversity of life, including humans. It is a Creation that God declares to be “very good.” I conclude the processes God employed to fashion the physical earth early in Creation week involved a vast amount of nuclear transmutation that ceased prior to His Creation of plant life on day 3. The Bible records that because human sin had become so rampant by Noah’s generation, God brought a cataclysmic judgment upon the earth, to which the fossil record today bears eloquent testimony. I am convinced this catastrophe was primarily tectonic in nature, enabled by weakening instabilities in the deformation properties of silicate rock that led to an episode of global runaway subduction. It was a cataclysm that profoundly transformed the face of the planet. Evidence I mentioned in the preceding section suggests that a minor pulse of accelerated nuclear decay accompanied this year-long, fossil-record generating event some 5000 years ago. A preliminary estimate of the amount of nuclear decay in this pulse may be as little as 200,000 years, which also is in the range estimated by *Gentry et al.* [1976] from $^{238}\text{U}/^{206}\text{Pb}$ ratios measured in halo radiocenters in coalified wood from the Colorado Plateau. To be sure, this sketch of earth history stands in stark contrast to the standard evolutionary picture of the past two centuries.

13. Conclusions

We have surveyed the results of geochemical studies of the earth’s composition and history from the last several decades. We observe that the continental crust contains extremely high concentrations of the so-called incompatible elements, including most of the radioactive ones,

relative to both mantle rocks as well as to meteorites. The evidence from the distribution of trace elements seems compelling that indeed the continental crust itself was derived from the earth's mantle rock via partial melting processes in the presence of water. Based on magmas we can readily sample at the earth's surface, such processes can be inferred to be operating today, albeit at very low rates. Guesses based on solar abundances of elements and on meteorite compositions relative to the earth's own elemental bulk composition suggest that about half of the major radioactive heat producing inventory presently resides in the continental crust. This implies a major aspect of the earth's formation involved the cycling of a major fraction of the mantle through a partial melting process near the planet's surface to produce the continental crust with its high concentrations of incompatible elements. This cycling presumably was driven by the mechanism of thermal convection, and this implies a vast amount of heat was removed from the earth's interior as a consequence. If such processes unfolded in a brief period of time as the account in Genesis 1 indicates, then this also places constraints on the nuclear decay histories of the radioactive elements. To me it seems an inescapable conclusion that nuclear decay processes also had to accompany the chemical differentiation and be commensurately rapid.

A pillar of materialist faith is the immutability of physical law. If the material cosmos is all there is, with no transcendent God who can intervene in His created world as He might choose, then the immutability of physical law is certainly a plausible assumption. On the other hand, if the God of the Bible, the God who has revealed Himself so unmistakably in human history, really does exist, there is no reason to hold to the idea of immutability of physical law. Woven into the very fabric of radioisotope dating methods is the assumption of the immutability of nuclear decay rates. If rates have been much higher in the past than they are at present, it must follow that the dates given by these methods are commensurately more recent. The fact that the long-standing enigma concerning the meaning of outcrop to outcrop correlation between surface heat flow and the radioactivity of surface rocks can be readily explained in terms of a recent episode of accelerated nuclear decay in my opinion is profoundly significant to the question of

the immutability of physical law and the correctness of radioisotope dating techniques. I am optimistic there are other similar clues of God's intervention during His creation of the heavens and the earth as well as His intervention during the Flood, as mentioned in II Peter 3, that He has preserved for us, which can be identified if we but look to Him for help.

References

- Anders, E., and N. Grevesse, Abundances of the elements: meteoritic and solar, *Geochimica et Cosmochimica Acta*, 53, 197–214, 1989.
- Arshavskaya, N. I., N. E. Galdin, E. W. Karus, O. L. Kuznetsov, E. A. Lubimova, S. Y. Milanovsky, V. D. Nartikoev, S. A. Semashko, and E. V. Smirnova, Geothermic investigations, in *The Superdeep Well of the Kola Peninsula*, edited by Y. A. Kozlovsky, Springer-Verlag, New York, pp. 387–393, 1987.
- Ashwal, L. D., P. Morgan, S. A. Kelley, and J. A. Percival, Heat production in an Archean crustal profile and implications for heat flow and mobilizing heat-producing elements, *Earth and Planetary Science Letters*, 85, 439–450, 1987.
- Austin, S. A., J. R. Baumgardner, D. R. Humphreys, A. A. Snelling, L. Vardiman, and K. P. Wise, Catastrophic plate tectonics: a global Flood model of Earth history, in *Proceedings of the Third International Conference on Creationism*, edited by R. E. Walsh, Creation Science Fellowship, Pittsburgh, Pennsylvania, pp. 609–621, 1994.
- Balling, N., K. G. Eriksson, O. Landstom, G. Lind, and D. Malmquist, *Naturgas, Vattenfall*, 57, Swedish State Power Board, Alvkärlab, Sweden, 1990.
- Baumgardner, J. R., Computer modeling of the large-scale tectonics associated with the Genesis Flood, in *Proceedings of the Third International Conference on Creationism*, edited by R. E. Walsh, Creation Science Fellowship, Pittsburgh, Pennsylvania, pp. 49–62, 1994a.
- Baumgardner, J. R., Runaway subduction as the driving mechanism for the Genesis Flood, in *Proceedings of the Third International Conference on Creationism*, edited by R. E. Walsh, Creation Science Fellowship, Pittsburgh, Pennsylvania, pp. 63–75, 1994b.
- Carlson, R. W., Mechanisms of earth differentiation: consequences for the

- chemical structure of the mantle, *Reviews in Geophysics*, 32, 337–361, 1994.
- Carslaw, H. S., and J. C. Jaeger, *Conduction of Heat in Solids*, second edition, Oxford University Press, p. 60, 1959.
- Chauvel, C., A. W. Hofmann, and P. Vidal, HIMU-EM: the French Polynesian connection, *Earth and Planetary Science Letters*, 110, 99–119, 1992.
- Clauser, C., P. Giese, E. Huenges, T. Kohl, H. Lehmann, L. Rybach, J. Safanda, H. Wilhelm, K. Windloff, and G. Zoth, The thermal regime of the crystalline continental crust: implications from the KTB, *Journal of Geophysical Research*, 102, 18417–18441, 1997.
- Dziewonski, A. M., and D. L. Anderson, Preliminary reference earth model, *Physics of the Earth and Planetary Interiors*, 25, 297–356, 1981.
- Gentry, R. V., W. H. Christie, D. H. Smith, J. F. Emery, S. A. Reynolds, R. Walker, S. S. Cristy, and P. A. Gentry, Radiohalos in coalified wood: new evidence relating to the time of uranium introduction and coalification, *Science*, 194, 315–318, 1976.
- Grand, S. P., R. D. van der Hilst, and S. Widiyantoro, Global seismic tomography: a snapshot of convection in the earth, *GSA Today*, 7, 1–7, 1997.
- Haenel, R., Geothermal investigations in the Rhenish massif, in *Plateau Uplift*, edited by K. Fuchs *et al.*, Springer-Verlag, New York, pp. 228–246, 1989.
- Hart, S. R., Heterogeneous mantle domains: signatures, genesis, and mixing chronologies, *Earth and Planetary Science Letters*, 90, 273–296, 1988.
- Hart, S. R., and G. A. Zindler, In search of a bulk-earth composition, *Chemical Geology*, 57, 247–267, 1986.
- Hart, S. R., E. H. Hauri, L. A. Oschmann, and J. A. Whitehead, Mantle plumes and entrainment: isotopic evidence, *Science*, 256, 517–520, 1992.
- Hauri, E. H., and S. R. Hart, Re-Os isotope systematics of HIMU and EM II oceanic island basalts from the south Pacific ocean, *Earth and Planetary Science Letters*, 114, 353–371, 1993.
- Hofmann, A. W., Mantle geochemistry: the message from oceanic volcanism, *Nature*, 385, 219–229, 1997.
- Hofmann, A. W., and W. M. White, Mantle plumes from ancient oceanic crust, *Earth and Planetary Science Letters*, 57, 421–436, 1982.
- Hofmann, A. W., K. P. Jochum, M. Seufert, and W. M. White, Nb and Pb in ocean basalts: new constraints on mantle evolution, *Earth and Planetary Science Letters*, 79, 33–45, 1986.
- Irifune, T., and A. E. Ringwood, Phase transformations in subducted oceanic crust and buoyancy relationships at depths 600–800 km in the mantle, *Earth and Planetary Science Letters*, 117, 101–110, 1993.

- Jeffreys, H., and K. E. Bullen, *Seismological Tables*, British Association for the Advancement of Science, London, 1940.
- Kellogg, L. H., B. H. Hager, and R. D. van der Hilst, Compositional stratification in the deep mantle, *Science*, 283, 1881–1884, 1999.
- Kesson, S. E., and J. D. Fitz Gerald, Partitioning of MgO, FeO, NiO, MnO and Cr₂O₃ between magnesian silicate perovskite and magnesiowuestite: implication for the origin of inclusions in diamond and the composition of the lower mantle, *Earth and Planetary Science Letters*, 111, 229–240, 1991.
- Kremenetsky, A. A., S. Y. U. Milanovsky, and L. N. Ovchinnikov, A heat generation model for continental crust based on deep drilling in the Baltic Shield, *Tectonophysics*, 159, 231–246, 1989.
- Lachenbruch, A. H., Crustal temperature and heat production: implications of the linear heat-flow relation, *Journal of Geophysical Research*, 75, 3291–3300, 1970.
- McDonough, W. F., and S.-s. Sun, The composition of the earth, *Chemical Geology*, 120, 223–253, 1995.
- McDonough, W. F., S.-s. Sun, A. E. Ringwood, E. Jagoutz, and A. W. Hofmann, Potassium, rubidium and cesium in the Earth and Moon and the evolution of the mantle of the Earth, *Geochimica et Cosmochimica Acta*, 56, 1001–1012, 1992.
- Palme, H., and K. G. Nickel, Ca/Al ratio and composition of the earth's upper mantle, *Geochimica et Cosmochimica Acta*, 49, 2123–2132, 1985.
- Pribnow, D. F. C., and H. R. Winter, Radiogenic heat production in the upper third of continental crust from KTB, *Geophysical Research Letters*, 24, 349–352, 1997.
- Ringwood, A. E., The chemical composition and origin of the earth, in *Advances in Earth Sciences*, edited by P. M. Hurley, MIT Press, Cambridge, Mass., 287–356, 1966.
- Ringwood, A. E., *Composition and Petrology of the Earth's Mantle*, McGraw-Hill, New York, 1975.
- Roy, R. F., D. D. Blackwell, and F. Birch, Heat generation of plutonic rocks and continental heat flow provinces, *Earth and Planetary Science Letters*, 5, 1–12, 1968.
- Rudnick, R. L., and D. M. Fountain, Nature and composition of the continental crust: a lower crustal perspective, *Reviews in Geophysics*, 33, 267–309, 1995.
- Sass, J. H., A. H. Lachenbruch, T. H. Moses, Jr., and P. Morgan, Heat flow from a scientific research well at Cajon Pass, California, *Journal of Geophysical Research*, 97, 4995–5015, 1992.

- Shaw, D. M., J. J. Cramer, M. D. Higgins, and M. G. Truscott, Composition of the Canadian Precambrian shield and the continental crust of the earth, in *The Nature of the Lower Continental Crust*, edited by J. B. Dawson *et al.*, 257–282, Geological Society of London, 1986.
- Stacey, F. D., *Physics of the Earth*, third edition, Brookfield Press, Brisbane, 1992.
- Stein, C. A., and S. Stein, Constraints on hydrothermal heat flux through the oceanic lithosphere from global heat flow, *Journal of Geophysical Research*, 99, 3081–3095, 1994.
- Sun, S.-s., Chemical composition and origin of the earth's primitive mantle, *Geochimica et Cosmochimica Acta*, 46, 179–192, 1982.
- van der Hilst, R. D., and H. Karason, Compositional heterogeneity in the bottom 1000 kilometers of earth's mantle: toward a hybrid convection model, *Science*, 283, 1885–1891, 1999.
- Waelenke, H., G. Dreibus, and E. Jagoutz, Mantle chemistry and accretion history of the earth, in *Archaean Geochemistry*, edited by A. Kroener, G. Hanson, and A. Goodwin, Springer, Berlin, 1–24, 1984.
- Weaver, B. L., The origin of ocean island basalt end-member compositions: trace element and isotopic constraints, *Earth and Planetary Science Letters*, 104, 381–397, 1991.
- Weaver, B. L., and J. Tarney, Empirical approach to estimating the composition of the continental crust, *Nature*, 310, 575–577, 1984.
- Wedepohl, K. H., The composition of the continental crust, *Mineralogical Magazine*, 58, supplement, 959–960, 1994.
- Zindler, A., and S. Hart, Chemical geodynamics, *Annual Reviews of Earth and Planetary Sciences*, 14, 493–571, 1986.

Chapter 4

Mineral Isochron Method Applied as a Test of the Assumptions of Radioisotope Dating

Steven A. Austin, Ph.D.*

Abstract. Three general methods of radioisotope dating have been applied to rocks and minerals: (1) “model age” method, (2) “whole-rock isochron” method, and (3) “mineral isochron” method. Of these three methods, only the last two have attempted to justify the initial condition assumption by rigorous geological argument. Thus, whole-rock and mineral isochrons are the best-documented ages for rocks. However, four categories of isochron discordance can be recognized within the published literature on geochronology. The most extraordinary category of discordance (here called “category four discordance”) occurs where the individual mineral isochron ages greatly exceed the whole-rock isochron ages for what arguably, by geologic context, are a cogenetic suite of rocks. Continental metamorphic and igneous rocks have been demonstrated to contain mineral isochron ages exceeding the whole-rock ages of their associated cogenetic suites. Two noteworthy examples of such “category four discordance” from the geochronology literature are the Lewisian Metamorphic Complex of Scotland (Archean) and the Guidong Granodiorite of China (Silurian). Such discordances are not easily explained in the conventional framework of assumptions in geochronology. Mineral and whole-rock ages for chondritic meteorites are approximately concordant. Thus, Pb-Pb mineral isochron ages for individual chondritic meteorites usually exceed slightly the associated Pb-Pb, Rb-Sr, and Ar-Ar whole-rock isochron ages of chondritic meteorites. Mineral isochron analysis needs to be performed on selected terrestrial rocks to discover if systematic “age” discordances exist. Scientific or statistical explanations need to be offered by creationists for both concordant and discordant isochrons. This challenge awaits future creationist research that seeks to reinterpret “ages” assigned by radioisotopes to rocks.

* *Chairman, Geology Department, Institute for Creation Research, Santee, California*

1. Introduction

Popular radioisotope techniques for dating rocks can be divided into three general methods for the purpose of discussion and analysis. These are the “model age” method, the “whole-rock isochron” method, and the “mineral isochron” method. These three general approaches to radioisotope dating involve frameworks of assumptions that are generally similar in that they each involve using the relative proportions of parent radioisotope to stable daughter isotope. However, the three methods are distinct in specific assumptions regarding the initial conditions.

2. Model Age Method

The first category is the “model age” method. This method employs measurement of the parent to daughter isotope ratios in a single rock or mineral, then makes an assumption of the initial ratio of parent to daughter, and finally uses the constant-decay-rate assumption to estimate the time it would take to acquire the measured isotope ratio from the assumed initial value. Potassium-argon dating, the most widely employed radioisotope procedure for dating rocks, applies the “model age” methodology. For K-Ar ages, the initial condition assumption is simple, elegant, but vulnerable. The quantity of radiogenic Ar ($^{40}\text{Ar}^*$) is assumed to be zero as the rock or mineral being dated originally formed. Lava flows, for example, cool to form rocks at the earth’s surface where gases such as Ar should naturally escape from the crystallization process. Therefore, the ratio of $^{40}\text{Ar}^*$ to ^{40}K in a rock is thought to begin at zero and steadily increase with age. The equation for the K-Ar age of a rock or mineral is given by *Faure* [1986]:

$$t = \frac{1}{5.543 \times 10^{-10}} \ln \left(\frac{^{40}\text{Ar}^*}{0.105 \ ^{40}\text{K}} + 1 \right) \quad (1)$$

where t is the age in years, $^{40}\text{Ar}^*$ is the abundance of radiogenic Ar in the rock, ^{40}K is the abundance of radioactive K, 5.543×10^{-10} is the estimate of the ^{40}K decay rate, and 0.105 is the fraction of ^{40}K which decays to ^{40}Ar .

Model ages are simple and are widely employed because of their low cost. A commercially available K-Ar determination costs about US\$350. However, when the K-Ar model age is discordant with what the geologist believes is the correct stratigraphic and paleontologic context, the model age is usually questioned and then discarded. Often one or more of the assumptions is suspected to be in error. Thus, K-Ar model ages are the most abundant dates published, but are the most frequently questioned and discarded.

Uranium-lead model ages are also widely applied to rocks, especially high-U mineral phases within rocks. The technique was first applied to uraninite and monazite, two U-rich minerals. These two minerals, however, are not very abundant in crustal rocks. Therefore, zircon, another U-rich mineral with much wider distribution, has been selected for U-Pb analysis. The most popular is called U-Pb “zircon” dating. For the system where U decays to Pb, the two rate equations given by *Dickin* [1995, p. 104] apply:

$$\left(\frac{{}^{206}\text{Pb}}{{}^{204}\text{Pb}}\right)_p = \left(\frac{{}^{206}\text{Pb}}{{}^{204}\text{Pb}}\right)_i + \left(\frac{{}^{238}\text{U}}{{}^{204}\text{Pb}}\right)_p \left(e^{\lambda_{238}t} - 1\right) \quad (2)$$

and

$$\left(\frac{{}^{207}\text{Pb}}{{}^{204}\text{Pb}}\right)_p = \left(\frac{{}^{207}\text{Pb}}{{}^{204}\text{Pb}}\right)_i + \left(\frac{{}^{235}\text{U}}{{}^{204}\text{Pb}}\right)_p \left(e^{\lambda_{235}t} - 1\right) \quad (3)$$

where subscripts p and i indicate present and initial isotope ratios, e is the natural base of logarithms (2.71828...), λ_{238} and λ_{235} are the decay constants for ${}^{238}\text{U}$ -decay and ${}^{235}\text{U}$ -decay, and t is the age in years. Zircon is a mineral very rich in U but strongly depleted in Pb when it crystallizes. For the procedure of zircon dating the value of $({}^{206}\text{Pb}/{}^{204}\text{Pb})_i$ and $({}^{207}\text{Pb}/{}^{204}\text{Pb})_i$, the initial radiogenic leads in the zircon, can be assumed to be essentially zero. Therefore, equations (2) and (3) simplify to:

$${}^{206}\text{Pb}^* = {}^{238}\text{U}_p \left(e^{\lambda_{238}t} - 1\right) \quad (4)$$

and

$${}^{207}\text{Pb}^* = {}^{235}\text{U}_p \left(e^{\lambda_{235}t} - 1\right) \quad (5)$$

where ${}^{206}\text{Pb}^*$ and ${}^{207}\text{Pb}^*$ are the abundances of radiogenic leads (that is,

the present measured abundances of ^{206}Pb and ^{207}Pb , because it is assumed that no initial ^{206}Pb and ^{207}Pb existed when the zircon crystallized).

A mineral that has remained closed to loss or gain of U and Pb should give concordant values of t when measured isotopic abundances are inserted into both equations (4) and (5). If concordant model ages from a zircon crystal are obtained by equations (4) and (5), the resultant “age” is usually considered trustworthy. Such ages are given a “concordia” interpretation [Wetherill, 1956]. Even discordance between the values of t using equations (4) and (5) can be interpreted by a “discordia” model [Dickin, 1995, pp. 107–111].

Ion microprobe analysis (an instrument nicknamed “SHRIMP”) allows inexpensive determinations of the U-Pb model ages of individual zircon crystals. The oldest radioisotopic age for a crustal rock was recently obtained using zircon in gneiss from western Slave Province, Canada, a date of 4.031 ± 0.003 Ga being obtained [Bowring and Williams, 1999].

Another significant model age method is the Pb-Pb method. Because the two U isotopes (^{238}U and ^{235}U) decay to two stable Pb isotopes (^{206}Pb and ^{207}Pb) at different rates, the proportion of the two radiogenic leads change with time. If the original ratio of the radiogenic leads is known or assumed, and the rock is assumed to have remained closed to U and Pb redistribution, the present ratio of the leads indicates the rock’s age. This produces a daughter-daughter model age, which is different from the more familiar parent-daughter model ages. The proportions of radiogenic Pb isotopes ^{206}Pb and ^{207}Pb are measured very accurately relative to non-radiogenic Pb (^{204}Pb) using a mass spectrograph. The present Pb isotope ratios are plugged into an equation with the assumed initial Pb isotope ratios and the two U-decay constants to calculate the Pb-Pb model age. The solution equation for the Pb-Pb model age is derived by combining equations (2) and (3) as described by Faure [1986, p. 288]:

$$\frac{\left(\frac{^{207}\text{Pb}}{^{204}\text{Pb}}\right)_p - \left(\frac{^{207}\text{Pb}}{^{204}\text{Pb}}\right)_i}{\left(\frac{^{206}\text{Pb}}{^{204}\text{Pb}}\right)_p - \left(\frac{^{206}\text{Pb}}{^{204}\text{Pb}}\right)_i} = \frac{1}{137.88} \left[\frac{e^{\lambda_{235}t} - 1}{e^{\lambda_{238}t} - 1} \right] \quad (6)$$

where subscript p and i indicate present and initial Pb isotope ratios, e is the natural base of logarithms (2.71828 . . .), λ_{235} and λ_{238} are the decay constants for ^{238}U -decay and ^{235}U -decay, and t is the age in years.

3. Whole-Rock Isochron Method

The “whole-rock isochron” method is the second general category of radioisotope dates. The whole-rock isochron dating method supposes what is called a “cogenetic suite of rocks.” If we select a number of rock samples from a single geologic unit, the various rocks should have all formed about the same time. Furthermore, geologic processes that operated to form the suite of rocks may have caused the various rocks to differ in the amounts of the radiogenic parent and daughter isotopes. However, the suite of rocks should be sufficiently mixed that there is uniformity among the different rocks with respect to the isotopic composition of the daughter. Over time the isotopic composition of the suite of rocks may have been altered by radioisotope decay. Essential to the whole-rock isochron method are the two ideas: (1) a cogenetic suite, and (2) uniformity within the suite of the daughter isotope ratio originally. These two assumptions replace the initial daughter isotope ratio that must be inserted into “model age” equations.

Figure 1 shows an application of the isochron method to a hypothetical radioisotope plot of measurements from six rocks from a cogenetic suite. A linear array with significant positive slope appears to be described by the isotopic measurements of six rocks in Figure 1c. One of the six isotopic analyses appears to lie off the line described by the other five, and it would usually be supposed to have been altered by a geologic process. The odd isotopic analysis is usually disregarded. Therefore, the interpretation offered in Figure 1a assumes a linear array with five rocks representative of the cogenetic suite. Rocks of the hypothetical cogenetic suite are given an “age” interpretation in Figure 1b, with the rocks when formed all having the same abundance of daughter (zero slope). After the passage of time the radioisotope decay of the parent has increased the quantity of daughter in a uniform manner according to the abundance of the parent. All points of equal age lie on the same line.

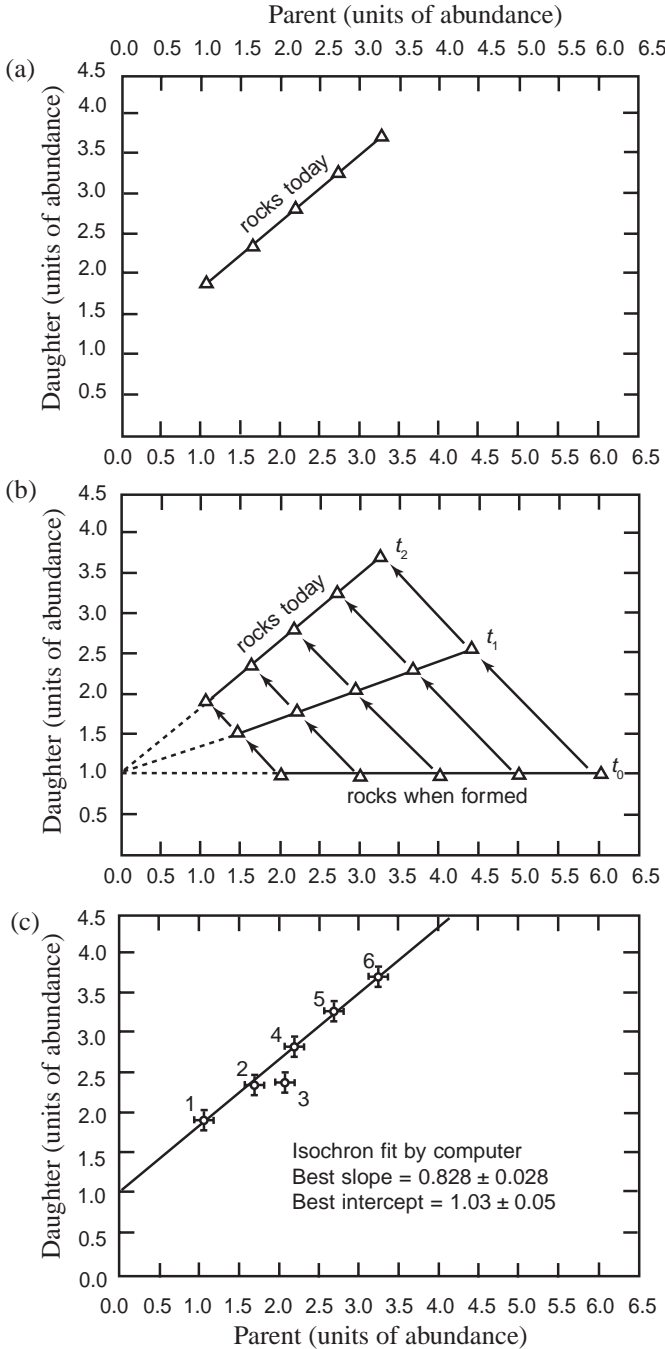


Figure 1 (opposite). The assumptions and methods of isochron dating are illustrated by diagrams depicting rocks of a hypothetical formation. (a) Study of five rocks of the formation indicates that their daughter-versus-parent compositions plot today as a linear array having positive slope. (b) The isochron model suggests that the five rocks, when they formed, all had the same abundance of daughter (1.0 “unit of abundance” in this case), but different abundances of parent. The compositions of the rocks today are assumed to have been derived by significant radioactive decay of parent and accumulation of daughter. (c) Six isotopic analyses of the rocks of the formation are plotted with error bars. A computer determines the “best-fit” line through the data points. The slope of the line can be used to estimate the “age” of these rocks. The greater the slope, the greater the “age”.

Thus, in Figure 1b, five of the six rocks appear to lie along a horizontal line at t_0 when the “cogenetic suite” formed. At some later time, t_1 , the five rocks describe a sloping line after significant radioisotope decay had occurred. Finally, Figure 1b shows the five rocks at later time t_2 , along another steeper line after even more decay has occurred. It is evident that the slope, or steepness of these lines, increases as the “age” of the samples increases. Each of these lines of “equal age” is called an “isochron” (from Greek, *isos*, equal; and *chronos*, time). *York* [1969] elaborated the statistical principles for plotting an “isochron” through isotopic data. *Ludwig* [1999] gave computer programs, now standard within the geochronology community, which plot isochrons and perform error analysis.

The whole-rock isochron dating method has been widely applied to indicate great ages of rocks. The frequently cited “age of the solar system” (4.55 ± 0.07 Ga) comes from a whole-rock ^{207}Pb - ^{206}Pb isochron for five meteorites [*Patterson*, 1956; *Allégre et al.*, 1995]. Figure 2 shows the now classic whole-rock isochron derived by *Patterson* [1956]. The “age” was derived from the $^{207}\text{Pb}/^{204}\text{Pb}$ versus $^{206}\text{Pb}/^{204}\text{Pb}$ plot of two iron meteorites (troilites) with three stony meteorites (two chondrites and a eucrite). The slope of the Pb-Pb line is converted to an “age” by a derivation from equation (6) as described by *Faure* [1986, p. 312]:

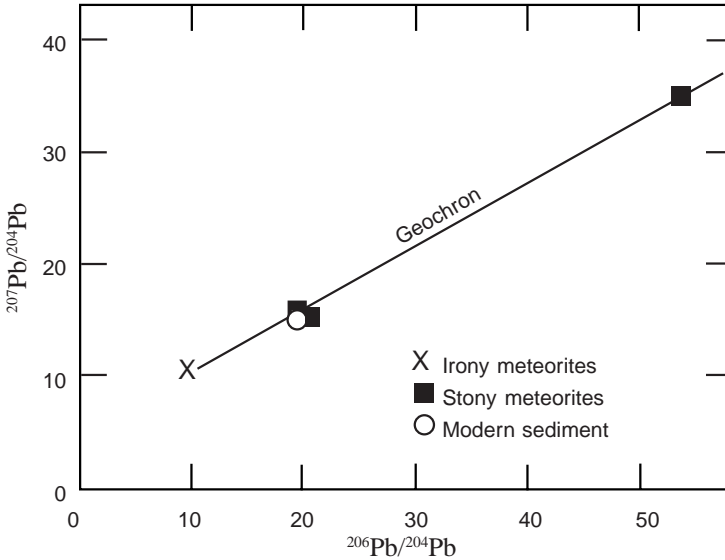


Figure 2. Lead-lead isochron plot of five meteorites used by *Patterson* [1956] to estimate the “age of the earth”. The Pb-Pb whole-rock isochron age of 4.49 ± 0.07 Ga (*Patterson*’s value, using new constants) has been recalculated using fifteen chondrites by *Huey and Kohman* [1973] as 4.505 ± 0.008 Ga.

$$m = \frac{1}{137.88} \left[\frac{e^{\lambda_{235}t} - 1}{e^{\lambda_{238}t} - 1} \right] \quad (7)$$

where m is the slope in units of rise divided by run. This equation, as with equation (6), cannot be solved directly for the “age” (t) by algebraic methods. This transcendental equation is best solved using a computer by the method of successive approximations.

Patterson [1956] employed the older decay constants for his solution to the “age of the solar system” using equation (7). When the newer decay constants for λ_{235} and λ_{238} are used in the recalculation, the “age of the solar system” is reduced to 4.49 ± 0.07 Ga [*Huey and Kohman*, 1973]. Making an argument from association, *Patterson* [1956] then transformed the meteorite whole-rock age into an “age-of-the-earth” estimate. His argument was that the earth contains average Pb isotopic

composition (indicated by Pb isotopes in Pacific Ocean sediment) that lies on the meteorite isochron. This age-of-the-earth calculation assumes that both the earth and the meteorites began billions of years ago with a common Pb isotope ratio. Thus the “age of the earth” is based on four assumptions: (1) a cosmological assumption of homogeneous Pb isotope ratios in the beginning, (2) the primitive value of Pb isotopes occurred in both the primitive earth and the primitive meteorites, (3) constant radioactive decay of U to Pb, and (4) a closed isotopic system within the rocks being dated.

For the case of the iron and chondritic meteorites dated by *Patterson* [1956], it is supposed that they all formed about the same time as the rest of the solar system from a mixture of pre-solar material that was isotopically homogeneous with respect to Pb. That Pb isotope ratio is essentially identical to that of the Canyon Diablo troilite, an iron meteorite with virtually an undetectable amount of U. Therefore, Canyon Diablo troilite is believed to be essentially identical to the primitive Pb isotope ratio.

The assumption involved in the age-of-the-earth calculation is elegant in its simplicity, but it has not gone unchallenged. Although selected meteorites describe a linear plot, many meteorites do not [*Gale et al.*, 1972]. Two questions are worth asking. First, was there isotopically homogeneous Pb in the beginning? Second, was the earth derived from the same Pb ratio? That first assumption of uniform Pb isotopes has been challenged by more meteorite data [*Tatsumoto et al.*, 1973; *Abranches et al.*, 1980] showing that many meteorites do not, statistically speaking, lie on the sloping line as supposed by *Patterson* [1956]. The data argue that leads were not, strictly speaking, homogeneous, but may have been approximately homogeneous.

The second assumption, that the Pb isotopes from earth and meteorites are from the same cogenetic suite, is not completely convincing. The strongest case comes from the elemental compositions of the earth and meteorites. Similarity in the elemental composition, especially the similarity of lithophile elements, of earth and meteorites support the idea of a cogenetic suite (see Chapter 3 by Baumgardner). But, the Pb isotopic compositions of ocean sediments have been measured with much

greater accuracy after Patterson's work. Ocean sediments consistently lie to the right of the meteorite whole-rock isochron [*Zindler and Hart, 1986, p. 507*]. Therefore, Patterson's original argument for the cogenetic suite based on ocean sediment is weak. The so-called "Pb paradox" arises from the recent studies of the interactive portions of the earth's mantle and the observation that no obvious terrestrial reservoir is known for Pb in the earth at the correct (meteorite linear array) isotopic composition [*Zindler and Hart, 1986, pp. 542–548*]. The earth's mantle has a Pb isotope signature lying to the right of the meteorite linear array. Where is the earth's undiscovered reservoir of Pb lying to the left of the linear array so the combined sum of terrestrial leads can lie on the linear array? Some scientists have suggested that the undiscovered reservoir of unique Pb resides in the earth's core. However, we have no direct measurements of the isotopes of Pb from the earth's core.

4. Mineral Isochron Method

Because the results of the "whole-rock isochron method" are tied to the debatable notion of a "cogenetic suite," a better isochron method of dating rocks needs to be devised. The mineral isochron method involves assumptions that are often less speculative. The minerals within a single rock could be argued by the geologic character of a rock to have been in an isotopically homogeneous condition when the rock formed. Three examples are provided here. First, a lava flow causes a mixing condition that should have produced homogeneous isotopes within a single rock as it cooled from the lava flow. The crystallization process that formed minerals as a lava flow cooled is recognized to have little ability to concentrate selectively daughter isotopes within certain minerals. Second, a diabase sill or dike that formed from magma injected rapidly into sedimentary strata should be well mixed isotopically. A rock extracted from such a sill or dike should have also been isotopically homogeneous in the beginning. Third, a metamorphic event which heated a rock to above 400°C would have caused recrystallization to occur throughout the rock, and that event would be expected to have caused local homogenization of isotopes within mineral phases as

recrystallization occurred.

Therefore, the concept of a “mineral isochron” within a rock may be geologically defensible and not as debatable as the notion of a “cogenetic suite” of rocks. This is why the mineral isochron method is superior to the whole-rock isochron method.

Because different mineral phases of a rock each have different chemical affinities for parent and daughter elements, each mineral phase should have its own characteristic parent-daughter isotopic ratio at the time of crystallization. However, each of the mineral phases is likely to have been isotopically homogeneous with respect to the daughter isotope in the beginning because of the geologic condition of mixing. Crystallization cannot selectively isolate just the radiogenic isotope within the various isotopes of the daughter element. This is a geologically more-believable initial condition established for isochron dating. Over time, the minerals within the rock will deviate from their assumed initial homogeneous values of the daughter isotope as significant radioisotope decay of the parent occurs. Over time the mineral phase within a single rock that has the largest quantity of parent will acquire the largest quantity of daughter. According to this theory, the degree of deviation within different mineral phases from the assumed initial value will be proportional to “age” of the rock. Furthermore, “mineral isochron ages” for different parent-daughter radioisotope pairs should give concordant “ages” if the two other assumptions of radioisotope dating apply (constancy of decay rates, and closed-system requirement).

Although the notion of a mineral isochron is elegant in the simplicity of its assumptions, the method is infrequently applied to rocks. The mineral isochron method requires extraction and separation of significant quantities of different mineral phases of a single rock. This is often a very tedious and time-consuming process involving significant skill in the laboratory. Heavy liquids and magnetism are the preferred techniques for separating minerals. Once different mineral phases of a single rock are isolated, they need to be analyzed isotopically on a mass spectrograph. These multiple isotope analyses that are required are difficult to perform and are costly.

Mineral isochron techniques find significant applications in testing

two assertions made by the millions-of-years chronology of conventional geology. The technique allows a test of (1) “model ages” and “whole-rock isochron ages” published in the geologic literature, and a test of (2) concordance of different radioisotope pairs that, it might be supposed, all concordantly date the rock to one age.

Ultimately, the mineral isochron method can be used as a partial test of the assumption of constant decay rate of radioisotopes in rocks. If the homogenization and closed system are assumed, then discordant mineral isochrons could argue for different decay rates between the various parent isotopes. Could α -emitting radioisotopes (U, Th, and Sm) have been accelerated to faster decay rates in the past than β -emitting radioisotopes (Rb and K)? This hypothesis could be testable by the mineral isochron method. If this hypothesis is correct, there should be systematic discordance within mineral isochrons.

5. Categories of Discordance

Isochron methods have been applied to dating of earth rocks. However, *mineral* isochron analyses published in the literature usually involve only one radioisotope parent and daughter. These published analyses rarely contain the “complete” condition of various radioisotopes within the mineral phases of a single rock. Does the peer-review process within the evolutionary literature prevent discordant mineral isochrons from being published? Much more common are the abundant whole-rock model ages and the occasional whole-rock isochron ages published in the geologic literature.

A variety of published data allow four categories of discordance to be defined. These four categories are defined here for the first time so that discussion of the nature of the discordance can be simplified. After these four categories of discordance are defined, examples are given.

Category One Discordance—A cogenetic suite of rocks with two or more discordant whole-rock isochron ages.

Category Two Discordance—A cogenetic suite of rocks that generates a whole-rock isochron age *older than* the associated mineral isochron ages from specific rocks.

Category Three Discordance—Two or more discordant mineral isochron ages from an individual rock.

Category Four Discordance—A cogenetic suite of rocks that generates a whole-rock isochron age *younger than* the associated mineral isochron ages from specific rocks.

5.1 Category One Discordance

Numerous authors [*Beckinsale et al.*, 1980; *Chauvel et al.*, 1985; *Crocker et al.*, 1993; *Shaw et al.*, 1997; *Pandey et al.*, 1997; *Mukasa et al.*, 1998; *Weber and Köhler*, 1999] document discordant whole-rock isochrons for Precambrian rocks of the continents. Discordance usually involves the Sm-Nd and Rb-Sr techniques, with the former giving older ages than the latter. However, discordance can also involve the Pb-Pb and K-Ar systems.

The deeply buried Cardenas Basalt of the Precambrian of Grand Canyon was dated at 1.103 ± 0.066 billion years by *Larson et al.* [1994] using the Rb-Sr whole-rock isochron method. However, Cardenas Basalt gives discordant Sm-Nd, Rb-Sr and K-Ar whole-rock isochron ages [*Austin and Snelling* 1998; *Austin*, unpublished data]. The seven new rocks [*Austin*, unpublished data] give the Rb-Sr whole-rock isochron age of 1.09 ± 0.03 billion years, being indistinguishable from the Rb-Sr ages obtained by *McKee and Noble* [1976] and *Larson et al.* [1994]. However, the same seven whole rocks [*Austin*, unpublished data] also give a Sm-Nd isochron age of 1.70 ± 0.16 billion years. Furthermore, the K-Ar whole-rock isochron appears to describe an age of 0.516 ± 0.030 billion years [*Austin and Snelling*, 1998]. The discordance between the three radioisotope systems for Cardenas Basalt indicates a fundamental problem with the assumptions of the whole-rock isochron method [*Austin*, 1994]. For example, how could the Sr isotopes in the cogenetic suite be homogenized 1.1 billion years ago without, at the same time, remixing the Nd isotopes? There appears to be no easy answer to the cause of this noteworthy discordance. Alternatives to the conventional dating assumptions need to be explored.

Specialists have offered a variety of explanations for the causes of

whole-rock discordances. Geologists have become very skillful in explaining discordant whole-rock isochrons. In addition to the popular time-dependent nuclear decay interpretation of linear-array plots, geologists have offered at least six alternative explanations for linear-array plots of daughter versus radioisotope parent. These six alternatives are:

- Inheritance of isotopic ratios directly from “aged” source rocks [*Brooks et al.*, 1976].
- Mixing or contamination of different quantities of two components within a two-component system [*Faure*, 1986].
- Partial melting of radiogenic minerals within source rocks [*G. B. Dalrymple*, unpublished and privately circulated manuscript, 1992].
- Selective diffusion of parent and/or daughter to/from the rock [*Austin and Snelling*, 1998].
- Correlation of errors developed by the isotopic measurement technique forming an “errorchron” [*Dickin*, 1995].
- Accelerated nuclear decay (see Chapter 7 by Humphreys).

5.2 Category Two Discordance

A cogenetic suite of rocks that generates a whole-rock isochron age *older than* the associated mineral isochron ages from specific rocks illustrates “category two discordance.” The modest amount of geologic literature on whole-rock and mineral isochrons shows that discordance between isochrons is not uncommon. When mineral isochron ages are significantly *younger* than the associated whole-rock isochron age, the discordance is often explained by local remobilization of the isotopes at the small scale, but without remobilization and homogenization on the large scale [*Li*, 1994; *Whitehouse et al.*, 1996]. The small scale of the individual rock is the domain of the mineral isochron. Within the rock, isotopes can be more easily mobilized by metamorphism than on the large scale. The large scale is the domain of the “cogenetic suite” and the whole-rock isochron. It takes a big event to homogenize isotopes over a wide area. Thus, “category two discordance” is rather easily accommodated within the conventional isochron methodology.

5.3 Category Three Discordance

Two or more discordant mineral isochron ages from an individual rock illustrate what is called “category three discordance.” *Zhao and McCulloch* [1993], *Unnikrishnan-Warrier* [1997], *Kruger et al.* [1998], and *Li et al.* [2000] give different examples of Sm-Nd mineral isochron ages exceeding Rb-Sr mineral isochron ages within the same rocks. The authors in these four different studies suggest that Sr isotopes were remobilized within the solid rocks by a heating event long after the original crystallization of these rocks. Garnet, a mineral phase controlling the Sm-Nd mineral isochron, is supposed to have a higher closure temperature than biotite, a mineral phase controlling the Rb-Sr mineral isochron. Supposedly, a lower temperature metamorphic event could homogenize the Sr but leave the Nd unmixed within the mineral phases of a rock. Thus, retrograde metamorphism has been offered as a likely explanation for observed examples where Sm-Nd mineral isochron ages significantly exceed Rb-Sr mineral isochron ages.

5.4 Category Four Discordance within Continental Magmatic Rocks

How are mineral isochrons older than their associated whole-rock isochrons interpreted within crustal rocks? Two examples illustrate “category four discordance” and possible interpretations. The Lewisian Metamorphic Complex of northwest Scotland was shown to contain two well-defined Sm-Nd whole-rock isochron ages, 2.943 ± 0.091 Ga and 2.846 ± 0.073 Ga [*Whitehouse et al.*, 1996]. These ages are shown graphically in Figure 3. These Sm-Nd whole-rock isochron ages are consistent with regional geology and so were accepted as the ages of the regional magma emplacement. However, all this changed when *Burton et al.* [1994] published what appear to be concordant Pb-Pb and Sm-Nd mineral isochrons from Lewisian amphibolites dating as 3.314 ± 0.064 Ga and 3.298 ± 0.073 Ga (Figure 4). Immediately, a great controversy began. Does the Lewisian Complex date to *ca.* 3.3 Ga and, therefore, represent “the oldest rocks of Europe” [*Galer*, 1994]? Is a radical reinterpretation of the Archean geology of Scotland required?

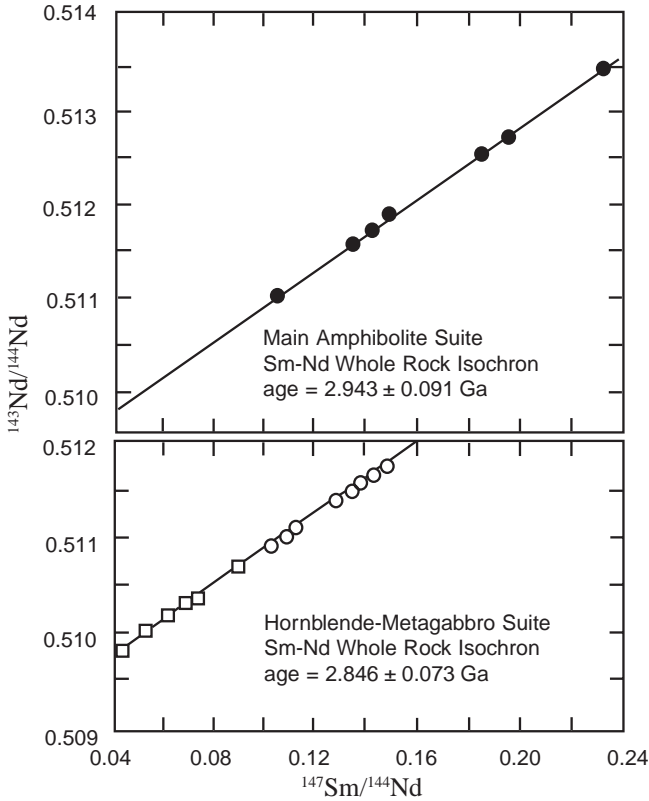


Figure 3. Samarium-neodymium whole-rock isochron ages for the Lewisian Metamorphic Complex of northwest Scotland [after *Whitehouse et al.*, 1996]. Open squares in lower diagram represent the Gruinard Bay trondhjemites. Only the Hornblende-Metagabbro Suite (represented by open circles in lower diagram) was used to calculate the regression line and age. The ages for the “Main Amphibolite Suite” and the “Hornblende-Metagabbro Suite” are concordant and seem to date the protolith from which the suite of rocks was derived at 2.9 Ga. However, Pb-Pb and Sm-Nd mineral isochron ages seem to date the “Main Amphibolite Suite” concordantly at 3.3 Ga (see Figure 4.)

Or is the regional geology well enough developed to exclude the older age? *Whitehouse et al.* [1996, p. 3086] say the discordance “can be explained only if the mineral isochrons or the whole-rock isochrons or

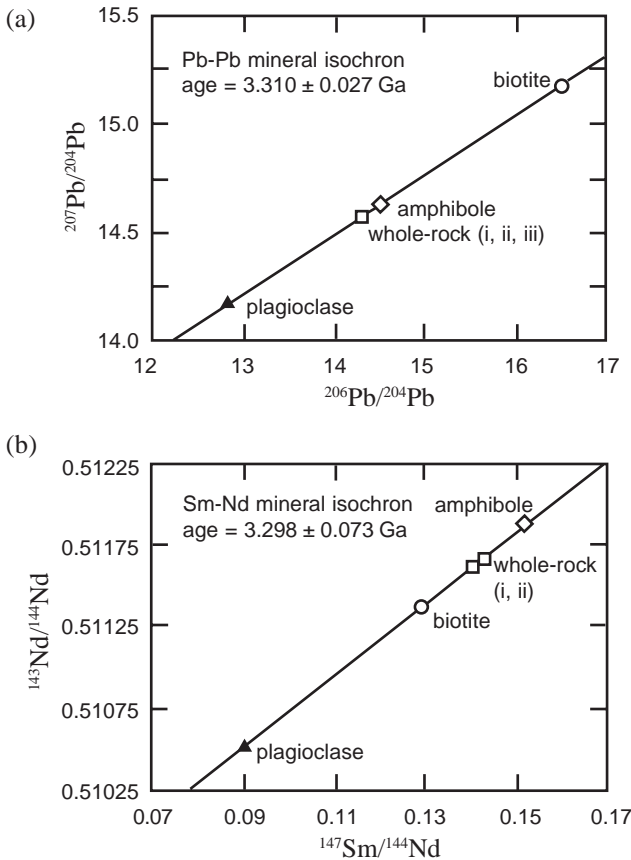


Figure 4. (a) Lead-lead and (b) samarium-neodymium mineral isochron ages for coexisting mineral phases in one amphibolite rock from the Lewisian Metamorphic Complex in northwest Scotland (sample GR 102 from Guinard Bay) [after *Burton et al.*, 1994]. The coexisting mineral phases within the rock seem to date concordantly the protolith from which the amphibolite was derived at 3.3 Ga. However, the Sm-Nd whole-rock isochron for the amphibolite suite is strongly discordant at 2.9 Ga (see Figure 3).

both are spurious.” They dispute the two mineral isochrons of *Burton et al.* [1994] as “spurious”, and they argue that their Sm-Nd whole-rock isochron is correct. In their dismissal of the Pb-Pb and Sm-Nd mineral

isochrons, however, *Whitehouse et al.* [1996] remain reticent to explain *scientifically* the linearity within the data of *Burton et al.* [1994].

A second example of mineral isochrons older than the associated whole-rock isochron comes from the Guidong Granodiorite of southeast China. *Li* [1994] describes the previously published whole-rock Rb-Sr isochron of 358 Ma. He then describes a U-Pb single-zircon date of 427 ± 3 Ma, a Rb-Sr mineral isochron age of 422 ± 14 Ma, and an impressive Sm-Nd mineral isochron age of 428 ± 12 Ma. According to *Li* [1994, p. 288], the whole-rock Rb-Sr isochron is exceedingly young, “probably caused by the combination of a number of factors, such as analytical problems, alteration of some analyzed samples and the heterogeneity of the source.”

One would expect the literature on geochronology to have ready explanations for “category four discordance.” Instead, we find researchers strangely reticent to explain obvious linearity within isotopic data. These researchers use words such as “spurious” and “probably caused by the combination of a number of factors,” without a ready explanation of the data they are discarding. “Category four discordance” between mineral and whole-rock isochrons needs a *scientific* or *statistical* explanation.

5.5 Possible Concordant Ages within Chondrites

Chondrites are common stony meteorites dominated by round granules imbedded within a finer matrix. They are thought to be among the most primitive and oldest of the meteorites. Magmatic and metamorphic processes, agents that have significantly altered terrestrial rocks, have not significantly transformed chondrites after their early formation. Thus chondrites are attractive for radioisotope study. Several Ca-Al-rich inclusions (CAIs) from Allende chondrite form a linear array on the ^{207}Pb - ^{206}Pb plot. The CAIs from Allende yield a ^{207}Pb - ^{206}Pb model age (relative to Canyon Diablo troilite) of 4.559 ± 0.004 Ga, and, according to *Tilton* [1989, p. 259], “yield the oldest high-precision meteorite date, thus providing the best estimate of the first condensation of matter in the solar system.” If eight CAIs of Allende are considered as an internal mineral isochron without reference to Canyon Diablo troilite, the

inclusions yield a ^{207}Pb - ^{206}Pb isochron age of 4.556 Ga [Tera and Carlson, 1999]. The matrix and chondrules of Allende indicate a slightly younger age, but Tilton [1989] believes “. . . no physical significance can be attached to the age difference . . .” According to Tilton [1989], we should not suppose a protracted interval for individual chondrite formation, say 50 million years or more. Thus, the internal Pb isotopic data indicate Allende formed rapidly about 4.56 Ga, the CAIs being “the oldest meteorite ages presently known” [Tilton, 1989]. Another chondrite named St. Severin contains the phosphate mineral whitlockite which gives the high-precision ^{207}Pb - ^{206}Pb age of 4.552 ± 0.003 Ga [Tilton, 1989]. Therefore, chondrites are regarded as a group to have Pb-Pb mineral isochrons and Pb-Pb model ages indicating formation within the narrow range of 4.53 to 4.56 Ga [Tilton, 1989]. This is now widely regarded as the “age of the solar system.”

The Pb-Pb mineral isochron ages reported above are apparently concordant with the original Pb-Pb whole-rock isochron age for meteorites, assuming the statistical errors assigned to the methods. The original 4.49 ± 0.07 Ga whole-rock “age of the solar system” was proposed for whole-rock meteorites by Patterson [1956] (age recalculated using new decay constants for U). Newer Pb isotopic data from chondrites are not exactly concordant. Huey and Kohman [1973] analyzed 15 chondrites to form a more-precise whole-rock Pb-Pb isochron yielding an age of 4.505 ± 0.008 Ga. Their data appear in Figure 5. Why is the more precise “age of the solar system” derived from Pb in whole rocks by Huey and Kohman [1973] (4.505 ± 0.008 Ga) slightly less than the mineral isochron ages for the chondrite Allende (4.556 ± 0.004 Ga)? Should any significance be attached to this discordance?

An interesting concordance exists within chondrites between the whole-rock Pb-Pb, Sm-Nd, Rb-Sr isochron and Ar-Ar systems. The Rb-Sr whole-rock isochron age is 4.498 ± 0.015 Ga for a very large suite of chondrites [Minster et al., 1982]. This Rb-Sr age is indistinguishable from the whole-rock Pb-Pb isochron of 4.505 ± 0.008 Ga [Huey and Kohman, 1973]. This Rb-Sr isochron appears in Figure 6. Because there is not a significant variation in Sm-Nd within chondrites, only an imprecise Sm-Nd whole-rock age of 4.21 ± 0.76 Ga was obtained

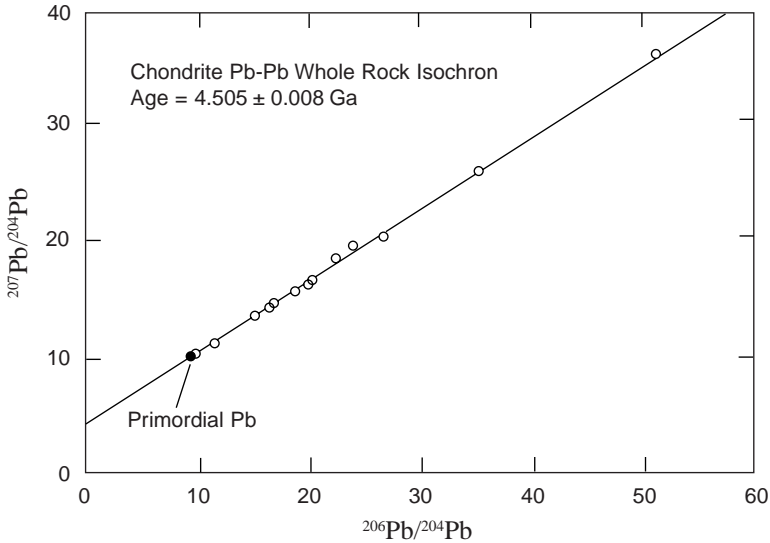


Figure 5. Lead-lead linear array plot for fifteen chondritic meteorites analyzed as whole rocks [after *Huey and Kohman, 1973*]. The Pb-Pb isochron age of 4.505 ± 0.008 Ga is concordant with the Rb-Sr whole-rock isochron for chondritic meteorites shown in Figure 6.

[*Jacobsen and Wasserburg, 1984*]. *Göpel et al.* [1994, p. 167] summarize the Ar-Ar model ages for chondrites. For twelve chondrites, eleven have Ar-Ar ages overlapping at 4.48 ± 0.04 Ga.

The Pb-Pb mineral isochron and Pb-Pb mineral model ages for chondrites appear to be slightly older than the associated whole-rock Pb-Pb, Rb-Sr and Ar-Ar ages. Similarities in ages may be caused by meteorites not having been strongly altered by magmatic process as have earth rocks. Most scientists would attribute the slight discordance to unaccounted-for errors in the analytical methods or uncertainties in the value of the decay constants. For example, faced with the older Pb-Pb mineral isochron ages with higher precision ^{235}U and ^{238}U decay constants, *Minster et al.* [1982] suggested that the younger Rb-Sr whole-rock isochron age of chondrites stems from an incorrect estimate of the decay constant of ^{87}Rb . Can a conclusion be offered for the near

concordance between α -emitters (U and Sm) and β -emitters (Rb and K) within chondrites? The data seem to be consistent with the notion, if radioisotope decay was accelerated at sometime in the past, that α -emitters (U and Sm) and β -emitters (Rb and K) within chondrites were both uniformly accelerated.

6. Continuing Research

The implications of concordant and discordant isochrons need to be explored. Especially important is the explanation of discordant isochrons as to their impact on the assumptions of radioisotope dating. Most appropriate is research on mineral isochron dating of rocks that, because of their geologic context, had a high probability of being isotopically homogeneous when they crystallized (for example, ancient lava flows,

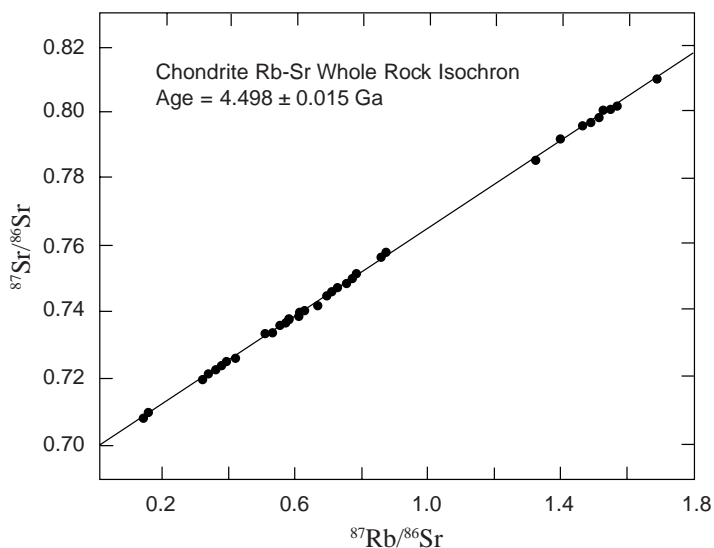


Figure 6. Rubidium-strontium linear array plot for twenty-three chondritic meteorites analyzed as whole rocks [after *Minster et al.*, 1982]. The graph includes multiple analyses on a single meteorite. The Rb-Sr isochron age of 4.498 ± 0.015 Ga is concordant with the Pb-Pb whole-rock isochron for chondritic meteorites shown in Figure 5.

ancient diabase sills, and ancient metamorphic crystallization events). Four mineral isochron applications for continuing research are suggested:

- **The Beartooth Andesitic Amphibolite, Wyoming**—This rock of the Beartooth Mountains of northwestern Wyoming is widely claimed to be one of the oldest rocks of the United States. An impressive Rb-Sr whole-rock isochron age of 2.790 ± 0.035 Ga [Wooden *et al.*, 1982] is believed to date the metamorphic event that recrystallized this rock. The precursor rock is suggested to be over 3.2 billion years old. The minerals quartz, plagioclase, biotite, hornblende, titanite and magnetite have been separated from a sample of the rock. A mineral isochron analysis should be performed to test for concordance of the different radioisotopic clocks. Will the various mineral isochron ages agree with the Rb-Sr whole-rock isochron?

- **Diabase Sill from the Precambrian of Grand Canyon**—The diabase of western Grand Canyon is an excellent target for mineral isochron analysis. Olivine, diopside and plagioclase are abundant minerals within the diabase. Whole-rock isochron ages need to be constructed from ten samples collected from the sill at Bass Rapids. Will Pb-Pb, Sm-Nd and Rb-Sr mineral and whole-rock isochrons be concordant? Study of the diabase is enhanced because the geochemistry is well understood and problems are evident in the K-Ar dating method.

- **Chert and Dolomite of the Redwall Limestone, Grand Canyon**—Interbedded chert and dolomite of the Thunder Springs Member of the Redwall Limestone have been demonstrated to have a significant variation in their Rb-Sr ratios. Hydrothermal sedimentary process appears to have homogenized Sr isotopes very early in the history of these rocks. The hydrothermal process transformed the original lime sediment either to dolomite or chert according to the texture of the original lime sediment. Today, because of the differences in abundances of Rb between chert and dolomite, a significant variation in Sr isotopes should be expected to exist between the chert and dolomite. Thus, a Rb-Sr isochron should be easily constructed. Whole-rock Rb-Sr, Sm-Nd and Pb-Pb isochrons should be attempted. Mineral concentrates from chert and dolomite could be made by acid treatment of the rock. Would any of these dates agree with the formation's conventional Mississippian assignment?

• **Lava Dams in Western Grand Canyon**—*G. Brent Dalrymple and W. K. Hamblin* [1998] have concluded recently that most of more than 60 published K-Ar model ages on Pleistocene basalts in western Grand Canyon are in error. What is the cause of this widespread error when the conventional K-Ar model age is produced? Could it be a mineral phase of these basaltic flows is retaining excess ^{40}Ar making them appear excessively old? Recently, *Rugg and Austin* [1998] concentrated olivine from a Pleistocene lava dam in western Grand Canyon and found it to yield an K-Ar “age” of 20.7 ± 1.3 million years. Could olivine be the mineral phase that is giving unacceptably old K-Ar model ages? This hypothesis needs to be tested by Ar isotopic analysis of individual mineral phases of Grand Canyon lava dams. The simple measurement of “excess Ar” in the olivine of the basalt disproves the zero Ar initial condition assumption of the conventional K-Ar dating method. How many more published K-Ar model ages await this simple yet profound challenge? *Snelling* [1999] summarized the “excess Ar” problem in volcanic rocks.

7. Conclusion

Mineral isochron analysis, a tedious procedure that is performed on a single rock, has significant applications to testing the “ages” of rocks assumed by evolutionists. The process of generating a “complete” mineral isochron using multiple parent-daughter systems potentially generates numerous model “ages” and multiple “mineral isochron ages” for a single rock. These ages should be concordant if evolutionary assumptions are true. An evolutionist should want to see this test completed so that the assumptions of the dating methods can be strengthened. The mineral isochron analysis provides the crucial and significant test of the evolutionary model. If there are significantly discordant “ages” within a single rock, creationists may be able to propose an alternate model. An adequate scientific or statistical reason needs to be given for each case of discordance.

Preliminary research on Grand Canyon rocks indicates that significant discordance exists between the “ages” calculated by different radioisotopes. How is this discordance to be explained? These research

challenges await creationists of the future who seek to reinterpret “ages” assigned by radioisotopes to rocks.

References

- Abranches, M. C. B., J. W. Arden, and N. H. Gale, Uranium-lead abundances and isotopic studies in the chondrites Richardton and Farmington, *Earth and Planetary Science Letters*, 46, 311–322, 1980.
- Allègre, C. J., G. Manhès, and C. Göpel, The age of the earth, *Geochimica et Cosmochimica Acta*, 59, 1445–1456, 1995.
- Austin, S. A. (editor), *Grand Canyon: Monument to Catastrophe*, Institute for Creation Research, Santee, California, pp. 111–131, 1994.
- Austin, S. A., and A. A. Snelling, Discordant potassium-argon model and isochron “ages” for Cardenas Basalt (Middle Proterozoic) and associated diabase of Eastern Grand Canyon, Arizona, in *Proceedings of the Fourth International Conference on Creationism*, edited by R. E. Walsh, Creation Science Fellowship, Pittsburgh, Pennsylvania, pp. 35–51, 1998.
- Beckinsale, R. D., N. H. Gale, R. J. Pankhurst, A. MacFarlane, M. J. Crow, J. W. Arthurs, and A. F. Wilkinson, Discordant Rb-Sr and Pb-Pb whole rock isochron ages for the Archaean basement of Sierra Leone, *Precambrian Research*, 13, 63–76, 1980.
- Bowring, S. A., and I. S. Williams, Priscoan (4.00–4.03 Ga) orthogneisses from northwestern Canada, *Contributions to Mineralogy and Petrology*, 134, 3–16, 1999.
- Brooks, C., D. E. James, and S. R. Hart, Ancient lithosphere: its role in young continental volcanism, *Science*, 193, 1086–1094, 1976.
- Burton, K. W., A. S. Cohen, R. O’Nions, and M. J. O’Hara, Archean crustal development in the Lewisian Complex of Northwest Scotland, *Nature*, 370, 552–555, 1994.
- Chauvel, C., B. Dupré, and G. A. Jenner, The Sm-Nd age of Kambalda volcanics is 200 Ma too old!, *Earth and Planetary Science Letters*, 74, 315–324, 1985.
- Crocker, C. H., K. D. Collerson, J. F. Lewry, and M. E. Bickford, Sm-Nd, U-Pb, and Rb-Sr geochronology and lithostructural relationships in the Southwestern Rae Province: constraints on crustal assembly in the Western Canadian Shield, *Precambrian Research*, 61, 27–50, 1993.
- Dalrymple, G. B., and W. K. Hamblin, K-Ar ages of Pleistocene Lava Dams in the Grand Canyon in Arizona, *Proceedings of the National Academy of Sciences*, 95, 9744–9749, 1998.
- Dickin, A. P., *Radiogenic Isotope Geology*, Cambridge University Press, New

- York, 452 p., 1995.
- Faure, G., *Principles of Isotope Geology*, second edition, Wiley, New York, 599 p., 1986.
- Gale, N. H., J. Arden, and R. Hutchison, Uranium-lead chronology of chondritic meteorites, *Nature Physical Sciences*, 240, pp. 56–57, 1972.
- Galer, S. J. G., Oldest rocks in Europe, *Nature*, 370, 505–506, 1994.
- Göpel, C., G. Manhès, and C. J. Allègre, U-Pb systematics of phosphates from equilibrated ordinary chondrites, *Earth and Planetary Science Letters*, 121, 153–171, 1994.
- Huey, J. M., and T. P. Kohman, ^{207}Pb - ^{206}Pb isochron and the age of chondrites, *Journal of Geophysical Research*, 78, 3227–3244, 1973.
- Jacobsen, S. B., and G. J. Wasserburg, Sm-Nd isotopic evolution of chondrites and achondrites, II, *Earth and Planetary Science Letters*, 67, 137–150, 1984.
- Kruger, F. J., B. S. Kamber, and P. D. Harris, Isotopic peculiarities of an Archaean pegmatite (Union Mine, Mica, South Africa): geochemical and geochronological implications, *Precambrian Research*, 91, 253–267, 1998.
- Larson, E. E., P. E. Patterson, and F. E. Mutschler, Lithology, chemistry, age and origin of the Proterozoic Cardenas Basalt, Grand Canyon, Arizona, *Precambrian Research*, 65, 255–276, 1994.
- Li, S., E. Jagoutz, Y. Chen, and Q. Li, Sm-Nd and Rb-Sr isotopic chronology and cooling history of ultrahigh pressure metamorphic rocks and their country rocks at Shuanghe in the Dabie Mountains, Central China, *Geochimica et Cosmochimica Acta*, 64, 1077–1093, 2000.
- Li, X., A comprehensive U-Pb, Sm-Nd, Rb-Sr and ^{40}Ar - ^{39}Ar geochronological study on Guidong Granodiorite, Southeast China: records of multiple tectonothermal events in a single pluton, *Chemical Geology*, 115, 283–295, 1994.
- Ludwig, K. R., *Isoplot/Ex Version 2.06: A Geochronological Toolkit for Microsoft Excel*, Berkeley Geochronology Center, Berkeley, California, 49 p., 1999.
- McKee, E. H., and D. C. Noble, Age of the Cardenas Lavas, Grand Canyon, Arizona, *Geological Society of America Bulletin*, 87, 1188–1190, 1976.
- Minster, J. F., J. L. Birck, and C. J. Allègre, Absolute age of formation of chondrites studied by the ^{87}Rb - ^{87}Sr method, *Nature*, 300, 414–419, 1982.
- Mukasa, S. B., A. H. Wilson, and R. W. Carlson, A multielement geochronologic study of the Great Dyke, Zimbabwe: significance of the robust and reset ages, *Earth and Planetary Science Letters*, 164, 353–369, 1998.

- Pandey, B. K., J. N. Gupta, K. J. Sarma, and C. A. Sastry, Sm-Nd, Pb-Pb and Rb-Sr geochronology and petrogenesis of the mafic dyke swarm of Mahabnagar, South India: implications for Paleoproterozoic crustal evolution of the Eastern Dharwar Craton, *Precambrian Research*, 84, 181–196, 1997.
- Patterson, C. C., Age of meteorites and the earth, *Geochimica et Cosmochimica Acta*, 10, 230–237, 1956.
- Rugg, S. H., and S. A. Austin, Evidences for rapid formation and failure of Pleistocene “Lava Dams” of the Western Grand Canyon, Arizona, in, *Proceedings of the Fourth International Conference on Creationism*, edited by R. E. Walsh, Creation Science Fellowship, Pittsburgh, Pennsylvania, pp. 475–486, 1998.
- Shaw, R. K., M. Arima, H. Kagami, C. M. Fanning, K. Shiraishi, and Y. Motoyoshi, Proterozoic events in the Eastern Ghats Granulite Belt, India: evidence from Rb-Sr, Sm-Nd systematics, and SHRIMP dating, *Journal of Geology*, 105, 645–656, 1997.
- Snelling, A. A., “Excess Argon”: The “Achilles’ Heel” of potassium-argon and argon-argon “dating” of volcanic rocks, *Institute for Creation Research Impact #307*, 4 p., 1999.
- Tatsumoto, M., R. J. Knight, and C. J. Allègre, Time differences in the formation of meteorites as determined from the ratio of lead-207 to lead-206, *Science*, 180, 1279–1283, 1973.
- Tera, F., and R. W. Carlson, Assessment of the Pb-Pb and U-Pb chronometry of the early solar system, *Geochimica et Cosmochimica Acta*, 63, 1877–1889, 1999.
- Tilton, G. R., Age of the solar system, in *Meteorites and the Early Solar System*, edited by J. F. Kerridge and M. S. Matthews, University of Arizona Press, Tucson, pp. 259–275, 1989.
- Unnikrishnan-Warrier, C., Isotopic signature of Pan-African rejuvenation in the Kerala Khondalite Belt, southern India: implications for East Gondwana reassembly, *Journal Geological Society of India*, 50, 179–190, 1997.
- Weber, B., and H. Köhler, 1999, Sm-Nd, Rb-Sr and U-Pb geochronology of a Grenville Terrane in Southern Mexico: origin and geologic history of the Guichicovi Complex, *Precambrian Research*, 96, 245–262, 1999.
- Wetherill, G. W., Discordant uranium-lead ages, *Transactions of the American Geophysical Union*, 37, 320–326, 1956.
- Whitehouse, M. J., M. B. Fowler, and C. R. L. Friend, Conflicting mineral and whole-rock isochron ages for the Late-Archaean Lewisian Complex of

northwest Scotland: implications for geochronology in polymetamorphic high-grade terrains, *Geochimica et Cosmochimica Acta*, 60, 3085–3102, 1996.

Wooden, J. L., P. A. Mueller, D. K. Hunt, and D. R. Bowes, Geochemistry and Rb-Sr geochronology of the Archean rocks from the interior of the southeastern Beartooth Mountains, Montana and Wyoming, *Montana Bureau of Mines and Geology Special Publication 84*, pp. 45–55, 1982.

York, D., Least squares fitting of a straight line with correlated errors, *Earth and Planetary Science Letters*, 5, 320–324, 1969.

Zhao, J., and M. T. McCulloch, Sm-Nd mineral isochron ages of Late Proterozoic dyke swarms in Australia: evidence for two distinctive events of mafic magmatism and crustal extension, *Chemical Geology (Isotope Geoscience Section)*, 109, 341–354, 1993.

Zindler, A., and S. Hart, Chemical geodynamics, *Annual Review of Earth and Planetary Sciences*, 14, 493–571, 1986.

Chapter 5

Geochemical Processes in the Mantle and Crust

Andrew A. Snelling, Ph.D.**

Abstract. Each of the radioisotopic systems used for rock “dating” (K-Ar, U-Th-Pb, Rb-Sr and Sm-Nd) when closely examined has its own peculiarities, but there are difficulties common to them all which raise questions as to their suitability as geochronometers. Daughter radiogenic ^{40}Ar is an inert gas that should not be present in rocks when they form, but should only accumulate from subsequent *in situ* radioactive decay of ^{40}K , yet “excess $^{40}\text{Ar}^*$ ” [see note below] is common in volcanic and crustal rocks yielding unacceptable old “ages.” Nearly all isotope pairs are mobile relative to one another in crustal fluids (ground and hydrothermal waters) leading to fractionation, gains and losses which disturb the radioisotopic systematics and produce erroneous “ages.” These problems are evident on all observational scales, even within mineral grains, and are often severe enough (with discordancies of up to almost 7500%) to raise doubts about all attempts at radioisotope dating. Yet because the definition of what are acceptable or unacceptable “ages” is based on stratigraphic and biostratigraphic settings and radioisotopic concordances within the uniformitarian time-frame, the end result is an apparent, internally consistent, self-fulfilling edifice of systematic “ages.”

However, the fact that modern mantle-derived oceanic volcanics consistently have radioisotopic signatures that yield excessively old “ages” has led to their use to identify geochemical reservoirs in the mantle. Such geochemical “fingerprinting” has also demonstrated that mixing of mantle and crustal sources produces crustal rocks which retain those radioisotopic signatures. The existence of these reservoirs has been combined with plate tectonics to produce a proliferation of mantle-crust geodynamics and plumbotectonics models. These are all built on the assumption of earth

Note: $^{40}\text{Ar}^*$ denotes radiogenic ^{40}Ar derived from radioactive decay of parent ^{40}K , the * symbol distinguishing it from primordial ^{40}Ar .

** *Geology Department, Institute for Creation Research, Santee, California*

accretion from the solar nebula at 4.57 Ga, but anomalies and discrepancies are still recognized even though the doubtful quality and integrity of the radioisotopic data being modeled is not. Alternately, most radioisotopic “ages” may have been produced as an artifact of systematic mixing of mantle and crustal sources endowed with fundamental geochemical signatures from the origin of the earth, geodynamics being catastrophic within a young-earth, global Flood framework.

1. Introduction

The methodology of the radioactive dating techniques begins with the collection of rock samples from outcrops or drillcores. The rock samples are then taken to the laboratory where after cleaning they are crushed. If the objective is to obtain “age” determinations on minerals within the rocks, the samples are only crushed to the particle size of the smallest mineral grains in them so that the result is a mixture of disaggregated mineral grains which can then be separated via various techniques into concentrates of each mineral phase in the rocks. Otherwise, rock samples are totally pulverized and homogenized for whole rock “age” determinations.

When the radioactive “age” determinations are finally made on either the constituent mineral concentrates or the whole rock powders from the original samples collected in the field, the technique is essentially a chemical analysis whereby the concentrations of particular radioactive elements, or radioisotopes, or the ratios of particular radioisotopes, are determined. From the numbers so produced calculations are made, based on various assumptions, to report “ages” for the constituent minerals or the whole rocks, or alternately, the results are plotted in order to determine isochron “ages.” Thus the “ages” so determined are not just a product of the physics of the nuclear processes involved in radioactive decay, because the “ages” are ultimately determined from the chemistry of the minerals and rocks. Consequently, it is not only necessary to understand the nuclear physics of radioactive decay, but also the chemistry of the rocks and their constituent minerals, plus the origin and history of the rocks being “dated” so that the resultant “ages” may be fully understood within their geological context. While there may be an underlying trend

in the radiometric data due to a systematic consequence of some change in the nuclear physics of the radioactive decay processes, such as accelerated decay rates, there will also be variations and “anomalies” (that of course depends on the selected criteria for what constitutes “normal”) which have been produced as a result of the geological origin of the rock samples and their mineralogy and geochemistry.

Therefore, it is essential to understand the geological, mineralogical and geochemical context of the rock and constituent mineral samples. Geochemical processes in the earth’s mantle and crust must be understood, as the rocks and their constituent minerals which are “dated” ultimately have their source in the mantle and/or are generated in the crust and reside there. These processes all have imposed second, third and even fourth order effects on any underlying first order trend in the radiometric data due to the nuclear physics of radioactive decay, and therefore it is essential to be able to characterize these second and subsequent order effects so that they may be removed from the data to reveal the true nature of the underlying first order trend. On the other hand, some of these geochemical processes may be responsible for the first order trend itself. Only in this way will it be possible to produce an alternative model for explaining the radioisotopic data within a young-earth creationist framework, as opposed to the prevailing multi-billion year “dates” within the uniformitarian belief system.

The purpose then in this chapter is to discuss various relevant geochemical processes in the mantle and crust, and to explore the effects they have on the radioisotopic systems used for “dating.” Because the different geochemical processes affect the various radioisotopic systems differently, and/or different geochemical processes are relevant only to individual radioisotopic systems, the following discussion deals with each radioisotopic system in turn.

2. The Potassium-Argon (K-Ar) Radioisotopic System

The K-Ar radioisotopic system is unique among the radioactive “dating” methods, primarily because Ar is a gas. One of the critical assumptions of radioactive “dating” is that the initial conditions are

known, which specifically means that the amounts of the parent and daughter radioisotopes initially in the rock or minerals is known and has only changed subsequently as a result of radioactive decay of the parent radioisotope into the daughter isotope. In the context of the K-Ar radioisotopic system this assumption is even more stringent, in that it is assumed no radiogenic Ar ($^{40}\text{Ar}^*$) was in the rocks and minerals when they formed and that all the $^{40}\text{Ar}^*$ now measured in the rocks and minerals has come as a result of radioactive decay of parent ^{40}K .

Geyh and Schleicher [1990] state:

What is special about the K-Ar method is that the daughter nuclide is a noble gas, which is not normally incorporated in the mineral and is not bound in the mineral in which it is found.

Similarly, *Dalrymple and Lanphere* [1969] state:

. . . a silicate melt will not usually retain the ^{40}Ar that is produced, and thus the potassium-argon clock is not “set” until the mineral solidifies and cools sufficiently to allow the ^{40}Ar to accumulate in the mineral lattice.

Dalrymple [1991] has recently put the argument more strongly:

The K-Ar method is the only decay scheme that can be used with little or no concern for the initial presence of the daughter isotope. This is because ^{40}Ar is an inert gas that does not combine chemically with any other element and so escapes easily from rocks when they are heated. Thus, while a rock is molten the ^{40}Ar formed by decay of ^{40}K escapes from the liquid.

2.1 Assumption Violated by “Excess” $^{40}\text{Ar}^*$

However, these dogmatic statements by Dalrymple are inconsistent with even his own work on historic lava flows [*Dalrymple*, 1969], some of which he found had non-zero concentrations of $^{40}\text{Ar}^*$ in violation of this key assumption of the K-Ar dating method. He went on to state that some cases of initial ^{40}Ar remaining in rocks have been documented but they are uncommon [*Dalrymple*, 1991]. Yet in his study of 26 historic subaerial lava flows [*Dalrymple*, 1969], five (almost 20%) of those flows contained “excess” Ar, so how can *Dalrymple* [1991] still claim “‘excess’ argon is rare”? It is only because of the independent historic cross-checks that we know that all the Ar in these lava flows is excess Ar which is

thus responsible for the grossly incorrect “ages.” The flows and their “ages” (where Ma = Mega-annum, that is, million years) were:

Hualalai basalt, Hawaii(AD 1800–1801)	1.6 ± 0.16 Ma
	1.41 ± 0.08 Ma
Mt. Etna basalt, Sicily (122 BC)	0.25 ± 0.08 Ma
Mt. Etna basalt, Sicily (AD 1792)	0.35 ± 0.14 Ma
Mt. Lassen plagioclase, California (AD 1915)	0.11 ± 0.03 Ma
Sunset Crater basalt, Arizona (AD 1064–1065)	0.27 ± 0.09 Ma
	0.25 ± 0.15 Ma

Far from being rare, there are numerous other examples reported in the literature of excess $^{40}\text{Ar}^*$ in recent or young volcanic rocks producing excessively old whole-rock K-Ar “ages.” Table 1 lists some of these. Among other studies, *Fisher* [1970] investigated submarine basalt from a Pacific seamount and found “the largest amounts of excess ^4He and ^{40}Ar ever recorded” (at that time). *McDougall* [1971] not only found “extraneous radiogenic argon present in three of the groups of basalt flows” on the young island of Réunion in the Indian Ocean, but “extraneous argon” was also “detected in alkali feldspar and amphibole in hypabyssal drusy syenites that are exposed in the eroded core of Piton des Niges volcano.” Significant quantities of excess $^{40}\text{Ar}^*$ have also been recorded in submarine basalts, basaltic glasses and olivine phenocrysts from the currently active Hawaiian volcanoes, Loihi Seamount and Kilauea, as well as on the flanks of Mauna Loa and Hualalai volcanoes, also part of the main island of Hawaii [*Honda et al.*, 1993; *Valbracht et al.*, 1996b], and in samples from the Mid-Atlantic Ridge, East Pacific Rise, Red Sea, Galapagos Islands, McDonald Seamount and Manus Basin [*Staudacher et al.*, 1989; *Marty and Humbert*, 1997]. *Patterson et al.* [1990] claimed that some of the initial Loihi analytical results were due to atmospheric contamination of the magma either during intrusion or eruption, but subsequent work [*Honda et al.*, 1993; *Valbracht et al.*, 1996b] has confirmed that the excess $^{40}\text{Ar}^*$ is not from atmospheric contamination at all.

It is quite obvious, therefore, that excess Ar can be retained in cooling

Table 1. Examples from the literature of recent or young volcanic rocks with excessively old whole-rock K-Ar “model ages” due to excess $^{40}\text{Ar}^*$ [after *Snelling, 1998*].

Lava Flow and Location	Known Age	K-Ar “Age”	Reference
Akka Water Fall flow, Hawaii	Pleistocene	32.3 ± 7.2 Ma	<i>Krummenacher, 1970</i>
Kilauea Iki basalt, Hawaii	AD 1959	8.5 ± 6.8 Ma	<i>Krummenacher, 1970</i>
Mt. Stromboli, Italy, volcanic bomb	September 23, 1963	2.4 ± 2 Ma	<i>Krummenacher, 1970</i>
Mt. Etna basalt, Sicily	May, 1964	0.7 ± 0.01 Ma	<i>Krummenacher, 1970</i>
Medicine Lake Highlands obsidian,	<500 years old	12.6 ± 4.5 Ma	<i>Krummenacher, 1970</i>
Glass Mountains, California	AD 1800–1801	22.8 ± 16.5 Ma	<i>Krummenacher, 1970</i>
Hualalai basalt, Hawaii	<800 years old	$0.15\text{--}0.47$ Ma	<i>McDougall et al., 1969</i>
Rangitoto basalt, Auckland, New Zealand	<30 Ma	95 Ma	<i>Fisher, 1971</i>
Alkali basalt plug, Benue, Nigeria	<0.3 Ma	18.0 ± 0.7 Ma	<i>Armstrong, 1978</i>
Olivine basalt, Nathan Hills, Victoria Land, Antarctica	1984	0.64 ± 0.03 Ma	<i>Esser et al., 1997</i>
Anorthoclase in volcanic bomb, Mt. Erebus, Antarctica	<200 years old	21 ± 8 Ma	<i>Noble and Naughton, 1968</i>
Kilauea basalt, Hawaii	<1,000 years old	42.9 ± 4.2 Ma	<i>Dalrymple and Moore, 1968</i>
Kilauea basalt, Hawaii	<1 Ma	30.3 ± 3.3 Ma	<i>Dalrymple and Moore, 1968</i>
East Pacific Rise basalt	<2.5 Ma	690 ± 7 Ma	<i>Funkhouser et al., 1968</i>
Seamount basalt, near East Pacific Rise	<0.6 Ma	580 ± 10 Ma	<i>Funkhouser et al., 1966</i>
East Pacific Rise basalt	<0.6 Ma	700 ± 150 Ma	<i>Fisher, 1972</i>
		24.2 ± 1.0 Ma	<i>Dymond, 1970</i>

lavas from the volcanic gases expelled from the same magma chamber as the lavas during their eruption. This is both open-system behavior and mixing, given that some of the volcanic Ar from the magma chamber represents Ar that was originally in the magma, perhaps even in isotopic equilibrium with parent K, but it is also mixing in the sense that the Ar is incorporated into the extruding lavas. Thus, *Snelling* [1998] obtained anomalous K-Ar “ages” for recent (1949, 1954, 1975) andesite flows at Mt. Ngauruhoe, central North Island, New Zealand, as high as 3.5 ± 0.2 Ma. Indeed, separate splits of the same sample from the same flow (June 30, 1954) yielded model ages of 0.8 ± 0.2 Ma and 3.5 ± 0.2 Ma, and two splits of another sample from the same flow yielded model ages of <0.27 Ma and 1.3 ± 0.3 Ma. Admittedly, it is difficult for the lab and its equipment to measure exceedingly low levels of Ar, and hence reproducibility is always going to be difficult to achieve. Nevertheless, each of these results was reported by the laboratory after duplicate runs had been made in each instance, and some samples were even reanalyzed months later. But in each case the initial results were confirmed, thus ruling out a systematic problem with the analytical procedure and the laboratory equipment. This indicates that the excess $^{40}\text{Ar}^*$ present in these lava flows occurs spasmodically through them, even at the hand specimen scale.

Austin [1996] investigated the 1986 dacite lava flow from the post-October 26, 1980 lava dome within the Mount St. Helens crater, and established that the 10-year-old dacite yields a whole-rock K-Ar model “age” of 0.35 ± 0.05 Ma due to excess $^{40}\text{Ar}^*$ in the rock. He also produced concentrates of the constituent minerals, which also yielded anomalous K-Ar model “ages” of 0.34 ± 0.06 Ma (plagioclase), 0.9 ± 0.2 Ma (hornblende), 1.7 ± 0.3 Ma (pyroxene) and 2.8 ± 0.6 Ma (pyroxene ultra-concentrate). Thus, even though these mineral concentrates were not ultra-pure, given the fine-grained glass in the groundmass and some Fe-Ti oxides, it is evident that the excess $^{40}\text{Ar}^*$ responsible for the anomalous K-Ar “ages” is retained within the different constituent minerals in different amounts.

2.2 Excess $^{40}\text{Ar}^*$ Occluded in Minerals

The excess $^{40}\text{Ar}^*$ is occluded therefore in the minerals within lava flows, rather than between the mineral grains. *Laughlin et al.* [1994] found that the olivine, pyroxene and plagioclase in Quaternary basalts of the Zuni-Bandera volcanic field of New Mexico contained very significant quantities of excess $^{40}\text{Ar}^*$, as did the olivine and clinopyroxene phenocrysts in Quaternary flows from New Zealand volcanoes [*Patterson et al.*, 1994]. Similarly, *Poths et al.* [1993] separated olivine and clinopyroxene phenocrysts from young basalts from New Mexico and Nevada, and then measured “ubiquitous excess argon” in them. *Damon et al.* [1967] reported several instances of phenocrysts with K-Ar “ages” 1–7 million years greater than that of the whole rocks, and one K-Ar “date” on olivine phenocrysts of greater than 110 Ma in a recent (<13,000 year old) basalt. *Damon et al.* [1967] thus suggested that large phenocrysts in volcanic rocks must contain the excess $^{40}\text{Ar}^*$ because their size prevents them from completely degassing before the flows cool, but *Dalrymple* [1969] concluded that there does not appear to be any correlation of excess $^{40}\text{Ar}^*$ with large phenocrysts or with any other petrological or petrographic parameter.

Thus most investigators have come to the obvious conclusion that the excess $^{40}\text{Ar}^*$ had to have been present in molten lavas when extruded, which then did not completely degas as they cooled, the excess $^{40}\text{Ar}^*$ becoming “trapped” in the constituent minerals, and in some instances, in the rock fabrics themselves. Laboratory experiments have tested the solubility of Ar in synthetic basalt melts and their constituent minerals near 1300°C at one atmosphere pressure in a gas stream containing Ar [*Broadhurst et al.*, 1990, 1992]. When quenched, synthetic olivine in the resultant material was found to contain 0.34 ppm $^{40}\text{Ar}^*$ (the Ar content of olivine is usually in the ppb range or undetectable). *Broadhurst et al.* [1990] commented that “the solubility of Ar in the minerals is surprisingly high,” and concluded that the Ar is held primarily in lattice vacancy defects within the minerals.

In different experiments, *Karpinskaya et al.* [1961] heated muscovite to 740°–860°C under high Ar pressures (2800–5000 atmospheres) for

periods of 3 to 10.5 hours. The muscovite absorbed significant quantities of Ar, producing K-Ar “ages” of up to 5 billion years, and the absorbed Ar appeared like ordinary radiogenic argon ($^{40}\text{Ar}^*$). *Karpinskaya* [1967] subsequently synthesized muscovite from a colloidal gel under similar Ar pressures and temperatures, the resultant muscovite retaining up to 0.5 wt% Ar at 640°C and a vapor pressure of 4000 atmospheres. This is approximately 2500 times as much Ar as is found in natural muscovite. These experiments show that under certain conditions Ar can be incorporated into minerals and rocks that are supposed to exclude Ar when they crystallize.

2.3 Cooling Rates and Potassium (K) Alteration

The rate of cooling of lavas is another factor that has been investigated. *Dalrymple and Moore* [1968] found that the 1 cm thick glassy rim of a pillow in a Kilauea submarine basalt had greater than 40 times more excess $^{40}\text{Ar}^*$ than the basalt interior just 10 cm below (see Figure 1). The glassy pillow rim is, of course, produced by rapid quenching of the hot basalt lava immediately as it contacts the cold ocean water, so the excess $^{40}\text{Ar}^*$ in the lava is rapidly trapped and retained. *Dymond* [1970] obtained similar results on four deep-sea basalt pillows from near the axis of the East Pacific Rise. *Dalrymple and Moore* [1968] also found that the excess $^{40}\text{Ar}^*$ contents of the glassy rims of basalt pillows increased systematically with water depth, leading them to conclude that the amount of excess $^{40}\text{Ar}^*$ is a direct function of both the hydrostatic pressure and the rate of cooling. Similarly, *Noble and Naughton* [1968] reported K-Ar “ages” from 0 to 22 Ma with increasing sample depth for submarine basalts probably less than 200 years old, also from the active Kilauea volcano.

Seidemann [1977] reported yet another intriguing relationship. He analyzed deep-sea basalt samples obtained from DSDP drillholes in the floor of the Pacific Ocean basin and found K-Ar “ages” increased with increasing K contents of the basalts, a relationship he noted also appeared in similar data published by DSDP staff. In basalt pillows the K content increases from the margin to a maximum at an intermediate distance into the pillows, whereas holocrystalline basalts (comprising crystals

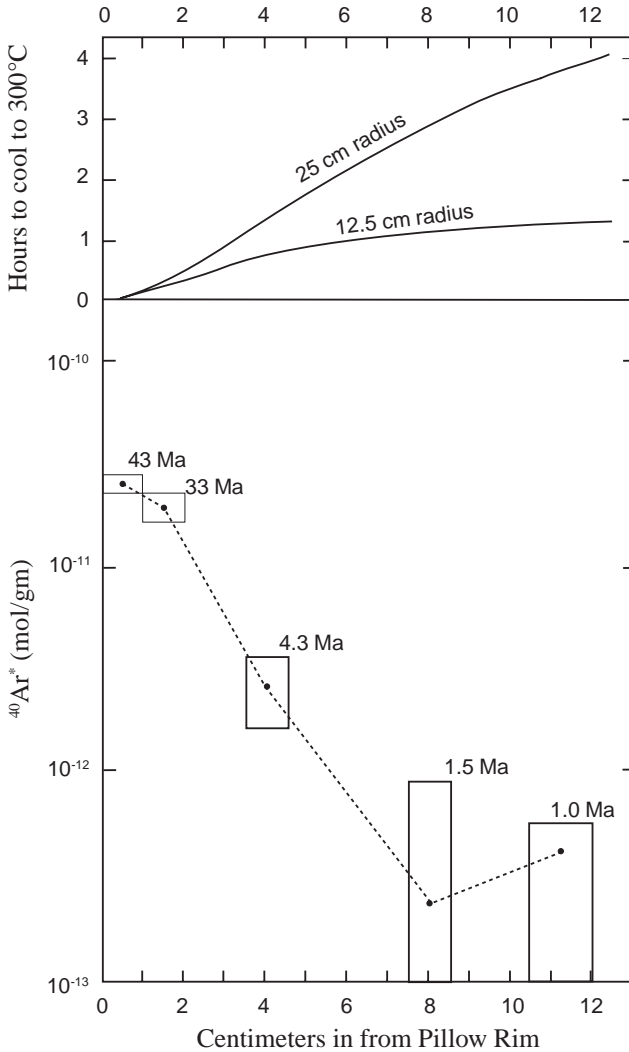


Figure 1. Excess content of radiogenic ^{40}Ar ($^{40}\text{Ar}^*$) and apparent age as functions of distance inwards from the rim of pillow sample 2590. Width of each box indicates thickness of analyzed sample; height of each box indicates 95% confidence limits. Top curves show the times required for spherical basalt pillows ($\kappa = 0.007$) to cool from 1200° to 300°C when one assumes a constant surface temperature of 0°C; Ma, million years [after *Dalrymple and Moore, 1968*].

and no glass) show a decrease of K inward from their margin [Hart, 1969]. *Seidemann* [1977] concluded, as had others before him, that submarine weathering adds K to the basalts, as does alteration at the time of formation, whereas the glassy pillow margins are largely impervious to seawater. Such an explanation is puzzling, given that seawater chemistry is dominated by Na, so experimental evidence is really needed to confirm it. The net result, however, is unreliable K-Ar “dates,” because the measured $^{40}\text{Ar}^*$ was probably not derived by radioactive decay of the measured ^{40}K contents. *Seidemann* also determined that sediment cover is not a significant barrier to the diffusion of K into basalt.

This same intriguing relationship between K contents of basalts and their K-Ar “ages” has also been noted in ancient lava flows, such as those of the Cardenas Basalt in the eastern Grand Canyon, Arizona. *Larson et al.* [1994] plotted the K content versus K-Ar “age” for seven samples from the upper member flows of the Cardenas Basalt and noted that the lower the K content the higher the K-Ar “age,” and that there was a clear curvi-linear trend in the data. They initially put this trend down to addition of K to the basalt flows during post-emplacement burial metamorphism, but discounted that because Rb should also have been enriched in the basalts and yet the Rb-Sr isochron has not been “disturbed” like the K-Ar isochron has for these same flows (see later). Thus they concluded that it must be due to the increased Ar loss associated with preferential burial alteration of those flows containing the higher contents of K.

Austin and Snelling [1998] provide data on an additional eight samples of the Cardenas Basalt, which data confirm that there is a curvi-linear trend between K content and K-Ar “ages” (Figure 2). It can be seen in this plot that there are some outliers from the main trend, but these are data from flows lower in the Cardenas Basalt sequence. *Austin and Snelling* found that the abundance of K in these basalts is related to the mineral constituents in these rocks, but could not find a direct correlation with the K-Ar data and the amount of glassy mesostasis/groundmass or the alteration mineralogy. On the other hand, the intriguing relationship reported by *Seidemann* [1977] was increasing K-Ar “ages” with

increasing K contents, the opposite to the trend in the Cardenas Basalt. *Austin and Snelling* [1998] suggested that there might be some correlation in the Cardenas Basalt with Ar loss, but this explanation was also found to be not consistent with the data (see later). Yet such trends remain and

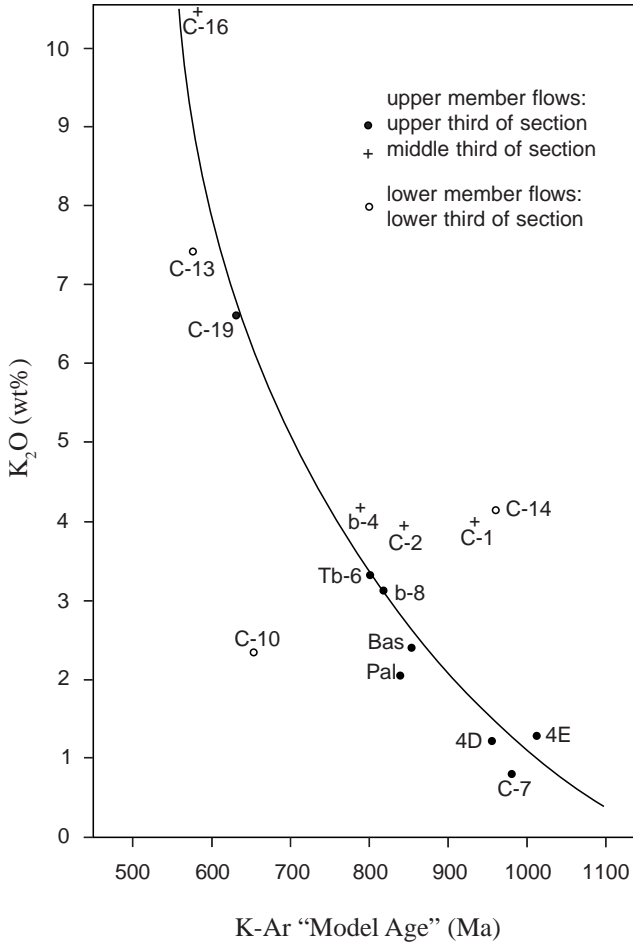


Figure 2. K-Ar "model ages" of the Cardenas Basalt, eastern Grand Canyon, Arizona, plotted against K₂O contents. The data are from *Austin and Snelling* [1998] and details of the samples are provided there. Except for three outliers there is a pronounced curvi-linear trend in the data of increasing K-Ar "model age" with decreasing K₂O content.

suggest that the K-Ar data are not simply “age” related.

Perhaps the key issues, though, are where this excess $^{40}\text{Ar}^*$ has come from, and whether it has been derived from radioactive decay of ^{40}K . One possibility is that excess $^{40}\text{Ar}^*$ can be accounted for by radioactive decay during long-term residence of magmas in chambers before eruption. *Esser et al.* [1997] discounted this option for the Mt. Erebus anorthoclase phenocryst. *Dalrymple* [1969] found that whereas the Mt. Lassen (1915) plagioclase phenocryst yielded excess $^{40}\text{Ar}^*$ and an anomalous K-Ar model “age,” a plagioclase from the 1964 eruption of Surtsey only had Ar whose isotopic composition matched that of air. Because phenocrysts are usually crystallized from lavas after eruption, they may arbitrarily trap excess $^{40}\text{Ar}^*$ during lava cooling, $^{40}\text{Ar}^*$ that would thus not be from *in situ* ^{40}K radioactive decay.

2.4 Negative “Ages” and Atmospheric Argon (Ar)

Another relevant consideration bearing on these issues is the observation noted by *Dalrymple* [1969] that some modern lava samples actually yield negative K-Ar model “ages,” apparently due to excess ^{36}Ar . Air has an $^{40}\text{Ar}/^{36}\text{Ar}$ ratio of 295.5, but some of *Dalrymple*’s samples had ratios less than 295.5 (and hence negative “ages”). According to the straightforward interpretation of the K-Ar dating methodology, this should be impossible. *Dalrymple* was not willing to attribute these anomalous ratios to experimental error, so he suggested three possible explanations that might account for the excess ^{36}Ar :

- (1) Incorporation of “primitive argon;”
- (2) Production of ^{36}Ar by the radioactive decay of ^{36}Cl ; or
- (3) Fractionation of atmospheric Ar by diffusion.

He rejected the possibility of significant ^{36}Ar formation *in situ* from nuclear reactions [option (2)] because the Cl content of basalts and the production rate of ^{36}Cl by cosmic-ray neutrons both are too low to account for any significant amount of ^{36}Ar . Instead, *Dalrymple* seemed to favor option (3), that when atmospheric Ar diffused back into lavas as they cooled, ^{36}Ar diffused in preferentially. However, he also recognized the weakness of this argument—it is difficult to explain why some lavas are

enriched in ^{36}Ar while others are not. To be consistent, if fractionation of atmospheric Ar occurred during diffusion, then this would mean that even supposedly “zero age” lavas actually have an apparent age, and that most lavas do not degas upon eruption. In fact, depending on how strong the fractionation of ^{36}Ar was during diffusion, it could even be that all lavas do not completely degas. (These implications have also been noted by *Giem* [1997].)

This only leaves Dalrymple’s option (1), that the lavas with the anomalously high ^{36}Ar come from areas of the mantle (and perhaps also the crust) which have primordial (or primitive) Ar that has not been diluted with radiogenic ^{40}Ar , and have not completely degassed. However, this means that there is no reason to assume that lavas whose Ar matches that in the atmosphere have degassed either, because they may have simply started with Ar which matches atmospheric Ar. Nevertheless, *Dalrymple and Moore* [1968] were convinced that “much of the volatile juvenile content may still be present in volcanic rocks quenched on the ocean floor.” Indeed, *Dalrymple and Lanphere* [1969] have specifically defined excess $^{40}\text{Ar}^*$ as ^{40}Ar that is not attributed to atmospheric Ar or *in situ* radioactive decay of ^{40}K . *Krummenacher* [1970] is more cautious, attributing anomalous $^{40}\text{Ar}/^{36}\text{Ar}$ ratios and excess $^{40}\text{Ar}^*$ to the “mass fractionation effect on argon of atmospheric isotopic composition” trapped in the lavas, as well as to the presence of “magmatic” Ar different in isotopic composition.

2.5 The Role of Xenoliths

Is the excess $^{40}\text{Ar}^*$ simply “magmatic” Ar, that is, Ar that collects in the magma and then is inherited by the lavas from it? *Funkhouser and Naughton* [1968] found that the excess $^{40}\text{Ar}^*$ in the 1800–1801 Hualalai flow, Hawaii, resided in fluid and gaseous inclusions in olivine, plagioclase and pyroxene in ultramafic xenoliths in the basalt. The quantities of excess $^{40}\text{Ar}^*$ were sufficient to yield K-Ar model “ages” from 2.6 Ma to 2960 Ma. However, *Dalrymple* [1969] subsequently only used the presence of ultramafic xenoliths and their excess $^{40}\text{Ar}^*$ contained in inclusions to explain partly the excess $^{40}\text{Ar}^*$ and anomalous K-Ar

model “ages” he obtained from the same 1800–1801 Hualalai flow, suggesting instead that the large single inclusions are not directly responsible for the excess Ar in the flows and that the $^{40}\text{Ar}^*$ is distributed more uniformly throughout the rocks. Nevertheless, those K-Ar and Ar-Ar geochronologists who are concerned about excess $^{40}\text{Ar}^*$ in their samples undermining their “dating” are careful to check for xenoliths and xenocrysts. *Esser et al.* [1997] did so and discounted xenocrystic contamination.

2.6 Noble Gases from the Mantle

Honda et al. [1993] have reported analyses of the isotopic concentrations and ratios of noble gases (including Ar) in submarine basalt glass samples from Loihi Seamount and Kilauea, Hawaii, and concluded that He and Ne isotopic ratios in particular, being uniquely different from atmospheric isotopic ratios, are indicative of the mantle source area of the plume responsible for the Hawaiian volcanism rather than from atmospheric contamination of the magma [*Patterson et al.*, 1990]. The $^{40}\text{Ar}/^{36}\text{Ar}$ ratios of up to 2536 (compared with the atmospheric $^{40}\text{Ar}/^{36}\text{Ar}$ ratio of 295.5) are consistent with the excess $^{40}\text{Ar}^*$ having also come with the magma from the mantle. *Valbracht et al.* [1996b] analyzed a larger suite of basalt glass samples, as well as samples of olivine phenocrysts, from the same and additional Hawaiian volcanoes, concluding that the isotopic systematics indicated that He and Ne had been derived from the mantle and had not been preferentially affected by secondary processes. Consequently, the excess $^{40}\text{Ar}^*$ also in these samples would have been carried also from the upper mantle source area of these basalts by the same magma plume responsible for the volcanism.

Moreira et al. [1998] have suggested, based on new experimental data from single vesicles in mid-ocean ridge basalt samples dredged from the North Atlantic, that the excess $^{40}\text{Ar}^*$ in the upper mantle may be almost double previous estimates [*Staudacher et al.*, 1989] (an $^{40}\text{Ar}/^{36}\text{Ar}$ ratio of 44,000 compared with an atmospheric $^{40}\text{Ar}/^{36}\text{Ar}$ ratio of 295.5—that is, an ^{40}Ar content almost 150 times more than the

atmospheric content relative to ^{36}Ar), and represents a primordial mantle component not yet outgassed. *Burnard et al.* [1997] obtained similar results on the same samples, but maintained that because some of the ^{36}Ar is probably surface-adsorbed atmospheric Ar, the upper mantle content of excess $^{40}\text{Ar}^*$ could be even ten times higher. Furthermore, *Burnard* [1999] has found that volatile compositions in basaltic glasses from the Mid-Atlantic Ridge vary from vesicle to vesicle in the same sample (for example, $^{40}\text{Ar}/^{36}\text{Ar}$ ratios of 1886 and 30,860). Further analyses of mid-ocean ridge basalt samples from the Mid-Atlantic, East Pacific, Indian Ocean, and the Red Sea [*Marty and Zimmermann*, 1999; *Nishio et al.*, 1999] have confirmed the high $^{40}\text{Ar}/^{36}\text{Ar}$ ratios (up to 19,000) and the excess $^{40}\text{Ar}^*$ brought from the upper mantle by the magmas. Some differences between the sample areas were concluded to be a reflection of mantle heterogeneity, and it was suggested that several types of fluid or fluid-bearing materials are transporting some of the volatiles (including excess $^{40}\text{Ar}^*$) within the mantle.

Similar results [*Valbracht et al.*, 1996a] have been obtained from ultramafic mantle xenoliths in basalts from the Kerguelen Archipelago in the southern Indian Ocean ($^{40}\text{Ar}/^{36}\text{Ar}$ ratios of up to 5910), and the measured considerable excess $^{40}\text{Ar}^*$ concluded to be a part of the mantle source signature of that hotspot volcanism. Analyzed samples from Iceland yielded $^{40}\text{Ar}/^{36}\text{Ar}$ ratios lower than typical mid-ocean ridge basalt values ($^{40}\text{Ar}/^{36}\text{Ar}$ ratios up to 6500), but the data suggest some atmospheric ^{36}Ar contamination has diluted the normal high upper mantle levels of excess $^{40}\text{Ar}^*$ [*Harrison et al.*, 1999]. Additionally, the data reflect the presence of a deep mantle component, consistent with bulk transfer for the deeper mantle via the Iceland Plume to mix hotspot with mid-ocean ridge volcanism. In contrast, plume volcanism which has produced ocean island basalts in the Polynesian region has much lower $^{40}\text{Ar}/^{36}\text{Ar}$ ratios (only up to 357) and thus much lower excess $^{40}\text{Ar}^*$, because the source mantle plume seems to have mixed subducted oceanic crust and upper mantle material with its lower mantle component [*Hanyu et al.*, 1999].

However, it has not only been the suboceanic mantle that has thus been sampled for its excess $^{40}\text{Ar}^*$ via such magma plumes. *Matsumoto*

et al. [1998] have reported high $^{40}\text{Ar}/^{36}\text{Ar}$ ratios (up to 5408) in spinel-lherzolites from five eruption centers in the youthful (<7 Ma) Newer Volcanics of southeastern Australia. These anhydrous lherzolites have compositions representative of the upper lithospheric mantle, and the significant excess $^{40}\text{Ar}^*$ in them indicates the presence of a sub-continental mantle reservoir with a very high $^{40}\text{Ar}/^{36}\text{Ar}$ ratio, and thus substantial excess $^{40}\text{Ar}^*$, similar to that found in mid-ocean ridge and plume/hotspot basalts. An even deeper mantle source tapped by a plume is now suggested as responsible for the carbonatites of the Kola region of Russia, based on analyses of rare gases in their fluid inclusions [*Marty et al.*, 1998]. The $^{40}\text{Ar}/^{36}\text{Ar}$ ratios obtained and the levels of excess $^{40}\text{Ar}^*$ are similar to those inferred for other plume sources, for example, Loihi (Hawaii) [*Valbracht et al.*, 1997], and are consistent with both a lower mantle origin for these carbonatitic fluids and a layered earth model in which regions are characterized by different refractory/volatile ratios (including Ar isotopes).

2.7 Sampling the Mantle with Diamonds and their Inclusions

Diamonds and their micro-inclusions are another means of “sampling” the mantle. Diamonds are thermodynamically stable in the pressure-temperature regime in the mantle at depths greater than 150 km, and their origin is believed to extend back to the Archean and the early crust of the earth [*Kesson and Ringwood*, 1989; *Kirkley et al.*, 1992]. They are formed in a number of processes associated with two rock types, eclogite and peridotite, xenoliths of which are also brought up into the upper crust with diamonds from the upper mantle below continental Precambrian shields (cratons) by kimberlite and lamproite “pipe” eruptions [*Gurney*, 1986, 1990; *Kirkley et al.*, 1992]. Even though the host kimberlite or lamproite may be relatively young (even in conventional terms), many diamonds date back to the Archean and thus the early history of the earth [*Richardson et al.*, 1984; *Kirkley et al.* 1992]. To account for all this evidence, it is postulated that the formation of most diamonds was closely associated with subduction of the Archean oceanic crust into the mantle [*Kesson and Ringwood*, 1989; *Kirkley et*

al., 1992], the required carbon, which was originally thought to be primordial carbon already in the mantle, is now believed to derive from sedimentary marine carbonates and biogenic carbon from bacteria/algae in the sediments subducted with the oceanic crust [Eldridge *et al.*, 1991; Kirkley *et al.*, 1991, 1992].

The noble gas contents of diamonds are consistent with their ancient and mantle origin, high He isotopic ratios (290 times the atmospheric ratio) being regarded as primordial and rivaling those measured for the Sun today [Ozima and Zashu, 1983; Gurney, 1986]. Of significance here is the postulation that He, Ar, K, Pb, Th and U are added to the convecting upper mantle circulation, and the proportions and isotopic compositions are strongly determined by entrainment from the lower mantle (below 670 km) [Harte and Hawkesworth, 1986; Gurney, 1990]. This is reflected in those Ar isotopic measurements that have been made on diamonds and their micro-inclusions.

Rather than focus on attempting to date only diamond micro-inclusions as others had done, Zashu *et al.* [1986] carefully selected 10 Zaire diamonds and examined them for purity before undertaking K-Ar dating analyses of the diamonds themselves. However, at the outset they noted that there had been almost no direct radiometric dating of diamonds except for conventional K-Ar dating, and the results had been questionable due to the possible presence of excess $^{40}\text{Ar}^*$. To avoid this problem, they used the K-Ar isochron dating method. Their experimental data showed good linear correlations, but these isochrons yielded an age of 6.0 ± 0.3 Ga, which of course was unacceptable because these diamonds would be older than the earth itself. Mistakes in the experimental procedure were easily discounted, so they were forced to conclude that excess $^{40}\text{Ar}^*$ was responsible, and that it needed to be in a fluid state to ensure the homogenization necessary to give such a constant $^{40}\text{Ar}/\text{K}$ ratio. Alternately, they speculated that the diamonds might differ in K isotopic composition from common K, but this was discounted in a follow-up study [Podosek *et al.*, 1988] in which it was found that ^{40}K was present in these diamonds in normal abundance. Because ^{40}Ar - ^{39}Ar analyses yielded the same unacceptable “age,” it was concluded that the excess $^{40}\text{Ar}^*$ was not generated *in situ* but was an inherited or “trapped”

component from the mantle reservoir when and where the diamonds formed.

These Zaire diamonds are not the only ones which have yielded excess $^{40}\text{Ar}^*$. *Phillips et al.* [1989] used a laser-probe to ^{40}Ar - ^{39}Ar date eclogitic clinopyroxene inclusions in diamonds from the Premier kimberlite, South Africa, and found moderate $^{40}\text{Ar}/^{36}\text{Ar}$ ratios indicative of much less excess $^{40}\text{Ar}^*$ than in the Zaire diamonds. The “age” of these eclogitic diamonds was thus determined to be 1.198 ± 0.014 Ga, much younger than the 3.3 Ga peridotitic diamonds at Kimberley and Finsch [*Kirkley et al.*, 1992], also in South Africa, so *Phillips et al.* [1989] interpreted the moderate excess $^{40}\text{Ar}^*$ as characteristic of mantle conditions prevailing at the time and in the region of Premier eclogitic diamond formation.

Zashu et al. [1986] postulated that the excess $^{40}\text{Ar}^*$ in the Zaire diamonds needed to be in a fluid state. Though *Navon et al.* [1988] did not analyze for Ar when they investigated fluids in micro-inclusions in diamonds from Zaire and Botswana, they found a high content of volatiles and incompatible elements in the uniform average composition of the micro-inclusions, with the amounts of water and CO_2 (in carbonates) almost an order of magnitude higher than the volatile contents of kimberlites and lamproites (host rocks to diamonds). At 1–3 wt% the chlorine levels were also much higher than those of kimberlites (<0.1%), although the bulk composition of micro-inclusions, including the high K_2O content (up to 29.7 wt%), resembled that of such potassic magmas. They concluded that these micro-inclusions represent the volatile-rich ($\approx 40\%$ volatiles) fluid or melt from the upper mantle in which the diamonds grew, and that because of the high volatile content in this hydrous mantle fluid, high levels of rare gases may also be expected and would explain the high $^{40}\text{Ar}/\text{K}$ ratios (the excess $^{40}\text{Ar}^*$) and anomalous “ages.”

As a result of continued investigation of those Zaire cubic diamonds, which produced ^{40}Ar - ^{39}Ar “age” spectra yielding a ≈ 5.7 Ga isochron, *Ozima et al.* [1989] discovered that just as there was an excellent correlation between their K contents and $^{40}\text{Ar}/^{36}\text{Ar}$ ratios, there is also a correlation between their Cl contents and ^{40}Ar . They concluded from their data “that the ^{40}Ar is an excess component which has no age

significance and that the ^{40}Ar and its associated K are contained in sub-micrometer inclusions of mantle-derived fluid.” *Turner et al.* [1990] also used the ^{40}Ar - ^{39}Ar technique through correlations with K, Cl and ^{36}Ar to unscramble the mixtures of radiogenic and parentless (excess) Ar components in fluid inclusions in “coated” Zaire diamonds and in olivine from an East African mantle xenolith. Their results proved conclusively that ^{40}Ar is present in a widespread Cl-rich component, which implies the existence of $\text{H}_2\text{O}/\text{CO}_2$ -rich phases with $^{40}\text{Ar}/\text{Cl}$ ratios that are “remarkably uniform over large distances,” with enrichments of these two incompatible elements by almost four orders of magnitude relative to the bulk upper-mantle values. These conclusions have been confirmed by *Johnson et al.* [2000], who analyzed the fluid inclusions in Canadian and other African diamonds and found $^{40}\text{Ar}/^{36}\text{Ar}$ ratios of 10,000–25,000 and $^{40}\text{Ar}^*$ poorly correlated with K, indicative of mantle-derived excess $^{40}\text{Ar}^*$ not produced by *in situ* radioactive decay of ^{40}K . Clearly, excess $^{40}\text{Ar}^*$ is abundant in the mantle and can be easily transported up into the crust.

2.8 Crustal Excess $^{40}\text{Ar}^*$

Is there only evidence then for excess $^{40}\text{Ar}^*$ in the mantle, gleaned from rocks (basalts and ultramafic xenoliths) and minerals (olivine, pyroxene, plagioclase and diamonds) that were formed in, or ascended from, the mantle? *Patterson et al.* [1993] envisage noble gases from the mantle (and the atmosphere) migrating and circulating through the crust (see Figure 3), so there should be evidence of excess $^{40}\text{Ar}^*$ in crustal rocks and minerals. In fact, noble gases in CO_2 -rich natural gas wells support such migration and circulation—that is, the isotopic signatures clearly indicate a mantle origin for the noble gases, including amounts of excess $^{40}\text{Ar}^*$ in some CO_2 -rich natural gas wells exceeding those in the mantle-derived mid-ocean ridge basalts [*Staudacher*, 1987; *Staudacher et al.*, 1989; *Ballentine*, 1997; *Burnard et al.*, 1997; *Moreira et al.*, 1998]. *Staudacher* [1987] also notes that the quantities of excess $^{40}\text{Ar}^*$ in the continental crust can be as much as five times that found in such mantle-derived mid-ocean ridge basalts [*Staudacher et al.*, 1989],

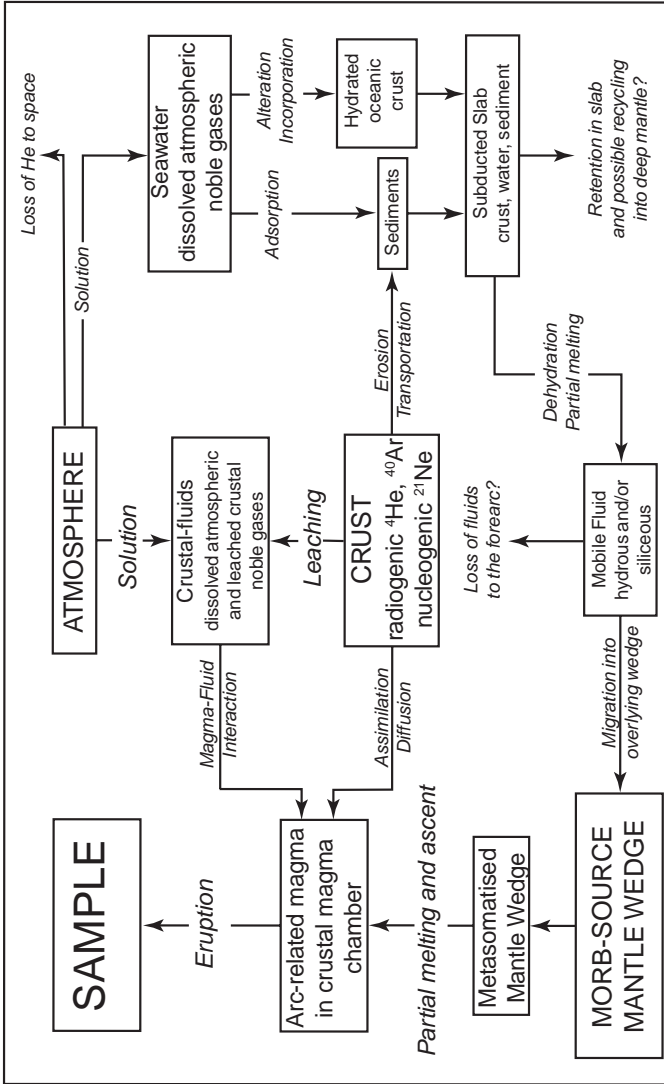


Figure 3. Schematic model of the pathways by which atmospheric, crustal and mantle-derived noble gases (including Ar) enter magmas. The three main components are shown in upper-case letters. MORB refers to Mid-Ocean Ridge Basalts, while SAMPLE refers to the noble gases trapped in samples as measured in laboratories. The arrows labelled in italics indicate the transport processes involved in moving noble gases through the system. The italic lettering not in boxes indicates pathways which remove noble gases from the system.

strongly suggesting that excess $^{40}\text{Ar}^*$ in crustal rocks and their constituent minerals could well be the norm rather than the exception, thus making all K-Ar (and Ar-Ar) dating questionable.

It has now been established that some diamonds (albeit micro-diamonds) can form in the crust—during high-grade metamorphism [Sobolev and Schatsky, 1990; Dobrzhinetskaya *et al.*, 1995] and via shock metamorphism as a result of meteorite or asteroid impact [Hough *et al.*, 1997]. The pressures and temperatures of high-grade metamorphism had been regarded as insufficient to produce diamonds, but the key ingredient was found to be volatile N_2 - CO_2 -rich fluids. Noble gas data on these diamonds are not yet available, due to their size and rarity, but such data have been definitive in establishing the crustal origin of carbonado diamonds [Ozima *et al.*, 1991]. Nevertheless, they still contain excess $^{40}\text{Ar}^*$.

Dalrymple [1991], referring to metamorphism and anatexis (melting) of rocks in the crust, commented, “If the rock is heated or melted at some later time, then some or all the ^{40}Ar may escape and the K-Ar clock is partially or totally reset.” In other words, $^{40}\text{Ar}^*$ escapes to migrate in the crust where it may then be incorporated in other minerals as excess $^{40}\text{Ar}^*$, just as $^{40}\text{Ar}^*$ degassing from the mantle does. Thus, for example, excess $^{40}\text{Ar}^*$ has been recorded in many minerals (some of which contain no ^{40}K) in crustal rocks, such as quartz, plagioclase, pyroxene, hornblende, biotite, olivine, beryl, cordierite, tourmaline, albite and spodumene [Damon and Kulp, 1958; Funkhouser *et al.*, 1966; Laughlin, 1969]—in pegmatites, metamorphic rocks, and lavas. And it is not just K-Ar dating analyses that detect excess $^{40}\text{Ar}^*$, as Lanphere and Dalrymple [1976] used the ^{40}Ar - ^{39}Ar method to confirm the presence of excess $^{40}\text{Ar}^*$ in feldspars and pyroxenes. Indeed, Pickles *et al.* [1997] obtained 128 Ar isotopic analyses from ten profiles across biotite grains in amphibolite-granulite facies metamorphic rock and apparent ^{40}Ar - ^{39}Ar “ages” within individual grains ranged from 161 to 515 Ma (see Figure 4). Pickles *et al.* [1997] concluded that these observations couldn’t be solely due to radiogenic build-up of $^{40}\text{Ar}^*$, but must be the result of incorporation by diffusion of excess $^{40}\text{Ar}^*$ from an external source, namely, $^{40}\text{Ar}^*$ from the mantle and other crustal rocks and

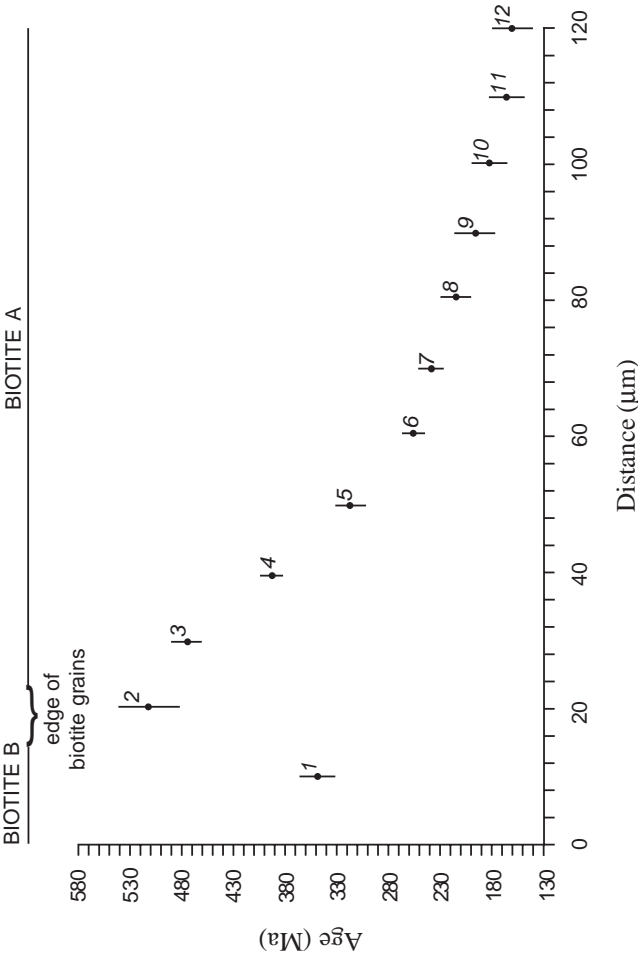


Figure 4. Apparent age versus distance profile across adjacent biotite grains in an amphibolite-granulite facies metamorphic rock from the Italian Alps [after *Pickles et al.*, 1997—their profile 8 across sample 85370]. The high spatial resolution profile is along a “trench” produced by the beam from an ultraviolet laser ablation microprobe which is parallel to the biotite cleavage and perpendicular to the grain boundary. Apparent ages range from 515 ± 27 Ma at the edge of biotite A to 161 ± 19 Ma $100 \mu\text{m}$ in from the edge of biotite A. The high apparent ages at the grain boundary cannot be attributed to alteration because scanning electron microscope (SEM) photographs discount it.

minerals. Thus, *Harrison and McDougall* [1980] were able to calculate a well-defined law for ^{40}Ar diffusion from hornblende in a gabbro due to heating. They also found that the excess $^{40}\text{Ar}^*$ which had developed locally in the intergranular regions of the host gabbro reached partial pressures in some places of at least 10^{-2} atm.

This crustal migration of $^{40}\text{Ar}^*$ is known to cause grave problems in attempted regional geochronology studies. In the Middle Proterozoic Musgrave Block of northern South Australia, *Webb* [1985] found a wide scatter of K-Ar mineral “ages” ranging from 343 Ma to 4493 Ma due to inherited (or excess) $^{40}\text{Ar}^*$, so that no meaningful interpretation could be drawn from the rocks (granulite, gneiss, pseudotachylyte, migmatite, granite and diabase). Of the diabase dikes which gave anomalous ages, he concluded that the “basic magmas probably formed in or passed through zones containing a high partial pressure of $^{40}\text{Ar}^*$, permitting inclusion of some of the gas in the crystallizing minerals.” Likewise, when *Baksi and Wilson* [1980] attempted to Ar date Proterozoic granulite-facies rocks in the Fraser Range (Western Australia) and Strangways Range (central Australia), they found that garnet, sapphirine and quartz in those rocks contained excess $^{40}\text{Ar}^*$ which rendered their Ar dating useless because of “ages” higher than expected. They also concluded that the excess $^{40}\text{Ar}^*$ was probably incorporated at the time of formation of the minerals, and their calculations suggested a partial pressure of ≈ 0.1 atm Ar in the Proterozoic lower crust of Australia, which extends over half the continent.

In a detailed ^{40}Ar - ^{39}Ar dating study of high-grade metamorphic rocks in the Broken Hill region of New South Wales (Australia), *Harrison and McDougall* [1981] found evidence of widely distributed excess $^{40}\text{Ar}^*$. The minerals most affected were plagioclase and hornblende, with step-heating ^{40}Ar - ^{39}Ar “age” spectra yielding results of up to 9.588 Ga (see Figure 5). Such unacceptable “ages” were produced by excess $^{40}\text{Ar}^*$ release, usually at temperatures of 350–650°C and/or 930–1380°C, suggesting the excess $^{40}\text{Ar}^*$ is held in sites within the respective mineral lattices with different heating requirements for its release. There are three principal trapping sites for Ar in solids—structural holes, edge dislocations and lattice vacancies. (Argon is also known to be held

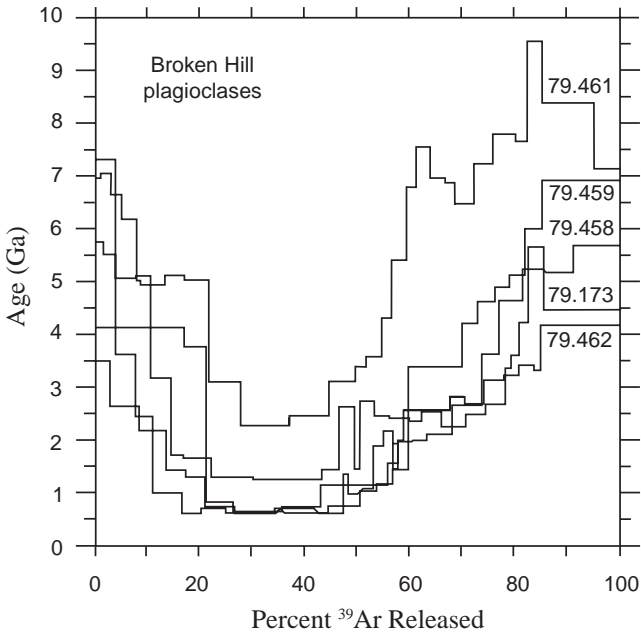


Figure 5. The ^{40}Ar - ^{39}Ar “age” spectra for plagioclases from mafic granulites near the North Broken Hill mine and at Black Bluff [after *Harrison and McDougall*, 1981]. All “age” spectra are characterized by a saddle-shape and each is labeled with its sample number. The plagioclase from sample 79.461 yields an apparent age of 9.588 Ga at over 80 percent ^{39}Ar released.

sometimes in some minerals in fluid inclusions.) Clearly, that study showed that at crustal temperatures, which are less than 930°C , some excess $^{40}\text{Ar}^*$ will always be retained in those trapping sites in minerals where it is obviously “held” more tightly, thus rendering K-Ar and ^{40}Ar - ^{39}Ar dating questionable. *Harrison and McDougall* [1981] were only able to produce a viable interpretation of the data because they made assumptions about the expected age of the rocks and of a presumed subsequent heating event (based on Pb-Pb and Rb-Sr dating), the latter being the time when they conjecture that accumulated $^{40}\text{Ar}^*$ was released from minerals causing a significant regional Ar partial pressure of $\approx 3 \times 10^{-4}\text{atm}$ to develop.

Several studies have now proved the existence of excess $^{40}\text{Ar}^*$ in some

of the most debated samples in the Dora Maira area of the Western Alps (Italy), and have suggested that this is a widely spread phenomenon in high pressure metamorphic terranes [Arnaud and Kelley, 1995; Scaillet, 1996]. Indeed, *Sherlock and Arnaud* [1999] performed ^{40}Ar - ^{39}Ar analyses on phengite (white mica) with a Rb-Sr “age” of 80.2 ± 1.6 Ma and on a whole-rock sample from high-pressure, low temperature metamorphic rocks from the Tavsanli Zone of northwest Turkey and obtained a convincing ^{40}Ar - ^{39}Ar plateau “age” of 107 ± 2 Ma and a $^{36}\text{Ar}/^{40}\text{Ar}$ versus $^{39}\text{Ar}/^{40}\text{Ar}$ isochron intercept “age” of 107.5 ± 2 Ma for the phengite. Whole-rock laser spot Ar-Ar “ages” ranged from 87 ± 4 to 100 ± 3 Ma. Assuming the validity of the Rb-Sr “age,” *Sherlock and Arnaud* [1999] concluded that due to excess $^{40}\text{Ar}^*$ in the phengite both the plateau and isochron “ages” are incorrect and have no geological meaning, and that:

The statistical tools have not been extensively explored in the forecast of such difficult applications, following the development of new sampling techniques and the increased awareness of excess argon, and the failure of some minerals to behave as a closed isochronous system. Failure to account for these possibilities will most likely lead to the generation of incorrect ages . . . We suggest that the use of the isochron and spectral approach in ^{40}Ar - ^{39}Ar geochronology cannot always be relied upon to prove or disprove the presence of excess argon, and therefore cannot ultimately be used to prove or disprove the validity of a plateau age.

Of course, having admitted that the presence of excess $^{40}\text{Ar}^*$ may go unnoticed and cannot be proved or disproved by this analytical method, the real benchmark is the assumption that the Rb-Sr “age” is correct and acceptable according to the uniformitarian timescale.

Nevertheless, direct measurements of crustal Ar have now been reported from the 9 km deep KTB drill-hole, Germany, as a consequence of the Continental Deep Drilling Project [Drescher *et al.*, 1998]. $^{40}\text{Ar}/^{36}\text{Ar}$ ratios varied from 550 to 37,200 (the atmospheric ratio is 295.5), which is indicative of enormous quantities of excess $^{40}\text{Ar}^*$. Furthermore, there was no apparent depth dependence in the $^{40}\text{Ar}/^{36}\text{Ar}$ ratios (and excess $^{40}\text{Ar}^*$), implying that the Ar is not due to atmospheric contamination but is generated and resident in crustal rocks as a result of radioactive decay and degassing of a primordial content. Different

rock types revealed slightly different isotopic characteristics, due to their K contents (gneisses had on average four times more excess $^{40}\text{Ar}^*$ than amphibolites). *Drescher et al.* [1998] thus estimated a loss rate or degassing flux of $1\text{-}6 \times 10^9$ atoms $\text{m}^{-2}\text{s}^{-1}$ for ^{40}Ar from crustal rocks, in good agreement with theoretical estimates from accumulated gases in crustal fluids.

2.9 Mantle-Crust Domains and Excess $^{40}\text{Ar}^*$

Harte and Hawkesworth [1986] have identified domains within the mantle and crust and described the interactions among them, all of which are relevant to the migration and circulation of Ar (and thus excess $^{40}\text{Ar}^*$) from the lower mantle to the crust and to lavas extruded on the earth's surface. The six domains are physically distinct units (see Figure 6) which show wide differences in average physical and chemical properties, as well as apparent age, structure and tectonic behavior. They are the lower mantle (below 660 km), upper mantle, continental mantle lithosphere, oceanic mantle lithosphere, continental crust and oceanic crust, and each is a distinct geochemical reservoir. Each domain may provide material for magmatic rocks, and particular geochemical features of magmas may be associated with particular domains. Thus the convecting upper mantle which comes to the surface at mid-ocean ridges may be identified as the source of most geochemical features of mid-ocean ridge basalts, including their excess $^{40}\text{Ar}^*$ contents. Similarly, the convecting lower mantle is regarded as the primordial or bulk earth geochemical reservoir, which may also contribute excess $^{40}\text{Ar}^*$ to mid-ocean ridge basalts, but is more important for its contribution to ocean island basalts (for example, Hawaii) and other plume-related basalts (continental alkali basalts and continental flood basalts). However, considerable complexity may be added to the deeper mantle geochemical structure as a result of localized accumulation of subducted oceanic lithosphere.

Porcelli and Wasserburg [1995] have proposed a steady-state upper mantle model for mass transfer of rare gases, including Ar. The rare gases in the upper mantle are derived from mixing of rare gases from

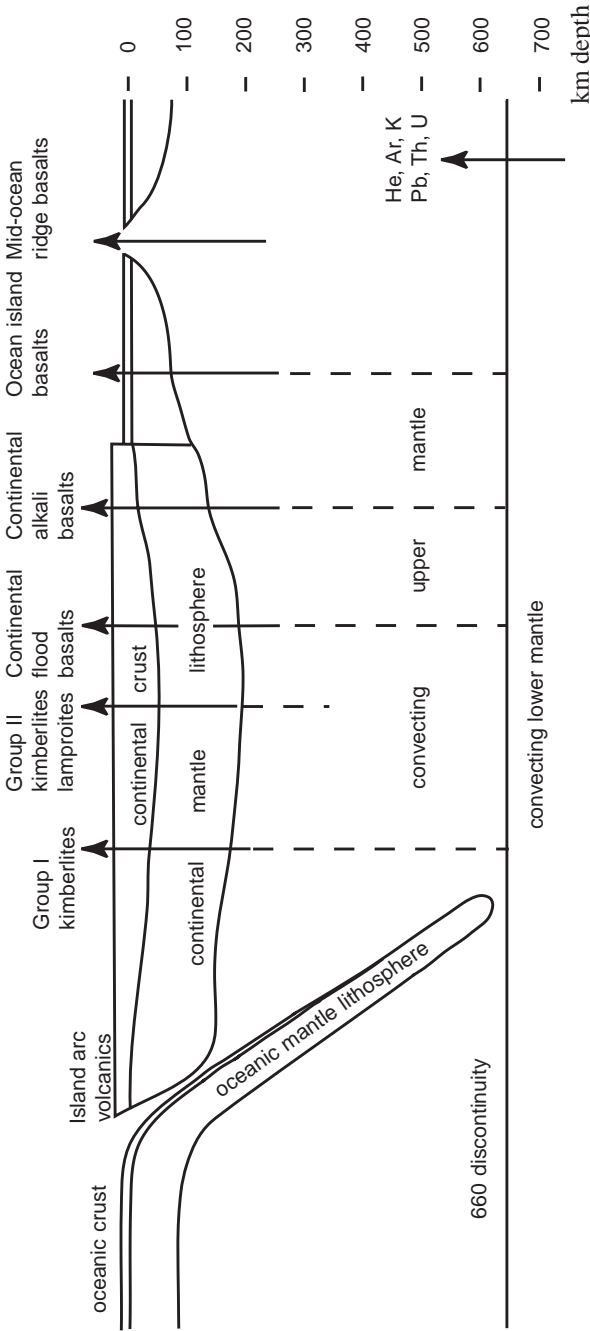


Figure 6. Mantle-crust domains and the distribution of mafic magmas [after *Harte and Hawkesworth, 1986*]. Helium (He), Ar, K, Pb, Th and U are the elements whose proportions and isotope compositions in the convecting upper mantle are strongly determined by entrainment from the lower mantle.

the lower mantle, subducted rare gases, and radiogenic nuclides produced *in situ*. Porcelli and Wasserburg claim that all of the ^{40}Ar in the closed-system lower mantle has been produced by ^{40}K decay in the lower mantle, but this claim is based on the assumption of a 4.5 Ga earth. In any case, they contradict themselves, because they also state that, the “lower mantle is assumed to have evolved isotopically approximately as a closed system with the *in situ* decay of ^{129}I , ^{244}Pu , ^{238}U , ^{232}Th , and ^{40}K adding to the complement of initial rare gases.” In other words, they admit that some of the ^{40}Ar must be primordial and not derived from radioactive ^{40}K . They then go on to claim that in the upper mantle, ^{40}K decay further increases the radiogenic ^{40}Ar from the lower mantle by a factor of ≈ 3 , but again this presupposes a 4.5 Ga earth and doesn’t allow for primordial ^{40}Ar that could well be also in the upper mantle if it is admitted to be in the lower mantle.

In the case of the continental and oceanic lithospheric domains, the lack of convective stirring means that different geological processes and events may implant in each domain a variety of geochemically distinct materials which will remain isolated from one another. Therefore, these domains do not have a single set of geochemical characteristics; thus identification of geochemically defined “sources” with particular physically defined crust-mantle domains is complex, and the geochemical definition of particular reservoirs cannot be regarded as simply definition of major physical entities. Nevertheless, excess $^{40}\text{Ar}^*$ will be added to these domains by the passage of basaltic magma plumes from the upper (and lower) mantle to the earth’s surface.

Furthermore, the processes of oceanic lithosphere formation from the convecting upper mantle in association with mid-ocean ridge activity mean that its isotopic characteristics everywhere will be largely similar to those of the convecting upper mantle and mid-ocean ridge basalts, including the addition of excess $^{40}\text{Ar}^*$. The corollary to this is that the oceanic crust is formed as part of these same processes. However, the oceanic crust generally has a thin veneer of sediments over it, and thick wedges of sediments adjacent to the domains of continental crust, whereas sections of the oceanic crust are hydrothermally altered. The compositions of these components of the oceanic crust may, therefore,

include a considerable contribution from continental detritus and ocean water, so that this oceanic crustal material may give rise to a distinct geochemical reservoir, the fate of which during subduction back into the upper mantle becomes critically important if it contributes to island arc volcanics, plume-related intra-plate magmas and mantle-derived xenoliths.

The complexity of continental crustal material is well known through direct observation, and the mantle lithosphere attached to it may be expected to show a similar complexity. Nevertheless, it is evident that excess $^{40}\text{Ar}^*$ also resides in the continental mantle lithosphere, as indicated by xenoliths [Matsumoto *et al.*, 1998]. Likewise, there is evidence of excess $^{40}\text{Ar}^*$ in crustal magmatic rocks (for example, gabbros [Harrison and McDougall, 1980], in pegmatites [Laughlin, 1969]), migrating through metamorphic terranes [Baksi and Wilson, 1980; Harrison and McDougall, 1981; Webb, 1985; Drescher *et al.*, 1998], and in natural gas in sedimentary reservoirs [Staudacher, 1987].

Thus the excess $^{40}\text{Ar}^*$ found in crustal rocks is in part primordial Ar not generated by radioactive decay of ^{40}K , but has been circulated up into the crustal rocks where it may continue migrating and building up regionally to partial pressure status. Because the evidence clearly points to this being the case, then when samples of crustal rocks are analyzed for K-Ar and Ar-Ar dating, the investigators can never really be sure that whatever $^{40}\text{Ar}^*$ is in their samples is from *in situ* radioactive decay of ^{40}K since the formation of the rocks, or whether some or all of it is from the “excess $^{40}\text{Ar}^*$ ” geochemical reservoirs in the lower and upper mantles. This could even be the case when K-Ar and Ar-Ar analyses yield dates compatible with other radioisotopic dating systems, and/or with fossil dating based on evolutionary assumptions. And there would be no way of knowing, because the $^{40}\text{Ar}^*$ from radioactive decay of ^{40}K cannot be distinguished analytically from primordial ^{40}Ar not derived from radioactive decay, except of course by external assumptions about the ages of the samples and of the earth. Therefore, these considerations call into question all K-Ar dating, whether model ages or isochron ages, and all Ar-Ar dating, as well as fossil dating that has been calibrated against K-Ar dates.

2.10 $^{40}\text{Ar}^*$ Loss

It is evident then that excess $^{40}\text{Ar}^*$, whether inherited or primordial, is a significant problem for K-Ar and Ar-Ar dating. However, for these “dating” methods to work successively the rocks and minerals to be dated must not only not contain any excess $^{40}\text{Ar}^*$, but they must have retained all of the $^{40}\text{Ar}^*$ produced within them by decay of ^{40}K . Yet $^{40}\text{Ar}^*$ loss from minerals is claimed to be a persistent problem. Because Ar is a noble (non-reactive) gas, it does not form bonds with other atoms in a crystal lattice, so no mineral phase preferentially takes up Ar and it is claimed that it can be readily lost from the minerals where it was originally produced. Argon also displays limited partition into fluids. *Faure* [1986] lists the causes to which Ar loss can be attributed:

- inability of the mineral lattice to retain Ar even at low temperatures and atmospheric pressure;
- either partial or complete melting of rocks followed by crystallization of new minerals from the resulting melt;
- metamorphism at elevated temperatures and pressures resulting in complete or partial Ar loss depending on the temperature and duration of the event;
- increase in temperature due to deep burial or contact metamorphism causing Ar loss from most minerals without producing any other physical or chemical changes in the rock;
- chemical weathering and alteration by aqueous fluids, leading not only to Ar loss but also to changes in the K content of minerals;
- solution and redeposition of water-soluble minerals; and
- mechanical breakdown of minerals, radiation damage, and shock waves (even excessive grinding during preparation of samples for “dating” by the K-Ar method may cause Ar loss).

However, it needs to be remembered that such explanations may often be resorted to in order to resolve conflicts between K-Ar and Ar-Ar dating results and expectations based on the evolutionary timescale, rather than being based on substantial experimental verification. Nevertheless, Ar is soluble in water [*Mazor and Fournier, 1973; Mauger, 1977*] and has a similar molecular diameter to water, so it can be removed from

minerals and rocks by ground and thermal waters.

A very good demonstration of apparent $^{40}\text{Ar}^*$ loss from different minerals in a thermal event is provided in the contact metamorphic zone associated with the Eldora stock in the Front Range of Colorado [Hart, 1964]. The 54 Ma quartz monzonite stock is intruded into Precambrian amphibolites and schists that are regarded as approximately 1350 Ma. Hart analyzed biotite, hornblende and K-feldspar at increasing distances from the intrusive contact and found that, even though there were only very minor mineralogical contact metamorphic effects and the petrographic alteration was of limited extent, there were profound effects on the K-Ar mineral “ages” as a result of losses of varying amounts of $^{40}\text{Ar}^*$ at large distances from the stock (see Figure 7) [Hart, 1964], based on the evolutionary timescale. The fraction of $^{40}\text{Ar}^*$ lost from each of the minerals decreased as a function of distance from the contact and reflected the differing retentivities of these minerals for $^{40}\text{Ar}^*$. The coarse biotite lost almost all of its $^{40}\text{Ar}^*$ and was largely reset out to a distance of about 100 m (300 feet) from the contact, and the effects of $^{40}\text{Ar}^*$ loss could be traced for more than 2 km beyond that distance. The K-Ar biotite “dates” finally stabilized at 1200 Ma at a distance of about 4.25 km from the contact. The K-feldspar “dates” increased somewhat erratically away from the contact and showed the effects of a substantial fraction of $^{40}\text{Ar}^*$ loss even at a distance of almost 7 km from the contact. This distance can hardly be said to be within the thermal aureole of the stock, and reflects the now widely accepted view that K-feldspars may lose Ar by diffusion even at ambient temperatures [Dickin, 1995]. However, hornblende displayed superior $^{40}\text{Ar}^*$ retention properties, with the loss of $^{40}\text{Ar}^*$ confined primarily to within approximately 3 m (10 feet) of the contact and then diminishing rapidly. Approximately 40 m (100 feet) from the contact the hornblende K-Ar “dates” reached a plateau value of 1200 Ma and ultimately rose to 1375 Ma about 4.3 km from the contact, which coincides approximately with the “date” for the regional metamorphism of the amphibolites and schists. (The variation in the Rb-Sr apparent “ages” in the coarse biotite will be discussed in Section 4.4.)

The Ar-Ar method is now routinely used, often in preference to the

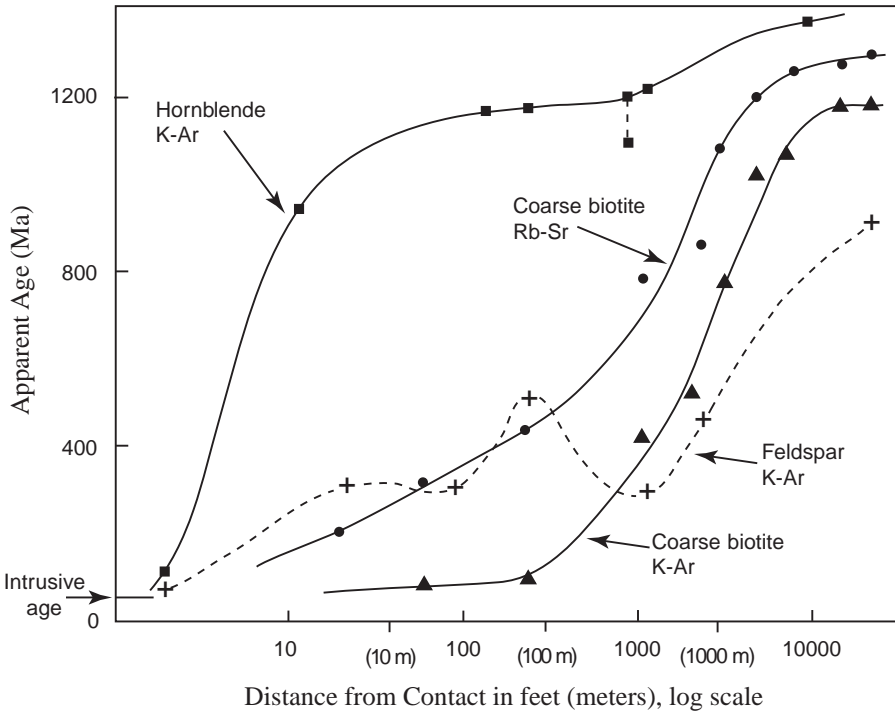


Figure 7. Plot of apparent mineral “ages” against outward distance from the contact of the Eldora stock, Colorado [after *Hart, 1964*].

K-Ar method, and depends on the diffusion of $^{40}\text{Ar}^*$ as minerals are heated in the “dating” laboratory. It has been found that when a K-bearing mineral is heated, the $^{40}\text{Ar}^*$ that has accumulated in it escapes by diffusion into the intergranular space, provided that the mineral remains stable under the experimental conditions. *Harrison* [1981] experimentally measured the $^{40}\text{Ar}^*$ loss from two compositionally contrasting hornblendes to determine the rate of $^{40}\text{Ar}^*$ diffusion. To be assured that the $^{40}\text{Ar}^*$ was released by diffusion, he heated the hornblendes under hydrothermal conditions at different temperatures and calculated the diffusion coefficients for Ar from the fraction of the $^{40}\text{Ar}^*$ released as a function of temperature. Coupled with geological data (that is, data such as that of *Hart* [1964] and *Harrison and McDougall* [1980] obtained

from field studies based on assuming the evolutionary timescale), *Harrison* [1981] obtained a value for the diffusion coefficient of Ar in hornblende of $0.024 (+0.053/-0.011) \text{ cm}^2\text{s}^{-1}$ and found that the ^{40}Ar diffusivity in hornblendes did not appear to be strongly dependent on the Mg/Fe ratio. He used these results to calculate closure temperatures (temperature below which the isotopic clock is “switched on,” or in other words, the temperature at which the mineral becomes a closed system with respect to loss by diffusion of radiogenic daughter products) for the hornblendes with diffusion radii on the order of 40–80 μm varying from about 580°C during “rapid” cooling to about 480°C for “slow” cooling. *Harrison et al.* [1985] conducted similar experiments to measure $^{40}\text{Ar}^*$ loss from hydrothermally treated biotite, calculating a diffusion coefficient of $0.077 (+0.21/-0.06) \text{ cm}^2\text{s}^{-1}$ over the temperature interval of 600–750°C and inferring an effective diffusion radius of approximately 140 μm , about double that of hornblende. They also found that ^{40}Ar diffusivity in biotites is strongly dependent on the Fe/Mg ratio, and predicted that Fe-rich biotite was significantly less retentive of $^{40}\text{Ar}^*$ than biotites of intermediate Fe/Mg compositions. This prediction was confirmed by *Grove and Harrison* [1996], who found that most biotite grains of intermediate composition possess comparable $^{40}\text{Ar}^*$ diffusion properties. However, in contrast to these diffusion experiments at elevated temperatures, *Fechtig and Kalbitzer* [1966] found from extensive experimentation that diffusion at room temperatures is always so small that no appreciable Ar losses occur.

Finally, it is worth considering an example of K-Ar “dating” of some “ancient” lava flows. Since we have seen that recent lava flows often contain excess $^{40}\text{Ar}^*$ it is conceivable that “ancient” lava flows would likewise have had excess $^{40}\text{Ar}^*$ at least initially, but both the experimental evidence of $^{40}\text{Ar}^*$ diffusion and the geological evidence of $^{40}\text{Ar}^*$ loss as described above would suggest “ancient” lava flows should exhibit a net $^{40}\text{Ar}^*$ loss. *Austin and Snelling* [1998] reported on K-Ar “dating” of the Middle Proterozoic Cardenas Basalt of the eastern Grand Canyon, Arizona, adding K-Ar data from seven samples previously analyzed by earlier investigators to eight samples of their own. Figure 8 is a plot of the $^{40}\text{Ar}^*$ versus ^{40}K data for the Cardenas Basalt with an isochron fitted

to the data yielding an age of 516 ± 30 Ma. This is less than half the accepted “age” of 1100 Ma derived from a 5-point Rb-Sr isochron by the *McKee and Noble* [1976] and from a 10-point Rb-Sr isochron by *Larsen et al.* [1994], which is thus now being widely regarded as the best “age” yet obtained for Grand Canyon strata. Based on the stratigraphic position in the overall Grand Canyon sequence the K-Ar isochron “age” (Cambrian) is clearly in error, but why? *Austin and Snelling* [1998] considered five possible explanations—Ar reset, Ar leakage, Ar inheritance, Ar mixing, and change of decay. Of significance here is that the first two models involve Ar loss and they have been the

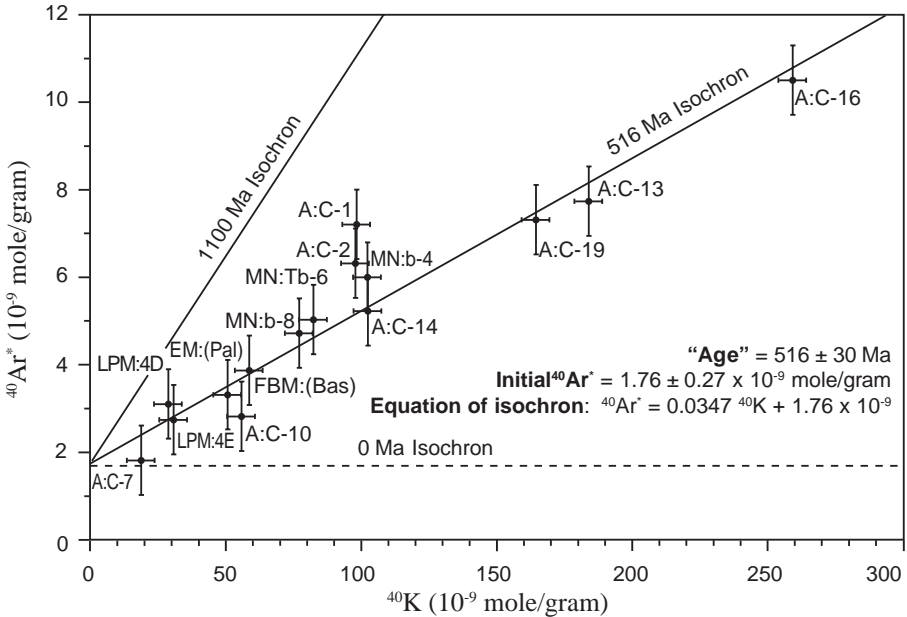


Figure 8. $^{40}\text{Ar}^*$ versus ^{40}K for the Middle Proterozoic Cardenas Basalt of the eastern Grand Canyon, Arizona [after *Austin and Snelling*, 1998]. “Isochron” and “age” calculated from 14 of 15 samples. One sample data point (A:C-1) was not included in the isochron calculation. Bars represent two-sigma uncertainties. The 1100 Ma isochron is included for comparison to show where the K-Ar isochron should be if the K-Ar data were in agreement with the Rb-Sr data.

usual explanation for this disparity between the K-Ar and Rb-Sr “ages,” but Austin and Snelling have demonstrated from the data that such explanations cannot explain the disparity. In fact, the y-intercept of the 516 Ma isochron through the K-Ar data indicates that there was some initial $^{40}\text{Ar}^*$ in these lava flows when they were extruded. The data are also fully compatible with no Ar diffusion from the flows after extrusion. All this is consistent with what we know of so many recent lava flows, but it still doesn’t explain conventionally why therefore the K-Ar “age” is less than half the Rb-Sr “age.” Therefore, if there has been no $^{40}\text{Ar}^*$ loss from these lava flows since their extrusion, then it could be argued that their K-Ar “age” is their maximum age, even though it is less than half of their conventional Rb-Sr “age”, and that given they instead contained excess $^{40}\text{Ar}^*$ when extruded, their true age could be even lower.

The assessment of what constitute acceptable/valid “dates,” of course, is based on their consistency within the uniformitarian/evolutionary timescale, which is hardly an objective yardstick. Thus, in the case of the Cardenas Basalt $^{40}\text{Ar}^*$ loss is conventionally offered for the apparent failure of K-Ar “dates” to match the acceptable Rb-Sr “date” consistent with the uniformitarian “age.” Similarly, *Mankinen and Dalrymple* [1972] rejected a 1.6 ± 0.1 Ma “date” from a K-Ar determination on the glassy matrix of a basalt because plagioclase phenocrysts in the same basalt had yielded a K-Ar “age” of 7.4 ± 0.2 Ma. Even though the glassy matrix constitutes 75% of the rock and also contains plagioclase laths, and the rock’s K_2O content is almost entirely concentrated in the glass which is described as unaltered, this “age” discrepancy was nonetheless blamed on $^{40}\text{Ar}^*$ loss from the glass. Because that conclusion is somewhat subjective, it could be equally argued that the maximum K-Ar “age” of this rock is only 1.6 ± 0.1 Ma, and the true age could be considerably less. By way of contrast, *Evernden et al.* [1964] analyzed several devitrified volcanic glasses of “known age” (that is, according to the uniformitarian timescale) and all yielded K-Ar ages that were “too young,” some being “virtually zero ages,” so they attributed this to $^{40}\text{Ar}^*$ loss due to devitrification. But how could $^{40}\text{Ar}^*$ be equally lost from unaltered glass and devitrified (altered) glass? Alternately, could it be

that the glass retains less inherited $^{40}\text{Ar}^*$ from the magma when the lavas cool, while the larger phenocrysts retain more? If so, then the K-Ar “ages” would be meaningless maximum ages due to differential inheritance, and the actual timescale involved would be drastically shorter.

Nevertheless, there is a steady loss of $^{40}\text{Ar}^*$ from crustal rocks to the atmosphere, on the order of $1\text{--}6 \times 10^9$ atoms $\text{m}^{-2}\text{s}^{-1}$ [Drescher *et al.*, 1998], which is a result of degassing of primordial ^{40}Ar and $^{40}\text{Ar}^*$ from radioactive decay of ^{40}K in the mantle and crust. However, it has been amply demonstrated that this $^{40}\text{Ar}^*$ flux produces a build-up of excess $^{40}\text{Ar}^*$ in both mantle-derived and crustal rocks, which thus yield excessively old “ages.” On the other hand, $^{40}\text{Ar}^*$ loss can clearly be a problem locally, resulting in “ages” much younger than expected. The key to assessing the acceptability of a K-Ar or Ar-Ar “date” is thus “knowing” what “age” is to be expected for the rocks being “dated,” which in the case of the Cardenas Basalt in the eastern Grand Canyon is the Rb-Sr “isochron age” that in turn has no independent reliability cross-check apart from a “stratigraphic age.” Therefore, when the $^{40}\text{Ar}^*$ contents of samples are measured there is no way of determining categorically whether there has been $^{40}\text{Ar}^*$ loss, or gain (via excess $^{40}\text{Ar}^*$), even when the calculated “ages” are compatible with other radioisotopic dating systems or expected “ages” based on stratigraphy, all of which renders such K-Ar and Ar-Ar “dates” questionable at best.

3. The Uranium-Thorium-Lead (U-Th-Pb) Radioisotopic System

Historically, U-Th-Pb “dating” was the first method to be used on minerals, in particular, U-bearing minerals. As the technology became available to measure these elements at trace levels and the isotopic ratios, the U-Th-Pb dating methods were also applied to whole rocks.

3.1 Open-System Behavior and U-Th-Pb Whole-Rock “Dating”

However, the early studies in whole-rock dating of crystalline rocks

showed the method to be of little value as a geochronological tool, because unfortunately the U-Pb and Th-Pb systems rarely stay closed due to the mobility of Pb, Th and especially U, under conditions of low-grade metamorphism and superficial weathering [Dickin, 1995]. Indeed, it was found that U appeared to have been lost from samples which exhibited no discernible effects of alteration, so that it was even suggested the leaching of U from surficial rocks might be a universal phenomenon [Stuckless, 1986]. For example, concentrations of U, Th and Pb, and the isotopic composition of Pb, for whole-rock samples of granitoids show:

- that open-system behavior is nearly universal in the surface and near-surface environment; and
- that elemental mobility is possible to depths of several hundred meters [Stuckless, 1986].

Several identified factors that control U and/or Pb mobility include:

- the mineralogical sites for U and its daughter products;
- access of ground water to these sites;
- the volume of circulating water; and
- the chemistry of the ground water.

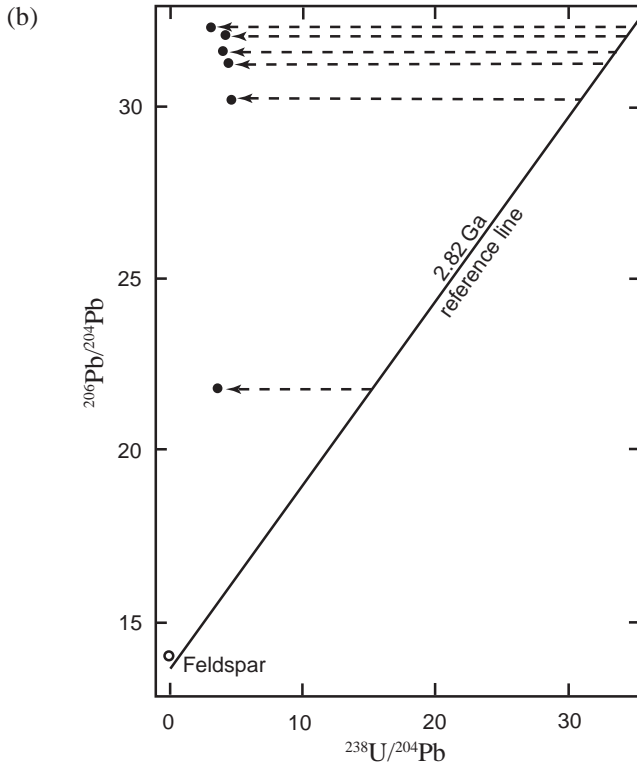
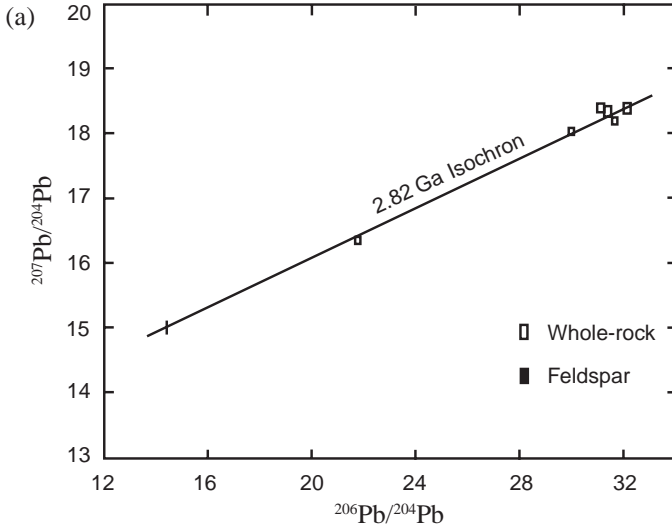
Rosholt and Bartel [1969] found that Th-Pb analyses of whole-rock samples from the Granite Mountains batholith of Wyoming yielded an approximate isochron age of 2.8 Ga, but on a U-Pb isochron diagram the system displayed disastrous U losses so that no age could be determined (see Figure 9 b and c). Surface and shallow drill-core (<30 m) samples of the granite of the Lankin Dome of the Granite Mountains batholith were found to have lost up to 90% of their U as a result of exposure to the near-surface environment [Rosholt *et al.*, 1973; Stuckless and Nkomo, 1978]. Yet in Figure 10 it can be seen that even samples that came from below 30 m depth are likewise depleted in U by up to more than 80%. Of course, these conclusions are based on the expectation of how much U should be in the samples if they are the claimed “age.” Analysis of minerals separated from U-depleted whole-rock samples showed an excess of radiogenic Pb in biotite and epidote, whereas analysis of these same minerals separated from a non-U-depleted sample recovered from a depth of 472 m showed that the biotite and epidote contain more than 60% of the total U and Th in the whole-rock [Stuckless

and Nkomo, 1978]. Furthermore, Ludwig and Silver [1977] noted that many K-feldspars separated from Precambrian rocks contained unsupported radiogenic Pb (that is, no parent isotopes in the mineral), but the composition of the unsupported Pb was compatible with the “age” of the host rock. This was interpreted as the Pb having been gained very late in the history of the feldspar, meaning that like the U loss, the Pb gain by K-feldspar must have occurred when the rocks were exposed to the near-surface environment. Nevertheless, in the Granite Mountains of Wyoming the Th-Pb system is closed and the U-Pb system is open on a whole-rock scale for samples that contain K-feldspar (Figure 9 b and c), but rocks that lack K-feldspar exhibit open-system behavior in both the Th-Pb and U-Pb systems [Stuckless and Nkomo, 1978; Stuckless et al., 1981].

In practice, therefore, the mobility of U, Th and Pb renders their use for simple U-Pb isochron dates very limited [Dickin, 1995]. This open-system behavior would largely invalidate U-Pb dating, but it is claimed that because a relationship exists between the parent ^{235}U and ^{238}U on the one hand, and daughter ^{207}Pb and ^{206}Pb nuclides on the other, and these nuclides show coherent chemical behavior, age information can still be obtained even from samples with disturbed systems. However, the focus has shifted back to using the U-Th-Pb dating technique on minerals, such that this has become the most popular and highly regarded radioisotopic dating method currently in use. The primary target minerals are grains of zircon (ZrSiO_4), baddeleyite (ZrO_2), titanite (CaTiSiO_5) and/or monazite ((Ce, La, Th) PO_4), though thorite (ThO_2), apatite ($\text{Ca}_5(\text{PO}_4)_3$), garnet and other minerals are sometimes used.

3.2 Pb Loss and Mineral U-Th-Pb “Dating”

The concentrations of U and Th in zircon, for example, range from a few hundred to a few thousand parts per million and average 1350 and 550 ppm respectively [Faure, 1986]. The presence of these elements in zircon can be attributed both to isomorphous replacement of Zr^{4+} (ionic radius = 0.87\AA) by U^{4+} (1.05\AA) and Th^{4+} (1.10\AA) and to the presence of inclusions of thorite, though the substitution of Zr^{4+} by U^{4+} and Th^{4+} is



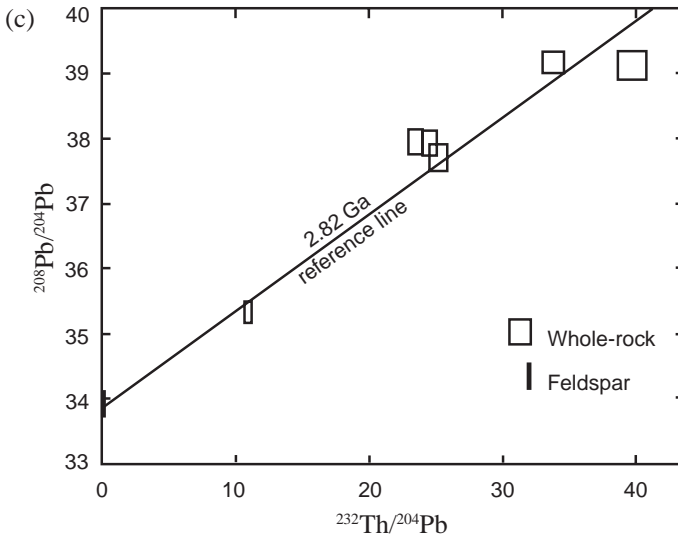


Figure 9 (a) and (b) opposite, and (c) above. Whole-rock plus mineral isochron diagrams for the Granite Mountains batholith, Wyoming [after *Rosholt and Bartel, 1969*]. (a) Pb-Pb isochron; (b) U-Pb system showing displacement of whole-rock data points far to the left of the 2.82 Ga reference line (derived from the Pb-Pb isochron) due to disastrous U losses; (c) Th-Pb “errorchron”.

limited by differences in their ionic radii. However, equally important is the fact that Pb^{2+} , which has an ionic radius of 1.32\AA , is excluded from zircon because of its large radius and lower charge. Therefore, zircon is believed to contain very little Pb at the time of its formation and thus supposedly has very high U/Pb and Th/Pb ratios, which enhances its sensitivity as a geochronometer. For this reason, zircon is the most frequently used mineral for U-Th-Pb radioisotopic dating, particularly in igneous rocks of acid to intermediate composition. More recently, baddeleyite has been used in dating mafic igneous rocks. Also, zircon grains are sometimes found in sedimentary rocks and so are analyzed to determine the supposed ages of the sediment source rocks.

It is assumed that when the zircon grains crystallized no radiogenic Pb was in them, and that all the radiogenic Pb now measured was derived by radioactive decay from U and Th. However, there are several lines of

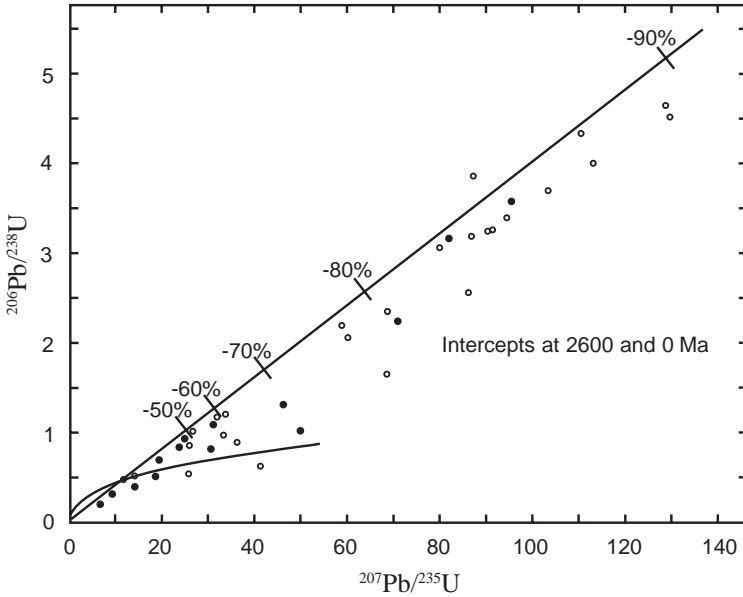


Figure 10. Concordia diagram for samples of the granite of Lankin Dome, Granite Mountains batholith, Wyoming [data from *Rosholt et al.*, 1973; *Stuckless and Nkomo*, 1978]. Circles represent samples from less than 30 m depth. A reference chord from 0 through the 2600 Ma equilibrium point on the concordia is marked with relative percentages of U loss, assuming closed-system behavior from 2600 Ma ago until 30 Ma ago. Scatter about the line is supposedly due to an average U loss of 20% ~1700 Ma ago [*Stuckless and Nkomo*, 1978]. The combined Proterozoic and recent U losses have left most surface and shallow drill-core samples with an apparent loss of greater than 80%. For most of these samples the recent U loss averages ~70%.

evidence that indicate radiogenic Pb can be inherited during crystallization of the mineral grains, and that open-system behavior is common, with radiogenic Pb loss by diffusion due to the way the Pb is held in the crystal lattices. Indeed, early dating work on U-rich minerals soon revealed that most samples yielded discordant $^{206}\text{Pb}/^{238}\text{U}$ and $^{207}\text{Pb}/^{235}\text{U}$ “ages,” which was attributed to Pb loss by *Holmes* [1954].

Ahrens [1955] found that monazite and uraninite from Zimbabwe (then Rhodesia) which yielded discordant U-Pb ages nevertheless defined a

linear array on the concordia diagram, which he attributed to Pb loss occurring by some kind of continuous diffusional process. Simultaneously, *Giletti and Kulp* [1955] demonstrated that radon (Rn) leakage by gaseous diffusion through microfissures in minerals such as uraninite could account for the disparity in U-Pb “ages.” Thus *Russell and Ahrens* [1957] postulated that intermediate members of the U-decay series were ejected into microfissures in mineral lattices by the recoil energy from α -particle emission, these nuclides and their decay products subsequently being removed by diffusion or leaching, which would account for continuous Pb loss.

Wetherill [1956a] advanced an alternative interpretation, now called the episodic Pb loss model, in which he argued that the upper intercept of the linear array with the concordia diagram corresponded to the time of formation of the minerals, whereas the lower intersection of the linear array represented the time when a thermal event caused the Pb loss from the minerals. *Wetherill* [1956b] evoked such open-system behavior because U-Pb “dates” that had been obtained had failed the crucial assumptions about initial conditions and a closed system for successful radioisotopic dating. Both *Wetherill* [1956b] and *Nicolaysen* [1957] independently developed graphical “solutions” consistent with the graphically observed results of loss of U-decay products, though *Wetherill* [1956b] preferred episodic Pb loss and *Nicolaysen* [1957] continuous Pb diffusion. *Wetherill* [1963] and *Wasserburg* [1963] subsequently derived equations to describe steady Pb loss and demonstrated its consistency with published U-Pb “age” data.

Tilton [1960] showed that U-rich minerals (primarily zircons) with similar formation “ages” from Archean shield areas on five continents all lay near a linear discordant array with a lower intersection that according to the episodic Pb loss model would imply a worldwide metamorphic event. Thus *Tilton* [1960] proposed that Pb loss was via continuous diffusion over “geological time” and supported his argument by experimentally demonstrating that Pb diffuses from zircon and U-bearing minerals at temperatures as low as 50°C.

Wasserburg [1963] also proposed that Pb loss by diffusion resulted from radiation damage to crystal lattices. This diffusional Pb loss model

was further developed by *Goldrich and Mudrey* [1972], who argued that radiation damage of U-rich minerals as a result of the α -decay of U, Th and their daughters was responsible for the formation of micro-capillary networks in the crystals which would thus become fluid filled. Lead which diffused into these fluids would be lost from the minerals when uplift and erosion of the basement rocks caused the pressure on the minerals to be released so that the micro-capillaries dilated and expelled their fluids together with the dissolved radiogenic Pb.

Meldrum et al. [1998] have confirmed that radiation damage can drastically increase the rate of Pb diffusion. Furthermore, while the diffusion rate is known to be slow [*Meldrum et al.*, 1998] and difficult to determine accurately [*Lee et al.*, 1997], higher temperatures induce faster diffusion [*Lee et al.*, 1997]. This is dramatically illustrated by the contact metamorphic effects of a Tertiary granite stock on zircon crystals in surrounding regionally metamorphosed Precambrian sediments and volcanics [*Davis et al.*, 1968]. Within 50 feet of the contact the ^{207}Pb concentration drops from 150 ppm to 30 ppm, with a corresponding drop in ^{238}U “ages” from 1405 Ma to 220 Ma (see Figure 11).

Silver and Deutsch [1963] made a pioneering case study of Pb loss from different zircon fractions in a single rock sample. They found that large zircon grains lost less Pb than smaller ones (due to the larger surface area/volume ratio of the latter), and that zircon grains with low U contents lost less Pb than high-U zircons. The latter effect was attributed to the greater radiation damage suffered by U-rich grains. In addition to losing Pb, metamict (altered due to radiation damage) zircons tend to incorporate impurities, including Fe.

Zircon crystals are often chemically and physically inhomogeneous (zoned) [*Lee et al.*, 1997], reflecting growth during crystallization from magma. Both zoned and unzoned zircon crystals may be found in the same rock. *Pidgeon* [1992] demonstrated that unzoned crystals can be the result of recrystallization of zoned crystals accompanied by loss of U, Th and Pb, and “resetting” of the U-Pb “ages.” Such recrystallization can be due to subsequent regional metamorphism. *Kröner et al.* [1994] found that high-grade metamorphism of granitic and related rocks reduced their U-Pb zircon “ages” from 1000 Ma down to 540 Ma, with

zircons even from a single sample yielding U-Pb “ages” between 1072 Ma and 539 Ma. Lead loss was severe and from entire grains. Similarly, *Ashwal et al.* [1999] obtained a spectrum of concordant U-Pb “ages” for zircons in a granulite facies (high-grade) metamorphosed anorthosite and concluded that this was indicative of high-temperature Pb loss during the metamorphism. There were marked correlations between zircon grain size and internal features, such that the oldest grains are larger and show relict magmatic zoning, whereas the youngest grains are small fragments containing high-U crack networks. Thus *Ashwal et al.* [1999] suggested volume diffusion and/or fracture-assisted diffusion was the dominant mechanism of Pb loss, and only minor episodic or continuous metamorphic zircon growth had occurred. Furthermore, they

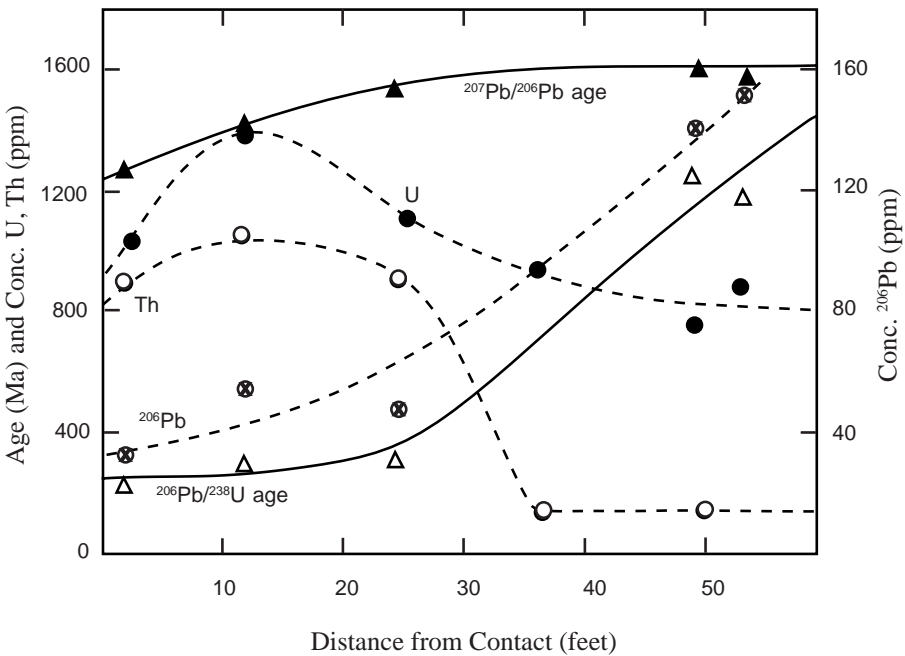


Figure 11. Change in $^{206}\text{Pb}/^{238}\text{U}$ and $^{207}\text{Pb}/^{206}\text{Pb}$ “ages” and in concentrations of U, Th and ^{206}Pb in zircons in Precambrian metasediments and metavolcanics as a function of distance from the contact with the Eldora Tertiary granite stock, Colorado [after *Davis et al.*, 1968].

added an obvious note of caution in the interpretation of zircon ages in meta-igneous rocks affected by high-grade metamorphism, which can be meaningless even when concordant.

3.3 Zircon “Inheritance” and Chemical Weathering

Another significant problem for zircon U-Pb “dating” are zircon crystals in some metamorphic and granitic rocks that yield much older “ages” than the accepted “ages” of the rocks. In metamorphic rocks this has been interpreted as inheritance of those zircon grains from the original sediment sources, zircons somehow surviving metamorphism without resetting of the U-Pb isotopic system [Froude *et al.*, 1983; Kröner *et al.*, 1994]. These “older” zircons in granitic rocks are likewise interpreted as being inherited from the source rocks that melted to produce the magmas [Williams *et al.*, 1983; Chen and Williams, 1990]. These situations are enigmatic, given the dramatic effect of similar temperatures during contact metamorphism [Davis *et al.*, 1968] (Figure 11). In some published studies the inherited zircons are 5–10 times “older” than those matching the accepted “ages” of the granites—for example, up to 1753 Ma in a 21 Ma Himalayan granite [Parrish and Tirrul, 1989], up to 3500 Ma in a 426 Ma south-east Australian granodiorite [Williams, 1992], and up to 1638 Ma in a 370 Ma New Zealand granite [Muir *et al.*, 1996].

However, if Pb is lost from some mineral grains, then it could be inherited by other crystals subsequent to the formation of the host rocks. Thus Ludwig and Silver [1977] found that many K-feldspars in Precambrian rocks contained unsupported or excess radiogenic Pb (that is, no parent isotope in the mineral), though the composition of the unsupported Pb was compatible with the supposed ages of the host rocks. On the other hand, Williams *et al.* [1984] found unsupported (excess) radiogenic Pb in a zircon crystal in an Antarctic gneiss, which thus produced anomalously high “ages.” Similar situations also result in “ages” hundreds of millions of years more than expected and are interpreted as due to excess radiogenic Pb, the origin of which is either explained as mixing from older source materials which melted to form

the magmas, and/or due to subsequent migration as a result of fluids, temperature and pressure [Zhang and Schärer, 1996; Copeland *et al.*, 1998]. This all begs the question—should “anomalously old” zircons be interpreted as inheritance of the zircon crystals, or of the “excess” radiogenic Pb *in* the crystals?

Furthermore, an additional problem is that originally encountered with whole-rock U-Th-Pb dating—chemical weathering. Stern *et al.* [1966] “dated” zircons removed from residual clay formed by chemical weathering of a gneiss in Minnesota and found that the weathered zircons appeared to have lost up to 85% of their radiogenic Pb. The “correct age” was already known from previous work on unweathered samples of the same gneiss, so this estimate of the amount of radiogenic Pb loss from the zircons due to chemical weathering was based on the assumption that their U content had remained unchanged. However, it could be argued that that assumption is rather tenuous, given the extreme mobility of U during weathering which is known to largely invalidate U-Pb dating, as already seen for the granites of the Granite Mountains batholith of Wyoming [Rosholt and Bartel, 1969] (see Figure 9).

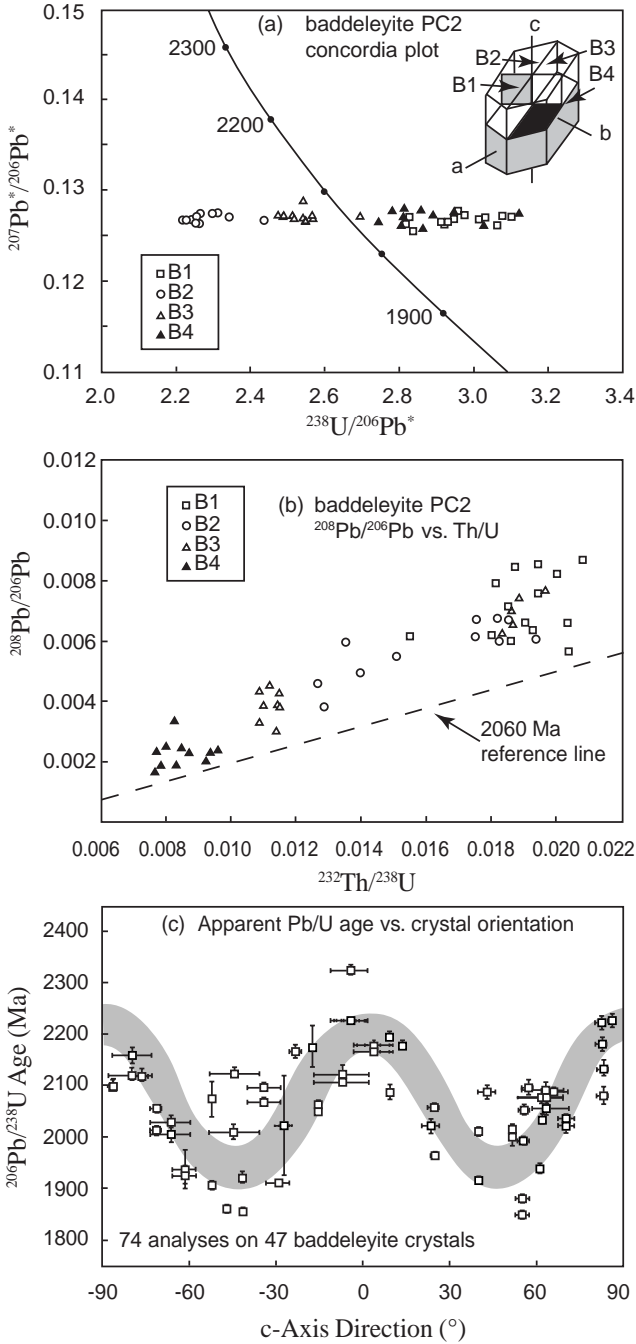
The advent of more sophisticated analytical technology has provided new means for the U-Th-Pb dating of zircons (and other minerals) to try to circumvent some of these problems. For example, Krogh [1982] took individual zircon grains separated from their host rock and abraded them in a pneumatic mill to remove the outer layers of the crystals, which are usually the most U-rich and therefore regarded as metamict. Because the results obtained in this manner showed spectacular increases in concordance, this technique has become a standard procedure in “conventional” zircon analysis. For example, when zircon crystals are interpreted as being inherited in a magma they may be overgrown by newer zircon crystal, so the old cores of the zircon grains can be recovered by hand-picking after the younger overgrowths have been removed by abrasion (Faure, 1986; Dickin, 1995). However, even though the improvement of U-Pb dates achieved by Krogh [1982] may have reduced the discordance of the results from 18.6% to 3.8%, the data still lie along a Pb-loss line that could equally be interpreted as a result of isotopic mixing.

3.4 Within Crystal U-Th-Pb “Dating”

A completely different approach to try to achieve concordant U-Pb ages is the *in situ* analysis of Pb isotopic compositions (and U/Pb ratios) in zircon grains by the ion microprobe, the most sophisticated instrument of this type being the SHRIMP (Sensitive High mass Resolution Ion MicroProbe). After being mounted the zircon or other crystals can be analyzed by the focusing of a very narrow ion beam onto the grains so that mass spectrometers can measure the ratios of the isotopes sputtered or vaporized from the targeted spots, which may be only 2 μm across. In this way even different growth zones in individual crystals can be analyzed and thus “dated.”

However, utilizing this SHRIMP *in situ* analytical technique, radiogenic Pb has been found to vary within most tested zircon grains on a 20 μm spatial scale [Compston, 1997]. Some spots were characterized by huge excesses of radiogenic Pb, up to 30 times the “expected” values. Furthermore, pronounced reproducible differences in radiogenic $^{206}\text{Pb}/^{238}\text{U}$ and thus apparent “ages” have been demonstrated between four differently oriented faces of a large baddeleyite crystal (Figure 12a), as well as correlated variation in radiogenic $^{208}\text{Pb}/^{206}\text{Pb}$ with $^{232}\text{Th}/^{238}\text{U}$ for the same four differently oriented faces (Figure 12b) [Wingate and Compston, 1997, 2000]. They concluded that the latter effect could be a primary crystal growth feature. In a second experiment, isotopic ratios were measured on the same crystal faces of 47 baddeleyite crystals but at different orientations with respect to the SHRIMP’s beam over a 180° range, the results revealing a striking, approximately sinusoidal, variation in $^{206}\text{Pb}/^{238}\text{U}$ apparent “ages” with orientation (Figure 12c) [Wingate and

Figure 12 (opposite). SHRIMP analytical results for baddeleyite, illustrating observed orientation effects [after Wingate and Compston, 1997, 2000]. (a) A U-Pb evolution (concordia) diagram showing apparent “ages” for four differently oriented surfaces (shown in inset) of a single baddeleyite crystal (PC2 from the Phalaborwa carbonatite, South Africa). (b) Correlated variation in total $^{208}\text{Pb}/^{206}\text{Pb}$ with $^{232}\text{Th}/^{238}\text{U}$ for the same surfaces measured in (a). (c) Variation of apparent $^{206}\text{Pb}/^{238}\text{U}$ “age” with orientation for (100) surfaces of 47 oriented baddeleyite crystals.



Compston, 1997, 2000]. However, similar significant differences in radiogenic $^{206}\text{Pb}/^{238}\text{U}$ or radiogenic $^{207}\text{Pb}/^{206}\text{Pb}$ related to orientation were not detected in zircon or monazite crystals (within the analytical statistics), although radiogenic $^{208}\text{Pb}/^{206}\text{Pb}$ and $^{232}\text{Th}/^{238}\text{U}$ both vary with orientation. These differences in radiogenic $^{208}\text{Pb}/^{206}\text{Pb}$ again correlated precisely with those in $^{232}\text{Th}/^{238}\text{U}$, which could be a real compositional variation reflecting zones of anisotropic primary crystal growth.

Furthermore, some monazite crystals have been found to contain random sub-microscopic blotchy patches that can vary up to 700 Ma in “age” from one another [*Cocherie et al.*, 1998]. Similarly, *Crowley and Ghent* [1999] obtained discordant U-Pb “ages” that still plotted as linear arrays on a concordia diagram for monazite grains in amphibolite facies metamorphic rocks, and high spatial resolution examination of the grains with an electron microprobe revealed domains with greatly contrasting U, Th and Pb concentrations. These were interpreted as small Tertiary domains existing along embayments into Proterozoic domains, in inclusion-rich zones, and in cracks. Because of the uniformity of the Proterozoic “ages” and the sharpness of the boundary between Proterozoic and Tertiary domains, *Crowley and Gent* [1999] claimed that Pb diffusion was negligible, despite the probable attainment of substantial temperatures (600–650°C) during the metamorphic event and the observation that the Tertiary domains are in locations where fluids clearly have locally dissolved and re-precipitated the monazite. Significantly, monazite grains can also yield negative “ages,” such as -97 Ma in a 20 Ma Himalayan granite that also contains zircons yielding “ages” up to 1483 Ma [*Parrish*, 1990], a discordancy of almost 7500%.

Clearly, the results of U-Th-Pb mineral dating are highly dependent on the investigators’ interpretations, which are usually based on expectations determined by the geological contexts of the rocks being “dated.” Radiogenic Pb is easily lost by diffusion from some crystals, and the process is accelerated by heat, water, radiation damage and weathering, while in other crystals it is inherited in excess. Uranium is readily dissolved by ground waters at considerable depths and leached from rocks and their constituent minerals. Thus without the geological context and thus the expected “ages” to guide the investigator, one cannot

be sure, as with whole-rock U-Th-Pb dating, that the analytical results and the derived “ages” are pristine and therefore represent the formation “ages” of the rocks under study. After all, apparent “ages” vary significantly within crystals at sub-microscopic scales, on different crystal faces and at different crystal orientations. These effects all combine to make U-Th-Pb “dating” of whole mineral grains and zones within them highly questionable, given that it is not always clear apart from outside assumptions as to what the “dates” really mean.

3.5 Patterns in Mineral U-Th-Pb “Ages”

As early as 1957 patterns were recognized in the U-Th-Pb “ages” obtained from different minerals. *Kulp and Eckelmann* [1957] found that whereas discordant U-Th-Pb “ages” were the norm for all the minerals “dated,” there were different patterns of discordance for the different minerals as shown in Table 2. Of course, the “probable age” is determined by the interpretation of the geological context so that *Kulp and Eckelmann* [1957] thus found that if adequately preserved, concordant “ages” could be attained from almost any radioactive mineral, though the mineral structures differed considerably in their stability to alteration.

Since these observations were made by *Kulp and Eckelmann* [1957] little attention has been paid to them, so the potential significance of these patterns has not been assessed. Furthermore, these observed

Table 2. Patterns of discordance between U-Th-Pb “ages” for different minerals [after *Kulp and Eckelmann*, 1957].

pitchblende:	$^{206}\text{Pb}/^{238}\text{U}$ “age” < $^{207}\text{Pb}/^{235}\text{U}$ “age” < probable age
uraninite:	$^{208}\text{Pb}/^{232}\text{Th}$ “age” < $^{206}\text{Pb}/^{238}\text{U}$ “age” < $^{207}\text{Pb}/^{235}\text{U}$ “age” < probable age
monazite,	
xenotime (YPO ₄):	$^{208}\text{Pb}/^{232}\text{Th}$ “age” < probable age < $^{207}\text{Pb}/^{235}\text{U}$ “age” < $^{206}\text{Pb}/^{238}\text{U}$ “age”
monazite:	$^{208}\text{Pb}/^{232}\text{Th}$ “age” < $^{206}\text{Pb}/^{238}\text{U}$ “age” < $^{207}\text{Pb}/^{235}\text{U}$ “age” < probable age
zircon and titanite:	$^{208}\text{Pb}/^{232}\text{Th}$ “age” << $^{206}\text{Pb}/^{238}\text{U}$ “age” < $^{207}\text{Pb}/^{235}\text{U}$ “age” < probable age
samarskite, thorite,	
titanite:	$^{208}\text{Pb}/^{232}\text{Th}$ “age” < $^{206}\text{Pb}/^{238}\text{U}$ “age” < $^{207}\text{Pb}/^{235}\text{U}$ “age” < probable age
euxenite:	$^{206}\text{Pb}/^{238}\text{U}$ “age” < $^{207}\text{Pb}/^{235}\text{U}$ “age” < $^{208}\text{Pb}/^{232}\text{Th}$ “age” = probable age

(samarskite and euxenite are complex Ca, U, Th, rare earth element, Ti oxides.)

patterns need to be further verified by surveying all the available mineral U-Th-Pb “dating” data available in the literature since 1957. As an example, it is immediately apparent that the pattern observed by *Kulp and Eckelmann* [1957] does indeed apply to the “model ages” obtained on five uraninite samples from the Koongarra uranium deposit of the Northern Territory of Australia [*Hills and Richards*, 1976], that is, the ^{232}Th “age” is less than the ^{238}U “age,” which is less than the ^{235}U “age,” which is less than the $^{207}\text{Pb}/^{206}\text{Pb}$ “age,” which in turn is less than the supposed “probable age.” This pattern holds true for each of the five uraninite samples, but why it is the case has not been determined. However, galena (PbS) is associated with the uraninite in the U ore, and not surprisingly it also contains radiogenic Pb which yields an almost identical Pb-Pb isochron “age” to that obtained on the uraninite [*Hills and Richards*, 1976; *Snelling*, 1994, 1995].

3.6 Whole-Rock Pb-Pb “Dating”

Even though the U-Pb isochron method for whole-rock dating has been discredited and so is now rarely utilized, Pb-Pb isochron whole-rock dating has continued to be used. The theory behind Pb-Pb isochron dating is straightforward. Because ^{235}U is always present with ^{238}U in a minor proportion always with a constant ratio, and because both U isotopes and their respective Pb isotope end members show coherent chemical behavior, “age” information can be derived from the Pb isotopes alone. Thus, it is argued, if a group of rock samples all have the same age and initial whole-rock Pb isotopic composition, then they will have developed with time different present-day, whole-rock Pb isotopic compositions according to their respective present-day U/Pb ratios [*Dickin*, 1995]. If the present-day, whole-rock Pb isotopic compositions of this suite of rock samples are then plotted, they are expected to form a straight-line array provided they have remained closed systems, the slope of the array being dependent on the “age” of the rocks.

Since the closed U-Pb system requirement remains, it might be wondered what advantage this whole-rock Pb-Pb isochron method offers over the discredited whole-rock U-Pb isochron method in view of the

known high mobility of U. However, we have already seen that the whole-rock Pb-Pb isochron for the granites of the Granite Mountains batholith of Wyoming gave the expected, geologically correct “age” of 2.82 Ga [Rosholt and Bartel, 1969] (see Figure 9a). Yet the U-Pb data for the same samples when plotted on a U-Pb isochron diagram (Figure 9b) showed that the samples had suffered disastrous U losses. It is then argued that the U-Pb whole-rock systems were effectively closed from the time of formation of the granite intrusions until very near the present day, when U was lost in recent weathering processes. This invalidates the U-Pb isochron method, but it is argued that since the Pb isotopic ratios in the rocks reflect the pre-weathering U concentrations, they are not upset by the recent weathering/alteration event.

3.7 Pb-Pb Isotopic Evolution Models

Now Pb is widely distributed throughout the earth and occurs not only as the radiogenic daughter of U and Th, but also forms its own minerals from which U and Th are excluded. Therefore, the isotopic composition of Pb varies between wide limits, from the highly radiogenic Pb in supposedly very old U, Th-bearing minerals to the “common” Pb in galena (PbS) and other minerals that have low U/Pb and Th/Pb ratios. Lead is also a trace element in all kinds of rocks, its isotopic composition being a record of the chemical environments in which the Pb has resided. These may include the mantle, crustal rocks, or Pb ores, each of these environments having different U/Pb and Th/Pb ratios that affect the isotopic evolution of Pb. Because the U/Pb and Th/Pb ratios are changed by magma generation and fractionation, by hydrothermal and metamorphic processes, and by weathering and other low-temperature processes at the earth’s surface, the Pb isotopic composition of a particular sample may have been modified both by decay of U and Th, and by mixing with Pb having different isotopic compositions. As a result, the isotopic compositions of Pb in rocks display complex patterns of variation that supposedly reflect their particular geologic histories, all of which is highly relevant to whole-rock Pb-Pb “dating.”

The first application of the whole-rock Pb-Pb dating technique was

actually on meteorites. *Patterson* [1956] calculated a Pb-Pb “age” of 4.55 ± 0.07 Ga on a suite of three stony meteorites and two iron meteorites, the least radiogenic sample analyzed being troilite (FeS) from the Canyon Diablo iron meteorite. The U/Pb ratio measured on this sample (0.025) was so low that Patterson concluded that no observable change in the isotopic composition of Pb could have resulted from radioactive decay after the meteorite was formed. Hence Canyon Diablo troilite is said to represent the “primordial” Pb isotope composition of the solar system and is regarded as an important benchmark for terrestrial Pb isotope evolution.

Previously, *Nier et al.* [1941] had reported isotopic analyses of Pb extracted from galenas from different ore deposits. They demonstrated conclusively that such leads have variable isotopic compositions and proposed that these variations resulted from mixing of radiogenic Pb with “primeval” Pb prior to the deposition of the galenas. Because the galena contains no U, there is no problem of U loss, and since there was no radioactive decay in the galena, the Pb isotopic composition is not measuring the “age” of the galena directly back from the present day, but instead is measuring the “age” of the galena source, from the formation of the earth until the isolation of the Pb into the galena. This approach was independently conceived by *Holmes* [1946] and *Houtermans* [1946]. The Holmes-Houtermans model seeks to account for the isotopic composition of any given sample of “common” Pb in terms of a single-stage history. It assumes that radiogenic Pb is produced by decay of U and Th in the source regions and that the resulting Pb (primeval plus radiogenic) is then separated from its parents and incorporated into ore deposits as galena. The isotopic composition of Pb in the galena then does not change because that mineral contains no U or Th. Subsequently “primeval” or “primordial” Pb became defined as the Pb isotopic composition of the Canyon Diablo troilite. Using these assumptions a Pb-Pb isochron can be drawn from the Pb isotopic composition of any galena sample back to the primeval Pb isotopic composition and so define the “age” of the galena, being the time when its Pb was supposedly extracted from its source rocks.

The major problem encountered with the Holmes-Houtermans model

was that as more galenas were analyzed they were found to scatter more and more widely on the Pb-Pb isochron diagram, some of the “ages” determined being clearly erroneous because they were in the future. Others, which were outliers to the main trend, often gave “ages” which could be shown to be geologically impossible. Given the complexity of the earth’s development, it was then realized that the country rock to a given galena ore was unlikely to have been a closed system since the formation of the earth. *Russell* [1956] considered the possibility that the mantle might be the reservoir for Pb isotopes and that it might not have been a closed system to U and Pb, such that it might have had a variable $^{238}\text{U}/^{204}\text{Pb}$ or μ value over time, due to some kind of differentiation mechanism. *Oversby* [1974] then proposed a model for an evolving mantle source of galena Pb with a progressive increase in μ value with time, approximated by a series of small increments in μ . This model was elaborated upon by *Cumming and Richards* [1975], who suggested a galena source with a linear increase in μ value. This change in thinking was necessitated by analyses which showed the presence of excess radiogenic Pb in many ore deposits, which was a clue that the U/Pb ratio of the source of the ore leads had probably increased with time.

Subsequently, *Stacey and Kramers* [1975] developed a two-stage model for Pb isotope history, but still starting with the assumed primordial Pb isotope ratios at the time of formation of the earth. They argued that at a more recent date the U/Pb ratio of the reservoir was changed by a worldwide geochemical differentiation event and then remained constant to the present. They argued that two closed systems were involved with different μ values separated in time by this worldwide differentiation event, the closed systems consisting of a combination of the upper mantle and upper crust (the lower crust, lower mantle and core were isolated). However, *Stacey and Kramers* [1975] recognized that their model was only an approximation of Pb isotopic development in the real earth.

However, it is not clear where the Pb isotopic reservoirs are actually located within the earth. As already noted, the mantle has long been regarded as the Pb isotopic reservoir, but it now appears that ore leads may have originated in sediments that were homogenized by repeated

cycles of erosion, transport and deposition before finally being melted in subduction zones [Faure, 1986]. Some of the Pb may have been extracted from the resulting magma in the course of volcanic activity as conformable ore deposits associated with interbedded volcanic and sedimentary rocks. In addition, Pb may have been transported by hydrothermal fluids from cooling plutons into the country rock for deposition in vein and replacement ore deposits. The Pb in such unconformable deposits is susceptible to contamination by mixing with other leads during transport, or by association with U, Th-bearing minerals after deposition. For this reason, leads in unconformable ore deposits frequently have variable Pb isotopic ratios that may define straight lines which appear to be isochrons, when in fact they are mixing lines caused by the addition of radiogenic Pb to common (or background) Pb, or by the mixing of common leads with two different isotopic compositions.

Efforts have continued in order to more accurately explain the Pb isotopic development within the earth with time. With the recognition of recycling of Pb isotopes between the crust and mantle, *Doe and Zartman* [1979] developed their “plumbotectonics” model. They defined three reservoirs: upper crust, lower crust and upper mantle (<500 km depth). Based on the interpreted evidence that continental accretion began early in the earth’s history, and that frequent orogenies mixed mantle and crustal sources to yield differentiated crustal blocks, *Doe and Zartman* [1979] modelled orogenies at regular intervals during earth history (at 400 Ma intervals), with a decreasing mantle contribution through time. Crustal contributions represented erosion and continental “foundering.” Orogenies instantaneously extracted U, Th and Pb from the three sources (upper crust, lower crust and upper mantle), mixed them, and then redistributed them back to the sources. Uranium fractionation into the upper crust represented granulite-facies metamorphism. Recycling of radiogenic upper crustal Pb into the mantle yields an apparent increase in mantle μ values with time. This process is balanced by the development of an unradiogenic lower crustal reservoir, due to the preferential retention of Pb relative to U during granulite-facies metamorphism of the lower crust.

3.8 Pb Isotopes in Ocean Basalts and Mantle Heterogeneity

The earth's mantle is increasingly being recognized as the key component of the earth's make-up, mantle convection not only being the driving force behind plate tectonics but the means by which rocks, minerals, elements and isotopes are mixed and differentiated into different reservoirs. The inaccessibility of the mantle, though, presents a severe problem for geochemical sampling. However, mantle-derived mafic magmas provide a prime source of evidence about the chemical structure of the mantle. Isotopic ratios are insignificantly affected by crystal fractionation, but they are susceptible to contamination in the continental lithosphere. Therefore the simplest approach to studying mantle chemistry through mafic magmas is to analyze oceanic volcanics, which are expected to have suffered minimal contamination in the thin oceanic lithosphere.

Isotopic analyses of ocean island basalts (OIBs) were the first used to demonstrate the existence of mantle heterogeneity. *Gast et al.* [1964] found significant differences among Pb isotopic ratios within suites of volcanic rocks from Gough and Ascension Islands in the Atlantic Ocean and also differences between the two islands. The Pb from these two islands was also found to contain excess radiogenic Pb. Subsequently, *Tatsumoto* [1966] found variations between the isotopic compositions of mid-ocean ridge basalts (MORBs) and OIBs. Many subsequent studies of the Pb isotopic compositions of OIBs found that they defined a series of arrays to the right of the so-called geochron on the Pb-Pb "isochron" diagram [*Sun*, 1980] (see Figure 13). The geochron is the isochron representing leads with isotopic compositions of zero "age," the slope being defined by the *Patterson* [1956] and subsequent analyses of Pb in meteorites, and the lower end being the Pb isotopic composition of the "primordial" Pb in the Canyon Diablo meteorite. The slopes of these OIB arrays in Figure 13 correspond to apparent "ages" of between 1 and 1.5 Ga for what are only recent lava flows. It is evident that the Pb in these OIBs is enriched in ^{206}Pb but deficient in ^{207}Pb . Moreover, the variations in Pb ratios on any given island indicates that the lava flows did not originate from a common magma chamber, but must have been

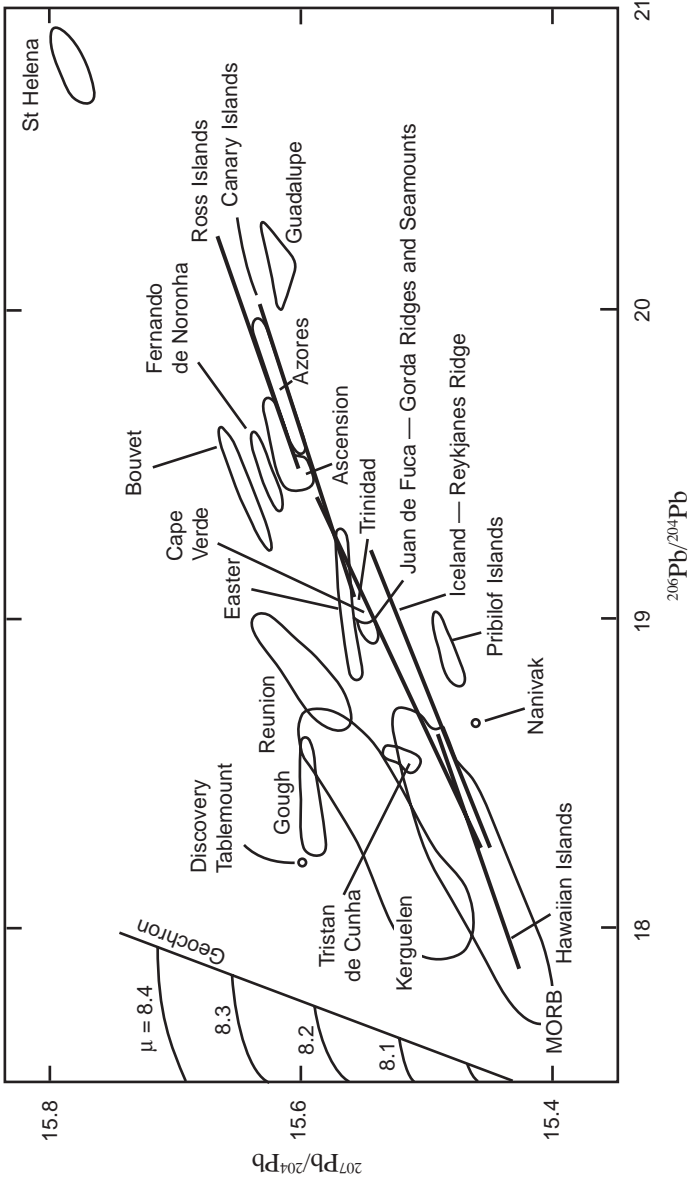


Figure 13. A Pb-Pb “isochron” diagram showing linear arrays of data defined by ocean island basalts [after Sun, 1980].

derived from source regions having different U/Pb ratios [Faure, 1986]. The differences in Pb ratios among volcanic rocks from different islands in the Atlantic and Pacific Oceans indicate that the apparent heterogeneity of the upper mantle is a worldwide phenomenon and is not restricted to one or two anomalous islands.

The linear arrays in the Pb-Pb data of OIBs in Figure 13 can be interpreted in three principal ways: as resulting from discrete mantle differentiation events, as the products of two-component mixing processes, or resulting from continuous evolution of reservoirs with changing μ values [Dickin, 1995]. Some have interpreted these linear arrays as isochrons [Faure, 1986], but each of these interpretations may be applicable to different magmatic suites! It seems clear that geochemical differentiation has variously depleted the mantle in U and Th, and that the Pb has subsequently assumed a range of isotopic compositions. Therefore, the isotope ratios of Pb in different parts of the mantle may exhibit the linear correlations expected for such systems [Faure, 1986]. On the other hand, the presence of Pb with different isotopic compositions in a heterogeneous mantle permits mixing to occur during formation of the basalt magmas [Sun *et al.*, 1975]. Therefore, the significance of linear data arrays for MORBs and OIBs on the Pb “evolution” diagram remains elusive. What is clear is that whole-rock Pb-Pb “dating” of these recent basalt lavas produces anomalously old “ages” which represent inheritance of Pb isotopic compositions from the mantle source areas of the magmas.

The distribution of OIB Pb-Pb arrays to the right of the geochron presents a problem in understanding Pb evolution in the earth as a whole, since it implies that the depleted mantle has an average composition more radiogenic than the geochron [Dickin, 1995]. This is the opposite of the expected behavior, since experimental evidence suggests that U is more incompatible than Pb, and should generate low U/Pb ratios in the depleted mantle [Tatsumoto, 1988]. This problem has been termed the “lead paradox.” A complementary reservoir with unradiogenic Pb has been postulated to exist to balance the radiogenic depleted mantle, but this other reservoir has proved hard to locate [Dickin, 1995].

It has been emphasized that Pb isotopic evolution in the mantle cannot

be described adequately by a series of closed systems because μ probably varied continuously throughout “geologic time” [Church and Tatsumoto, 1975]. Moreover, the possibility of mixing the leads of differing isotopic compositions in the mantle, and perhaps also between the mantle and the crust as a result of subduction of crustal material, must also now be recognized [Faure, 1986]. The effect of mixing of Pb from sources in the crust and mantle was more clearly recognized in the Pb isotopic ratios of volcanic rocks from subduction zones than in oceanic basalts.

3.9 Pb-Pb Isochrons and Pb Isotopic Mixing

The Pb isotopic compositions of volcanic rocks on the continents also form linear arrays that have also been interpreted as mixtures derived from the crust and mantle. A classic example of this Pb isotopic mixing effect was reported by *Moorbath and Welke* [1969] from the study of the igneous rocks on the Isle of Skye in northwest Scotland. This area is well known because it contains a wide variety of plutonic and volcanic rocks of early Tertiary age whose petrogenesis has been the subject of much discussion. *Moorbath and Welke* [1969] found that both the acid and mafic igneous rocks from Skye lay on a strong linear array on the $^{207}\text{Pb}/^{204}\text{Pb}$ versus $^{206}\text{Pb}/^{204}\text{Pb}$ diagram, with a slope of approximately 3 Ga (see Figure 14a). They interpreted the linear array as a mixing line between radiogenic mantle-derived Pb and very unradiogenic Archean crustal Pb of the basement Lewisian Complex. By plotting $^{208}\text{Pb}/^{204}\text{Pb}$ versus $^{206}\text{Pb}/^{204}\text{Pb}$ ratios (see Figure 14b) it is possible to resolve three components in the Skye Tertiary igneous rocks [Thompson, 1982]. The lavas are therefore interpreted as mantle-derived magmas that have suffered strong contamination in the granulite-facies lower crust, while the granites are attributed to similar precursors which underwent further differentiation and contamination in shallower amphibolite-facies crust under Skye. In other words, the Pb isotopic compositions of the igneous rocks of Skye favor the hypothesis that significant proportions of their contained Pb were derived from the basement Lewisian Complex, and that at least some of the granitic magma could have been derived by partial melting of that basement complex.

Faure [1986] offers an important word of caution—“not all linear arrays on the Pb-Pb diagram are isochrons.” Linear correlations of Pb isotopic ratios can also result from mixing of leads of different isotopic

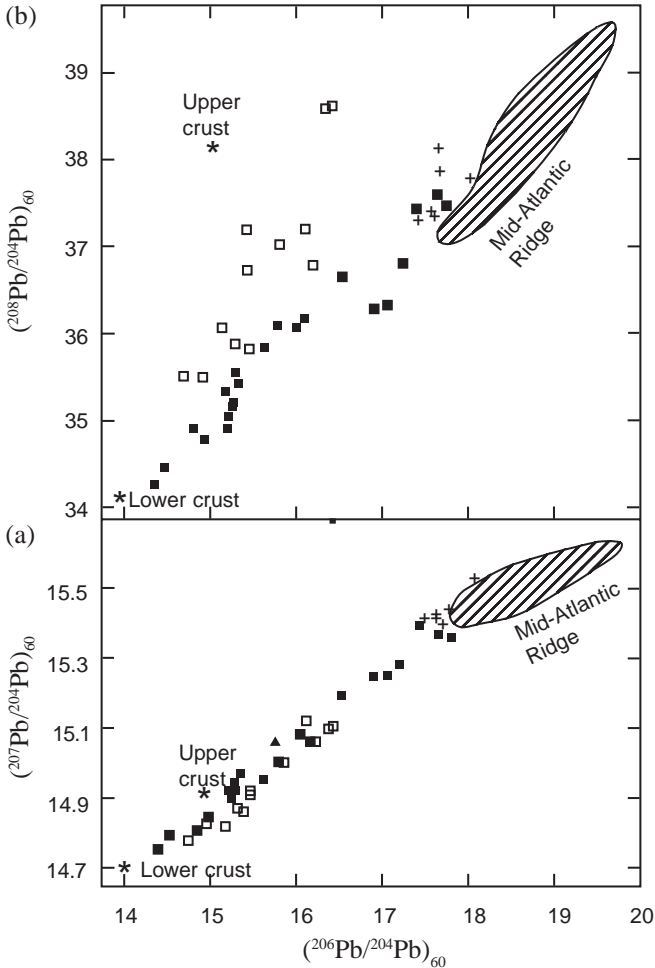


Figure 14. Plot of initial Pb isotope ratios (at 60 Ma) for Tertiary igneous rocks from the Isle of Skye, NW Scotland, to show evidence for three-component mixing in their genesis [after *Thompson*, 1982]. Symbols: (*) = crustal end-members; (■) = lava suite; (□) = granites; (+) = low-K tholeiites; (subscript 60) = at 60 Ma. Mid-Atlantic Ridge approximates Hebridean mantle composition.

compositions in varying proportions. The problem of distinguishing mixing lines from isochrons affects the interpretation of ore leads, as well as Pb in young volcanic rocks. In both examples the linear patterns of Pb ratios imposed by mixing is preserved to “haunt” us. In “older” rocks the initial colinearity of isotopic ratios on mixing lines may be destroyed by subsequent decay of U and Th, which ultimately scatters the ratios off the line. Nevertheless, the original initial colinearity due to mixing remains significant, because the present-day U-Th-Pb isotopic ratios therefore do not represent the “ages” of the rocks, and may result in false isochrons.

An extreme example of a false isochron produced by mixing of leads of different isotopic compositions graphically illustrates the pitfalls in whole rock Pb-Pb isochron dating generally. The Pb-Pb isochron “ages” of the uraninites and galenas in the U ore at Koongarra in the Northern Territory, Australia [*Hills and Richards, 1976*] are nearly identical. The Pb in the galenas is clearly radiogenic Pb and is interpreted as being derived from an older generation of uraninite whose U had been remobilized at approximately 870 Ma, the U-Pb isochron “age” of the uraninites. Subsequent to this formation of the primary ore, erosion of the land surface exposed the ore to weathering, the U being dispersed downslope in the weathered horizon from the intersection of the primary ore with the base of weathering in the direction of groundwater flow [*Snelling, 1990*]. It is hardly surprising, therefore, that the soils overlying the ore zones and the immediate areas of host rocks carry anomalous U and Pb concentrations compared to background levels [*Snelling, 1984*]. That the ground waters have been responsible for dispersing U and Pb into the surrounding soils is also clearly demonstrated by analyses down through the soil profile. Furthermore, *Dickson et al.* [1985, 1987] found the Pb isotopic signature of the U ore in the soils above a second orebody which is concealed by about 40 m of barren overburden, and in the soils to the south of the main orebody within the U hydrogeochemical halo found by *Giblin and Snelling* [1983]. *Dickson et al.* [1985, 1987] not only collected soil samples from above the mineralization at Koongarra and from the immediate surrounding areas, but from as far afield as 17 km from the known U mineralization, yet all 113 soil samples were

highly correlated ($r = 0.99986$) on a $^{207}\text{Pb}/^{206}\text{Pb}$ versus $^{204}\text{Pb}/^{206}\text{Pb}$ diagram, yielding an apparent isochron representing an “age” of 1445 ± 20 Ma for the soil samples (see Figure 15) [Dickson *et al.*, 1987]. Most of the soil samples consisted of detritus eroded from sandstone which overlies the schists hosting the U ore, so because the samples from near the mineralization gave a radiogenic Pb signature this false

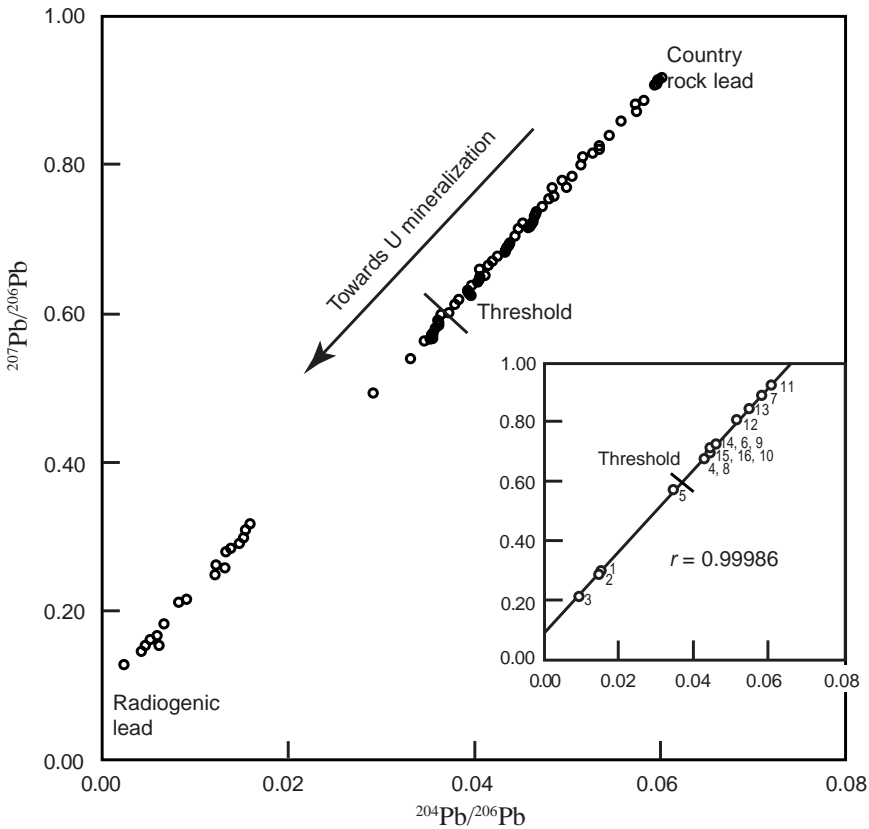


Figure 15. Plot of $^{207}\text{Pb}/^{206}\text{Pb}$ versus $^{204}\text{Pb}/^{206}\text{Pb}$ for the combined data sets of Dickson *et al.* [1985, 1987] of Pb isotopic ratios in soils from the area around the Koongarra uranium orebody, Northern Territory, Australia, indicating the high correlation ($r = 0.99986$) between the two variables. Insert shows data collected in the Dickson *et al.* [1987] study plotted on the fitted regression line.

isochron was interpreted as being due to mixing of radiogenic Pb from the U ore with the “common” or country rock Pb of the sandstone. However, even though several of the soil samples consisted of either weathered schist or basement granite (which contains accessory zircon and uraninite) up to 17 km from the known U ore, those soil samples still plotted on the same apparent “isochron,” which is nevertheless geologically meaningless.

3.10 Some Conclusions

It has to be concluded, therefore, that U-Th-Pb “dating” involves many pitfalls which are really only surmounted by making further assumptions and by dependence on uncertain cross-checks. It is rather arbitrary to assume that the Pb isotopic composition of a mineral in one small meteorite fragment constitutes the earth’s primordial signature, but that assumption yields the 4.57 Ga “age” for the earth and is necessary to salvage U-Th-Pb “dating.” Both U and Pb mobility undermine whole-rock “dating,” and Pb migration within, and loss from, individual mineral grains is so prevalent that interpreting the resultant isotopic data is largely dependent upon the bias of the investigators to ultimately make the technique work, that is, to produce the desired outcome. In this way an entire edifice has been built which from the outside looks impregnable and internally consistent.

Yet fundamental problems remain. Modern ocean basalts reveal inconsistent Pb isotopic heterogeneities in their mantle sources, even for suites of flows on a single island, which yield vastly erroneous old “ages” and which are totally at variance with all models of Pb isotopic evolution built on the assumed primordial Pb signature and with the erected interpretative framework (growth curves). Isotope inheritance, migration and mixing in the U-Th-Pb system is a prevalent chronic problem at all observational scales, and what is known of patterns in U-Th-Pb “ages” hints at some underlying fundamental, non-time-dependent process which would render all “age” interpretations invalid. Clearly, even though the constructed “age” system edifice looks internally consistent, the individual “dating” results within it are nevertheless

questionable, and the foundations it is built on probably are systematically in error.

4. The Rubidium-Strontium (Rb-Sr) Radioisotopic System

The Rb-Sr radioisotopic system is still one of the most widely used for isotopic whole-rock “dating,” because most crustal rocks contain sufficient Rb and Sr (anywhere between 10 and 1000 ppm) to make the chemical separation of the elements and the mass spectrometry relatively straightforward. The method has been applied to a wide range of whole-rock compositions, as well as to individual minerals. However, the results of Rb-Sr geochronology have not always been easy to interpret because it is claimed that both Rb and Sr are relatively mobile elements, so that the isotopic system may be readily disturbed either by the influx of fluids or by a later thermal event [Rollinson, 1993]. On the other hand, *Hanson and Gast* [1967] have stated that:

It is significant that no one has so far been able to thermally induce radiogenic strontium-87 to leave its host mineral in quantities commensurable to the loss of argon under geologically reasonable conditions even though it is not uncommon to find biotites in nature which have lost both radiogenic argon-40 and strontium-87 due to a thermal event.

Thus if the experimental evidence does not show ^{87}Sr loss can be thermally induced, then geological interpretation of ^{87}Sr loss due to thermal events may in contrast only be demanded by the required consistency with the evolutionary timescale.

Nevertheless, if an Rb-Sr isochron is obtained it can usually be attributed to a definite event, such as the “age” of metamorphism or alteration, or the “age” of diagenesis in sedimentary rocks, even if the primary “age” cannot be determined. Biotite and muscovite are the minerals most commonly dated by the Rb-Sr method. Such mineral “ages” are calculated using a 2-point isochron, in which a mineral with low Rb concentration such as plagioclase, or better the whole rock, is used as a control on the initial ratio [Rollinson, 1993].

4.1 Anomalous Rb-Sr Isochrons

However, some of the basic assumptions of the method are now being questioned [Zheng, 1989]. As first developed the method assumed a suite of cogenetic rock samples to have:

- the same age;
- the same initial $^{87}\text{Sr}/^{86}\text{Sr}$ ratio; and
- acted as a closed system.

The goodness of fit of the analytical data points in the plot of $^{87}\text{Sr}/^{86}\text{Sr}$ versus $^{87}\text{Rb}/^{86}\text{Sr}$ has always served as a check of these assumptions. As the method was applied to an increasing number of geological situations, it soon became apparent that linear relationships between $^{87}\text{Sr}/^{86}\text{Sr}$ and $^{87}\text{Rb}/^{86}\text{Sr}$ ratios could sometimes yield anomalous isochrons which have no distinct geological meaning, even when there is an excellent goodness of fit of the isochrons to the data.

It is now recognized that a primary mafic magma should inherit the isotopic composition of its mantle source, and in some instances the parent/daughter ratio also [Dickin, 1995]. If different magma batches were cogenetic and sampled the elemental and isotopic compositions of different source domains, then it is argued that this might lead to the eruption of an “isochron” suite. For example, *Sun and Hansen* [1975] found that the Rb-Sr data for 14 different ocean island basalts (OIBs) when plotted on an isochron diagram yielded a positive correlation with a slope “age” of approximately 2 Ga. The basalts on individual ocean islands sometimes also defined arrays with positive slopes. Sun and Hansen attributed these positive correlations between Rb/Sr and isotopic composition to mantle heterogeneity, suggesting that the apparent “ages” represented the time since mantle domains were isolated from the convecting mantle. *Brooks et al.* [1976a] used the term “mantle isochrons” for these “ages.”

The mantle isochron concept was extended to continental igneous rocks by *Brooks et al.* [1976b]. They studied 30 examples taken from the literature of both volcanic and plutonic continental igneous rock suites. Because these were all regarded as “ancient” unlike most OIBs which are recent, *Brooks et al.* then corrected the measured $^{87}\text{Sr}/^{86}\text{Sr}$ ratios of

the samples in each suite back to their calculated initial ratios at the time of magmatism (“known” from independent information) before plotting them against their Rb/Sr ratios. The resultant data for each of the rock suites studied formed roughly linear arrays, so Brooks *et al.* termed these plots “pseudo-isochron diagrams.” Brooks *et al.* rejected the possibility that these pseudo-isochrons were mixing lines produced by crustal contamination of mantle-derived mafic magmas, instead believing them to “date” mantle differentiation events which had established domains of different Rb/Sr ratios in the subcontinental lithosphere.

Another example of correlated $^{87}\text{Sr}/^{86}\text{Sr}$ and $^{87}\text{Rb}/^{86}\text{Sr}$ ratios was reported by *Bell and Powell* [1969] for potassic lava flows from the Birunga and Toro-Ankole fields along the borders of Uganda, Zaire (now the Congo Republic) and Rwanda of East Africa. These two volcanic centers are about 160 km from each other and are located along the western rift north of Lake Tanganyika and west of Lake Victoria. The lava flows are known to be quite young (Pliocene to Recent) and there is evidence of volcanic activity in historical times. Because these volcanic rocks are therefore very young, they should form an isochron having a slope approaching zero. However, *Bell and Powell* [1969] found a significant positive correlation between the average $^{87}\text{Sr}/^{86}\text{Sr}$ and Rb/Sr ratios of different rock types among these lava flows. Indeed, when plotted the $^{87}\text{Sr}/^{86}\text{Sr}$ ratios of these rocks are positively correlated with their $^{87}\text{Rb}/^{86}\text{Sr}$ ratios, the line which can arbitrarily be drawn through the cluster of data points probably representing a mixing line. It cannot be an isochron because the slope of the line represents an “age” of 773 Ma, when the rocks are supposed to be all less than 1 Ma. This date is of course fictitious, as is the “isochron,” because in this case the $^{87}\text{Sr}/^{86}\text{Sr}$ ratios of these rocks are probably the result of a mixing process and are not due to decay of ^{87}Rb in the rocks after their formation. Thus this positive correlation of initial $^{87}\text{Sr}/^{86}\text{Sr}$ ratios of igneous rocks and their Rb/Sr ratios could be interpreted as evidence of long-term heterogeneity in the upper mantle.

A fundamental assumption of the mantle isochron model is that neither isotopic nor elemental ratios are perturbed during magma ascent through

the crust. However, it is now generally accepted that this assumption is not upheld with sufficient reliability to attribute “age” significance to so-called “erupted” isochrons. Breakdown in the mantle isochron model can also be caused by low degrees of melting in the mantle source, leading to fractionation between Rb, an ultra-incompatible element, and Sr, a moderately incompatible element. Hence *Dickin* [1995] concluded that only isotope-isotope mantle isochrons, such as those provided by the Pb isotopic system, can reliably be interpreted as dating the “ages” of mantle differentiation events.

Faure and Powell [1972] demonstrated that in “modern” volcanic rocks there is an overall approximate inverse correlation between their initial $^{87}\text{Sr}/^{86}\text{Sr}$ ratios and their Sr contents. In other words, volcanic rocks with high Sr contents have low $^{87}\text{Sr}/^{86}\text{Sr}$ ratios, whereas volcanic rocks (and dunites and peridotites) with high $^{87}\text{Sr}/^{86}\text{Sr}$ ratios have low Sr contents. It has also been shown that in a general way the $^{87}\text{Sr}/^{86}\text{Sr}$ ratios of oceanic basalts, including sea-floor basalts, correlate positively with their relative K contents (defined by $\text{K}_2\text{O}/(\text{K}_2\text{O} + \text{Na}_2\text{O})$) [*Peterman and Hedge*, 1971]. This is not unexpected as Rb is an alkali metal like K and therefore will correlate with the K content of rocks and minerals, the decay of ^{87}Rb thus increasing the ^{87}Sr content relative to ^{86}Sr . Yet another observed trend in some basaltic rocks has been suggested as due to contamination with sialic material, because their initial $^{87}\text{Sr}/^{86}\text{Sr}$ ratios increase with their increasing SiO_2 contents [*Faure et al.*, 1971].

4.2 Initial Rb/Sr—Differences and Subsequent Behavior

Faure and Powell [1972] reported that an increasing number of apparently cogenetic suites of both oceanic and continental volcanic rocks were being discovered to have significant within-suite variations in initial $^{87}\text{Sr}/^{86}\text{Sr}$ ratios. They suggested that in general these variations could have been caused by either

- differences in the initial $^{87}\text{Sr}/^{86}\text{Sr}$ ratios of the source regions of the rocks in the upper mantle and lower crust, or
- variable contamination of their parent magmas with “foreign” Sr via bulk assimilation, wall-rock reaction, selective migration of radiogenic

Sr, and/or isotopic exchange and equilibration.

Indeed, *McCarthy and Cawthorn* [1980] have argued the assumption that all rocks in a comagmatic igneous complex started with the same initial $^{87}\text{Sr}/^{86}\text{Sr}$ ratio may be invalid, particularly if the period of initial crystallization was very protracted such that a fractionated melt with a high Rb/Sr ratio was able to accumulate radiogenic ^{87}Sr before eventually crystallizing. Variations in the initial $^{87}\text{Sr}/^{86}\text{Sr}$ ratios for suites of young lavas from a single volcano have been found [*Cortini and Hermes*, 1981], which suggests that the assumption of a well-defined initial ratio for many suites of rocks would be difficult to defend.

Magma contamination is a case in point. In contaminated plutonic rocks, one cannot assume that all the Sr of the contaminants has been uniformly mixed into the magma, and hence the assumption that all rocks initially had the same $^{87}\text{Sr}/^{86}\text{Sr}$ ratio cannot be justified. Contamination is in fact one of the main sources of mineralogical and geochemical variation in granitic rocks, and all main types of likely contaminant have compositions which would lead to an under-estimation of the initial $^{87}\text{Sr}/^{86}\text{Sr}$ ratio of the magma and an overestimation of the "age" of crystallization of the magma [*Hall*, 1987]. Furthermore, granitic rocks form as products of a number of different processes, such as differentiation of basaltic parent magmas, partial melting rocks of different compositions in the crust, and metasomatic reactions involving recrystallization and diffusion of ions on a large scale. Thus if a granite has been derived by fractional crystallization of basalt magma or by partial melting of deep crust or upper mantle, its initial $^{87}\text{Sr}/^{86}\text{Sr}$ ratio should be low, like the ratios of most basalts. On the other hand, if the granite has been derived from older crustal material, it should have inherited as its initial $^{87}\text{Sr}/^{86}\text{Sr}$ ratio the relatively higher ratio of that older crustal material at the time the granite was produced. Then there is also sampling bias, given that because of the necessity of obtaining samples with a spread of $^{87}\text{Rb}/^{86}\text{Sr}$ ratios in order to produce a viable isochron and to calculate its slope, investigators may deliberately sample highly contaminated rocks in order to extend the Rb/Sr range, which may thus yield a misleading or even erroneous determination of the initial $^{87}\text{Sr}/^{86}\text{Sr}$ ratio.

Obviously the nature of the Rb-Sr system at the initial instance of time in the formation of a rock is of crucial importance in understanding the meaning of an isochron. Yet even a suite of samples which do not have identical “ages” and initial $^{87}\text{Sr}/^{86}\text{Sr}$ ratios can be fitted to isochrons [Köhler and Müller-Sohnius, 1980; Haack *et al.*, 1982]. Furthermore, supposed multi-stage development of a geological system increases the complexity of interpreting Rb-Sr data for “dating” purposes. For example, Compston *et al.* [1982] suggested a two-stage ^{87}Sr development for the Stockdale rhyolite of the Lake District, England, in order to account for its anomalous whole-rock Rb-Sr isochron “age” (the initially-determined isochron “age” did not agree with the biostratigraphic “age”). Certain samples having very high Rb-Sr were deleted during interpretation of the data so as to remove most of the excess scatter in the data, the high Rb/Sr of the deleted samples being interpreted as a net loss in Sr during hydrothermal alteration subsequent to extrusion of the rhyolite. This example illustrates how the interpretation of Rb-Sr “dating” data is influenced by factors external to the actual Rb-Sr radioisotopic system. In another example, “rotation of the isochron” was used to describe the perceived distortion of the Rb-Sr system in German volcanics due to presumed post-magmatic processes [Schleicher *et al.*, 1983].

Allègre [1987] has pointed out that variations in initial $^{87}\text{Sr}/^{86}\text{Sr}$ ratios may have resulted from Rb/Sr fractionation (differentiation). Since Rb is an alkali metal and Sr an alkaline-earth metal, the $^{87}\text{Sr}/^{86}\text{Sr}$ variations are a reflection of the alkali/alkaline-earth fractionation (differentiation) inside the family of lithophile elements [Hedge and Walthall, 1963]. The present-day observed $^{87}\text{Sr}/^{86}\text{Sr}$ variations may well be partly a function of time because radiogenic ^{87}Sr has accumulated due to the decay of ^{87}Rb , but the geochemical behavior between Rb and Sr also needs to be taken into account. Zheng [1989] maintains that the three variables ^{87}Sr , ^{86}Sr and ^{87}Rb are not independent of each other, and as a result the measured $^{87}\text{Sr}/^{86}\text{Sr}$ and $^{87}\text{Rb}/^{86}\text{Sr}$ ratios are not necessarily two independent variables on an Rb-Sr isochron diagram. Furthermore, Zheng shows by detailed argumentation that because a geological system cannot have had a homogeneous ^{86}Sr distribution, and because the ^{86}Sr is used as a common variable in the conventional isochron equation, the

observed isochronous correlation in the plot of $^{87}\text{Sr}/^{86}\text{Sr}$ versus $^{87}\text{Rb}/^{86}\text{Sr}$ is generally enhanced to some extent. Thus correlations between ^{87}Rb and ^{87}Sr may be negative, positive or non-existing, but good positive correlations have usually been induced between $^{87}\text{Sr}/^{86}\text{Sr}$ and $^{87}\text{Rb}/^{86}\text{Sr}$ ratios due to the function of ^{86}Sr as the common denominator.

The Rb-Sr isochron method assumes a constant $^{87}\text{Sr}/^{86}\text{Sr}$ ratio at the initial instance of time for all samples in a given suite. However, it has already been noted that all samples in a comagmatic suite may not have the same initial $^{87}\text{Sr}/^{86}\text{Sr}$ ratio. It is thus possible that for a comagmatic suite the initial $^{87}\text{Sr}/^{86}\text{Sr}$ ratios of samples may not only be variable, but linearly correlated with the $^{87}\text{Rb}/^{86}\text{Sr}$ ratios, and thus the determination of both “age” and initial ratio from the isochron method may be seriously in error. The present-day observed linear array on an isochron diagram is in fact a combination of the initial linear relationship between $^{87}\text{Sr}/^{86}\text{Sr}$ and $^{87}\text{Rb}/^{86}\text{Sr}$ ratios, corresponding to the pseudo-isochrons defined by *Brooks et al.* [1976a, b], and the accumulation of radiogenic ^{87}Sr since the time of rock formation. Thus the observed isochron is only an apparent isochron.

Therefore, it can be argued that the nature of the initial Rb-Sr system has considerable influence on the validity of an isochron, and that a valid isochron may have been rotated by this inherited initial Rb-Sr array in either a clockwise or anticlockwise direction [*Zheng*, 1989], which changes the slope of the isochron and therefore the resultant calculated apparent “age.” The reason why such inherited arrays could be present in geological systems is complicated, but they are probably due to either partial melting, fractional crystallization, mixing, the original sediments, or because of metamorphism. Indeed, partial melting and fractional crystallization can give rise to a given geochemical correlation between ^{87}Rb and ^{86}Sr .

4.3 Isotopic Mixing from Sources—An Australian Example

An illustration of the effects of some of these processes on a geological system is the granitic rocks of the Lachlan Fold Belt of south-eastern Australia. Regional variations of isotopic and chemical

compositions of the granitic rocks have been demonstrated for the batholiths of south-eastern Australia, not too dissimilar to the granitic rocks in the batholiths of southern California. *Chappell and White* [1974] use mineralogical and chemical criteria of these granitic rocks to distinguish I-type (igneous) from S-type (sedimentary) granites, the former being attributed to fusion of the mantle or mantle-derived rocks, with the latter being derived from pelitic sedimentary rocks. Such a two-fold classification of granites would seem to be at variance with the evidence that granitic batholiths are blends of both mantle and crustal sources, and thus while I-type and S-type granites may be the extremes of possible petrogenetic provenance, most large-scale granitic batholiths appear to be intermediate in origin.

Debate over the source rocks and mode of formation of these granitic rocks in south-eastern Australia has continued and isotopic studies have been at the forefront of justifying proposed models. *Compston and Chappell* [1978] reported that the granitoids exhibited well-fitted linear variation lines inversely correlating Sr with SiO₂, which they interpreted as evidence of physical unmixing of a felsic melt from the refractory residue after melting of the source rocks. Using this interpretation they calculated the average chemistry of the source rocks in terms of the individual melts and refractory residues for each granitoid, plus the fractional amount of minimum-melt component in each particular source. The next step was to calculate the approximate Rb/Sr ratios for the particular rocks that had been partially melted to form each granitoid, and using the initial ⁸⁷Sr/⁸⁶Sr of each granitoid as a measure of the mean ⁸⁷Sr/⁸⁶Sr of the source rocks at the time of melting, they were able to plot these data on a source Rb/Sr isochron diagram and derive a “source isochron” for these rocks that melted to form these granitoids. Whereas the age of the granitoids was regarded as 420 Ma, the source isochron yielded an “age” for the source rocks of 1100 Ma, suggesting that Precambrian continental material was present in the lower crust of south-eastern Australia during the early Paleozoic. This interpretation would appear to be consistent with the “ages” of supposedly inherited zircon grains in these granitoids [*Chen and Williams, 1990; Williams, 1992*].

Clearly, the isotopic data suggested mixing of crustal and mantle

components to form these granitic rocks, which other investigations appear to have confirmed. *McCulloch and Chappell* [1982] calculated the epsilon (ϵ) values from the initial $^{143}\text{Nd}/^{144}\text{Nd}$ and $^{87}\text{Sr}/^{86}\text{Sr}$ ratios of the granitic rocks and xenoliths of the Berridale and Kosciusko Batholiths and found that they plotted along a curved trajectory that is typical of binary mixtures (see Figure 16). The granitic rocks were classified into I- and S- types and were thus found to separate into two overlapping clusters on the isotope correlation diagram. However, both types fit the

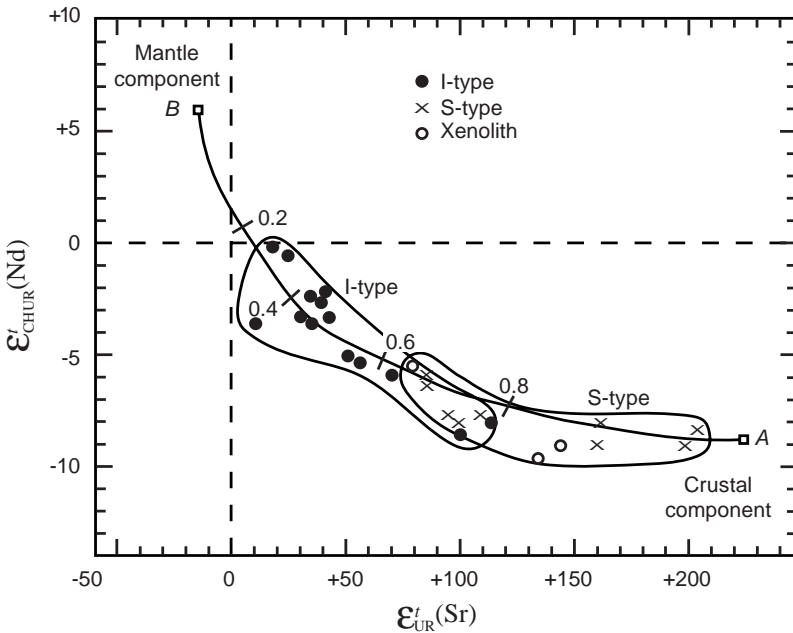


Figure 16. Epsilon (ϵ) values of Nd and Sr, corrected for decay, of granitic rocks and xenoliths from the Berridale and Kosciusko Batholiths of southeastern Australia [after *McCulloch and Chappell*, 1982]. Both I-type (igneous) and S-type (sedimentary) granitic rocks fit the same mixing line, indicating that both are mixtures of two components derived from “depleted” mantle and from the continental crust. The curve was fitted using the following end-member compositions: Crustal component (A): $\epsilon(\text{Nd}) = -9.0$, $\text{Nd} = 28.0$ ppm, $\epsilon(\text{Sr}) = 227.2$, $\text{Sr} = 140$ ppm; Mantle component (B); $\epsilon(\text{Nd}) = +6.0$, $\text{Nd} = 14.0$ ppm, $\epsilon(\text{Sr}) = -14.20$, $\text{Sr} = 470$ ppm.

same mixing curve formed from a crustal component and a depleted-mantle component. Therefore, it was concluded that even I-type granites may contain between 20% and 80% of the crustal component. Nevertheless, *McCulloch and Chappell* [1982] found that the chemical compositions of these granitic rocks deviated from those predicted by the mixing model, so they concluded that the sources were chemically heterogeneous and that more than two components were involved in the petrogenesis of these batholiths.

Keay et al. [1997] agreed that the Sr-Nd isotopic models of two-component crust-mantle mixing based on an apparent simple hyperbolic array have failed to account for the geochemical and isotopic features of granitoids from the Lachlan Fold Belt of south-eastern Australia. Instead, they showed that a three-component mixture of mantle-derived magma and two contrasting crustal components could successfully explain the isotopic compositions of the granitoids (see Figure 17). New isotopic data on granitoids of the Fold Belt had revealed a separate isotopic trend at the primary end of the Sr-Nd array, defined by a depleted mantle component and a mafic crustal component with similar isotopic characteristics to Cambrian greenstones within the Fold Belt. Combined with data from the ubiquitous Ordovician turbidites which host the granitoids, *Keay et al.* [1997] constructed three-component isotopic mixing curves that enclose all the granitoids of the Fold Belt (Figure 17), indicating that contributions from the Ordovician turbidites, Cambrian greenstones, and a depleted mantle component could produce the isotopic characteristics of the granitoids. *Keay et al.* concluded that some important implications of their model are that

- S- and I-type granites appear to be mixtures of, rather than unique products from, contrasting sources; and
- the granitoids may have formed where magmatism promoted crustal fusion and crust-mantle mixing.

Furthermore, the previously inferred Precambrian continental basement beneath the Fold Belt is unnecessary, *Keay et al.* [1997] suggesting the zircon inheritance in the granitoids could equally be from zircons inherited in the Ordovician turbidites during sedimentation.

Magma mixing as a major petrogenetic process has thus received

considerable attention, and contamination/assimilation of mantle-derived magma with crustal rocks during emplacement has been accepted as a possible mixing mechanism. Resultant effects of this mixing on Rb-Sr chronology have therefore been recognized [Zheng, 1989]. Thus the

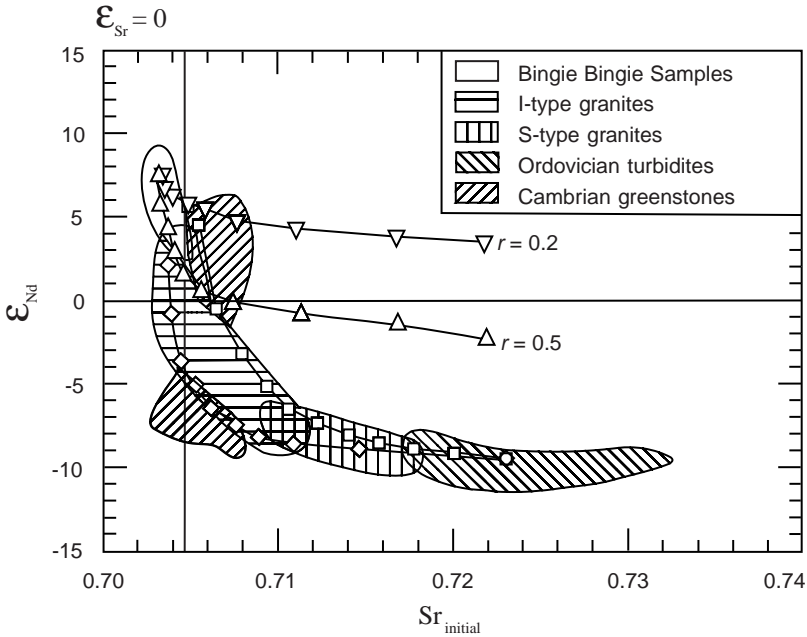


Figure 17. Hyperbolic Sr-Nd isotopic array for Lachlan Fold Belt (LFB) rocks; separate fields delineate Bingie Bingie Point samples, S- and I-type granites, Ordovician turbidites, and Cambrian greenstones [after Keay *et al.*, 1997]. Superimposed on these fields are isotopic mixing curves [DePaolo and Wasserburg, 1979a] calculated for assimilation of Ordovician turbidites by mantle-source magma (open diamonds) from Bingie Bingie Point and by greenstone melt (open squares). Fractional crystallization during assimilation of Ordovician turbidites is modeled by two additional curves ($r = 0.2$, $r = 0.5$) [DePaolo, 1981b]. These curves do not fit available data, indicating fractional crystallization was of minor importance in production of the LFB Sr-Nd isotopic array. Each symbol along the mixing and assimilation-fractional crystallization curves, approaching Ordovician turbidite composition, represents assimilation of 10% additional crustal material.

present-day measured Rb-Sr data may not define a valid isochron, that is, an apparent isochron will be produced which can be a mixing isochron or an inherited linear array. However, this will only be known if the isochron produced is not in accord with independent assumptions about what the “age” should be.

4.4 The Rb-Sr System During Metamorphism

Mineral and whole-rock Rb-Sr systems may respond differently to metamorphic events. Strontium-87 generated by Rb decay occupies unstable lattice sites in Rb-rich minerals and tends to migrate out of the crystal if subjected to a thermal pulse, even of a magnitude well below the melting temperature. However, if fluids in the rock remain static, Sr released from Rb-rich minerals such as micas and K-feldspar will tend to be taken up by the nearest Sr sink, such as plagioclase or apatite [Dickin, 1995].

Individual minerals, therefore, are regarded as open systems during metamorphism, and thus a mineral isochron yields the “age” of cooling from the thermal event, when each mineral is supposed to again become a closed system. However, a whole-rock domain of a certain minimum size is regarded as remaining an effective closed-system during the thermal event, and thus is regarded as being useful in “dating” the initial crystallization of the rock. A possible complication involves limited Rb re-mobilization. Rubidium-rich minerals tend to suffer some Rb loss, while Rb-poor phases may be contaminated by the growth of Rb-rich alteration products, leading to some unpredictability.

After Rb-Sr mineral systems have been opened in the thermal pulse of a regional metamorphic event, there is a point in time when the mineral systems are supposed to again be closed to element mobility. Thus it is argued that by dating the closure or “blocking” of different mineral systems, Rb-Sr “ages” give information about the cooling history of metamorphic terranes. These blocking temperatures have been determined experimentally, but can also be determined theoretically based on the temperature-dependence of volume diffusion processes [Dodson, 1979]. This blocking temperature is dependent on the cooling

rate, since the slower the cooling, the longer will be the time since partial loss of daughter ^{87}Sr occurred, and the lower will be the apparent “age.” Thus, in a slow-cooling regional metamorphic terrane there is a continuous transition from a high-temperature regime, when radiogenic ^{87}Sr escapes from crystal lattices by diffusion ideally as fast as it is formed by Rb decay, to low-temperature conditions when there is supposedly negligible ^{87}Sr escape.

If a mineral is in contact with a fluid phase which can remove radiogenic ^{87}Sr from its surface, then the rate of loss of ^{87}Sr depends on the rate of volume diffusion across a certain size of lattice. In the case of biotite, this diffusion will be predominantly parallel to the cleavage planes rather than across them. *Dodson* [1979] found that diffusion geometry is independent of grain size, and that Sr loss is controlled by the rate at which radiogenic atoms leave the sites in which they were formed. Thus the susceptibility of Sr to mobilization by fluids increases complexity in the interpretation of the Sr blocking temperature and therefore the Rb-Sr “age” data.

A classic example of the effect of the temperatures of metamorphism, in this case contact metamorphism, is seen in the apparent mineral “ages” with outward distance from the contact of the Eldora stock in the Front Range of Colorado (see Figure 7 again) [*Hart*, 1964]. The coarse biotites in the Precambrian amphibolites and schists, which had been intruded by a Tertiary quartz monzonite stock, showed even greater disturbance of the Rb-Sr system than the K-Ar system due to the heat of the intruding magma. *Hart* [1964] calculated that the coarse biotite only 20 feet (just over 6 m) from the contact had lost 88% of its radiogenic ^{87}Sr , while the loss at 14,100 feet (4.3 km) was essentially zero.

In a subsequent study, *Hanson and Gast* [1967] also investigated the effects of thermal metamorphism, on K-Ar and Rb-Sr ages of biotite, muscovite and K-feldspar and K-Ar ages of hornblende in a 2.6 Ga granitic stock near its contact with the 1.05 Ga Duluth Gabbro in Minnesota, and on Rb-Sr and K-Ar ages of biotite and K-Ar ages of hornblende in a 2.6 Ga amphibolite where intruded by a 800 Ma diabase dike in the Beartooth Mountains of Wyoming. The apparent loss of $^{40}\text{Ar}^*$ and ^{87}Sr from biotite took place over the temperature range from 720 to

450°C near and out to 20 m from the Wyoming dike, and from 500 to 350°C near and out to 5 km from the Duluth Gabbro. Volume diffusion, and zero and first order chemical reaction rate models were used to describe the apparent rate of loss of $^{40}\text{Ar}^*$ and ^{87}Sr from the minerals, the loss of $^{40}\text{Ar}^*$ from hornblende taking place at higher temperatures than the loss from biotite. *Hanson and Gast* [1967] concluded that the relative stability of mineral “ages” in a contact metamorphic zone appeared to be hornblende K-Ar > muscovite Rb-Sr > muscovite K-Ar > biotite Rb-Sr > biotite K-Ar, although for the micas the Rb-Sr and K-Ar ages were essentially concordant. Thus, if uniformitarian timescale assumptions are ignored and the isotopic ratios are simply interpreted as a geochemical signature of the rocks, then it would appear that the heat of these intrusions was responsible for some migration and redistribution of ^{87}Sr in commensurate quantities to $^{40}\text{Ar}^*$, even though experimental confirmation of this at laboratory scales is apparently contradictory.

However, in a more recent study of regional and contact metamorphism in the Laramie Mountains of Wyoming, *Patel et al.* [1999] found contrasting responses in the Rb-Sr radioisotopic system. Whereas the Rb-Sr isotopic data require that Sr was redistributed during amphibolite facies (>650°C, >7 kbar) regional metamorphism on a scale of at least tens of meters, during subsequent contact metamorphism (at >800°C) isotopic mobility appears to have been restricted to centimeter-scale or less. The independent “yardstick” which was used to establish these scales of Sr mobility was a whole-rock Sm-Nd isochron based on analyses of the same samples, which yielded an older “age” interpreted as that of the protoliths because of the presumed relative immobility of Sm and Nd during metamorphism. Yet the Sm-Nd radioisotopic system is fraught with its own problems (see later). Nevertheless, *Patel et al.* [1999] concluded that the regional metamorphism involved fluid transport which facilitated Sr isotopic resetting, whereas the contact metamorphism occurred in a relatively dry environment in which isotopic mobility was restricted. Without doubt, fluids can and will facilitate isotopic mobility at all observational scales, particularly when their chemistry and temperature make them more reactive.

4.5 Open-System Behavior and Whole-Rock Isochrons

The whole-rock Rb-Sr method was widely used as a “dating” tool for igneous crystallization “ages” during the 1960s and 1970s, but lost credibility during the 1980s as evidence of whole-rock open-system behavior mounted [Dickin, 1995]. For example, Rb-Sr isochrons in metamorphic terrains can yield good linear arrays whose slope is nevertheless a meaningless average of the protolith and metamorphic “ages.” Whole-rock Rb-Sr systems can be disturbed and reset to give good-fit secondary isochrons even by relatively low-grade metamorphism when there may be little field evidence and only relatively minor mineralogical alteration [Zheng, 1989]. Such an outcome is, of course, desirable in the uniformitarian timeframe, for otherwise the timescale would be grossly expanded, so explanations such as this for “ages” that are “too young” are readily adopted. In any case, this problem may probably be caused by the need to sample over a relatively large geographical area in order to maximize the range of Rb/Sr ratios. A good example is provided by the gneisses in southern Norway [Field and Raheim, 1979a, b, 1980]. Whole-rock open-system behavior can occur at even lower grades of metamorphism in fine-grained acid volcanic rocks. Such units have been attractive for “absolute” calibration of the stratigraphic record because they are conformable with the sedimentary strata. They also tend to have large and variable Rb/Sr ratios, thus yielding good isochrons. However, experience has shown that they are particularly susceptible to radiogenic ^{87}Sr loss. Indeed, the Rb-Sr systems in metamorphic rocks are complicated by two factors, whether:

- initial $^{87}\text{Sr}/^{86}\text{Sr}$ ratios have been homogenized by metamorphism, or
- Rb and Sr elemental abundances have been redistributed during the metamorphism.

Because of the mobility of radiogenic ^{87}Sr in non-lattice positions (formed by the *in situ* radioactive decay of ^{87}Rb), the ^{87}Sr can easily migrate during metamorphism.

An example of this is the case of the Stockdale rhyolite in the Lake District of England, already cited. The 16-point whole-rock isochron initially determined on this fine-grained flow-banded lava yielded an

“age” which was inconsistent with its presumed age based on biostratigraphy and other “dating” methods. Thus it has been argued that the whole unit was probably disturbed by some kind of hydrothermal event after extrusion and subsequent burial, and so *Compston et al.* [1982] sought to verify this supposed re-setting event post-dating extrusion of the lava. They found that if the four samples with the highest Rb/Sr ratios were removed, along with one sample with an anomalously high Sr content, then all of the other samples lay close to the reference line for the preferred “age.” Thus because a separate isochron with a lower “age” could be calculated from this discarded data, this “age” was interpreted as the time of hydrothermal alteration of the whole rhyolite rock unit when there was supposed to have been a net loss of ^{87}Sr which was nevertheless only selective in its effects.

Other investigators have also observed that, as in the case of the Stockdale rhyolite, samples with the highest Rb/Sr ratios seem to have been the most obviously affected during metamorphism. Because the $^{87}\text{Sr}/^{86}\text{Sr}$ ratios of either igneous terranes or sedimentary strata are relatively heterogeneous from site to site due to varying Rb/Sr distribution, there seems to be a tendency for the Sr isotopes to undergo re-equilibration during metamorphism. In reality, few systems are perfectly homogenized during metamorphism [*Zheng, 1989*]. Furthermore, minerals separated from single whole-rock specimens may yield distorted internal mineral isochrons also dependent on the degree of Sr isotopic homogenization.

Thus the evidence for open-system Rb-Sr systematics in numerous environments has now discredited the Rb-Sr isochron method as a “dating” tool [*Dickin, 1995*]. In some cases, gain or loss of Rb and Sr from the rocks is so regular that a linear array can be produced on the conventional isochron diagram, and biased isochron results give spurious “age” and initial $^{87}\text{Sr}/^{86}\text{Sr}$ ratio estimates [*Zheng, 1989*]. Similarly, *Cameron et al.* [1981] concluded that the wide scatter commonly observed in whole-rock Rb-Sr isochrons from polymetamorphic terranes may arise in principle in three different ways:

- open-system behavior of the samples during later metamorphism;
- variation in the initial $^{87}\text{Sr}/^{86}\text{Sr}$ owing to heterogeneity in the protolith

rocks; and

- inclusion of rocks of different primary “ages.”

Zheng [1989] thus concluded that:

As it is impossible to distinguish a valid isochron from an apparent isochron in the light of Rb-Sr isotopic data alone, caution must be taken in explaining the Rb-Sr isochron age of any geological system.

The example of the isotopic investigation by *Kruger et al.* [1998] of an Archean pegmatite in South Africa will suffice to illustrate that the validity of an Rb-Sr isochron can only be determined by its consistency or not with other isotopic data. In this example, Pb-Pb and Sm-Nd isotopic data suggested an “age” for this pegmatite of approximately 2915 Ma, whereas an Rb-Sr K-feldspar-garnet-albite isochron yielded an approximate 2023 Ma “age.” This disparity was thus interpreted in terms of the Rb-Sr isochron corresponding to a later (hydro)thermal overprint subsequent to pegmatite formation. *Kruger et al.* [1998] suggested that Sr isotope resetting was incomplete and resulted in open-system behavior of the pegmatite, with K-feldspar almost quantitatively losing its (radiogenic) ^{87}Sr . On the other hand, Sr loss from muscovite was variable but also incomplete, as indicated by a wide range in “ages” (2088–2744 Ma). While *Kruger et al.* claim that only insignificant portions of this migrating Sr were incorporated into adjacent albite grains, the outer edge of one of those grains in contact with a muscovite grain yielded an apparent “age” of 5852 Ma, while its core yielded an apparent “age” of 3067 Ma. They concluded that not only was Sr lost from the system and the Rb/Sr ratio of the whole-rock was changed as a result, but the preferential Sr loss by far exceeded predictions based on volume diffusion experiments, perhaps occurring by means of “fast-path transport,” which of course is a convenient explanation to account for these gross “age” discrepancies beyond experimental verification. Clearly *Zheng* [1989] is correct in concluding that:

... an observed isochron does not certainly define a valid age information for a geological system, even if a goodness of fit of the experimental data points is obtained in plotting $^{87}\text{Sr}/^{86}\text{Sr}$ vs. $^{87}\text{Rb}/^{86}\text{Sr}$. This problem cannot be overlooked, especially in evaluating the numerical time scale.

4.6 The Rb-Sr System in Sedimentary Rocks

The Rb/Sr method has also been used on sedimentary rocks, because the “absolute date” of the time of deposition of sedimentary rocks is an important problem, but one that is very difficult to solve [*Dickin*, 1995]. Accurate “dates” depend on thorough re-setting of isotopic clocks. Hence Rb-Sr dating of sediments rests on the assumption that Sr isotope systematics in the rock were homogenized during deposition or early diagenesis, and therefore remained as a closed system until the present day. However, these two requirements may be mutually exclusive.

In principle, sedimentary rocks may be divided into two groups according to the nature of the Rb-bearing phase present. Allogenic (detrital) minerals are moderately resistant to open-system behavior during burial metamorphism, but problems arise from inherited isotopic signatures. Authigenic minerals are deposited directly from seawater and hence display good initial Sr isotopic homogeneity. However, it can be conveniently claimed that they are highly susceptible to recrystallization after burial and may not remain closed systems when the “dates” obtained are in disagreement with uniformitarian expectations and independent experimental confirmation of such behavior is lacking.

Detrital Rb-bearing minerals such as micas, K-feldspar, clay minerals, etc., can be expected to contain inherited “old” radiogenic Sr, so that “dating” of such material should in theory give an average of the provenance “ages” of the sedimentary constituents. Fine-grained, detrital sedimentary rocks such as shales consist primarily of mineral particles that formed prior to deposition of the sediment and therefore may have extensive prior histories, but it has been demonstrated many times that such fine-grained detrital sedimentary rocks form linear arrays on Rb-Sr isochron diagrams [*Faure*, 1986]. However, the “dates” determined from such isochrons have proven difficult to interpret because isotopic homogenization is not necessarily associated with the time of deposition, but may result from diagenesis, structural deformation, and recrystallization during incipient metamorphism. All of these processes post-date deposition by varying periods of time. On the other hand, the presence of “old” detrital minerals resistant to isotopic equilibration

(for example, muscovite) may result in “dates” that exceed the time of deposition of the sediment. Nevertheless, *Dickin* [1995] maintains that if sufficiently fine-grained shales are sampled, then it appears that the constituent minerals (mainly the clay mineral illite) often suffer substantial Sr exchange during post-depositional diagenesis, and so may develop an almost homogeneous initial Sr isotope composition soon after deposition, thereafter remaining effectively closed systems until the present day.

Compston and Pidgeon [1962] pioneered whole-rock Rb-Sr dating of shale, and found that in some circumstances the above conditions were closely approached, while in other cases gross inherited $^{87}\text{Sr}/^{86}\text{Sr}$ variations remained, preventing the calculation of a meaningful “age.” *Compston and Pidgeon* attributed this to undecomposed detrital micas, probably sericite. *Whitney and Hurley* [1964] found that the major source of error in Rb-Sr “age” determinations on whole-rock samples of shales was the presence of inherited radiogenic Sr in the detrital minerals. They concluded that the magnitude of this effect was dependent upon the provenance of the detritus and the degree to which it had been altered during weathering, transportation and sedimentation.

Some recent work on the dating of shales has sought to avoid problems of contamination with detrital micas and feldspars by analyzing separated clay-mineral fractions, whose purity is checked by x-ray defraction [*Dickin*, 1995]. *Clauer* [1979] compared Rb-Sr whole-rock and clay mineral analyses of a Precambrian shale from West Africa. He found that four clay fractions defined a linear array which yielded a somewhat acceptable “age” with an initial ratio consistent with associated dolomite. A whole-rock sample free of detrital feldspar also lay on this “isochron,” but two whole-rock analyses with traces of feldspar lay slightly above it and a fourth sample with abundant feldspar was displaced well above the “isochron.” *Dickin* [1995] concluded from this example that it would appear whole-rock Rb-Sr dating of shales is an unreliable geochronometer, but that analysis of separate illite fractions may give meaningful “ages” of diagenesis or low-grade metamorphism. However, there is always a danger that the detrital component may not be completely eliminated from the illite fraction.

On the other hand, the mineral glauconite seemingly offers an attractive possibility of “dating” sedimentary rocks directly, due to its high Rb content, easy identification and widespread stratigraphic distribution. Glauconite is a micaceous mineral similar to illite which is best developed in macroscopic pellets, probably formed by the alteration of a very fine-grained clay precursor intermixed with organic matter beneath the sediment-water interface in the marine environment. During this process the K contents of the pellets increase, as determined by the study of pellets on the present-day ocean floor. According to *Clauer* [1979, 1981] and *Bonhomme* [1982] some glauconite only produces acceptable “ages” when its grain size is less than 2 μm . When the grain size is larger, the glauconite yields inflated “ages.” Given that glauconite is deposited under water where Sr mobility should be at or near its maximum, Sr isotopic homogeneity should occur, but it obviously does not, nor is there good evidence for resetting. On the other hand, *Thompson and Hower* [1973] lamented the low radioisotopic “ages” yielded by glauconites, which they maintained could be explained by the occurrence of K (and by inference Rb) in interpreted hexagonal voids in the basal plane of glauconite’s hydrated layers and exchange sites from where K, and therefore Rb, can be readily extracted, and from where Ar and Sr would predictably be also lost.

Rubidium-strontium analyses of Holocene (zero-age) glauconite pellets by *Clauer et al.* [1992] have shown that Sr isotope equilibrium with seawater is achieved only slowly as the K content increases. Thus the Rb-Sr data can be used to calculate a model Sr-“age” for the pellets by making the initial ratio equal to the isotopic composition of seawater Sr at the time of sedimentation. A zero-age pellet starts with a high apparent model “age” due to a large content of Sr in detrital mineral phases. However, as it matures the pellet homogenizes with seawater so that the model “age” falls to zero in a fully equilibrated pellet (see Figure 18) [*Clauer et al.*, 1992]. Thus there is a correlation between decreasing K content and increasing apparent Rb-Sr model “age.”

Finally, there is another important implication for the Rb-Sr isotope systematics of sedimentary rocks. Given that the allochthonous minerals often have inherited Sr isotopic signatures, and authigenic minerals such as

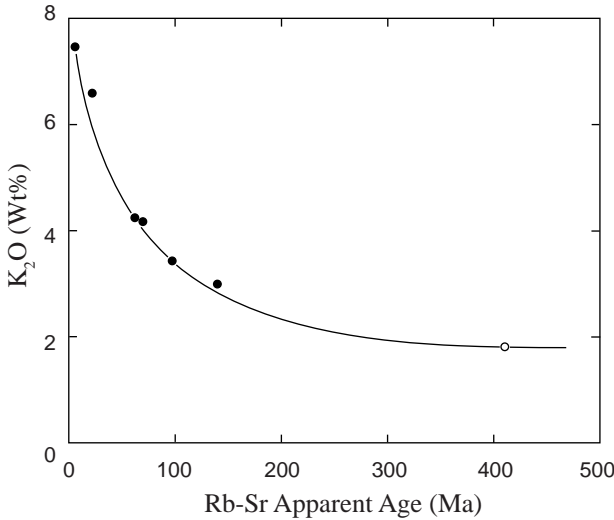


Figure 18. Rb-Sr model “ages” of Holocene (zero-age) glauconite pellets as a function of K content [after *Clauer et al.*, 1992]. Open symbol indicates the clay fraction.

glauconite can initially have a large content of Sr and a high apparent Rb-Sr model “age,” during subsequent metamorphism open-system behavior may occur in some phases while other phases are moderately resistant to such open-system behavior. Therefore the resultant metamorphic rock may not have homogenized radiogenic Sr and may likewise inherit apparent Rb-Sr model “ages,” while the previously highlighted susceptibility of Sr to mobilization by fluids will also lead to uncertainty in the interpretation of the Rb-Sr data of the rocks after metamorphism.

4.7 The Effects of Weathering

All of the above conclusions regarding the suitability for Rb-Sr “dating” of rocks and minerals apply only when the rocks and their minerals have not been altered by chemical weathering at or near the surface of the earth. Because most rocks that are used for “dating” are usually collected from outcrops, the effects of chemical weathering on the

^{87}Rb - ^{87}Sr decay scheme may be important.

Dasch [1969] measured the concentrations of Rb and Sr and $^{87}\text{Sr}/^{86}\text{Sr}$ ratios in several weathering profiles developed on igneous and metamorphic rocks. He found that progressive chemical weathering caused an increase in the Rb/Sr ratio due to the loss of Sr and concurrent increase in the Rb concentration of the rocks. The $^{87}\text{Sr}/^{86}\text{Sr}$ ratio, however, was found to remain constant, or increased only slightly. *Bottino and Fullagar* [1968] reported similar results for a granite in Virginia. They showed that in the weathered zone Li and Ca are depleted by about 50%, while Na, Mg and Sr are depleted by about 25% compared to fresh rock samples. Potassium showed no change, but Rb was enriched by about 20%. Thus the average Rb/Sr ratio of the weathered granite was found to be about 70% higher than that of the fresh rock. It can thus be concluded that chemical weathering of igneous and metamorphic rocks tends to increase the Rb/Sr ratios, moving them to the right on an isochron diagram. As a result, "dates" derived from chemically weathered rocks or minerals by the Rb-Sr method may be lower than the "true ages."

A graphic example of the effects of chemical weathering on Rb-Sr and K-Ar "dates" of biotite was reported by *Goldich and Gast* [1966]. They separated biotite grains from residual clay formed by chemical weathering of a gneiss in Minnesota. Rubidium-strontium "dates" of these biotites were about 75% lower than "dates" derived from unweathered biotite samples. In contrast, the K-Ar "dates" of the weathered biotites were only 25% lower, which was an unexpected but interesting anomaly. This disparity between the Rb-Sr and K-Ar "dates" of biotites has been attributed to a process of base exchange by *Kulp and Engels* [1963] and *Kulp* [1967]. They suggested that Ca-bearing ground water can remove K and radiogenic ^{40}Ar quantitatively from biotite, leaving the $^{40}\text{Ar}^*/^{40}\text{K}$ ratio unchanged. In this process radiogenic ^{87}Sr may be exchanged for other Sr isotopes in the water and is thus removed from the mineral. In addition, Rb^+ ions may replace K^+ ions, thereby increasing the Rb concentration of the biotite. The net result of these exchange reactions would be that the Rb-Sr "dates" of biotite are lowered significantly while the K-Ar "dates" remain relatively

unaffected. Their experiments suggested that 50% of the K can be removed together with the associated radiogenic ^{40}Ar without affecting K-Ar “dates,” whereas Rb-Sr “dates” can be lowered significantly simply by treating the biotite with a solution containing Rb and Ca. Thus they concluded that if sufficient Rb is present in ground water, Rb will be added to biotite while radiogenic ^{87}Sr is removed, lowering the Rb-Sr “age” relative to the K-Ar “age.”

Brooks [1968] investigated the open-system behavior of co-existing plagioclase and K-feldspar in a granite and was able to show that altered plagioclase gained significant amounts of radiogenic ^{87}Sr , ^{86}Sr and ^{87}Rb which had been derived from the K-feldspar. The significance of these results is that the alteration involved not only the movement of radiogenic ^{87}Sr , but also of Rb and normal (non-radiogenic) Sr.

Of course, outcrops that are clearly weathered and altered are not usually sampled for “dating.” What is therefore of even greater concern is how easily and quickly Rb and Sr can be leached from fresh rock. *Irber et al.* [1996] carried out leaching experiments on German granites containing biotite and muscovite. A mildly acidic (self-adjusting to pH 3) leaching solution was reacted with powdered samples of the granites for durations of 2, 5 and 20 hours. The results revealed extreme differences in the leaching behavior of Rb-Sr and the Sr isotopes which was mineralogically controlled, with the release of ^{87}Sr also depending on the leaching of Rb. *Irber et al.* [1996] found that large amounts of Rb were leached from the biotite in the biotite granite, while the less leachable feldspars contributed only minor amounts of Sr to the leaching solution. In fact, the Rb was about 10 times more leachable than Sr, and hence the $^{87}\text{Sr}/^{86}\text{Sr}$ ratio of the leaching solution was controlled by the leached Rb-fraction (and ^{87}Sr) which resulted in a higher $^{87}\text{Sr}/^{86}\text{Sr}$ in solution compared to the rock. Thus when the calculated isotopic compositions of the leached rock samples were plotted on an isochron diagram they shifted down along the isochron produced by the fresh rock samples. In complete contrast, *Irber et al.* [1996] found that the solution leached large amounts of Sr from the accessory apatite and calcite in the muscovite-K-feldspar-albite granites, while the less leachable muscovites and feldspars contributed only minor amounts of

Rb and Sr to the solution. In general, Sr was up to 50 times more leachable than Rb, and hence the $^{87}\text{Sr}/^{86}\text{Sr}$ ratio of the solution was controlled by the Sr-fraction whose isotopic composition was that of “common” ^{86}Sr , similar to the initial $^{87}\text{Sr}/^{86}\text{Sr}$ ratio of the granite and lower compared to the present-day fresh whole-rock ratio. The calculated isotopic compositions of the leached rocks plotted away from the isochron produced by the fresh rock samples, effectively rotating the isochron.

The significance of these results lies in the fact that most rocks in outcrop will show only subtle effects of chemical weathering and alteration due to their exposure to the atmosphere and meteoric water (which is often slightly acidic). *Irber et al.* [1996] maintain that investigations of alteration sequences have shown that during most common types of alteration a spread of Rb/Sr whole-rock ratios occurs due to drastic loss of Sr, whereas the Rb increases due to sericitization. Only in the case of strong albitization is the Rb/Sr whole-rock ratio lowered due to the removal of phyllosilicates and K-feldspar, and the fixation of some Sr in newly-formed albite. Because such changes are systematic, false isochrons can be generated which therefore may not be distinguishable from the “true” isochrons and “ages” that themselves may be artifacts of mixing, contamination or inheritance.

4.8 More Conclusions

All of these considerations combine to cast a “shadow” over the Rb-Sr radioisotopic system as a reliable geochronometer. The repeatedly demonstrated mobility of both Sr and Rb in fluids and at elevated temperatures invariably disturbs the Rb-Sr systematics, which combined with fractionation then yields invalid or meaningless “ages.” Much is made of the significance of initial $^{87}\text{Sr}/^{86}\text{Sr}$ ratios, yet these are known to vary within apparently cogenetic suites of both oceanic and continental volcanic rocks, even from a single volcano, perhaps due to contamination. In any case, volcanic rocks can inherit their Rb-Sr systematics, and even “ages,” from their source areas which thus demonstrates heterogeneities in the mantle (and crust), while plutonic rocks are clearly the result of mixing of such sources. Anomalous and false isochrons are prolific,

their status only being apparent when such results are compared with other radioisotopic systems (such as Sm-Nd) and/or the stratigraphic setting. Thus recognition of inheritance, open-system behavior, contamination and mixing, and the later effects of weathering, together have increasingly caused Rb-Sr radioisotopic “dating” to be regarded as unreliable and therefore rejected.

5. The Samarium-Neodymium (Sm-Nd) Radioisotopic System

Neodymium (Nd) and samarium (Sm) are light rare earth elements with ionic radii of 1.08Å and 1.04Å respectively, and an ionic charge of 3+ like the other rare earth elements. Samarium is less abundant than Nd, which is consistent with the general decrease in abundance of the elements with increasing atomic number. The ratio of Sm to Nd concentrations in terrestrial rocks and minerals varies only from about 0.1 to 0.5 because the similarity of their chemical properties inhibits more extensive separation of Nd from Sm by geological processes.

The rare earth elements occur in high concentrations in several minerals, such as bastnaesite (CeFCO_3), monazite (CePO_4), and cerite ($(\text{Ca, Mg})_2(\text{Ce})_8(\text{SiO}_4)_7 \cdot 3\text{H}_2\text{O}$). The rare earth elements also occur as trace elements in common rock-forming minerals, in which they replace major ions. In addition, they may reside in inclusions of apatite, zircon, and other accessory minerals. Minerals exercise a considerable degree of selectivity in admitting rare earth elements into their crystal structures. Feldspars, biotite, and apatite tend to concentrate the light rare earth elements (the Ce group), whereas pyroxenes, amphiboles and garnet commonly concentrate the heavy rare earth elements (the Gd group). Furthermore, the concentrations of both Sm and Nd in the common rock-forming silicate minerals increase in the sequence in which they crystallize from magmas—olivine, pyroxene, amphibole and biotite, and in the feldspars from plagioclase to K-feldspar. The Sm/Nd ratios of most minerals range from about 0.37 (pyroxene) to (0.15) (K-feldspar), although garnet has a high ratio of about 0.54. Thus, the selectivity of the rock-forming minerals for the light or heavy rare earth elements affects the rare earth element concentrations of the rocks in which these

minerals occur.

The concentrations of both Nd and Sm in igneous rocks increase with increasing degree of differentiation, but their Sm/Nd ratios decrease. Thus, for example, the Sm/Nd ratio of a mid-ocean ridge basalt (MORB) is 0.32, whereas granites have a ratio of only 0.19. Alkali igneous rocks are enriched both in Sm and Nd compared to silica-saturated rocks and their Sm/Nd ratios range from 0.10 to 0.20, on average. Furthermore, in general, Nd is concentrated relative to Sm in the course of fractional crystallization of magma so that typical crustal rocks have lower Sm/Nd ratios than rocks derived from the upper mantle. Similarly, when silicate liquids form by partial melting of rocks in the mantle or crust, the liquid phase is enriched in Nd relative to Sm. This is because Nd^{3+} has a larger radius than Sm^{3+} which gives it a lower ionic potential (charge/radius) than Sm^{3+} , so that Nd^{3+} forms weaker ionic bonds that are broken more easily than those of Sm^{3+} .

5.1 Sm-Nd “Dating” and Its Limitations

“Age” determinations by the Sm-Nd method are usually made by analyzing separated minerals or cogenetic suites of rocks whose Sm/Nd ratios vary sufficiently to define the slope of an isochron in co-ordinates of $^{143}\text{Nd}/^{144}\text{Nd}$ and $^{147}\text{Sm}/^{144}\text{Nd}$. The Sm-Nd method is best suited for dating mafic and ultramafic igneous rocks, whereas the Rb-Sr method is more applicable to “dating” of acidic and intermediate igneous rocks that are enriched in Rb and depleted in Sr. Furthermore, the rare earth elements including Sm and Nd are much less mobile than Rb, Sr, Th, U and Pb during regional metamorphism, hydrothermal alteration and chemical weathering, so the Sm-Nd method is often used to supposedly “see through” younger events in rocks whose Rb-Sr and Pb-Pb isotopic chemistry has been disturbed. Thus it is claimed that rocks may be “dated” reliably by the Sm-Nd method even though they may have gained or lost Rb and Sr, or where the rocks are not suitable for dating by the Rb-Sr method, either because they have low Rb/Sr ratios or because they have not remained closed to Rb or Sr. Thus the Sm-Nd technique is often chosen as the best whole-rock method for determining “crust

formation ages,” which are supposed to be the times of formation of new segments of continental crust by fractionation of material from the mantle [Rollinson, 1993]. Whole-rock Sm-Nd “dating” therefore has an advantage over mineral Sm-Nd “dating” in that the scale of sampling is much larger (meters or kilometers instead of millimeters or centimeters), so that the possibility of post-crystallization isotopic re-equilibration between samples is reduced [DePaolo, 1988].

The chief limitations on the Sm-Nd technique are the long half-life of ^{147}Sm (106 Ga), so that it is only really applicable to supposedly “old” rocks, and the relatively small variations in Sm/Nd ratios found in most cogenetic rock suites. This latter problem has led some investigators to combine a wide range of lithologies on the same isochron in order to obtain a spread of Sm/Nd ratios [Rollinson, 1993]. However, that procedure has resulted in samples extracted from different sources and with very different histories being plotted on the same isochron and producing some spurious results. Thus a significant problem with whole-rock Sm-Nd “dating” is determining if the rocks are both isochronous and have the same initial $^{143}\text{Nd}/^{144}\text{Nd}$ ratio, which is considered an important geochemical parameter. However, it is difficult to obtain precise initial $^{143}\text{Nd}/^{144}\text{Nd}$ ratios because no common minerals have $^{147}\text{Sm}/^{144}\text{Nd}$ near zero, so on isochron plots long extrapolations are usually made in order to determine the intercepts, which result in relatively large uncertainties [DePaolo, 1988]. Furthermore, variations in initial ratios for suites of young lavas from a single volcano have been found [Chen and Frey, 1983], which suggests that the assumption of a well-defined initial ratio for many suites of rocks is difficult to defend. This is particularly problematic for Sm-Nd whole-rock “dating” because the relatively small range of $^{143}\text{Nd}/^{144}\text{Nd}$ ratios in most rock suites means that any differences in the initial ratio that are larger than the analytical uncertainty could affect the “age” substantially. Thus if a rock suite has variable initial ratios, and especially if the Sm/Nd ratios and the initial ratios are correlated, as is often the case, both the determined “age” and the initial ratio may be seriously in error. For example, rocks of very nearly the same “age” (± 15 Ma) from the Peninsular Ranges Batholith of southern California exhibit variations in initial $^{143}\text{Nd}/^{144}\text{Nd}$ of some

0.14%, equal in magnitude to the total range of $^{143}\text{Nd}/^{144}\text{Nd}$ expected along a typical isochron [DePaolo, 1981c]. Furthermore, the $^{143}\text{Nd}/^{144}\text{Nd}$ initial ratios are roughly correlated with $^{147}\text{Sm}/^{144}\text{Nd}$ in the rocks, so that the data scatter about an apparent “isochron” of 1.7 Ga, even though the “crystallization age” is about 0.1 Ga! This problem should be less severe in supposedly older (Archean) rock suites where smaller ranges of initial $^{143}\text{Nd}/^{144}\text{Nd}$ ratios would be expected. Nevertheless, any scatter about a whole-rock isochron clearly must be critically assessed, since it could be an indication that both the determined “age” and initial $^{143}\text{Nd}/^{144}\text{Nd}$ ratio are in error, even in Archean rock suites [Chauvel *et al.*, 1985].

5.2 The Problems Obtaining a Spread of Sm/Nd Ratios

Most early Sm-Nd work was focused on the determination of “crystallization ages” for Archean igneous rocks where the Rb-Sr or K-Ar methods had often failed to yield an accurate “crystallization age” due to remobilization of the parent or daughter elements during subsequent metamorphism. A good example of this application was the “dating” of the Stillwater Complex (Montana-Wyoming) by DePaolo and Wasserburg [1979b]. Rubidium-strontium data on three separated minerals from a single unit of the Stillwater layered series formed a scatter which did not define an isochron. However, Sm-Nd data on the same mineral samples yielded an excellent linear array from which an “age” was calculated. In order to test for possible mineralogical re-setting of Sm and Nd, DePaolo and Wasserburg also analyzed six whole-rock samples from different layers of the intrusion with a wide range of plagioclase/pyroxene abundances. This Sm-Nd data fell within the analytical uncertainty of the mineral isochron, thus suggesting to them that the mineral isochron yielded a true “crystallization age” for the intrusion, and that the magma had homogeneous initial Nd isotope composition. However, Sm-Nd analyses of whole-rock samples from a wider stratigraphic range within the intrusion demonstrated wider variations in the initial ratios [Lambert *et al.*, 1989]. In any case, the initial ratio of DePaolo and Wasserburg [1976b] falls well away from the supposed estimated mantle values at 2.7 Ga, which was explained

(away) as due to contamination of the magma by “old” crustal Nd from the nearby Wyoming Craton.

The above example emphasizes the importance of combined mineral and whole-rock isochrons to test the “age” interpretation of the Sm-Nd data. However, this approach is not possible for fine-grained rocks such as Archean basalts and komatiites. In these situations, whole-rock analyses have often been used alone, but subtle effects on the slope of whole-rock isochrons can be caused by analyzing samples with apparent slight variations in presumed crustal contamination. Another danger, mentioned previously, is the combining of a wide range of lithologies on the same isochron in order to obtain a spread of Sm/Nd ratios. A good example of these problems is provided by the Kambalda volcanics of Western Australia. *McCulloch and Compston* [1981] determined a composite Sm-Nd isochron on a suite of rocks comprising the ore-bearing Kambalda ultramafic unit, the footwall and hanging-wall basalts, and an “associated” sodic-granite and felsic porphyry. Although the whole suite yielded a good isochron “age” of 2790 ± 30 Ma, the mafic and ultramafic samples alone gave an older best-fit “age” of 2910 ± 170 Ma.

The danger of constructing this “composite” Sm-Nd isochron of felsic, mafic and ultramafic rocks which might not be co-magmatic was pointed out by *Claoue-Long et al.* [1984], who attempted to “date” the Kambalda lavas by the Sm-Nd method without utilizing felsic rocks. However, they were forced to combine analyses from komatiites and basalts in order to achieve a good spread of Sm/Nd ratios. After the exclusion of one komatiite sample from Kambalda and a suite of basalt lavas from 40 km south of the main Kambalda sequence, ten data points yielded an “age” of 3262 ± 44 Ma, which *Claoue-Long et al.* interpreted as the time of eruption. *Chauvel et al.* [1985] challenged this interpretation on the basis of Pb-Pb “dating” of the Kambalda volcanics and associated sulfide mineralization at 2726 ± 34 Ma, which they argued was resistant to re-setting by later events. They attributed the apparent 3.2 Ga Sm-Nd “age” to either variable crustal contamination of the magma suite by older basement, or possibly a heterogeneous mantle source, all of which is a matter of interpretation. Furthermore, U-Pb “dating” of interpreted zircon xenocrysts (literally, foreign crystals) in one of the hanging-wall

basalts subsequently appeared to confirm the contamination model [Compston *et al.*, 1985], but with an “age” of 3.4 Ga it was problematic as to what was the real “age” of this so-called contamination or whether these isotopic ratios have no “age” meaning at all! Dickin [1995] maintained that, in retrospect, “danger signals” should have been seen in the whole-rock Sm-Nd data, since only the hanging-wall basalts defined a slope of 3.2 Ga and those were the samples which could have suffered the most contamination.

Similar effects have been demonstrated for komatiites and basalts in the Abitibi Belt of Ontario, Canada. Cattell *et al.* [1984] obtained an apparent “age” of 2.83 Ga from a whole-rock Sm-Nd isochron on these rocks, but a maximum “eruption age” of 2697 ± 1 Ma was also provided by U-Pb zircon “dating” of an underlying volcanoclastic rock. So they plotted initial $^{143}\text{Nd}/^{144}\text{Nd}$ ratios at 2697 Ma against $^{147}\text{Sm}/^{144}\text{Nd}$, which suggested an “erupted” Sm-Nd isochron with an apparent “age” of only 130 ± 64 Ma! Of course, no age significance was attached to this pseudo-isochron, because they attributed this to the magma sampling a very depleted mantle source and/or contamination by older crustal rock. Since such interpretations can arbitrarily be applied to the isotopic data as an explanation when the “age” produced is invalid (not as anticipated), then it could potentially be argued that such interpretations might always be more valid than any “age” significance.

5.3 Metamorphism and Sm-Nd Mobility

The Sm-Nd method has frequently been applied to “dating” the supposed “igneous” protolith “age” of high-grade metamorphic basement rocks where other radioisotopic systems have been reset. For example, whole-rock Rb-Sr, whole-rock Pb-Pb and U-Pb zircon “ages” on granulite-facies and amphibolite-facies Lewisian gneisses of north-west Scotland were found to be roughly concordant, yet these gneisses are generally very Rb- and U-depleted, suggesting that even large whole-rock samples were probably open systems for these elements during some “depletion event.” A suite of whole-rock samples was Sm-Nd “dated” by Hamilton *et al.* [1979] to see whether the Sm-Nd isotopic

system had remained undisturbed during the metamorphism which the other isotopic systems had presumably “dated.” The Sm-Nd isotopes yielded an older “age” by about 250 Ma, which seemed to suggest to the investigators that the gneisses had remained closed systems for Sm-Nd during granulite-facies metamorphism. They therefore interpreted this “age” as the time of protolith formation, which therefore supposedly occurred about 250 Ma before the interpreted closing of the U-Pb zircon and the whole-rock Rb-Sr and Pb-Pb isotopic systems subsequent to the presumed peak of metamorphism.

There were obviously two problems with the sampling to produce this Sm-Nd isochron “age”—the combining of amphibolite- and granulite-facies gneisses in the sample suite, and also the inclusion of samples from a bimodal suite of tonalitic gneisses and mafic rocks from a layered complex. Nevertheless, because this combination of samples yielded statistically compatible Sm-Nd data the resultant isochron “age” was deemed acceptable. However, more detailed investigation by *Whitehouse* [1988] showed that the mafic rocks of the layered complex had “retained” the older Sm-Nd isochron “age,” whereas the Sm-Nd whole-rock systems in the non-mafic rocks seem to have been “reset” to the same “age” as the U-Pb zircon and other whole-rock isotopic systems. Thus it was concluded that the Sm-Nd isotopic system had only remained closed in the mafic rocks during the metamorphic event, the Sm-Nd in the other gneisses being disturbed. This is contrary to the oft-repeated claim that the less mobile Sm and Nd are not disturbed by events subsequent to the initial formation of their host rocks. If these isotopes are mobile in ways similar to the other isotopic systems, then the reliability of Sm-Nd “ages” is equally questionable.

Although some studies have shown that the Sm-Nd isotopic system is not remobilized during hydrothermal alteration of felsic rocks, *Poitrasson et al.* [1995] maintain that the rare earth element mobility caused by certain hydrothermal conditions does perturb the Sm-Nd system. They investigated hydrothermally altered rhyolites and granite, and found that although these rocks were initially very homogeneous as regards their Nd isotopes, some samples displayed very contrasting Nd isotopic signatures, such as comparatively low initial $^{143}\text{Nd}/^{144}\text{Nd}$ ratios which

were anomalous. Furthermore, the isotopically perturbed rocks were invariably associated with peculiar rare earth element patterns that were also difficult to explain in terms of differentiation or contamination of the parent magmas, so they concluded that the Sm-Nd isotopic system had been perturbed by the hydrothermal alteration. Although the net result of this hydrothermal alteration was leaching of the rare earth elements from the rocks, the perturbation of the Sm-Nd isotopic system could not be solely explained by a modification of the Sm/Nd ratio significantly after emplacement of these rocks, which led to the conclusion that the isotopic compositions were modified by a component introduced from the hydrothermal fluid which had contrasting $^{143}\text{Nd}/^{144}\text{Nd}$ ratios. *Poitrasson et al.* [1995] thus found that rare earth elements were transported over distances exceeding several tens to hundreds of meters, even where mineralized fractures were absent in the granite they studied. Furthermore, isotopically perturbed samples could not be discriminated readily from unperturbed samples in the field because of the lack of obvious indicators of different degrees of fluid-rock interactions. Thus Sm and Nd are not as immobile as is often claimed, nor does the Sm-Nd isotopic system escape being significantly perturbed, which raises similar doubts about the reliability of the Sm-Nd “dating” system as with the other radioisotopic dating systems.

5.4 Sm-Nd Mineral “Dating”

Another area where the Sm-Nd isochron method has been widely applied is to the “dating” of high-grade metamorphic minerals. Mineral isochrons have the advantage that variations in partition coefficients between minerals have caused moderately large variations in Sm/Nd ratios, unlike whole-rock systems. Thus, it is claimed that “precise ages” may be determined. Garnet-bearing mineral assemblages offer the best potential, because garnets have high Sm/Nd ratios in contrast to clinopyroxene or plagioclase, which results in a large range in Sm/Nd and thus allows better statistics in determining the “age” from the slope of such a mineral isochron. Garnet “ages” are determined on 2-point isochrons between garnet and one or more of the minerals plagioclase,

orthopyroxene or clinopyroxene and hornblende, the classic example being that of eclogite, a garnet-clinopyroxene rock which has thus been a major focus of Sm-Nd mineral “dating.” Mineral isochrons which do not involve garnet show a smaller range of Sm/Nd ratios, but still are regarded as yielding reasonably “precise ages.” However, the oft-claimed relative immobility of the rare earth elements, which is said to be an asset in “dating” igneous crystallization, is a problem in using the Sm-Nd method to date metamorphism. Mineral systems may be opened sufficiently to disrupt the original igneous chemistry, but are thought not to be open enough to completely overprint the system.

The crucial consideration with respect to mineral systems being open to element mobility is the so-called blocking temperatures of the minerals, the principal control on the retentivity of radiogenic isotopes in minerals. As previously discussed, the blocking temperature is the point at which the mineral becomes a closed system with respect to a particular daughter isotope. Different minerals will close at different temperatures, and different isotopic systems in the same mineral will also close at different temperatures. Otherwise known as the closure temperature, it is defined as “the temperature of a system at the time of its apparent age” [Dodson, 1979]. It is thus the temperature below which the isotopic clock is switched on.

When a cooling mineral is close to its temperature of crystallization, the daughter isotope in question will diffuse out of the mineral as fast as it is produced and so cannot accumulate. On cooling the mineral enters a transition stage in which some of the daughter isotope is lost and some is retained, until finally at low temperatures the rate of escape is negligible and all of the daughter isotope is presumably retained. It is therefore important to determine the closure temperatures for the different isotopic systems in the different minerals in a metamorphic rock, the postulated temperature of the metamorphism thus indicating how reliable a mineral isochron for that metamorphic rock might be.

The blocking temperature for Nd diffusion in garnet is regarded as being about 700°C [Windrim and McCulloch, 1986], and thus Nd mobility would appear to only be a problem in garnet at the very highest grade of metamorphism. However, the closure temperature of the

Sm-Nd system in metamorphic garnet has been the subject of continued debate, with estimates varying from approximately 400°C to 800°C [Ganguly *et al.*, 1998]. Indeed, experimental determinations of the diffusion coefficients of Sm and Nd in garnet and theoretical considerations show that a sufficiently restricted range of closure temperature cannot be assigned to the Sm-Nd decay system in garnet [Ganguly *et al.*, 1998]. Nevertheless, Ganguly *et al.* [1998] used the Sm-Nd “cooling age” of garnet from their experimental data to calculate both the cooling rate and the closure temperature predicated on knowing the temperature and “age” at the peak of metamorphic conditions. This obviously involves circular reasoning regarding the uniformitarian validity of the Sm-Nd isotopic system.

Yet resetting of the Sm-Nd isotopic system in garnet does take place, as Hensen and Zhou [1995] found in granulite-facies metamorphic rocks in Antarctica. They claimed an effective diameter for diffusion of only 1 mm, but admitted that chronological constraints are essential for the unambiguous interpretation of reaction textures, an admission that the reliability of garnet Sm-Nd “dating” is needed (and therefore often assumed) in order to provide these chronological constraints in spite of diffusion and resetting. Another frequently-used method for providing chronological constraints on the Sm-Nd isotopic system in garnets has been U-Th-Pb dating of the garnets. However, the study by DeWolf *et al.* [1996], in which U content in a garnet lattice was directly measured, found that essentially all the U in garnets was hosted in inclusions, and this was subsequently confirmed by Vance *et al.* [1998], who demonstrated that the U-Th-Pb systematics of garnets are controlled by inclusions of zircon, monazite and allanite. As noted by Vance *et al.* [1998], this then has implications regarding the closure temperature for the Sm-Nd system in garnets, because the U-Th-Pb “dating” constraints often used for garnets are actually dating their inclusions, which will invariably be older than the garnets. However, Mezgar *et al.* [1993] estimated a closure temperature for Sm-Nd in garnets of about 570°C calibrated against U-Pb “ages” on titanite and an Ar-Ar “age” on hornblende, so this implies Sm-Nd mobility at higher temperatures. Nevertheless, calibrations are still dependent on the reliability of the

other radioisotopic dating systems and their consistency with the uniformitarian timescale.

In any case, *Poitrasson et al.* [1998] have shown from a study of Sm-Nd isotopic systematics in the minerals of two granites that the fluids of hydrothermal convection interacting with country rocks at the end of granite crystallization are capable of carrying lanthanides including Sm and Nd in the crust over distances of at least 1 km. The minerals in both granites produced two statistically acceptable alignments able to be satisfactorily interpreted as mineral isochrons, but one each of these “isochrons” in each granite produced an otherwise meaningless “age,” which had to be interpreted as either inherited or due to hydrothermal convection long after crystallization of the granites. Ironically, *Poitrasson et al.* [1998] claimed that, in spite of the obvious disparity in the Sm-Nd isotopic data of different minerals within the same rock due to large-scale fluid movements of these isotopes, nonetheless the Sm-Nd systematics at the whole-rock scale were not perturbed! Such a claim is both arbitrary and convenient, but they are still admitting that the Sm-Nd systematics in minerals are just as weakly resistant to hydrothermal fluids as the K-Ar and Rb-Sr isotopic systems, and that it may be Sm that is more susceptible to migration than Nd. Clearly, the Sm-Nd isotopic “dating” system in both whole-rocks and minerals is not as “foolproof” as is often claimed, sometimes being arbitrarily subject to resetting and disturbance due to diffusion and fluid migration at all scales.

5.5 Sm-Nd “Model Ages”

Of considerable importance in the use of the Sm-Nd isotopic system are “model ages.” A “model age” is defined as an estimate of the time at which a sample separated from its mantle source region, or put another way, a measure of the length of time a sample has been separated from the mantle from which it was originally derived [*Rollinson, 1993*]. This, of course, assumes:

- knowledge of the isotopic compositions of mantle sources,
- absence of parent/daughter isotopic fractionation after extraction from

the mantle sources, and

- the immobility of parent and daughter isotopes.

In the case of Sr isotopes none of these criteria is usually fulfilled with any certainty either for igneous rocks or for sediments [*Goldstein, 1988*], and so “model ages” are not now frequently calculated for the Rb-Sr system.

“Model ages” are most commonly quoted for the Sm-Nd isotopic system, and are regarded as valuable because they can be calculated for an individual rock from a single pair of parent-daughter isotopic ratios. They must, however, be interpreted with care [*Rollinson, 1993*]. The basis of all “model age” calculations is an assumption about the isotopic compositions of the mantle source regions from which the samples were originally derived. In the case of Nd isotopes there are two frequently quoted “models” for the mantle reservoir—CHUR (the CHondritic Uniform Reservoir) and Depleted Mantle (DM).

5.5.1 CHUR “Model Ages.” The CHUR model [*DePaolo and Wasserburg, 1976a*] assumes that the earth’s primitive mantle had the same isotopic composition as the average chondritic meteorite at the formation of the earth, which in this case is taken to be 4.6 Ga. For Nd isotopes CHUR is synonymous with the composition of the bulk earth. *DePaolo and Wasserburg [1976a]* made the first Nd isotope determinations on terrestrial igneous rocks. When they plotted the “ages” and initial $^{143}\text{Nd}/^{144}\text{Nd}$ ratios of these units on a diagram of Nd isotope “evolution” against time, they found that Archean plutons had initial ratios which were remarkably consistent with the evolution of CHUR. Since the initial ratios of co-magmatic rock suites are traditionally determined from isochron intercepts, it should be remembered that the poor spread of Sm/Nd ratios in most rock suites combined with the long extrapolations involved causes error-magnifications which can lead to quite significant errors in the determination of these initial $^{143}\text{Nd}/^{144}\text{Nd}$ ratios.

The claimed isotopic “evolution” of Nd in the earth according to the CHUR model is illustrated in Figure 19. Note again that the whole basis of this model are the assumptions of a 4.6 Ga “age” for the earth and an origin from the “solar nebula.” Partial melting of CHUR gave rise to

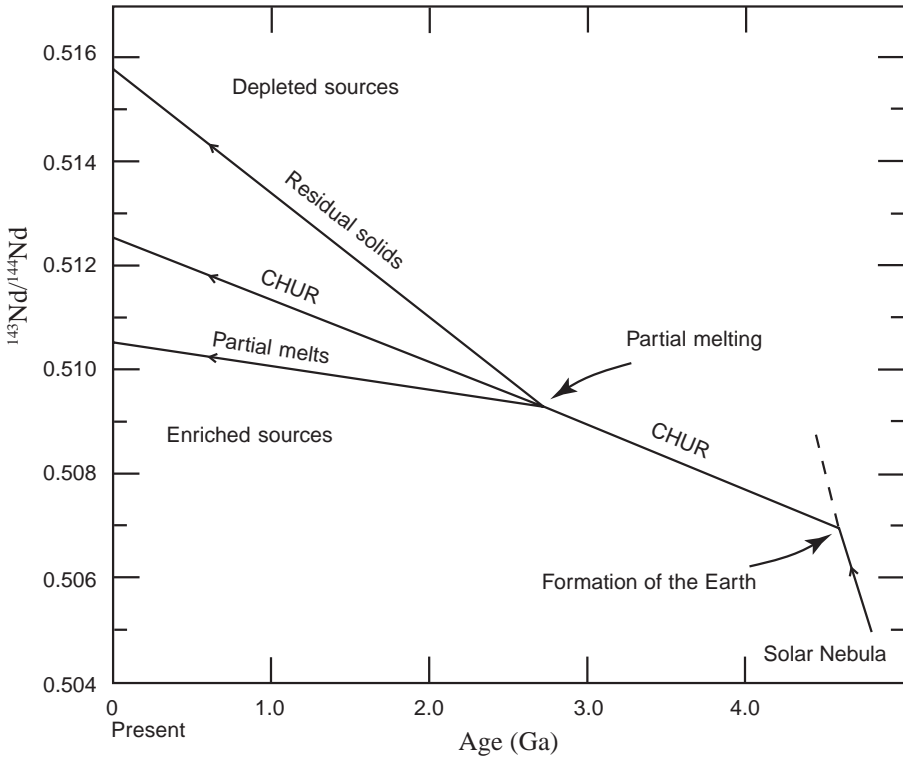


Figure 19. Isotopic evolution of Nd in a chondritic uniform reservoir (CHUR) [after *Faure*, 1986]. Magma formed by partial melting has a lower Sm/Nd ratio than CHUR, whereas the residual solids have a higher Sm/Nd ratio. As a result, the present day $^{143}\text{Nd}/^{144}\text{Nd}$ ratio of the rocks formed from the silicate liquid is less than that of CHUR, whereas the $^{143}\text{Nd}/^{144}\text{Nd}$ ratio of the residual solids is higher. If magma forms by a second episode of melting of such “depleted” mantle, the resulting igneous rocks have initial $^{143}\text{Nd}/^{144}\text{Nd}$ ratios that are greater than CHUR.

magmas having lower Sm/Nd ratios than CHUR, the igneous rocks forming from such magmas therefore having lower present-day $^{143}\text{Nd}/^{144}\text{Nd}$ ratios than CHUR. The residual solids that remained behind after withdrawal of the magmas have correspondingly higher Sm/Nd ratios than the chondritic reservoir. Consequently, these “depleted” regions of the reservoir have higher $^{143}\text{Nd}/^{144}\text{Nd}$ ratios than CHUR at the

present time. The differences in the Sm/Nd ratios of partial melts and residual solids as indicated in Figure 19 are consistent with the geochemical properties of Sm and Nd. Those parts of the chondritic reservoir that remained undisturbed by magma-forming events continued to contain Nd whose isotopic composition “evolved” without interruption right up to the present. The straight line in Figure 19 that represents these undisturbed regions thus serves as a reference for the isotopic “evolution” of Nd in the rocks which formed from magma generated within the reservoir in the past. Thus it is possible to compare the initial $^{143}\text{Nd}/^{144}\text{Nd}$ ratios of igneous and metamorphic rocks in the earth’s crust with the corresponding $^{143}\text{Nd}/^{144}\text{Nd}$ ratios of CHUR at the presumed time of crystallization of the rocks, particularly if the initial $^{143}\text{Nd}/^{144}\text{Nd}$ ratios of different kinds of rocks are higher or lower than those of CHUR at the appropriate “geological” times.

The differences in the isotopic ratios are quite small, and for that reason *DePaolo and Wasserburg* [1976a] introduced the epsilon (ϵ) parameter. A positive ϵ value is said to indicate that the rocks were derived from residual solids in the reservoir after magma had been withdrawn at an earlier time. Such parts of the reservoir are said to be “depleted” in the large ion lithophile elements (K, Rb, Ba, Th, U, etc.) that are preferentially partitioned into the liquid phase during partial melting. A negative ϵ value is said to indicate that the rocks were derived from sources that had a lower Sm/Nd ratio than the chondritic reservoir, meaning that such rocks were derived from, or assimilated, “old” crustal rocks whose Sm/Nd ratio had been lowered originally when they separated from CHUR. If the ϵ value is 0, then the isotopic composition of Nd in the rock is said to be indistinguishable from that in the chondritic reservoir, from which it is concluded that the rocks could have been derived directly from that reservoir (CHUR).

DePaolo and Wasserburg [1976b] argued that if the CHUR evolution line defines the initial ratios of continental igneous rocks through “geological” time, then measurement of $^{143}\text{Nd}/^{144}\text{Nd}$ and $^{147}\text{Sm}/^{144}\text{Nd}$ in any crustal rock would yield a “model age” for the formation of that rock (or its precursor) from the chondritic reservoir, provided that there was sufficient Nd/Sm fractionation during the process of crustal

extraction from the mantle to give a reasonable divergence. A “model age” calculated relative to CHUR, therefore, is the time in the past when the sample suite is supposed to have separated from the mantle reservoir and acquired a different Sm/Nd ratio. It is also the time at which the sample supposedly had the same $^{143}\text{Nd}/^{144}\text{Nd}$ ratio as CHUR. This is illustrated in Figure 20, in which the present-day $^{143}\text{Nd}/^{144}\text{Nd}$ composition of a sample is extrapolated back in time until it intersects the CHUR evolution line. This gives the T_{CHUR} “model age.” The evolution curve for the sample is constructed from the present-day $^{143}\text{Nd}/^{144}\text{Nd}$ ratio, and the T_{CHUR} “model age” is calculated from the present-day (measured) $^{147}\text{Sm}/^{144}\text{Nd}$ and $^{143}\text{Nd}/^{144}\text{Nd}$ isotope ratios of the sample with a standard equation. Care has to be taken to choose the correct CHUR value because different laboratories use different normalizing values [Rollison, 1993].

“Model ages” are also sensitive to the difference in Sm/Nd between the sample and CHUR, and only fractionated samples with Sm/Nd ratios which are sufficiently different from the chondritic value will yield “precise ages.” “Dates” calculated by this method have potential geological significance only when the Sm/Nd ratio of the rock which is to be “dated” did not change since the time of separation of Nd from the chondrite reservoir (Figure 19). It would seem that this condition is better satisfied by Sm and Nd than by Rb and Sr, because the geochemical properties of these rare earth elements are much more similar to one another than the geochemical properties of the alkali metal (Rb) and the alkaline earth (Sr). It is claimed that in general the Sm/Nd ratios of crustal rocks are not changed by metamorphism, or even by erosion and redeposition, and therefore, the “model ages” calculated can be regarded as estimates of the length of time the Nd in the rocks has resided in the crust. However, as already noted, both Sm and Nd can be transported by hydrothermal fluids in the crust over distances of at least 1 km and some separation of Sm from Nd can occur [Poitrasson *et al.*, 1998], which potentially nullifies the claimed significance of these “model ages.”

5.5.2 Depleted Mantle “Model Ages.” While observing the good fit of Archean plutons to the CHUR Nd isotope evolution line, *DePaolo and Wasserburg* [1976b] also noted that young mid-ocean ridge basalts (MORBs) lay well above the CHUR evolution line. However, they

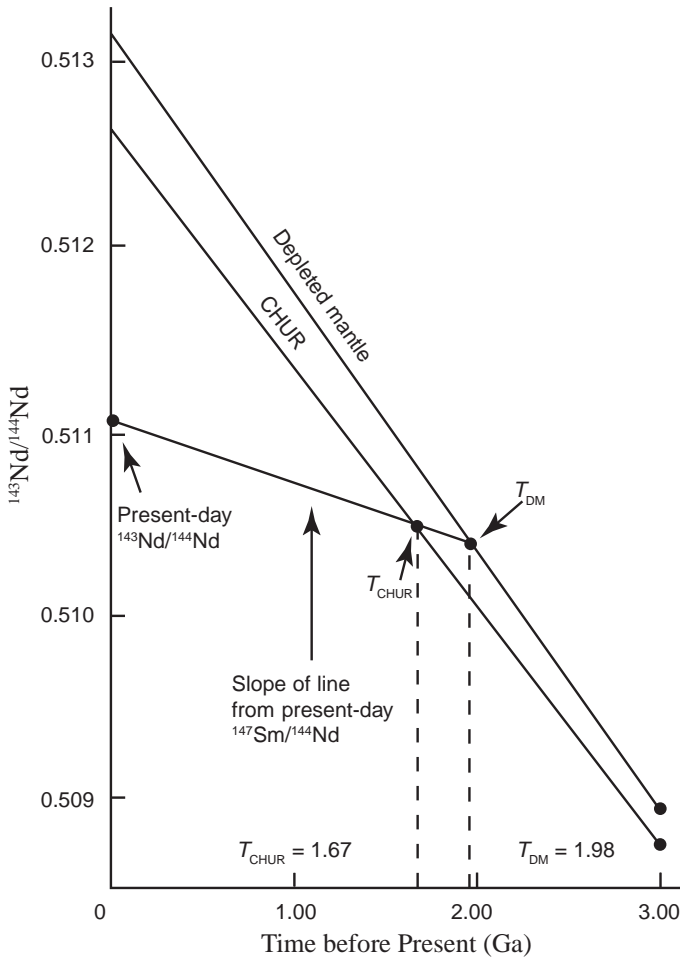


Figure 20. The evolution of $^{143}\text{Nd}/^{144}\text{Nd}$ with time in an individual sample compared with two models of the mantle—CHUR (the chondritic uniform reservoir) and depleted mantle (DM) [after *Rollinson, 1993*]. A model Nd age is the time at which the sample had the same $^{143}\text{Nd}/^{144}\text{Nd}$ ratio as its mantle source. In this case there are two possible solutions, depending upon which mantle model is preferred. The T_{CHUR} “model age” is approximately 1.67 Ga and the T_{DM} “model age” is approximately 1.98 Ga. A similar diagram can be constructed using the ϵ notation in place of $^{143}\text{Nd}/^{144}\text{Nd}$.

recognized that Archean continental igneous rocks which fell within the error of the CHUR evolution line could conceivably lie on a depleted mantle evolution line characterized by progressively increasing Sm/Nd and $^{143}\text{Nd}/^{144}\text{Nd}$. Subsequent studies of the initial $^{143}\text{Nd}/^{144}\text{Nd}$ ratios from other Precambrian terranes, including Proterozoic metamorphic basement, suggested that the mantle which supplied the continental crust had “evolved” since “earliest times” with an Sm/Nd ratio greater than that of CHUR. Thus *DePaolo* [1981a] found that the Proterozoic metamorphic basement of the Colorado Front Range plotted on a depleted mantle evolution curve linked to modern island arc volcanics, which thus represented the supposed Nd isotope evolution of a progressively depleted reservoir which was the source area for calc-alkaline magmatism. This curve is close to the CHUR evolution line in the early Archean, but diverges progressively to the present day, as in Figure 20. Three “younger” granitoid plutons in the Colorado Front Range yielded progressively “younger” initial $^{143}\text{Nd}/^{144}\text{Nd}$ ratios which lay on a $^{143}\text{Nd}/^{144}\text{Nd}$ evolution line diverging from the depleted mantle evolution curve at the “age” of the metamorphic basement, suggesting that these granitoids contain a large fraction of re-melted basement. Thus Sm-Nd “model ages” for the continental crust are usually calculated with reference to this depleted mantle (DM) reservoir curve rather than CHUR and are denoted T_{DM} . *DePaolo* [1981a] argued that T_{DM} model “ages” would be a more accurate indication of “crustal formation age” than T_{CHUR} . These “depleted mantle model ages” are calculated by substituting the appropriate DM values in place of $(^{143}\text{Nd}/^{144}\text{Nd})_{\text{CHUR}}$ and $(^{147}\text{Sm}/^{144}\text{Nd})_{\text{CHUR}}$ in the standard “model age” equation. A graphical solution of a T_{DM} “model age” calculation is illustrated in Figure 20.

Since the development of the concept of Proterozoic depleted mantle by *DePaolo* [1981a], new analyses have prompted several reinterpretations of the “evolution” of the depleted mantle reservoir. For example, *DePaolo* [1983] calculated a more depleted mantle evolution curve with a sinusoidal form, using newly published data for Precambrian basalts. Subsequently, *Nelson and DePaolo* [1984] proposed using a convex upward depleted mantle curve on the basis of Proterozoic basalt compositions, but both these curves were made obsolete by subsequent

new data. An alternative to *DePaolo's* [1981a] model was proposed by *Goldstein et al.* [1984]. Their model assumes linear depletion of the mantle and provides a good fit to early Proterozoic greenstones, the most depleted ϵ_{Nd} values in these suites probably representing flood basalts erupted in drifting environments that suffered little crustal contamination. However, the *Goldstein et al.* [1984] model is not the most appropriate mantle model for calculating “crustal extraction ages” of tonalitic crust-forming rocks generated in arc settings. Consequently, there has been a tendency for a proliferation of depleted mantle models as new data for different geographical areas become available. Nevertheless, the models of *DePaolo* [1981a] and *Goldstein et al.* [1984] have had the widest application. Thus when a “depleted mantle model age” is calculated it is important that the depleted mantle model evolution curve used must also be specified.

5.6 Sm-Nd “Model Ages”—Problems and Limitations

It is important to remember the assumptions upon which these calculated “model ages” are based and that these assumptions are not always fulfilled [*Rollinson*, 1993]. First, assumptions are made about the isotopic composition of the reservoir which is being sampled—either CHUR or depleted mantle. This aspect of “model age” calculations in itself raises three further problems:

- the correct choice of reservoir is important, for as Figure 20 shows, there can be as much as 300 Ma difference between Nd CHUR and DM “model ages”;
- there is a variety of possible models for the depleted mantle, as highlighted above; and
- there is great confusion over the actual numbers that should be used for mantle values.

These difficulties have arisen because the Sm-Nd technique developed very rapidly and different laboratories used different normalization schemes in parallel. In practical terms, however, provided the same set of values is consistently used, the overall effect on calculated “model ages” is not great.

A second assumption used in “model age” calculations is that the Sm/Nd ratio of the sample has not been modified by fractionation after its separation from the mantle source. In the case of Nd isotopes, this is usually regarded as a reasonable assumption to make. Nevertheless, as has been noted, hydrothermal fluids can redistribute Sm and Nd and thus disturb the Sm/Nd ratios. Finally, the third assumption is that all material came from the mantle in a single event, which may not always be the case.

The meaning of these “model ages” is somewhat problematic, as an example will illustrate. Table 3 shows Nd CHUR and depleted mantle “model ages” for granulites and gneisses from central Australia, as reported by *Windrim and McCulloch* [1986]. Sample no. 234 is the plotted example in Figure 20. The minimum difference between the

Table 3. Model Nd “ages” calculated for CHUR and depleted mantle for granulites and gneisses from the Strangeways Range, central Australia [from *Windrim and McCulloch*, 1986].

Sample No.	$\frac{^{147}\text{Sm}}{^{144}\text{Nd}}$	$\frac{^{143}\text{Nd}}{^{144}\text{Nd}}$	$T_{(\text{CHUR})}^{\text{Nd}} (\text{Ga})$	$T_{(\text{DM})}^{\text{Nd}} (\text{Ga})$
<i>Mafic granulites</i>				
226	0.1853	0.511772 ± 36	0.856	2.203
234	0.1251	0.511049 ± 30	1.672	1.975
551	0.2134	0.512122 ± 36	2.596	2.950
868	0.2046	0.512013 ± 24	3.388	2.491
<i>Quartzofeldspathic and calc-silicate rocks</i>				
501A	0.1248	0.511006 ± 28	1.755	2.034
507	0.1310	0.511039 ± 24	1.844	2.115
503	0.1248	0.510967 ± 32	1.837	2.093
512	0.1150	0.510794 ± 32	1.938	2.145

Notes:

1. Nd isotopes normalized to $^{146}\text{Nd}/^{142}\text{Nd} = 0.636151$.
2. DM values for Nd are $(^{143}\text{Nd}/^{144}\text{Nd})_{\text{today}} = 0.51235$, $(^{147}\text{Sm}/^{144}\text{Nd})_{\text{today}} = 0.225$.
3. Calculations made using the standard Nd model age equation.

CHUR and depleted mantle “model ages” is 207 Ma, while the maximum difference is 1347 Ma. There is clearly more of an inconsistency in the CHUR “model ages,” particularly for the mafic granulites, which range from 856 Ma to 3.388 Ga, whereas the range of CHUR “model ages” for the quartzofeldspathic and calc-silicate rocks is very much narrower, from 1.755 Ga to 1.938 Ga. On the other hand, the depleted mantle “model ages” for the quartzofeldspathic and calc-silicate rocks averaged to 2.097 Ga, which is virtually indistinguishable from the Sm-Nd whole-rock “isochron age” of 2.07 ± 0.125 Ga for the full suite of eight samples [Windrum and McCulloch, 1986]. The depleted mantle “model ages” for the mafic granulites, on the other hand, averaged to 2.405 Ga, which is 308 Ma above the whole-rock “isochron age.” Clearly, the Nd isotopic composition of these rocks more closely fits the depleted mantle reservoir interpretation, but it should be the mafic granulites whose depleted mantle “model age” matches the Sm-Nd whole-rock “isochron age.” In any case, it should be remembered that the same isotopic data from the rock samples are used to calculate both the whole-rock “isochron age” and the “model ages,” so there should be internal consistency virtually by definition.

“Model ages” of granitoids are sometimes used to estimate the “age” of their source. In the case of mantle-derived granites, the “model ages” supposedly give the times of mantle fractionation of the basaltic precursors to the granites. These are usually assumed to be very close in time to the “crystallization ages” of the granites. Granitoids which are derived by the melting of older continental crust will give “model ages” which are indicative of the “ages” of the crustal sources. This is possible because the intracrustal fractionation process is regarded as not greatly disturbing the Sm/Nd ratios of the sources. Often, however, granites are a mixture of crustal and mantle sources. When this is the case, as in the example depicted in Figure 21, calculated “model ages” may give very misleading results [Arndt and Goldstein, 1987]. These mixing processes are being increasingly recognized from Nd and Sr isotopic studies, as illustrated earlier in Figures 16 and 17. Clearly, there is therefore no way of knowing for sure whether any calculated Sm-Nd “age,” whether isochron or model, is real or whether it is an artifact of mixing of sources,

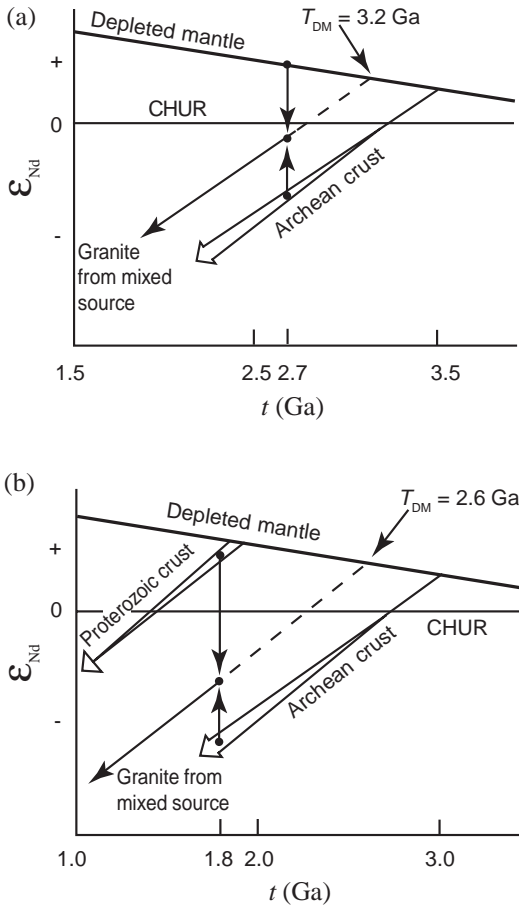


Figure 21. The evolution of $^{143}\text{Nd}/^{144}\text{Nd}$ (expressed as ϵ units) with time, for depleted mantle and continental crust. Relative to CHUR the depleted mantle shows increasing $^{143}\text{Nd}/^{144}\text{Nd}$ (increasingly positive ϵ -values), whereas the continental crust shows retarded $^{143}\text{Nd}/^{144}\text{Nd}$ evolution (increasingly negative ϵ -values). (a) The depleted mantle “model age” for a granite formed at 2.7 Ga from a mixture of a juvenile component derived from the depleted mantle and from Archean crust formed at 3.5 Ga will be 3.2 Ga. (b) The depleted mantle “model age” of a granite formed by the mixture of Proterozoic (1.9 Ga) and Archean (3.0 Ga) crustal sources at 1.8 Ga is 2.6 Ga. The “model ages” have little real meaning for they neither reflect the “crystallization age” of the granite nor the “age” of the crustal source [after Arndt and Goldstein, 1987].

be they crustal or mantle, or both, or even interpretative processes which appear to be internally self-fulfilling.

“Model ages” for clastic sedimentary rocks (sandstones, shales, etc.) are thought to provide an estimate of their “crustal residence age” [O’Nions *et al.*, 1983], for minimal fractionation of Sm/Nd is believed to accompany their generation. However, since many continental sediments are a mixture of materials from different sources, Nd “model ages” are in reality the average “model ages” of the sediments and thus are believed to provide minimum estimates of the “crustal residence ages” or average “crustal residence ages.” Nevertheless, such interpretations are conjectural, given that the nature of the mixture of materials cannot always be quantified, nor can the complex histories of the different sources be always elucidated.

5.7 Sm-Nd “Model Ages” and Basement “Age” Mapping

As already noted, Sm-Nd “model ages” are calculated to determine “crustal-extraction ages” or “crust-formation ages.” The Sm-Nd isotopic “dating” technique is often used on whole-rock samples because it is believed to be capable of “seeing back” through erosion, sedimentation, high-grade metamorphism and even crustal melting which may have re-set other isotopic “dating” systems. However, these processes can cause complications in the interpretation of “model ages,” as already noted. For example, in sediments the microscopic clay-mineral fraction can be re-set during diagenesis due to mobilization of rare earth elements on the mineralogical scale [Stille and Clauer, 1986; Bros *et al.*, 1992]. It is claimed that this does not imply open Sm-Nd systems on a whole-rock scale, but such a claim is hard to justify when it is known that fluids are capable of transporting the rare earth elements distances of at least 1 km [Poitrasson *et al.*, 1998]. Such remobilization acts upon the rare earth element patterns inherited by the sediment particles from their original sources, including their Sm-Nd “model ages.” Furthermore, metamorphism even to granulite-facies has been demonstrated to cause Sm-Nd isotopic re-setting [Whitehouse, 1988], which thus necessitates careful interpretation of sample analyses.

Nelson and DePaolo [1985] have attempted to place upper limits on the disturbance of “model ages” under conditions of intracrustal reworking by considering the limiting case of crustal anatexis, and have thus estimated that the maximum amount of Sm/Nd fractionation likely to arise by intracrustal melting processes could be as much as 20% of the pre-existing fractionation between sample Sm/Nd and CHUR Sm/Nd. Nevertheless, *Nelson and De Paolo* [1985] and *Bennett and DePaolo* [1987] used the Nd isotopic data of granitic plutons across the USA to determine “crustal formation ages” on associated country rocks (assuming that the granites are the products of anatexis of those country rocks) and to therefore map the presumed Precambrian basement “age” structure across the continental USA (see Figure 22). However, there are weaknesses in this approach, particularly when “model ages” do not correspond to igneous “crystallization ages.” The 2.0–2.3 Ga “model

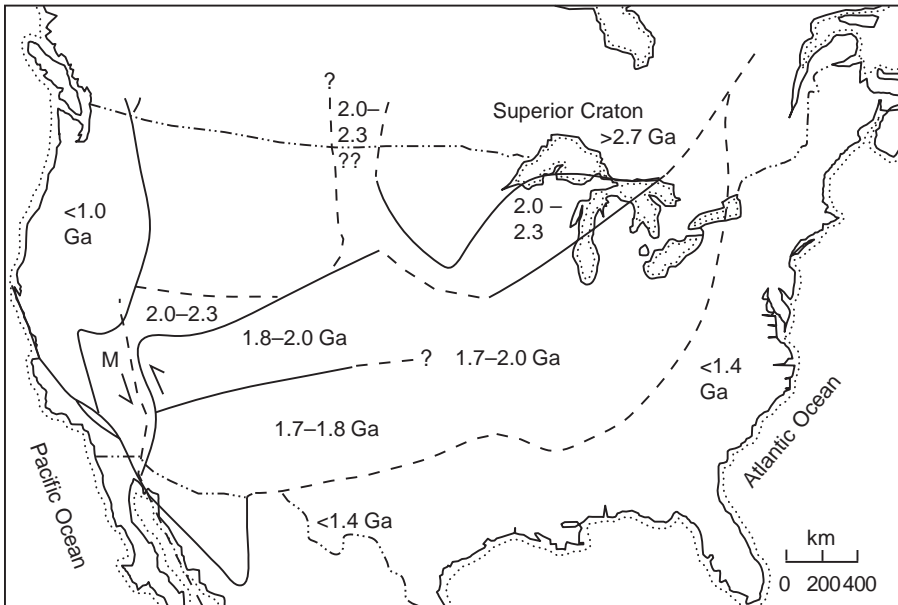


Figure 22. Map of the USA, showing the distribution of Nd “model age” provinces [after *Bennett and DePaolo*, 1987]. M indicates the Mojavia terrane and the adjacent dashed curve is the inferred location of a Proterozoic shear.

ages” of the “Mojavia” and “Penokean” terranes in Figure 22 exemplify this problem, because it is believed they represent Proterozoic mantle-derived magmas which mixed with large quantities of re-melted Archean crust to generate mixed “model ages” which have no meaning as “crustal extraction ages,” as illustrated already in Figure 21 [Arndt and Goldstein, 1987].

Likewise, *DePaolo et al.* [1991] admitted that the establishment of Sm-Nd “model ages” or “mantle separation ages” for crustal rock reservoirs requires the “precise” geochronological information typically provided by U-Pb isotopic measurements of zircons, plus models for:

- Nd isotopic evolution in the mantle sources of continental crust;
- Nd isotopic evolution of crustal reservoirs subsequent to formation;
- petrogenesis of certain types of granitic rocks in the crust;
- the mechanisms of formation of hybrid crust (mixtures of material newly differentiated from the mantle with material derived from older crust); and
- the evolution of the lower parts of the continental crust during continental margin magmatism and intracontinental extension.

They added that the greatest uncertainties came from a lack of adequate information on the lower crustal processes and composition. Clearly, the usefulness of the Sm-Nd “dating” method is very much dependent on interpretative models and the other isotopic “dating” systems that have their own sets of problems.

In a similar study, *McCulloch* [1987] demonstrated that large areas of Australian basement have Nd “model ages” of 2.1–2.2 Ga. In contrast, he rejected a mixing model between Archean and Proterozoic components for three reasons:

- the consistency of intermediate “ages,”
- the problems of assimilating large fractions of Archean material, and
- the absence of inherited Archean zircons.

However, *Arndt and Goldstein* [1987] answered the latter two objections by arguing that the mixing process need not have involved assimilation of solid crust by a magma, and by pointing out that the zircon argument is invalidated by the lack of 2.1–2.2 Ga zircons. Thus *Dickin* [1995] concluded that while Nd “model age” mapping of gneiss

terrane may be a powerful method to delineate the geographical extent of different crustal provinces, geochronological confirmation of the resultant “model age” provinces must be provided by other isotopic “dating” methods.

Ironically, such attempts to map the “age” structure of the continents are not new, the first being that of *Hurley et al.* [1962], who used the Rb-Sr isotopic “dating” method that was then in vogue, well before the development of the Sm-Nd method. They compared Rb-Sr “isochron ages” with Sr “model ages” calculated assuming a mantle $^{87}\text{Sr}/^{86}\text{Sr}$ ratio of 0.708 (the mantle “growth curve” is now said to be less radiogenic than this). On average the “isochron ages” and “model ages” were correlated (just as Nd “isochron ages” and Nd “model ages” are often somewhat correlated), leading them to suppose that the “isochron ages” dated the time of crustal extraction from a mafic source. Thus *Hurley et al.* [1962] applied the method to the North American continent in order to calculate the approximate areas of crustal basement attributed to different “age” provinces, as depicted in Figure 23. At the time this seemed a good approach, but as *Dickin* [1995] points out we now know that the Rb-Sr system is too easily re-set to yield reliable “crustal extraction ages” for “old” terranes. Yet, as just noted above, *Dickin* [1995] had likewise concluded the Nd “model age” method requires geochronological confirmation by other isotopic “dating” methods because of the problem of mixing of Sm/Nd isotopes. Thus each of the isotopic “dating” methods has its problems and reaches a point in the history of its usage where the increasingly arising problems bring limits and doubts upon its usage.

6. The Strontium-Lead-Neodymium (Sr-Pb-Nd) Radioisotopic System

It is now well recognized that the isotopic ratios in a magma are characteristic of the source region from which the magma was extracted, and the ratios appear to remain unchanged during subsequent fractionation events [*Rollinson*, 1993]. While this may be because the mass difference between any pair of these radiogenic isotopes is so small

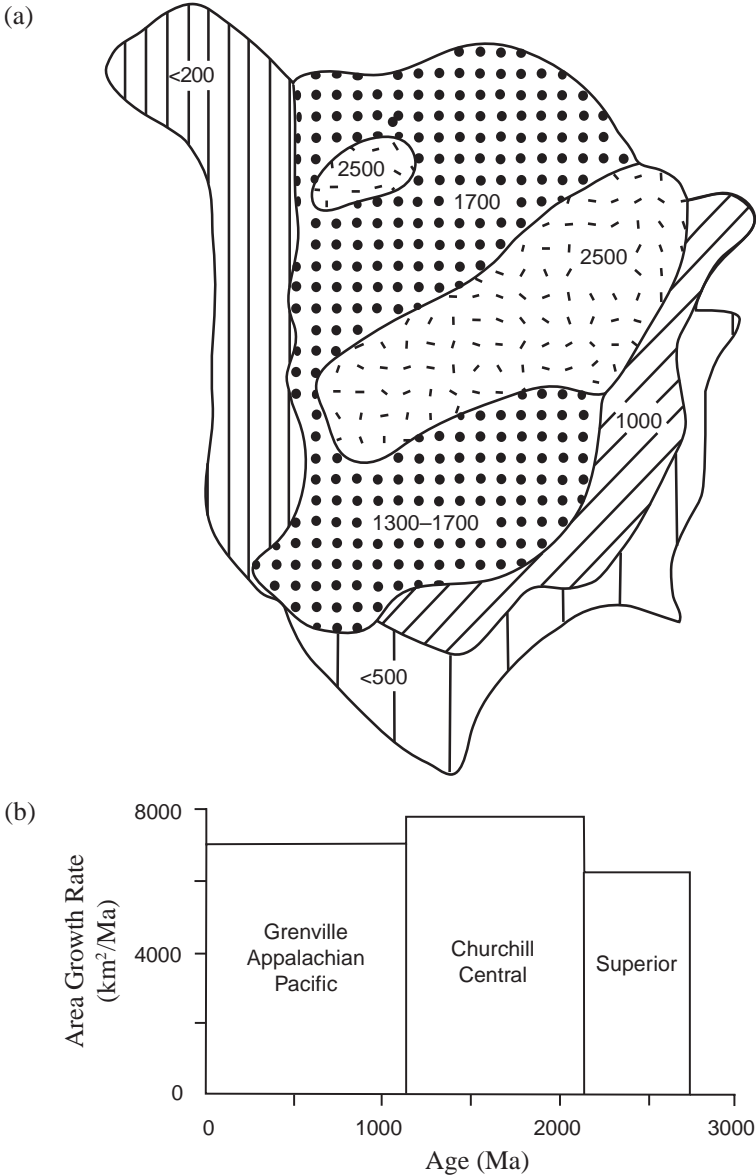


Figure 23. Estimated area of North American crustal basement attributable to different Rb-Sr “age” provinces [after *Hurley et al.*, 1962]. (a) Map showing provinces of different “ages” in Ma; (b) Histogram of “growth rate” against time.

that the isotope-pair cannot be fractionated by processes controlled by crystal-liquid equilibria, there is nonetheless evidence at the small scale of some differences in some isotopic ratios even on different faces of the same crystal [*Wingate and Compston, 1997, 2000*]. Thus during partial melting a magma is usually presumed to have the same isotopic character as its source region. This assumption has led to two important developments in isotope geochemistry. Firstly, distinct source regions can ideally be recognized with their own unique isotopic character, and secondly, mixing can potentially be recognized between isotopically-distinct sources. Thus one of the main quests of isotope geology is to identify the different isotopic reservoirs in the crust and mantle, and to characterize them for as many isotopic systems as is possible. This has obvious ramifications for radioisotopic “dating,” as we have already seen with the K-Ar and Ar-Ar, U-Th-Pb, Rb-Sr and Sm-Nd radioisotopic systems.

The larger and more difficult question of how the reservoirs acquired their own identities leads into the question of crust and mantle geodynamics. It is claimed that a wealth of mixing and contamination processes can be recognized in and between sources, although these can normally be reduced to two essentially different types of processes [*Hawkesworth and van Calsteren, 1984*]. First, radiogenic isotopes are being used to identify components from different sources which have contributed to a particular magmatic suite—for example, the contamination of continental flood basalt with “old” continental crust. Of course, all of this work presupposes millions-of-years timescales, but these contamination processes are recognized as of short duration. However, the radiogenic isotopic ratios can still be used for “fingerprinting” sources and source regions rather than stipulating “ages.” The second application is to constrain models for the development of source regions of magmatic rocks. For example, it is claimed that there are several sources of oceanic basalts in the upper mantle, so it is of some importance to discover how and when these supposed separate sources acquired their separate identities, and thus how their isotopic signatures have affected the radioisotopic “ages” assigned to crustal rocks.

6.1 The Role of Different Isotopic Systems in Identifying Reservoirs and Processes

The different elements used in radiogenic isotope studies vary greatly in their chemical and physical properties, so much so that different isotope systems vary in their sensitivity to particular petrological processes. This variability may show itself in two ways. First, the parent and the daughter elements may under certain circumstances behave in different ways so that the two become fractionated. The order of incompatibility for the elements of interest is

$$\text{Rb} > \text{Th} > \text{U} > \text{Pb} > \text{Nd} > \text{Sr}, \text{Sm}$$

These values indicate the extent to which an element is fractionated into the crust relative to the depleted mantle. For example, Rb is the element most concentrated in the crust relative to the depleted mantle, whereas Sr and Sm are the least concentrated. Alternately, a parent-daughter element-pair may behave coherently and not be fractionated, and yet behave in a very different manner from the parent-daughter pair of another isotopic system. A good example is the contrast between the Sm-Nd system, in which both elements share very similar chemical and physical characteristics, and the Rb-Sr system, in which the elements are strongly fractionated from one another. The properties of the five isotopic systems of usual interest are briefly reviewed with respect to the isotopic character of crust and mantle reservoirs in Table 4.

Samarium and Nd isotopes are not significantly fractionated within the continental crust by metamorphic or sedimentary processes and thus appear to preserve the parent/daughter ratio of their source region. In this respect the Sm-Nd system seems to differ markedly from Rb-Sr, U-Pb and Th-Pb systems. Samarium and neodymium are thought to be immobile under hydrothermal conditions (though there is now evidence to the contrary), and so their isotopic composition is believed to reflect the actual proportions of rock or magma involved in specific petrological processes. The Sm-Nd system, however, has the disadvantage that small amounts of recycled crust mixed with a large proportion of a mantle component become isotopically invisible.

Lead isotopes are more complex because of the three different decay schemes— ^{238}U - ^{206}Pb , ^{235}U - ^{207}Pb and ^{232}Th - ^{208}Pb . In general, U and Pb are relatively mobile in crustal processes, particularly in magmatic/hydrothermal situations, whereas Th is highly insoluble. Both U and Pb are incompatible elements in silicates, although U enters a melt more readily than Pb. In detail, the two isotopes of Pb produced from U, ^{206}Pb and ^{207}Pb , show contrasting behavior as a consequence of their differing radioactive decay rates. Early in the claimed history of the earth ^{235}U appears to have decayed rapidly relative to ^{238}U so that ^{207}Pb evolved rapidly with time. Lead-207 abundances therefore are regarded as an extremely sensitive indicator of an apparent old source. Today, however, ^{235}U is supposed to be largely extinct so that in the recent history of the earth ^{238}U decay is more prominent, and consequently ^{206}Pb abundances show a greater spread than ^{207}Pb . This difference in behavior between the different isotopes of Pb allows the identification of several isotopic reservoirs. The crustal reservoirs are best sampled by studying the isotopic composition of a mineral such as feldspar with a low U/Pb or low Th/Pb ratio and which preserves the “initial” Pb composition of the source. This approach was developed by *Doe and Zartman* [1979].

Strontium is usually regarded as relatively immobile under hydrothermal conditions, although Rb is often more mobile. Thus Sr is believed to reflect fairly closely the original bulk composition of a suite of rocks, and Rb less so. Furthermore, the Rb-Sr system shows the most extreme differences in incompatibility between the parent and daughter elements. Rubidium and strontium are easily separated, so that there is extreme fractionation between crust and mantle leading to the apparent accelerated Sr isotope evolution of the continental crust relative to the mantle. Within the continental crust Rb and Sr are further separated by remelting, metamorphism and sedimentation, with Sr being partitioned into and retained by plagioclase, whereas Rb is preferentially partitioned into the melt or fluid phase.

Table 4. The isotopic character of crust and mantle reservoirs (present-day isotope ratios shown in parentheses) [after *Rollinson, 1993*].

	$^{87}\text{Rb}-^{86}\text{Sr}$	$^{147}\text{Sm}-^{143}\text{Nd}$	$^{238}\text{U}-^{206}\text{Pb}$	$^{235}\text{U}-^{207}\text{Pb}$	$^{232}\text{Th}-^{208}\text{Pb}$
Continental Crustal Sources					
Upper crust	High Rb/Sr; high $^{87}\text{Sr}/^{86}\text{Sr}$	Low Sm/Nd; low $^{143}\text{Nd}/^{144}\text{Nd}$ (negative epsilon)	High U/Pb; high $^{206}\text{Pb}/^{204}\text{Pb}$	High U/Pb; high $^{207}\text{Pb}/^{204}\text{Pb}$	High Th/Pb; high $^{208}\text{Pb}/^{204}\text{Pb}$
Middle crust	Mod. high Rb/Sr (0.2–0.4); $^{87}\text{Sr}/^{86}\text{Sr} =$ (0.72–0.74)	Retarded Nd evolution in the crust relative to chondritic source	U-depleted; low $^{206}\text{Pb}/^{204}\text{Pb}$	U-depleted; low $^{207}\text{Pb}/^{204}\text{Pb}$	Mod. high Th; mod. high $^{208}\text{Pb}/^{204}\text{Pb}$
Lower crust	Rb depletion; Rb/Sr <ca 0.04; lower $^{87}\text{Sr}/^{86}\text{Sr}$ 0.702–0.705		Severe U depletion; very low $^{206}\text{Pb}/^{204}\text{Pb}$ (ca 14.0)	Severe U depletion; very low $^{207}\text{Pb}/^{204}\text{Pb}$ (ca 14.7)	Severe Th depletion; very low $^{208}\text{Pb}/^{204}\text{Pb}$
Subcontinental lithosphere					
Archean	Low Rb/Sr	Low Sm/Nd			
Proterozoic to Recent	High Rb/Sr	Low Sm/Nd			

	⁸⁷ Rb- ⁸⁶ Sr	¹⁴⁷ Sm- ¹⁴³ Nd	²³⁸ U- ²⁰⁶ Pb	²³⁵ U- ²⁰⁷ Pb	²³² Th- ²⁰⁸ Pb
Oceanic Basalt Sources [Zindler and Hart, 1986]					
<u>Depleted mantle (DM)</u>	Low Rb/Sr; low ⁸⁷ Sr/ ⁸⁶ Sr	High Sm/Nd; high ¹⁴³ Nd/ ¹⁴⁴ Nd (positive epsilon)	Low U/Pb; low ²⁰⁶ Pb/ ²⁰⁴ Pb (ca 17.2-17.7)	Low U/Pb low ²⁰⁷ Pb/ ²⁰⁴ Pb (ca 15.4)	Th/U = 2.4 ± 0.4; low ²⁰⁸ Pb/ ²⁰⁴ Pb (ca 37.2-37.4)
<u>HIMU (high μ = U/Pb)</u>	Low Rb/Sr; low ⁸⁷ Sr/ ⁸⁶ Sr (= 0.7029)	Intermediate Sm/Nd (<0.51282)*	High U/Pb; high ²⁰⁶ Pb/ ²⁰⁴ Pb (>20.8)	High U/Pb; high ²⁰⁷ Pb/ ²⁰⁴ Pb	High Th/Pb
<u>Enriched mantle (EM)</u>					
<u>EM I</u>	Low Rb/Sr; ⁸⁷ Sr/ ⁸⁶ Sr = ± 0.705	Low Sm/Nd; ¹⁴³ Nd/ ¹⁴⁴ Nd < 0.5112*	Low U/Pb; ²⁰⁶ Pb/ ²⁰⁴ Pb = (17.6-17.7)	Low U/Pb; ²⁰⁷ Pb/ ²⁰⁴ Pb = (15.46-15.49)	Low Th/Pb; ²⁰⁸ Pb/ ²⁰⁴ Pb = (38.0-38.2)
<u>EM II</u>	High Rb/Sr; ⁸⁷ Sr/ ⁸⁶ Sr > 0.722	Low Sm/Nd; ¹⁴³ Nd/ ¹⁴⁴ Nd = (0.511-0.5121)*	High ²⁰⁷ Pb/ ²⁰⁴ Pb and ²⁰⁸ Pb/ ²⁰⁴ Pb at a given ²⁰⁶ Pb/ ²⁰⁴ Pb		
<u>PREMA (Prevalent mantle)</u>	⁸⁷ Sr/ ⁸⁶ Sr = 0.7033	¹⁴³ Nd/ ¹⁴⁴ Nd = 0.5130*	²⁰⁶ Pb/ ²⁰⁴ Pb = (18.2-18.5)		
<u>Bulk earth</u>	⁸⁷ Sr/ ⁸⁶ Sr = 0.7052	¹⁴³ Nd/ ¹⁴⁴ Nd = 0.51264* (= chondrite)	²⁰⁶ Pb/ ²⁰⁴ Pb = 18.4 ± 0.3	²⁰⁷ Pb/ ²⁰⁴ Pb = 15.58 ± 0.08	Th/U = 4.2; ²⁰⁸ Pb/ ²⁰⁴ Pb = 38.9 ± 0.3

* Normalized to ¹⁴⁶Nd/¹⁴⁴Nd = 0.7219.

6.2 Recognizing Isotopic Reservoirs

Three isotopic reservoirs have been recognized in the continental crust, characterized with respect to Nd, Sr and Pb isotopes [*Taylor et al.*, 1984]. Furthermore, five end-member compositions have been delineated in the mantle [*Zindler and Hart*, 1986], which by a variety of mixing processes are regarded as capable of explaining all the observations on mid-ocean ridge and ocean-island basalts (MORBs and OIBs). The composition of each of these sources is summarized in Table 4 and plotted on a series of generalized isotope correlation diagrams in Figures 24–27.

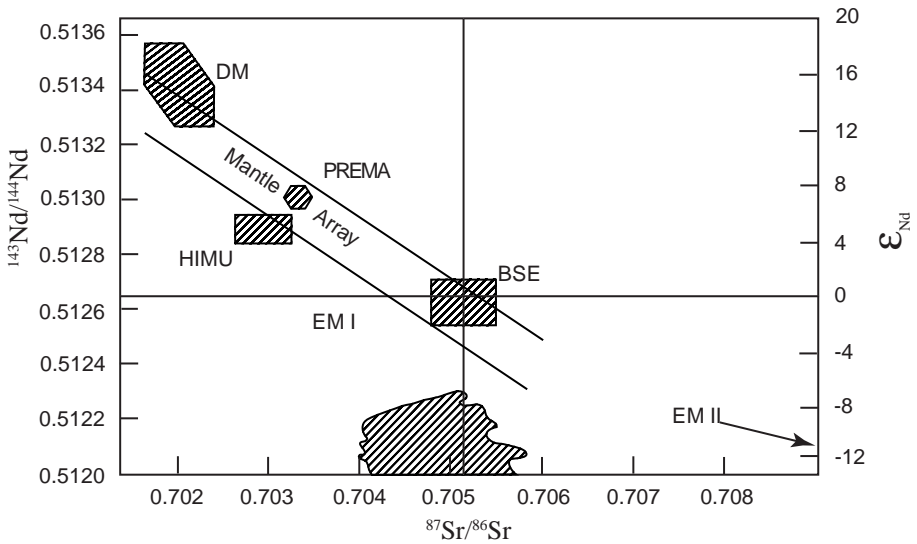


Figure 24. A $^{143}\text{Nd}/^{144}\text{Nd}$ versus $^{87}\text{Sr}/^{86}\text{Sr}$ isotope correlation diagram, showing the main oceanic mantle reservoirs of *Zindler and Hart* [1986]: DM, depleted mantle; BSE, bulk silicate earth; EM I and EM II, enriched mantle; HIMU, mantle with high U/Pb ratio; PREMA, frequently observed PREvalent MANTle composition. The mantle array is defined by many oceanic basalts, and a bulk earth value for $^{87}\text{Sr}/^{86}\text{Sr}$ can be obtained from this trend. ϵ_{Nd} is defined as the deviation in parts per 10^4 of the initial $^{143}\text{Nd}/^{144}\text{Nd}$ ratios from the CHUR evolution line [*DePaolo and Wasserburg*, 1976a].

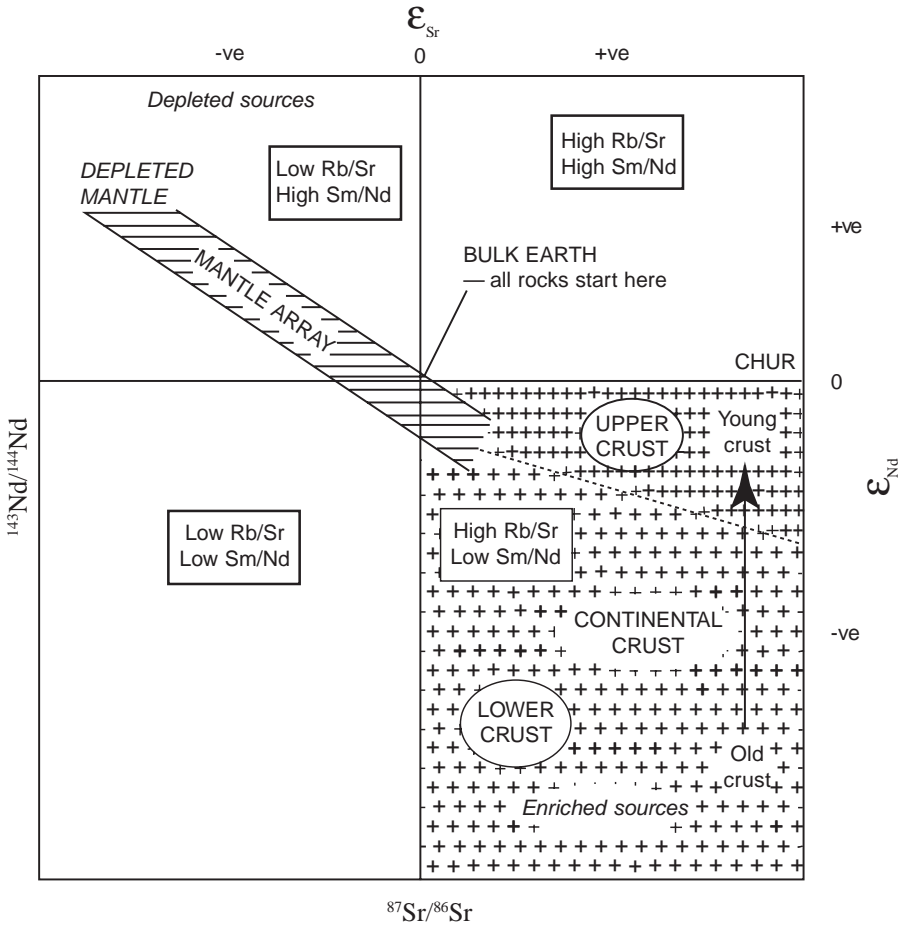


Figure 25. A $^{143}\text{Nd}/^{144}\text{Nd}$ versus $^{87}\text{Sr}/^{86}\text{Sr}$ (ϵ_{Nd} versus ϵ_{Sr}) isotope correlation diagram showing the relative positions of depleted and enriched mantle sources [after DePaolo and Wasserburg, 1979a]. Most non-enriched mantle reservoirs plot in the upper left “depleted” quadrant (cf. Figure 24), whereas most crustal rocks plot in the lower right “enriched” quadrant. Upper and lower crust tend to plot in different positions in the crustal quadrant. “-ve” and “+ve” refer to negative and positive ϵ_{Sr} and ϵ_{Nd} values respectively.

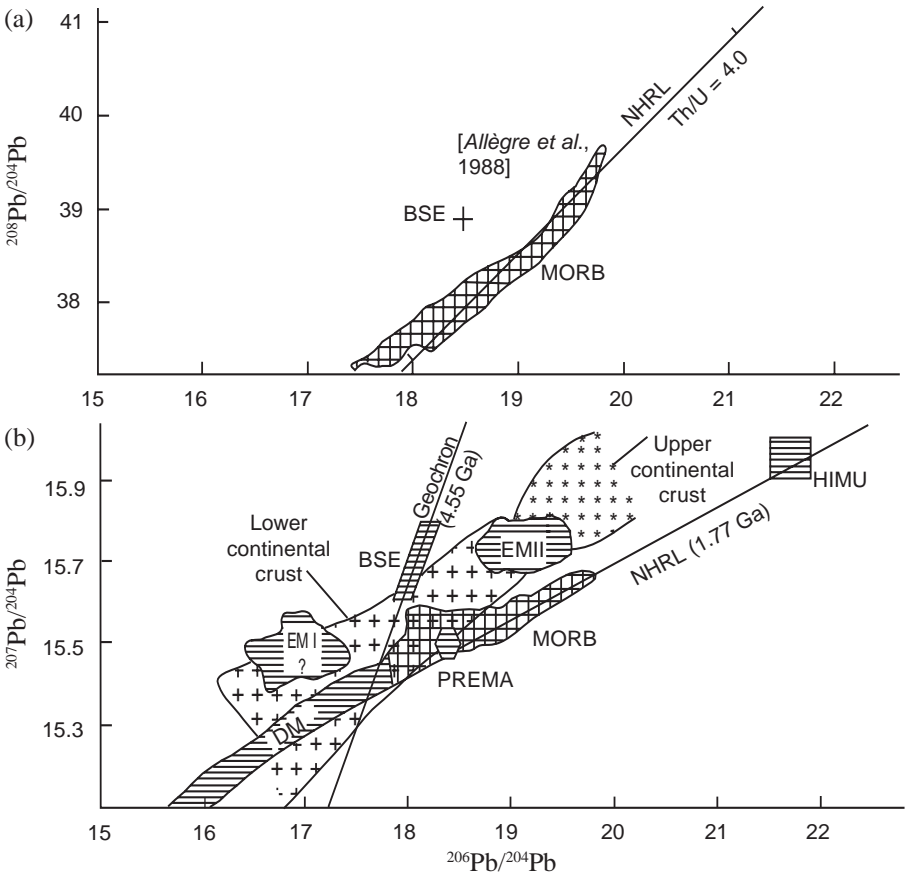


Figure 26. (a) $^{208}\text{Pb}/^{204}\text{Pb}$ versus $^{206}\text{Pb}/^{204}\text{Pb}$ isotope correlation diagram showing the position of the northern hemisphere reference line (NHRL) with $\text{Th}/\text{U} = 4.0$. The bulk silicate earth value (BSE) is from Allègre et al. [1988]. The field of MORB is shown with crosshatching. (b) $^{207}\text{Pb}/^{204}\text{Pb}$ versus $^{206}\text{Pb}/^{204}\text{Pb}$ isotope correlation diagram showing the position of the northern hemisphere reference line (NHRL), the slope of which has an age significance of 1.77 Ga, and the geochron. Volcanic rocks which plot above the NHRL are said to have a DUPAL signature. The mantle reservoirs of Zindler and Hart [1986] are plotted as follows: DM, depleted mantle; BSE, bulk silicate earth; EM I and EM II, enriched mantle; HIMU, mantle with high U/Pb ratio; PREMA, frequently observed PREvalent MANTle composition. EM II also coincides with the field of oceanic pelagic sediment. The fields of the upper and lower continental crust are shown with crosses, and the field of MORB with cross-hatching. [After Rollinson, 1993].

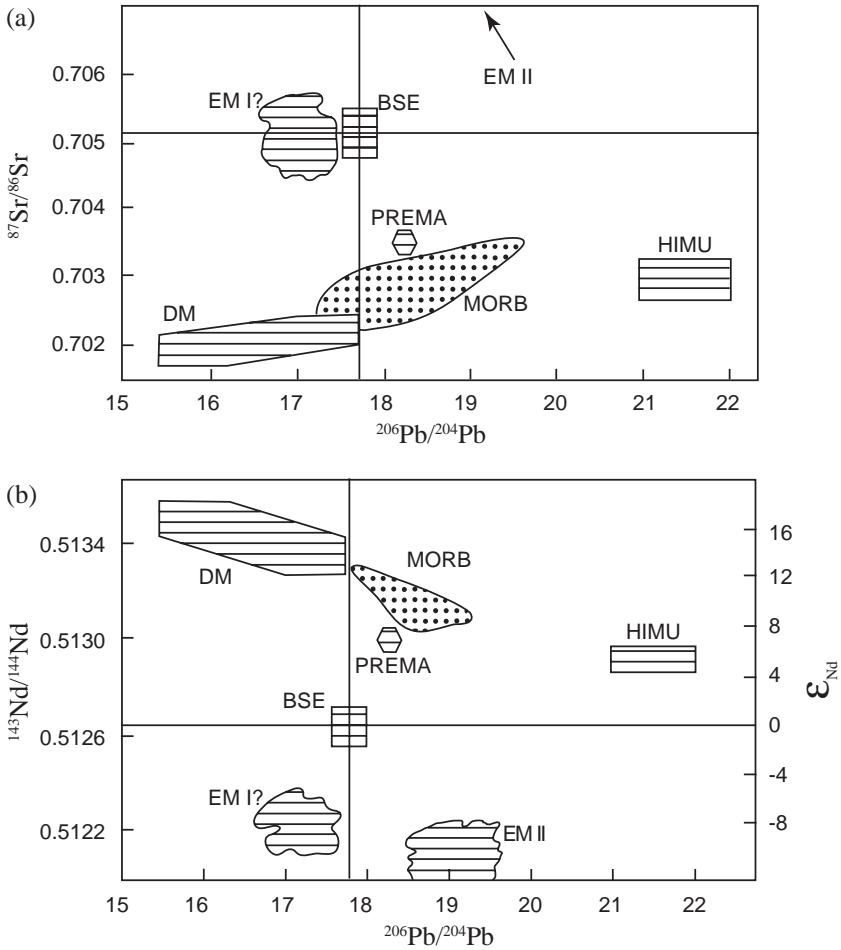


Figure 27. (a) $^{87}\text{Sr}/^{86}\text{Sr}$ versus $^{206}\text{Pb}/^{204}\text{Pb}$ isotope correlation diagram; (b) $^{143}\text{Nd}/^{144}\text{Nd}$ versus $^{206}\text{Pb}/^{204}\text{Pb}$ isotope correlation diagram. Both diagrams show the positions of the mantle reservoirs identified by Zindler and Hart [1986]: DM, depleted mantle; BSE bulk silicate earth; EM I and EM II, enriched mantle; HIMU, mantle with high U/Pb ratio; PREMA, frequently observed PREvalent MANTle composition. The stippled field is mid-ocean ridge basalts (MORBs). The $^{206}\text{Pb}/^{204}\text{Pb}$ value of the bulk earth differs from the value in Table 4, which is taken from Allègre *et al.* [1988].

6.2.1 Oceanic Mantle Sources. Young magmatic rocks record the isotopic composition of their source directly. This is because there is insufficient time for the parent isotope present in a newly formed magma to decay and produce additional daughter isotopes to add to those inherited from the source. Thus the present-day isotopic compositions of recent oceanic basalts were used by *Zindler and Hart* [1986] to identify five possible end-member mantle reservoirs (see Figures 24–27). Their possible locations in the mantle are given diagrammatically in Figure 28.

The five possible end-member mantle reservoirs and their isotopic compositions are:

- **Depleted Mantle (DM).** Depleted mantle is characterized by high $^{143}\text{Nd}/^{144}\text{Nd}$, low $^{87}\text{Sr}/^{86}\text{Sr}$ and low $^{206}\text{Pb}/^{204}\text{Pb}$. It is regarded as the dominant component in the source of many mid-ocean ridge basalts (MORBs) (see Figures 24, 26 and 27).
- **HIMU Mantle (Mantle with High U/Pb ratio).** The very high $^{206}\text{Pb}/^{204}\text{Pb}$ and $^{208}\text{Pb}/^{204}\text{Pb}$ ratios observed in some ocean-island basalts (OIBs), coupled with low $^{87}\text{Sr}/^{86}\text{Sr}$ (*ca* 0.7030) and intermediate $^{143}\text{Nd}/^{144}\text{Nd}$, suggest this mantle source that is enriched in U and Th relative to Pb without an associated increase in Rb/Sr. A number of models have been proposed to explain the origin of this mantle reservoir—the mixing into the mantle of altered oceanic crust (possibly contaminated with seawater), the loss of Pb from part of the mantle into the earth's core, and the removal of Pb (and Rb) by metasomatic fluids in the mantle.
- **Enriched Mantle (EM).** Enriched mantle has variable $^{87}\text{Sr}/^{86}\text{Sr}$, low $^{143}\text{Nd}/^{144}\text{Nd}$, and high $^{207}\text{Pb}/^{204}\text{Pb}$ and $^{208}\text{Pb}/^{204}\text{Pb}$ at a given value of $^{206}\text{Pb}/^{204}\text{Pb}$. Differentiation has also been made [*Zindler and Hart*, 1986] between enriched mantle type-I (EM I) with low $^{87}\text{Sr}/^{86}\text{Sr}$, and enriched mantle type-II (EM II) with high $^{87}\text{Sr}/^{86}\text{Sr}$. One striking and large-scale example of enriched mantle (EM II) has been identified in the southern hemisphere by *Hart* [1984] and is known as the DUPAL anomaly (named after the authors *DUPre and ALLègre* [1983] who first identified this isotopic anomaly). The enriched mantle was identified with respect to a North Hemisphere Reference Line (NHRL) defined by the linear arrays

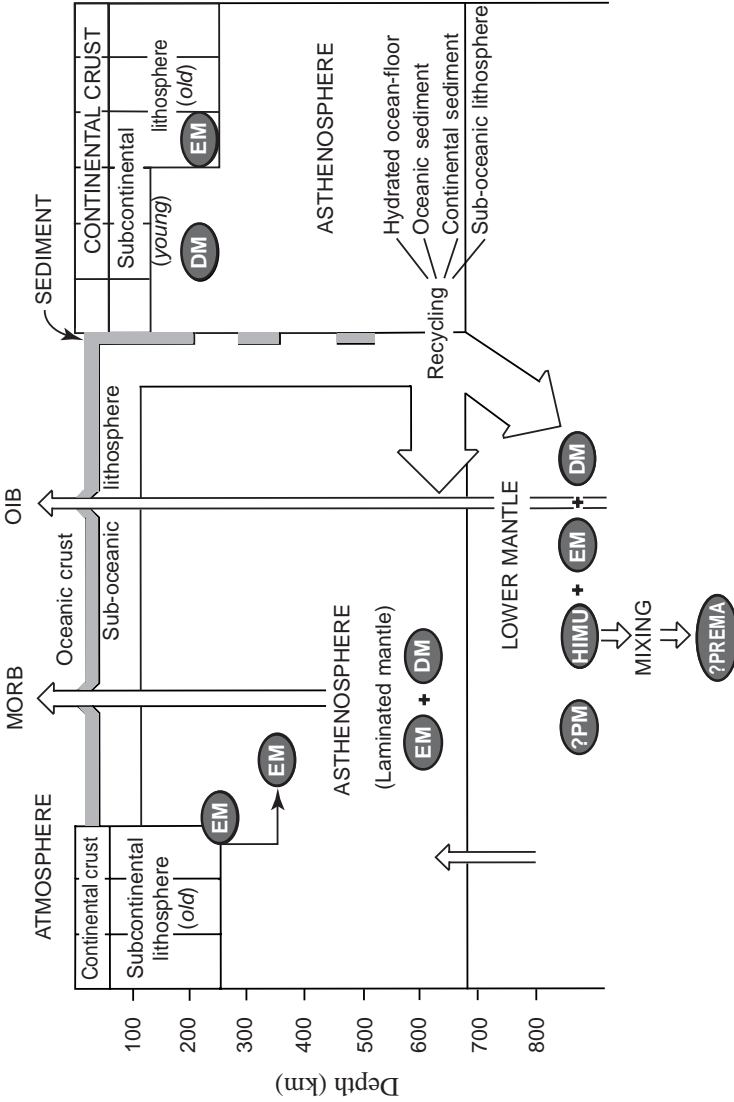


Figure 28. Cartoon diagram showing the different crust and mantle reservoirs and the possible relationship among them, based upon the observations of isotope geochemistry [after *Rollinson, 1993*]. The mantle reservoirs are identified using the nomenclature of *Zindler and Hart [1986]*: EM, enriched mantle; DM, depleted mantle; HIMU, mantle with high U/Pb ratio; PREMA, prevalent mantle; PM, primitive mantle.

on $^{207}\text{Pb}/^{204}\text{Pb}$ versus $^{206}\text{Pb}/^{204}\text{Pb}$ and $^{208}\text{Pb}/^{204}\text{Pb}$ versus $^{206}\text{Pb}/^{204}\text{Pb}$ plots for MORBs and OIBs (see Figure 26).

There are a number of models which explain the origin of enriched mantle. In general terms enrichment is likely to be related to subduction, whereby crustal material is injected into the mantle (see Figure 28). EM II has affinities with the upper continental crust and may represent the recycling of continentally-derived sediment, continental crust, altered oceanic crust or OIB crust. An alternative model is based upon the similarity between enriched mantle and the subcontinental lithosphere, and suggests that the enrichment is due to the mixing of the subcontinental lithosphere into the mantle. EM I has affinities with the lower crust and may represent recycled lower crustal material, but an alternative hypothesis suggests that it is enriched by mantle metasomatism. Another proposal [Weaver, 1991] is that EM I and EM II are produced by mixing between HIMU mantle and subducted oceanic sediment.

- **Frequently observed PREvalent MAntle (PREMA).** The great frequency of basalts from ocean islands, intra-oceanic island arcs and continental basalt suites with $^{143}\text{Nd}/^{144}\text{Nd} = 0.5130$ and $^{87}\text{Sr}/^{86}\text{Sr} = 0.7033$ suggests that there is an identifiable mantle component with this isotopic character. This has been referred to as the frequently observed PREvalent MAntle (PREMA) [Zindler and Hart, 1986]. It has $^{207}\text{Pb}/^{204}\text{Pb} = 18.2$ to 18.5.

- **Bulk Silicate Earth (BSE), bulk earth or primary Uniform Reservoir (UR).** It can be argued that there is a mantle component which has the chemistry of the Bulk Silicate Earth (the earth without the core). This composition is said to be equivalent to that of a homogeneous primitive mantle which supposedly formed during the degassing of the planet and during core formation, prior to the formation of the continents. Some oceanic basalts have isotopic compositions which closely approximate to the composition of the bulk earth, although at present there are no geochemical data which require that such a mantle reservoir still survives.

The recognition of a variety of possible mantle reservoirs for the source of oceanic basalts has led to an appreciation of the complexity of mantle

processes, particularly beneath ocean islands. For example, a study of the island Gran Canaria in the Canary Islands by *Hoernle et al.* [1991] showed that at least four different mantle components (HIMU, DM, EM I and EM II) have contributed to the production of these volcanic rocks since the so-called Miocene. Furthermore, the isotopic evidence indicates that the different reservoirs have made their contributions to the lava pile at different times in the history of the volcano.

Following the work of *Zindler and Hart* [1986], a number of workers have sought to characterize further the proposed mantle end-member compositions in terms of their trace element concentrations. Ranges of values currently in use for highly incompatible trace element ratios in the crust and mantle reservoirs have been compiled by *Saunders et al.* [1988] and *Weaver* [1991].

6.2.2 Continental Crustal Sources. The isotopic compositions of rocks from the continental crust are extremely variable, and it is said that isotope ratios are only strictly comparable if the samples are all of the same “age.” Thus it has been decided that compositional differences are best considered relative to a normalizing parameter which takes into account the “age” of the sample. One such reference point is the chondritic model of earth composition (CHondrite Uniform Reservoir or CHUR) and its claimed evolution through time. Thus crustal samples are often plotted on a graph of isotopic composition versus time relative to a reference line such as the CHUR reservoir. For Nd isotopes this is quantified in terms of the epsilon (ϵ) notation. The general isotopic characteristics of crustal reservoirs also are given in Table 4 and are:

- **Upper Continental Crust.** The upper continental crust is characterized by high Rb/Sr and consequently has high $^{87}\text{Sr}/^{86}\text{Sr}$ ratios. Nd isotope ratios, on the other hand, are low relative to mantle values as a consequence of the light rare earth element enrichment and the low Sm/Nd ratios which characterize the continental crust. Uranium and thorium are enriched in the upper continental crust and give rise to high ^{206}Pb , ^{207}Pb and ^{208}Pb isotope ratios.

- **Middle Continental Crust.** The middle continental crust is represented by extensive areas of amphibolite facies gneisses found in granite-gneiss terranes. These rocks have retarded $^{143}\text{Nd}/^{144}\text{Nd}$ as

discussed above, and $^{87}\text{Sr}/^{86}\text{Sr}$ ratios lower than in the upper crust. Uranium, however, is depleted and $^{206}\text{Pb}/^{204}\text{Pb}$ and $^{207}\text{Pb}/^{204}\text{Pb}$ ratios may be lower than in the mantle. Thorium levels are lower than those in the upper crust but not as depleted as U.

• **Lower Continental Crust.** The lower continental crust is characterized by granulite facies metamorphism and is often strongly Rb depleted. Thus it has low $^{87}\text{Sr}/^{86}\text{Sr}$ ratios which are not greatly different from modern mantle values. This means that a modern granite derived from the lower crust and one derived from the mantle will have very similar $^{87}\text{Sr}/^{86}\text{Sr}$ initial ratios. Uranium/lead and Th/Pb ratios in the lower crust are lower than modern mantle values, so that ^{206}Pb , ^{207}Pb and ^{208}Pb isotope ratios are all very low and may be used to distinguish between lower crust and mantle reservoirs.

• **Subcontinental Lithosphere.** The subcontinental lithosphere is not so easily characterized as other domains, for it is extremely variable in isotopic composition. For example, the subcontinental lithosphere beneath Scotland shows extreme Nd/Sr isotopic heterogeneity which encompasses both of the enriched mantle domains EM I and EM II [Menzies and Halliday, 1988]. Some of the variability may be correlated with the presumed “age” of the subcontinental lithosphere. The Archean subcontinental lithosphere is normally underlain by enriched lithosphere (EM I—low Rb/Sr, low Sm/Nd), but depleted examples are also known. The lithosphere beneath Proterozoic mobile belts, however, more closely resembles the depleted mantle found beneath older ocean basins [Menzies, 1989]. Proterozoic to Phanerozoic subcontinental lithosphere is characterized by enrichment in Rb and the light rare earth elements, resulting in radiogenic Sr and non-radiogenic Nd isotopes. This is similar to enriched mantle EM II.

6.3 Mantle Reservoirs through Time and Isotope Correlations

The isotopic compositions of mantle source regions are believed to change with time according to the parent/daughter element ratio, particularly if one is starting with the assumption of millions of years of elapsed time. Consequently, these changes are plotted on isotopic

evolution diagrams to show the changes in isotopic compositions of the reservoirs with time. Such diagrams are constructed for each isotopic system by measuring the isotopic composition of the mantle at the present day from modern lavas, and by calculating the initial ratios from isochron diagrams of ancient mantle melts (that is, ancient lavas). Diagrams of this type are considered particularly useful for depicting the isotopic evolution of crustal rocks of differing “ages,” and with different parent/daughter isotope ratios. It should be noted, however, that as yet there are insufficient data to draw detailed mantle evolution diagrams for all the postulated mantle reservoirs of *Zindler and Hart* [1986].

6.3.1 Sr Isotopes. We do well to realize that while the observational evidence indicates variations in the radioisotopic ratios laterally and with depth in the crust and within the mantle, the existence of these so-called reservoirs as distinct physical units is very much open to conjecture. Also, there is the underlying assumption in all of this interpretative work that there have been millions of years of elapsed time, and that the earth is 4.57 Ga old. Furthermore, various meteorites are assumed to represent the primordial earth condition. Thus, for example, the starting point for the evolution of Sr isotopes, the $^{87}\text{Sr}/^{86}\text{Sr}$ ratio at the formation of the earth, is taken to be the isotopic composition of basaltic achondrite meteorites, which are assumed to have a composition approximating that of the solar nebula at the time of planetary formation in the current secular cosmological model. It is usually referred to as BABI (Basaltic Achondrite Best Initial), and the measured value is 0.69897 ± 0.000003 .

Estimates of $^{87}\text{Sr}/^{86}\text{Sr}$ for the bulk earth today vary, but are between 0.7045 and 0.7052 indicating Rb/Sr ratios between 0.03 and 0.032. This gives a broad band for the $^{87}\text{Sr}/^{86}\text{Sr}$ evolution curve for the bulk earth (see Figure 29). *Bell et al.* [1982] estimated the composition of the depleted mantle source beneath the Superior Province, Canada, which appears to have evolved supposedly from the primitive mantle at around 2.8 Ga, although this differs from the depleted mantle evolution curve of *Ben Othman et al.* [1984] and the present-day composition of the depleted mantle of *Zindler and Hart* [1986] (see Figure 29). Estimates for enriched mantle [*Zindler and Hart*, 1986] suggest present-day

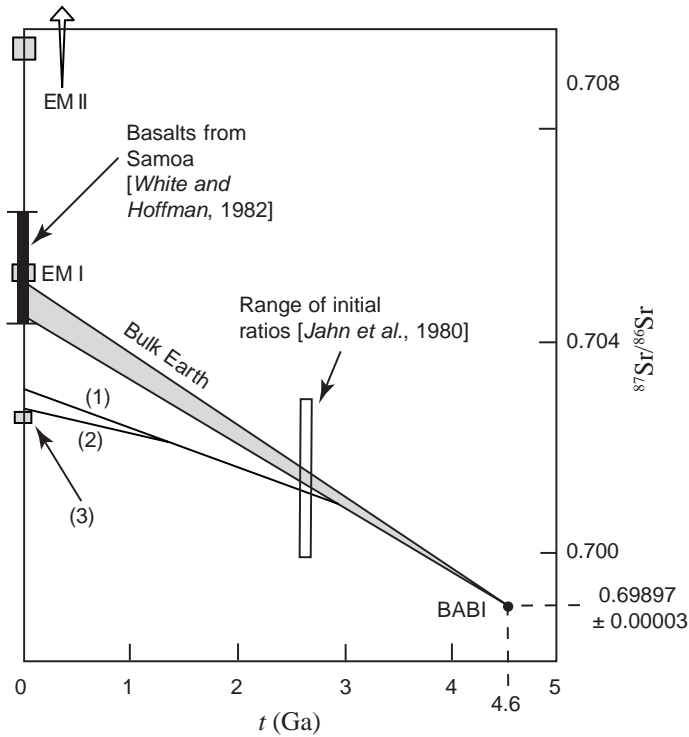


Figure 29. The “evolution” of Sr isotopes with time [after *Rollinson, 1993*]. The shaded field indicates the “evolution” of the bulk earth from 4.6 Ga to the present-day value of between 0.7045 and 0.7052, reflecting Rb/Sr ratios of between 0.03 and 0.032. The depleted mantle curve (1) is from *Bell et al. [1982]* and indicates the separation of a depleted mantle reservoir from the primitive mantle at *ca* 2.8 Ga beneath the Superior Province, Canada. Depleted mantle curve (2) is from *Ben Othman et al. [1984]* and is based upon the data from MORBs, ophiolites, komatiites and meteorites. It represents the equation $(^{87}\text{Sr}/^{86}\text{Sr}) = At^2 + Bt + C$ where $A = -1.54985776 \times 10^{-4}$, $B = -1.6007234$ and $C = 0.70273029$, where t is time from the present in Ga. (3) is the present-day depleted mantle value of *McCulloch and Black [1984]*. The present-day enriched mantle compositions (EM I and EM II) are from *Zindler and Hart [1986]* and the composition of enriched basalts from Samoa from *White and Hofmann [1982]*. The spread of initial ratios from 2.7 to 2.6 Ga is for mafic and felsic igneous rocks, from *Jahn et al. [1980]*.

$^{87}\text{Sr}/^{86}\text{Sr}$ ratios of about 0.705 and about 0.722. Measured values in present-day basalts from Samoa [White and Hofmann, 1982] scatter about the lower of these two values.

Jahn *et al.* [1980] showed that $^{87}\text{Sr}/^{86}\text{Sr}$ ratios for Archean mafic and felsic igneous rocks scatter above and below the bulk earth curve, supposedly indicating that there may have been a variety of mantle sources with different compositions even in the Archean. However, mantle $^{87}\text{Sr}/^{86}\text{Sr}$ ratios need to be interpreted with great caution, especially in “old” rocks, because the high ratios can result from metasomatic processes. For this reason studies of mantle evolution are better based on other isotopic systems where the parent and daughter isotopes are less mobile; this is why the study of Nd isotopes has become so popular over the last decade or so.

A number of authors, for example, Faure [1986], have proposed on the basis of measured initial ratios that the growth of $^{87}\text{Sr}/^{86}\text{Sr}$ in the mantle with time defines a curvilinear path (compared with Figure 29), and that this reflects the irreversible loss of Rb from the mantle into the crust during the formation of the continental crust. The loss of Rb from the mantle and its enrichment in the continental crust lead to very different patterns of Sr isotope evolution in the two reservoirs as a consequence of their different Rb/Sr ratios (see Figure 30). The high Rb/Sr ratios found in the continental crust give rise to an accelerated increase in $^{87}\text{Sr}/^{86}\text{Sr}$ with time, whereas the low Rb/Sr of the depleted mantle gives rise to only a small increase in $^{87}\text{Sr}/^{86}\text{Sr}$ since the formation of the earth.

There are many examples in the literature of authors who have used mantle evolution diagrams of the type illustrated in Figure 30 to plot the initial Sr isotope ratios of measured samples relative to supposed mantle and crustal evolution curves, in order to determine their likely source region. For example, it can be seen on Figure 30 that a suite of rocks produced by partial melting of the mantle at 1.0 Ga will have a very different initial ratio ($^{87}\text{Sr}/^{86}\text{Sr} = 0.7034$) from rocks produced by partial melting of the crust at that same time ($^{87}\text{Sr}/^{86}\text{Sr} = 0.7140$). It is this principle which is regarded as being useful to identify the source of magmatic rocks of known “age.” Of course, the key is that the “age” of the rocks must first be known.

6.3.2 Nd Isotopes. The $^{143}\text{Nd}/^{144}\text{Nd}$ isotopic composition of the bulk earth is thought to be approximated by the composition of chondritic meteorites, the CHondritic Uniform Reservoir (CHUR). The supposed linear evolution of CHUR with time is shown in Figure 31. Studies of modern oceanic basalts and both ancient and modern granitic rocks have suggested that many igneous rocks could be derived from a mantle composition which has a higher Sm/Nd than CHUR, is enriched in $^{143}\text{Nd}/^{144}\text{Nd}$ relative to CHUR, but which is known as depleted mantle.

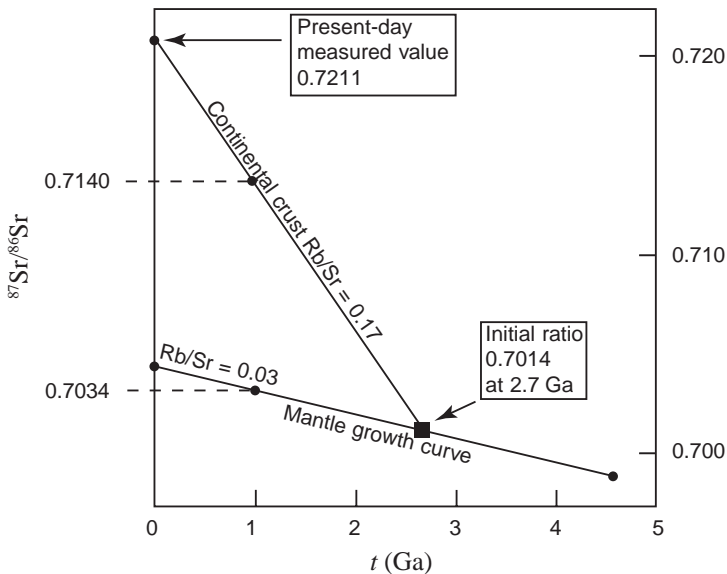


Figure 30. The evolution of $^{87}\text{Sr}/^{86}\text{Sr}$ with time in the continental crust and mantle [after Rollinson, 1993]. At 2.7 Ga mantle differentiation supposedly led to the formation of a new continental crust. The new crust inherited an initial $^{87}\text{Sr}/^{86}\text{Sr}$ ratio of 0.7014 from its parent mantle, but acquired a substantially different Rb/Sr ratio (0.17) compared with 0.03 in the mantle. The higher Rb/Sr ratio in the continental crust led to an accelerated growth of $^{87}\text{Sr}/^{86}\text{Sr}$ with time in the continental crust relative to that in the mantle, so that the present-day measured value in the crust is 0.7211 compared with 0.7045 in the mantle. The $^{87}\text{Sr}/^{86}\text{Sr}$ ratios shown on the left-hand side of the diagram indicate the initial ratios in melts formed from continental crust at 1.0 Ga (0.7140) and from the mantle at 1.0 Ga (0.7034).

Currently there are several models for this depleted mantle source, the main differences between them being:

- the time at which the depleted mantle supposedly differentiated from the bulk earth, and
- whether the depletion of the mantle was linear or whether it varied with time.

Liew and McCulloch [1985] proposed that the light REE (rare earth elements) depletion from the chondritic reservoir took place between 2.5 and 3.0 Ga at the time of a major episode of crust generation, and they proposed a linear evolution of $^{143}\text{Nd}/^{144}\text{Nd}$ in the depleted mantle

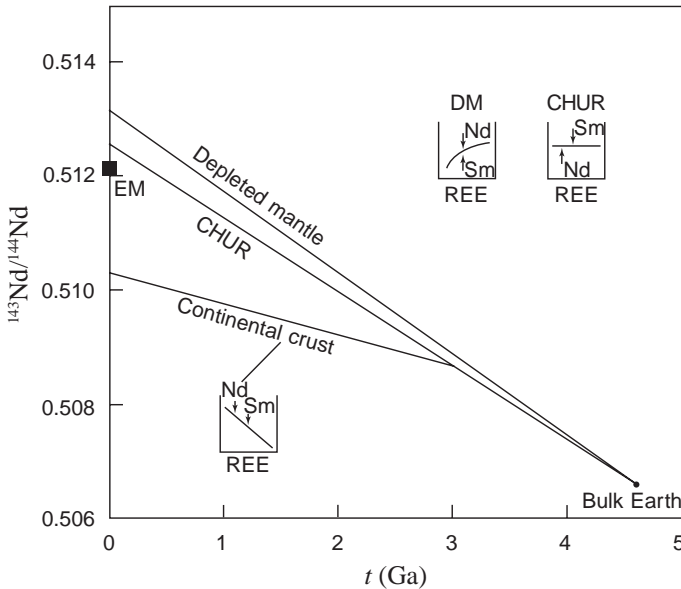
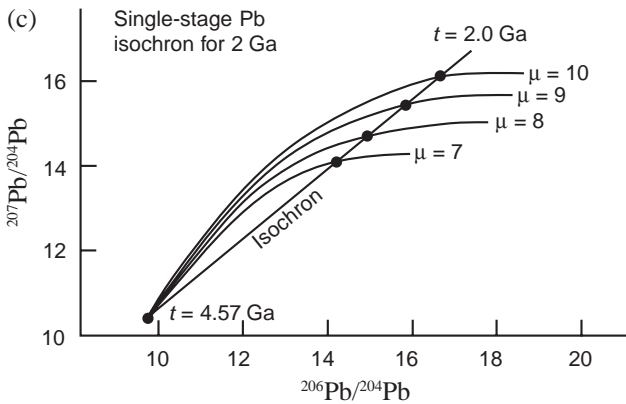
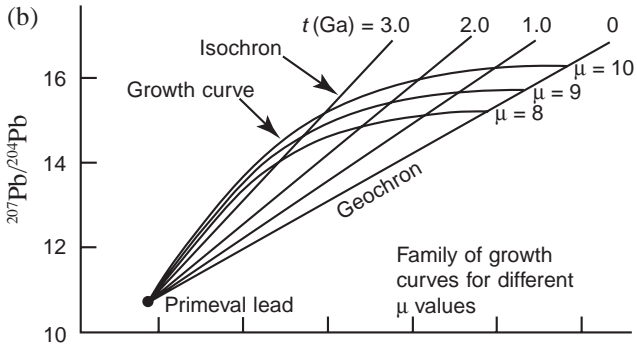
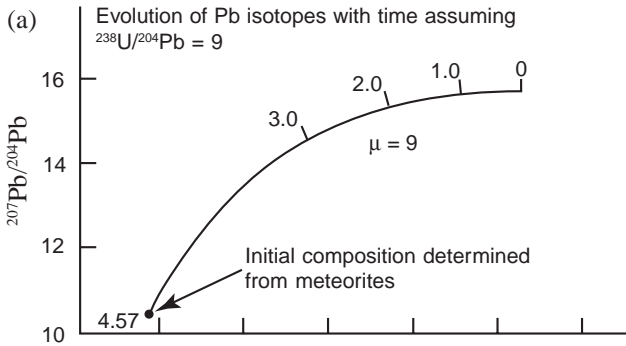


Figure 31. The evolution of $^{143}\text{Nd}/^{144}\text{Nd}$ isotopes with time in the mantle, the continental crust and the bulk earth [after *Rollinson, 1993*]. Relative to the bulk earth (CHUR) in which the fractionation of Sm/Nd is normalized to unity, the depleted mantle (DM) has a high Sm/Nd ratio and shows higher $^{143}\text{Nd}/^{144}\text{Nd}$. The continental crust has lower Sm/Nd and shows a retarded $^{143}\text{Nd}/^{144}\text{Nd}$ evolution with time. Enriched mantle (EM) shows some affinity with the continental crust inasmuch as it also has a retarded isotopic evolution, while in the Rb-Sr system it shows accelerated evolution relative to the bulk earth and mantle.



between this time and the present. *Goldstein et al.* [1984] preferred a linear evolution between the present day and the formation of the earth. *DePaolo* [1981a] and *Nelson and DePaolo* [1984] plotted curves which decrease to zero at 4.6 Ga, while the curve of *Allègre and Rousseau* [1984] and *Ben Othman et al.* [1984] reduces to an ϵ value of +2.5 at 4.0 Ga. Some support for this supposed depleted mantle very early in the history of the earth comes from the work of *Collerson et al.* [1991].

The Sm/Nd ratio of the continental crust is highly fractionated (<1.0) relative to CHUR and shows retarded $^{143}\text{Nd}/^{144}\text{Nd}$ evolution with time. This is the opposite of the Rb/Sr system, where the Sr-isotopic evolution of the crust shows accelerated evolution with time relative to the mantle.

6.3.3 Pb Isotopes. Because there are so many variables in Pb isotopic systems (since there are three different decay schemes), it is not convenient to display the data on the same type of time versus isotope ratio diagram as is used for Sr and Nd isotopes, so the concordia diagram is a better choice. On this diagram families of concordia or growth curves can be drawn for different $^{238}\text{U}/^{204}\text{Pb}$ ratios (μ values) (see Figure 32).

Figure 32 (opposite). The evolution of Pb isotopes with time [after *Rollinson*, 1993]. (a) The growth curve for $^{207}\text{Pb}/^{204}\text{Pb}$ and $^{206}\text{Pb}/^{204}\text{Pb}$ through time. The locus of points is a curve because the two isotopes are produced at different rates. The starting composition at the formation of the earth (4.57 Ga) is taken from the isotopic composition of troilite in the Canyon Diablo meteorite. This growth curve assumes a $^{238}\text{U}/^{204}\text{Pb}$ ratio (μ value) of 9.0. (b) A family of growth curves for Pb isotopes identical to that depicted in (a), showing Pb isotopic growth from the assumed primeval composition at 4.57 Ga until the present for $\mu = 8, 9$ and 10. Isochrons for 0, 1.0, 2.0 and 3.0 Ga are the lines which join the 0, 1.0, 2.0 and 3.0 Ga points on each growth curve. The 0 Ga isochron is known as the geochron. (c) A single-stage Pb isochron for 2.0 Ga. The isochron line joins the 2.0 Ga points on the growth curves for four different μ values and passes through the primeval Pb composition at 4.57 Ga; it represents a suite of samples which evolved from 4.57 Ga until 2.0 Ga, when they were isolated from U. These values have supposedly remained frozen in the rocks since 2.0 Ga. The growth curves in these diagrams are based upon the assumption that the isotopes of Pb have evolved uninterrupted since the formation of the earth. This is thought to be a simplification and normally a more complex model of Pb isotope evolution is adopted [*Cumming and Richards*, 1975; *Stacey and Kramers*, 1975].

Based on the assumptions implicit in U-Th-Pb “dating,” each curve can be calibrated for time, and equal time points can be joined to give isochrons. *Brevart et al.* [1986] used Pb isotope initial ratios to demonstrate mantle heterogeneity at 2.7 Ga and constructed a depleted mantle curve from 2.7 Ga to the present day from initial ratios of komatiites and basalts on a ^{206}Pb - ^{207}Pb isotope evolution diagram.

6.3.4 Isotope Correlations. Isotope correlation diagrams are used to display the contrasting compositions of crust and mantle reservoirs, and they can equally be a means of investigating mixing processes between sources of contrasting compositions. *Zindler et al.* [1982] proposed a three-dimensional Sr-Pb-Nd isotopes plot for oceanic basalts and showed that averaged data define a planar surface, implying coherence between Sr-Pb-Nd isotopes in the source of the oceanic basalts. However, this appears to be an oversimplification, as is apparent from the Pb-Sr-Nd-Hf study of *Stille et al.* [1983] who showed that data from Hawaii do not plot in the mantle plane of *Zindler et al.* [1982], and who suggested that U-Pb fractionation may be decoupled from Rb-Sr, Sm-Nd and Lu-Hf fractionation.

Trends on such isotope correlation diagrams are most commonly interpreted as mixing lines. The mixing may be in the source region, in a magma chamber or between a melt and a “contaminant,” such as the wall-rock into which a magma is emplaced or through which it has traveled. *Langmuir et al.* [1978] described a general mixing equation which can be applied to isotope ratios. Compositions resulting from mixing normally lie on a hyperbolic curve, but if the ratios have a common denominator (as in the case of $^{87}\text{Sr}/^{86}\text{Sr}$ versus $^{87}\text{Rb}/^{86}\text{Sr}$ and $^{207}\text{Pb}/^{204}\text{Pb}$ versus $^{206}\text{Pb}/^{204}\text{Pb}$), then mixing will produce a linear trend.

• **Mixing between sources.** For a number of years, the isotopic compositions of oceanic basalts have been regarded as the result of mixing of a variety of mantle sources. This is borne out by linear and curvilinear arrays on isotope correlation diagrams, such as the Nd-Sr mantle array (see Figures 24 and 25) and the Pb-Pb isotope NHRL (see Figure 26). Similar principles apply to mixing between crust and mantle sources.

Many authors portray mixing on an Nd-Sr isotope correlation diagram

following the principles outlined by *DePaolo and Wasserburg* [1979a]. For instance, *McCulloch et al.* [1983] used this diagram (see Figure 33) to show how the compositions of kimberlites and lamproites may be derived by the mixing of MORB-type depleted mantle and an enriched mantle similar to EM II. *McCulloch and Chappell* [1982] also used the Nd-Sr diagram to explain the contrasting isotope chemistry of S- and I-type granites in terms of mixing between depleted mantle and a sedimentary crustal component (Figure 16). More complex examples of mixing between three end-members are discussed by *Shirey et al.* [1987] and *Ellam and Hawkesworth* [1988] in studies of oceanic basalt and subduction-related magmas respectively.

The identification of mixing as an important process both in the mantle and between the crust and the mantle inevitably leads to more profound questions about mechanisms in mixing and how they relate to major

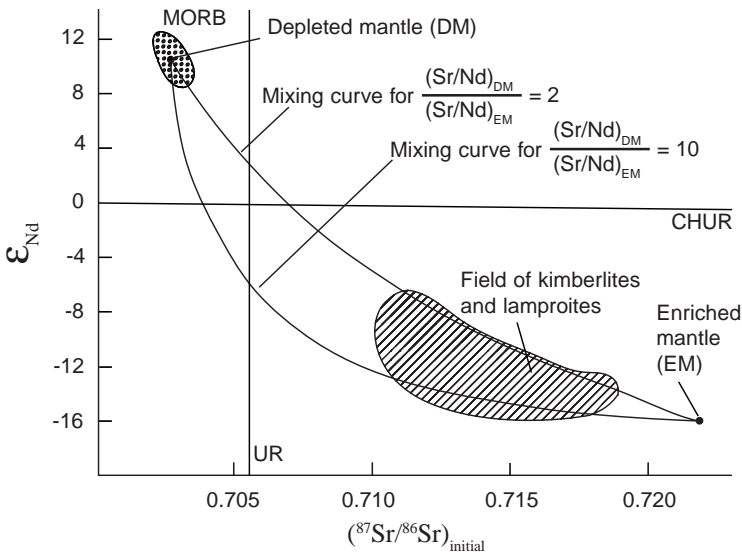


Figure 33. A $^{143}\text{Nd}/^{144}\text{Nd}$ versus $^{87}\text{Sr}/^{86}\text{Sr}$ correlation diagram showing two hyperbolic mixing curves for different ratios of $(\text{Sr}/\text{Nd})_{\text{EM}}/(\text{Sr}/\text{Nd})_{\text{DM}}$ between depleted mantle (DM) and enriched mantle (EM) [after *McCulloch et al.*, 1983]. The mixing can account for the range of $^{143}\text{Nd}/^{144}\text{Nd}$ and $^{87}\text{Sr}/^{86}\text{Sr}$ values observed in kimberlites and lamproites from Western Australia.

plate tectonic processes. This is the field of geodynamics.

- **Mixing in a magma chamber.** *Sharpe* [1985] showed that Sr isotopes can be used to model the magma mixing and multiplicity of magmas in a layered intrusion. He documented the Sr isotopic change with stratigraphic height within the Bushveld layered intrusion (South Africa) and showed that there is a gradual increase in initial $^{87}\text{Sr}/^{86}\text{Sr}$ with height up the intrusion, and that there is a marked increase in initial ratio in the central part of the layered intrusion—the Main Zone (see Figure 34). The gradual change in $^{87}\text{Sr}/^{86}\text{Sr}$ from 0.7065 at the base of the intrusion to 0.7073 at the top is interpreted as magma addition and mixing. The high initial ratio of the Main Zone (0.7085) represents a different liquid layer (probably contaminated with shales) intruded into the density-stratified magma pile near the base of the magma chamber.

- **Contamination of magmas by the continental crust.** The expression “crustal contamination” can have a number of different meanings. Most normally it means “contamination of mantle-derived melts by continental crust after they have left the source region” [*Hawkesworth and van Calsteren*, 1984]. However, it can also be used in the sense of a mantle source region from which magmas are derived which was contaminated by crustal material at some time in the past by, for example, the incorporation of subducted sediment into the mantle. One of the problems is that it is not always easy to discriminate between the two processes on the basis of rock chemistry.

Crustal contamination may arise in a variety of ways. Mechanisms include the bulk assimilation of crustal material, the assimilation of a partial melt derived from crustal materials, and the selective exchange of specific elements aided by the transfer of fluids from crust to melt. The more “evolved” members of an igneous suite are more likely to show evidence of contamination, for they have spent the longest time in the continental crust.

Stable isotopes, particularly oxygen isotopes, are probably the most sensitive of all isotopic systems to the process of crustal contamination [*Hawkesworth and van Calsteren*, 1984]. Of the radiogenic isotopes Nd isotopes are the least sensitive to this process, whereas Sr and particularly Pb isotopes are of great value. The ability of Pb isotopes to detect the

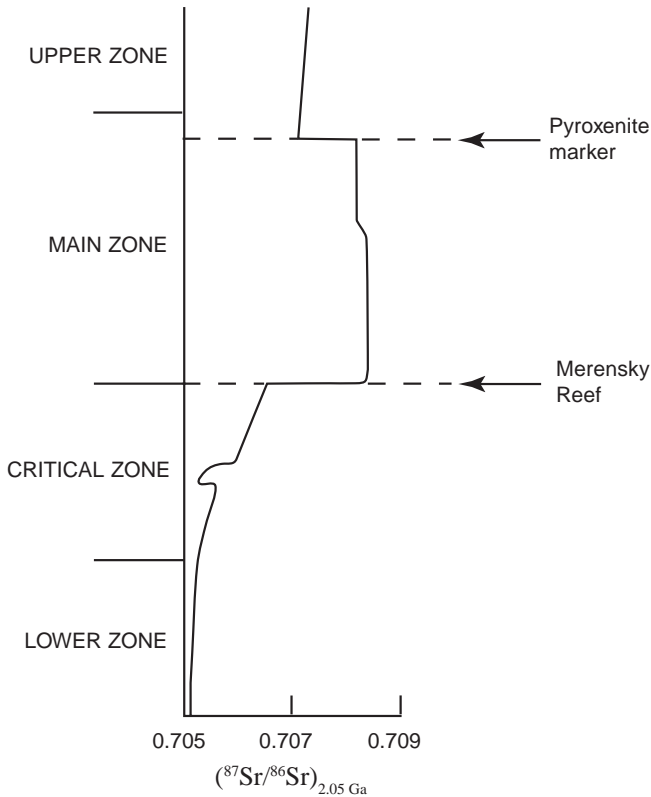


Figure 34. Change in $^{87}\text{Sr}/^{86}\text{Sr}$ with stratigraphic height in the Bushveld intrusion, South Africa [after *Sharpe*, 1985]. The gradual increase in $^{87}\text{Sr}/^{86}\text{Sr}$ with stratigraphic height reflects the addition and mixing of a magma with a higher $^{87}\text{Sr}/^{86}\text{Sr}$ ratio. The marked increase in isotopic composition between the pyroxenite marker and the Merensky Reef marks the influx of a new pulse of magma.

contamination of mantle-derived melts by “old” continental crust has been elegantly demonstrated by *Taylor et al.* [1980]. They showed that the late Archean (2.85 Ga) Nuk gneisses of west Greenland were contaminated to a varying extent by the Pb derived from the early Archean (3.7 Ga) Amitsoq gneisses. In contrast, the Sr isotopic compositions in those same rocks are low, even in the most contaminated rocks, indicating

that the contamination was selective, which led *Taylor et al.* [1980] to suggest that the contamination process was probably related to a fluid phase. Differentiating between contamination in the source region and contamination during transport through the continental crust can be difficult using isotope correlation diagrams alone, and additional information, such as that from stable isotope studies and from radiogenic isotope-trace element plots, is necessary.

- **Crustal contamination and AFC processes.** *DePaolo* [1981b] has shown that Assimilation and Fractional Crystallization (AFC), a popular mechanism of contamination, may shift compositions on an isotope correlation diagram far from what might be expected on the basis of simple mixing. On an Nd-Sr isotope correlation diagram simple mixtures will define a straight line trend between the magma and contaminant, whereas in AFC processes when the bulk solid/liquid distribution coefficient for Nd and Sr differ markedly then there is a significant departure from a simple mixing curve. *Powell* [1984] inverted the equations of *DePaolo* [1981b] in an attempt to calculate the composition of the contaminant from an AFC trend on an isotope correlation diagram.

- **Contamination with seawater.** The high $^{87}\text{Sr}/^{86}\text{Sr}$ ratio of seawater relative to mantle values as seen in oceanic basalts means that the exchange of Sr between seawater and ocean crust in a mid-ocean ridge system has the capacity to produce relatively radiogenic $^{87}\text{Sr}/^{86}\text{Sr}$ ratios even in young MORB and associated sulfides [*Spooner et al.*, 1977; *Vidal and Clauer*, 1981]. Nd isotopes are in contrast relatively insensitive to this type of contamination, and a plot on an Nd-Sr diagram shows enhanced $^{87}\text{Sr}/^{86}\text{Sr}$ at constant $^{143}\text{Nd}/^{144}\text{Nd}$. The length of the vector is proportional to the effective water/rock mass ratio. Lead isotopes are less predictable. *Vidal and Clauer* [1981], in a study of recent sulfides from the East Pacific Rise, found that the Sr isotopes showed evidence of seawater contamination, whereas the Pb isotopes did not. *Spooner and Gale* [1982], however, in a similar study of larger Cretaceous mid-ocean ridge sulfide deposits, did find evidence of contamination from seawater Pb. *Chivas et al.* [1982] used Sr isotopes to calculate water/rock ratios in diorites and granodiorites altered by seawater using an equation analogous to that used by *Taylor* [1974] for oxygen isotopes.

6.3.5 Isotopes versus Trace Elements. Since an isotope ratio cannot be fractionated by crystal-liquid equilibria and therefore is indicative of the magmatic source, the correlation between an isotope ratio and a major or trace element can be used as a guide to the major element or trace element composition of the source. Typically, ratios of highly incompatible trace elements are the most useful in characterizing the elemental composition of the source region. Thus, correlations between isotope ratios and ratios of highly incompatible trace elements are likely to indicate mixing between compositionally distinct sources.

The equations of *Langmuir et al.* [1978] predict that data plotted on an isotope ratio versus trace element diagram with a common denominator (for example, $^{87}\text{Sr}/^{86}\text{Sr}$ versus $1/^{86}\text{Sr}$) will define a straight line. Mixing diagrams of this type, however, can give rise to spurious correlations because of the common denominator effect [*Dodson*, 1982]. An additional problem with the $^{87}\text{Sr}/^{86}\text{Sr}$ ratio versus $1/^{86}\text{Sr}$ diagram, highlighted by *Mensing et al.* [1984], is that, in the case of basaltic lavas undergoing fractional crystallization and assimilating crustal material (AFC), the composition of the contaminant does not lie on the magma evolution trajectory. Thus the linear mixing trend cannot be used to determine the composition of the contaminant.

6.4 Mantle-Crust Geodynamics

The ultimate outcome of defining crust and mantle isotopic reservoirs should be a model which explains how the reservoirs interact and how they obtained their present-day compositions. Such unifying models have been proposed, and they link reservoir compositions to the processes that govern plate tectonics. There are two types of approach. Models based upon Pb isotopes and which chiefly emphasize crustal reservoirs are known as plumbotectonics models. Models which emphasize mixing processes in the mantle, and which are based upon a number of different isotope systems, are described as geodynamic models.

Plumbotectonics models [*Doe and Zartman*, 1979] are based on variations in initial Pb isotopic compositions which are related to tectonic setting. The upper continental crust, the lower continental crust and the

upper mantle reservoirs can be characterized by their concentrations of U, Th and Pb. As indicated in Table 4, U, Th and Pb are concentrated in the upper crust, with U and Th enriched relative to Pb so that the upper crust “evolves” radiogenic Pb. The lower crust is depleted in Th and U and “evolves” unradiogenic Pb. The mantle has lower concentrations of U, Th and Pb than the continental crust, but has U/Pb and Th/Pb ratios which lie between the two crustal reservoirs and so “evolves” Pb of an intermediate character. The mixing of Pb in its three reservoirs takes place in “orogenies” (or orogenes) producing a fourth “mixed” reservoir. Curves are plotted to show the Pb isotopic evolution of the four reservoirs with time [Zartman and Haines, 1988] (see Figure 35). The $^{207}\text{Pb}/^{204}\text{Pb}$ versus $^{206}\text{Pb}/^{204}\text{Pb}$ plot discriminates well between the upper crust and the lower crust/mantle, while the $^{208}\text{Pb}/^{204}\text{Pb}$ versus $^{206}\text{Pb}/^{204}\text{Pb}$ plot discriminates between the lower crust and the upper crust/mantle.

However, it has long been known that the measured Th/U of mid-ocean ridge basalts and, by inference, the upper mantle, is much lower than the time-integrated Th/U ratio of the upper mantle, but Elliott *et al.* [1999] are convinced that this mismatch can be readily explained by *in situ* decay of U and Th. Their resolution of the conundrum suggests near constant Th/U of the upper mantle in early earth history followed by a steady decrease after the Archean, due to post-Archean recycling of U into the mantle preferentially relative to insoluble Th. (The claimed dramatic increase in atmospheric oxygen at the end of the Archean is said to have made U highly soluble, resulting in it being readily weathered from the continents and then incorporated into altered oceanic crust from sea water.) This flux of recycled U calculated by Elliott *et al.* [1999] to appropriately lower upper mantle Th/U is within the bounds obtained by integrating present-day fluxes of subducted “excess” U for about 2 Ga, and thus appears to provide a solution to the Th/U conundrum that does not require the Pb isotope ratios of the upper mantle to predominantly reflect the signature of entrained material from another, deeper reservoir such as the lower mantle. On the other hand, this apparent conundrum is solely due to assuming the validity of the uniformitarian timescale, because in reality there is no mismatch between the measured Th/U of mid-ocean ridge basalts and the Th/U ratio of

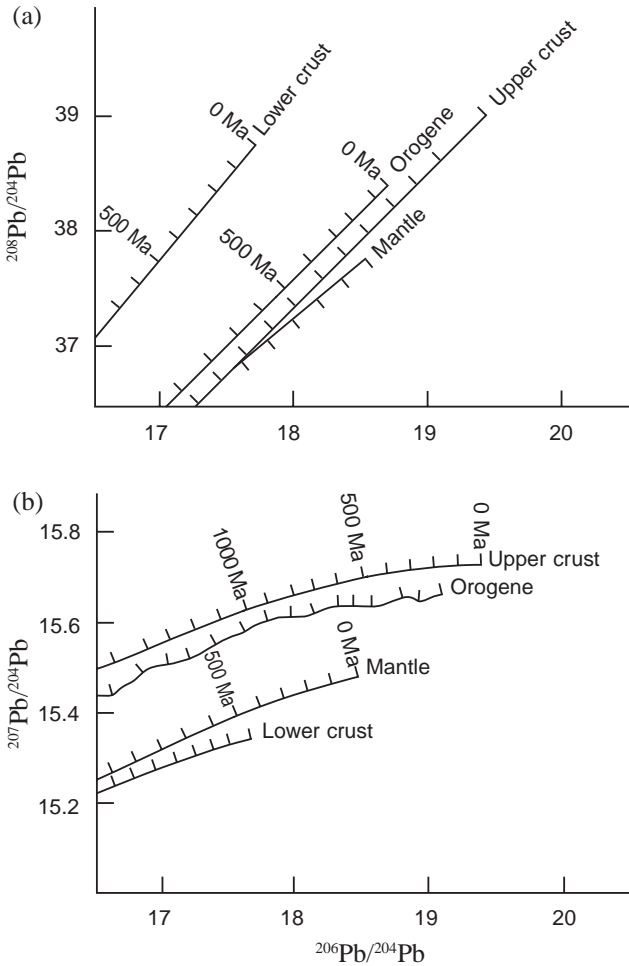


Figure 35. Lead isotope evolution curves for the lower crust, upper crust, mantle and orogene plotted for (a) $^{208}\text{Pb}/^{204}\text{Pb}$ versus $^{206}\text{Pb}/^{204}\text{Pb}$ and (b) $^{207}\text{Pb}/^{204}\text{Pb}$ versus $^{206}\text{Pb}/^{204}\text{Pb}$ for plumbotectonics version IV [after Zartman and Haines, 1988]. The ticks on each curve are at 100 Ma intervals and time flows from right to left on each curve commencing at 0 Ma.

their upper mantle source.

Geodynamics models are tectonic models for the chemical structure of the earth, and are constrained both by the isotopic data and our present understanding of plate tectonic processes. When the Nd-Sr compositions of the continental crust and oceanic basalts were plotted relative to the composition of the bulk earth (Figure 25), it was found that oceanic basalts are enriched in Nd and depleted in Sr relative to the bulk earth, while the continental crust shows the opposite relationship. This suggests that the continental crust and the mantle source of oceanic basalts are complimentary reservoirs of Nd and Sr, and that the continental crust has been extracted from the earth's mantle leaving a reservoir enriched in Nd and depleted in Sr. In a similar way, the isotopic compositions of crust and mantle reservoirs have been interpreted by means of a series of mass balance equations between crust, mantle and the presumed original composition of the Bulk Silicate Earth (BSE). By this means the interrelationships between different reservoirs have been explored, limits set on the proportion of mantle involved in the formation of the continental crust, and insights into the nature of mantle convection have been gained [Allègre *et al.*, 1983a, b; Galer and O'Nions, 1985; Zindler and Hart, 1986; Allègre, 1987]. Figure 28 is a cartoon diagram illustrating a possible way in which the different reservoirs interact.

Further development of geodynamics models has increasingly been tied into geophysical elucidation of mantle and crustal structure and its application to plate tectonics. Also, rare gas data (including $^{40}\text{Ar}^*$), which likewise have been used independently to define geochemical reservoirs in the crust and mantle, are now being employed in refinement of mantle-crust geodynamics. Thus Albarède [1998] has taken into account evidence from high-resolution seismic tomography that lithospheric plates penetrate the 660 km discontinuity, the boundary between the lower and upper mantle, to evaluate a time-dependent geochemical model for the earth with a mineralogically layered mantle, but with substantial exchange amounting to 50% of the lithospheric plate flux across the 660 km discontinuity. His model involved four reservoirs (lower and upper mantle, crust, atmosphere), with low concentration levels of U, Th and K in the lower mantle relative to the upper mantle, and the lower

mantle depleted in rare gases. Albarède thus reproduced the best estimates of the modern $^{40}\text{Ar}/^{36}\text{Ar}$ ratios in each reservoir, but his model is dependent on a lower figure for the terrestrial K/U ratio than what has been measured in crustal rocks. Whereas such geodynamics models also take into account the fractionation and recycling of other isotopes (Nd, Sr, Hf) due to crustal growth, subduction, descending lithospheric plates into the lower mantle, plumes, etc., they are nonetheless based on assumptions about the earth's initial geochemical makeup inherent in evolutionary models for the earth's formation from the solar nebula, and on a 4.57 Ga uniformitarian timescale.

The generally preferred uniformitarian geochemical paradigm for development of rare gases (including $^{40}\text{Ar}^*$) in the mantle is that the lower mantle has remained an isolated and undegassed reservoir throughout at least the past 4.35 Ga of earth history, because ~50% of the $^{40}\text{Ar}^*$ produced by ^{40}K -decay appears to still reside within the mantle [Allègre *et al.*, 1996; O'Nions and Tolstikhin, 1996; Phipps Morgan, 1998]. Nevertheless, Phipps Morgan [1998] maintains that simple models of Ar evolution within a convecting mantle demonstrate that whole-mantle convection can retain 25–60% of the $^{40}\text{Ar}^*$ produced during earth evolution without the need for postulating an isolated and undegassed lower mantle. Thus these models suggest that the $^{40}\text{Ar}^*$ constraint should be reinterpreted to instead be that ~50% of the mantle (and possibly the crust also) has been undegassed since the $^{40}\text{Ar}^*$ was produced within it. Such a conclusion avoids the evidence of abundant excess $^{40}\text{Ar}^*$ circulating in the mantle and crust, which seems more consistent with a young earth and catastrophic plate tectonics [Austin *et al.*, 1994].

Furthermore, Davies [1999] maintains that a gas-rich lower mantle would severely limit the permissible mass flow rate into the upper mantle, and conflicts with evidence from refractory trace elements and their isotopes that most of the mantle has been processed, consistent with increasingly strong geophysical evidence for a large mass flow between the upper and lower mantle. Therefore, he proposes a degassed lower mantle, which requires, assuming the total amount of ^{40}Ar is unknown, either that the earth has 50% less ^{40}K than is usually estimated, the ^{40}Ar

is sequestered in the core, or that ^{40}Ar has been lost from the earth entirely. The latter two possibilities are implausible, leaving a 50% lower K/U ratio in the earth as the preferred option to remove the apparent discrepancy, a resultant model which is similar to that of *Albarède* [1998]. However, measurements of the terrestrial K/U ratio in crustal rocks do not support this model, and estimates of the earth's total ^{40}Ar budget projected from measurements are not unreasonable. This still leaves the apparent discrepancy, but that in reality is an artifact of the assumed uniformitarian timescale and evolutionary origin for the earth.

A more complicated model for geochemical reservoirs using transport balances to reconcile data in the Th-U-Pb system was developed by *Kramers and Tolstikhin* [1997] and features four continental crust reservoirs, the oceanic crust reservoir, upper and lower mantle reservoirs, and the core reservoir, plus a prototerrestrial material reservoir representing the earliest terrestrial material to have formed during conjectured earth accretion (see Figure 36). *Tolstikhin and Marty* [1998] adapted this model with the addition of an atmosphere reservoir to develop an evolutionary model for identifying and quantifying processes supposedly able to reproduce rare gas and nitrogen isotopic abundances in the main terrestrial reservoirs.

Similarly, *Nägler and Kramers* [1998] utilized the same model for the terrestrial evolution of the Sm-Nd system (Figure 36), which they suggested essentially operates in the upper mantle, oceanic crust and continental crust. To simplify modeling, *Nägler and Kramers* [1998] admitted that the model describes internally fully homogeneous reservoirs, so that a scatter of real data around the model development curves was to be expected as a result of imperfect mixing. Such modeling is invariably limited in trying to describe and accommodate all the complexities and variabilities of the real isotopic and geochemical data from countless rock samples. Nevertheless, *Nägler and Kramers* [1998] still proposed a third order polynomial curve for depleted upper mantle evolution as a new reference for Nd_{DM} "model age" calculations, while admitting there were clear anomalies apart from true mantle heterogeneity and some whole-rock mixing relationships in the rock Nd isotopic data, and strong apparent discrepancies between Sm-Nd

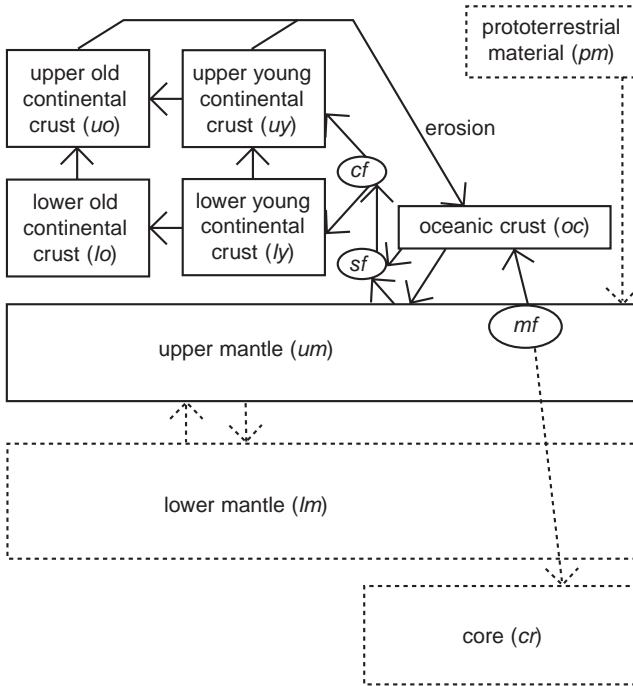


Figure 36. Reservoirs (with abbreviations) and fluxes (arrows) of the transport balance model of *Kramers and Tolstikhin [1997]*. Ellipses denote fractionation loci: *mf* mantle fractionation (melting) zone giving rise to oceanic crust; *sf* subduction (mixing-melting) fractionation zone where protocrust originates; *cf* intracrustal fractionation zone formally giving rise to upper crust (as melt) and lower crust (as residue). Stippled arrows: fluxes without fractionation; solid arrows: fluxes with fractionation. Reservoirs with stippled outlines are not important for Sm-Nd modeling: the “prototerrestrial” and “core” reservoirs are effectively closed since 4.5 Ga ago; the fluxes between upper and lower mantle are also negligible for Sm-Nd since that time [after *Nägler and Kramers, 1998*].

systematics and zircon U-Pb ages.

Recognizing the difficulties of modeling the complexities in the geochemical and isotopic data, *Phipps Morgan and Morgan [1999]* sought to simplify the task by just focusing on the effects on the mantle of the production of mid-ocean ridge basalts (MORBs) and ocean-island basalts (OIBs). Thus they proposed a geochemical model for mantle

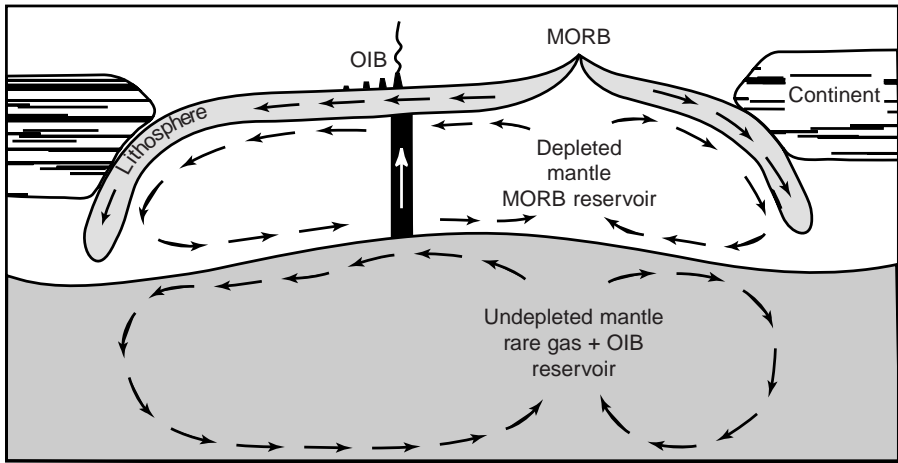


Figure 37. Cartoon of stratified mantle convection that is consistent with the observed geochemistry of mid-ocean ridge basalt (MORB) and continental crust. This paradigm is often invoked to explain observed rare-gas differences between ocean island basalt (OIB) and MORB, observed isotopic depletion of MORB and isotopic enrichment of continental crust, and trace element contrasts between MORB and continental crust. However, it does not seem to be consistent with geophysical evidence for significant present-day flow between the upper and lower mantle. [After *Phipps Morgan and Morgan*, 1999].

evolution in which a sequence of hotspot and ridge upwellings has melted the mantle to make hotspot and mid-ocean ridge basalts and their residues, and plate subduction has recycled and stirred all of these differentiation products back into the mantle. After the assumed billions of years they claim this process would have mixed various “plums” of incompatible-element rich veins within a matrix made from the residues of melting that have been depleted in incompatible elements. *Phipps Morgan and Morgan* [1999] propose that the mantle flows upward and melts in a two-stage process. They maintain that the observed trace element, rare gas and isotopic contrasts between ocean-island and mid-ocean ridge basalts can thus be produced by a recipe which assumes that throughout earth history these two sequential stages of deep plume and shallower ridge melting have both created and reprocessed the plums

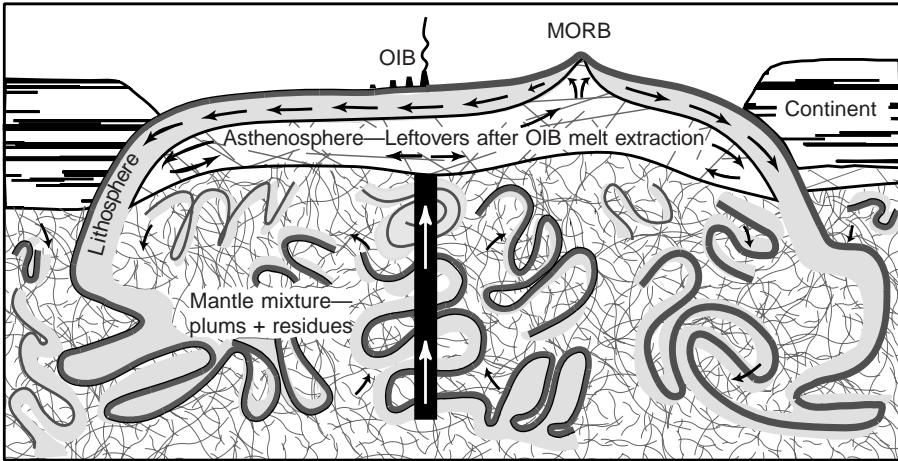


Figure 38. Alternative paradigm of whole mantle convection that may prove to be consistent with both geochemical and geophysical evidence. In this scenario the mantle is a “plum-pudding” mixture of recycled basalts and continental sediments, rich in incompatible elements, that have been stirred by convection into recycled residues from plume and ridge melt-extraction and surviving “primitive” mantle. The asthenosphere “MORB-source” is derived from typical plum-pudding mantle by melting an upwelling plume—the plume melts become an OIB, while the depleted leftovers from plume-melting pond beneath the lithosphere to supply the asthenosphere. When this depleted asthenosphere upwells and melts a second time beneath a ridge, its melt becomes a MORB. [After Phipps Morgan and Morgan, 1999].

and residues that make up the present-day mantle. Rather than stratified mantle convection, with a depleted upper mantle MORB reservoir and an undepleted lower mantle rare gas and OIB reservoir (see Figure 37), their paradigm involves convection of the whole mantle that is a mixture of plums and residues, which they suggest also seems consistent with geophysical evidence for significant present-day flow between the upper and lower mantle (see Figure 38). Significantly, if the assumption of uniformitarian process rates over billions of years is rejected, then this melting and mixing model could conceivably be still accomplished with catastrophic plate tectonics [Austin *et al.*, 1994] within a young-earth timeframe.

7. Discussion

The proliferation of crust-mantle geodynamics models for isotopic/geochemical reservoirs in a burgeoning literature is testimony to the difficulties encountered in finding meaningful trends in the plethora of isotopic data now available. However, two crucial considerations need to be recognized:

- The quality and integrity of the radioisotopic data.

The available evidence clearly demonstrates the relative mobilities of the elements involved in all the relevant radioisotopic systems (K-Ar, U-Th-Pb, Rb-Sr, and even Sm-Nd) in crustal fluids, particularly at elevated temperatures (hydrothermal fluids) and due to weathering, not just in the rocks but within the constituent minerals themselves. This mobility results in either inheritance of excess radiogenic daughter isotopes or even extra radioactive parent isotopes in some cases, or in loss of radiogenic daughter and/or radioactive parent isotopes. Thus the quality and integrity of the radioisotopic data upon which these models have been built are highly questionable—that is, not the isotopic ratios themselves, but the interpretation of them. Quite obviously the main criterion for accepting or rejecting radioisotopic data is whether the resultant “ages” are consistent with the stratigraphic and biostratigraphic setting and with other radioisotopic “ages” (concordances), all within the uniformitarian time framework. This makes the edifice that has been built internally consistent by definition and therefore self-fulfilling, with no independent measure of objectivity. Yet the problems with the quality and integrity of the radioisotopic data remain, with no way of knowing whether even the “good” data yielding acceptable “ages” are likewise suspect.

- The role of the mantle in yielding old “ages” in modern lavas.

It was in large part the discovery that modern lavas, particularly oceanic basalts, yielded old radioisotopic “ages” which led to the recognition and definition of the mantle geochemical reservoirs, and then plumbotectonics and mantle-crust geodynamics. And yet these “ages” are only anomalously old because the radioisotopic signatures in these modern lavas have been interpreted in terms of “ages.” In fact, they may

only represent further fundamental geochemical characteristics of the mantle and thus the rocks. Furthermore, if modern lavas are artificially old because of being sourced from these heterogeneous mantle reservoirs, then is it not possible that “ancient” lavas also sourced from the mantle may likewise be artificially old? Mixing from mantle and crustal sources to produce all crustal rocks has been amply demonstrated by using as fundamental geochemical “fingerprints” these same radioisotopic systems which have also yielded the self-consistent and systematic, vast radioisotopic “ages.” So could it be that these radioisotopic “ages” are really only an artifact of systematic mixing from mantle and crustal sources, sources which were endowed with fundamental geochemical signatures at the origin of the earth? Very different radioisotopic signatures in successive flows from the same volcanoes would seem to be consistent with such mixing processes. Vast timespans of slow-and-gradual uniformitarian plate tectonics are unnecessary to produce the required mixing, crustal growth and mantle stirring, because catastrophic plate tectonics has the potential to explain, and be consistent with, even more of the real-world data, but within a young-earth timeframe [*Austin et al.*, 1994]. Indeed, state-of-the-art computer modeling of plate tectonics has demonstrated that the processes of subduction, plate movements and mantle convection, and therefore crustal growth, occur catastrophically over a drastically shortened timescale [*Baumgardner*, 1994a, b].

The recognition that there are many anomalies and discrepancies in the uniformitarian radioisotopic data, and that geochemical modeling of the mantle’s contribution to crustal growth can explain the radioisotopic ratios found in crustal rocks, suggests that there is scope for attempting a fresh “big picture” analysis of the radioisotopic data within a young-earth, global Flood/catastrophic plate tectonics framework. The quality and integrity of the radioisotopic data may often be doubtful on the one hand, but the concordances and a systematic consistency within the uniformitarian edifice remain. The solution may therefore involve the geochemical and catastrophic tectonic (geodynamic) processes in the mantle and crust that have unmistakably produced their geochemical and radioisotopic signatures in the earth’s

crustal rocks, signatures that have been wrongly interpreted as old “ages.” Nevertheless, some radioactive decay has occurred, sufficient to produce, for example, mature (fully-formed) ^{238}U radiohalos, as will be discussed in Chapter 8.

The assumption of the uniformitarian timescale undergirds the interpretation of radioisotopic analyses, because consistency with that timescale distinguishes “dates” that are acceptable from “anomalies” that need to be explained by open-system behavior, inheritance, etc. Thus it is difficult to quantify just how significant are multiple isotope concordances and what appears to be a consistent overall trend of lower strata in the geologic record dating older than upper strata. However, the impression gained from the foregoing detailed examination of the primary radioisotopic “dating” systems is that if the uniformitarian timescale assumption were removed, where more than one radioisotope system has been utilized to “date” specific rock strata, isotope discordances would be in the majority. That such discordances are often the case has already been discussed by Austin in Chapter 4. However, a relevant example here is that of the Cardenas Basalt of eastern Grand Canyon which has yielded a Rb-Sr isochron “age” of 1107 ± 70 Ma, but a K-Ar isochron “age” of 516 ± 30 Ma [Austin and Snelling, 1998]. Furthermore, what is also highly significant with respect to this example is that no practical explanation can be found for why the K-Ar isochron “age” is “anomalous,” and thus, if it weren’t for the assumed uniformitarian “age” of this basalt, perhaps the Rb-Sr isochron “age” would be deemed “anomalous.” Without an objective “yardstick” both isochron “ages” could even be “anomalous.” Using the same reasoning, there is therefore no guarantee that even when and where isotopic concordances do occur the resultant “dates” are somehow objectively correct.

However, if there is one conclusive observation to be made, it is that the “ages” derived from the radioisotopic systems can really only be regarded as maximum ages given the evidence of open-system behavior, mixing, inheritance, etc., and thus that the true ages of the strata may be considerably, or even drastically, younger. Of course, this puts intolerable strain on the evolutionary timescale for uniformitarians, because it not

only argues that the conventional interpretation of radioisotopic dating is not secure, but that the evidence actually points towards a much younger earth. One relevant example of radioisotopic analyses indicating a drastically reduced timescale for a significant thickness of rock strata is that provided by *Gentry et al.* [1976]. They showed that the $^{238}\text{U}/^{206}\text{Pb}$ ratios in embryonic radiohalo centers in coalified wood in Jurassic and Triassic strata of the Colorado Plateau yielded “ages” for the strata more recent by at least factors of 270 and 760, respectively, than the conventional “ages.” Furthermore, the presence of accompanying dual ^{210}Po halos signified U infiltrated these strata at the same time soon after deposition and rapid compaction, which is only possible if the Jurassic and Triassic strata were essentially contemporaneous, instead of conventionally being separated by tens of millions of years.

Nevertheless, the challenge of explaining the apparent overall “younging” trend stratigraphically upwards through the geologic record within a young-earth timeframe remains. One suggested possibility is that there was a burst of accelerated radiodecay during the Flood, and/or a burst during Creation (see Chapter 7 by Humphreys). Thus, the radioisotopic ratios produced, if interpreted in terms of today’s radiodecay rates, would suggest that the rocks are very old, when in fact most of the radiodecay occurred extremely rapidly. If this occurred during the Flood, then the deepest strata would have more accelerated decay products accumulated in them than shallower strata deposited later in the Flood, and so would yield radioisotopic “dates” that were much older. Also, the physical evidence of radioactive decay, such as fission tracks and radiohalos, would be accounted for by the large amount of radiodecay that actually occurred, albeit extremely rapidly.

However, just how much radiodecay has occurred can really only be calculated from the physical evidence. Thus, for example, as discussed in Chapters 7 and 8, the development of fully-formed ^{238}U radiohalos would seem to require only 10–150 million years of radioactive decay at constant decay rates at today’s values. This is drastically short of the claimed 4.57 billion years of radioactive decay interpreted from radioisotopic ratios. Therefore, there is ample scope for an alternative explanation for the radioisotopic ratios measured in the earth’s crustal

rocks. Furthermore, it is important to seek an alternative model that also explains the apparent overall trend in radioisotopic “dates” through the geologic record.

Damon and Kulp [1958] found excess $^{40}\text{Ar}^*$ in beryl crystals recovered from pegmatites and other magmatic rocks of various uniformitarian “ages” and geological locations. Beryl is a mineral that usually contains no ^{40}K whatsoever, so all the $^{40}\text{Ar}^*$ measured (significant quantities in fact) had to have been inherited as excess $^{40}\text{Ar}^*$ from the magmas and magmatic/hydrothermal fluids. It is therefore highly significant that *Damon and Kulp* [1958] reported a one hundred-fold difference in excess $^{40}\text{Ar}^*$ content between beryl crystals formed in the early Precambrian (with an “age” of about 3 Ga) and those from the Paleozoic (with “ages” of 280–320 Ma). They found no significant variation in the total volume of the volatile constituents in the beryl crystals and thus eliminated formation pressure as a direct cause of this “age” correlation. In fact, there is a systematic trend in the data, between the absolute amounts of excess $^{40}\text{Ar}^*$ in the beryl crystals and the uniformitarian/radioisotopic “ages” of the beryl crystals. *Damon and Kulp* [1958] interpreted this correlation as due to a more extensive mobilization of the lower crust and mantle in the past (in the earlier phases of earth history) with a consequent greater rate of degassing of inert gases than at present.

The significance of these observations within a young-earth timeframe should be readily apparent. In the Biblical framework of earth history there were two clearly-stated periods of non-uniformitarian, accelerated geological processes—Creation and the Flood (II Peter 3:3–7). It is abundantly clear from copious measurements that there have been enormous quantities of excess $^{40}\text{Ar}^*$ in the earth’s mantle which have been transferred to crustal rocks during the earth’s history. Inheritance of excess $^{40}\text{Ar}^*$ by crustal rocks has been amply demonstrated. Thus it is conceivable that the apparent overall systematic K-Ar and Ar-Ar radioisotopic “age” trend through the geologic record might be explained by systematic inheritance of excess $^{40}\text{Ar}^*$ during these periods of accelerated geological processes at Creation and the Flood when the vast majority of the geologic record was formed. A lot of outgassing would have occurred during Creation week especially with crustal

formation and tectonics on day 3 to produce the dry land, so rocks inheriting a lot of excess $^{40}\text{Ar}^*$ at that time would now appear to be vastly older than rocks formed subsequently during the Flood when less outgassing was occurring. Similarly, there would have been more outgassing and excess $^{40}\text{Ar}^*$ inheritance at the beginning of the Flood, with the breaking up of “the fountains of the great deep” (Genesis 7:11), than during later phases of the Flood, so that early Flood rocks would now appear to be much older than late Flood rocks higher up the geologic record. The excess $^{40}\text{Ar}^*$ in beryl data are consistent with this model.

Furthermore, plumbotectonics and mantle-crust geodynamics models have demonstrated that the radioisotopic ratios interpreted as “ages” could conceivably have been derived from progressively tapping into an increasingly stirred mantle with geochemical reservoirs consisting of compositional plums and melt residues, which included different U-Th-Pb, Rb-Sr, Sm-Nd isotopic signatures and excess $^{40}\text{Ar}^*$ contents. Accelerated geological processes during Creation and the Flood, including catastrophic plate tectonics at least during the latter event, would guarantee that the present condition of the mantle and the crustal geologic record, which uniformitarians claim to have developed over 4.57 Ga, would have instead developed within a young-earth timeframe of 6000–10,000 years. Obviously, the radioisotopic data are complicated by open-system behavior and have been filtered with the uniformitarian timescale assumption. Therefore, a lot of work is needed to reprocess the huge volume of data now available and to thus develop this radioisotopic mixing and inheritance model so as to explain those radioisotopic concordances which occasionally exist, and the apparent overall trend in radioisotopic “dates” through the geologic record. Another concurrent approach is to undertake exhaustive radioisotopic “dating” case studies on specific, strategic rock units whose geologic and tectonic contexts are well characterized. The data generated should then be used to compare the radioisotopic systems, isochron “ages” and model “ages” (both whole-rock and mineral where possible) to test for radioisotopic concordances, and to determine whether the overall trend in radioisotopic “dates” through the geologic record is only apparent or is real, or whether a radioisotopic mixing and inheritance, catastrophic

mantle-crust geodynamics model can better explain the radioisotopic data. Such case studies are being pursued (see Appendix) concurrently with continued literature research.

One other consideration is important, and that is the initial geochemical makeup of the earth at its creation. Uniformitarians assume the earth accreted from the solar nebula at 4.57 Ga and that the earth's initial bulk geochemical composition was that of the average chondritic meteorite, which then becomes the starting condition for isotopic evolution through subsequent earth history. As argued by Baumgardner in Chapter 3, the plethora of geochemical data now available and the robustness of geochemical and geophysical modelling strongly suggest that at its creation the earth's bulk geochemical composition was probably that of the average chondritic meteorite. Of course, any associated inference about accretion from a solar nebula is totally rejected, given the unequivocal Biblical statements that the Earth was in fact created before the Sun. Therefore, our quest to model the radioisotopic data in the framework of catastrophic mantle-crust geodynamics is potentially greatly aided by starting with the same initial bulk geochemical composition and utilizing the same plate tectonics processes for stirring the mantle and extracting the crustal geologic record, but of course in the context of catastrophic accelerated geological processes at Creation and during the Flood.

Therefore, in this catastrophic mixing and inheritance model to explain the radioisotopic data, it is envisaged that the earth started after Creation with a radioisotopic signature equivalent to an "age" of almost 4.57 Ga, with only a comparatively small amount of radioactive decay having occurred subsequently, as evidenced by mature ^{238}U radiohalos, for example. Accelerated global tectonic processes during Creation week to produce the dry land on day 3 would then have extracted from the "primitive" mantle the necessary crustal material. Because sequential extraction to build the crust was involved, and thus progressively more fractionation and mixing, the resulting radioisotopic signatures in the sequences of crustal rocks so formed could have conceivably displayed a "younging" trend. Then with catastrophic plate tectonics, and renewed mantle stirring and crustal growth, triggered by the breaking up of "the

fountains of the great deep” at the outset of the Flood, the sequence of “new” crustal rocks progressively formed could conceivably have been endowed with even younger “ages” as the Flood event continued. However, radioisotopic “age” anomalies would also have increasingly developed as oceanic crust and some ocean floor sediments were recycled back into the mantle, mixing their radioisotopic signatures with those in the mantle, especially where melting occurred to produce magmas that then added new magmatic rocks to the crust again. Quite clearly, the “picture” that emerges is one of increasing complexity as these accelerated geological and tectonic processes continued. Repeated stirring of the mantle, extraction of magmas from it, and also recycling of crustal rocks back into it, would have progressively complicated the pattern of radioisotopic signatures in an increasingly “plum-pudding” mantle mixture. Migration of radioisotopes in crustal fluids would also produce “age” anomalies. Thus the description of this mixing and inheritance model is still very rudimentary. Continued research is therefore crucial to test the viability of this model, to further identify and define the trends in the radioisotopic data, and thus to begin “fleshing out” the model with a more detailed description of the development through earth history of the radioisotopic ratios found in crustal rocks.

8. Overall Conclusions

This review of each of the major long-age radioisotopic “dating” methods has shown that two of the three basic assumptions which underpin these methods face easily demonstrated difficulties. First, open-system behavior is rife, being readily recognized in weathered and hydrothermally altered samples. It is also subtly present even in otherwise fresh rocks, often enough to suggest that all chosen samples could be affected to varying degrees. All parent-daughter pairs suffer at least some fractionation and/or disturbance as a result of the mobility of these isotopes in crustal fluids (ground and hydrothermal waters) and during metamorphism, including the Sm-Nd system which is usually claimed to be immobile even under metamorphic conditions. Furthermore, isotopic differences, migration and gains or losses are found at all

observational scales down to zones within mineral crystals and different crystal faces. Resetting is therefore common.

Second, the initial conditions can be either uncertain or variable for cogenetic suites of rock samples. In the K-Ar system, excess $^{40}\text{Ar}^*$ occurs in modern lavas which thus yield anomalously old “ages,” but this same problem now has been documented in volcanic and crustal rocks of all “ages.” Because $^{40}\text{Ar}^*$ is indistinguishable from non-radiogenic ^{40}Ar , there is no way of knowing whether the $^{40}\text{Ar}^*$ measured in all samples has been produced by *in situ* radioactive decay of ^{40}K , is primordial ^{40}Ar inherited from the mantle, or is mobile $^{40}\text{Ar}^*$ acquired from other crustal rocks via fluid transport. Whereas the isochron technique is supposed to provide by extrapolation the initial ratios (and therefore initial conditions) for the Rb-Sr and Sm-Nd systems in cogenetic rock suites, significant problems do arise. The ranges of $^{143}\text{Nd}/^{144}\text{Nd}$ ratios are usually so small that the necessary long extrapolations are within the analytical uncertainties of the samples, thus amplifying the error margins for the determined initial ratios and introducing substantial uncertainties. In any case, variations in initial $^{87}\text{Sr}/^{86}\text{Sr}$ or $^{143}\text{Nd}/^{144}\text{Nd}$ ratios for cogenetic suites of young lavas from single volcanoes have been found, meaning that the assumption of well-defined initial ratios for many suites of rocks is difficult to defend.

Third, not all linear arrays on Rb-Sr, Sm-Nd and Pb-Pb diagrams are true isochrons. Linear correlations are known to arise from mixing of the isotopic signatures of mantle and crustal sources, contamination, fractionation and/or sampling bias. Recent lavas on ocean islands plot along Rb-Sr and Pb-Pb isochrons which correspond to exceedingly old “ages,” so it is recognized that these inconsistent isotopic signatures represent characteristics of heterogeneous mantle sources rather than true “ages” of the lavas. The Pb-Pb system in these lavas is also totally at variance with all models of Pb isotopic evolution built on the assumed primordial Pb isotopic composition of a mineral in one small meteoritic fragment which yields the earth’s 4.57 Ga “age.” Similarly, Sm-Nd “model ages” are based on the assumption that Nd isotopic evolution commenced with a bulk earth composition at its 4.6 Ga origin of the average chondritic meteorite. Thus the edifice of radioisotopic “dating”

is ultimately built on the foundation of assumed earth accretion from the solar nebula at 4.57 Ga. Furthermore, what constitutes accepted “ages” within the uniformitarian time framework is determined by consistency with the stratigraphic and biostratigraphic settings and with other radioisotopic “ages.” Such concordances appear to occur systematically through the geologic record.

The common thread among all the radioisotopic systems is the role of geochemical reservoirs in the mantle as the source of isotopic inheritance and mixing to give crustal rocks their isotopic signatures. Thus a number of isotopic reservoirs have been characterized—at least five in the mantle and four in the crust—but what they actually represent is still uncertain. Nevertheless, plumbotectonics and mantle-crust geodynamics models have sought to link the reservoir compositions to the processes of plate tectonics. Thus complex mixing has occurred through time as the upper and lower mantles have been stirred by subduction of plates, convection and the ascent of plumes. Crustal growth has resulted. Burgeoning in number, these models are all generalizations of the complexities of the isotopic data and begin with earth accretion from the solar nebula at 4.57 Ga.

However, if modern lavas have radioisotopic signatures which yield old “ages” because of being sourced in heterogeneous mantle reservoirs, then “ancient” lavas may likewise appear artificially old because of being similarly sourced. Isotopic mixing from mantle and crustal reservoirs thus can explain the radioisotopic signatures in crustal rocks, so it is conceivable that the radioisotopic “ages” in most crustal rocks are an artifact of systematic mixing of mantle and crustal sources endowed with fundamental radioisotopic/geochemical signatures at the fiat creation of the earth. This possible alternative mantle-crust geodynamics model could be feasible within the framework of a young earth, a global Flood and catastrophic plate tectonics, and thus needs to be developed and tested. Rather than perturbing the radioisotopic systems, in this model complex, multi-faceted open-system behavior may be able to explain how radiogenic daughter isotopes are in association with their radioactive parent isotopes in the proportions necessary to yield a false interpretation of long ages. The physical evidence of radioactive decay, such as fission

tracks and radiohalos, may be explained by only a limited period of minor accelerated decay very early in the Creation week, rather than by long ages of radioactive decay. Subsequent geochemical mixing of the inherited primordial radioisotopic ratios may then account for the apparent radioisotopic “ages” in the earth’s crustal rocks. Much work obviously needs to be done to now specify in more detail, and then quantify, all these concepts within such a geodynamics mixing model to explain the apparent systematic radioisotopic “age” trend in the geologic record.

References

- Ahrens, L. H., Implications of the Rhodesia age pattern, *Geochimica et Cosmochimica Acta*, 8, 1–15, 1955.
- Albarède, F., Time-dependent models of U-Th-He and K-Ar evolution and the layering of mantle convection, *Chemical Geology*, 145, 413–429, 1998.
- Allègre, C. J., Isotope geodynamics, *Earth and Planetary Science Letters*, 86, 175–203, 1987.
- Allègre, C. J., and D. Rousseau, The growth of the continents through geological time studied by the Nd isotopic analysis of shales. *Earth and Planetary Science Letters*, 67, 19–34, 1984.
- Allègre, C. J., S. R. Hart, and J.-F. Minster, Chemical structure and evolution of the mantle and continents determined by inversion of Nd and Sr isotopic data, I. Theoretical models. *Earth and Planetary Science Letters*, 66, 177–190, 1983a.
- Allègre, C. J., S. R. Hart, and J.-F. Minster, Chemical structure and evolution of the mantle and continents determined by inversion of Nd and Sr isotopic data, II. Numerical experiments and discussion. *Earth and Planetary Science Letters*, 66, 191–213, 1983b.
- Allègre, C. J., E. Lewin, and B. Dupre, A coherent crust-mantle model for the uranium-thorium-lead isotope system, *Chemical Geology*, 70, 211–234, 1988.
- Allègre, C. J., A. Hofmann, and R. K. O’Nions, The argon constraints on mantle structure, *Geophysical Research Letters*, 23, 3555–3557, 1996.
- Armstrong, R. L., K-Ar dating: Late Cenozoic McMurdo volcanic group and dry valley glacial history, Victoria Land, Antarctica, *New Zealand Journal of Geology and Geophysics*, 21(6), 685–698, 1978.
- Arnaud, A. O., and S. P. Kelley, Evidence for excess argon during high pressure

- metamorphism in the Dora Maira Massif (Western Alps, Italy) using an ultraviolet laser ablation microprobe ^{40}Ar - ^{39}Ar technique, *Contributions to Mineralogy and Petrology*, 121, 1–11, 1995.
- Arndt, N. T., and S. L. Goldstein, Use and abuse of crust-formation ages, *Geology*, 15, 893–895, 1987.
- Ashwal, L. D., R. D. Tucker, and E. K. Zinner, Slow cooling of deep crustal granulites and Pb-loss in zircon, *Geochimica et Cosmochimica Acta*, 63, 2839–2851, 1999.
- Austin, S. A., Excess argon within mineral concentrates from the new dacite lava dome at Mount St. Helens volcano, *Creation Ex Nihilo Technical Journal*, 10(3), 335–343, 1996.
- Austin, S. A., J. B. Baumgardner, D. R. Humphreys, A. A. Snelling, L. Vardiman, and K. P. Wise. Catastrophic plate tectonics: a global Flood model of earth history, in *Proceedings of the Third International Conference on Creationism*, edited by R. E. Walsh, pp. 609–621, Creation Science Fellowship, Pittsburgh, Pennsylvania, 1994.
- Austin, S. A., and A. A. Snelling, Discordant potassium-argon model and isochron “ages” for Cardenas Basalt (Middle Proterozoic) and associated diabase of eastern Grand Canyon, Arizona, in *Proceedings of the Fourth International Conference on Creationism*, edited by R.E. Walsh, pp. 35–51, Creation Science Fellowship, Pittsburgh, Pennsylvania, 1998.
- Ballentine, C. J., Resolving the mantle He/Ne and crustal $^{21}\text{Ne}/^{22}\text{Ne}$ in well gases, *Earth and Planetary Science Letters*, 152, 233–249, 1997.
- Baksi, A. K., and A. F. Wilson, An attempt at argon dating of two granulite-facies terranes, *Chemical Geology*, 30, 109–120, 1980.
- Baumgardner, J. R., Computer modeling of the large-scale tectonics associated with the Genesis Flood, in *Proceedings of the Third International Conference on Creationism*, edited by R. E. Walsh, pp. 49–62, Creation Science Fellowship, Pittsburgh, Pennsylvania, 1994a.
- Baumgardner, J. R., Runaway subduction as the driving mechanism for the Genesis Flood, in *Proceedings of the Third International Conference on Creationism*, edited by R. E. Walsh, pp. 63–75, Creation Science Fellowship, Pittsburgh, Pennsylvania, 1994b.
- Bell, K., and J. L. Powell, Strontium isotopic studies of alkalic rocks: the potassium-rich lavas of the Birunga and Toro-Ankole regions, east and central equatorial Africa, *Journal of Petrology*, 10, 536–572, 1969.
- Bell, K., J. Blenkinsop, T. J. S. Cole, and D. P. Menagh, Evidence from Sr isotopes for long lived heterogeneities in the upper mantle. *Nature*, 298,

- 251–253, 1982.
- Ben Othman, D., M. Polve, and C. J. Allègre, Nd-Sr isotopic composition of granulites and constraints on the evolution of the lower continental crust, *Nature*, 307, 510–515, 1984.
- Bennett, V. C., and D. J. DePaolo, Proterozoic crustal history of the western United States as determined by neodymium isotopic mapping, *Geological Society of America Bulletin*, 99, 674–685, 1987.
- Bonhomme, M G., The use of Rb-Sr and K-Ar dating methods as a stratigraphic tool applied to sedimentary rocks and minerals, *Precambrian Research*, 18, 5–25, 1982.
- Bottino, M. L., and P. D. Fullagar, The effects of weathering on whole-rock Rb/Sr ages of granitic rocks, *American Journal of Science*, 266, 661–670, 1968.
- Brevart, O., B. Dupre, and C. J. Allègre, Lead-lead age of komatiite lavas and limitations on the structure and evolution of the Precambrian mantle, *Earth and Planetary Science Letters*, 77, 293–302, 1986.
- Broadhurst, C. L., M. J. Drake, B. E. Hagee, and T. J. Benatowicz, Solubility and partitioning of Ar in anorthite, diopside, fosterite, spinel, and synthetic basaltic liquids, *Geochimica et Cosmochimica Acta*, 54, 299–309, 1990.
- Broadhurst, C. L., M. J. Drake, B. E. Hagee, and T. J. Benatowicz, Solubility and partitioning of Ne, Ar, Kr and Xe in minerals and synthetic basaltic melts, *Geochimica et Cosmochimica Acta*, 56, 709–723, 1992.
- Brooks, C., Relationship between feldspar alteration and the precise post-crystallization movement of rubidium and strontium isotopes in a granite, *Journal of Geophysical Research*, 73, 4751–4757, 1968.
- Brooks, C., S. R. Hart, A. Hofmann, and D. E. James, Rb-Sr mantle isochrons from oceanic regions, *Earth and Planetary Science Letters*, 32, 51–61, 1976a.
- Brooks, C., D. E. James, and S. R. Hart, Ancient lithosphere: its role in young continental volcanism, *Science*, 193, 1086–1094, 1976b.
- Bros, R., P. Stille, F. Gauthier-Lafaye, F. Weber, and N. Clauer, Sm-Nd isotopic dating of Proterozoic clay material: an example from the Francevillian sedimentary series, Gabon, *Earth and Planetary Science Letters*, 113, 207–218, 1992.
- Burnard, P., The bubble-by-bubble volatile evolution of two mid-ocean ridge basalts, *Earth and Planetary Science Letters*, 174, 199–211, 1999.
- Burnard, P., D. Graham, and G. Turner, Vesicle-specific noble gas analyses of “popping rock”: implications for primordial noble gases in earth, *Science*, 276, 568–571, 1997.

- Cameron, M., K. D. Collerson, W. Compston, and R. Morton, The statistical analysis and interpretation of imperfectly-fitted Rb-Sr isochrons from polymetamorphic terrains, *Geochimica et Cosmochimica Acta*, 45, 1087–1097, 1981.
- Cattell, A., P. E. Krogh, and N. T. Arndt, Conflicting Sm-Nd whole rock and U-Pb zircon ages for Archean lavas from Newton Township, Abitibi Belt, Ontario, *Earth and Planetary Science Letters*, 70, 280–290, 1984.
- Chappell, B. W., and A. J. R. White, Two contrasting granite types, *Pacific Geology*, 8, 173–174, 1974.
- Chauvel, C., B. Dupre, and G. A. Jenner, The Sm-Nd age of Kambalda volcanics is 500 Ma too old!, *Earth and Planetary Science Letters*, 74, 315–324, 1985.
- Chen, C.-Y., and F. A. Frey, Origin of Hawaiian tholeiite and alkalic basalt, *Nature*, 302, 785–789, 1983.
- Chen, Y. D., and I. S. Williams, Zircon inheritance in mafic inclusions from Bega Batholith granites, south-eastern Australia: an ion microprobe study, *Journal of Geophysical Research*, 95, 17,787–17,796, 1990.
- Chivas, A.R., A.S. Andrew, A.K. Sinha, and J.R. O’Neil, Geochemistry of a Pliocene-Pleistocene oceanic-arc plutonic complex, Guadalcanal, *Nature*, 300, 139–143, 1982.
- Church, F.E., and M. Tatsumoto, Lead isotope relations in oceanic ridge basalts from the Juan de Fuca-Gorda Ridge area, NE Pacific Ocean, *Contributions to Mineralogy and Petrology*, 53, 253–279, 1975.
- Claoue-Long, J.C., M.F. Thirlwall, and R.W. Nesbitt, Revised Sm-Nd systematics of Kambalda greenstones, Western Australia, *Nature*, 307, 697–701, 1984.
- Clauer, N., A new approach to Rb-Sr dating of sedimentary rocks, in *Lectures in Isotope Geology*, edited by E. Jäger and J.C. Hunziker, pp. 30–51, Springer-Verlag, Berlin, 1979.
- Clauer, N., Rb-Sr and K-Ar dating of Precambrian clays and glauconies, *Precambrian Research*, 15, 331–352, 1981.
- Clauer, N., E. Keppens, and P. Stille, Sr isotopic constraints on the process of glauconitization, *Geology*, 20, 133–136, 1992.
- Cocherie, A., O. Legendre, J. J. Peucat, and A. N. Kouamelan, Geochronology of polygenetic monazites constrained by *in situ* electron microprobe Th-U-total lead determination: implications for lead behaviour in monazite, *Geochimica et Cosmochimica Acta*, 62, 2475–2497, 1998.
- Collerson, K. D., L. M. Campbell, B. L. Weaver, and Z. A. Palacz, Evidence

- for extreme mantle fractionation in early Archaean ultramafic rocks from northern Labrador, *Nature*, 349, 209–214, 1991.
- Compston, W., Variation in radiogenic Pb/U within the SL13 standard, *Research School of Earth Sciences Annual Report 1996*, pp. 118–121, Australian National University, Canberra, Australia, 1997.
- Compston, W., and B. W. Chappell, Estimation of source Rb/Sr for individual igneous-derived granitoids and the inferred age of the lower crust in southeast Australia, *US Geological Survey, Open-File Report 78-701*, 79–81, 1978.
- Compston, W., and R. T. Pidgeon, Rubidium-strontium dating of shales by the total-rock method, *Journal of Geophysical Research*, 67, 3493–3502, 1962.
- Compston, W., I. McDougall, and D. Wyborn, Possible two-stage ^{87}Sr evolution in the Stockdale rhyolite, *Earth and Planetary Science Letters*, 61, 297–302, 1982.
- Compston, W., I. S. Williams, I. H. Campbell, and J. J. Gresham, Zircon xenocrysts from the Kambalda volcanics: age constraints and direct evidence for older continental crust below the Kambalda-Norseman greenstones, *Earth and Planetary Science Letters*, 76, 299–311, 1985.
- Copeland, P., R. R. Parrish, and T. M. Harrison, Identification of inherited radiogenic Pb in monazite and its implications for U-Pb systematics, *Nature*, 333, 760–763, 1988.
- Cortini, M., and O. D. Hermes, Sr isotopic evidence for a multi-source origin of the potassic magmas in the Neapolitan area (S. Italy), *Contributions to Mineralogy and Petrology*, 77, 47–55, 1981.
- Crowley, J. L., and E. D. Ghent, An electron microprobe study of the U-Th-Pb systematics of metamorphosed monazite: the role of Pb diffusion versus overgrowth and recrystallization, *Chemical Geology*, 157, 285–302, 1999.
- Cumming, G. L., and J. R. Richards, Ore lead isotope ratios in a continuously changing earth, *Earth and Planetary Science Letters*, 28, 155–171, 1975.
- Dalrymple, G. B., $^{40}\text{Ar}/^{36}\text{Ar}$ analyses of historic lava flows, *Earth and Planetary Science Letters*, 6, 47–55, 1969.
- Dalrymple, G. B., *The Age of the Earth*, 474 pp., Stanford University Press, Stanford, 1991.
- Dalrymple, G. B., and M. A. Lanphere, *Potassium-Argon Dating: Principles, Techniques and Applications to Geochronology*, 258 pp., W. H. Freeman, San Francisco, 1969.
- Dalrymple, G. B., and J. G. Moore, Argon 40: excess in submarine pillow basalts from Kilauea Volcano, Hawaii, *Science*, 161, 1132–1135, 1968.

- Damon, P. E., A. W. Laughlin, and J. K. Precious, Problem of excess argon-40 in volcanic rocks, *Radioactive Dating Methods and Low-Level Counting*, International Atomic Energy Agency, Vienna, pp. 463–481, 1967.
- Damon, P. E., and J. L. Kulp, Excess helium and argon in beryl and other minerals, *American Mineralogist*, 43, 433–459, 1958.
- Dasch, E. J., Strontium isotopes in weathering profiles, deep-sea sediments, and sedimentary rocks, *Geochimica et Cosmochimica Acta*, 33, 1521–1552, 1969.
- Davies, G.F., Geophysically constrained mantle mass flows and the ^{40}Ar budget: a degassed lower mantle?, *Earth and Planetary Science Letters*, 166, 149–162, 1999.
- Davis, G. L., S. R. Hart, and G. R. Tilton, Some effects of contact metamorphism on zircon ages, *Earth and Planetary Science Letters*, 5, 27–34, 1968.
- DePaolo, D. J., Neodymium isotopes in the Colorado Front Range and crust-mantle evolution in the Proterozoic, *Nature*, 291, 193–196, 1981a.
- DePaolo, D. J., Trace element and isotopic effects of combined wallrock assimilation and fractional crystallisation, *Earth and Planetary Science Letters*, 53, 189–202, 1981b.
- DePaolo, D. J., A neodymium and strontium isotopic study of the Mesozoic calc-alkaline granitic batholiths of the Sierra Nevada and Peninsular Ranges, California, *Journal of Geophysical Research*, 86, 10,470–10,488, 1981c.
- DePaolo, D. J., The mean life of continents: estimates of continental recycling rates from Nd and Hf isotopic data and implications for mantle structure, *Geophysical Research Letters*, 10, 705–708, 1983.
- DePaolo, D. J., *Neodymium Isotope Geochemistry: An Introduction*, 187 pp., Springer-Verlag, Berlin, 1988.
- DePaolo, D. J., and G. J. Wasserburg, Nd isotopic variations and petrogenetic models, *Geophysical Research Letters*, 3, 249–252, 1976a.
- DePaolo, D. J., and G. J. Wasserburg, Inferences about magma sources and mantle structure from variations of $^{143}\text{Nd}/^{144}\text{Nd}$, *Geophysical Research Letters*, 3, 743–746, 1976b.
- DePaolo, D. J., and G. J. Wasserburg, Petrogenetic mixing models and Nd-Sr isotopic patterns, *Geochimica et Cosmochimica Acta*, 43, 615–627, 1979a.
- DePaolo, D. J., and G. J. Wasserburg, Sm-Nd age of the Stillwater Complex and the mantle evolution curve for neodymium, *Geochimica et Cosmochimica Acta*, 43, 999–1008, 1979b.
- DePaolo, D. J., A. M. Linn, and G. Schubert, The continental crustal age

- distribution: method of determining mantle separation ages from Sm-Nd isotopic data and application to the south-western United States, *Journal of Geophysical Research*, 96, 2071–2088, 1991.
- DeWolf, C. P., C. J. Zeissler, A. N. Halliday, K. Mezger, and E. J. Essene, The role of inclusions in U-Pb and Sm-Nd garnet geochronology: stepwise dissolution experiments and trace uranium mapping by fission track analysis, *Geochimica et Cosmochimica Acta*, 60, 121–134, 1996.
- Dickin, A. P., *Radiogenic Isotope Geology*, 452 pp., Cambridge University Press, Cambridge, England, 1995.
- Dickson, B. L., B. L. Gulson, and A. A. Snelling, Evaluation of lead isotopic methods for uranium exploration, Koongarra area, Northern Territory, Australia, *Journal of Geochemical Exploration*, 24, 81–102, 1985.
- Dickson, B. L., B. L. Gulson, and A. A. Snelling, Further assessment of stable lead isotope measurements for uranium exploration, Pine Creek Geosyncline, Northern Territory, Australia, *Journal of Geochemical Exploration*, 27, 63–75, 1987.
- Dobrzhinetskaya, L. F., E. A. Eide, R. B. Larsen, B. A. Sturt, R. G. Trønnes, D. C. Smith, W. R. Taylor, and T. V. Posukhova, Microdiamond in high-grade metamorphic rocks in the western gneiss region, Norway, *Geology*, 23, 597–600, 1995.
- Dodson, M. H., Theory of cooling ages, in *Lectures in Isotope Geology*, edited by E. Jäger and J. C. Hunziker, pp. 194–202, Springer-Verlag, Berlin, 1979.
- Dodson, M. H., On “spurious” correlations in Rb-Sr isochron diagrams, *Lithos*, 15, 215–219, 1982.
- Doe, B. R., and R. E. Zartman, Plumbotectonics, in *Geochemistry of Hydrothermal Ore Deposits*, 2nd edition, edited by H. L. Barnes, chapter 2, pp. 22–70, Wiley, New York, 1979.
- Drescher, J., T. Kirsten, and K. Schäfer, The rare gas inventory of the continental crust, recovered by the KTB Continental Deep Drilling Project, *Earth and Planetary Science Letters*, 154, 247–263, 1998.
- Dupre, B., and C. J. Allègre, Pb-Sr isotope variation of Indian Ocean basalts and mixing phenomena, *Nature*, 303, 142–146, 1983.
- Dymond, J., Excess argon in submarine basalt pillows, *Geological Society of America Bulletin*, 81, 1229–1232, 1970.
- Eldridge, C. S., W. Compston, I. S. Williams, J. W. Harris, and J. W. Bristow, Isotope evidence for the involvement of recycled sediments in diamond formation, *Nature*, 353, 649–653, 1991.
- Ellam, R. M., and C. J. Hawkesworth, Elemental and isotopic variations in

- subduction related basalts: evidence for a three component model, *Contributions to Mineralogy and Petrology*, 98, 72–80, 1988.
- Elliott, T., A. Zindler, and B. Bourdon, Exploring the kappa conundrum: the role of recycling in the lead isotopic evolution of the mantle, *Earth and Planetary Science Letters*, 169, 285–302, 1999.
- Esser, R. P., W. C. McIntosh, M. T. Heizler, and P. R. Kyle, Excess argon in melt inclusions in zero-age anorthoclase feldspar from Mt Erebus, Antarctica, as revealed by the $^{40}\text{Ar}/^{39}\text{Ar}$ method, *Geochimica et Cosmochimica Acta*, 61, 3789–3801, 1997.
- Evernden, J. F., D. E. Savage, G. H. Curtis, and G. T. James, Potassium-argon dates and the Cenozoic mammalian chronology of North America, *American Journal of Science*, 262, 145–198, 1964.
- Faure, G., *Principles of Isotope Geology*, 2nd edition, 589 pp., Wiley, New York, 1986.
- Faure, G., and J. L. Powell, *Strontium Isotope Geology*, 188 pp., Springer-Verlag, Berlin, Germany, 1972.
- Faure, G., R. L. Hill, L. M. Jones, and D. H. Elliot, Isotope composition of strontium and silica content of Mesozoic basalt and dolerite from Antarctica, *SCAR Symposium*, University Press, Oslo, Norway, 1971.
- Fechtig, H., and S. Kalbitzer, The diffusion of argon in potassium-bearing solids, in *Potassium-Argon Dating*, edited by D. A. Schaeffer and J. Zähringer, pp. 68–106, Springer-Verlag, Berlin, 1966.
- Field, D., and A. Raheim, Rb-Sr total rock isotope studies on Precambrian charnockitic gneisses from south Norway: evidence for isochron resetting during a low-grade metamorphic-deformational event, *Earth and Planetary Science Letters*, 45, 32–44, 1979a.
- Field, D., and A. Raheim, A geological meaningless Rb-Sr total rock isochron, *Nature*, 282, 497–499, 1979b.
- Field, D., and A. Raheim, Secondary geological meaningless Rb-Sr isochrons, low $^{87}\text{Sr}/^{86}\text{Sr}$ initial ratios and crustal residence times of high-grade gneisses, *Lithos*, 13, 295–304, 1980.
- Fisher, D. E., Heavy rare gases in a Pacific seamount, *Earth and Planetary Science Letters*, 9, 331–335, 1970.
- Fisher, D. E., Excess rare gases in subaerial basalt from Nigeria, *Nature*, 232, 60–61, 1971.
- Fisher, D. E., U/He ages as indicators of excess argon in deep sea basalts, *Earth and Planetary Science Letters*, 14, 255–258, 1972.
- Froude, D. O., T. R. Ireland, P. O. Kinny, I. S. Williams, and W. Compston,

- Ion microprobe identification of 4100–4200 Ma-old terrestrial zircons, *Nature*, 304, 616–618, 1983.
- Funkhouser, J. G., and J. J. Naughton, Radiogenic helium and argon in ultramafic inclusions from Hawaii, *Journal of Geophysical Research*, 73, 4601–4607, 1968.
- Funkhouser, J. G., I. L. Barnes, and J. J. Naughton, Problems in the dating of volcanic rocks by the potassium-argon method, *Bulletin of Volcanology*, 29, 709–717, 1966.
- Galer, S. J. G., and R. K. O’Nions, Residence time of thorium, uranium and lead in the mantle with implications for mantle convection, *Nature*, 316, 778–782, 1985.
- Ganguly, J., M. Tirone, and R. L. Hervig, Diffusion kinetics of samarium and neodymium in garnet, and a method for determining cooling rates of rocks, *Science*, 281, 805–807, 1998.
- Gast, P. W., G. R. Tilton, and C. Hedge, Isotopic composition of lead and strontium from Ascension and Gough Islands, *Science*, 145, 1181–1185, 1964.
- Gentry, R. V., W.H. Christie, D. H. Smith, J. F. Emery, S. A. Reynolds, R. Walker, S. S. Cristy, and P. A. Gentry, Radiohalos in coalified wood: new evidence relating to the time of uranium introduction and coalification, *Science*, 194, 315–318, 1976.
- Geyh, M. A., and H. Schleicher, *Absolute Dating Methods*, Springer-Verlag, Berlin, 1990.
- Giblin, A. M., and A. A. Snelling, Application of hydrogeochemistry to uranium exploration in the Pine Creek Geosyncline, Northern Territory, Australia, *Journal of Geochemical Exploration*, 19, 33–55, 1983.
- Giem, P. A. L., *Scientific Theology*, 291 pp., La Sierra University Press, Riverside, California, 1997.
- Giletti, B. J., and J. L. Kulp, Radon leakage from radioactive minerals, *American Mineralogist*, 40, 481–496, 1955.
- Goldich, S. S., and P. W. Gast, Effects of weathering on the Rb-Sr and K-Ar ages of biotite from the Morton Gneiss, Minnesota, *Earth and Planetary Science Letters*, 1, 372–375, 1966.
- Goldich, S. S., and M. J. Mudrey, Jr, Dilatancy model for discordant U-Pb zircon ages, in *Contributions to Recent Geochemistry and Analytical Chemistry*, edited by A. I. Tugrainov, pp. 415–418, Nauka Publishing Office, Moscow, 1972.
- Goldstein, S. L., Decoupled evolution of Nd and Sr isotopes in the continental

- crust, *Nature*, 336, 733–738, 1988.
- Goldstein, S. L., R. K. O’Nions, and P. J. Hamilton, A Sm-Nd isotopic study of atmospheric dusts and particulates from major river systems, *Earth and Planetary Science Letters*, 70, 221–236, 1984.
- Grove, M., and T. M. Harrison, $^{40}\text{Ar}^*$ diffusion in Fe-rich biotite, *American Mineralogist*, 81, 940–951, 1996.
- Gurney, J. J., Diamonds, in *Kimberlites and Related Rocks, Vol. 2: Their Mantle/Crust Setting, Diamonds and Diamond Exploration*, pp. 935–965, Proceedings of the Fourth International Kimberlite Conference, Geological Society of Australia Special Publication No. 14, 1986.
- Gurney, J. J., The diamondiferous roots of our wandering continent, *South African Journal of Geology*, 93, 423–437, 1990.
- Haack, U., J. Hoefs, and E. Gohn, Constraints on the origin of Damaran granites by Rb/Sr and $\delta^{18}\text{O}$ data, *Contributions to Mineralogy and Petrology*, 79, 279–289, 1982.
- Hall, A., *Igneous Petrology*, 573 pp., Longman, Essex, England, 1987.
- Hamilton, P. J., R. K. O’Nions, N. M. Evensen, and J. Tarney, Sm-Nd systematics of Lewisian gneisses: implications for the origin of granulites, *Nature*, 277, 25–28, 1979.
- Hanson, G. N., and P. W. Gast, Kinetic studies in contact metamorphic zones, *Geochimica et Cosmochimica Acta*, 31, 1119–1153, 1967.
- Hanyu, T., I. Kaneoka, and K. Nagao, Noble gas study of HIMU and EM ocean island basalts in the Polynesian region, *Geochimica et Cosmochimica Acta*, 63, 118–1201, 1999.
- Harrison, D., P. Burnard, and G. Turner, Noble gas behaviour and composition in the mantle: constraints from the Iceland Plume, *Earth and Planetary Science Letters*, 171, 199–207, 1999.
- Harrison, T. M., Diffusion of ^{40}Ar in hornblende, *Contributions to Mineralogy and Petrology*, 78, 324–331, 1981.
- Harrison, T. M., and I. McDougall, Investigations of an intrusive contact, northwest Nelson, New Zealand—II. Diffusion of radiogenic and excess ^{40}Ar in hornblende revealed by $^{40}\text{Ar}/^{39}\text{Ar}$ age spectrum analysis, *Geochimica et Cosmochimica Acta*, 44, 2005–2020, 1980.
- Harrison, T. M., and I. McDougall, Excess ^{40}Ar in metamorphic rocks from Broken Hill, New South Wales: implications for $^{40}\text{Ar}/^{39}\text{Ar}$ age spectra and the thermal history of the region, *Earth and Planetary Science Letters*, 55, 123–149, 1981.
- Harrison, T. M., I. Duncan, and I. McDougall, Diffusion of ^{40}Ar in biotite:

- temperature, pressure and compositional effects, *Geochimica et Cosmochimica Acta*, 49, 2461–2468, 1985.
- Hart, S. R., The petrology and isotopic-mineral age relations of a contact zone in the Front Range, Colorado, *Journal of Geology*, 72, 493–525, 1964.
- Hart, S. R., K, Rb, Cs contents and K/Rb, K/Cs ratios of fresh and altered submarine basalts, *Earth and Planetary Science Letters*, 6, 295–303, 1969.
- Hart, S. R., A large-scale isotope anomaly in the southern hemisphere mantle, *Nature*, 309, 753–757, 1984.
- Harte, B., and C. J. Hawkesworth, Mantle domains and mantle xenoliths, in *Kimberlites and Related Rocks, Vol. 2: Their Mantle/Crust Setting, Diamonds and Diamond Exploration*, pp. 649–686, Proceedings of the Fourth International Kimberlite Conference, Geological Society of Australia Special Publication No. 14, 1986.
- Hawkesworth, C. J., and P. W. C. van Calsteren, Radiogenic isotopes—some geological applications, in *Rare Earth Element Geochemistry*, edited by P. Henderson, pp. 375–431, Elsevier, Amsterdam, 1984.
- Hedge, C. E., and F. G. Walthall, Radiogenic strontium-87 as an index of geological processes, *Science*, 140, 1214–1217, 1963.
- Hensen, B. J., and B. Zhou, Retention of isotopic memory in garnets partially broken down during an overprinting granulite-facies metamorphism: implications for the Sm-Nd closure temperature, *Geology*, 23, 225–228, 1995.
- Hills, J. H., and J. R. Richards, Pitchblende and galena ages in the Alligator Rivers Region, Northern Territory, Australia, *Mineralium Deposita*, 11, 133–154, 1976.
- Hoernle, K., G. Tilton, and H.-U. Schmincke, Sr-Nd-Pb isotopic evolution of Gran Canaria: evidence for shallow enriched mantle beneath the Canary Islands, *Earth and Planetary Science Letters*, 106, 44–63, 1991.
- Holmes, A., An estimate of the age of the Earth, *Nature*, 157, 680–684, 1946.
- Holmes, A., The oldest dated minerals of the Rhodesian Shield, *Nature*, 173, 612–617, 1954.
- Honda, M., I. McDougall, D. B. Patterson, A. Doulgeris, and D. A. Clague, Noble gases in submarine pillow basalt glasses from Loihi and Kilauea, Hawaii: a solar component in the earth, *Geochimica et Cosmochimica Acta*, 57, 859–874, 1993.
- Hough, R. M., I. Gilmour, C. T. Pillinger, F. Langenhorst, and A. Montanari, Diamonds from the iridium-rich K-T boundary layer at Arroyo El Mimbral, Tamaulipas, Mexico, *Geology*, 25, 1019–1022, 1997.

- Houtermans, F. G., Die isotoopen-haufigkeiten im natürlischen blei und das Alter des urans, *Naturwissenschaften*, 33, 185–187, 1946.
- Hurley, T. M., H. Hughes, G. Faure, H. W. Fairbairn, and W. H. Pinson, Radiogenic strontium-87 model of continent formation, *Journal of Geophysical Research*, 67, 5315–5334, 1962.
- Irber, W., W. Siebel, P. Möller, and S. Teufel, Leaching of Rb and Sr ($^{87}\text{Sr}/^{86}\text{Sr}$) of Hercynian peraluminous granites with application to age determination, in *V.M. Goldschmidt Conference, Journal of Conference Abstracts, Vol. 1* (1), 281, 1996.
- Jahn, B.-M., P. Vidal, and G. R. Tilton, Archaean mantle heterogeneity: evidence from chemical isotopic abundances in Archaean igneous rocks, *Philosophical Transactions of the Royal Society of London*, A297, 353–364, 1980.
- Johnson, L. H., R. Burgess, G. Turner, H. J. Milledge, and J. W. Harris, Noble gas and halogen geochemistry of mantle fluids: comparison of African and Canadian diamonds, *Geochimica et Cosmochimica Acta*, 64, 717–732, 2000.
- Karpinskaya, T. B., Synthesis of argon muscovite, *International Geology Review*, 9, 1493–1495, 1967.
- Karpinskaya, T. B., I. A. Ostrovskiy, and L. L. Shanin, Synthetic introduction of argon into mica at high pressures and temperatures, *Isv Akad Nauk S.S.S.R. Geology Series*, 8, 87–89, 1961.
- Keay, S., W. J. Collins, and M. T. McCulloch, A three-component Sr-Nd isotopic mixing model for granitoid genesis, Lachlan Fold Belt, eastern Australia, *Geology*, 25, 307–310, 1997.
- Kesson, S. E., and A. E. Ringwood, Slab-mantle interactions 2. The formation of diamonds, *Chemical Geology*, 78, 97–118, 1989.
- Kirkley, M. B., J. J. Gurney, and A. A. Levinson, Age, origin and emplacement of diamonds: a review of scientific advances in the last decade, *Canadian Institute of Mining Bulletin*, 84, 48–57, 1992.
- Kirkley, M. B., J. J. Gurney, M. L. Otter, S. J. Hill, and L. R. Daniels, The application of C isotope measurements to the identification of the sources of C in diamonds: a review, *Applied Geochemistry*, 6, 477–494, 1991.
- Köhler, H., and D. Müller-Sohnius, Rb-Sr systematics on paragneiss series from the Bavarian Moldanubium, Germany, *Contributions to Mineralogy and Petrology*, 71, 387–392, 1980.
- Kramers, J. D., and I. N. Tolstikhin, Two terrestrial lead isotope paradoxes, forward transport modelling, core formation and the history of the continental crust, *Chemical Geology*, 139, 75–110, 1997.

- Krogh, T. E., Improved accuracy of U-Pb zircon ages by the creation of more concordant systems using the air abrasion technique, *Geochimica et Cosmochimica Acta*, 46, 637–649, 1982.
- Kröner, A., P. J. Jaekel, and I. S. Williams, Pb-loss patterns in zircons from a high-grade metamorphic terrain as revealed by different dating methods, U-Pb and Pb-Pb ages for igneous and metamorphic zircons from northern Sri Lanka, *Precambrian Research*, 66, 151–181, 1994.
- Kruger, F. J., B. S. Camber, and P. D. Harris, Isotopic peculiarities of an Archaean pegmatite (Union Mine, Mica, South Africa): geochemical and geochronological implications, *Precambrian Research*, 91, 253–267, 1998.
- Krummenacher, D., Isotopic composition of argon in modern surface volcanic rocks, *Earth and Planetary Science Letters*, 8, 109–117, 1970.
- Kulp, J. L., Concordance and discordance between K-Ar and Rb-Sr isotopic ages from micas, in *Chemistry of the Earth's Crust*, edited by A. P. Vinogradov, Vol. II, pp. 592–606, Israel Program for Scientific Translations, Jerusalem, 1967.
- Kulp, J. L., and W. R. Eckelmann, Discordant U-Pb ages and mineral type, *American Mineralogist*, 42, 154–164, 1957.
- Kulp, J. L., and J. Engels, Discordances in K-Ar and Rb-Sr isotopic ages, in *Radioactive Dating*, pp. 219–238, International Atomic Energy Agency, Vienna, 1963.
- Lambert, D. D., J. W. Morgan, R. J. Walker, S. B. Shirey, R. W. Carlson, M. L. Xientek, and M. S. Koski, Rhenium-osmium and samarium-neodymium isotopic systematics of the Stillwater Complex, *Science*, 244, 1169–1174, 1989.
- Langmuir, C. H., Geochemical consequences of *in situ* crystallisation, *Nature*, 340, 199–205, 1989.
- Langmuir, C. H., R. D. Vocke, G. N. Hanson, and S. R. Hart, A general mixing equation with applications to Icelandic basalts, *Earth and Planetary Science Letters*, 37, 380–392, 1978.
- Lanphere, M. A., and G. B. Dalrymple, Identification of excess ^{40}Ar by the $^{40}\text{Ar}/^{39}\text{Ar}$ age spectrum technique, *Earth and Planetary Science Letters*, 12, 359–372, 1976.
- Larson, E. E., P. E. Patterson, and F. E. Mutschler, Lithology, chemistry, age, and origin of the Proterozoic Cardenas Basalt, Grand Canyon, Arizona, *Precambrian Research*, 65, 255–276, 1994.
- Laughlin, A. E., J. Poths, H. A. Healey, S. Reneau, and G. WoldeGabriel, Dating of Quaternary basalts using the cosmogenic ^3He and ^{14}C methods with

- implications for excess ^{40}Ar , *Geology*, 22, 135–138, 1994.
- Laughlin, A. W., Excess radiogenic argon in pegmatite minerals, *Journal of Geophysical Research*, 74, 6684–6690, 1969.
- Lee, J. K. W., I. S. Williams, and D. J. Ellis, Determination of Pb, U and Th diffusion rates in zircon, *Research School of Earth Sciences Annual Report 1996*, pp. 121–122, Australian National University, Canberra, Australia, 1997.
- Liew, T. C., and M. T. McCulloch, Genesis of granitoid batholiths of Peninsular Malaysia and implications for models of crustal evolution: evidence from a Nd-Sr isotopic and U-Pb study, *Geochimica et Cosmochimica Acta*, 49, 587–600, 1985.
- Ludwig, K. R., and L. T. Silver, Lead isotope inhomogeneties in Precambrian igneous K-feldspars, *Geochimica et Cosmochimica Acta*, 41, 1457–1471, 1977.
- Mankinen, E. A., and G. B. Dalrymple, Electron microprobe evaluation of terrestrial basalts for whole-rock K-Ar dating, *Earth and Planetary Science Letters*, 17, 89–94, 1972.
- Marty, B., and F. Humbert, Nitrogen and argon isotopes in oceanic basalts, *Earth and Planetary Science Letters*, 152, 101–112, 1997.
- Marty, B., I. Tolstikhin, I. L. Kamensky, V. Nivin, E. Balaganskaya, and J.-L. Zimmermann, Plume-derived rare gases in 380 Ma carbonatites from the Kola region (Russia) and the argon isotopic composition in the deep mantle, *Earth and Planetary Science Letters*, 164, 179–192, 1998.
- Marty, B., and J.-L. Zimmermann, Volatiles (He, C, N, Ar) in mid-ocean ridge basalts: assessment of shallow-level fractionation and characterization of source composition, *Geochimica et Cosmochimica Acta*, 63, 3619–3633, 1999.
- Matsumoto, T., M. Honda, I. McDougall, and S. Y. O'Reilly, Noble gases in anhydrous lherzolites from the Newer Volcanics, southeastern Australia: a MORB-like reservoir in the subcontinental mantle, *Geochimica et Cosmochimica Acta*, 62, 2521–2533, 1998.
- Mauger, R. L., K-Ar ages of biotites from tuffs in Eocene rocks of the Green River, Washakie and Uinta Basins, Utah, Wyoming, and Colorado, *Contributions to Geology, University of Wyoming*, 15, 17–41, 1977.
- Mazor, E., and R. O. Fournier, More on noble gases in Yellowstone National Park hot waters, *Geochimica et Cosmochimica Acta*, 37, 515–525, 1973.
- McCarthy, T. S., and R. G. Cawthorn, Changes in initial $^{87}\text{Sr}/^{86}\text{Sr}$ ratio during protracted fractionation in igneous complexes, *Journal of Petrology*, 21, 245–264, 1980.

- McCulloch, M. T., Sm-Nd isotopic constraints on the evolution of Precambrian crust in the Australian continent, in *Proterozoic Lithospheric Evolution*, edited by A. Kröner, pp. 115–130, *American Geophysical Union, Geodynamics Series 17*, 1987.
- McCulloch, M. T., and W. Compston, Sm-Nd age of Kambalda and Kanowna greenstones and heterogeneity in the Archean mantle, *Nature*, *294*, 322–327, 1981.
- McCulloch, M. T., and B. W. Chappell, Nd isotopic characteristics of S- and I-type granites, *Earth and Planetary Science Letters*, *58*, 51–64, 1982.
- McCulloch, M. T., A. L. Jacques, D. R. Nelson, and J. D. Lewis, Nd and Sr isotopes in kimberlites and lamproites from Western Australia: an enriched mantle origin, *Nature*, *302*, 400–403, 1983.
- McCulloch, M. T., and L. P. Black, Sm-Nd isotopic systematics of Enderby Land granulites and evidence for the redistribution of Sm and Nd during metamorphism, *Earth and Planetary Science Letters*, *71*, 46–58, 1984.
- McDougall, I., The geochronology and evolution of the young volcanic island of Réunion, Indian Ocean, *Geochimica et Cosmochimica Acta*, *35*, 261–288, 1971.
- McDougall, I., H. A. Polach, and J. J. Stipp, Excess radiogenic argon in young subaerial basalts from the Auckland volcanic field, New Zealand, *Geochimica et Cosmochimica Acta*, *33*, 1485–1520, 1969.
- McKee, E. H., and D. C. Noble, Age of the Cardenas lavas, Grand Canyon, Arizona, *Geological Society of America Bulletin*, *87*, 1188–1190, 1976.
- Meldrum, A., L. H. Boatner, W. J. Weber, and R. C. Ewing, Radiation damage in zircon and monazite, *Geochimica et Cosmochimica Acta*, *62*, 2509–2520, 1998.
- Mensing, T. M., G. Faure, L. M. Jones, J. R. Bowman, and J. Hoefs, Petrogenesis of the Kirkpatrick basalt, Solo Nunatak, northern Victoria Land, Antarctica, based upon isotopic compositions of strontium, oxygen and sulfur, *Contributions to Mineralogy and Petrology*, *87*, 101–108, 1984.
- Menzies, M. A., Cratonic, circumcratonic and oceanic mantle domains beneath the western United States, *Journal of Geophysical Research*, *94*, B7899–B7915, 1989.
- Menzies, M. A., and A. Halliday, Lithospheric domains beneath the Archaean and Proterozoic crust of Scotland, *Journal of Petrology*, Special Lithosphere Issue, 275–302, 1988.
- Mezger, K., E. J. Essene, and A. N. Halliday, Closure temperatures on the Sm-Nd system in metamorphic garnets, *Earth and Planetary Science Letters*,

- 113, 397–409, 1993.
- Moorbath, S., and H. Welke, Lead isotope studies on igneous rocks from the Isle of Skye, northwest Scotland, *Earth and Planetary Science Letters*, 5, 217–230, 1969.
- Moreira, M., J. Kunz, and C. J. Allègre, Rare gas systematics in popping rock: isotopic and elemental compositions in the upper mantle, *Science*, 279, 1178–1181, 1998.
- Muir, R. J., T. R. Ireland, S. D. Weaver, and J. D. Bradshaw, Ion microprobe dating of Paleozoic granitoids: Devonian magmatism in New Zealand and correlations with Australia and Antarctica, *Chemical Geology*, 127, 191–210, 1996.
- Nägler, T. F., and J. D. Kramers, Nd isotopic evolution of the upper mantle during the Precambrian: models, data and the uncertainty of both, *Precambrian Research*, 91, 233–252, 1998.
- Navon, O., I. D. Hulcheon, G. R. Rossman, and G. J. Wasserburg, Mantle-derived fluids in diamond micro-inclusions, *Nature*, 335, 784–789, 1988.
- Nelson, B. K., and D. J. DePaolo, 1,700 Myr greenstone volcanic successions in southwestern North America and isotopic evolution of Proterozoic mantle, *Nature*, 312, 143–146, 1984.
- Nelson, B. K., and D. J. DePaolo, Rapid production of continental crust 1.7 to 1.9 b.y. ago: Nd isotopic evidence from the basement of the North American mid-continent, *Geological Society of America Bulletin*, 96, 746–754, 1985.
- Nicolaysen, L. O., Solid diffusion in radioactive minerals and the measurement of absolute age, *Geochimica et Cosmochimica Acta*, 11, 41–59, 1957.
- Nier, A. O., R. W. Thompson, and B. F. Murphy, The isotopic constitution of lead and the measurement of geological time III, *Physical Review*, 60, 112–117, 1941.
- Nishio, Y., T. Ishii, T. Gamo, and Y. Sano, Volatile element isotopic systematics of the Rodrigues Triple Junction Indian Ocean MORB: implications for mantle heterogeneity, *Earth and Planetary Science Letters*, 170, 241–253, 1999.
- Noble, C. S., and J. J. Naughton, Deep-ocean basalts: inert gas content and uncertainties in age dating, *Science*, 162, 265–267, 1968.
- O’Nions, R. K., P. J. Hamilton, and P. J. Hooker, A Nd isotope investigation of sediments related to crustal development in the British Isles, *Earth and Planetary Science Letters*, 63, 229–240, 1983.
- O’Nions, R. K., and I. N. Tolstikhin, Limits on the mass flux between lower and upper mantle and stability of layering, *Earth and Planetary Science*

- Letters*, 139, 213–222, 1996.
- Oversby, V. M., A new look at the lead isotope growth curve, *Nature*, 248, 132–133, 1974.
- Ozima, M., and S. Zashu, Primitive helium in diamonds, *Science*, 219, 1067–1068, 1983.
- Ozima, M., S. Zashu, Y. Takigami, and G. Turner, Origin of the anomalous ^{40}Ar - ^{39}Ar age of Zaire cubic diamonds: excess ^{40}Ar in pristine mantle fluids, *Nature*, 337, 226–229, 1989.
- Ozima, M., S. Zashu, K. Tomura, and Y. Matsuhisa, Constraints from noble-gas contents on the origin of carbonado diamonds, *Nature*, 351, 472–474, 1991.
- Parrish, R. R., U-Pb dating of monazite and its applications to geological problems, *Canadian Journal of Earth Sciences*, 27, 1431–1450, 1990.
- Parrish, R. R., and R. Tirrul, U-Pb age of the Baltoro Granite, northwest Himalaya, and implications for monazite U-Pb systematics, *Geology*, 17, 1076–1079, 1989.
- Patel, S. C., C. D. Frost, and B. R. Frost, Contrasting responses of Rb-Sr systematics to regional and contact metamorphism, Laramie Mountains, Wyoming, USA, *Journal of Metamorphic Geology*, 17, 259–269, 1999.
- Patterson, C. C., Age of meteorites and the Earth, *Geochimica et Cosmochimica Acta*, 10, 230–237, 1956.
- Patterson, D. B., M. Honda, and I. McDougall, Atmospheric contamination: a possible source for heavy noble gases in basalts from Loihi Seamount, Hawaii, *Geophysical Research Letters*, 17, 705–708, 1990.
- Patterson, D. B., M. Honda, and I. McDougall, The noble gas cycle through subduction systems, *Research School of Earth Sciences Annual Report 1992*, pp. 104–106, Australian National University, Canberra, Australia, 1993.
- Patterson, D. B., M. Honda, and I. McDougall, Noble gases in mafic phenocrysts and xenoliths from New Zealand, *Geochimica et Cosmochimica Acta*, 58, 4411–4427, 1994.
- Peterman, Z. E., and C. E. Hedge, Related strontium isotopic and chemical variations in oceanic basalts, *Geological Society of American Bulletin*, 82, 493–500, 1971.
- Phillips, D., T. C. Onstott, and J. W. Harris, $^{40}\text{Ar}/^{39}\text{Ar}$ laser-probe dating of diamond inclusions from the Premier Kimberlite, *Nature*, 340, 460–462, 1989.
- Phipps Morgan, J., Thermal and rare gas evolution of the mantle, *Chemical Geology*, 145, 431–445, 1998.

- Phipps Morgan, J., and W. J. Morgan, Two-stage melting and the geochemical evolution of the mantle: a recipe for mantle plum-pudding, *Earth and Planetary Science Letters*, 170, 215–239, 1999.
- Pickles, D. S., S. P. Kelley, S. M. Reddy, and J. Wheeler, Determination of high spatial resolution argon isotope variations in metamorphic biotites, *Geochimica et Cosmochimica Acta*, 61, 3809–3833, 1997.
- Pidgeon, R. T., Recrystallisation of oscillatory zoned zircon: some geochronological and petrological implications, *Contributions to Mineralogy and Petrology*, 110, 463–472, 1992.
- Podosek, F. A., J. Pier, O. Nitoh, S. Zashu, and M. Ozima, Normal potassium, inherited argon in Zaire cubic diamonds, *Nature*, 334, 607–609, 1988.
- Poitrasson, F., C. Pin, and J.-L. Duthou, Hydrothermal remobilization of rare earth elements and its effect on Nd isotopes in rhyolite and granite, *Earth and Planetary Science Letters*, 130, 1–11, 1995.
- Poitrasson, F., J.-L. Paquette, J.-M. Montel, C. Pin, and J.-L. Duthou, Importance of late-magmatic and hydrothermal fluids on the Sm-Nd isotope mineral systematics of hypersolvus granites, *Chemical Geology*, 146, 187–203, 1998.
- Porcelli, D., and G. J. Wasserburg, Transfer of helium, neon, argon, and xenon through a steady-state upper mantle, *Geochimica et Cosmochimica Acta*, 59, 4921–4937, 1995.
- Poths, J., H. Healey, and A. W. Laughlin, Ubiquitous excess argon in very young basalts, *Geological Society of America Abstracts with Programs*, 25, A-462, 1993.
- Powell, R., Inversion of the assimilation and fractional crystallisation (AFC) equations: characterisation of contaminants from isotope and trace element relationships in volcanic suites, *Journal of the Geological Society of London*, 141, 447–452, 1984.
- Richardson, S. H., J. J. Gurney, A. J. Erlank, and J. W. Harris, Origin of diamonds in old enriched mantle, *Nature*, 310, 198–202, 1984.
- Rollison, H., *Using Geochemical Data: Evaluation, Presentation, Interpretation*, 352 pp., Longman, Harlow, Essex, England, 1993.
- Rosholt, J. N., and A. J. Bartel, Uranium, thorium and lead systematics in Granite Mountains, Wyoming, *Earth and Planetary Science Letters*, 7, 14–17, 1969.
- Rosholt, J. N., R. E. Zartman, and I. T. Nkomo, Lead isotope systematics and uranium depletion in the Granite Mountains, Wyoming, *Geological Society of America Bulletin*, 84, 989–1002, 1973.

- Russell, R. D., Lead isotopes as a key to the radioactivity of the earth's mantle, *Annals of the New York Academy of Sciences*, 62, 435–448, 1956.
- Russell, R. D., and L. H. Ahrens, Additional regularities among discordant lead-uranium ages, *Geochimica et Cosmochimica Acta*, 11, 213–218, 1957.
- Saunders, A. D., M. J. Norry, and J. Tarney, Origin of MORB and chemically depleted mantle reservoirs: trace element constraints, *Journal of Petrology*, Special Lithosphere Issue, 415–445, 1988.
- Scaillet, S., Excess ^{40}Ar transport scale and mechanism in high-pressure phengites: a case study from an eclogitised metabasite of the Dora-Maira nappe, western Alps, *Geochimica et Cosmochimica Acta*, 60, 1075–1090, 1996.
- Schleicher, H., H. J. Lippolt, and I. Raczek, Rb-Sr systematics of Permian volcanites in Schwarzwald (SW-Germany), part II. Age of eruption and the mechanism of Rb-Sr whole-rock age distortions, *Contributions to Mineralogy and Petrology*, 84, 281–291, 1983.
- Seidemann, D. E., Effects of submarine alteration on K-Ar dating of deep-sea igneous rocks, *Geological Society of America Bulletin*, 88, 1660–1666, 1977.
- Sharpe, M. R., Strontium isotope evidence for preserved density stratification in the main zone of the Bushveld Complex, South Africa, *Nature*, 316, 119–126, 1985.
- Sherlock, S. C., and N. O. Arnaud, Flat plateau and impossible isochrons: apparent ^{40}Ar - ^{39}Ar geochronology in a high-pressure terrain, *Geochimica et Cosmochimica Acta*, 63, 2835–2838, 1999.
- Shirey, S. B., J. F. Bender, and C. H. Langmuir, Three-component isotopic heterogeneity near the Oceanographer Transform, Mid-Atlantic Ridge, *Nature*, 325, 217–223, 1987.
- Silver, L. T., and S. Deutsch, Uranium-lead isotopic variations in zircons: a case study, *Journal of Geology*, 71, 721–758, 1963.
- Snelling, A. A., A soil geochemistry orientation survey for uranium at Koongarra, Northern Territory, *Journal of Geochemical Exploration*, 22, 83–99, 1984.
- Snelling, A. A., Koongarra uranium deposits, in *Geology of the Mineral Deposits of Australia and Papua New Guinea*, edited by F. E. Hughes, pp. 807–812, The Australasian Institute of Mining and Metallurgy, Melbourne, Australia, 1990.
- Snelling, A. A., U-Th-Pb “dating”: an example of false “isochrons,” in *Proceedings of the Third International Conference on Creationism*, edited by R. E. Walsh, pp. 497–504, Creation Science Fellowship, Pittsburgh,

- Pennsylvania, 1994.
- Snelling, A. A., The failure of U-Th-Pb “dating” at Koongarra, Australia, *Creation Ex Nihilo Technical Journal*, 9(1), 71–92, 1995.
- Snelling, A. A., The cause of anomalous potassium-argon “ages” for recent andesite flows at Mt Ngauruhoe, New Zealand, and the implications for potassium-argon “dating,” in *Proceedings of the Fourth International Conference on Creationism*, edited by R. E. Walsh, pp. 503–525, Creation Science Fellowship, Pittsburgh, Pennsylvania, 1998.
- Sobolev, N. V., and V. S. Schatsky, Diamond inclusions in garnets from metamorphic rocks: a new environment for diamond formation, *Nature*, 343, 742–746, 1990.
- Spooner, E. T. C., and N. H. Gale, Pb-isotopic composition of ophiolitic volcanogenic sulphide deposits, Troodos Complex, Cyprus, *Nature*, 296, 239–242, 1982.
- Spooner, E. T. C., H. J. Chapman, and J. D. Smewing, Strontium isotopic composition and oxidation during ocean floor hydrothermal metamorphism of the ophiolitic rocks of the Troodos Massif, Cyprus, *Geochimica et Cosmochimica Acta*, 41, 873–890, 1977.
- Stacey, J. S., and J. D. Kramers, Approximation of terrestrial lead isotope evolution by a two-stage model, *Earth and Planetary Science Letters*, 26, 207–221, 1975.
- Staudacher, T., Upper mantle origin of Harding County well gases, *Nature*, 325, 605–607, 1987.
- Staudacher, T., P. Sarda, S. H. Richardson, C. J. Allègre, I. Sagna, and L. V. Dimitriou, Noble gases in basalt glasses from a Mid-Atlantic Ridge topographic high at 14°N: geodynamic consequences, *Earth and Planetary Science Letters*, 96, 119–133, 1989.
- Stern, T. W., S. S. Goldich, and M. F. Newell, Effects of weathering on U-Pb ages of zircon from the Morton Gneiss, Minnesota, *Earth and Planetary Science Letters*, 1, 369–371, 1966.
- Stille, P., and N. Clauer, Sm-Nd isochron-age and provenance of the argillites of the Gunflint Iron Formation in Ontario, Canada, *Geochimica et Cosmochimica Acta*, 50, 1141–1146, 1986.
- Stille, P., D. M. Unruh, and M. Tatsumoto, Pb, Sr, Nd and Hf isotopic evidence of multiple sources for Oahu, Hawaii basalts, *Nature*, 304, 25–29, 1983.
- Stuckless, J. S., Applications of U-Th-Pb isotope systematics to the problems of radioactive waste disposal, *Chemical Geology*, 55, 215–225, 1986.
- Stuckless, J. S., and I. T. Nkomo, Uranium-lead isotope systematics in

- uraniferous alkali-rich granites from the Granite Mountains, Wyoming, implications for uranium source rocks, *Economic Geology*, 73, 427–441, 1978.
- Stuckless, J. S., I. T. Nkomo, and B. R. Doe, U-Th-Pb systematics in hydrothermally altered granites from the Granite Mountains, Wyoming, *Geochimica et Cosmochimica Acta*, 45, 635–645, 1981.
- Sun, S. S., Lead isotopic study of young volcanic rocks from mid-ocean ridges, ocean islands and island arcs, *Philosophical Transactions of the Royal Society of London*, A297, 409–445, 1980.
- Sun, S. S., and G. N. Hansen, Evolution of the mantle: geochemical evidence from alkali basalt, *Geology*, 3, 297–302, 1975.
- Tatsumoto, M., Genetic relations of oceanic basalts as indicated by lead isotopes, *Science*, 153, 1094–1101, 1966.
- Tatsumoto, M., U, Th and Pb abundances in Hawaiian xenoliths, *Conference on the Origin of the Earth*, Lunar and Planetary Institute, pp. 89–90, 1988.
- Taylor, H. P., The application of oxygen and hydrogen isotope studies to problems of hydrothermal alteration and ore deposition, *Economic Geology*, 69, 843–883, 1974.
- Taylor, P. N., N. W. Jones, and S. Moorbath, Isotopic assessment of relative contributions from crust and mantle sources to magma genesis of Precambrian granitoid rocks, *Philosophical Transactions of the Royal Society of London*, A310, 605–625, 1984.
- Taylor, P. N., S. Moorbath, R. Goodwin, and A. C. Petrykowsky, Crustal contamination as an indicator of the extent of early Archaean continental crust: Pb isotopic evidence for the late Archaean gneisses of west Greenland, *Geochimica et Cosmochimica Acta*, 44, 1437–1453, 1980.
- Thompson, G. R., and J. Hower, An explanation for low radiometric ages for glauconite, *Geochimica et Cosmochimica Acta*, 37, 1473–1491, 1973.
- Thompson, R. N., Magmatism of the British Tertiary Volcanic Province, *Scottish Journal of Geology*, 18, 49–107, 1982.
- Tilton, J. R., Volume diffusion as a mechanism for discordant lead ages, *Journal of Geophysical Research*, 65, 2933–2945, 1960.
- Tolstikhin, I. N., and B. Marty, The evolution of terrestrial volatiles: a view from helium, neon, argon and nitrogen isotope modelling, *Chemical Geology*, 147, 27–52, 1998.
- Turner, G., R. Burgess, and M. Bannon, Volatile-rich mantle fluids inferred from inclusions in diamond and mantle xenoliths, *Nature*, 344, 653–655, 1990.

- Valbracht, P. J., M. Honda, T. Matsumoto, N. Mattielle, I. McDougall, R. Ragettli, and D. Weis, Helium, neon and argon isotope systematics in Kerguelen ultramafic xenoliths: implications for mantle source signatures, *Earth and Planetary Science Letters*, 138, 29–38, 1996a.
- Valbracht, P. J., H. Staudigel, M. Honda, I. McDougall, and G. R. Davies, Isotopic tracing of volcanic source regions from Hawaii: decoupling of gaseous from lithophile magma components, *Earth and Planetary Science Letters*, 144, 185–198, 1996b.
- Valbracht, P. J., T. Staudacher, A. Malahoff, and C. J. Allègre, Noble gas systematics of deep rift zone glasses from Loihi Seamount, Hawaii, *Earth and Planetary Science Letters*, 150, 399–411, 1997.
- Vance, D., M. Meier, and F. Oberli, The influence of high U-Th inclusions on the U-Th-Pb systematics of almandine-pyrope garnet: results of a combined bulk dissolution stepwise-leaching, and SEM study, *Geochimica et Cosmochimica Acta*, 62, 3527–3540, 1998.
- Vidal, Ph., and N. Clauer, Pb and Sr isotopic systematics of some basalts and sulfides from the East Pacific Rise at 21°N (project RITA), *Earth and Planetary Science Letters*, 55, 237–246, 1981.
- Wasserburg, G. J., Diffusion processes in lead-uranium systems, *Journal of Geophysical Research*, 68, 4823–4846, 1963.
- Wetherill, G. W., An interpretation of the Rhodesia and Witwatersrand age patterns, *Geochimica et Cosmochimica Acta*, 9, 290–292, 1956a.
- Wetherill, G. W., Discordant uranium-lead ages, I, *Transactions of the American Geophysical Union*, 37, 320–326, 1956b.
- Wetherill, G. W., Discordant uranium-lead ages, 2. Discordant ages resulting from diffusion of lead and uranium, *Journal of Geophysical Research*, 68, 2957–2965, 1963.
- Weaver, B. L., The origin of ocean island basalt end-member compositions: trace element and isotopic constraints, *Earth and Planetary Science Letters*, 104, 381–397, 1991.
- Webb, A. W., Geochronology of the Musgrave Block, *Mineral Resources Review, South Australia*, 155, 23–27, 1985.
- White, W. M., and A. W. Hofmann, Sr and Nd isotope geochemistry of oceanic basalts and mantle evolution, *Nature*, 296, 821–825, 1982.
- Whitehouse, M. J., Granulite facies Nd-isotopic homogenisation in the Lewisian Complex of northwest Scotland, *Nature*, 331, 705–707, 1988.
- Whitney, P. R., and P. M. Hurley, The problem of inherited radiogenic strontium in sedimentary age determinations, *Geochimica et Cosmochimica Acta*, 28,

- 425–436, 1964.
- Williams, I. S., Some observations on the use of zircon U-Pb geochronology in the study of granitic rocks, *Transactions of the Royal Society of Edinburgh*, 83, 447–458, 1992.
- Williams, I. S., W. Compston, and B. W. Chappell, Zircon and monazite U-Pb systems and histories of I-type magmas, Berridale Batholith, Australia, *Journal of Petrology*, 24, 76–97, 1983.
- Williams, I. S., W. Compston, L. P. Black, T. R. Ireland, and J. J. Foster, Unsupported radiogenic Pb in zircon: a cause of anomalously high Pb-Pb, U-Pb and Th-Pb ages, *Contributions to Mineralogy and Petrology*, 88, 322–327, 1984.
- Windrim, D. P., and M. T. McCulloch, Nd and Sr isotopic systematics of central Australian granulites: chronology of crustal development and constraints on the evolution of the lower continental crust, *Contributions to Mineralogy and Petrology*, 94, 289–303, 1986.
- Wingate, M. T. D., and W. Compston, Crystal orientation effects during SHRIMP analysis of mineral targets, *Research School of Earth Sciences Annual Report 1996*, pp. 116–118, Australian National University, Canberra, Australia, 1997.
- Wingate, M. T. D., and W. Compston, Crystal orientation effects during ion microprobe U-Pb analysis of baddeleyite, *Chemical Geology*, 168, 75–97, 2000.
- Zartman, R. E., and S. M. Haines, The plumbotectonic model for Pb isotopic systematics among major terrestrial reservoirs—a case for bidirectional transport, *Geochimica et Cosmochimica Acta*, 52, 1327–1339, 1988.
- Zashu, S., M. Ozima, and O. Nitoh, K-Ar isochron dating of Zaire cubic diamonds, *Nature*, 323, 710–712, 1986.
- Zhang, L. S., and U. Schärer, Inherited Pb components in magmatic titanite and their consequence for the interpretation of U-Pb ages, *Earth and Planetary Science Letters*, 138, 57–65, 1996.
- Zheng, Y.-F., Influences of the nature of the initial Rb-Sr system on isochron validity, *Chemical Geology*, 80, 1–16, 1989.
- Zindler, A., and S. R. Hart, Chemical geodynamics, *Annual Review of Earth and Planetary Sciences*, 14, 493–571, 1986.
- Zindler, A., E. Jagoutz, and S. Goldstein, Nd, Sr and Pb isotopic systematics in a three-component mantle: a new perspective, *Nature*, 298, 519–523, 1982.

Chapter 6

Theoretical Mechanisms of Accelerated Radioactive Decay

Eugene F. Chaffin, Ph.D.*

Abstract. Data, for instance, isochron and fission track data, indicate that a large amount of decay has occurred in lunar and earth rocks. This chapter examines physical mechanisms for accelerated decay as well as possible explanations for fission track data in terms of short-lived, fissioning nuclides. The data are examined in attempts to rid the discussion of the assumptions of the uniformitarian philosophy, and to formulate views of the relevant theories of physics which are not hampered by an anti-Biblical worldview.

1. Introduction

Within physics research today, there are various theoretical models being considered which involve variable “constants,” and hence could lead to accelerated nuclear decay. The models include variable fine-structure constant, cosmological constant, dielectric permittivity, speed of light, gravitational coupling G , strong nuclear coupling g , etc. [Damour and Dyson, 1996; Okun, 1996; Wyss, 1997; Barrow and Magueijo, 1998a, b; Li and Gott, 1998; Barrow, 1999; Ivanchik et al., 1999]. I have not attempted to separate the list of the previous sentence in terms of which constants vary, since variation of one constant can be linked with, or in some cases be viewed as, variations of others. On the one hand, experimental and observational limits on possible recent variation of these so-called “constants” keep getting tighter, as physicists consider more situations as evidence of non-variation. On the other hand, new bodies of theory keep appearing which may indicate that variation of these

* Professor of Physics, Bob Jones University, Greenville, South Carolina

parameters is possible. Usually, conventional science restricts these variations to the time of the early universe, soon after the big bang. As has been noted [*Chaffin*, 1990, 1994], episodic or transient variations are more difficult to rule out, as opposed to linear extrapolations of assumed variations into the past. Thus these episodic variations may be needed to explain isotopic abundances found in rocks within a young-earth timeframe.

2. Motivation for Studies of Variable Constants

Studies of fission track dating, isochrons using various isotopes, etc. keep turning up data which appear to be convergent upon an old age for a rock, contrary to what a young-earth creationist might at first expect. We also find that various data which give old ages for recent rocks, that is, the Kilauea lava flows measured in the 1970s, the Austin data for Grand Canyon rocks [see *Austin and Snelling*, 1998] etc., indicate that apparent “age” can be inherited from parent magmas. What we seek is a creationist theory of the isotopic abundances in the earth, including the source regions for these magmas. Where physics enters the picture is in explaining, or attempting to explain, the isotopic abundance variations with time. If there has been accelerated decay at some points in earth history, it will be impossible to successfully explain the data without recognizing and modeling this fact.

Various models of accelerated decay exist already in the conventional literature, but have not been adapted to the creationist worldview. For example, *Olson and Jordan* [1987] considered the effect of a variation in the cosmological constant on the age of the universe, but ruled out *a priori* any ages less than several billion years. The reason they did that was not due to any inherent difficulties within their model, but due to their assumption that this would be inconsistent with other bodies of knowledge about earth history. What we propose to do in this project is to examine various theoretical models without allowing this bias to color the results.

Chaffin [1994] presented results of a numerical study, using a simple computer program, which allowed the depth of the nuclear potential well to vary. The radius of the nucleus and the depth of the potential

well represent two variables which are tied to the energy of the emitted α -particle and the decay constant. In this simple model a constraint is needed, which may be taken to be the approximate constancy of radioactive halo radii (see Chapter 8 by Snelling for a discussion of halos). If the energy of the α -particle is held constant, then the halo radius will also be constant. Since the radius of a halo ring is slightly dependent on the dose of radiation and the size of the halo inclusions, an exact constraint on the α -particle energy cannot be maintained. For a 5 MeV change in the potential well depth, with the α -energy held exactly constant, the computer program shows that the decay constant will change by only one power of ten. If the α -particle is allowed to change by 10% or so, then the decay constant changes by about 10^5 . In Chapter 2 by DeYoung, it was shown that a change in the decay constant of the order of 10^9 may be required, if the accelerated decay is restricted to the one year period of the Genesis Flood. Thus, these considerations seem to indicate that a one year episode of accelerated decay at the time of the Flood may not be enough. Other episodes during Creation week or during the Fall may also be necessary.

In this chapter, we examine the theories which exist already in the physics literature, examine the extent to which they can be useful to a young-earth viewpoint, and develop where necessary the equations and theory needed to extend these results to the parts of parameter space appropriate to the young-earth viewpoint. If new theories suggest themselves which have not already been developed, we pursue those theories until it becomes apparent whether they work.

Theories may turn out to be dead-end streets. For example, *Georgi and Glashow* [1974] proposed the SU(5) group as the basis for unifying strong, weak, and electromagnetic forces. It predicted that the same coupling strength, the fine-structure constant, characterize all three kinds of interaction. The theory was very successful, and is still accepted as a good approximation to the real world of particle physics. However, it predicted decay of the proton, a prediction which is still not verified, and in fact evidence has accumulated that the half-life for this decay, if not infinite, is much longer than the SU(5) theory requires. Consequently, theorists look for alternatives to this theory to represent the real world. We would like to

play this same “game” from a young-earth perspective, primarily because of the relation to our interest in accelerated decay.

3. Beta-Decay Theory as Fundamental Physics

Beta-decay, as opposed to α -decay or spontaneous fission, involves the changing of neutrons into protons or the opposite, protons changing into neutrons. The theory of these processes consequently goes to the most basic level of our understanding of particle physics, and involves the introduction of poorly understood “coupling constants.”

Barrow [1999], while considering the effect of the variation of the speed of light and/or the fine-structure constant during the early universe, realized that these changes could affect other dimensionless coupling constants as well. He wrote:

A more far-reaching aspect of c -variation is the fact that a fall in the value of c at very early times would lead to a strengthening of dimensionless gauge couplings unless other changes in the structure of physics could offset this. Thus, attempts to reconstruct the history of the very early universe could not count on the applicability of asymptotic freedom and the ideal gas condition at early times in the usual way.

To explain what this means for young-earth creationists, I will review a little history.

In 1956 Lee and Yang proposed that parity was not conserved in β -decay [*Lee and Yang*, 1956, 1957]. This was later confirmed by experiments of *Wu et al.* [1957]. In the theory of β -decay, the non-conservation of parity led to the simultaneous presence of certain terms in the Hamiltonian which had not been previously thought compatible.

Previously, Hamiltonians were constructed by demanding that the analytical form of the interaction be composed of linear combinations of five types of *bilinear covariants*: scalar, vector, tensor, axial vector, and pseudoscalar [*Lee and Yang*, 1956, appendix; *Rose*, 1961, pp. 61–64). From the five bilinear covariants we form the interaction Hamiltonian:

$$H_{int} = \Sigma C_i (\bar{\psi}_p \Gamma_i \psi_n) (\bar{\psi}_e \Gamma_i \psi_\nu) \quad (1)$$

where the Γ_i are the matrices needed to form the scalar, vector, tensor, etc. forms of the interactions. The five forms provide a complete basis for writing the interaction, and any others may be written as linear combinations of these bases. One sees, however, that the theory contains five parameters C_i which must be determined by experiment and are not given by the theory. The C_i values combine to give the expressions for the decay constants of nuclei which undergo β -decay, and these decay constants may be measured experimentally.

Lee and Yang were awarded the Nobel prize for physics in 1957. However, their theory was modified by some more recent Nobel prize-winning work. The 1979 physics prize went to Sheldon Glashow, Steven Weinberg, and Abdus Salam for their work on the gauge field theory unifying electromagnetic and weak interactions, based on the group $SU(2) \times U(1)$. It is significant that this theory led to the idea of *spontaneous symmetry breaking* and the inflationary big bang cosmology. The basic theory involves only leptons, photons, and the W and Z bosons. It replaces the C_i parameters of Lee and Yang's theory by a smaller set of g and g' coupling constants associated with the $SU(2)$ and $U(1)$ groups, respectively, and a mixing angle θ_w [Bailin and Love, 1993, chapter 14]. The g and g' are the gauge coupling constants mentioned in the quote of Barrow above. Spontaneous symmetry breaking causes the charged leptons, the electron, muon, and tau, to acquire a mass, which can be matched to the experimental values thus eliminating some of the parameters. The masses of the W and Z bosons are used in similar fashion [Bailin and Love, 1993, p. 249]. However, one might note that this procedure matches the *present-day* values of the free parameters, hence if the g and g' values had varied in the early universe's history, the actual number of free parameters would not necessarily be determined without a more all-encompassing theoretical framework.

An important idea involved in spontaneous symmetry breaking is the Higgs mechanism, named after P. W. Higgs [Higgs, 1964a,b]. This mechanism involves the Higgs fields, which are postulated as a new type of scalar field added for the purpose of breaking the symmetry. *Scalar* fields, unlike electric and magnetic fields, do not point in any particular direction. For example, the temperature at different points on

earth may be thought of as a scalar field: temperature does not point in any particular direction. When the Higgs field has a value of zero, the symmetry is unbroken, and the universe is said to be in the state of the *false vacuum*. However, the theory is built to imply that a lower energy density is possible when the Higgs fields have a non-zero value. Then the universe would be in the state of the *true vacuum*. The transition to non-zero Higgs fields is analogous to a liquid (spherically symmetric) to a crystalline (not spherically symmetric) phase transition. For the electroweak theory of combined electromagnetic and weak interactions, there would exist new particles, as yet undiscovered, called the Higgs bosons, with masses of the order of 100 GeV. The phase transition causes the mass of the Higgs particles to change from zero to the 100 GeV value, and also causes charged leptons to acquire mass. Without the Higgs mechanism we would not have a successful (renormalizable) theory of weak interactions.

Linde [1979, 1984] was one of the originators of the idea of the inflationary universe model, a modified big bang origin of the universe. The Higgs mechanism is what makes the *inflation* possible, and the inflationary scenario is what enables cosmologists to solve problems such as the horizon problem. The horizon problem has to do with the fact that, since the speed of light is a limiting speed for all interactions, then distant regions of the universe possibly could not have had time to come to equilibrium with other regions before their separation became so large that they could not interact any more. Rapid expansion, driven essentially by the Higgs mechanism, is one possibility which cosmologists highly favor for solving this problem. *Linde* [1979, p. 434] stated that: "Phase transitions [in gauge theories] . . . lead to a time dependence of the masses of particles, of coupling constants, and of the cosmological term in the expanding universe, . . ." This sounds like what we need to cause accelerated decay. However, there is a problem with this.

The problem is that all this variation stops immediately after the phase transition. Hence, the variation would occur before neutrons and protons existed, and in fact before nuclei were formed in the big bang scenario. Hence, from a Creation viewpoint, if for no other reason, this stopping of the variation would seem to limit the applicability of the Higgs

mechanism, etc. to provide accelerated decay.

Are there ways around this problem? Possibly. One recent series of articles [*Barrow and Magueijo, 1998a, b; Albrecht and Magueijo, 1999; Barrow, 1999*] presents interesting alternatives. Varying constants make sense only if viewed in terms of variations in dimensionless ratios [*Chaffin, 1994; Albrecht and Magueijo, 1999*]. For example, a variation in the fine-structure constant may be viewed as a variation in the speed of light, a variation in the permeability of the vacuum, or a variation in the fundamental charge e . However, a variation in one of these which does not change the dimensionless ratio (the fine-structure constant) amounts to a variation of units and would not correspond to any real process. A recent observation of quasar spectra in fact may be indicating that the fine-structure constant is different at large red shifts [*Webb et al., 1999*]. Whether this is so or not, these new types of models provide a way to have accelerated decay at times when nuclei do exist and when observed abundance ratios of isotopes may be affected. This is one component of what young-earth creationism needs to establish a viable model.

Other methods of extending the variation in decay rates beyond the phase transitions may involve the size of extra dimensions. Extra dimensions were first introduced to physics by *Kaluza [1921]* and *Klein [1926]*. Einstein's general theory of relativity, when extended to five dimensions, led naturally to a description of electric and magnetic fields in terms of extra components of the "metric tensor." The theory had previously included only gravitation, and electricity and magnetism included only as afterthoughts, entering through their energy and momentum contributions. However, the Kaluza-Klein approach led naturally to the same equations for electricity and magnetism as had been discovered by James Clerk Maxwell in the 1800s. While this is a step forward for the theory, the difficulty at the time was how to relate the fifth dimension to our everyday world, and the theory had no provision for studying the dynamics of changes in size of the fifth dimension. Klein proposed that his fifth dimension was smaller than the size of a particle, or in modern terms we would say that it was compactified. Only recently, with the discovery of superstring theory, have methods

of studying the dynamics of extra dimensions been possible. Recently, various workers, *Dienes* [1998], *Antoniadis and Pioline* [1999], and *Randall and Sundrum* [1999a, b], have proposed that the extra dimensions may not be as small as has been thought. This may have the consequence of extending the variation of coupling constants beyond the phase transitions [*Chaffin*, 2000].

Modern physics seeks to find a unified theory to explain all the types of force, now including gravitational, electrical, magnetic, weak nuclear, strong nuclear forces under one umbrella. Modern string theory is searching for the “vacuum” state that corresponds to the real world. Such a state would reproduce the particle spectrum, masses, and coupling constants of standard particle physics. It would also determine the correct “cosmological constant” and explain the expansion of the universe as a function of time. Specialists in modern superstring theory are at present experiencing new discoveries about the theory at a very fast pace, and it is hoped that the unified theory will soon be forthcoming. Meanwhile there remain challenges such as explaining whether or not there is a small probability for proton decay, smaller than present experimental limits.

Conventional wisdom said that the extra dimensions were all “rolled up” to a very small size, smaller than an elementary particle. This has recently been challenged. New ideas say that all the extra dimensions may not be felt equally by all of the particles and forces of nature. According to this idea, the Large Hadron Collider (LHC) being planned for completion in Europe in a few years will see some new physics that was not originally foreseen. For creationists, this may also mean that thoughts of variable decay may receive some support from theory.

Some young-earth creationists might ask whether radioisotope data can be explained without variable decay constants. One piece of evidence that Creation viewpoints need accelerated decay has to do with spontaneous fission decay. Spontaneous fission is, of course, the fission of a nucleus that occurs without being induced by absorption of some outside particle. It is similar to the difference between spontaneous applause and an audience which is acting on cue from a stage signal. The rate of these spontaneous decays depends on the delicate balance

between the strong nuclear force between nuclear particles and the coulomb repulsion between protons. The strong nuclear force has a separate coupling constant from that of β -decay, but there are still close analogies between the weak and strong nuclear forces. Hence, the next few sections will discuss evidence which is related to spontaneous fission and α -decay, with the goal of determining whether these data indicate variable decay constants and hence variable coupling constants.

4. Fission Track Data as a Motivation

When fission of a nucleus occurs, the two fragment nuclei travel off at speeds of the order of one-tenth of the speed of light. According to the ion-explosion spike model of track formation [*Fleischer et al.*, 1965], the fission fragments are highly charged, massive particles which violently repel electrons away from a cylindrical tube surrounding their path (Figure 1). This leaves positive ions at the lattice sites along the path, and mutual repulsion between these positive ions separates them and forces them into the surrounding lattice, leaving a cylindrical region of damage. If the solid in which the tracks form is an insulator at low temperature, the tracks may be preserved for times comparable to the age of the universe. Conventional science based on uniformitarian philosophy has attributed most of these tracks to spontaneous fission of ^{238}U , with some tracks in some meteorites and moon rocks assigned to ^{244}Pu [*Crozaz et al.*, 1972; *Hutcheon and Price*, 1972; *Macdougall*, 1976]. Since the half-life of ^{238}U is 4.468 billion years, and that of ^{244}Pu 82 million years, techniques have been developed to interpret track counts as indicating long ages for the rocks in which they are found. *Fleischer et al.* stated [1965, p. 2703]: “If, starting from the end of nucleosynthesis, meteoritic crystals were formed and then cooled in a time interval comparable to the 7.6×10^7 years [*sic: this was the accepted value in 1965*] half-life for ^{244}Pu decay, they should contain large numbers of ^{244}Pu spontaneous fission tracks. On any reasonable cosmological model it can be shown that ^{238}U is the only other isotope that need be considered as a source of spontaneous fission tracks.” Of course, the phrase “reasonable cosmological model” refers only to those based on

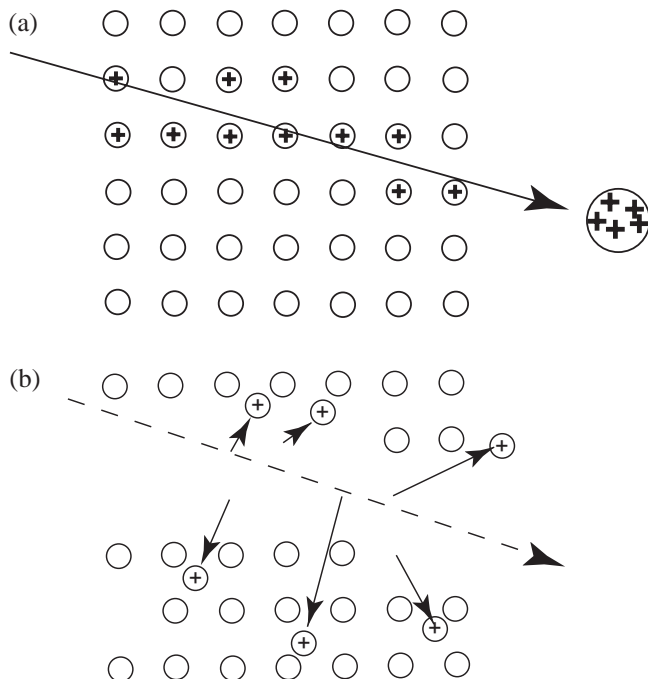


Figure 1. The ion-explosion spike model of fission track formation. In part (a), a fission fragment plows through the crystal, leaving some nuclei devoid of some electrons, or having a very large positive charge. In (b), the positively-charged nuclei repel each other, leaving a tube or cylinder of radiation damage in the crystal. Etching later enlarges this track for microscopic examination.

uniformitarian presumptions. As the techniques were perfected, corrections were discovered for effects of cosmic rays and cosmic-ray induced spallation [Crozaz *et al.*, 1972]. Spallation reactions occur at energies greater than 50 MeV when a nucleon strikes a nucleus causing nucleons or groups of nucleons to emerge (α -particles, deuterons, etc.) In some meteorites the cosmic ray induced spallation tracks are more numerous than the fission tracks.

Creationists have not gone on record with many statements about fission track dating. Chaffin [1987], in a review article concerning radioactive dating, discussed the possibility that fission track dates could

be assigned to other isotopes with shorter half-lives than ^{238}U or ^{244}Pu . *Bielecki* [1994] wrote a thesis for the Institute for Creation Research in which he examined fission track densities in obsidian from Resting Spring Range located near Shoshone, California. Since the rocks are placed in the Miocene of the uniformitarian geologic column, but were thought to be post-Flood rocks according to Bielecki, it was initially thought that the fission track densities might be smaller than what would be imparted by a million-year age. However, the data did not support this hypothesis.

Can we determine what type of nuclide could produce these fission tracks within the timeframe of the young earth, and assuming that fission decay “constants” were truly the same throughout earth history? The possibility that the half-lives varied episodically in the past has been previously discussed [*Chaffin*, 1985, 1987, 1990, 1994]. A theoretical basis seems to exist for this possibility, but what is needed is to determine if data exist in support of the variation. For the present, I will attempt to explain the existing fission track densities without invoking variable half-lives for spontaneous fission. If this proves to be impossible, then the evidence might lead to variable half-lives. However, in the next few paragraphs I will do my best to avoid invoking variable half-lives at all.

5. The Fission Track Method

Fission track densities ρ are the sum of components due to fission and those due to cosmic rays. Various techniques can be used to separate the cosmic ray components [*Crozaz et al.*, 1972; *Hutcheon and Price*, 1972]. This leads to an equation for the fission track density ρ_f :

$$\rho_f = \left(\frac{\lambda_f}{\lambda_D} \right) \left(e^{\lambda_D T} - 1 \right) R_F N_0 C_X \quad (2)$$

where: λ_f = the spontaneous fission decay constant of the nuclide producing the tracks

λ_D = the total decay constant including α -decay for this same nuclide

N_0 = the number of atoms per cubic centimeter

C_x = the atomic concentration of the unknown nuclide,
measured at the present (modern) time

T = the total storage time of the fission tracks

R_f = the effective range of fission fragments.

As example of the application of this equation, we might consider the lunar rock 12064 from the Apollo 14 mission to the Fra Mauro region of the Moon. *Crozaz et al.* [1972] reported that 17.3×10^7 tracks per square centimeter of this sample were attributable to spontaneous fission. The effective range of fission fragments in this sample, a crystal of whitlockite, is about 9.4×10^{-4} cm. Since the density of whitlockite is 3.123 grams per cubic centimeter, N_o is 5.53×10^{17} atoms per cubic centimeter. The present-day, measured concentration of ^{238}U varies from 60 to 90 parts per million, which is consistent with an age of about 3.3 billion years according to the above equation. However, *Crozaz et al.* [1972] concluded from the slope of a plot of fission track density versus U concentration that the real age was probably 4.2 billion years.

If one abandons uniformitarian assumptions, other isotopes besides ^{238}U and ^{244}Pu become possible candidates for producing these tracks. What sort of nuclide would provide a reasonable alternative?

6. A Graph for Showing Acceptable Half-Lives

If the age of the solar system is only 6000–10,000 years, then nuclides with total decay half-lives greater than about 1500 years would, if present at Creation, still be present in measurable abundances. Of course, this is assuming there has never been a time period of accelerated decay during solar system history. Also, this assumes there are no other production mechanisms of any significance for these nuclides, which seems to be the case for the ones we will consider. Now for many heavy nuclides the dominant decay mode is α -decay, with spontaneous fission being a strong competitor. When one adds too many protons or neutrons to a nucleus, β -decays and/or electron capture becomes predominant. To keep matters simple, I shall assume that the neutron and proton numbers are adjusted to keep β -decays and electron capture out of the picture. We can always go back and consider their effect later. This leaves us with the necessity

of having to consider a total decay half-life T , which is the combination of that due to α -decay T_α and that due to spontaneous fission T_{sf} :

$$\frac{1}{T} = \frac{1}{T_{sf}} + \frac{1}{T_\alpha} \tag{3}$$

The hyperbola on Figure 2 shows a curve for which the total half-life is restricted to be 1500 years. If we postulate that a short half-life nuclide made the fission tracks and then decayed away so as to leave no measurable traces, then we are restricted to the region to the left and below this curve.

A second restriction is that the decay constant for spontaneous fission must not be smaller than about one-ten thousandth of the decay constant for α -decay, otherwise the nuclide will decay away before a sufficient number of fission tracks can be made. This ratio equals the half-life for α -decay divided by the half-life for spontaneous fission, since the natural logarithm of two cancels out of the ratio. Hence, Figure 2 shows a line starting at the origin and heading above and to the right with a slope of

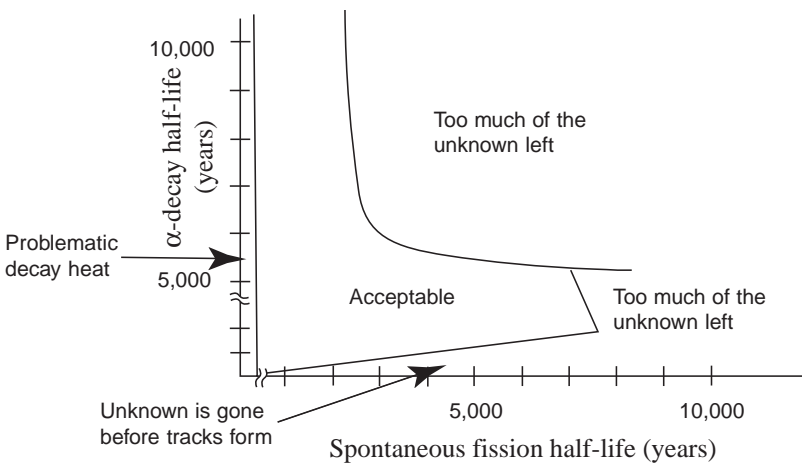


Figure 2. A graph of a decay half-life versus spontaneous fission half-life. Only certain nuclei fall in the acceptable region, and thus could explain fission tracks, in a young-earth paradigm, without accelerated decay. See the text for discussion.

10^{-4} . Only nuclides above this line are acceptable.

To the right of the acceptable region there is another line which must be drawn when the half-life for spontaneous fission becomes too large to produce enough fission tracks during the history of the rock in question. The precise position of this line depends on the concentration of the unknown.

A fourth restriction is that the half-life for spontaneous fission cannot be too small, since the rock would melt due to the rapid decay, annealing away the tracks. Reasonable assumptions about the energy released per fission, the thermal conductivity of these insulating rocks, and the annealing temperature produce an order-of-magnitude estimate of a few minutes for the lowest acceptable half-lives.

Figure 2 thus delineates what type of nuclei could have made the fission tracks on the basis of a young-earth model. One might ask, why should we not just attribute the tracks to ^{238}U as in the uniformitarian model? The answer is that, according to equation (1), and an assumption of several thousand years for the age of the earth, ^{238}U could only produce about 17 tracks per square centimeter, as compared to the measured amount of ten million times greater magnitude (for lunar rock 12064 previously discussed). Thus, on the assumption of constant half-lives, we are forced to seek another candidate.

7. Consideration of Known Nuclei with Spontaneous Decay Modes

Consulting the Knolls Atomic Power Company Chart of the Nuclides, or various software packages such as Periodic Table 2.03, one ends up with only a few candidates which fall within the range of acceptability. Table 1 shows what are probably the best candidates, three isotopes of Cf.

For ^{254}Cf , spontaneous fission is the predominant decay mode, with α -decay occurring 0.31% of the time. Since the total half-life of ^{254}Cf is 60.5 days, it could produce plenty of fission tracks before disappearing below detectable concentrations. However, the 0.31% of decays that follow the α -decay mode would produce small concentrations of ^{250}Cm

Table 1. Alternative fission track producers.

Nuclide	α -Decay Half-Life	Spontaneous Fission Half-Life	Possible Problems
^{254}Cf	? (α -decay occurs 0.31% of the time)	60.5 ± 0.2 days	The daughter nuclide ^{250}Cm has a long half-life of 7400 years.
^{252}Cf	2.64 years	85.5 ± 0.5 years	The daughter nuclide ^{248}Cm has a long half-life of 350,000 years. ^{244}Pu should also be produced.
^{250}Cf	13.1 years	$17,300 \pm 600$ years	The daughter nuclide ^{244}Cm has a long half-life of 4713 years.
Superheavy	?	?	?

(half-life 7400 years). Hence, it would be interesting to try to find detectable amounts of ^{250}Cm in some of these rocks.

For ^{252}Cf , the predominant decay mode is α -decay, but the total half-life is only 2.64 years. The partial half-life for spontaneous fission is 85.5 ± 5 years [Vandenbosch and Huizenga, 1973, p. 47]. This places this nuclide in the acceptable part of Figure 2, and a concentration of about 0.91 parts per billion could have produced the track density in lunar rock 12064 and then decayed away before modern times.

For ^{250}Cf , the story is similar, with the total half-life being 13.1 years

and the partial half-life for spontaneous fission being $17,300 \pm 600$ years [Vandenbosch and Huizenga, 1973, p. 47]. A concentration of about 37 parts per billion could have produced the tracks in lunar rock 12064 in the process of decaying away.

8. Superheavy Nuclei

In the mid-1970s the author of this chapter was a postdoctoral researcher involved in studying the theory of fission [Chaffin and Dickmann, 1976]. This involved reducing the theory to computer programs for evaluation on IBM computers. In the early 1970s, various groups had begun to map out the potential energy of heavy nuclei as a function of nuclear shape, and had found that some as yet undiscovered nuclei might be stable [Nix, 1972]. The calculations indicated that nuclei with about $Z = 114$ might have half-lives of the order of 10^{15} years, and hence might be found in nature if mechanisms to produce them had been in operation according to our cosmological model. However, as time went on additional effects were considered, such as axial asymmetry of the nucleus on the path to separation into fragments. This had the unfortunate effect of drastically reducing the predicted half-lives of these unknown superheavy nuclei [Patyk *et al.*, 1989; Sobiczewski, Patyk and Cwiok, 1989; Seaborg and Loveland, 1990, pp. 273–274]. The latest theory has some nuclei at $N = 182$ to 184 with α -decay half-lives of around 12 days and spontaneous fission half-lives in the range from 10^4 to 10^8 years. For the spontaneous fission half-lives of around 10^4 years, a concentration of a few parts per million could have produced fission tracks in rocks such as 12064 and then decayed away. Experimental groups in Germany, Russia, and California are actively trying to produce these nuclei at present [Lazerev *et al.*, 1994; Hofmann *et al.*, 1996; Stone, 1999). Recent successes have produced nuclides with $Z = 110$, 112, and 114, but so far the neutron numbers have not matched the values needed for the greatest stability. We shall see what turns up.

9. Fissiogenic Xenon (Xe)?

In the early 1970s the majority of scientists studying meteorites thought that a large component of the noble gas Xe present in meteorites, and in particular carbonaceous chondrites, might be due to fission [*Alexander et al.*, 1971; *Drozd et al.*, 1972; *Lewis et al.*, 1975; *Kuroda*, 1982, p. 102]. This idea had originated with *Kuroda* [1960]. Laboratory experiments seemed to show that the proportions of the isotopes ^{131}Xe , ^{132}Xe , ^{134}Xe , and ^{136}Xe produced from fission of ^{244}Pu matched that of a component of the Xe found in meteorites. However, further study revealed that the light isotopes ^{124}Xe and ^{126}Xe were also enriched in the same host phases in these meteorites. Since the fission hypothesis could not explain the production of these isotopes, it was abandoned [*Lewis and Anders*, 1983; *Lewis et al.*, 1987; *Jorgensen*, 1988; *Lewis, Anders and Draine*, 1989; *Huss*, 1991]. This means that some Xe comes from fission, but that the bulk of the Xe must, in most cases, be explained in some other fashion, not from ^{244}Pu . *Steinberg and Wilkins* [1978] show that short-lived superheavy elements could possibly be produced in the r-process inside a supernova, but they would fission before the supernova material could be incorporated into meteorites. Hence, the non-creationist cosmological theories of the origin of Xe do not rely on fission after the formation of meteoroids, the Moon, and other solar system bodies.

For the young-earth creationist, this means that Xe isotopic compositions are difficult to explain. They do not point, as had once been thought, to ^{244}Pu fission. Furthermore, they are not evidence against the Creation model since the evolutionists have difficulty explaining them, and also since the bulk of the Xe is in carbonaceous phases which do not normally involve fissiogenic elements.

10. Can Different Parent Nuclei of Fission Tracks be Distinguished?

It might be thought that the tracks produced by different parent nuclei, for example ^{238}U versus ^{252}Cf , should be distinguishable. However, a wide family of nuclei undergo asymmetric fission similar to what ^{238}U

does [Vandenbosch and Huizenga, 1973, chapters 10 and 11]. In this type of asymmetric fission, there is a double peaked graph of the yield for different masses versus mass number. Some 80 or more different nuclei are produced in sizable yields, so that any one fission may yield different fragment nuclei than the next one. Experimentally, it is found that the kinetic energy of the fission fragments depends on $Z^2/A^{1/3}$, where Z is the number of protons in the fissioning nucleus and A is its mass number. However, this energy will usually be divided unevenly among the fragments. Also, in using fission tracks we do not know which fragment nuclei produced the individual tracks, and there is a wide statistical variation in the individual kinetic energies. Hence, the length of the tracks is, in practice, not a very helpful method of distinguishing between tracks produced from ^{238}U or ^{252}Cf .

Huang and Walker [1967] discovered that tracks produced by the recoil of the parent nucleus from α -decay could, in certain cases, be revealed by etching techniques similar to that for fission tracks. The α -recoil tracks are much shorter, consisting of shallow pits of only about 100 Å (angstroms) length, but there are more of them per unit area of etchable surface, and the use of phase contrast microscopes could reveal them. The increased track density is due to the fact that ^{238}U undergoes α -decay 99.99% of the time versus spontaneous fission only 0.001% of the time. Huang and Walker [1967] noted that possible ^{244}Pu contributions to the track densities could be checked by examining both α -recoil data and fission track data. Spontaneous fission of ^{244}Pu occurs in 0.13% of all decays, a slightly larger value than for ^{238}U , but more significantly, the half-life of ^{244}Pu is much shorter.

Gentry [1967, 1968] used the α -recoil techniques to gather more data on certain samples containing radioactive halos. The data provided evidence against the idea that Po halos were produced by radioactive precursors migrating along conduits or cracks. From the data, Gentry found no evidence for ^{244}Pu tracks. In particular, fission tracks were found emanating from U halos, and the total number of tracks agreed with the number consistent with the halo coloration, without the necessity of postulating ^{244}Pu contributions. In other areas of the etchable surface, not associated with halos, the α -recoil track density gave an approximate

upper limit to the ^{244}Pu contribution, and no real positive evidence for ^{244}Pu tracks.

If ^{252}Cf , a superheavy nucleus, or another candidate were responsible for excess fission tracks, it may be possible to use α -recoil data to account for the situation. In the case of ^{254}Cf , for example, spontaneous fission is the predominant decay mode, with α -decay occurring only 0.31% of the time. Hence, if an appreciable fraction of the tracks were due to ^{254}Cf , the α -recoil density should be much less than in the pure ^{238}U case. The ratio of ^{238}U tracks to ^{254}Cf or other tracks may vary from sample to sample, so Gentry's results do not necessarily rule this out.

These considerations narrow the field of possible producers of fission tracks down to only a few candidates. The theory that these nuclides are responsible can be falsified by searching for the products of their decay chains, using equipment capable of detecting concentrations of only a few parts per trillion. Fission track data by itself thus seems to be explainable, pending further results, in this fashion without accelerated decay. However, wider considerations may not support this conclusion.

In Biblical Creation models, nucleosynthesis need not be predominantly a work of the big bang or of supernova explosion scenarios. Scriptures such as Genesis 1, John 1, and Hebrews 11:3 indicate that the appearance of the elements out of nothing seems to be the correct concept. The primeval fireball is not mentioned or necessarily implied in Scripture. Also, the long times required would not fit our scenario. If accelerated decay occurred early in earth history, it would tend to eliminate the short-lived fission track sources that we have been talking about. However, accelerated nuclear decay may also imply accelerated induced reactions. *Fowler, Greenstein, and Hoyle* [1962] studied a model in which gigantic solar flares associated with the early history of the Sun would produce high energy protons and neutrons which would react with other material in the solar system. They discussed, for example, the formation of ^{107}Pd and ^{129}I in this way. While the Creation model would not incorporate the scenario for the formation of the Sun which these authors advocated, the nuclear reactions which they proposed could still possibly occur in giant flares associated with the early history of the Sun. Alternately, the mechanisms that cause

accelerated decay may also cause nuclear reactions, thus synthesizing other elements.

Evidence, such as mature ^{238}U halos in Precambrian rocks, indicates a large amount of nuclear decay subsequent to early earth history (see Snelling, Chapter 8 and Humphreys, Chapter 7). It is doubtful whether the U in the halo inclusions is mobile enough to allow the explanation of these halos in terms of the present-day, measured U concentrations, without accelerated decay. *Ramdohr* [1960, 1969] discussed lattice destructions which occur in the immediate vicinity of strongly radioactive minerals. These lattice destructions then pave the way for dissolution or replacement of the affected areas. When one thinks of the fission tracks and α -particle damage that should be expected in the inclusions of a U halo, it is hard to deny that some U migration must have occurred. However, the fact that the halos still exist argues that the U concentrations have not been too large since otherwise the damage would be of the more extensive type that *Ramdohr* documents. Hence, large amounts of nuclear decay coming from a small amount of U appears to be a reasonable conclusion. If we attribute this to an accelerated decay episode, this implies that any short-lived nuclei such as the Cf we have discussed would not be present. The reason is that the Cf would also have experienced accelerated decay. Thus, these wider considerations may imply that fission tracks cannot be attributed to short-lived nuclides.

Another possibility is that presently stable nuclides, such as those of Pb, could have become unstable during one or more of the accelerated decay episodes and have contributed to the inventory of observed fission tracks. This is a matter deserving future study.

11. Conclusions

While other possibilities exist, such as the above discussion indicates for the case of fission tracks, accelerated decay models need investigation. On the one hand, experimental data are needed to link the theories with the real world. Hence, it is important to get involved in the study of things like fission tracks, since they seem to offer interesting aspects that are not present just in the study of some isochrons in isolation from

other data. On the other hand, real experimental data are not likely to completely specify the generalized theories. One needs to consider all the promising avenues for theories of accelerated decay.

References

- Albrecht, A., and J. Majueijo, Time varying speed of light as a solution to cosmological puzzles, *Physical Review*, *D59*, 043516, 1999. Also available as preprint astro-ph/9811018.
- Alexander, E. C. Jr., R. S. Lewis, J. H. Reynolds, and M. C. Michel, Plutonium-244: confirmation as an extinct radioactivity, *Science*, *172*, 837–840, 1971.
- Antoniadis, I., and B. Pioline, Large dimensions and string physics at a TeV, preprint hep-ph/9906480, presented at the conference *Fundamental Interactions: from Symmetries to Black Holes* in honor of Francois Englert, Brussels, March 25–27, 1999 and *Beyond the Desert 99*, Castle Ringberg, Tegenersee, Germany, June 6–12, 1999.
- Austin, S. A., and A. A. Snelling, Discordant potassium-argon and model and isochron “ages” for Cardenas Basalt (Middle Proterozoic) and associated diabase of eastern Grand Canyon, Arizona, in *Proceedings of the Fourth International Conference on Creationism*, edited by R. E. Walsh, pp. 35–51, Creation Science Fellowship, Pittsburgh, Pennsylvania, 1998.
- Bailin, D., and A. Love., *Introduction to Gauge Field Theory*, Institute of Physics Publishing, Bristol and Philadelphia, 1993.
- Barrow, J. D., Cosmologies with varying light-speed, *Physical Review*, *D59*, 043515, 1999. Also available as preprint astro-ph/9811022.
- Barrow, J. D., and J. Magueijo, Varying-alpha theories and solutions to the cosmological problems, *Physics Letters*, *B443*, 104–110, 1998a. Also available on the Los Alamos preprint server (xxx.lanl.gov) as paper astro-ph/9811072.
- Barrow, J. D., and J. Magueijo, Solutions to the quasi-flatness and quasi-lambda problems, *Physics Letters*, *B447*, 246–250, 1998b. Also available on the Los Alamos preprint server (xxx.lanl.gov) as paper astro-ph/9811073.
- Bielecki, J. W., *A Study in Spontaneous Fission Track Density in Resting Spring Range Obsidian (Miocene) near Shoshone, California*, Unpublished Master’s dissertation, Graduate School, Institute for Creation Research, 1994.
- Chaffin, E.F., The Oklo natural uranium reactor: evidence for a young earth, *Creation Research Society Quarterly*, *22*, 10–16, 1985.

- Chaffin, E. F., A young earth?—a survey of dating methods, *Creation Research Society Quarterly*, 24, 109–117, 1987.
- Chaffin, E. F., The difficulty in obtaining realistic conclusions about variable “constants”, *Creation Research Society Quarterly*, 27, 6–9, 1990.
- Chaffin, E. F., Are the fundamental “constants” of physics really variables? in *Proceedings of the Third International Conference on Creationism*, edited by R. E. Walsh, Creation Science Fellowship, Pittsburgh, Pennsylvania, pp. 143–150, 1994.
- Chaffin, E. F., A mechanism for accelerated radioactive decay, *Creation Research Society Quarterly*, 37, 3–9, 2000.
- Chaffin, E. F., and F. Dickmann, Validity of the adiabatic cranking model when applied to fission, *Physical Review Letters*, 37, 1738–1740, 1976.
- Crozaz, G., R. Drozd, H. Graf, C. M. Hohenberg, M. Monnin, D. Ragan, C. Ralston, M. Seitz, J. Shirck, R. M. Walker, and J. Zimmerman, Uranium and extinct ^{244}Pu effects in Apollo 14 materials, in *Proceedings of the Third Lunar Science Conference*, Supplement 3, *Geochimica et Cosmochimica Acta*, vol. 2, edited by D. Heymann, pp. 1623–1636, Chemical and Isotope Analyses, Organics Chemistry, MIT Press, Cambridge, Massachusetts, 1972.
- Damour, T., and F. Dyson, The Oklo bound on the time variation of the fine-structure constant, *Nuclear Physics*, B480, 37–54, 1996. Also available on the Los Alamos preprint server (xxx.lanl.gov) as paper hep-ph/96066486.
- Dienes, K. R., E. Dudas, T. Gherghetta, and A. Riotto, Cosmological phase transitions and radius stabilization in higher dimensions, *Nuclear Physics*, B543, 387–422, 1998.
- Drozd, R., C. M. Hohenburg, and D. Ragan, Fission xenon from extinct ^{244}Pu in 14301, *Earth and Planetary Science Letters*, 15, 338–346, 1972.
- Fleischer, R. L., P. B. Price, and R. M. Walker, Spontaneous fission tracks from extinct ^{244}Pu in meteorites and the early history of the solar system, *Journal of Geophysical Research*, 70, 2703–2707, 1965.
- Fleischer, R. L., P. B. Price, and R. M. Walker, Tracks of charged particles in solids, *Science*, 149, 383–393, 1965.
- Fowler, W. A., J. L. Greenstein, and F. Hoyle, Nucleosynthesis during the early history of the solar system, *Geophysical Journal of the Royal Astronomical Society*, 6, 148–220, 1962.
- Gentry, R. V., Extinct radioactivity and the discovery of a new pleochroic halo, *Nature*, 213, 487–489, 1967.
- Gentry, R. V., Fossil alpha-recoil analysis of certain variant radioactive halos, *Science*, 160, 1228–1230, 1968.

- Georgi, H., and S. L. Glashow, Unity of all elementary-particle forces, *Physical Review Letters*, 32, 438–441, 1974.
- Higgs, P. W., Broken symmetries, massless particles and gauge fields, *Physics Letters*, 12, 132–133, 1964a.
- Higgs, P. W., Broken symmetries and the masses of gauge particles, *Physical Review Letters*, 13, 508–509, 1964b.
- Hofmann, S., V. Ninov, F. P. Heberger, P. Armbruster, H. Folger, G. Münzenberg, H. J. Schött, A. G. Popeko, A. V. Yeremin, S. Saro, R. Janik, and M. Leino, The new element 112, *Zeitschrift für Physik*, A354, 229–230, 1996.
- Huang, W. H., and R. M. Walker, Fossil alpha-recoil tracks: a new method of age determination, *Science*, 155, 1103–1106, 1967.
- Huss, G. R., Meteorite, in *McGraw Hill Yearbook of Science and Technology 1991*, McGraw Hill, New York, pp. 235–237, 1991.
- Hutcheon, I. D., and P. B. Price., ^{244}Pu fission tracks: evidence in a lunar rock 3.95 billion years old, *Science*, 176, 909–911, 1972.
- Ivanchik, A. V., A. Y. Potekhin, and D. A. Varshalovich, The fine-structure constant: a new limit on its cosmological variation and some theoretical consequences, *Astronomy and Astrophysics*, 343, 439, 1999. Also available on the Los Alamos preprint server (xxx.lanl.gov) as paper astro-ph/9810166.
- Jorgensen, U. G., Formation of Xe-HL-enriched diamonds in grains in stellar environments, *Nature*, 332, 702–705, 1988.
- Kaluza, Th., von, Zum unitätsproblem der physik, *Sitzungsberichte der Preußische Akademie der Wissenschaften zu Berlin, Physikalisch-Mathematische Klasse*, 1, 966–972, 1921.
- Klein, O., Quantentheorie und fünfdimensionale relativitätstheorie, *Zeitschrift für Physik*, 37, 895–906, 1926.
- Kuroda, P. K., Nuclear fission in the early history of the earth, *Nature*, 187, 36–38, 1960.
- Kuroda, P. K., *The Origin of the Chemical Elements and the Oklo Phenomenon*, Springer-Verlag, New York, 1982.
- Lazerev, Yu. A., Yu. V. Lobanov, V. K. Oganessian, V. K. Utyonkov, F. Sh. Abdullin, G. V. Buklanov, B. N. Gikal, S. Iliev, A. N. Mezentsev, A. N. Polyakov, I. M. Sedykh, I. V. Shirokovsky, V. G. Subbotin, A. M. Sukhov, Yu. S. Tsyganov, V. E. Zhuchko, R. W. Loughheed, K. J. Moody, J. F. Wild, E. K. Hulet, and J. H. McQuaid, Discovery of enhanced nuclear stability near the deformed shells $N = 162$ and $Z = 108$, *Physical Review Letters*, 73, 624–627, 1994.

- Lee, T. D., and C. N. Yang, Question of parity conservation in weak interactions, *Physical Review*, 104, 254–258, 1956.
- Lee, T. D., and C. N. Yang, Errata: question of parity conservation in weak interactions, *Physical Review*, 106, 1371, 1957.
- Lewis, R. S., B. Srivivasan, and E. Anders, Host phase of a strange xenon component in Allende, *Science*, 190, 1251–1262, 1975.
- Lewis, R. S., and E. Anders, Interstellar matter in meteorites, *Scientific American*, 249(2), 66–77, 1983.
- Lewis, R. S., T. Ming, J. F. Wacker, E. Anders, and E. Steel, Interstellar diamonds in meteorites, *Nature*, 326, 160–162, 1987.
- Lewis, R. S., E. Anders, and B. T. Draine, Properties, detectability, and origin of interstellar diamonds in meteorites, *Nature*, 339, 117–121, 1989.
- Li, L.-X., and J. R. Gott, III, Inflation in Kaluza-Klein theory: relation between the fine-structure constant and the cosmological constant, *Physical Review*, D58, 102513, 1998. Also available on the Los Alamos preprint server (xxx.lanl.gov) as astro-ph/9804311.
- Linde, A. D., Phase transitions in gauge theories and cosmology, *Reports on Progress in Physics*, 42, 390–437, 1979.
- Linde, A. D., The inflationary universe, *Reports on Progress in Physics*, 47, 925–986, 1984.
- Maccougall, J. D., Fission-track dating, *Scientific American*, 235(2), 114–122, 1976.
- Nix, J. R., Predictions for superheavy nuclei, *Physics Today*, 25(4), 30–38, 1972.
- Okun, L. B., Fundamental constants of nature, invited paper to appear in the *Proceedings of the Fifteenth International Conference on Atomic Physics: Zeeman-Effect Centenary*, held at the Wan der Waals-Zeeman Laboratory, University of Amsterdam, August 5–9, 1996. Also available on the Los Alamos preprint server (xxx.lanl.gov) as paper astro-ph/9612249.
- Olson, T. S., and T. F. Jordan, Ages of the universe for decreasing cosmological constants, *Physical Review*, D35, 3258, 1987.
- Patyk, Z., J. Skalski, A. Sobiczewski, and S. Cwiok, Potential energy and spontaneous fission half-lives for heavy and superheavy nuclei, *Nuclear Physics*, A502, 591c–600c, 1989.
- Ramdohr, P., Neue Beobachtungen an radioaktiven Höfen in verschiedenen Mineralien mit kritischen Bemerkungen zur Auswertung der Höfe zur Altersbestimmung, *Geologische Rundschau*, 49, 253–263, 1960.
- Ramdohr, P., *The Ore Minerals and their Intergrowths*, Pergamon Press, New York, 1969.
- Randall, L., and R. Sundrum, A large mass hierarchy from a small extradimension,

- Physics Letters*, 83, 3370–3373, 1999a.
- Randall, L., and R. Sundrum, An alternative to compactification, *Physics Letters*, 83, 4690–4693, 1999b.
- Rose, M. E., *Relativistic Electron Theory*, John Wiley and Sons, New York, 1961.
- Seaborg, G. T., and W. D. Loveland, *The Elements Beyond Uranium*, John Wiley and Sons, New York, 1990.
- Sobiczewski, A., Z. Patyk, and S. Cwiok, Deformed superheavy nuclei, *Physics Letters*, B224, 1–4, 1989.
- Steinberg, E. P., and B. D. Wilkins, Implications of fission mass distributions for the astrophysical r-process, *The Astrophysical Journal*, 223, 1000–1014, 1978.
- Stone, R., Element 114 lumbers into view, *Science*, 283, 474, 1999.
- Vandenbosch, R., and J. R. Huizenga, *Nuclear Fission*, Academic Press, New York, 1973.
- Webb, J. K., V. V. Flambaum, C. W. Church, M. J. Drinkwater, and J. D. Barrow, A search for time variation of the fine structure constant, *Physical Review Letters*, 82, 884–887, 1999. Also available as preprint astro-ph/9803165.
- Wu, C. S., E. Ambler, R. W. Hayward, D. D. Hoppes, and R. P. Hudson, Experimental test of parity conservation in beta decay, *Physical Review*, 105, 1413–1415.
- Wyss, W., The speed of light as a dilaton field, available on the Los Alamos preprint server (xxx.lanl.gov) as paper gr-qc/9711065, 1997.

Bibliography

- Ahlen, S. P., P. B. Price, and G. Tarlé, Track-recording solids, *Physics Today*, 34 (9), 32–39, 1981.
- Allaert, E., C. Wagemans, G. Wegener-Penning, A. J. Deruytter, and R. Barthélémy, Energy and mass distributions for $^{241}\text{Pu}(n_{\text{th}}, f)$, $^{242}\text{Pu}(s.f.)$, and $^{244}\text{Pu}(s.f.)$ fragments, *Nuclear Physics*, A380, 61–71, 1982.
- Bardsley, W. E., Random errors in fission-track dating, *Journal of the International Association for Mathematical Geology*, 14, 545–546, 1982.
- Cwiok, S., W. Nazarewicz, J. X. Saladin, W. Plociennik, and A. Johnson, Hyperdeformations and clustering in the actinide nuclei, *Physics Letters*, B322, 304–310, 1994.
- Fields, P. R., H. Diamond, D. N. Metta, D. J. Rokop, and C. M. Stevens, ^{237}Np , ^{236}U , and other actinides on the Moon, in *Proceedings of the Third Lunar*

- Science Conference*, Supplement 3, *Geochimica et Cosmochimica Acta*, vol. 2, edited by D. Heymann, pp. 1637–1644, Chemical and Isotope Analyses, Organics Chemistry, MIT Press, Cambridge, Massachusetts, 1972.
- Fields, P. R., H. Diamond, D. N. Metta, C. M. Stevens, and D. J. Rokop, Isotopic abundances of actinide elements in Apollo 12 samples, in *Proceedings of the Second Lunar Science Conference*, Supplement 2, *Geochimica et Cosmochimica Acta*, vol. 2, edited by A. A. Levinson, pp. 1571–1576, Chemical and Isotope Analyses, Organics Chemistry, MIT Press, Cambridge, Massachusetts, 1971.
- Fields, P. R., A. M. Friedman, J. Lerner, C. M. Stevens, D. Metta, and W. K. Sabine, Decay properties of ^{244}Pu , and comments on its existence in nature, *Nature*, 212, 131–134, 1966.
- Fleischer, R. L., P. B. Price, E. M. Symes, and D. S. Miller, Fission-track ages and track-annealing behaviour of some micas, *Science*, 143, 349–351, 1964.
- Gentner, W., D. Storzer, R. Gijbels, and P. R. Van der Linden, Calibration of the decay constant of ^{238}U spontaneous fission, *American Nuclear Society Transactions*, 15, 125–126, 1972.
- Hermann, G., The search for superheavy elements in nature, *Physica Scripta*, 10A, 71–76, 1974.
- Hoffman, D. C., F. O. Lawrence, J. L. Mewherter, and F. M. Rourke, Detection of ^{244}Pu in nature, *Nature*, 234, 132–134, 1971.
- Keller, O. L., Jr., D. C. Hoffman, P. A. Penneman, and G. O. Choppin, Accomplishments and promise of transplutonium research, *Physics Today*, 37(3), 35–41, 1984.
- Märk, E. M., Pahl, M., and T. D. Märk, Fission track annealing behavior of apatite, *American Nuclear Society Transactions*, 15, 126–127, 1972.
- Nilsson, S. G., Introduction, *Physica Scripta*, 10A, 1–2, 1974.
- Podosek, F. A., and J. C. Huneke, Isotopic composition of ^{244}Pu fission xenon in meteorites: reevaluation using lunar spallation xenon systematics, *Earth and Planetary Science Letters*, 12, 73–82, 1971.
- Price, P. B., and R. M. Walker, Fossil tracks of charged particles in mica and the age of minerals, *Journal of Geophysical Research*, 68, 4847–4861, 1963.
- Randrup, J., S. E. Larsson, P. Möller, A. Sobiczewski, and A. Lukasiak, Theoretical estimates of spontaneous fission half-lives for superheavy elements based on the modified-oscillator model, *Physica Scripta*, 10A, 60–64, 1974.
- Ter-Akopian, G. M., J. H. Hamilton, Yu. Ts. Oganessian, A. V. Daniel, J. Kormicki, A. V. Ramayya, G. S. Popeko, B. R. S. Babu, A.-H. Lu,

- K. Butler-Moore, W.-C. Ma, S. Cwiok, S. W. Nazarewicz, K. K. S. D. Deng, J. Kilman, M. Morhac, J. D. Cole, R. Aryaeinejad, N. R. Johnson, I. Y. Lee, F. K. McGowan, and J. X. Saladin, New spontaneous fission mode for ^{252}Cf : indication of hyperdeformed $^{144,145,146}\text{Ba}$ at Scission, *Physical Review Letters*, 77, 32–35, 1996.
- Unik, J. P., J. E. Gindler, L. E. Glendenin, K. F. Flynn, A. Gorski, and R. K. Sjoblom, Fragment mass and kinetic energy distributions for fissioning systems ranging from mass 230 to 256, in *Proceedings of the Third Symposium on the Physics and Chemistry of Fission*, Rochester, 1973, International Atomic Energy Agency, New York, pp. 17–33, 1974.
- Wesolowski, J. J., W. John, and D. Nease, A search for superheavy elements in lunar material, in *Proceedings of the Second Lunar Science Conference*, Supplement 2, *Geochimica et Cosmochimica Acta*, vol. 2, edited by A. A. Levinson, pp. 1585–1589, Chemical and Isotope Analysis, Organic Chemistry, MIT Press, Cambridge, Massachusetts, 1971.

Accelerated Nuclear Decay: A Viable Hypothesis?

D. Russell Humphreys, Ph.D.*

Abstract. Geoscience and nuclear data strongly imply that “billions of years” worth of nuclear decay took place within thousands of years ago. To explain this, I propose that since Creation, one or more episodes occurred when nuclear decay rates were billions of times greater than today’s rates. Possibly there were three episodes: one in the early part of the Creation week, another between the Fall and the Flood, and the third during the year of the Genesis Flood. I outline the scientific and Biblical evidence for accelerated nuclear decay, investigate theoretical ways God may have chosen to cause the acceleration, review problems with this hypothesis, and offer preliminary scientific predictions to test it.

1. Introduction

In this chapter I offer scientific and Biblical evidence that atomic nuclei have decayed much faster in the past than they do today. This is a shocking idea today, since we have all been conditioned to think of radioactivity as immutable, one of the few constants in a world of change. To shatter that myth, let me point out a little-known fact: researchers have repeatedly changed nuclear decay rates in the laboratory.

For example, one survey of the scientific literature cites over two dozen experiments reporting changes in nuclear decay rates, changes caused by the chemical or physical environment of the decaying nuclei [*Hahn, Born and Kim, 1976*]. Such changes are not surprising to nuclear theorists, and the same survey reports over a score of theoretical studies predicting or explaining rate perturbations. A more recent experiment gives similar results [*Huh, 1999; Kerr, 1999*].

* Sandia National Laboratories, Albuquerque, New Mexico

Most of the rate changes cited were between a few tenths of a percent to a few percent, but several were greater than twenty percent. More recently, a researcher reported a change as high as forty percent [Reifenschweiler, 1994]. However, these human-produced rate changes are minuscule compared to the million-fold or greater acceleration of decay rates which (I will show below) is required by the evidence for a young earth. Therefore we should not be surprised if we find evidence that God has supernaturally intervened, either directly or indirectly, to produce such large changes.

For those who feel that allowing the possibility of God's intervention in the natural world is incompatible with science, let me point out several things which might broaden their definition of "science." First, if God has indeed so intervened, then all theories related to the results of that intervention must take account of it—if they are to be correct. It would thus be foolish to exclude *a priori* the possibility of God causing an acceleration of nuclear decay.

Second, there is nothing preventing us from looking for evidence in the natural world of the scientific consequences of accelerated decay. I will show below how observational data point strongly to accelerated decay in the recent past.

Third, if we can find hints about accelerated decay in Scripture, and Scriptural reasons for God to cause it, then our case is stronger. I will show such below. Fourth, if we can show several possible theoretical links in the chain of causation, from nuclear theory to the hand of God, that would also strengthen the case, especially if the chain leads to events recorded in Scripture. I will sketch that reasoning below.

This hypothesis of accelerated decay is not without problems, and I will discuss some below, as well as outlining possible solutions. The hypothesis is testable, the more so as we flesh out the theory. I will outline the type of predictions we would expect from the theory and the kind of tests we can make.

What I want to show in this paper is that accelerated nuclear decay is a good answer to the problems posed by geoscience and nuclear data. I will show that the data require it, Scripture suggests it, theory allows it, and observations can test it.

2. Much Nuclear Decay has Occurred

Some people suggest that God created daughter isotopes near parent nuclei to give an “apparent age” to rocks. One problem with that view is the *large variety* of decay effects involved. If we survey the wealth of nuclear geoscience data, it is difficult to escape the conclusion that large amounts of nuclear decay have occurred in the past—millions of times more than can be accounted for in 6000 years of decay at today’s rates. For me, one of the most compelling individual items of such evidence is the existence of mature radiohalos formed from ^{238}U -decay.

Figure 1 shows such a halo in a crystal of mica. As Chapter 8 explains in more detail, the ring-like halos are discolorations produced by α -particles (He nuclei) emitted by decaying nuclei in a tiny grain, the radiocenter, at the common center of the halos. Each of the rings requires at least 5×10^7 α -decays to form it fully [Gentry, 1973, pp. 350, 360]. A typical one-micron radiocenter contains up to 5×10^9 members of the ^{238}U -decay chain (reasoning from Po halo data) [Gentry, 1974, p. 63]. The innermost ring comes from the α -decay of ^{238}U , which presently has a half-life of 4.47 billion years. For five billion of those U nuclei to undergo fifty million α -decays would require, at the present rate of decay, over 150 million years. Thus these halos are visible marks of decay, direct evidence for at least “hundreds of millions” of years worth of

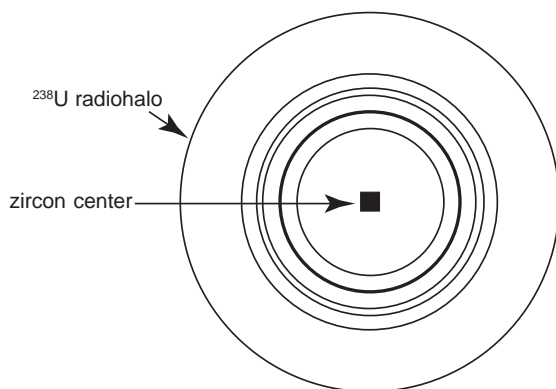


Figure 1. Mature ^{238}U radiohalo with all eight rings produced by α -particles.

nuclear decay.

Moreover, ion microprobe studies of the radiocenters show the amounts of daughter isotopes we would expect from ^{238}U -decay, particularly ^{206}Pb , the particular isotope of Pb produced by the ^{238}U -decay chain. Larger (~100 micron) crystals of one type of radiocenter material, zircon (zirconium silicate), retain the right order of magnitude of ^4He atoms we would expect from the amount of α -decay, since α -particles are He nuclei. Thus we seem to have on hand the actual α -particles of the decays!

The zircons also contain many, if not all, of the fifteen isotopes in the ^{238}U -decay chain, namely, ^{238}U , ^{234}Th , ^{234}Pa , ^{234}U , ^{230}Th , ^{226}Ra , ^{222}Rn , ^{218}Po , ^{214}Pb , ^{214}Bi , ^{214}Po , ^{210}Pb , ^{210}Bi , ^{210}Po , and finally ^{206}Pb [*Gentry et al.*, 1973]. The multiple rings in radiohalos also testify to the presence of these isotopes. It is difficult to conceive of non-nuclear scenarios which would, all over the world, insert the necessary isotopes into all the microscopic radiocenters and zircons in approximately the right proportions. Thus the radioisotopes in these items offer strongly supporting evidence for at least “hundreds of millions” of years worth of nuclear decay.

There is also nuclear fission to consider. Fission is very similar to α -decay, except that the emitted particle is much larger, roughly half the mass of the parent nucleus. For more details see Chapter 6, Sections 4 and 5. When a nucleus embedded in a rock crystal splits, the resulting two fission fragments move violently away from each other, tearing up the crystal lattice. The resulting damage to the lattice is great, and thus easy to detect. The usual technique is to apply a suitable solvent to the surface of the crystal, which etches the damaged parts preferentially. Then the researcher inspects the surface under a microscope, looking for the characteristic tracks. Even for the slow rate of spontaneous (not triggered by neutrons) fission of ^{238}U , there are enough such atoms to produce a large number of tracks. A creationist study of Miocene volcanic glass shows thousands of times more fission tracks than could be accounted for by spontaneous ^{238}U fission in thousands of years at today's rates [*Bielecki*, 1994]. Thus fission tracks seem to be visible evidence for “millions” of years worth of decay by nuclear fission.

As Chapter 3, Section 11 shows, another by-product of nuclear decay is heat. As the decay particles slow to a stop in the surrounding rock,

they heat it up. This heat normally takes a long time to leave its place of origin (millions of years to go hundreds of meters), since rocks conduct heat only slowly. Geoscientists have long known that heat flow from the earth's surface is closely correlated with the amount of radioactivity in the rocks near or at the surface; the more radioactivity, the greater the heat flow [*Lachenbruch*, 1970]. The amount of heat flow is consistent with “millions” of years worth of nuclear decay at today's rates.

Thus we observe a wide spectrum of nuclear decay effects: (1) daughter isotopes along the whole decay chain, (2) visible scars (halos) from α -decay, (3) the α -particles themselves (He nuclei), (4) visible tracks from decay by fission, and (5) the heat produced by nuclear decay. The most reasonable hypothesis is that all these products of nuclear decay were indeed produced by nuclear decay! But the amounts of those products we observe are much greater than thousands of years could produce—at today's rates.

3. Little Time for the Decay to Occur

One response to the data above is the evolutionist interpretation: the earth is old enough for all the nuclear decay to have occurred at today's rates. But that approach ignores the large amount of evidence against an old earth, both Biblical and scientific.

The Biblical evidence for a young earth seems very clear. Not only is there strong evidence in Genesis, but also throughout the rest of Scripture. Table 1 lists some of those Scriptures.

Some of these items, such as numbers 4 and 5, are very clear and direct. But others are less direct and need some explanation. The verses of items 3 and 13 describe a global cataclysm whose logical consequence would be to produce most of the fossil-bearing geologic strata [*Whitcomb and Morris*, 1961], thus casting doubt on the whole idea of “geologic ages.” The verses of item 6 imply (but, I acknowledge, do not absolutely require) that there was essentially no time between God's commands and their results, thus making His creating much more awesome (verse 8) than a slow process taking billions of years.

In the verse of item 9, Christ was referring to Genesis 1:1, “From the

Table 1. Biblical evidence for a young world.

Item	Verse	Comments
1	Genesis 1:5	God's definition of the word "day" in the context of Genesis 1
2	Genesis 1:1–2:3	21 times: day + number, evening/morning, day/night, days, etc.
3	Genesis 6:13–8:19	Consequences of worldwide Flood eliminate "geologic ages"
4	Exodus 20:11	Universe created in six ordinary days of the week
5	Exodus 31:17	Universe created in six ordinary days of the week
6	Psalms 33:6–9	Implies Creation happened as fast as God spoke
7	Matthew 19:4	Implies man has been here since the beginning of Creation
8	Matthew 24:21	Implies tribulations occur since the beginning of the world
9	Mark 10:6	Implies man has been here since the beginning of Creation
10	Luke 11:50	Implies human bloodshed near the foundation of the world
11	John 8:44	Implies murder occurred near the beginning
12	Romans 1:20	Implies God's power seen by men for most of world history
13	II Peter 3:6	Consequences of worldwide Flood eliminate "geologic ages"
14	Whole Bible	Total absence of positive verses for billions of years

beginning of creation . . .," and to Genesis 1:26 ". . . God made them male and female." Those two events occurred on days one and six. By putting them together under the general heading "the beginning," Christ is strongly implying that the time between the two events was short compared to the thousands of years which have elapsed since Adam. That leaves no room for the evolutionary view, that billions of years elapsed between the beginning of the cosmos and the relatively recent advent of mankind. Items 7, 8, 10, 11, and 12 use similar reasoning. That is, the verses they cite all suggest that mankind has been around for nearly the entire history of the universe.

Item 14 points out the fact that old-earthers have no verse as explicit as Exodus 20:11 and its context. The verses they cite are indirect and have simple alternative interpretations. (For example, in II Peter 3:8, the word "as" means "similar to," not "equal to".) Since the Israelites were familiar with long-age mythologies (such as that of the Egyptians) and had suitable words in their own language, God would not have shocked them if he had told them clearly the world was billions (in Hebrew, "hundreds of thousands of myriads") of years old. That He did so nowhere in His Word weighs against an old world, especially when contrasted

Table 2. Scientific evidence for a young world.

Item	Description	Reference
1	Sodium is deposited in the sea rapidly	<i>Austin and Humphreys</i> [1990]
2	Tight folds and clastic dikes formed rapidly	<i>Austin and Morris</i> [1986]
3	“Squashed” radiohalos show fast deposition	<i>Gentry</i> [1992, pp. 53–58]
4	Earth’s magnetic field loses energy rapidly	<i>Humphreys</i> [1990, p. 138]
5	Sediment accumulates on seafloors rapidly	<i>Vardiman</i> [1995]
6	Polystrate fossils show deposition was rapid	<i>Morris</i> [1994, pp. 100–102]
7	Features on strata surfaces show rapid burial	<i>Morris</i> [1994, pp. 94–100]
8	History started recently	<i>Morris</i> [1994, pp. 69–70]
9	Human population grows very rapidly	<i>Morris</i> [1994, pp. 70–71]
10	Scarcity of stone-age graves shows short times	<i>Morris</i> [1994, p. 71]
11	Fossil “graveyards” show rapid burial	<i>Whitcomb and Morris</i> [1961]
12	Small Pb diffusion shows recentness of strata	<i>Gentry et al.</i> [1982a]
13	Small He diffusion shows recentness of strata	<i>Gentry et al.</i> [1982b]
14	Scarcity of radiogenic He in air shows youth	<i>Vardiman</i> [1990]

with all the verses supporting a young world.

The geoscience evidence for a young earth is also very strong, as creationists have been showing for many years. Table 2 shows just a few of the many possible examples of such evidence.

Creationists have produced large lists of such evidence [*Morris*, 1974; *Brown*, 1995, pp. 19–36]. These data are at least as numerous and weighty, and more varied, than old-earth evidence. We cannot ignore such a large body of evidence for a young world, because a truly scientific explanation must include *all* the data relevant to the age issue.

4. Biology Seems to Allow Fast Decay Only at Certain Times

According to Section 2 a large amount of nuclear decay has occurred, and according to the evidence in Section 3 the time for it to occur was brief. Therefore nuclear decay must have been accelerated sometime in the past. Using the usual 4.5 billion year radiometric age of the earth as an estimate of the maximum amount of decay observed, and the 6000-year Biblical age for the actual time available, we get an average acceleration factor α :

$$\alpha = \frac{4.5 \times 10^9 \text{ radiometric years}}{6 \times 10^3 \text{ real years}} = 7.5 \times 10^5 \quad (1)$$

That is, on the average, the decay rates had to be about 750,000 times greater than today's rates to accomplish the observed amount of decay. If the periods of accelerated decay were much shorter than 6000 years, the peak acceleration factor would be much greater than the average above.

If we spread out the acceleration uniformly over almost all the 6000 years, there would be severe consequences for living creatures. At today's low decay rates, the background dose most creatures on earth receive from radioactivity in the environment (not counting cosmic rays and man-made sources) is about 2.6 milliSieverts per year [*Schleien et al.*, 1998, pp. 1–4]. (1 milliSievert = 100 millirem.) Equation (1) means that, during the 6000 years of accelerated nuclear decay, living creatures would receive nearly 2000 Sieverts per year. Such a level would kill humans within weeks [*Schleien et al.*, 1998, pp. 15–4].

However, there are three periods in the earth's history when radioactivity in the earth's crust might not have harmed living creatures:

- From the first instant of Creation to, say, midway into the third day. During that period, God had not yet created any plants or animals.
- During the 1656 years which elapsed from Creation, or the Fall of man, to the Genesis Flood—*provided* that during that time all the naturally-occurring radioactive elements were deep within the earth's crust and not accessible to life at the surface of the earth. The decay rates would have to be below the intensities at which they would cause life-extinguishing geologic upheavals at the surface.
- During the year of the Genesis Flood, when over a mile of water shielded the ark from radioactive rocks below, and the thick walls of the ark would shield the creatures within from any radioactive elements leaching from the rocks below into the waters outside the ark. In a section below I will present reasons for thinking that during the Flood there were very few radioactive atoms in the tissues of the creatures themselves.

Figure 2 shows these three periods and approximate decay rates relative to today's rates.

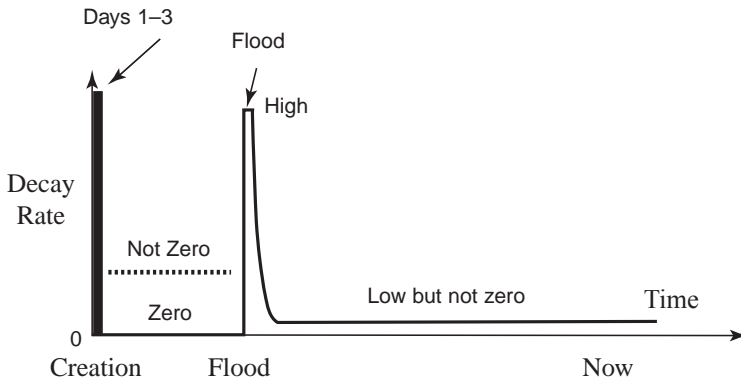


Figure 2. Possible history of nuclear decay rates, showing several possible episodes of accelerated rates during: (1) early Creation week, (2) the 1656 years between Creation and the Genesis Flood, and (3) the year of the Genesis Flood. The vertical scale is compressed logarithmically.

5. Fast Decay Explains both Trend and Deviations in Data

Figure 3 plots published radioisotopic ages of samples from Phanerozoic (fossil-bearing) strata versus the accepted biostratigraphic (fossil-determined) ages for each sample [Woodmorappe, 1979]. The dotted line shows where each point would fall if its radioisotopic and stratigraphic ages were equal. Although the creationist who collated these data did so to show how often the radioisotopic ages deviate from the line, and how large the deviations can be, we still see an overall trend. How can we explain both the trend and large deviations?

One very common creationist explanation of the trend is that evolutionists either knowingly or unknowingly filter the data, thus imposing an artificial trend on the data. This could happen either by informing the radioisotopic laboratories what the approximate “right age” should be, or by simply not publishing highly deviant data—things we know do happen [Woodmorappe, 1999; Snelling, Chapter 5 of this book]. According to this view, if *all* the data were plotted in the same way as Figure 3, we would not see a trend at all, but simply a random scattering of points all over the graph. The deviations would then simply

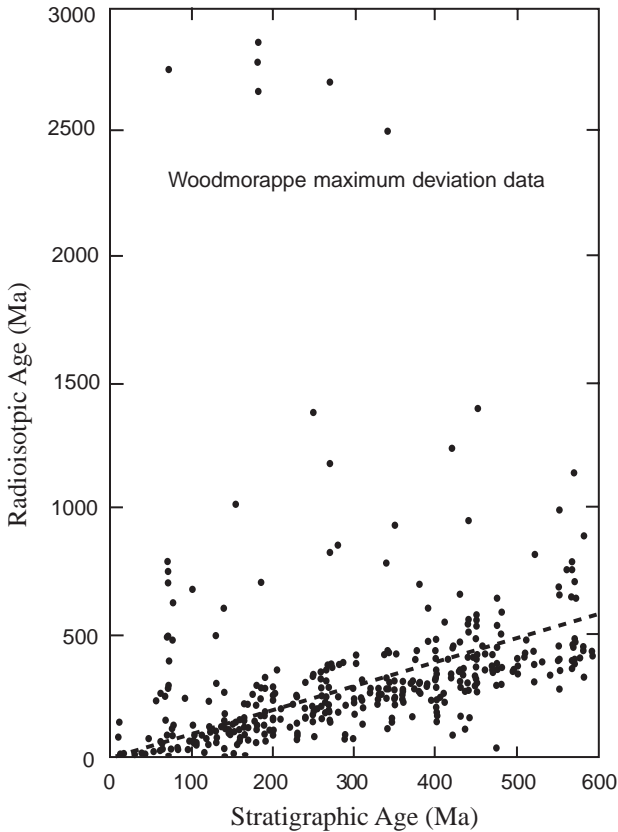


Figure 3. Published radioisotopic ages of samples related to their published age according to geologic stratum. Selected for their deviations from the dotted line [Woodmorappe, 1979], these points nonetheless show a clear trend, as well as large deviations from the trend.

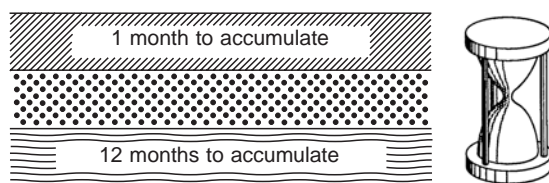
be published by more honest researchers who were willing to let the data fall where they may.

Attractive as this explanation may be for some people, I have one problem with it: how did the radioisotopic timescale get established in the first place? For example, how did geoscientists come to a consensus that Cambrian strata ought to be between 500 and 600 million years old? If I understand the history of that question correctly, there was no consensus on a timescale until the first crude (no isotopic separation)

U-Pb dates were done around the turn of this century [Holmes, 1911]. Those measurements gave approximately the same timescale we have today. If other radioisotopic observations had resulted in greatly different dates, my impression is that researchers of that time would be under no particular ideological pressure to make their dates conform to one scale or another. The fact that a consensus emerged before such pressure would exist supports the existence of a trend.

Is there a real trend or not? Several approaches could resolve this question. One would be a historical study. How widely did timescales vary before radioisotopic dating? In the early years, were there ideological pressures to conform to one particular scale? Were there dissenters? The second way is to collect our own samples, submit them to radioisotopic laboratories without bias, and publish *all* the results. Steve Austin and Andrew Snelling are doing just that (see Chapter 4), but it will be a long and expensive process before we have enough data.

The point I want to make is this: if an acceleration of decay rates did occur, I would expect the data to look like Figure 3. There would be both a general trend and many large deviations from that trend. Figure 4 suggests why. Just for simplicity, imagine that all decay rates were exactly a half-billion times higher than normal for exactly twelve months during the Genesis Flood, afterwards dropping down to today's rates. A lava



Deeper layers give “older” dates

Figure 4. Lava flows deposited at different times during the year of the Genesis Flood would experience different amounts of accelerated nuclear decay. The flow shown at the bottom would accumulate decay products for nearly twelve months, whereas the flow near the top would accumulate decay products for less than one month. As interpreted normally, this would cause the radiometric ages of the two strata to differ by nearly “460 million years”.

flow laid down at the end of the first month of the Flood would be near the bottom of the fossil strata. It would undergo eleven months of the accelerated decay, and it would accumulate “460 million years” worth of decay products.

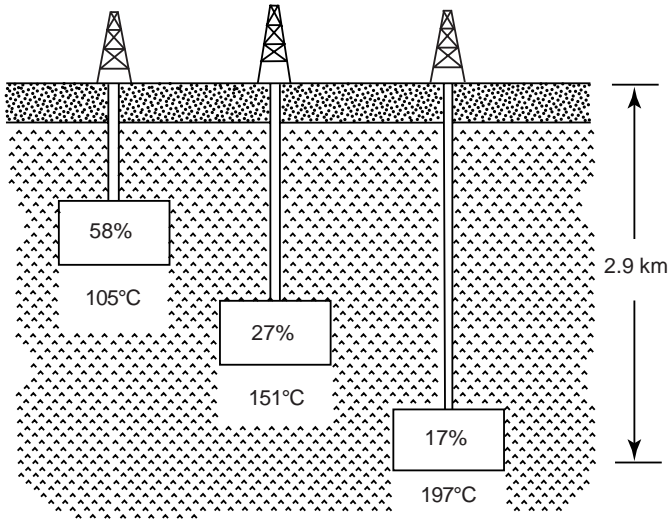
Another lava flow occurring at the beginning of the last month of the Flood would be near the top of the strata. It would have only one month of accelerated decay left to it, so it would accumulate “42 million years” worth of decay products. Thus the upper strata would be radiometrically much younger than the deeper strata; there would be a trend of radioisotopic age with depth, and thus with biostratigraphy. The difference in radioisotopic ages from top to bottom would be “500 million years,” but the true age difference would only be one year.

In summary, nuclear decay acceleration would cause a general trend in the data. See Don DeYoung’s analysis in Chapter 2, Section 5. Radioisotopic dates would then generally reflect the order and timing of events during the Genesis Flood. But the timescale would shrink from megayears down to months!

The rapidity of events would also cause large scatter in the data. The usual assumption in radioisotopic dating is that rock formation happens slowly enough to reset the radioisotopic “clocks” to zero. For example, lava flowing from deep underground over many years might separate concentrations of ^{40}K from concentrations of its daughter isotope, ^{40}Ar , before it finally cools and hardens into basalt. But if things happened quickly, that assumption could be incorrect in many cases. For example, a lava flow at the top of Grand Canyon might show similar radioisotopic ages as its possible parent body near the bottom of the canyon, just as recent research demonstrates [Austin, 1994, pp. 120–126]. So the accelerated decay hypothesis leads us to expect large, and possibly frequent, deviations from the general trend, just as Figure 3 shows.

6. Helium Retention Supports Fast Nuclear Decay

One of the strongest pieces of evidence I know of for accelerated decay is the high retention of radiogenic ^4He in microscopic zircons. Figure 5 summarizes the data [Gentry *et al.*, 1982b]. These zircons, about 75



Jemez Caldera, Fenton Lake, New Mexico
 Precambrian basement granodiorite
 Zircons in biotite
 1.5 billion years Pb/Pb

Figure 5. Zircons in a Precambrian granitic formation retain unusually high amounts of radiogenic He [Gentry, *et al.*, 1982b], suggesting accelerated nuclear decay within thousands of years ago.

microns long, are embedded in crystals of biotite (black mica). In turn, the biotite is embedded in hot Precambrian basement granodiorite (granitic rock) below the Jemez volcanic caldera near Los Alamos, New Mexico. Radioisotopic (Pb-Pb) dating of zircons recovered from deep boreholes in the formation give an age of “1.5 billion years” [Zartman, 1979].

The surprising thing is this: although these zircons are tiny and were in hot rock, they have retained *very large percentages* of the ^4He which the radioactive atoms in the zircons would have emitted by α -decay at normal rates over the alleged 1.5 billion years, as Table 3 shows. This is surprising to evolutionists because, over a billion years, they would expect most of the He to escape such small zircons by diffusion (He atoms wriggling through the crystal lattice), especially at high temperatures.

Table 3. Helium retention in Jemez zircons [*Gentry et al.*, 1982b].

Depth (km)	Temperature (°C)	Helium (cc/kg)	Retention (%)
0.96	105	86	58
2.17	151	36	27
2.90	197	28	17
3.50	239	0.76	1.2
3.93	277	~0.2	~0.1

Diffusion rates of radiogenic He through *bare* zircons, not embedded in other crystals, have been measured, as Figure 6 shows [*Magomedov*, 1970]. Those rates are too fast to retain the He for more than a few decades even at room temperatures. However, the biotite crystals in which the Jemez zircons were embedded could “bottle up” the He in the zircons, causing longer retention times. So the real question is: how fast does He diffuse through biotite?

Unfortunately, I have found no measurement in the literature of He diffusion in biotite. However, there are measurements of *argon* diffusion in biotite, at least for high temperatures [*Grove and Harrison*, 1996]. Like He, Ar is a noble gas which does not chemically bond to other atoms. Argon atoms are larger and heavier than He atoms, so we would expect He to diffuse through a given material faster than Ar. That is, we can scale diffusion rates in any given mineral from the size and mass of the diffusing atoms [*Fortier and Gilletti*, 1989]. Argon and helium measurements on other materials support such scaling [*Carrol*, 1991]. From those data we can very roughly extrapolate the Ar-in-biotite data to He-in-biotite, getting a band of estimated He diffusion rates for biotite.

We can then compare the scaled He-in-biotite rates to two simple models for the Jemez He retention:

- *Evolution model*—steady low-rate radioactive decay, He production, and He diffusion for 1.5 billion years at today’s temperatures in the formation.
- *Creation model*—a short burst of high-rate radioactive decay and He production, followed by 6000 years of He diffusion at today’s temperatures in the formation.

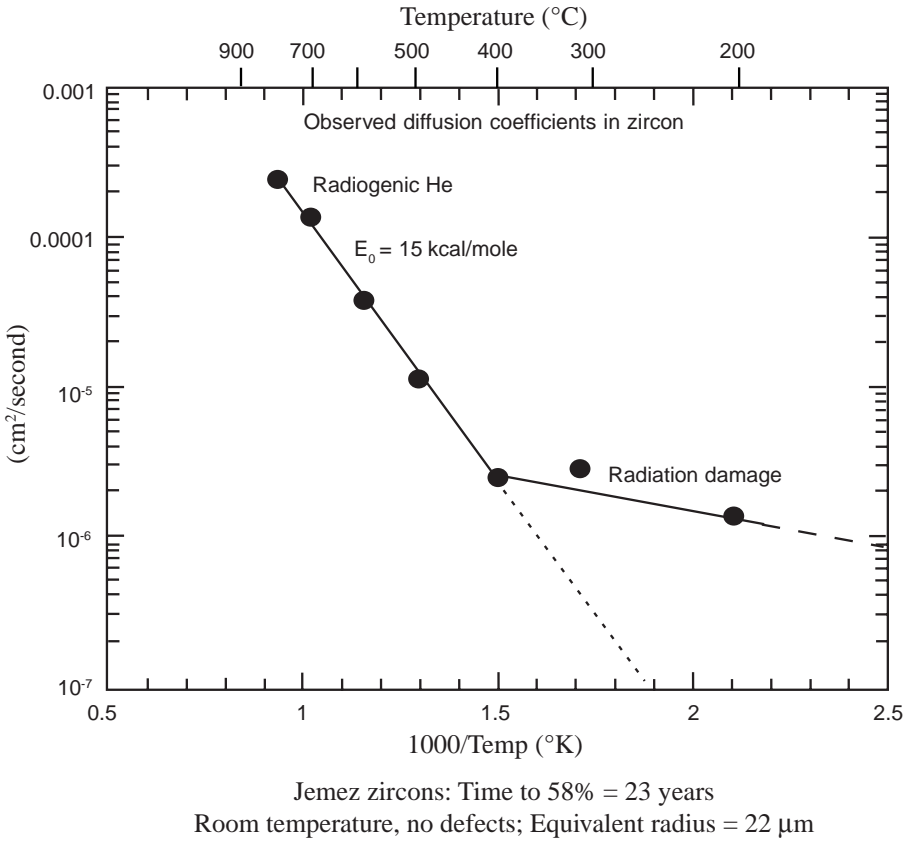


Figure 6. Helium diffuses very rapidly, within decades, out of bare zircons not embedded in biotite crystals [after *Magomedov*, 1970]. That suggests the surrounding biotite was the main restraint upon He diffusion out of the Jemez zircons.

Next we can plug each of these models into the well-understood equations for diffusion [*Carslaw and Jaeger*, 1959, pp. 234–235]. For simplicity, I assume the zircons to be He-filled spherical cavities in the biotite. The cavity diameters are 44 microns, to match the surface areas of the zircons. Then for each temperature, I calculate what diffusion coefficient in the biotite is necessary to get the observed percent He retention in the zircons during the time allotted by each of the two models. Figure 7 exhibits the calculated model-required diffusion coefficients

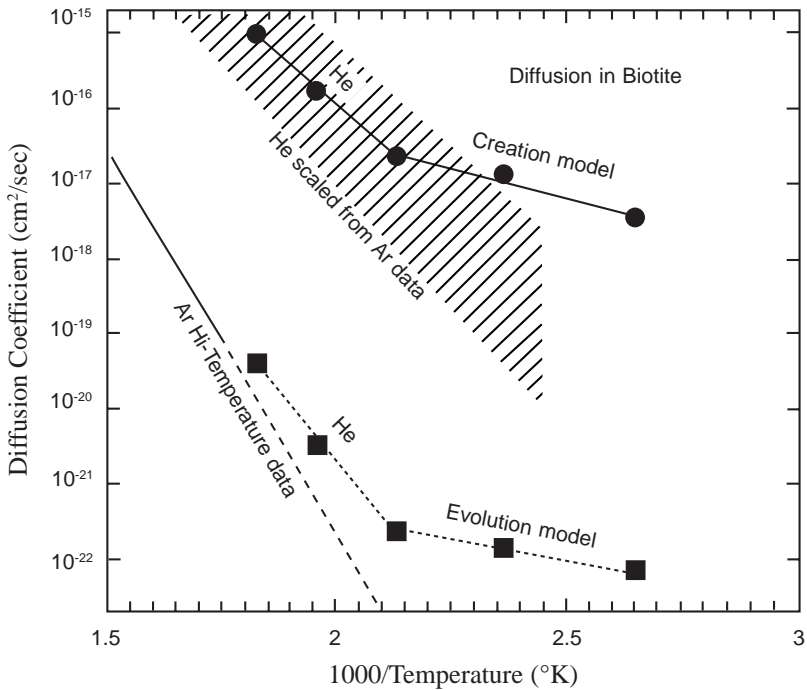


Figure 7. Predictions of yet-future experiments on He diffusion through biotite, using the observed He retention in Jemez zircons in two very different theoretical models. An evolutionist model (gigayear timescale) predicts the line with square points. A creationist model (kiloyear timescale) predicts the line with round points. The solid line shows experimentally-measured Ar diffusion in biotite [*Grove and Harrison, 1996*], extrapolated down by the dashed line from high temperatures to these temperatures. Rough extrapolations from those data using He and Ar diffusion observed in other minerals [*Carroll, 1991; Lippolt and Weigel, 1988*] suggest that the He-in-biotite measurements will fall into the shaded band shown. Thus He diffusion measurements in biotite are likely to reject the evolutionist model and confirm the creationist model.

and their dependence on temperature. The small squares and finely dotted line show the He diffusion rates in biotite *required* by the evolution model to get the observed Jemez He retentions. The small filled circles and solid line show the He-in-biotite rates *required* by the Creation model to get the observed He retentions. The solid line at the left shows the

observed high-temperature data for Ar in biotite. The dashed line joined to the solid line qualitatively shows the expected behavior of the low-temperature Ar data, excluding the effect of defects and impurities, which would reduce the slope of the right-hand part of the dashed line [Girifalco, 1964, p. 102]. The shaded band shows the estimated He-in-biotite rates roughly scaled (as mentioned above) from the Ar-in-biotite data, and the Ar/He data in other minerals, especially muscovite [Lippolt and Weigel, 1988].

The exciting thing about Figure 7 is this: the shaded band overlaps the Creation model and is far above the evolution model. That is, our estimates of what the experimental He-in-biotite rates should be are entirely consistent with a burst of accelerated nuclear decay only thousands of years ago. Moreover, the estimates exclude, by many orders of magnitude, the evolution model. That is, if the formation were really 1.5 billion years old, most of the He should have diffused out of the zircons.

Of course, estimates are not as good as experiments. I propose that careful experimental measurements be done on He diffusion in the actual Jemez biotites. We can take the “He Creation Model” line in Figure 7 as an approximate *prediction* of what the experimental results would be if accelerated decay occurred. I say “approximate” because my Creation model is very simple. For example, it does not take account of possible changes in the formation temperature with time, nor does it take into account that the time since the burst of decay might be only 4300 years (from the Flood) instead of 6000 years (from Creation). But I would expect the simple Creation model to be within an order of magnitude of future experimental results if the accelerated decay hypothesis is correct.

The evolution model I have used is also very simple; for example, it also does not account for temperature variations in the formation. But since the evolution model differs from the estimated He-in-biotite rates by four to five orders of magnitude, I seriously doubt whether any clever patches on the model could ever bring it into agreement with the shaded area.

Figure 7 shows a clear difference between evolutionist and creationist predictions, one which a well-performed experiment could resolve

decisively. Future theoretical and experimental results on Ar-to-He scaling could also shed more light. In the meantime we have every reason to be optimistic. We could summarize the He retention data as follows:

- Over a billion years worth of nuclear decay occurred within thousands of years ago!
- Accelerated nuclear decay appears to explain the above summary very well.

7. Other Data Support the Helium Retention Data

Several other lines of evidence are in good accord with the He retention data, thus strengthening the case for accelerated decay. One of these is the scarcity of radiogenic ^4He in the earth's atmosphere [*Vardiman*, 1990]. Even after accounting for the slow rate of escape of He from the atmosphere into space, there is far less He in the air than we would expect after billions of years of nuclear decay in the crust. One simple calculation in the secular literature, which as far as I know has not been refuted in over four decades, indicates that the atmosphere contains less than 0.01% of the ^4He evolutionists would expect after ~5 billion years [*Cook*, 1957]. It appears from Section 6 that much of the He has not had time to even leave the zircons where it originated, much less move up through the crust into the air. The scarcity of He in the atmosphere and the excess of it in the zircons work together to support the case that large amounts of nuclear decay have occurred while only thousands of years have elapsed.

Studies of Pb diffusion from the Jemez zircons give similar results as the He diffusion study [*Gentry et al.*, 1982a; *Gentry*, 1992, pp. 257–260, 340–352]. In particular, if we extend Gentry's diffusion calculation [*Gentry et al.*, 1982a, p. 298, note 16] down to the deepest and hottest sample (313°C), we find at that temperature most of the radiogenic Pb would diffuse out of a bare zircon of this small size in only a few hundred thousand years. Yet the deepest samples still retained essentially all their Pb. Our only problem is that the calculation does not include the “bottling” effect of the biotite, so we need to do calculations on Pb diffusion in biotite to be certain of its agreement with the He

retention.

Other evidences for accelerated decay are the famous “orphan” Po radiohalos: ^{218}Po , ^{214}Po , and ^{210}Po radiohalos with no rings from any parent isotopes [Gentry, 1992, pp. 36–31]. If the Po was not created instantaneously in solid rock, then according to one hypothesis, the orphan halos suggest drastic changes in nuclear decay rates [Humphreys, 1986].

8. Deuteronomy Suggests God Kindled Nuclear Fire

Several Scriptures offer support for the idea of accelerated nuclear decay. My favorite is Deuteronomy 32:22. There God said, through Moses, the following to the people of Israel gathered on the plains of Moab, just before they were to cross the Jordan river:

*“For a fire **has been kindled** in My anger,
And burns to the lowest Sheol,
And consumes the earth with its yield,
And sets on fire the **foundations of the mountains.**”*

The translation above [Young, 1898, p. 143; Green, 1979, vol. 1, p. 550] clarifies the verb tenses. In the Hebrew text, the first verb, “has been kindled” [קדַח *qadach*, to break out, ignite], is in the perfect tense, which generally refers to action completed before the time of reference. The last three verbs, “burn,” “consume,” and “set on fire,” are all in the imperfect tense. With the word “and” [וַ *waw*] preceding them, they refer to consequences of the first verb action which are still continuing at the time of reference [Yates, 1938, p. 104; Weingreen, 1959, pp. 90–91]. The context suggests that the time of reference was the time when Moses was speaking. So the first verb suggests that at some time before Moses’ speech God kindled a fire [עֵשׂ *esh*]. Then at the time of Moses’ speech this fire was in the process of burning, consuming, and setting on fire.

Many people might assume the verse above is only a metaphor, that God was not referring to a literal fire. I prefer not to make such an assumption automatically, for the simple reason that from other verses I have learned interesting new scientific facts by looking for a

straightforward meaning first [*Humphreys*, 1994, pp. 55–57]. Furthermore, this particular passage uses five different Hebrew words related to “fire” or “burning,” thus putting a major emphasis on that concept.

Seeking a straightforward meaning, then, what kind of fire could God mean? Consider what the fire does. First, it is burning [יָקַדַּ *yaqad*] down to the lowest part of the earth, if we take Sheol as a physical location [Numbers 16:30–33, Amos 9:2]. Second, it is consuming [אָכַל *akal*, to eat] the earth with its yield [יָבוּל *y^evul*, produce of the soil]. Since the earth and its produce still exist today, the fire has not completely destroyed them.

Third, it sets on fire [לָהַט *lahat*, to devour, scorch] the foundations of the mountains. This is very significant, since geoscientists today have much evidence that the roots of the mountains, deep within the earth’s continental crust, are heated by *nuclear decay*. For example, volcanoes, fed by magma from deeper parts of the crust, release large amounts of radioactive ²²²Rn gas, one of the isotopes in the ²³⁸U decay chain. This suggests that the “fire” in Deuteronomy 32:22 is *heat from nuclear decay*.

Such heat is indeed scorching the whole earth down to its center, and it produces microscopic but significant damage to living creatures and plants which presently contain radioactive atoms. And yet neither the earth nor its biological produce are completely destroyed by this fire of nuclear decay; it merely eats away at them. Taken straightforwardly, the verse is a graphic and accurate picture of the effects of nuclear decay.

Note carefully that this nuclear fire was “kindled” at some time in Moses’ past. That implies there was a time before the igniting when the fire had not been burning. At that time nuclei would be entirely stable, not decaying. Then at some specific time, nuclei began decaying. This switch from zero to non-zero rates is an *infinite* percentage change—quite a drastic acceleration of nuclear decay!

9. Scripture Hints at a Decay Speedup During the Genesis Flood

Psalm 18:7–8 (NAS) suggests one occasion when God kindled the

nuclear fires:

*“Then the earth shook and quaked;
And the **foundations of the mountains** were trembling
And were shaken, because He was angry.
Smoke went up out of His nostrils,
And **fire** from his mouth devoured;
Coals were kindled by it.”*

Second Samuel 22 is almost identical to Psalm 18, and the above passage is almost identical to II Samuel 22:8–9. This two-fold repetition by the true Author of Scripture, the Spirit of God, suggests that this magnificent song contains important information. David is the human author, and at first the psalm appears to reflect his personal experience. However, verses 7–8 (above) and 11–16 (below) appear to refer to much more cataclysmic events than ever occurred in David’s life:

*“Darkness of waters, thick clouds of the skies
. . . thick clouds . . . hailstones and coals of fire.
The LORD also thundered in the heavens . . .
Hailstones and coals of fire.
And lightning flashes in abundance . . .
Then the **channels of water** appeared,
And the **foundations of the world** were laid bare . . .
He sent from on high, He took me;
He drew me out of **many waters**.” [Psalm 18:11–16]*

While these are undoubtedly metaphors for David’s real experiences, and also prophetic allusions to the future experiences of Jesus Christ [Gaebelein, 1965, p. 84], the metaphors and allusions appear to be built on past physical manifestations of God’s great power. The biggest such event which fits is the Genesis Flood.

Another suggestive passage is Habakkuk 3:8–10, 15 (NAS):

*“Did the LORD rage against [lit. **burn in**] the rivers,
Or was Thine anger against the rivers,
Or was Thy wrath against the sea . . .
Thou didst **cleave the earth** with rivers.
The mountains saw Thee and quaked;
The **downpour of waters** swept by.*

*The deep uttered forth its voice;
It lifted high its hands . . .
Thou didst tread on the sea with Thy horses,
On the surge of many waters.”*

Caveat: In contrast to most of the items in Table 1, the passages in this section are not Hebrew prose, but rather are poetry. While understanding the colorful and dramatic images of such passages is often tricky, I take these Scriptures as a hint—certainly not as an iron-clad requirement—that the Genesis Flood was at least one occasion when God kindled nuclear fire which shook the foundations of the mountains and caused other cataclysmic events. If these passages don’t help you, just ignore them.

10. The New Testament Also Suggests Nuclear Decay Changes

For those who feel more comfortable with the familiar New Testament than with the oft-neglected Old Testament, we can study the words of the apostle Peter. After discussing the former heavens and earth which were created by the word of God and then destroyed during the Genesis Flood, Peter says in II Peter 3:7(NAS):

*“But the present heavens and earth by His word **are being reserved for fire . . .**”*

A more literal translation of the emphasized words would say that the present heavens and earth “having been stored up, are [on, with, to] fire,” since the Greek text has no preposition here and the word translated “fire” [πυρ *pur*, as in pyre] is in the dative case. One scholar gives the following exegesis of the passage [*Wuest*, 1972, pp. 68–69] “. . . the deposit of fire with which they were stored resides in them as a permanent deposit.”

This suggests that in destroying the antediluvian world, God somehow stored up “fire” in the heavens and the earth. A few verses later we find a clue as to how:

*“. . . looking for and hastening the coming of the day of God, on account of which the heavens will be destroyed by burning and **the elements will melt with intense heat!**”* [II Peter 3:12, NAS]

Surprisingly, it turns out that the Greek verb translated “will melt” [τήκω *teko*, to make liquid] in the emphasized phrase above is actually in the *present* tense [Thayer, 1889, p. 621]. To repeat:

- The verb for “melt” above is not future but *present* tense.

It differs from the preceding verb “will be destroyed,” which is indeed future tense in the Greek. The verb for “melt” is also in the passive voice. I would translate the phrase as, “. . . the elements, being feverishly hot, are being melted [right now]!” A well-known Bible scholar also translates the phrase in the present tense [Wuest, 1972, p. 74]: “. . . the elements burning up are being melted.”

I am emphasizing this phrase because it relates to nuclear decay. The word translated “elements” [στοιχείον *stoicheion*, member of a series] includes the meaning the Greek philosophers would have assigned to it: “the elements from which all things have come, the material causes of the universe” [Thayer, 1889, p. 589]. Here it implies the basic building blocks of the physical world, the elementary particles, nuclei, and atoms which constitute a well-ordered series, the periodic table of the elements. At the time Peter wrote, these elements were hot and *being melted*. This is a very appropriate word picture of the nuclei of atoms, which the well-known “liquid drop” model says are like a liquid [Roy and Nigam, 1967, pp. 166–172]. The measured temperatures of these tiny drops of molten matter are between 2 and 6 *billion* degrees Kelvin [Melby *et al.*, 1999]. Nuclei are thermodynamically isolated from the atomic and molecular world around them, so their high temperatures usually don’t affect us.

Also notice that II Peter 3:12 ascribes the molten condition of the elements to the *present* heavens and earth, not to the previous world before the Genesis Flood. This implies that at some time before the Genesis Flood, all atomic nuclei were stable. Using the language of thermodynamics, perhaps at that time all nuclei were in a solid state, like tiny crystals. Then God changed things, and now the nuclei are molten drops of hot liquid. Some of them have temperatures near their boiling point, so they occasionally evaporate particles—which is the process of nuclear decay.

We usually think of melting things by adding energy to raise their

temperature. However, another way is to lower the melting point, such as by using salt to melt ice. A change in nuclear forces could similarly lower the melting points of nuclei.

Going back to the seventh verse, notice that this change in nuclei applies to the *heavens* as well as the earth. It was not just a local change in the vicinity of the earth; it affected the whole cosmos.

We should not be reluctant to attribute technical accuracy to these verses, since the Spirit of God, whom Peter himself says moved the writers of Scripture [II Peter 1:21], is the Creator who designed the nuclei and the laws governing them! He is fully entitled to change the decay rates, as this passage and the previous passages appear to imply.

11. Did God Change Nuclear Decay to Change the World?

People often ask at this point, “Why would God change decay rates?” Some seem to feel the only reason to do such would be to confuse the interpreters of nuclear data. But “God is not the author of confusion” [I Corinthians 14:33], and it appears He had much better reasons for His actions.

First of all, nuclear decay is a very important energy source within the interiors of planets, and in their crusts. Heat controls the viscosity and buoyancy of various rock layers in the earth. An abrupt increase of radioactivity could well have triggered the cataclysmic tectonic events which resulted in the Genesis Flood [*Baumgardner*, 1994]. Thus, nuclear decay acceleration could be the means God chose to cause Noah’s Flood.

Second, a decay acceleration could also have caused catastrophes in the solar system, such as cratering, volcanoes, and the past tectonic activity on Mars and Venus [*Spencer*, 1994]. Third, since nuclear fusion rates are related to decay rates, it could increase the activity of stars, causing some to be more turbulent, others to generate cosmic rays, and yet others to explode. I will speak more about the effects on stars below.

Fourth, nuclear decay affects living creatures, both by the soil, in tissues, and by star-produced cosmic-ray particles hitting the earth’s atmosphere. It could well be one means God used to bring about mortality and curse the ground, as the necessary consequence of Adam’s sin

[Genesis 3:17–19, 22]. All four of the above reasons fall into the general category of God’s judgment for man’s sin, as Romans 8:20–22 (NAS) summarizes:

*“For the creation was subjected to **futility**, not of its own will, but because of Him who subjected it, in hope that the creation itself also will be set free from its slavery to **corruption** into the freedom of the glory of the children of God. For we know that the whole creation groans and suffers the pains of childbirth together until now.”*

The Greek word translated “corruption” [φθορα *phthora*] includes the idea of “decay,” which of course brings to mind the decay of nuclei. Also notice that God subjected the *whole* Creation to futility and decay, not just the earth. From all this, I surmise that nuclei were completely stable from at least the last part of day three of the Creation week until the fall of man. After that, nuclei may have decayed at a moderate rate for 1656 years, until God accelerated the decay to start the Genesis Flood.

12. Nuclear Theory Favors Changes in Alpha-Decay Rates

Alpha (α)-decay of nuclei is fairly well understood. The protons and neutrons in a nucleus tend to cluster together in groups of four, two neutrons and two protons. These clusters are α -particles, which are ${}^4\text{He}$ nuclei. Figure 8 shows the potential energy “well” experienced by an α -particle at various distances from the center of the nucleus. The steeper the slope of the well, the stronger the force it exerts on the α -particle, just as if the particle were moving uphill. The horizontal dotted line represents the total energy of a particular α -particle in the nucleus, typically about 5 MeV (1 MeV = 1 million electron volts, a handy unit of energy in nuclear physics).

When the particle is near the center of the nucleus (near radius zero), the potential well is at its maximum depth, typically about -60 MeV. In this region the attraction due to the strong nuclear force is much greater than electrostatic repulsion. The kinetic energy of the α -particle is the difference between the line representing the potential and the horizontal dotted line, the difference at the center being about 65 MeV. That means the α -particle is moving at nearly 20% of the speed of light, which is

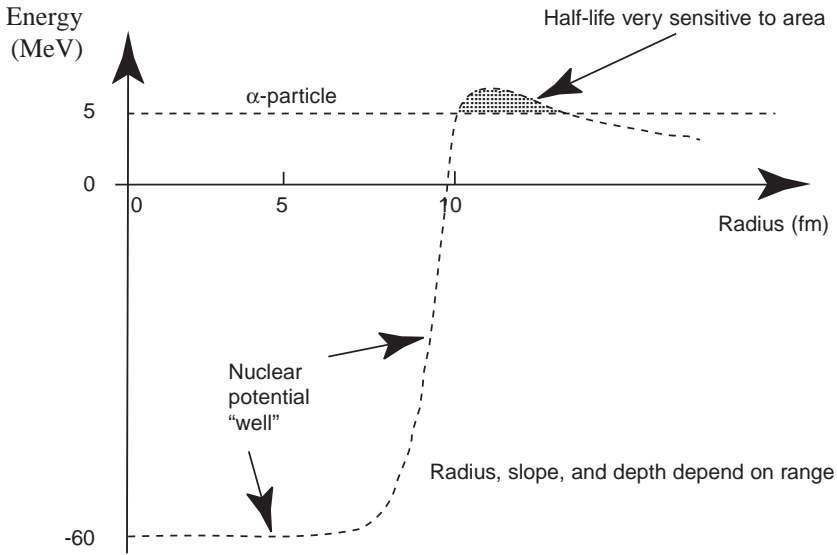


Figure 8. Some α -particles in a nucleus have nearly enough energy to surmount the “coulomb barrier” (shaded area) keeping them in the nucleus. The rate at which the particles can quantum-mechanically “tunnel” through the barrier is extremely sensitive to the height and thickness of the barrier region. Small changes in the nuclear potential “well” (dashed line) could thus cause billion-fold accelerations of nuclear decay rates.

rather fast for nuclear physics.

Near the center, the slope of the well is small, so the α -particle experiences little net force. When the α -particle starts approaching the wall of the well from the inside, it encounters a steeper slope in the potential. That means the rest of the nucleus is trying to pull the α -particle back toward the center. The increase of potential energy decreases the kinetic energy of the particle, meaning it slows down. When the potential energy equals the total energy, at a radius of about 10 fm (1 fm = 1 femtometer = 10^{-15} meter, often called a “Fermi”) here in my illustration, the particle stops completely.

Normally the α -particle rebounds from the wall, so it spends most of its life in the nucleus bouncing back and forth between the walls of the potential well. However, quantum fluctuations in the various energies

occasionally allow the particle to “tunnel” through the shaded area, called the *coulomb barrier*.

When the α -particle emerges outside the barrier, it finds itself in a region where the potential energy slopes downward and outward. That means the nucleus is now pushing the α -particle outward, mainly because of the electrostatic (“coulomb”) repulsion between the positive electric charge of the α -particle and the positive electric charge of the nucleus. As it moves outward, the α -particle picks up speed and kinetic energy. Eventually, when it is far away from its parent nucleus, it has a kinetic energy of 5 MeV and is moving at about 5% of the speed of light.

Nuclear theorists have calculated the probability with which the α -particles can penetrate the coulomb barrier [Evans, 1955, pp. 72–75, 874–877]. The resulting half-life (inversely proportional to decay rate) for α -decay can be approximated as:

$$T_{\alpha} \approx T_c e^{\gamma}, \text{ where } \gamma = a - b\sqrt{R} \quad (2a, b)$$

where R is the radius of the nucleus, T_c is roughly the time between collisions of the α -particle with the barrier, and a and b are constants which depend on the atomic number Z of the nucleus and the velocity v of the α -particle within the nucleus (v can change if nuclear potentials change):

$$T_c \approx \frac{R}{v} \ln 2 \approx 10^{-21} \text{ sec}, \quad a = \frac{Ze^2}{\hbar\epsilon_0 v}, \quad b = \frac{4e}{h} \sqrt{\frac{\pi}{\epsilon_0} Zm_{\alpha}} \quad (3a, b, c)$$

The other constants are the electron charge e , the permittivity of space ϵ_0 , Planck’s constant h , the reduced Planck’s constant $\hbar = h/2\pi$ and the mass of the α -particle m_{α} . The radius of the nucleus depends on its atomic weight A [Evans, 1955, p. 77],

$$R = R_0 A^{1/3}, \quad (4)$$

where the nuclear unit radius $R_0 \approx 1.3$ fm is a constant which is proportional to the *range*, r_0 , of the strong nuclear force. In meson theories of nuclear forces, the range of a force determines how sharply the force drops off with increasing distance r from a particle [Brink, 1965, pp. 83–118]. Mesons are short-lived nuclear particles most of

whose masses are intermediate between electrons and protons. They are a subset of a class of particles called “bosons” which have different amounts of spin than electrons, protons, and neutrons. The force-mediating ones are now called “gauge bosons.” “Range” in a meson theory means that in addition to factors like r^{-2} , the expressions for the force F between particles also have an exponential factor containing the range r_o , such as:

$$F \propto \frac{1}{r^2} \exp\left(-\frac{r}{r_o}\right) \quad (5)$$

According to quantum chromodynamics (quark theory) and experiments, the most relevant force for the nucleus is the one generated by the exchange of just one π meson between nuclear particles. The resulting range is

$$r_o = \frac{\hbar}{m_\pi c}, \quad (6)$$

where m_π is the mass (nearly the same) of any one of the three π mesons (positive, negative, and uncharged), and c is the speed of light. Using equations (4) and (6) with the proportionality of r_o and R_o tells us that R depends on the mass of the π meson and the atomic mass A of the nucleus:

$$R \propto \frac{A^{1/3}}{m_\pi} \quad (7)$$

The inverse proportionality of range with meson mass in equation (6) comes from very basic theory, and is supported by experiment. As we will see below, one suggestion, offered as a tentative working hypothesis, is that God changed meson masses, and possibly other factors to a lesser degree. If meson masses were to become smaller, the ranges of nuclear forces would increase, the nuclear unit radius R_o in equation (4) would increase, and the radius R of the nucleus would increase. If the radius R of the nucleus increases, then equations (2,a,b) say that the half-life for α -decay would decrease very much.

Figure 9 shows how equation (2) says the half-life of ^{226}Ra would change with changes in the nuclear unit radius R_o [Evans, 1955, p. 77, Figure 6.1], and thus with changes in meson masses. For $R_o = 1.49$ fm, the graph gives the presently observed half-life of 1620 years. Doubling

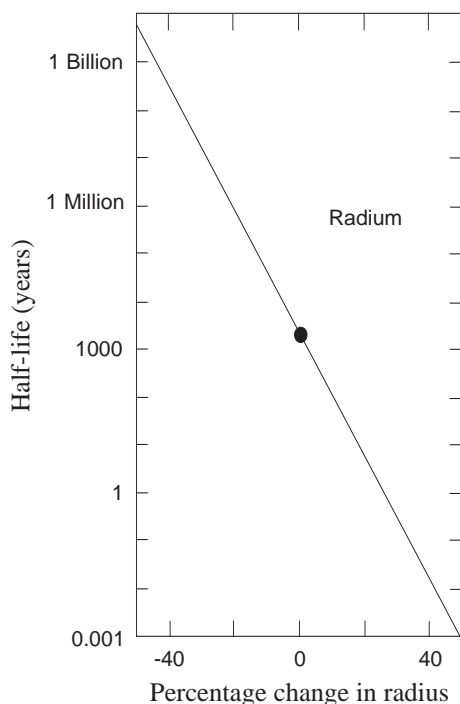


Figure 9. The α -decay half-life of ^{226}Ra predicted by quantum mechanics depends very strongly on the radius of the Ra nucleus [Evans, 1955, p. 77]. The radius of a nucleus is directly proportional to the range (see text) of the strong nuclear force.

R_0 from 1.0 fm to 2.0 fm would decrease the half-life by a factor of *trillions*, dropping it from gigayears down to days!

The reason for this extremely strong dependence of α -decay rates on the radius of the nucleus is that the nuclear radius affects both the height and width of the coulomb barrier, the shaded region in Figure 8, and the rate with which α -particles penetrate the barrier depends *exponentially* on the area in the shaded region. Thus α -decay rates are extremely sensitive to meson masses.

Other suggestions might involve variation of the radius of one of the dimensions of compactified string theory. Or one might consider the variation of so-called coupling constants. A coupling constant is a number

which specifies the strength with which a particle is coupled to the field it produces or responds to. These include the strong coupling constant α_s and the weak coupling constant α_w . If the variation occurred before the Creation of life, during the first 2½ days of Creation week, a variation of the electromagnetic coupling constant might be possible [Chaffin, 2000]. The electromagnetic coupling constant may be expressed in terms of the dimensionless ratio commonly called the fine-structure constant. When it varies relative to gravitation, accelerated decay results.

We can use equations (2), (3), and (7) to give us a relation telling us how α -decay half-lives should depend on Z , A , and meson mass. The result is that the ratio of the half-life of a particular nucleus now, $T_\alpha(\text{now})$, to the half-life of the same nucleus during an accelerated period, $T_\alpha(\text{acc})$, will depend on the meson mass now, $m_\pi(\text{now})$ and the meson mass during the accelerated period, $m_\pi(\text{acc})$:

$$\frac{T_\alpha(\text{now})}{T_\alpha(\text{acc})} = \exp \left[(3.65)\sqrt{Z}A^{1/6} \left(\sqrt{\frac{m_\pi(\text{now})}{m_\pi(\text{acc})}} - 1 \right) \right] \quad (8)$$

This equation allows us to make scaling relations between various types of radiometric dating methods using α -decay.

13. Beta-Decay Also Depends on Gauge Boson Masses

Atomic nuclei frequently transmute themselves by β -decay, that is, by emitting an electron along with an elusive neutrino. Does β -decay also depend strongly on meson masses? Probably. Unfortunately, β -decay does not seem to be nearly as well-understood at a fundamental level as α -decay is. That is because β -decay originates at a deeper level than α -decay, within the neutrons or protons themselves. See Eugene Chaffin's summary of the history of β -decay research in Chapter 6, Section 3. The force involved is called the "weak" nuclear force, although now it appears that it is about as strong as the electromagnetic force, but with an extremely short range. Field theorists have made good progress in understanding the weak force, but they have thus far failed to reduce the complexities to as clear an intuitive picture as we have of α -decay.

In my opinion, the β -decay equations and predictions which follow are not as firmly founded in fundamental theory as those for α -decay

Until the last few decades, the only theory of weak interactions we had was that of Enrico Fermi. His theory was frankly phenomenological. That is, it did not offer any details about the weak force itself and how it might depend on other factors. Instead, his theory lumped all the essential qualities of the weak force into a single number, the Fermi constant G . This “coupling constant” connects the weak force with the particles it affects, much like the charge of the electron, e , connects the electromagnetic force to the particles it affects. Fermi succeeded in showing that G is the same number for all the weak force interactions we know of. In fact, it may be universal, that is, the same for interactions between all particles [*Halzen and Martin*, 1984, pp. 253–257].

From the Fermi theory and experiments [*Evans*, 1955, pp. 558–559] we can say that the half-life T_β for β -decay in the nucleus depends on the Fermi constant G , the Z of the nucleus, and the radius R of the nucleus approximately as follows:

$$T_\beta \propto \frac{R \left(\frac{Z}{137} \right)^2}{G^2} \quad (9)$$

Equation (7) tells us how R depends on the atomic mass A and the π meson mass. But how should G depend on boson masses? We now have a theory, the rather non-intuitive Weinberg-Salam “electroweak” theory, which unifies electromagnetism and the weak force at the cost of simplicity. Its bottom line is that the Fermi constant G is related to the electron charge e as follows [*Halzen and Martin*, 1984, pp. 257, 297]:

$$G = \frac{\sqrt{2} e^2}{8M_w^2 \sin^2 \theta_w} \quad (10)$$

where M_w is the mass of the W^\pm particle, the “intermediate vector boson,” which, along with the Z^0 particle, mediates the weak force; M_w is large, being experimentally measured to have a rest mass energy of about 80 GeV (1 GeV = 1,000 MeV) [*Halzen and Martin*, 1984, p. 337]. That means the weak force has an extremely short range. The other parameter, θ_w , is the Weinberg, or “weak mixing,” angle; it is such that $\sin^2 \theta_w \approx 1/4$

[Halzen and Martin, 1984, p. 304–305]. If we assume that e and θ_w remained unchanged during an acceleration period, then equations (7), (9), and (10) give us a proportionality describing how β -decay half-lives should depend on Z , A , and boson masses:

$$T_\beta \propto M_w^4 \left(\frac{A^{1/3}}{m_\pi} \right)^{\left(\frac{Z}{137} \right)^2} \quad (11)$$

For a particular nucleus, we can relate β -decay half-lives and boson masses for both now and during an accelerated period:

$$\frac{T_\beta(\text{now})}{T_\beta(\text{acc})} = \left[\frac{M_w(\text{now})}{M_w(\text{acc})} \right]^4 \left[\frac{m_\pi(\text{acc})}{m_\pi(\text{now})} \right]^{\left(\frac{Z}{137} \right)^2} \quad (12)$$

Since most β -decaying nuclei of geological interest have a Z less than 39, the exponent of the second factor (the one with the π meson masses) is usually less than 0.081. The first factor, the one with the intermediate vector boson mass, has a much larger exponent, namely 4, so it should dominate the above equation. Thus we would expect smaller gauge boson masses to accelerate β -decay rates.

We can use equations (8), (11), and (12) to predict trends and relationships between various kinds of radioisotopic dates. The predictions would be more precise if we could theoretically determine how much each boson mass changed during an acceleration period. But that awaits a theory probing to a deeper level. The next section sketches the beginnings of such a theory.

14. Cosmic Expansion may have Accelerated Nuclear Decay

In sorting out different theories for the decay, one principle to consider is that of *economy of action* on God's part. That is, changing pervasive physical constants (such as c , e , or h) could profoundly affect the physical processes on which human life depends. That gets the theorist into a much wider arena, and he would have much more explaining to do. Instead, I prefer to start with theories in which God would make a very

precise change, in order to limit the effects to just those which would accomplish His purposes, some of which I suggested in Section 11. (However, Eugene Chaffin has proposed an alternative approach which would cause other physical phenomena to change besides nuclear forces [Chaffin, 2000]. As he points out, such changes would be acceptable during early Creation week, before God created life.)

Thus we should seek a theory in which only nuclear (weak and strong) forces would be affected during an acceleration period. That way, the forces which most directly relate to human life, gravity and electromagnetism, would not change. If God *changed the ranges of all forces by a multiplying factor*, or a set of various multiplying factors, only the nuclear forces would change. To see this, refer back to equation (5) and think of it as applying to all four types of force, but with different ranges for each force.

For gravity and electromagnetism, observations indicate that the ranges are infinite, or nearly so. An infinite range makes the exponential factor in equation (5) equal to one, so that it drops out and leaves only the inverse-square factor. Multiplying an infinite range by any given factor would leave the range still infinite. So gravity and electromagnetic forces would be left unchanged, and life could continue relatively unaffected. The weights of objects and the orbits of planets would continue as before. The outer electronic structure of atoms (determining chemical reactions, light emission and reception, molecular structure, etc.) would continue as before. Only deep within the atoms, in a region closely confined around their very centers, would things be different. Changing ranges by a multiplying factor (or set of factors) would accomplish that.

From the very basic physics theory which leads to equation (6), we can say that the ranges of forces are directly related to the masses of the gauge bosons which mediate the forces. For example, the gauge boson related to the electromagnetic force is the photon, which all measurements indicate has zero rest mass, or very close to it. Zero rest mass in equation (6) leads to infinite range, which is what we appear to observe for electromagnetic forces. The smaller the mass, the longer the range. The previous sections indicate that we need longer ranges for acceleration of α - and β -decay. So for nuclear forces, we would expect

that the masses of their gauge bosons, for example the π mesons and the W^\pm , to be *reduced* during periods of accelerated decay.

Here is a *very important caveat*. Present quantum field theory says that gauge boson masses are closely related to the masses of protons, neutrons, and electrons. Thus a change in only the gauge boson masses might change the total gravitational mass of atoms, planets and stars. That would change things on a large scale, at least during the periods of accelerated decay. However, there are other factors which enter into nuclear forces, such as the strong force coupling coefficient and the weak force Weinberg angle. My equations do not spell out all of these factors. It is possible that: (a) all of the factors automatically work together to keep the total energy (mass) of the nuclei constant, (b) God actively intervened to keep the total energy constant, or (c) He allowed the energy to change. My suggestions, in order of decreasing confidence and increasing specificity, are: (1) *Something* changed in nuclear forces, (2) Possibly ranges changed, (3) Possibly gauge boson masses changed, (4) Possibly other constants changed, (5) Possibly all these were related to cosmological changes, as I suggest below. At any point in our exploration, we could easily diverge from that sequence of suggestions as we learn more. Thus these steps toward a theory are *very tentative*.

At this point, I find that many people ask, “But how would God change the boson masses?” Let’s stop and assess what we are doing here. We are following a theoretical chain of causation backwards. It goes from the observation of the effects of accelerated decay back to a possible cause, change of boson masses. If we now find a prior cause, x , for the boson mass changes, then the same people might ask, “But what caused x ?” Perhaps then we will find that a yet previous cause, y , produced x as an effect. If we could follow this chain (or any other) backwards far enough, we might find a point where God has intervened supernaturally. That should not surprise us, because Colossians 1:17 says that Christ is not only the Creator of all things, but also the Sustainer of all the forces between them:

*“And He is before all things, and in Him all things **hold together**.”*

The Greek word here translated “hold together” [$\sigma\upsilon\nu\iota\sigma\tau\eta\mu\iota$ *sunistemi*, to place or bind together] appears in II Peter 3:5 to include nuclear

transformations [Humphreys, 1983]. It appears that Christ already has direct control of the nuclear (and other) forces, and furthermore that He is intimately involved with them. So even if we cannot follow all the links in the chain of causes back past a certain point, we can be confident that Jesus Christ is not only at the end of it, but at every link along the way. The point I am trying to make is that we should avoid the pitfall of insisting on completely naturalistic explanations for accelerated decay. Instead, my approach is to push the science we think we know as far as is reasonable, but remain ready at every point to see that God has intervened, and is intervening.

However, I think He encourages us to try to trace the chain as far back as we can [Proverbs 22:17, Psalm 111:2, etc.]. Let us try to do so by considering that we can interpret quantum field theory as meaning space itself is a *material*. The “vacuum” of field theory would be an “ether” or “fabric” we do not perceive directly [Wilczek, 1999]. It would sustain the perceivable objects which exist in it, and move unhindered through it. The Bible appears to uphold this view of space, calling it “the heavens” [Humphreys, 1994, pp. 67–68]. According to field theory, space is the medium through which propagate all forces between particles. If space changes, the forces could change.

As a more concrete example, in Figure 10 I picture space as partly consisting of a lattice of quarks and antiquarks, held together by strings of “gluons” under tension. A prominent field theorist says of such a string between quark-antiquark pairs, “The *tension strength* of a string is a constant of Nature: about 14 *tons* of force” [‘t Hooft, 1997, p. 91, his italics].

While some theorists may think of “Nature” as obligingly keeping things constant, the God who made nature is under no such constraint. He may have changed the tension. Since recent cosmological observations support the idea that space itself is under tension [Straumann, 1999], a change of tension could start the expansion of the cosmos, or change the rate of expansion. This may be how God “stretched out the heavens” as mentioned in many Old Testament passages, such as Isaiah 40:22 [Humphreys, 1994, pp. 66–67].

It is very interesting to note that at least two of the periods when

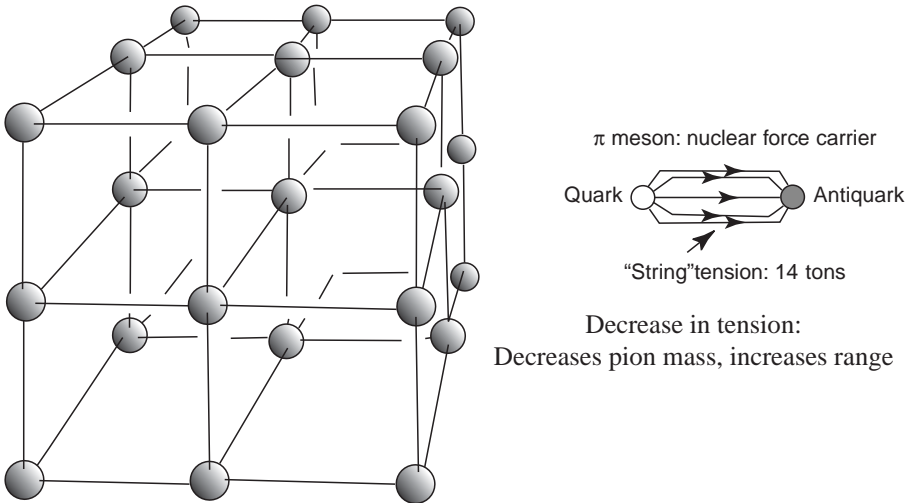


Figure 10. The “vacuum” of quantum field theory pictured as a lattice of quark-antiquark pairs. The tension, right now about 14 tons [*t Hooft*, 1997], of the “strings” holding each pair together determines the mass of π mesons, and thus the range of the strong nuclear force. A small reduction in the tension would greatly accelerate nuclear decay rates.

accelerated decay is feasible also appear to be associated with a stretching-out of the heavens. The first period is early in Creation week, when God stretched out the “expanse” [רַקִּיעַ *raqia*, something expanded, spread-out] as mentioned in Genesis 1:6,7 [*Humphreys*, 1994, pp. 58–59, 68]. The other is during the Genesis Flood [*Humphreys*, 1994, p. 68]. As I mentioned in Section 9, Psalm 18 appears to be describing events during the Flood, including God’s kindling of nuclear fires. The 17th verse of that Psalm says of God:

“He stretched out the heavens also, and came down . . .”

Many translations render the emphasized words as “bowed,” but that is a tertiary meaning, according to lexicons. Here I have translated the Hebrew word [נָטָה *natah*, to stretch out, extend] with its most basic meaning [*Davidson*, 1970, p. 546; *Holladay*, 1971, p. 235; *Brown, Driver, and Briggs*, 1979, pp. 639–640]. This suggests that God caused an episode of expanding space at the beginning of the Flood. In the earth’s timescale, this expansion would have to be very rapid [*Humphreys*, 1994].

A rapid expansion could have caused an acceleration of nuclear decay, and consequently the catastrophic plate tectonic events which brought about the Genesis Flood.

If God did change the tension of space (to cause expansion), how would this affect boson masses? According to quantum chromodynamics, a quark-antiquark pair and the stretched string between them constitute a π meson [Halzen and Martin, 1984, p. 6]. We can think of each of the quark-antiquark pairs in the lattice of Figure 10 as such a meson. According to quark theory, the string tension greatly affects the mass of the meson. Thus if God changed the tension of space, the mass of π mesons would also change with it. As we have seen, that would change nuclear decay rates.

The above is not a theory, only the crude beginnings of a sketch of one. Physics still awaits a detailed theory for the structure of the “vacuum,” and I would not expect such a theory to be any less complex than the microscopic physics of solid or liquid materials which are perceivable. In its application to nuclear forces, such a theory would have to account not only for how the tension of space affects gauge bosons, but also how it affects electrons, protons, neutrons, and the basic “constants,” such as c , e , and h .

I encourage creationist physicists who are called of God and gifted in this area to pursue and develop quantum field theory. I haven't yet found a practitioner of that theory who could communicate to me a deep understanding of the meaning underlying that theory's equations—though I admit that the fault could be in me! However, I hope that a deeper synthesis can be made which would allow more of us to see clearly the beauty and wonder of God's works in the sub-nuclear realm.

15. Heat and other problems

The most obvious problem with the hypothesis of accelerated nuclear decay is: what to do with all the heat? A simple calculation shows that crustal rocks with their present amount of radioactivity would melt many times over if decay rates were accelerated. However, I would like to emphasize here that *all* creationist Creation or Flood models I know of

have serious problems with heat disposal [Baumgardner, 1986, p. 21]. There is simply too much geological work to be done in too short a time. So the solution I outline here should be useful to *any* creationist geological model.

The solution takes advantage of a little-known but well-established consequence of the expansion of the cosmos: *it makes energy disappear!* That includes heat energy. A rapid expansion, such as outlined in the previous section, makes heat disappear fast enough to alleviate our problem, perhaps solving it.

The well-known red shifts of light from distant galaxies offer a simple illustration of the effect. Consider a photon leaving a distant galaxy on its way toward us. According to general relativity, and contrary to popular misconception, the photon suffers no Doppler red shift as it leaves [Harrison, 1981, pp. 245–248]. A simple way of understanding that is that the galaxy is not moving with respect to the fabric of space in its vicinity, but rather moving *with* the expansion. According to Einstein's famous photoelectric formula, the photon's energy E_1 as it starts its journey is:

$$E_1 = h \frac{c}{\lambda_1} \quad (13)$$

where λ_1 is the wavelength the photon has when it starts; h and c are Planck's constant and the speed of light. According to general relativity, the expansion of space as the photon travels toward us stretches out the wavelength of the photon, so when it reaches earth it has a longer (redder) wavelength λ_2 . By Einstein's formula, the photon now has an energy

$$E_2 = h \frac{c}{\lambda_2} \quad (14)$$

Since the received wavelength λ_2 is greater than the starting wavelength λ_1 , then the received energy E_2 of the photon is *less* than the energy E_1 the photon had when it started. Somehow the photon lost an energy $\delta E = E_1 - E_2$. Since the photons we see generally suffer no collisions (otherwise they would be scattered away from our line of sight) on the way to us through an *empty* vacuum, how could they lose energy? Should physicists resort to a non-constant c or h to account for the change?

The answer is that they don't have to. There is a well-understood but poorly publicized mechanism in general relativity that accounts for the loss. The result of calculations using that mechanism is [Robertson and Noonan, 1968, p. 356]: "Therefore, the radiation energy which is lost in an expanding universe is used up *as work in aiding the expansion.*"

I offer the following simple way of thinking about the effect. For photons moving in a curved space, their momentum pushes on the "fabric" of space, trying to straighten it out. If space increases its radius of curvature while the photons are pushing, the photons then impart some of their energy to the motion of the fabric, increasing its kinetic energy. To fully visualize the direction of the pushing and the motion of the fabric requires visualizing—by analogy—an additional spatial dimension [Humphreys, 1998, p. 204]. But even without visualizing the extra dimension, especially for those who want to view that dimension as "fictitious," one can simply imagine some of the energy of the photons disappearing from the three-dimensional space we can perceive. However we want to interpret the mathematics, the equations insist on the result—disappearing energy.

This effect doesn't apply merely to photons, but to *any* free particle in an expanding space. Eventually a moving free particle with non-zero rest mass will come to a stop with respect to the space in its vicinity, losing all its kinetic energy [Robertson and Noonan, 1968, p. 344; Landau and Lifshitz, 1983, pp. 374–375].

All relativists think that while the expansion of space sweeps galaxies apart, the galaxies themselves (and smaller objects) do not change size with the expansion. One explanation (I know of no other) for why that should be so is that the force associated with the expansion is much smaller than the forces binding together stars in a galaxy (or particles in planets, people, and atoms) [Pachner, 1964; Noerdlinger and Petrosian, 1971]. The expansion is only strong enough to overcome the feeble gravitational forces between galaxies. By that view, the fabric of space between particles bound to each other, whether within stars or atoms, continues to expand, sliding past the particles essentially without friction.

The calculations leading to equation (14) were for free particles, because that is easier to calculate and to demonstrate no energy losses

by normal means. What about *bound* particles, such as ions thermally vibrating in a solid crystal lattice? That is harder to calculate, but a simple *gedanken* experiment suggests the same effect applies to bound particles as well as free ones. Imagine a large box with perfectly reflecting sides. One particle, say a molecule, bounces around in the box in a vacuum. The box itself does not change size, for the reason I offered above, so the molecule does not lose energy to the walls of the box as it bounces off them.

Except for the tiny fraction of time the molecule spends in bouncing off the walls, it is perfectly free. During the free part of its flight, it is just like the free particle in empty space, and the molecule imparts some of its energy to the fabric of space. The molecule is bound within the box, and yet it loses energy which does not go into the walls of the box. Now shrink the box to the size of a unit cell in the crystal. Again the molecule loses energy to the fabric of space. In a real crystal, the vibrating ions transfer energy back and forth with their neighboring ions, but as each ion moves, it will also lose some kinetic energy to the fabric of space within which it is moving. From our viewpoint, the energy does not go in any of the three directions we perceive; it simply disappears.

From the relativistic equations [*Landau and Lifshitz*, 1983, pp. 374–375], we can easily show that a non-relativistic (speed much less than c) particle of kinetic energy E loses energy at a rate determined by the radius of curvature of space R and its rate of change:

$$\frac{\dot{E}}{E} = -2 \frac{\dot{R}}{R} \quad (15)$$

where the dot represents the time derivative (time measured in a reference frame at rest with respect to the fabric of space in the vicinity). If the specific heat does not change, and there is no input or output of heat, we can integrate this equation to specify the temperatures T of an isolated system before and after an episode of expansion:

$$\frac{T_{after}}{T_{before}} = \left(\frac{R_{before}}{R_{after}} \right)^2 \quad (16)$$

For example, if there were a two-fold expansion during the year of the

Genesis Flood [*Humphreys*, 1994, p. 68] assuming the possibility of time dilation during that period, the system would undergo a four-fold loss of temperature during that year. Of course, if the system is a radioactive rock or a person, we also have to account for all the usual inputs and outputs of heat. But equation (15) represents an additional loss of heat that would be important in situations where normal heat outflows are slow.

A final note on heat flow is that it is not only a problem but also a benefit for creationists. As John Baumgardner shows in Chapter 3, Section 11, the character of heat flow from the earth's crust is beginning to look like strong evidence for accelerated decay.

Now let's briefly consider another possible problem: were there radioactive atoms in the tissues of the creatures aboard the ark? The main ones today are ^{40}K and ^{14}C . If creatures aboard the ark had the same percentages of those isotopes we have in our tissues today, and the acceleration applied to them as well as to everything else, they might not have survived.

Carbon 14 does not seem to be a problem. There are several good reasons to think the percentage of ^{14}C in the air and living creatures was much lower before the Flood than it is today [*Humphreys*, 1994, pp. 62–63]. So Noah and the other creatures aboard the ark would have acquired only a small amount of ^{14}C by the time the Flood began.

However, ^{40}K is a problem. Even though ^{40}K represents only about 0.01% of all the K we have in our tissues today (the other 99.99% is ^{39}K), that would be enough to kill Noah if he underwent more than a few million radioisotopic years worth of nuclear decay. Of course, Noah may not have experienced more nuclear decay than that if most of the accelerated decay occurred during the first part of Creation week, a model we are just beginning to consider. However, let us consider where we get ^{40}K today. Most of it comes from material which was deposited as soil or in the sea after being eroded from continental granites *during the Genesis Flood*. Noah, however, got his K from pre-Flood soil, soil which God had designed for a perfect world. Would God have included in that soil isotopes which He knew would become radioactive, and which would harm the creatures aboard the ark? I'm inclined to say "no."

That “no” also places a constraint upon the geology of the antediluvian world. To keep radioactive atoms out of the tissues of the ark creatures, the biosphere, both soil and water, would have to remain separate from the (at least potentially) radioactive atoms of what would become the continental granites after the Flood.

Another possibility to consider is the effect upon stars. Thermonuclear fusion is like α -decay in reverse. Thus a change which accelerates α -decay rates could also accelerate nuclear fusion in stars. Some theoreticians think it would take millions of years for the effects of a moderate change in the core of a star like our Sun to reach the surface [Noyes, 1999, p. 66], but a larger change might take effect more quickly. Nearby stars, including the Sun, might have been more turbulent during the Genesis Flood, emitting more light and more cosmic rays. Some types of stars may have become novas or supernovas. After the Flood, cosmic-ray bombardment of the earth may have been more intense than today, generating ^{14}C in the earth’s atmosphere faster than now. That would affect our estimates of the age of the radiocarbon inventory of the earth, and perhaps bring it more into line with other indicators of a young age for the earth [Aardsma, 1990, pp. 2, 12].

Last I want to consider a non-problem sometimes encountered in the scientific literature. There authors often allege that if nuclear decay rates change, the energies of α -particles would change significantly, so the size of radiohalo rings would be different from the ones which would form today. However, an excellent study of that allegation showed that “decay rates may vary without significantly changing the radii of radiohalos” [Chaffin, 1994, pp. 143–146.] Also see Eugene Chaffin’s related comments in Chapter 6 of this book.

16. Conclusion

I hope I have convinced you, the reader, that acceleration of nuclear decay is a viable hypothesis. The data require it, theory allows it, the Bible supports it, problems with it seem solvable, and we can test it experimentally. The theory needs to be worked out in detail, but we can already make some predictions. In particular, experimental He diffusion

rates in Jemez biotite should turn out to be within an order of magnitude of the “Creation model” line in Figure 7. Trends in radioisotopic dates should be governed by the equations in sections 12 and 13.

For a research program, I would like to see (1) He-in-biotite diffusion measured, (2) continuing efforts to get unbiased radioisotopic ages, (3) a historical and literature study done of the efforts to establish the presently accepted timescale, (4) an improved theoretical study of the rate issue, particularly for β -decay, and (5) tests of the trends predicted by the theory. I am looking forward to seeing such a program bear fruit, and I have every confidence it can do so.

References

- Aardsma, G. E., Radiocarbon, dendrochronology, and the date of the Flood, in *Proceedings of the Second International Conference on Creationism*, edited by R. E. Walsh and C. L. Brooks, vol. 2, pp. 1–15, Creation Science Fellowship, Pittsburgh, Pennsylvania, 1990.
- Austin, S. A., and D. R. Humphreys, The sea’s missing salt: a dilemma for evolutionists, in *Proceedings of the Second International Conference on Creationism*, edited by R. E. Walsh and C. L. Brooks, vol. 2, pp. 17–33, Creation Science Fellowship, Pittsburgh, Pennsylvania, 1990.
- Austin, S. A., and J. D. Morris, Tight folds and clastic dikes as evidence for rapid deposition and deformation of two very thick stratigraphic sequences, in *Proceedings of the First International Conference on Creationism*, edited by R. E. Walsh, C. L. Brooks and R. S. Crowell, vol. 2, pp. 3–15, Creation Science Fellowship, Pittsburgh, Pennsylvania, 1986.
- Austin, S. A., Are Grand Canyon rocks one billion years old?, in *Grand Canyon: Monument to Catastrophe*, edited by S. A. Austin, pp. 111–131, Institute for Creation Research, Santee, California, 1994.
- Austin, S. A., J. R. Baumgardner, D. R. Humphreys, A. A. Snelling, L. Vardiman, and K. P. Wise, Catastrophic plate tectonics: a global flood model of earth history, in *Proceedings of the Third International Conference on Creationism*, edited by R. E. Walsh, pp. 609–621, Creation Science Fellowship, Pittsburgh, Pennsylvania, 1994.
- Bielecki, J. W., *A Study of Spontaneous Fission Track Densities in Resting Spring Range Obsidian (Miocene) near Shoshone, California*, 77 pp., Masters Thesis, Institute for Creation Research, Santee, California, 1994.

- Baumgardner, J. R., Numerical simulation of the large-scale tectonic changes accompanying the Flood, in *Proceedings of the First International Conference on Creationism*, edited by R. E. Walsh, C. L. Brooks and R. S. Crowell, vol. 2, pp. 17–30, Creation Science Fellowship, Pittsburgh, Pennsylvania, 1986.
- Baumgardner, J. R., Runaway subduction as the driving mechanism for the Genesis Flood, in *Proceedings of the Third International Conference on Creationism*, edited by R. E. Walsh, pp. 63–75, Creation Science Fellowship, Pittsburgh, Pennsylvania, 1994.
- Brink, D. M., *Nuclear Forces*, Pergamon Press, Oxford, 1965.
- Brown, F., S. R. Driver, and C. A. Briggs, *The New Brown-Driver-Briggs-Genesius Hebrew and English Lexicon*, Hendrickson Publishers, Peabody, Massachusetts, 1979.
- Brown, W., *In the Beginning*, Center for Scientific Creation, Phoenix, Arizona, 1995.
- Carroll, M. R., Diffusion of Ar in rhyolite, orthoclase and albite composition glasses, *Earth and Planetary Science Letters*, 103, 156–168, 1991.
- Carslaw, H. S., and J. C. Jaeger, *Conduction of Heat in Solids*, second edition, Clarendon Press, Oxford, 1959. The solutions apply just as well to diffusion of He as they do to diffusion of heat. Apply case IV, p. 235, to eq. (8) on p. 234.
- Chaffin, E. F., Are the fundamental “constants” of physics really variables?, in *Proceedings of the Third International Conference on Creationism*, edited by R. E. Walsh, pp. 143–150, Creation Science Fellowship, Pittsburgh, Pennsylvania, 1994.
- Chaffin, E. F., A mechanism for accelerated decay, *Creation Research Society Quarterly*, 37, 3–9, 2000.
- Cook, M. A., Where is the earth’s radiogenic helium?, *Nature*, 179, 213, 1957.
- Davidson, B., *The Analytical Hebrew and Chaldee Lexicon*, second edition, Zondervan, Grand Rapids, Michigan, 1970.
- Evans, R. D., *The Atomic Nucleus*, McGraw-Hill, New York, 1955.
- Fortier, S. M., and B. J. Giletti, An empirical model for predicting diffusion coefficients in silicate minerals, *Science*, 245, 1481–1484, 1989.
- Gaebelein, A. C., *The Psalms*, Loizeaux Brothers, Neptune, New Jersey, 1965.
- Gentry, R. V., Radioactive halos, *Annual Review of Nuclear Science*, 23, 347–362, 1973.
- Gentry, R. V., Radiohalos in a radiochronological and cosmological perspective, *Science*, 184, 62–66, 1974.

- Gentry, R. V., *Creation's Tiny Mystery*, third edition, Earth Science Associates, Knoxville, Tennessee, 1992.
- Gentry, R. V., S. S. Cristy, J. F. McLaughlin, and J. A. McHugh, Ion microprobe confirmation of Pb isotope ratios and search for isomer precursors in polonium radiohaloes, *Nature*, 244, 282–283, 1973.
- Gentry, R. V., T. J. Sworski, H. S. McKown, D. H. Smith, R. E. Eby, and W. H. Christie, Differential lead retention in zircons: implications for nuclear waste management, *Science*, 216, 296–298, 1982a.
- Gentry, R. V., G. L. Glish, and E. H. McBay, Differential helium retention in zircons: implications for nuclear waste containment, *Geophysical Research Letters*, 9, 1129–1130, 1982b.
- Girifalco, L. A., *Atomic Migration in Crystals*, Blaisdell, New York, 1964.
- Grove, M., and T. M. Harrison, $^{40}\text{Ar}^*$ diffusion in Fe-rich biotite, *American Mineralogist*, 81, 940–951, 1996.
- Green, J., *The Interlinear Hebrew/Greek English Bible*, Associated Publishers, Lafayette, Indiana, 1979.
- Hahn, H.-P., H.-J. Born, and J. I. Kim, Survey on the rate perturbation of nuclear decay, *Radiochimica Acta*, 23, 23–37, 1976.
- Halzen, F., and A. D. Martin, *Quarks and Leptons*, John Wiley and Sons, New York, 1984.
- Harrison, E. R., *Cosmology*, Cambridge University Press, Cambridge, 1981.
- Holladay, W. L., *A Concise Hebrew and Aramaic Lexicon of the Old Testament*, Eerdmans, Grand Rapids, Michigan, 1971.
- Holmes, A., The association of lead with uranium in rock-minerals, and its application to the measurement of geologic time, *Proceedings of the Royal Society, Series A*, 85, 248–256, 1911.
- Huh, C.-A., Dependence of the decay rate of ^7Be on chemical forms, *Earth and Planetary Science Letters*, 171, 325–328, 1999.
- Humphreys, D. R., The creation of the earth's magnetic field, *Creation Research Society Quarterly*, 20, 89–94, 1983.
- Humphreys, D. R., Discussion, in *Proceedings of the First International Conference on Creationism*, edited by R. E. Walsh, C. L. Brooks and R. S. Crowell, vol. 2, p. 102, Creation Science Fellowship, Pittsburgh, Pennsylvania, 1986.
- Humphreys, D. R., Physical mechanism for reversals of the earth's magnetic field during the Flood, in *Proceedings of the Second International Conference on Creationism*, edited by R. E. Walsh and C. L. Brooks, vol. 2, pp. 129–142, Creation Science Fellowship, Pittsburgh, Pennsylvania,

- 1990.
- Humphreys, D. R., *Starlight and Time*, Master Books, Green Forest, Arizona, 1994.
- Humphreys, D. R., New vistas of space-time rebut the critics, *Creation Ex Nihilo Technical Journal*, 12, 195–212, 1998.
- Kerr, R. A., Tweaking the clock of radioactive decay, *Science*, 286, 882–883, 1999.
- Lachenbruch, A. H., Crustal temperature and heat production: implications of the linear heat–flow relation, *Journal of Geophysical Research*, 75, 78–87, 1970.
- Landau, L. D., and E. M. Lifshitz, *The Classical Theory of Fields*, fourth English edition, Pergamon Press, 1983.
- Lippolt, H. J., and E. Weigel, ^4He diffusion in ^{40}Ar -retentive minerals, *Geochimica et Cosmochimica Acta*, 52, 1449–1458, 1988.
- Magomedov, Sh. A., Migration of radiogenic products in zircon, *Geokhimiya*, 2, 263–267, 1970. In Russian. English abstract in *Geochemistry International*, 7, 203, 1970. English translation available from D. R. Humphreys.
- Melby, E., L. Bergholt, M. Guttormsen, M. Hjorth-Jensen, F. Ingebretsen, S. Messelt, J. Rekstad, A. Schiller, S. Siem, and S. W. Ødegard, Observation of thermodynamical properties in the ^{162}Dy , ^{166}Er , and ^{172}Yb nuclei, *Physical Review Letters*, 83, 3150–3153, 1999.
- Morris, J. D., *The Young Earth*, Master Books, Colorado Springs, Colorado, 1994.
- Morris, H. M., The young earth, *Institute for Creation Research Impact #17*, 1974.
- Noyes, R. W., *The Sun, Our Star*, 263 pp., Harvard University Press, Cambridge, Massachusetts, 1982.
- Noerdlinger, P. D., and V. Petrosian, The effect of cosmological expansion on self-gravitating ensembles of particles, *Astrophysical Journal*, 168, 1–9, 1971.
- Pachner, J., Nonconservation of energy during cosmic evolution, *Physical Review Letters*, 12, 117–118, 1964.
- Robertson, H. P., and T. W. Noonan, *Relativity and Cosmology*, W. B. Saunders Company, Philadelphia, 1968.
- Reifenschweiler, O., Reduced radioactivity of tritium in small titanium particles, *Physics Letters*, A184, 149–153, 1994.
- Roy, R. R., and B. P. Nigam, *Nuclear Physics*, John Wiley and Sons, New York, 1967.
- Schleien, B., L. A. Slaback, and B. K. Birky, editors, *Handbook of Health*

- Physics and Radiological Health*, third edition, Williams and Wilkins, Baltimore, 1998.
- Spencer, W. R., The origin and history of the solar system, in *Proceedings of the Third International Conference on Creationism*, edited by R. E. Walsh, pp. 513–523, Creation Science Fellowship, Pittsburgh, Pennsylvania, 1994.
- Straumann, N., The mystery of the cosmic vacuum energy density and the accelerated expansion of the Universe, *European Journal of Physics*, 20, 419–427, 1999.
- Stacey, F. D., *Physics of the Earth*, John Wiley and Sons, New York, 1969.
- 't Hooft, G., *In Search of the Ultimate Building Blocks*, Cambridge University Press, Cambridge, 1997.
- Thayer, J. H., *Thayer's Greek-English Lexicon of the New Testament*, corrected edition, Associated Publishers, Grand Rapids, Michigan, 1889.
- Vardiman, L., *The Age of the Earth's Atmosphere*, Institute for Creation Research, El Cajon, California, 1990.
- Vardiman, L., *Sea Floor Sediment and the Age of the Earth*, Institute for Creation Research, El Cajon, California, 1995.
- Weingreen, J., *A Practical Grammar for Classical Hebrew*, second edition, Clarendon Press, Oxford, 1959.
- Wilczek, F., The persistence of ether, *Physics Today*, 52, 13–14, January 1999.
- Whitcomb, J. C., and H. M. Morris, *The Genesis Flood*, Baker Book House, Grand Rapids, Michigan, 1961.
- Woodmorappe, J., Radiometric geochronology reappraised, *Creation Research Society Quarterly*, 16, 102–129, 147–148, 1979.
- Woodmorappe, J., *The Mythology of Modern Dating Methods*, Institute for Creation Research, El Cajon, California, 1999.
- Wuest, K. S., *In These Last Days*, Eerdmans, Grand Rapids, Michigan, 1954.
- Yates, K. M., *The Essentials of Biblical Hebrew*, revised edition, Harper and Row, New York, 1954.
- Young, R., *Young's Literal Translation of the Holy Bible*, third edition, Bethany Fellowship, Minneapolis, 1898.
- Zartman, R. E., Uranium, thorium, and lead concentrations and lead isotopic composition of biotite granodiorite (Sample 9527-2b) from LASL Drill Hole GT-2, *Los Alamos Science Laboratory Report Number LA-7923-MS*, 1979.

Chapter 8

Radiohalos

Andrew A. Snelling, Ph.D.*

Abstract. An extensive review of all types of radiohalos confirms their radioactive origin, but the observed probable constancy of radiohalo radii does not necessarily imply constancy of radioactive decay rates. The identity of U and Th halos is beyond question, but the radioisotopes responsible for variant dwarf, giant, and other intermediate-sized varieties has still not been conclusively established. Most attention and controversy has surrounded the Po halos, because isotopic analyses of the radiocenters indicate the Po isotopes responsible for the halos were “parentless” (that is, no traces of their precursors are found). Debate has centered on whether the Po halos are secondary, due to fluid transport of Ra, Rn and/or Po isotopes along fractures, defects and cleavage planes, or primordial, due to the fleeting existence of ^{218}Po (half-life of 3 minutes) and ^{214}Po (half-life of 164 microseconds) thus suggesting fiat creation of the Po isotopes in place with the host minerals and rocks. Secondary Po halos are known in coalified wood and along fractures in minerals, “parentless” ^{210}Po is known to have been rapidly transported in hydrothermal fluids and ground waters, and there appears to be a correlation between Po halos and immediately adjacent U sources. Furthermore, the Po halos are not just in Precambrian and granitic rocks, some hosts intruding Phanerozoic fossil-bearing (Flood-related) strata. However, the apparent absence of α -recoil tracks and the uniform background distribution of fission tracks are still problematical to the secondary origin hypothesis. Since radiohalos provide a tangible, physical record of nuclear decay in crustal rocks through earth history further field and laboratory work is recommended, focusing on the geological documentation of known and new Po halo localities, but also on documentation of the geological distribution of mature (fully-formed) U (and Th) halos in order to confirm whether such halos are indeed absent from Phanerozoic granitic rocks (as tentatively proposed).

* *Geology Department, Institute for Creation Research, Santee, California*

1. Introduction

Radiohalos (or radioactive halos) were first called “pleochroic halos” because they represented circular areas in some minerals as minute zones of color or darkening surrounding tiny central mineral crystals or inclusions [Bates and Jackson, 1980]. They are best seen in certain minerals, notably biotite, in rock thin sections. Upon microscopic examination, within the zone of discoloration can be seen concentric dark and light circles with diameters between about 10 and 40 μm (micron) and centered on the tiny mineral inclusion [Gentry, 1973].

These halos were first reported between 1880 and 1890, but their origin was a mystery until the discovery of radioactivity. In 1907 Joly [1907] and Mügge [1907] independently suggested that the central inclusions were radioactive and that the alpha (α) emissions from them damaged the surrounding mineral and produced concentric shells of discoloration around them (the circular patterns observed in thin sections are, of course, simply planar sections through concentric spheres centered around the tiny inclusions) (see Figure 1). Thus the earliest name, pleochroic, was partially a misnomer, since these halos were later found in minerals which are isotropic (have the same characteristics in all three dimensions)

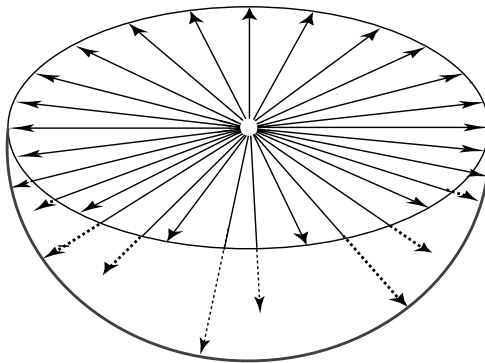


Figure 1. Sunburst effect of α -damage trails. The sunburst pattern of α -damage trails produces a spherically colored shell around the halo center. Each arrow represents 5 million α -particles emitted from the center. Halo coloration initially develops after 100 million α -decays, becomes darker after 500 million, and very dark after 1 billion [after Gentry, 1988].

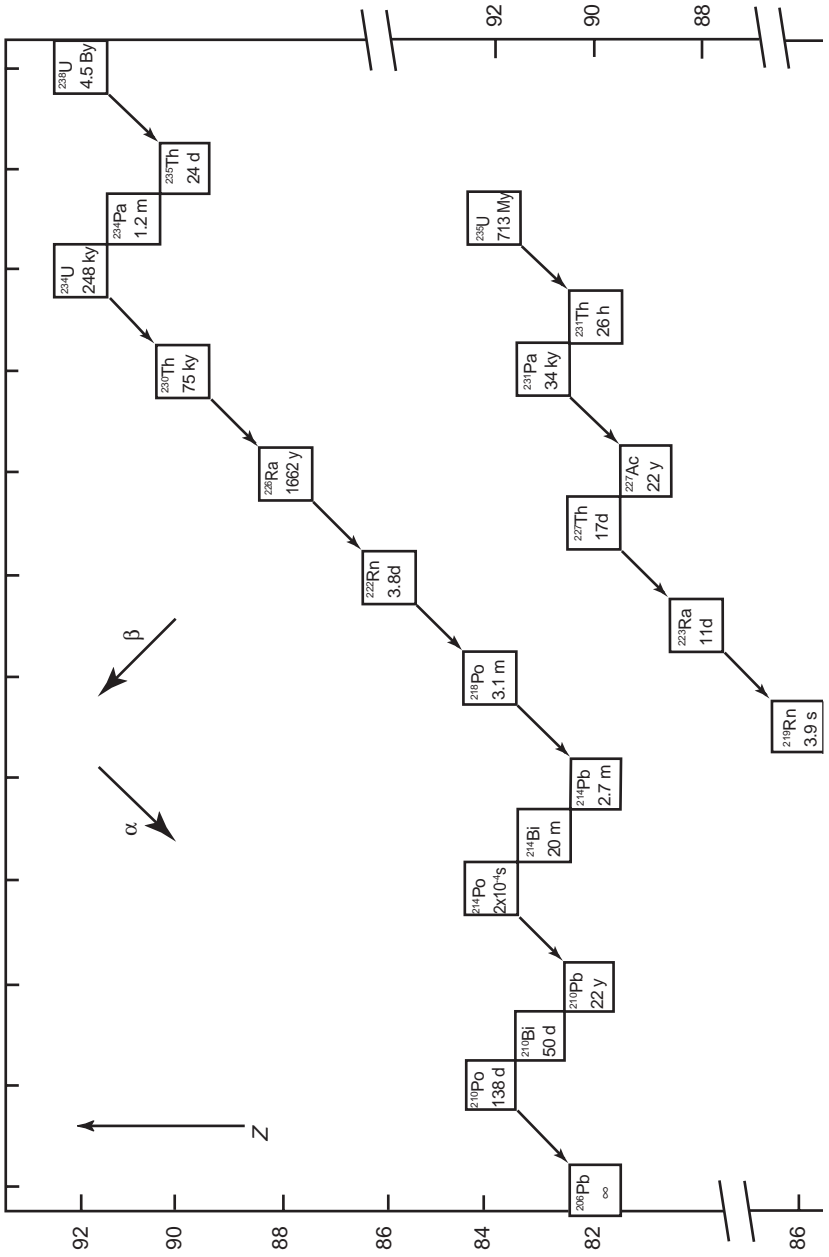
and which therefore do not show pleochroism (the ability to differentially absorb various wavelengths of transmitted light in various crystallographic directions, and thus to show different colors in different directions [*Bates and Jackson, 1980*]).

The significance of radiohalos is not so much in their attractiveness as mineralogical oddities, but because they are a physical, integral and historical record of radioactive decay in minerals that has occurred over a period of time. Most importantly, this record is detailed enough for us to allow estimation of the decay energies involved and to identify the radionuclides which have decayed (through energies and through genetic connections). In the context of radioactive dating of rocks and the age of the earth, therefore, the radiohalos, their origin and their history are of the utmost importance. Yet in spite of this, there are classes of halos which would appear to correspond to no presently-known radionuclides. Therefore, excluding the possibility of a non-radioactive origin, these could be evidence for as yet undiscovered or presently extinct radionuclides.

2. The Radioactive Origin of Halos

So radioactive halos may be generally defined as any type of discolored, radiation-damaged region within a mineral, usually resulting from α -emissions from a central radioactive inclusion. When the central inclusions, or radiocenters, are small (about 1 μm), the U and Th daughter α -emitters produce a series of discolored concentric spheres, which in thin section appear microscopically as concentric rings whose radii correspond to the ranges of the α -emitters in the mineral [*Gentry, 1984, 1986*].

The most compelling evidence to support the Joly-Mügge hypothesis of the radioactive origin for radiohalos is the correspondence between halo dimensions and the ranges of typical α -particles (extrapolated from air to mica). This is suggestive of a cause and effect connection. An even stronger qualitative argument is the correspondence between the number of α -emitters in the ^{238}U (or ^{232}Th) series and the number of rings in the corresponding halos. Figure 2 is a diagrammatic



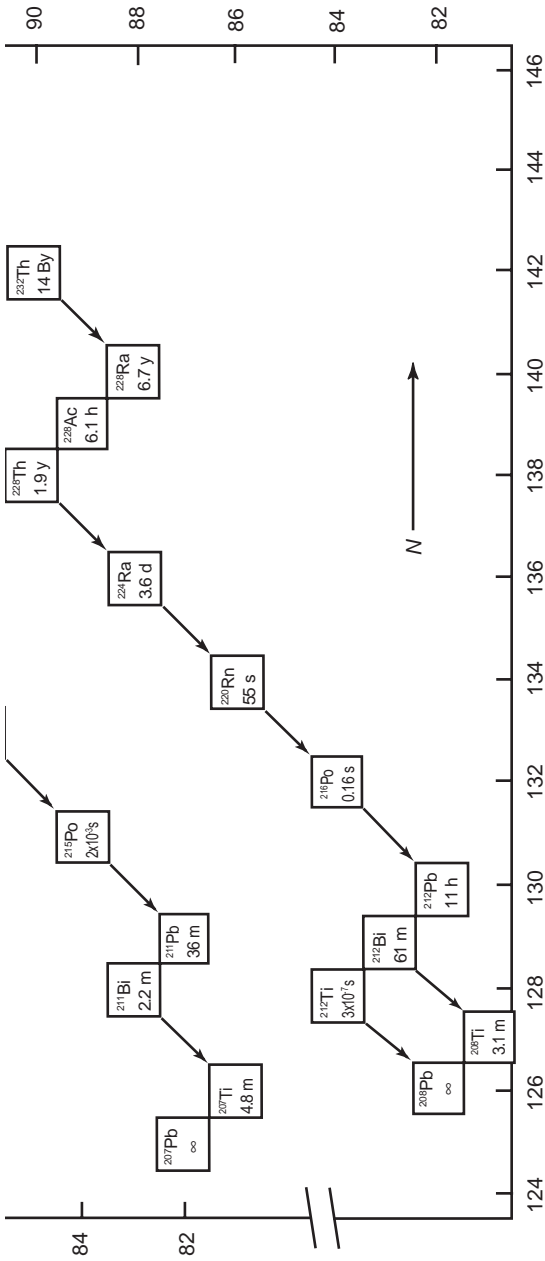


Figure 2. Part of the chart of the nuclides, in terms of Z (atomic number) against N (number of neutrons), to show species in the Th- and U-series decay chains and their half-lives. Before the chemistry of the decay series nuclides was investigated, many of the species were given provisional names which are now obsolete. The only one of these much used today is ionium (^{230}Th). The latter nomenclature will be used here.

representation of part of the chart of the nuclides, showing the species in the U- and Th-series decay chains and their half-lives, and arrows depicting which decay steps are due to α -emissions. Since large concentrations of the parent radionuclides are needed to produce the concentric ring structures of the halos, the parent ^{235}U radionuclide can be discounted as it only constitutes about 0.7% of naturally-occurring U. Figure 3 therefore is a schematic drawing of a ^{238}U halo (a) and a ^{232}Th halo (b) based on the ranges of the respective α -particles in air and their energies, the latter being appropriately listed. It is a simple matter of then comparing such a drawing with published halo photomicrographs to establish the correspondence of the ring patterns, which is compelling evidence for identifying the naturally-occurring radiohalos as being

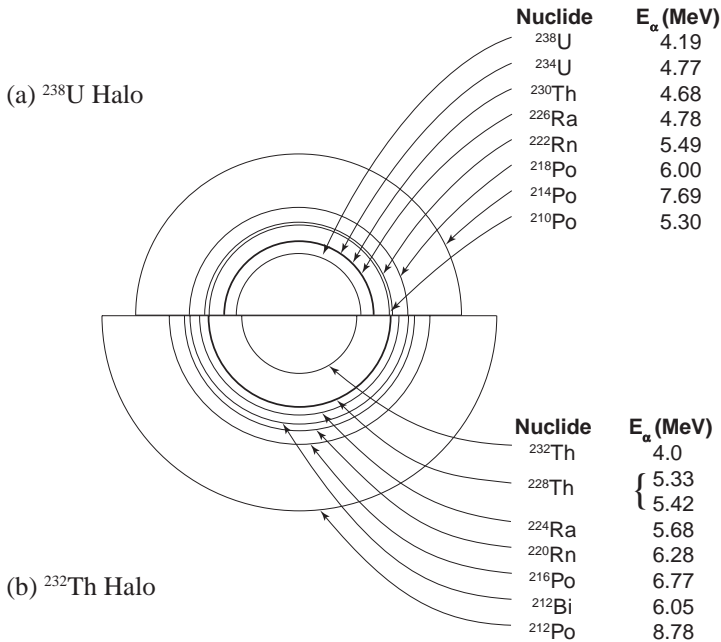


Figure 3. Schematic drawing of (a) a ^{238}U halo, and (b) a ^{232}Th halo, with radii proportional to the ranges of α -particles in air. The nuclides responsible for the α -particles and their energies are listed for the different halo rings [after Gentry, 1973].

derived from the ^{238}U and ^{232}Th series decay of these parent radionuclides originally concentrated in the central tiny inclusions (or radiocenters) [Gentry, 1973].

Rutherford [1910] and Joly and Rutherford [1913] initially provided evidence for the radioactive decay origin of the halos by showing that α -radioactivity could produce halo-like coloration in solids. In 1910 Rutherford reported that radon (Rn) enclosed in a soda-lime glass capillary tube produced a colored annulus whose breadth approximated the range of Rn α -particles in glass. Then in 1913 Joly and Rutherford reported that a dose of 1.5×10^{13} α -particles/cm² produced a halo-like coloration in biotite.

Results from using newer methods permit observation of single fission tracks in biotite [Fleischer *et al.*, 1965]. After appropriate etching (with hydrofluoric acid), an embryonic U halo (only the first ring visible) exhibits a cluster of 20–30 ^{238}U fossil fission tracks [Gentry, 1968a], implying that approximately 5×10^7 ^{238}U atoms have decayed [Gentry, 1973]. Thus at the first U ring radius of 13 μm the natural α -dose approximates that determined by Joly and Rutherford. This limited agreement in diverse samples is accidental, because different biotites may show wide coloration threshold responses. By irradiating halo-containing biotites with ^4He ions, Gentry [1968a, 1970] found that natural and induced coloration thresholds compare favorably enough to suggest that for some biotites the discoloration is approximately independent of dose rate, up to an α -flux of 10 nA/mm².

Ordinary radiohalos can be defined therefore as those which initiate with ^{238}U and/or ^{232}Th α -decay [Gentry, 1973], irrespective of whether the actual U or Th halo closely matches the respective idealized α -decay patterns. In a few instances the match is very good, the real size agreeing very well with the ^4He ion accelerator-induced coloration bands in biotite, fluorite and cordierite (see Table 1) [Gentry, 1973, 1974]. In general, a halo ring can be assigned to a definite α -emitter with confidence only when the halo radiocenter is about 1 μm in size [Gentry, 1984, 1986].

However, in other cases, such as halos in fluorite, much work was required before these halos could be reliably associated with U α -decay [Gentry, 1974]. As Gentry explained, reversal effects accompanying

extreme radiation damage can cause the appearance of rings that cannot be associated with definite α -emitters of the U-decay chain. (Reversal effects occur when the dose of radiation producing the halos is so intense and the resultant damage so extreme that the coloration inside the halos can be reversed, with normal dark rings being obliterated by total “bleaching” of the host crystal, and different diffuse dark rings, “ghost” rings, left where there would be normal light areas.) Thus some halos may exhibit a ring structure different from the idealized U and/or Th

Table 1. Comparison of sizes of ^4He induced coloration bands with halo radii. The ^4He ion energies at which the induced coloration bands were formed, or the α -particle energies of the corresponding radionuclides, are listed. Thus the radionuclide or α -particle energy which produced any halo ring can be recognized. The letters K-L, H, S, M and G represent halo measurements by Kerr-Lawson [1928], Henderson [1939], Henderson and Bateson [1934], Henderson and Sparkes [1939], Henderson and Turnbull [1934], Henderson, Mushkat and Crawford [1934], Schilling [1926], Mahadevan [1927] and

^4He Induced Coloration Band Sizes (μm)					E (MeV)	Nuclide	U Halo Radii (μm)		
Biotite		Fluorite	Cordierite				Biotite		
G_L ↓	G_M ↓	G_D ↓	G ↓	G ↓	↓	↓	$K-L$ ↓	H ↓	G ↓
13.4	13.8	14.2	14.1	16.2	←4.2	^{238}U →	12.3	12.7	12.2→13.0
NM	16.7	NM	17.3	19.2	←4.77	^{226}Ra →	15.4	15.3	14.8→15.8
NM	NM	NM	NM	NM	←4.66	^{230}Th →	NR	NR	NR
NM	16.7	NM	17.3	19.2	←4.78	^{234}U →	15.4	15.3	14.8→15.8
NM	19.3	20.0	19.6	22.5	←5.3	^{210}Po →	NR	NR	NR
NM	20.5	21.1	NM	NM	←5.49	^{222}Rn →	18.6	19.2	18.1→19.0
NM	23.0	23.9	23.6	26.7	←6.0	^{218}Po →	22.0	23.0	21.5→22.7
33.1	33.9	34.4	34.6	38.7	←7.69	^{214}Po →	33.0	34.1	30.8→33.0

α -decay patterns because of reversal effects. Furthermore, even though most other halos exhibit blurred ring structures due to the large sizes of the inclusions, nevertheless the outer dimensions allow them to be classified as U and/or Th types.

Modern analytical techniques such as Scanning Electron Microscope X-Ray Fluorescence (SEM-XRF) and Ion Microprobe Mass Spectrometry (IMMA) have been utilized to show that U and Th and their respective end-product isotopes of Pb are contained within the U and Th halo

Gentry [1974]. Subscripts L, M and D indicate light, medium (dose 10 to 20 times coloration threshold) and dark (dose about 50 times coloration threshold) induced bands; L→D and L→M indicate light to dark and light to medium (these were visually determined). Gentry's measurements were made with a filar micrometer readable to 0.07 μm . The estimated overall uncertainty was $\pm 0.3 \mu\text{m}$. Other abbreviations: NM not measured, NR not resolved, and NP not present.

U Halo Radii (μm)			Po Halo Radii (μm) in Biotite						Po Halo Radii (μm) in Fluorite	
Fluorite	Cordierite		^{210}Po		^{214}Po		^{218}Po		^{210}Po	^{218}Po
<i>S</i> ↓	<i>G</i> ↓	<i>M</i> ↓	<i>H</i> ↓	<i>G</i> _{L→D} ↓	<i>H</i> ↓	<i>G</i> _{L→M} ↓	<i>H</i> ↓	<i>G</i> _M ↓	<i>G</i> ↓	<i>G</i> ↓
14.0	14.2	16	NP	NP	NP	NP	NP	NP	NP	NP
16.9	17.1	19	NP	NP	NP	NP	NP	NP	NP	NP
15.8	NR	NR	NP	NP	NP	NP	NP	NP	NP	NP
16.9	17.1	19	NP	NP	NP	NP	NP	NP	NP	NP
19.3	19.5	NR	19.8	18.3→19.9	20.0	18.1→19.1	19.9	19.3	19.8	19.8
20.5	20.5	23.5	NP	NP	NP	NP	24.0	NP	NP	NP
23.5	23.5	26.5	NP	NP	NP	NP	NP	23.3	NP	23.7
34.5	34.7	38.5	NP	NP	34.5	32.5→33.8	34.0	34.0	NP	34.9

radiocenters [*Gentry*, 1971, 1974; *Gentry et al.*, 1973, 1974, 1976, 1978], as they would be expected to be.

3. Radiohalo Occurrence

Radiohalos usually are found in igneous rocks, even being in some igneous fragments which occasionally occur interspersed in sedimentary rocks [*Stark*, 1936]. However, there are reports of halos in gneisses from southern India [*Mahadevan*, 1927; *Gentry*, 1971; *Wise*, 1989], and in South Africa [*Hallbauer*, 1969]. Another exception is their occurrence in coal and asphaltized wood [*Jedwab*, 1966], and in coalified wood [*Gentry et al.*, 1976]. While mineralogists have found over 40 minerals in which radiohalos occur, their distribution within these minerals is very erratic [*Ramdohr*, 1933, 1957, 1960; *Stark*, 1936]. Biotite is quite clearly the major mineral in which radiohalos occur, and when they do they are prolific where found. Other minerals include fluorite and cordierite, but there are reports of radiohalos being present and especially common in quartz [*Laemmlein*, 1945; *Owen*, 1988; *Rink and Odom*, 1989; *Odom and Rink*, 1989]. While radiohalos have also been observed in orthoclase and microcline associated with radionuclide-bearing minerals [*Hallbauer*, 1969], they have not been seen in calcite or plagioclase [*Owen*, 1988]. However, radiohalos have also been found in diamonds [*Armitage*, 1995]. Furthermore, radiohalos in opaque minerals, such as ilmenite, of course are visible only in reflected light and exhibit poorly defined ring structure, partly due to smearing effects produced by large (approximately 10 μm) halo inclusions [*Ramdohr*, 1933, 1957, 1960]. Only those minerals that are transparent in 30 mm sections are suitable for detailed ring analysis, but even in these considerable microscope scanning time is required to locate good halo specimens [*Gentry*, 1973].

Ease of thin section preparation and fairly good registration properties have made biotite an ideal choice for numerous radiohalo investigations, namely, those of *Joly* [1917a, b, 1923, 1924], *Lingen* [1926], *Iimori and Yoshimura* [1926], *Kerr-Lawson* [1927, 1928], *Wiman* [1930], *Henderson and Bateson* [1934], *Henderson and Turnbull* [1934], *Henderson et al.*

[1934], and *Gentry* [1968a, 1970]. The three-dimensional nature of a halo is demonstrated when a biotite specimen is prepared for microscope examination [*Gentry*, 1973]. Because of its perfect cleavage properties, the leaves of a book of biotite (as with other micas) are easily separated with scotch tape, each successive section revealing a ring pattern of increasing size until the diametral section is obtained. (The molecular sheet structure of biotite is only about 10 Å thick, so leaves can be very thin.) Ring sizes have to be measured in diametral sections, and the most accurate measurements result from specimens having exceptionally small inclusions as their radiocenters.

As good as some radiohalos in certain biotite specimens are, investigations of *Hirschi* [1920, 1924], *Gudden* [1924], *Schilling* [1926] and *Gentry* [1974] have shown that radiohalos in fluorite afforded even better microscopic resolution of the halo rings. *Mahadevan* [1927] and *Gentry* [1974] have shown that radiohalos in cordierite may also yield suitable ring structure for accurate radii measurements, as has also been done by *Owen* [1988] for quartz.

The radiohalo inclusions occur as accessory minerals and have been identified as zircon, xenotime, monazite, allanite, sphene (titanite), apatite, uraninite and thorite [*Joly*, 1917a, b, 1923, 1924; *Ramdohr*, 1933, 1957, 1960; *Hutton*, 1947; *Snetsinger*, 1967; *Gentry*, 1970, 1971]. However, their small size sometimes prevents use of petrologic identification techniques.

Uranium, Th and other specific halo types have been observed mainly in Precambrian rocks [*Joly*, 1917a, b, 1923, 1924; *Iimori and Yoshimura*, 1926; *Kerr-Lawson*, 1927, 1928; *Wiman*, 1930; *Henderson and Bateson*, 1934; *Henderson and Turnbull*, 1934; *Henderson et al.*, 1934; *Gentry*, 1968a, 1970, 1971; *Owen*, 1988], but much remains to be learned about their occurrence in rocks from other geological periods. However, studies have shown that halos do exist in rocks stretching from the Precambrian to the Tertiary [*Holmes*, 1931; *Stark*, 1936; *Wise*, 1989], but unfortunately in most instances the halo types, whether U, Th or Po, etc., existing in the rocks investigated were not identified by comparing the observed halo ring structures with the ideal ring structures of the known halo types. Nevertheless, according to the data so far available (see Table 5

later), it would seem that Po halos mainly occur in Precambrian rocks, but it may be premature to conclude this until more Phanerozoic rocks have been examined.

4. Evidence Regarding Constancy of Radioactive Decay Rates

Because radiohalos are integral α -radiographs, an early interest was to ascertain whether U and Th halo radii were the same sizes in rocks from different geological periods. Any unaccounted for non-uniformity was thought would imply different decay energies and perhaps suggest a different value of λ , the decay constant. Such investigations were based on the premise that well-defined halo rings could be associated with specified α -energies [*Gentry, 1973*].

In other words, have radioactive decay rates remained invariant during the course of earth history? If they have, then geochronologists might seem justified in interpreting various parent/daughter isotope ratios found in rocks in terms of elapsed time. If on the other hand there have been periods in earth history where the decay rate was higher (that is, during a singularity), then in general the isotope ratios in rocks would not reflect elapsed time, except in specific cases where secondary rocks or minerals containing only the parent radionuclides formed at the end of the most recent singularity (for example, the Flood).

Even though most of Joly's measurements of U and Th halos showed their radii were about the sizes expected from the α -decay energies of the U and Th decay chains [*Joly, 1917a, b, 1923, 1924*], and perhaps not realizing all the subtle factors which may influence halo radii sizes, he announced in 1923 that U halo radii were indeed variable in rocks from different geological periods and claimed these slight discrepancies suggested that the radioactive decay rate had not been constant over geological time. But in 1926–1928, other investigators [*Iimori and Yoshimura, 1926; Schilling, 1926; Kerr-Lawson, 1927, 1928*] reported that U and Th halo radii in biotite, cordierite and fluorite approximated the expected values (within experimental error). However, these measurements were made on radiohalos within the same host rock and did not in themselves counter Joly's claim of variable halo radii in rocks

from different geological periods.

Even so, *Kerr-Lawson* [1927, 1928] made an important observation. In very thin biotite flakes he saw the inner ^{238}U ring resolved from the subsequent U halo rings (see Figure 3). Since Joly had not reported this inner ring, Kerr-Lawson inferred Joly's mineral sections containing the radiohalos were too thick to permit good ring resolution and so attributed Joly's variable halo radii to a confusion in measuring the inner U halo rings. *Gentry* [1973] confirmed this point by personal examination of some of Joly's thin sections.

In the 1930s Henderson and co-workers [*Henderson and Bateson*, 1934; *Henderson and Turnbull*, 1934; *Henderson et al.*, 1934] performed a classic series of experiments using a halo photometer for direct recording of radiohalo ring patterns. With little theoretical justification Henderson and his co-workers compared, as had *Joly* [1917a, b, 1923, 1924], *Iimori and Yoshimura* [1926] and *Kerr-Lawson* [1927, 1928], halo ring sizes with the minima of the composite curve formed by superimposing all the ^{238}U -decay chain Bragg ionization curves. There were inherent problems because a single composite curve could at best represent only one of the many radiohalo growth stages [*Gentry*, 1973]. Yet this approach seemed partially successful, for the composite curve did resemble the photometric scan of a U halo which showed all rings.

Further attempts to compare radiohalo radii with equivalent mineral ranges derived from α -ranges in air are also unsatisfactory because of uncertainties in the air-mineral conversion factor [*Gentry*, 1973]. Now newer techniques do allow appropriate standards to be developed.

Another aspect to the accurate determination of ring radii for radiohalo identification is the development of the radiohalos through different growth stages. In the case of a U halo, in its embryonic form only the first two rings are prominent (the ^{238}U and ^{234}U rings, as seen in Figure 3). Then there is the normal or intermediate stage when all rings may be detected. However, if the inner halo region is overexposed, then there can be coloration reversal and the formation of a diminutive ghost ring in the center. Alternately, all the inner rings may be completely obliterated. In other instances further spurious ghost rings unrelated to the terminal α -ranges may develop. Clearly, there are many traps for the

unwary. Thus investigators such as *Schilling* [1926], *Ramdohr* [1933, 1957, 1960] and *Gentry* [1967, 1971] at one time erred in inventing new α -activity to account for some of these ghost rings. Undoubtedly, a one-to-one correspondence between halo radius and α -energy is not always valid.

The most direct technique for developing reliable standards for halo radii comparisons is to irradiate halo-containing minerals with a sufficient dose of mono-energetic ^4He ions until halo-like coloration develops [*Gentry*, 1970, 1974]. If the development of the coloration is somewhat independent of the dose rate, then the ^4He ions will produce a coloration band that in theory is equivalent in depth or size to a halo radius produced by α -particles of the same energy. The experiment can then be repeated with ^4He ions of a different energy. The induced coloration band sizes then form the standards against which halo radii may be compared. However, in some minerals, especially biotite, the radiohalo radii are somewhat dose dependent, so that darker rings show slightly higher radii than faint rings [*Gentry*, 1974]. This dose effect is often masked by subtle halo radius variations produced by attenuation of the α -particles emitted within the inclusion itself. For example, when the inclusion, such as zircon, is more dense than the host mineral (biotite), slightly smaller radii result in embryonic halos, and extreme values are reached only after a heavy dose. However, a heavy dose produces a dark halo which tends to obscure the inner halo rings, making measurements difficult.

Although the finite inclusion size renders all radii measurements uncertain to a degree, there are two cases when the need for a correction is minimized. For densely colored radiohalos surrounding large inclusions, the only reasonable radius measurements are those made from the inclusion edge. On the other hand, for radiohalos in biotite with only tiny 1 μm inclusions, no correction for inclusion size is really necessary. However, in the case of fluorite the effect of finite inclusion size is minimized because some halos exist with radiocenters only 0.5 μm in diameter. Furthermore, in contrast to radiohalos in biotite, there is evidence that in some cases in fluorite the radioactivity is sufficiently distributed on the inclusion, implying radiohalo radii should be measured

from the inclusion edge. Fortunately, the radiohalo ring size in fluorite is only very minimally dependent on the α -dose, so that even embryonic halo rings form at practically maximum size [Gudden, 1924; Schilling, 1926; Gentry, 1974].

Table 1 shows U halo radii measurements in biotite, fluorite and cordierite [Schilling, 1926; Mahadevan, 1927; Kerr-Lawson, 1927, 1928; Henderson and Bates, 1934; Henderson and Turnbull, 1934; Henderson *et al.*, 1934; Gentry, 1973, 1974], as well as the coloration band sizes produced by accelerator ^4He ion beams of varying energy in the same minerals [Gentry, 1974]. Note that the comparison between fluorite coloration band sizes and halo radii is quite good, while in biotite the halo radii are somewhat smaller than the equivalent coloration band sizes. This deviation in biotite is likely due to the effects of a finite inclusion size, plus the dose-dependent radius effect, rather than a change in α -energy. Note also the comparison between coloration band sizes and halo radii in cordierite. The agreement is fair, even though the U halos in cordierite are developed around large inclusions which necessitated that the halo radii be measured from the inclusion edge [Mahadevan, 1927].

Finally, therefore, with respect to the question of whether radioactive decay rates have been constant throughout geological time, Spector [1972] has argued that the differences between the halo radii measurements made by Henderson and his co-workers and the equivalent air-mineral ranges do not present a case for the constancy of radioactive decay rates over geological periods of time, but if anything, imply the opposite (variable λ). However, in view of the experimental uncertainties with halo radii measurements this conclusion is not necessarily valid. On the other hand, Gentry [1974] has shown that even exact agreement between halo radii and corresponding coloration band sizes does not necessarily imply an invariant λ , and in fact uncertainties in radius measurements alone preclude establishing the stability of λ for ^{238}U to more than 35%.

The basis for the thinking that standard size U and Th halos imply invariant radioactive decay rates throughout geological time has proceeded from the quantum mechanical treatment of α -decay, which

in general shows that the probability for α -decay for a given radionuclide is dependent on the energy with which the α -particle is emitted from the nucleus [Gentry, 1984, 1986]. This in turn has been thought to mean that the higher the energy of the α -particles emitted from a particular radioisotope, the greater is the probability of α -decay and thus the shorter the half-life (decay rate) of that radioisotope. Table 2 illustrates this relationship between α -particle energies and half-lives. The argument then has been that if the radioactive decay rates have varied in the past, the U and Th halo rings would be of different sizes now because the energies of the α -particles would have been different during the period (or periods) of change.

Unfortunately, such notions were proposed before the advent of modern nuclear physics and the development of the technology to investigate α -particle emission during radioactive decay. Thus *Brown* [1990] insisted that, because of the sharpness of the radiohalo rings and the ease of

Table 2. Half-lives and energies of the α -particles emitted by radioisotopes in the ^{238}U and ^{232}Th decay chains (y = years, d = days, m = minutes, s = seconds).

Radioisotope	Half-life ($t_{1/2}$)	α -Particle Energy (MeV)
^{238}U	4.5×10^9 y	4.19
^{234}U	2.48×10^5 y	4.77
^{232}Th	1.4×10^{10} y	4.0
^{230}Th	7.5×10^4 y	4.68
^{228}Th	1.9 y	5.33, 5.42
^{226}Ra	1622 y	4.78
^{224}Ra	3.6 d	5.68
^{222}Rn	3.8 d	5.49
^{220}Rn	55 s	6.28
^{218}Po	3.1 m	6.00
^{216}Po	0.16 s	6.77
^{214}Po	2×10^{-4} s	7.69
^{212}Bi	61 m	6.05
^{212}Po	3×10^{-7} s	8.78
^{210}Po	138 d	5.30

identifying them with the α -particle sources that produced them, radioisotope half-lives over a range of 21 orders of magnitude have not varied by more than a factor of two during the time the geological formations of the earth which contain radiohalos have been in existence. Furthermore, *Brown* [1990] also deduced that this implied there has been no significant variation in the nuclear long-range force, the nuclear short-range force, or the electrical interaction force during this time interval. *Gentry* [1990] rejected *Brown*'s conclusions because of their dependence on uniformitarian assumptions, on the uniformity of physical laws, and on the validity of quantum mechanics at all past times. Understandably, *Brown* [1991] responded to affirm that the uniformity of physical laws was essential to our ability to "do science" because God has permitted the world to operate generally on that basis (unless He chooses to intervene), so that His original conclusions were justified. However, as explained by *Humphreys* in Chapter 7, the α -decay rate is extremely sensitive to the range of the strong nuclear force. Furthermore, a modest change in the range of the strong nuclear force can alter decay rates by orders of magnitude while hardly affecting the energies of the emitted α -particles and thus the diameters of radiohalo rings. Indeed, *Chaffin* [1994] has already demonstrated that if the depth of the potential energy "well" is increased with a corresponding increase in the decay constant λ , then the decay energy of the α -particle may be held the same with only a slight change in the nuclear radius, so that the radii of radiohalos also would remain the same while the decay constant λ changed (that is, the decay rate increased). Therefore the observed probable constancy of radiohalo radii does not necessarily imply an invariant λ (constant decay rates), and thus cannot preclude the possibility of accelerated decay rates (that is, shorter half-lives) in the past.

There is one last important relevant consideration here. Earlier it has been noted (see Figure 1) that halo coloration initially develops after 100 million α -decays, becomes darker after 500 million, and very dark after 1 billion α -decays [*Gentry*, 1988]. Embryonic U halos are sometimes observed (for example, in fluorite [*Gentry*, 1988]), but most U halos in biotites (for instance) are fully developed or mature, having thus apparently required on the order of 500 million–1 billion α -decays.

Therefore, the development of mature U halos in biotites suggests either a large amount of radioactive decay has actually occurred, or if the rocks were created, God created those rocks with the appearance of much radioactive decay.

Furthermore, if a large amount of radioactive decay has actually occurred, then within the Biblical, young-earth creationist timeframe such large quantities of radioactive decay had to occur in a drastically shorter period of elapsed time than the constancy at today's decay rates assumed by uniformitarians would allow. This in turn would thus imply that there had to have been a period, or periods, of accelerated radioactive decay during earth history (for example, early in Creation week and/or during the Flood). However, as already noted, accelerated α -decays (or shorter half-lives) do not result from higher α -particle energies concurrently producing larger halo ring radii. Thus if there had been a period of accelerated α -decay, then radiohalos produced during that period would not have larger ring radii than those corresponding radiohalos produced at today's decay rates outside of that period. Unfortunately, therefore, the ring radii measurements are not able to confirm either the constancy or non constancy of decay rates, and do not preclude the possibility that such a period of accelerated decay has occurred.

5. Variant Halos

Whereas ordinary radiohalos have been defined as those initiated by ^{238}U and/or ^{232}Th α -decay, there are variant halos which exhibit ring patterns different from the now well recognized ring structure and radii of U and Th halos. Some are due to α -decay from known radionuclides, while others present diverse ring structures unlike any currently known α -decay sequence. It is these variant halos which still require detailed explanation and which therefore provide the biggest challenge, and potentially the most fruitful areas, for research into whether the rates of radioactive decay have changed over geological time.

5.1 Dwarf Halos

Joly [1917a, b, 1923, 1924] reported the existence of dwarf halos with radii of approximately 5.2 and 8.5 μm in the biotites from the pegmatite quarried at Ytterby near Stockholm, Sweden. One rather unsatisfactory attempt has been made to identify the 5.2 μm dwarf halo with ^{147}Sm α -decay ($E_{\alpha} = 2.24 \text{ MeV}$) [*Picciotto and Deutsch*, 1960]. Dwarf halos are extremely rare and erratically distributed even in the few biotite samples which contain them [*Gentry*, 1973]. *Joly* considered their radioactive origin beyond question and attributed their bleached appearance to radiation overexposure or to elevated temperatures.

Gentry [1971] has also found dwarf halos in biotite specimens from Ytterby, and the sizes are difficult to correlate with the α -decay systematics of known radioactive nuclides. The smallest dwarf halos range from only 1.5 to about 2.5 μm with associated α -energies in the 1 MeV range. The half-lives of known radionuclides are in excess of 10^{13} years for α -decay energies of 2 MeV or less. Such weakly active radionuclides almost escape detection and would hardly be expected to produce halos. Other dwarf halos with radii from 3 to 11 μm correspond to α -energies of approximately 1.1 to 3.4 MeV. Some of these dwarf halos reflect coloration differences possibly due to varying amounts of parent radionuclides in the central inclusions. In this respect the occurrence of dual-ring dwarf halos also suggests a radioactive origin. Although *Gentry* has not yet seen dwarf halos in cordierite, *Mahadevan's* report [1927] of equivalent dwarf sizes in this mineral lends much credence to the radioactive origin of such halos. Whether there exists a causal relationship between the dwarf halos and the previously reported, though unconfirmed, low-energy α -activity found by *Brukl et al.* [1951] is presently open to question. However, it should be noted here that the dwarf rings which *Henderson* and his co-workers [*Henderson and Bateson*, 1934; *Henderson and Turnbull*, 1934; *Henderson et al.*, 1934] reported in some U halos appear to have been only artifacts of the coloration process.

Nevertheless, several lines of evidence which indicate the enigmatic dwarf halos were produced by some presently unidentified radioactivity

have been summarized by *Gentry* [1971, 1973] and *Gentry et al.* [1978]. The rapid etch from hydrofluoric acid and the K/Ca inversion in these dwarf halos are strongly characteristic of highly radiation-damaged regions. Furthermore, *Gentry et al.* [1978] reported that the peripheries of the dwarf halos were more rapidly etched than the central parts. This suggests the emission of particles from the halo centers caused greater damage (higher specific ionization) near the ends of their paths, which is characteristic of α -particles.

5.2 X Halos and Other Intermediate-Sized Varieties

Still rarer than the dwarf halos are the X halos first reported by *Joly* [1917a, b, 1923, 1924] in the biotites from Ytterby (Sweden) and Arendal (Norway). Later, *Lingen* [1926] reported halos of similar dimensions occurring in a granite near Cape Town (South Africa). According to *Joly* the inside ring of the X halo may be somewhat diffused and measures about 8.5 to 9.8 μm in radius, corresponding to an E_α of about 2.9 to 3.2 MeV. The bleached rings extend out to a radius of about 14 to 15 μm , and sometimes an adjacent dark ring is evident at about 17 μm ($E_\alpha = 4.4$ to 5.0 MeV). The outer wide band extends to approximately 28 μm , corresponding to an E_α of 6.7 to 6.9 MeV. Despite some similarities with Th halos there is no known α -decay sequence corresponding to these energies. Although well documented (and photographed) by *Joly*, no other investigator has yet found any X halos even after the scanning of thousands of sections of biotites from Ytterby, Arendal and Cape Town [*Gentry*, 1973]. Furthermore, the quite obscure reports of *Schintlmeister and Hernegger* [1940, 1941] and *Schintlmeister* [1941, 1942] of genetically related α -decay of 3 MeV and 4.5 MeV are interesting, but they remain unconfirmed. Therefore any association with the very elusive X halo is only speculation.

Gentry [1966b] reported the existence of a halo with rings apparently due to α -energies of about 4.4 to 5.4 MeV. However, the relatively large size of the central inclusion of this halo (6 μm in diameter) necessitates its re-examination. It is possible that the inner disc of this halo is a ghost ring resulting from α -particle attenuation within the inclusion. If so, the

halo may then be of the ^{210}Po variety (to be discussed below). *Gentry* [1967] has also reported a halo possibly due to ^{211}Bi α -decay, which is in the ^{235}U decay chain (see Figure 2). Since only two of these halos have thus far been reported, more specimens obviously are needed to confirm the identity of this type of halo.

Another unusual halo was the so-called D halo reported by *Henderson* [1939] and *Henderson and Sparks* [1939] to exhibit a diffuse boundary at a radius of approximately 16 μm . Henderson tentatively attributed this halo to ^{226}Ra α -decay because the radius approximated the size of the ^{226}Ra ring in the U halo. The absence of other rings, which should have appeared from daughter product α -activity, was explained by assuming that the immediate ^{222}Rn product (radon being a gas) diffused from the central inclusion before it decayed. This is contrary to the situation observed in normal ^{238}U halos. *Gentry* [1973] examined such halos, both in Henderson's original thin sections and in other biotites, and they generally possess central inclusions several microns in diameter and are without detailed ring structure. While Gentry felt they could not be explained on the basis of ^{226}Ra α -decay, the presence of fossil fission tracks indicated that U series α -emitters produced part of the coloration in this halo type.

In addition to U and Th halos, *Iimori and Yoshimura* [1926] reported three halo sizes which they designated as Z_1 , Z_2 and Z_3 halos. They attributed these halos to actinium (^{235}U) series α -emitters. *Gentry* [1973] examined some of the original slides, as well as separate Japanese biotite samples in which such halos had been reported. He observed that many halos in these biotites are very dark, so that it was necessary to prepare very thin sections in order for the central inclusions in the halos to be seen. Some of the original Iimori and Yoshimura thin sections containing Z halos were simply too thick to permit accurate halo radii measurements. Gentry concluded that the Z_1 and Z_2 halos could be explained as U halos and/or a combination of U-Th halos without postulating the presence of actinium (^{235}U) α -emitters, while the Z_3 halo was actually a ^{210}Po halo, as were the "emanation" halos reported by *Joly* [1917b, 1924] and *Mahadevan* [1927].

5.3 Giant Halos

Although *Hirschi* [1920, 1924] was apparently the first to report giant halos, the report by *Wiman* [1930] of halos within biotite with radii of approximately 55 μm and 67 μm was better documented. Even so, on the basis of a rather cursory examination *Höppe* [1959] was unable to confirm *Wiman's* results. However, *Gentry* [1970] later found, after examination of more than 1000 thin sections [*Gentry*, 1973], that giant halos do exist in the rocks described by *Wiman*.

A more abundant source of giant halos was found in biotite from Madagascar. In this specimen *Gentry* [1970] reported seven different groups of giant halos ranging from 45 μm to 110 μm (see Table 3). An unanswered question is whether these halos originated with high energy α -emitters in the range from 9.5 MeV to 15 MeV. One group in particular with radii between 50 and 58 μm *Gentry* tentatively attributed to the low-abundance (1:5500), high-energy (10.55 MeV) α -particles of ^{212}Po , the last α -emitter in the Th decay chain [*Gentry*, 1966a]. Tentatively, this low-abundance group was associated with the 55 μm radius giant halos in the granites which *Wiman* studied.

No other known radionuclides occur with sufficient energy and/or abundance to produce the other groups of giant halos. Therefore, seven other possibilities were considered by *Gentry* [1970] as explanations

Table 3. Frequency of halo sizes of radii 32 to 110 μm in a Madagascan biotite [*Gentry*, 1970].

Group	Interval of halo radius (μm)	Maximum energy of α -particles (MeV)	Total number of halos
I	32–35	7.68	22
II	37–43	8.78	274
III	45–48	≈ 9.5	28
IV	50–58	≈ 10.6	130
V	60–67	≈ 11.7	69
VI	70–75	≈ 12.3	58
VII	80–85	≈ 13.2	30
VIII	90–95	≈ 14.1	10
IX	100–110	≈ 15.1	5

for the giant halos. These were:

- variations in α -particle range due to structural changes in biotite;
- diffusion of a pigmenting agent from the central inclusion into the matrix;
- diffusion of radioactivity from the inclusion to the matrix;
- channeling along cleavage planes;
- β -radiation instead of α -emission;
- long-range α -particles from spontaneous fission; and
- α -particles or protons from (neutron, α -particle) or (α -particle, proton) reactions.

Gentry [1970] has shown that it would appear none of the above alternatives are very probable, implying that the giant halos may represent unknown α -radioactivity. In this respect, the giant halos in cordierite reported (and photographed) by *Krishnan and Mahadevan* [1930] are very significant. The “Th” giant halos they reported may be due to the low abundance α -particles from ^{212}Po . In contrast, the “U” giant halos they reported correspond to an E_α of about 9.5 MeV and do not appear to be explained on the basis of a low-abundance ^{238}U -decay series α -emitter.

Gentry [1973] has also suggested that high spin or shape isomers (structurally different atoms of the same isotope) which exhibit high energy α -decay may be responsible for the giant halos [*Gentry*, 1970], an hypothesis which was investigated by *Gentry et al.* [1973]. *Gentry et al.* [1976] analyzed the monazite radiocenters in some of the giant halos using proton-induced x-ray emission and concluded that the observed x-ray energy spectra were best explained by the presence of a number of superheavy elements. However, there is practically nothing else to suggest a superheavy element connection [*Gentry*, 1970]. Furthermore, *Holbrow* [1977] suggested that the giant halos might have been produced by the α -particles that occasionally accompany the spontaneous fission of ^{244}Pu , and that under ideal circumstances such giant halos might be as large as 100 μm , with the proton-induced x-rays from the monazite radiocenters not being due to superheavy elements, but possibly due to K x-rays of Te fission fragments.

The characteristics of these giant halos found in the Madagascan biotite

have been summarized by *Gentry* [1970, 1973], the radii of several hundred halos having been measured with a precision of about $\pm 1.5 \mu\text{m}$. The grouping of different radii sizes, the α -particle energies thus represented, and the frequency of the occurrence of each radii grouping are listed in Table 3. It may be significant to note that for halos with large inclusions the actual radius of the halo as measured from the inclusion edge to the halo perimeter varied up to around 5 to 6 μm , with the variation dependent upon the stage of halo development [*Gentry*, 1970], perhaps because a greater fraction of the α -particles are being emitted within the outermost micron of the large inclusions. Furthermore, he found variations of 1 μm in halo radii even with point-like inclusions, possibly resulting from maximum ionization (coloration) occurring at slightly less than end-point ranges. Non-uniform halo boundaries also occurred and may have resulted from non-uniform distributions of radioactivity in the inclusions. Other uncertainties in the radii measurements could have arisen if the inclusions were inclined with respect to the cleavage planes in which the radii were being measured.

The maximum energy values of the α -particles were tabulated by *Gentry* [1970] for purpose of comparison only and were *not* meant to necessarily imply that the respective halo groups originated with α -particles of that energy. There were a few halos which did not fall into any of the categories listed in Table 3, but *Gentry* found the number of this type was only a small percentage of the total (2%).

Radiohalos in groups I and II were the normal U and Th halos, whose maximum radii are identified with the respective daughter α -emitters ^{214}Po ($E_\alpha = 7.68 \text{ MeV}$) and ^{212}Po ($E_\alpha = 8.78 \text{ MeV}$) of these decay series respectively (see Figure 3). As indicated above, *Gentry* also thought that the halos in group IV may be associated with the low-abundance, long-range α -particles from ^{212}Po ($E_\alpha = 10.55 \text{ MeV}$) in the Th decay series. Two other observations by *Gentry* are worth noting. First, *Gentry* [1970] showed a photomicrograph with a radiohalo which was a combination of both U and Th series decay, with an inner ring from ^{214}Po (^{238}U decay chain) and an outer ring produced by ^{212}Po (^{232}Th decay chain). In this instance the central inclusion had a diameter of about 20 μm . The second observation *Gentry* [1973] made was that unlike

overexposed Th halos in ordinary biotite which are dark, the Th halos in the Madagascan biotite had lighter rather than darker coloration. Furthermore, in both the Th and U halos in the same biotite the internal ring structures are missing, often due to the large central inclusions.

While no definitive evidence as yet exists for a radioactive origin of all the giant, unexplained halos, some of those with opaque central inclusions in the Madagascan biotite exhibit isotopic anomalies which raise questions about the uniformity of U and Th α -decay. For example, the mass scans and x-ray fluorescence analyses of both monazite and opaque central inclusions in the Madagascan giant halos [Gentry, 1984, 1986] clearly indicate that, whereas both the monazite and opaque inclusions exhibit ^{206}Pb and ^{207}Pb from ^{238}U and ^{235}U decay respectively, the opaque inclusions exhibit a marked deficiency of ^{208}Pb from ^{232}Th decay. Of course, when the central inclusions are monazite, then because of their high concentrations of Th as well as significant U, the occurrence of the combined U and Th halos are accounted for.

The subsequent work by Gentry *et al.* [1978] on giant halos found in certain biotites from granites at Arnö and Rickaby (Sweden) has furnished data with implications for the radioactive origin of both the giant halos, and the enigmatic dwarf halos found in biotites from the pegmatite at Ytterby, Sweden (as already discussed). Gentry *et al.* [1978] found that the majority of U and Th halos in these Swedish biotites exhibited darkening which extended to the maximum halo radii (approximately 38 to 40 μm for the Th halos). However, about 1% of the halos had an inner bleached region which varied from approximately 2 to 25 μm in radius surrounding highly radioactive inclusions. Generally, when the bleached region was small (less than or equal to 8 μm), no change was evident in the dimensions of the halos. However, in those halos in which the bleached regions were more intense and of larger radius (approximately 15 μm), somewhat weakly colored diffuse rings were generally observed outside the normal boundaries of U and Th halos.

These are the giant halos which were reported by Gentry [1970] to surround only dense Th halos and which were tentatively attributed to the low-abundance, high-energy α -particles from ^{212}Po in the ^{232}Th decay chain. However, Gentry *et al.* [1978] reported that diffuse, abnormally

large rings also surrounded dense U halos in these Swedish biotites, and as there are no high energy α -particles of any significant abundance in the ^{238}U decay chain, they therefore considered that hypothesis as possibly untenable. Instead, they explored the possibility that these bleached interior regions were somehow associated with the formation of the giant halos.

Even though these giant halos were found by *Gentry et al.* [1978] in granite specimens obtained from the same locations as *Wiman* [1930], the giant halos described by *Gentry et al.* [1978] are different from those reported by *Wiman* [1930]. The *Gentry et al.* [1978] giant halos surround U and/or Th rich inclusions and have diffuse boundaries which may vary from approximately 42 to approximately 55 μm in radius. In contrast, *Wiman* [1930] reported giant halos around zircon inclusions showing normal size inner rings and somewhat weak, but rather sharply defined, outer rings of 57 μm and more rarely 67 μm .

Combining results of applying optical microscope, electron microprobe x-ray fluorescence and ion microprobe mass spectrometer techniques, *Gentry et al.* [1978] were able to show that the regions corresponding to the bright, inner bleached areas of their giant halos as seen under the optical microscope are diminished in K by about a factor of 10 and slightly enhanced in Ca compared to the surrounding biotite. Because the radius of the bright, inner circular bleached regions around the central inclusions approximated the range of the predominant lower energy α -particles of the U and Th decay chains, *Gentry et al.* [1978] suggested that extreme radiation damage effects may have first produced a partial decomposition of the biotite in these regions, with secondary effects then inducing the migration of K out of and Ca into these regions, the latter migrating inwards from the outer halo regions which showed Ca depletion. Some mineralogical aspects relating to part of this phenomenon have been reported by *Rimsaite* [1975].

The giant halos therefore probably did not result from diffusion of radioactivity into the biotite because ion microprobe mass spectrometer studies showed U, Th and Pb were confined to the central inclusions [*Gentry et al.*, 1978]. Instead, the large K depletion in the central regions may have sufficiently reduced the total mass there at a crucial period of

time to allow the highest normal energy α -particles of the Th and U decay chains (8.73 MeV and 7.68 MeV respectively) to penetrate beyond the normal boundaries of the halos because of having first passed through regions of lower density. (Because of the large K depletion and slight Ca enrichment, these regions would have had a slightly lower density than the adjacent biotite.)

Although there are thus unanswered questions about this phenomenon, it seems that the bleached areas are high radiation damaged regions. This observation itself is significant, because under the microscope the dwarf halos exhibit the same type of bleached appearance as is shown by the inner bleached regions of the giant halos [*Gentry*, 1971, 1973]. Thus when *Gentry et al.* [1978] analyzed the Ytterby dwarf halo centers for the presence of some recognizable parent and/or daughter radionuclides, it became evident that the same type of K-Ca inversion phenomenon was showing up throughout the dwarf halo regions, which they considered as additional evidence for a radioactive origin of the dwarf halos.

Finally, the suggestions made by *Fowler and Lang* [1977], though listed by *Gentry* [1970] and regarded as improbable, are worth considering. *Fowler and Lang* [1977] maintained that the large inclusions/radiocenters of the giant halos would generate cracks both normal and parallel to the biotite cleavage due in part to radiation damage induced swelling of the inclusions. These cracks in turn may help extend the volume exposed to radiation damage by allowing α -particles entering or crossing the cracks to travel further than their normal ranges, and enhance the capabilities of diffusion of Rn isotopes liberated from the inclusions. Based on these suggestions, *Chaudhuri and Iyer* [1980] proposed a diffusion of gaseous Rn isotopes model for all variant halos. They claimed that the radiation damaged and cracked areas around the U- and Th-rich inclusions would have diffusion coefficients of about 10^{-7} to 10^{-11} cm^2s^{-1} compared with 10^{-22} cm^2s^{-1} for solid crystals, but they based their calculations on a millions-of-years timescale. Thus much still needs to be resolved before a satisfactory explanation for the formation of giant halos, consistent with all the data (including α -recoil evidence), is produced.

5.4 Polonium (Po) Halos

Of the four types of unusual halos that appear distinct from those formed by U and/or Th α -decay, only the Po halos can presently be identified with known α -radioactivity [Gentry, 1968a, 1971, 1973, 1974; Gentry *et al.*, 1973, 1974]. There are three Po isotopes in the ^{238}U -decay chain (see Figure 2)— ^{218}Po (half-life of 3 minutes), ^{214}Po (half-life of 164 microseconds) and ^{210}Po (half-life of 138 days). Figure 4 shows schematic drawings of the idealized structures of the three different Po halos in comparison with the ^{238}U halo. Note that the Po halos only exhibit Po rings and are designated by the first (or only) Po α -emitter in the decay sequence, these Po α -emitters being end members in the ^{238}U -decay chain.

All three different Po halos occur in biotites, while according to the

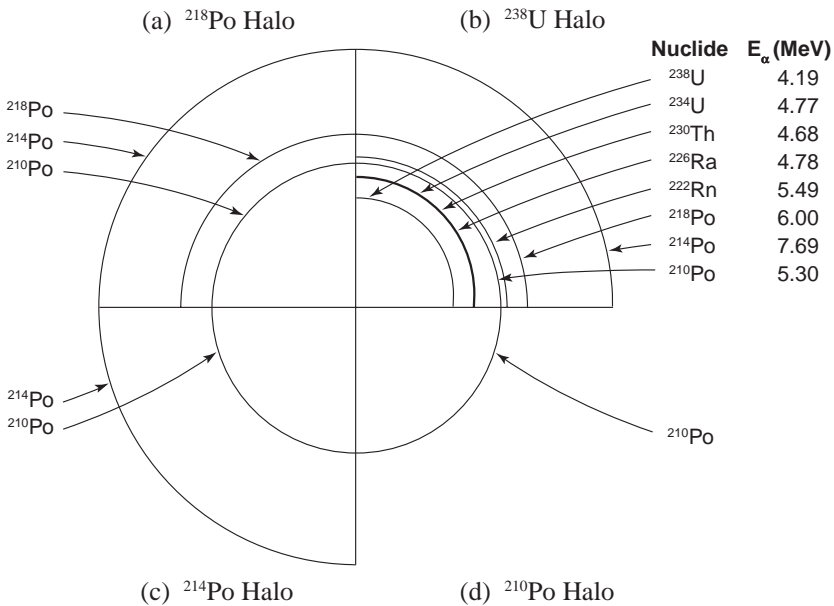


Figure 4. Composite schematic drawing of (a) a ^{218}Po halo, (b) a ^{238}U halo, (c) a ^{214}Po halo and (d) a ^{210}Po halo with radii proportional to the ranges of α -particles in air. The nuclides responsible for the α -particles and their energies are listed for the different halo rings [after Gentry, 1973].

data available thus far it would appear that only ^{218}Po and ^{210}Po halos occur in fluorite, and only ^{210}Po halos in cordierite [Gentry, 1968a, 1971, 1973, 1974, 1984, 1986, 1988; Gentry *et al.*, 1973, 1974; Wise, 1989]. Comparison of photomicrographs of these Po halos with the schematic drawings in Figure 4 enables easy identification because the similarities are clearly evident. Where several ^{210}Po are in the same field of view within biotite and fluorite the effect of different α -doses is obvious. When very dark and light halos are compared, the darker halos have slightly larger radii, which are attributable to higher α -doses.

The data in Table 1 give measurements of Po halos in biotite and fluorite by Gentry [1973, 1974], and Henderson and Sparks [1939]. Henderson's measurements were made using the halo photometer, while the rest were made under the optical microscope with a calibrated ocular micrometer. For comparison purposes Table 1 includes measurements of Po halos in biotite that exhibit radius variations due to dose effects. However, the table still shows the correspondence between Po halo radii and the induced coloration band sizes, leaving little doubt that the Po halo ring structures do indeed match the respective Po α -emitters. Note the very good agreement between Po and ^{238}U halo radii in fluorite. In biotite the ^{238}U halo radii must be compared with very light Po halos in order to minimize radii differences from dose effects. Although not shown in Table 1, Po halo radii measurements in cordierite [Mahadevan, 1927] also agree with the coloration band sizes.

An important observation from Figure 4 is that, in the idealized ^{238}U and ^{218}Po halo patterns, it is evident that the ^{222}Rn ring is missing from the ^{218}Po halo but present in the ^{238}U halo. This is confirmed by photomicrographs of these halos in both fluorite and biotite [Gentry, 1984, 1986], which show the presence of the ^{222}Rn ring in the ^{238}U halo in contrast to its absence in the ^{218}Po halo. However, because the ^{222}Rn ring in the ^{238}U halo can closely approximate the ^{210}Po ring or even overlap it, observation of the optical image of the rings alone may not conclusively identify a ^{218}Po halo, so ion microprobe confirmation may be needed. Nevertheless, this may still be unequivocal evidence that the ^{218}Po halos were initiated by ^{218}Po in the tiny central inclusions, rather than with an earlier α -emitter in the ^{238}U decay chain such as ^{222}Rn or its

parent ^{226}Ra . Likewise, it can be noted that the ring patterns of the ^{214}Po and ^{210}Po halos indicate that they were initiated by ^{214}Po and ^{210}Po respectively. This is critical in determining the origin and mode of formation of these Po halos.

Joly [1917b, 1924] was probably the first to investigate ^{210}Po halos and he was clearly baffled by them, calling them “emanation” halos. Because *Schilling* [1926] saw Po halos located only along cracks in his Wölsendorf fluorite sample, he suggested that they originated from preferential deposition of Po from U-bearing solutions. (*Gentry* [1973] reported that he also found Po halos in the same fluorite, but separated from conduits.) Following on from *Joly*’s work, *Henderson* [1939] and *Henderson and Sparks* [1939] invoked a similar but more quantitative hypothesis to explain Po halos along conduits in biotite. Those Po halos he found occurring away from conduits, similar to those found by *Gentry* [1973, 1974], were more difficult to account for, but he proposed a very qualitative laminar flow hypothesis.

Now the reason for these and other attempts to account for Po halos by some sort of secondary process is quite simple—the half-lives of the respective Po isotopes are far too short to be reconciled with slow magmatic cooling rates for the rocks such as granites which contain the Po-halo bearing biotites (for example, the half-life for ^{218}Po is 3 minutes). This is not the only formidable obstacle encountered by endeavoring to explain the Po halos by secondary transport of Po separated from U. First, there is the problem of how isotopic separation of several Po isotopes, or their β -decay precursors [*Gentry et al.*, 1973], from parent ^{238}U could have occurred naturally. Second, a straightforward explanation of ^{218}Po halos implies that the 1 μm radiocenters of very dark halos of this type initially contained as many as 5×10^9 atoms (a concentration of more than 50%) of the ^{218}Po isotope [*Gentry*, 1974]. *Gentry* [1984, 1986] maintains that in most cases the minerals (presumably those in which the halos occur) contain only ppm abundances of U, which means only a negligible supply of Po daughter atoms is available for capture at any given time. To form a halo these daughter atoms must migrate or diffuse so they can be captured at a collecting site, a problem which is compounded by the low diffusion rates in minerals [*Gentry*, 1968a, 1975;

Fremlin, 1975].

Yet *Gentry* [1968a], by using fission-track and α -recoil techniques, reported that he had found no evidence for a secondary origin for the three types of Po halos in biotite, which occurred apart from conduits. Consistent with the ring structures, fission-track analyses of the Po halo inclusions showed very little, if any, fission of U had occurred in the rocks. Furthermore, the α -recoil technique [*Huang and Walker, 1967*], which permits the observation of a single α -recoil pit in biotite, was employed to measure the distribution of decayed α -radioactivity in regions both adjacent to and far removed from Po halo inclusions. No differences in α -recoil density were noted in the two areas. If U daughter α -activity had fed the Po inclusions, a significantly higher α -recoil density would presumably have been in evidence.

One solution to this dilemma was initially suggested by *Gentry* [1973], that the parent radionuclides of the Po in the halo inclusions were long half-life β -decaying isomers that may yet exist. The halo ring structures would allow for this, because β -radiation produces no coloration in halos in biotite, fluorite or cordierite. If such isomers existed, Po, U and Th halos could all be explained by assuming that minute quantities of the respective radionuclides were incorporated into separate halo inclusions, either before or coincident with the host rock crystallization. However, *Gentry et al.* [1973] investigated the possible existence of such isomers, and then *Gentry* [1974] decided that because no trace had yet been found this hypothesis was untenable.

The identity of U, Th and Po halos in biotite and fluorite samples has been confirmed by *Gentry* [1970, 1971, 1974] and *Gentry et al.* [1973, 1974], who used scanning electron microscope x-ray fluorescence (SEM-XRF), and ion microprobe mass spectrometric (IMMA), techniques to analyze *in situ* the various types of halo radiocenters, including even the smallest halo inclusions. Many U and Th inclusions were analyzed in order to obtain isotopic data against which the results from the radiocenters in the variant halos, particularly the Po halos, could be compared.

Because the Po halos were all initiated by Po isotopes which decay to terminate with ^{206}Pb , the radiocenters should reflect an excess of this Pb

isotope. Furthermore, because the ring structures and fission-track analyses show only small amounts, if any, of U, mass analyses of such Po halo inclusions should be consistent with these observations also. Generally then, while any given Po halo inclusion might have initially contained varying amounts of different Po isotopes, halo rings would have developed only if approximately 10^8 atoms of a specific radionuclide were present. This implies Po isotope ratios may be variable even when examining different Po halos of the same general type. (In principle this is similar to the case where varying amounts of Th are found in halo inclusions around which only U-decay chain rings appear.)

Overall, the studies of various Po halo radiocenters in biotite and fluorite have shown little or no U in conjunction with anomalously high $^{206}\text{Pb}/^{207}\text{Pb}$ and/or Pb/U ratios which would be expected from the decay of Po without the U precursor which normally occurs in U radiohalo centers [Gentry, 1974; Gentry *et al.*, 1974]. Specifically, the ion probe analyses revealed one ^{210}Po halo inclusion that contained Pb without any detectable ^{204}Pb , U or Th; the $^{206}\text{Pb}/^{207}\text{Pb}$ ratio was approximately 20 or more. Gentry [1973] maintained that the absence of U and Th meant this Pb was not radiogenically derived from those elements, while the absence of ^{204}Pb meant this Pb could not be so-called primordial or common Pb as those terms are usually defined. He therefore concluded that while these values were inexplicable on the basis of known isotopic mixtures of Pb, they definitely agreed with the isotopic mixture of Pb which would be expected by derivation from Po decay independent of U or Th.

In other Po inclusions the $^{206}\text{Pb}/^{207}\text{Pb}$ ratio has been determined as about 10, 12, 18, 22, 25, 40, 62 and 80. The theoretical maximum possible radiogenic $^{206}\text{Pb}/^{207}\text{Pb}$ ratio, based on an instantaneous production of Pb from normal isotopic decay of U, is 21.8. Therefore, $^{206}\text{Pb}/^{207}\text{Pb}$ ratios greater than 21.8 not only reflect the existence of a seemingly abnormal mixture of Pb isotopes, but in a different way confirm the existence of Pb derived from Po decay independent of the normal U-decay chain [Gentry, 1971; Gentry *et al.*, 1973].

After carefully considering the data he had gathered, Gentry advanced the hypothesis that the three different types of Po halos in biotite, fluorite

and cordierite represent the decay of primordial Po, in which case the rocks that host these halos, that is, the Precambrian granites, must be primordial rocks [Gentry, 1979, 1980, 1982, 1983]. By this reasoning, Gentry identifies the Precambrian granites as the rocks that were created almost instantly as a part of the Creation event recorded in Genesis 1:1, rather than as rocks which are the product of the evolution of the earth.

6. Secondary Radiohalos

According to Gentry [1984, 1986], all the various types of halos already discussed would be termed primary halos because they developed from α -activity emanating from small accessory inclusions which were presumably present when the host minerals (for example, biotite) crystallized. However, what are clearly secondary radiohalos also exist in pieces of coalified wood buried in sandstones and associated with “roll front” U deposits of the Colorado Plateau area [Breger, 1974; Gentry *et al.*, 1976]. There is abundant evidence that ground waters have leached U from granitic and other Precambrian basement rocks and carried it in solution, infiltrating through sandstone beds in the region in front of an alteration or roll front marking the boundary at the redox interface between the advancing oxygenated ground waters and the normal reducing conditions in the sandstone beds [Adler, 1974; Granger and Warren, 1974]. At the same time the wood buried in the sandstones was still in a permeable condition [Gentry *et al.*, 1976]. When the U-bearing ground water passed through the pieces of wood, certain active sites within the wood preferentially collected U, while other sites collected Se, Po and Pb. Harshman [1974] found that there was an anomalous concentration of Se present in the U orebodies with which the coalified logs were associated, and the Se had been deposited in narrow zones at the outer edges of the altered tongues, astride the edges, or in reduced sandstone close to the edges just in front of the advancing U-mineralizing roll/redox fronts. The altered sandstone behind the roll fronts contains ferroselite (FeSe_2), while the reduced sandstone in front of the advancing U mineralization contains native Se. Because Se concentrations are at least one order of magnitude greater in the altered

sandstone compared with the unmineralized reduced sandstone, significant amounts of Se had to have been introduced into the sandstone with the U by the advancing groundwater flow.

It is quite significant that the U halos, which developed around the tiny U-sites, are all under-developed and typically embryonic, that is, they do not generally exhibit the outer ^{214}Po ring characteristic of fully developed U halos in biotite and fluorite [Gentry, 1973]. Such under-developed halos would normally imply a low U concentration in the radiocenters, but electron microprobe x-ray fluorescence (EMXRF) and ion microprobe mass spectrometer (IMMA) analyses revealed that many such radiocenters contain large amounts of U, with low Pb abundance [Gentry *et al.*, 1976]. Thus the $^{238}\text{U}/^{206}\text{Pb}$ ratios obtained for the U halo radiocenters were extremely high—approximately 2230, 2520, 8150, 8300, 8750, 18,700, 19,500, 21,000, 21,900 and 27,300 (corrected for different ionization efficiencies). These data, including the under-developed/embryonic state of the U halos, suggest it has only been a relatively short time since U infiltrated the coalified wood, specifically within the last several thousand years [Gentry *et al.*, 1976].

The variations in the $^{238}\text{U}/^{206}\text{Pb}$ ratio values obtained have been explained as resulting from the addition of varying amounts of “old” radiogenic Pb to a constant amount of ^{206}Pb generated *in situ* in these radiocenters from decay of ^{238}U [Gentry *et al.*, 1976]. These varying amounts of “old” radiogenic Pb are of course consistent with radiogenic Pb also being leached with the U from the granitic and other Precambrian basement rocks by ground waters and carried in solution as the ground waters infiltrated through the host sandstone beds. However, even without attempting to subtract this “old” ^{206}Pb , a $^{238}\text{U}/^{206}\text{Pb}$ value of 27,300 is indicative of a formation time for the radiocenter more recent by a factor of at least 270 than the minimum (Cretaceous), and of a factor of 760 than the maximum (Triassic), geological age estimated for the introduction of the U into the coalified logs [Rosholt, 1958; Stern and Stieff, 1959]. In fact, a $^{238}\text{U}/^{206}\text{Pb}$ value of 27,300 would have been produced by only about 240,000 years of radioactive decay at today’s observed rates. Some $^{238}\text{U}/^{206}\text{Pb}$ ratios that more accurately reflect the amount of Pb from *in situ* U decay were obtained by searching for sites

with even higher ratios but containing negligible amounts of extraneous Pb. Two such U halo radiocenters were found. Such ratios are consistent with both the initial U infiltration and the coalification having occurred within the past several thousand years. On the other hand, it may be argued that some U may have been added or Pb may have been selectively removed, or both, by groundwater circulation after coalification producing variable U/Pb ratios, but the highest ratio would then simply reflect the last time when U or Pb mobilization, or both, occurred. However, even though this hypothesis has been used to account for U disequilibrium in bulk U ore samples [*Rosholt*, 1958; *Stern and Stieff*, 1959], it is inconsistent with the observation that nearly all the U halos are embryonic. The evidence overwhelmingly indicates that the U radiocenters formed during the initial introduction of U to the sandstones, so if this were as long ago as the Triassic or Jurassic are generally claimed to be, then the resultant U halos should not only be fully developed, but also over-exposed [*Gentry et al.*, 1976].

In order to determine whether these phenomena were characteristic only of the coalified wood associated with the U deposits in the Colorado Plateau sandstones, *Gentry et al.* [1976] investigated coalified wood fragments found in the Devonian Chattanooga shale. They only observed embryonic U halos, and the $^{238}\text{U}/^{206}\text{Pb}$ ratios were much too high to correlate with the standard geological age of this Devonian formation. Furthermore, they found that the low U content of the shale rules out subsequent U mobilization/infiltration as responsible for the very high isotopic ratios, which thus seems to rule out additional U mobilization/infiltration as an explanation for the high isotopic ratios in the Colorado Plateau U halo centers.

Another class of more sharply defined halos was also discovered in the Colorado Plateau coalified wood samples [*Gentry et al.*, 1976]. These halos possessed smaller inclusions than the U halos, and these inclusions or radiocenters exhibited a distinct metallic-like reflectance in reflected light. EMXRF analyses showed these halo radiocenters consisted mainly of Pb and Se, which represents the metallic mineral clausthalite (PbSe). Three different varieties of these halos exist; one with a circular cross-section, another with an elliptical cross-section with variable major and

minor axes, and a third most unusual one that is actually a dual halo, being a composite of a circular and an elliptical halo around exactly the same radiocenter.

Although the elliptical halos differ radically from the circular halos, the latter resemble the ^{210}Po halos found in minerals such as biotite, and the variations in the radii of the circular halos approximate the calculated penetration distances (approximately 26–31 μm) of the ^{210}Po α -particle (energy $E_\alpha = 5.3$ MeV) in this coalified wood [Gentry *et al.*, 1976]. Henderson [1939] and Henderson and Sparks [1939] theorized that Po halos might form in minerals where U-daughter Po isotopes (or their β -precursors, for example, ^{210}Pb) were preferentially accumulated into small inclusions from some nearby U sources. According to Gentry *et al.* [1976] and Gentry [1986] this hypothesis has not been confirmed for the origin of ^{218}Po , ^{214}Po and ^{210}Po halos in U-poor minerals [Gentry, 1968, 1973, 1974], but it does seem to provide a reasonable explanation for the origin of the ^{210}Po halos in the U-rich coalified wood.

The composition of the halo radiocenters (clausthalite, PbSe) is conducive to the secondary accumulation hypothesis because both of the U daughters, ^{210}Po (half-life of 138 days) and its β -precursor ^{210}Pb (half-life of 22 years), possess the two characteristics that are vitally essential for the hypothesis:

- chemical similarity with the elements in the inclusion, and
- half-lives sufficiently long to permit accumulation prior to decay, a requirement related to the nuclide transport rate.

In the matrix of minerals the diffusion coefficients are so slow that there is a negligible probability that ^{210}Po or ^{210}Pb atoms would migrate even 1 μm before decaying, but a solution-saturated wood in a permeable condition would exhibit a much higher transport rate as well as unusual geochemical conditions which might favor the accumulation of ^{210}Po and ^{210}Pb nuclides. Because most of the resultant Po halos have been plastically deformed in elliptical shapes, this accumulation must have been essentially finished prior to complete coalification, for after coalification the wood probably would not have been as amenable to plastic deformation, and it would be much more difficult to account for such rapid and widespread migration of the radionuclides within the

138 day half-life of ^{210}Po (due to the coalified wood being less permeable). *Gentry et al.* [1976] reported that 100 or more ^{210}Po halos were sometimes evident in a single thin section (2 cm x 2 cm) of coalified wood, and they occurred quite generally in the thin sections examined.

Positive identification of the ^{210}Po halos comes from IMMA analyses, which showed that the ^{238}U content was low, the $^{238}\text{U}/^{206}\text{Pb}$ ratios varying from 0.001 to 2.0. This small ^{238}U content implies that only an extremely small amount of Pb could have been generated by *in situ* U decay, while the negligible ^{204}Pb eliminates common Pb as the source of the ^{206}Pb . Because the $^{206}\text{Pb}/^{207}\text{Pb}$ ratios varied from 8 to 16.4, the best explanation for the data is that an increment of ^{206}Pb generated by *in situ* ^{210}Po decay was added to the isotopic composition of “old” radiogenic Pb. Thus it is evident that ^{210}Pb accumulated with Se from the ground waters passing through the sandstones permeating the fossil wood to form these clauthalite radiocenters, with some ^{206}Pb also secondarily accumulating via groundwater transport from a previous “old” accumulation of *in situ* U decay elsewhere.

What then is the meaning of these Po halos? The variations in shapes can be attributed to plastic deformation which is believed to have occurred prior to coalification of the wood, deformation possibly being due to compaction of both the enclosing sandstones and the wood. The model for formation of the ^{210}Po halos which is most consistent with the data envisions that both ^{210}Po and ^{210}Pb accumulated simultaneously in the clauthalite (PbSe) inclusions and thus spherical ^{210}Po halos would have developed within six months to one year from the ^{210}Po atoms initially present, while second similar ^{210}Po halos would then develop within 25 to 50 years as the ^{210}Pb atoms were slowly β -decayed to produce another generation of ^{210}Po atoms. If there was no deformation of the coalified wood matrix between these periods, then the two ^{210}Po halos would simply coincide. If, however, the matrix was deformed between the two periods of halo formation, then the first halo would have been compressed into an ellipsoid and the second halo would be a normal sphere. The result would be a dual “halo.” The widespread occurrence of these dual halos in both Triassic and Jurassic specimens [*Gentry et al.*, 1976] could be considered corroborative evidence for only one period of introduction

of U into the host sandstones, because it is then possible to account for the structure of the dual halos on the basis of a single specifically timed event, be it compaction of the sandstones or a tectonic event. *Gentry et al.* [1976] report that in fact the dual halos occur in only about one out of 100 single ^{210}Po halos, which they suggest is due to the clausthalite radiocenters rarely accumulating large enough quantities of ^{210}Pb to subsequently generate second outer circular ^{210}Po halos. Furthermore, the likely progress of coalification accompanying the deformation would then reduce the sensitivity of the wood to the α -induced coloration and thus possibly require an α -dose 50 to several hundred times higher from the ^{210}Pb decay sequence to produce even the light outer circular ^{210}Po halos compared to the darker first-formed elliptical ^{210}Po halos.

Thus *Gentry et al.* [1976] have established that secondary ^{210}Po halos occur in coalified wood as a result of fluid transport separating the ^{210}Po and its β -precursor ^{210}Pb from their parent U and preferentially concentrating them in suitable clausthalite radiocenters (because of the chemical affinity of Pb, Po and Se). However, *Gentry* [1986, 1988] is convinced that Po halos in biotite, fluorite and cordierite are not secondary halos caused by U-bearing solutions, and that his experiments have yielded unequivocal evidence that those Po halos have no connection to any U-bearing solutions flowing through the cracks and cleavage planes in biotite, fluorite and cordierite [*Gentry*, 1968a, 1973, 1974; *Gentry et al.*, 1973]. As already noted, it was *Henderson* [1939] and *Henderson and Sparks* [1939] who first suggested that ^{218}Po , ^{214}Po and ^{210}Po halos were formed by natural processes involving U-bearing solutions flowing through biotite selectively depositing Po at various sites where it further decayed to form the Po halos.

Yet there is evidence that secondary ^{210}Po halos do occur in biotites. *Gentry* [1996] has conceded that the microscopic examination of biotite sections in some instances reveals evidence of fluid infiltration. In those areas the biotites show cracks where some type of radioactive fluid has passed through, because along the cracks and around the edges of the adjacent biotite the discoloration usually associated with halos appears as wide dark lines that follow the conduits and cracks. These wide dark lines would have been caused by α -particle radioactivity in solution. In

many cases halos, including both U and Po halos, are found along these cracks or conduits. However, *Gentry* [1996] also noted that halos are also found that do not appear to lie along any conduits or areas of visible discoloration from radioactive solutions.

Similar observations were first made by *Henderson and Sparks* [1939], who published a number of photomicrographs illustrating this phenomenon. They claimed that they had found all types of halos along veins or channels in biotites with their “type D” halos predominating. *Henderson and Sparks* [1939] specifically mentioned and illustrated ^{218}Po , ^{210}Po , U and embryonic Th halos along fractures and these type D halos, which they tentatively attributed to ^{226}Ra . *Gentry* [1973] was uncertain of their identity even though fossil fission tracks indicated that U series α -emitters produced part of the discoloration. Because they generally possess large central inclusions and are without detailed ring structure they are still enigmatic, but still may be ^{226}Ra halos produced by ^{226}Ra separated in the fluids from parent ^{238}U , with the daughter ^{222}Rn and the rest of the decay chain likewise having been separated from the ^{226}Ra . Clearly, fluids with the right chemistry are capable of producing secondary halos of all types, and are thus capable of separating Po and their β -precursors from U and the upper portion of the U-decay series.

Henderson and Sparks [1939] also observed that the halos along a fracture are often connected by a darkened zone of discoloration which appears to be tubular along the axis of the fracture with a diameter equal to the diameter of the halos along the fracture. This “vein” may sometimes consist of several concentric tubes whose diameters are equal to those of the halo rings. Thus *Henderson and Sparks* [1939] recorded U discoloration bands along fractures and fluid transport conduits, while *Meier and Hecker* [1976] recorded both U and Po bands along conduits in biotite. *Gentry et al.* [1974] also noted that single halos are observed around discrete inclusions lodged in conduits or cleavage cracks, while vein halos formed from a continuous distribution of radioactivity apparently deposited from hydrothermal solutions along conduits. However, *Meier and Hecker* [1976] have postulated that the fluids responsible for these secondary halos are of low-temperature supergene

origin due to weathering and chemical leaching processes.

7. Discussion

Debate over the origin of the Po radiohalos has been waged ever since Gentry and his co-workers correctly identified them and sought to demonstrate that their presence was evidence of the fiat creation of the Po and the rocks containing the Po halos. In particular, Gentry and his colleagues sought to show by experimental evidence that, for example, there were no U-decay chain precursors to ^{218}Po in the radiocenters of ^{218}Po halos and that therefore the ^{218}Po had to be primordial. Thus because the half-life of ^{218}Po is three minutes, then the time for the ^{218}Po halos to form would be fleeting and the rocks themselves which contain these halos would likewise have to be primordial. Of course, Gentry had to be circumspect about these implications of the Po halos when he first published his results in the open scientific literature. Thus he postulated the possibility of long-lived precursors to the Po isotopes that were now extinct. Yet at the same time he hinted at fiat creation as the explanation by asking leading questions such as,

. . . can they [the Po halos] be explained by presently accepted cosmological and geological concepts relating to the origin and development of Earth? [Gentry, 1974].

7.1 Responses

There have been a number of different responses to Gentry's propositions regarding the Po halos. *Moazed et al.* [1973], for example, argued that Henderson and his co-workers, and by inference therefore Gentry, had incorrectly identified the Po halos, all the evidence for which they sought to demonstrate was equally consistent with the interpretation that these are variants of the standard U halos. Other protagonists such as *Damon* [1979], *York* [1979] and *Dutch* [1983] all accepted that the Po halos had been correctly identified. Their main objection was that the implications of Gentry's claims regarding the Po halos (that is, fiat creation) conflict completely with the accepted abundant interwoven evidence of the established multi-billion year geochronology.

Moazed et al. [1973] though raised one valid important issue, namely, the potential uncertainties of the ion microprobe analyses of the halo radiocenters, analyses which Gentry (and his co-workers) had used to conclude that the Po that formed the Po halos was “parentless” and thus potentially primordial. The ion microprobe is essentially a surface technique with a maximum resolution of 2 μm . In order to study the composition of a halo inclusion, it would be necessary to ascertain that the inclusion lies on the surface of the thin section and that it is large enough and placed accurately enough within the instrument to ensure that the microprobe would not be detecting a significant portion of the host environment. Since the inclusions central to Po halos are approximately 2 μm (or less) in diameter and are generally embedded within the biotites (which are usually 15–20 μm thick), and the microprobe must operate at the extreme limits of its capability, it is possible the microprobe was examining the host environments along with the inclusions. Nevertheless, the publications by Gentry (and his co-workers) demonstrate that due care was taken and other techniques such as scanning electron microscope x-ray fluorescence were employed for comparison of analyses to rule out such effects [*Gentry et al.*, 1974, for example].

In contrast to others, *Feather* [1978] endeavored to produce an objective assessment of the two hypotheses contending to explain the Po halos—the first which adopts the natural assumption that the Po must arrive ultimately from the disintegration of “primordial” U and postulates preferential deposition of Po from hydrothermal solutions [*Henderson and Sparkes*, 1939] or supergene solutions [*Meier and Hecker*, 1976] containing the long-lived parents; and the second which attributes the derivation of the Po to the slow decay of hitherto-unknown long-lived isomers of Po or Bi originally present in the active inclusions [*Gentry et al.*, 1973]. In his synopsis Feather stated:

Ever since the discovery of Po-halos in old mica (Henderson and Sparks 1939) the problem of their origin has remained essentially unsolved. Two suggestions have been made (Henderson 1939; Gentry et al. 1973), but neither carried immediate conviction. These suggestions are examined critically and in detail, and the difficulties attaching to the acceptance of either are

identified. Because these two suggestions appear to exhaust the logical possibilities of explanation it is tempting to admit that one of them must be basically correct, but whoever would make this admission must be fortified by credulity of a high order.

Feather [1978], of course, did not know at the time that *Gentry* [1979, 1983, 1986, 1988] would later conclude that the Po and the host rocks were primordial, produced by fiat creation only 6000 or so years ago.

7.2 Fluid Transport and Diffusion Rates

However, while *Feather* [1978] did not state which of these hypotheses he favored, others such as *Fremlin, Hashemi-Nezhad et al.* [1979], *York* [1979], *Wakefield* [1988c] and *Wise* [1989] support the hypothesis of *Henderson and Sparks* [1939] that hydrothermal fluids probably carried the Po along fractures and cleavage planes and deposited it in the Po radiocenters, and *Chaudhuri and Iyer* [1980] and *Dutch* [1983] suggest diffusion of the relevant radioisotopes necessary to produce the Po halos. However, *Gentry* has many times pointed out the difficulties and apparent conflicting evidence for fluid transport and diffusion [*Gentry*, 1968a, 1973, 1974, 1975, 1980, 1986, 1989, 1998; *Gentry et al.*, 1976]. The major obstacle is the very short half-lives of the Po isotopes and their immediate precursors, plus the painstakingly slow diffusion rates in minerals. For example, *Gentry* [1975] chose a simple calculation which highlights this problem. Since the root mean squared distance, x , that an atom of diffusion coefficient, D , will migrate in time, t , is $x = (2Dt)^{1/2}$ and the maximum value of D for Pb at 20°C in seven different minerals, for example, is $10^{-18} \text{ cm}^2\text{s}^{-1}$, then a ^{210}Pb atom, which is the precursor to ^{210}Po and with a half-life of 22 years, would migrate, on average, about 10^{-5} cm before decay. Even at 1038°C when the D value is drastically increased to $10^{-11} \text{ cm}^2\text{s}^{-1}$ the ^{210}Pb still only migrates a negligible distance of 0.1 cm in feldspar before decaying. However, the minerals containing the Po halos have not suffered such high temperatures since their formation and during the time of Po halo formation, yet even in fluorite at a more realistic temperature of 300°C, the D value for Pb is less than $10^{-22} \text{ cm}^2\text{s}^{-1}$ such that a ^{210}Pb atom would migrate only about 10^{-7} cm

before decay [Gentry, 1975]. Similarly, Gentry *et al.* [1976] maintain that in minerals the diffusion coefficients are so low that there is a negligible probability that ^{210}Po or ^{210}Pb atoms would migrate even 1 μm before decaying. Thus, if Po or Pb radionuclides were migrating to Po halo radiocenters, most would have decayed in transit and produced a large excess of α -recoil tracks close to the radiocenters, which is contrary to observation [Gentry, 1968a]. Yet in many instances the Po halos are located in the interior of large crystals and even small mica flakes where they appear to often be more than 10 cm or more away from a potential significant U source [Gentry, 1975]. Furthermore, the magnitude and seeming impossibility of the task of diffusing all the necessary Po into the radiocenters is highlighted by the estimate that, for example, a very dark ^{218}Po halo with a 1 μm radiocenter would have initially contained as many as 5×10^9 atoms (a concentration of more than 50%) of the ^{218}Po isotope which only has a half-life of three minutes [Gentry, 1974], yet there may be as many as 20,000–30,000 ^{218}Po and ^{210}Po halos per cm^3 [Gentry, 1968a] or 5000–10,000 ^{218}Po and ^{214}Po halos per cm^3 [Gentry, 1975] in minerals from some locations.

However, Hashemi-Nezhad *et al.* [1979] performed experiments at temperatures of 250–600°C to test Pb diffusion rates along the cleavage planes of mica (muscovite) and reported that their experiments showed Pb diffusion in the mica to be a fairly rapid process with the Pb traversing at least 1 cm in 24 hours over the temperature range. They noted that for the three most common minerals containing Po halos, biotite, fluorite and cordierite, all have cleavage properties, and they did not rule out the possibility that the diffusion of Po itself may be a contributory, or even the main, cause of Po halo formation, with higher mobilities of Pb and Po at elevated temperatures. Thus to circumvent Gentry's observation of the lack of excess α -recoil tracks around Po radiocenters as contrary evidence [Gentry, 1968a, 1975], they pointed to the annealing of fossil fission tracks even at 20°C, more substantial annealing at 150°C, and the fact that α -recoil tracks fade more easily than fission tracks. In other words, not only would elevated temperatures have induced fairly rapid diffusion of Po and Pb along cleavages to concentrate in radiocenters, but the elevated temperatures would also have annealed the α -recoil

tracks produced during the transport process. However, these suggestions ignore the experiments of *Poole* [1928a, b] on the effect of heat on both radiohalos and host biotite. He found that after 15 minutes heating at 610°C the halos had completely disappeared and the biotite very rapidly darkened. Similarly, *Armitage and Back* [1994] found that heating Po radiohalo-bearing biotite from 250° to 750°C for up to five hours causes variable but significant changes and damage to biotite, and can erase both structural defects and radiohalos. This would seem to rule out moderate to high temperatures being involved in any claimed Pb or Po diffusion into the radiocenters, or occurring subsequent to Po halo formation, because such temperatures would not only anneal the α -recoil tracks left behind by that claimed diffusion, but erase the Po halos and damage the biotite host. Of course, this does not necessarily rule out lower temperature supergene or even hydrothermal transport.

Nevertheless, *Chaudhuri and Iyer* [1980] maintained that the experimental support of *Hashemi-Nezhad et al.* [1979] for Pb diffusion at high temperatures and the formation of Po halos from α -active Pb precursors may explain the relatively large number of ^{210}Po halos but cannot account for the formation of halos from short-lived ^{218}Po and ^{214}Po nuclei. Thus *Chaudhuri and Iyer* [1980] proposed the migration of ^{222}Rn away from its parent U by gaseous diffusion/transport and its accumulation in voids in other regions in the matrix, where it subsequently decayed to Po and other daughter products, as the explanation of how Po could get separated from U sources. Because at any time the number of Rn atoms per unit volume would be much more in the voids than in the matrix, Po would accumulate in the voids over time, which would then become the Po radiocenters. Furthermore, whereas there would be a uniform α -recoil track density in regions away from and adjacent to the resultant Po halos due to the gaseous diffusion of the Rn through the bulk matrix of the host mineral, the α -recoil track density would be very high in and around the void region where the Po accumulated and became the Po radiocenter. But track revelation and density measurements are not possible at that close range within the Po halos, so this argument appears to circumvent the observation of uniform α -recoil track densities by *Gentry* [1968a, 1975]. However, *Chaudhuri*

and Iyer [1980] neglected to quantify the diffusion rate and relied on the accumulation of Po in the voids over “geological time,” which of course is precluded by the three minute half-life of ^{218}Po .

Collins [1992] also contended that Po halos formed as a result of diffusion of ^{222}Rn in “ambient” fluids, and maintained that all of the granites in which Po halos have been found also contain myrmekite (an intergrowth of plagioclase feldspar and vermicular quartz, generally replacing potassium feldspar). He therefore suggested that these granites were formed by replacement of precursor rocks such as gabbros, the process involving fracturing and shearing accompanied by voluminous hydrothermal fluids, which could thus have introduced the U and then transported the Rn that deposited Po in what became radiocenters within biotite crystals. However, the consensus among granite specialists is that myrmekite only forms by localized metasomatism (volume for volume replacement) after granites have almost completely crystallized from magmas, often associated with increased hydrothermal activity accompanied by deposition of ore minerals (containing U, Pb, Cu, Au, Sn, Bi, S, Se, etc.) [*Pitcher*, 1993]. Nevertheless, *Collins* [1992] correctly observed that the crystal lattice of biotite contains sites where negatively charged fluoride (F^-) or hydroxyl (OH^-) ions can be accommodated, and these lattice sites being relatively large provide space where similar-sized, negatively charged ions such as the polonide (Po^{2-}) ion [*Bagnall*, 1957] could potentially enter and take up lattice positions. However, this does not explain how the 10^8 – 10^9 Po atoms required to produce each dark Po halo [*Gentry*, 1988] were rapidly concentrated in tiny radiocenters before they α -decayed, unless *Collins* [1992] is implying that large volumes of hydrothermal fluids continued to flush Rn and Po through the biotite crystals over a longer period, the Po being scavenged from the fluids to progressively replenish the Po concentrations in the radiocenters as the Po already there α -decayed. But what would continually scavenge the Po from the fluids causing it to be deposited in the tiny radiocenters? There would really need to be tiny inclusions, along cleavage planes within the biotite crystals, of an element (or elements) able to readily bond with Po, because Po atoms held in lattice sites would be scattered through biotite crystals rather than being

concentrated in the observed tiny radiocenters.

Brown [1997] also favored the penetration of hydrothermal fluids along crystal lattice planes to deposit the Po in radiocenters, but he suggested ^{226}Ra was the radioisotope separated from parent U and transported. In support of this secondary origin for Po halos, *Brown* [1997] reiterated the observation that it is only the Po isotopes which are the radioactive daughters of U and Th that are found to have produced Po halos, and not other Po isotopes such as ^{208}Po , ^{209}Po and ^{213}Po which are most probably primordial. However, of greater significance is his report of inclusions of native Cu 0.002–0.1 μm thick and up to 1.0 μm in diameter found in favored lattice planes of some biotites in granitic rocks hosting hydrothermally-produced porphyry Cu ore deposits [*Ilton and Veblen*, 1988]. As indicated by *Brown* [1997], these tiny Cu inclusions were clearly deposited from Cu-bearing hydrothermal fluids that flowed along the lattice planes of the biotite crystals. Therefore, it is reasonable to expect that hydrothermal fluids are similarly capable of depositing tiny inclusions of other elements along the lattice planes of biotites, and in particular, elements such as Pb, Se, and S which are known to readily form compounds with Po [*Bagnall*, 1957], and which would thus form tiny Po-scavenging radiocenters. Furthermore, *Brown* [1997] calculated that, given a constant supply of ^{226}Ra in a hydrothermal fluid, and hence a constant supply of ^{218}Po , equilibrium concentrations in the fluid of all three Po isotopes would be reached in about 100 years after the zero-level starting point, whereas the equilibrium concentration of ^{214}Po would be reached in only about 200 minutes. Thus for this process of hydrothermal transport of Ra and Po to have succeeded in depositing Po in tiny radiocenters along biotite lattice planes, so as to have subsequently produced Po halos, would have depended on the speed of fluid flow, on a constant supply of Ra and Po, and on the presence of favorable conditions at deposition sites which would have had to continuously scavenge the Po from the fluids.

7.3 Po Halos Along Fluid Conduits?

Wise [1989] maintained that most of the Po halos are found along

conduits, fractures and dislocations in crystal structures as reported by *Joly* [1917a, b], *Schilling* [1926] and *Meier and Hecker* [1976]. Indeed, all Irish halos [*Joly*, 1917a, b] and Wölsendorf halos [*Schilling*, 1926] were claimed by the original investigators to have occurred *only* along cracks or conduits. *Henderson and Sparks* [1939] suggested that the way in which the halos are located in the biotite is of importance as evidence bearing on the genesis of the halos. They found that in most cases it appeared that the halos were concentrated in planes parallel to the planes of cleavage. When a book of biotite was split into thin leaves, most of the leaves would be blank until a certain depth was reached, when signs of halos became manifest. A number of halos were then found in central sections in a single leaf, while the leaves on either side of it showed off-center sections of the same halos. The same mode of occurrence was often found at intervals within the book of biotite. Across a single leaf or flake the halos often appeared scattered apparently at random, with however, a definite tendency for them to be thicker near the edge of the biotite crystal or near its junction with gross inclusions. Such edges, they said, were sometimes heavily darkened by radioactive staining. In other cases, particularly where the halos were frequent, some of them they found to lie along lines of crystal symmetry, and occasionally they could see vestiges of straight conduits connecting these linearly arranged halos.

Meier and Hecker [1976] also pointed out that the Po halos they found had a distinctly different origin than the U and Th halos. They observed that the nuclei of U and Th halos are usually formed by tiny accessory minerals such as apatite, zircon and monazite, whereas a lot of Po halos were without any visible microscopic centers. Thus they concluded that there was an important difference between the genesis of U and Th halos on the one hand, being connected with inclusions of U and Th nuclides into the lattices of tiny accessory minerals during their crystallization from magmas and before the later crystallization of biotite, and the genesis of Po halos on the other hand, not being formed by any entry of Po isotopes into the lattices of accessory minerals during magmatic crystallization. Instead they argued for the accumulation of Po halos at distorted areas and cracks within biotite, suggesting that Po isotopes

must therefore be deposited at defects within the biotite at a later stage, the Po isotopes being adsorbed onto tiny inclusions.

Understandably, *Gentry* [1989, 1998] asserted the insinuation that Po halos occur only along cracks or conduits is firmly denied by the photographic evidence even in Henderson's reports as well as his own reports [*Gentry*, 1967, 1968a, 1971, 1973, 1974, 1984; *Gentry et al.*, 1974] and especially by the color photographs in his book [*Gentry*, 1988]. *Gentry*, of course, recognizes that even when halos are photographed without any sign of defects or cracks it is because the halos are actually on a cleavage plane, the halos being exposed to view by peeling away of the overlying biotite flakes along the plane of cleavage, or of the overlying fluorite also along the cleavage plane. So while the photographs do not show any cracks or defects, the halos are in fact still along cleavage planes. As *Wise* [1998] maintains, biotite is composed of crystals in the form of sheets that are only one molecule thick (approximately 10 Å), and therefore in biotite one is never more than one-half a molecule thickness away from a cleavage plane. Yet *Henderson and Sparks* [1939], as already noted above, observed that halos were not found on every cleavage plane in biotite, but only on certain cleavage planes within a book of biotite flakes. However, *Gentry* [1998] has responded by reporting that the vast majority of "perfect" crystals of biotite he has worked with do not exhibit basal cleavage separations unless something is done in splitting the biotite during specimen processing to find and view Po halos. Furthermore, he claimed to have demonstrated this both by visual inspection before and after prolonged immersion of the biotite crystals into an aqueous dye solution, before proceeding with either peeling the biotite with scotch tape, or mechanically with a sharp blade. Clearly, either of these procedures can induce cleavage separations. However, whether there are separations or not, even where biotite crystals appear to be perfect and defect-free, the biotite will nonetheless be made up of flakes one molecule thick stacked on top of one another with cleavage planes between them.

Wise [1998] also noted that the possible Po halos in a diamond photographed by *Armitage* [1995] are along what clearly appear to be cracks or at the termini of strange, bent, hollow tubes, which is suggestive

of fluid transport of Po or its precursors. However, *Armitage* [1998] maintained that only a few of the strange tubes observed in the diamond even ascended close to the surface of the processed (cut) diamond (none made contact with the surface), and claimed that the structures Wise interpreted as cracks are not cracks, but appear to be solid inclusions also not in contact with the surface of the diamond. Thus, in contrast to potential fluid transport of Po along cleavage planes in biotite, the case for fluid transport of Po along conduits in this diamond is arguable, being dependent on unequivocal identification of the structures with which the observed halos are associated.

7.4 Quantification of Fluid Transport

Putting aside the debate over whether Po halos are always found in proximity to cracks, defects and cleavages, the detailed analysis by *Feather* [1978] of fluid transport of the relevant radionuclides is instructive. In summary, Feather found that if the hydrothermal solution is assumed to take up ^{226}Ra preferentially from the U source, and if two types of inclusion are present in the biotite, one type providing deposition centers for the isotopes of Po, and other centers for the depositions of the isotopes of Bi (or, alternately, of Pb), then ideal situations may be identified in which Po halos of each of the three types might develop. Basically, the discriminating factor is the time of transit of the hydrothermal solution from U source to deposition sites. Transit times ranging upwards from about 20 days favor the development of ^{210}Po halos, transit times less than five days are required for the development of ^{218}Po halos, and even shorter transit times are necessary (five hours or less) if ^{214}Po halos are to be formed. To this extent, says Feather, the fluid transport hypothesis achieves formal success in producing secondary Po halos. However, in the first place the model assumes “scavenging” properties for the inclusions which are highly specific. In the second, the model’s requirements as to transit time are fairly sensitive. Of course, because of his uniformitarian assumptions, Feather believes this movement of radioelements had to occur over a period of 10 million years or more during halo development. Otherwise, he noted, the fact

that a single small sample of biotite frequently contains Po halos of more than one type cannot be disregarded, for if these had to develop concurrently then the model would be in considerable difficulty. Finally, *Feather* [1978] suggested that the *Meier and Hecker* [1976] supergene hypothesis which postulates Po deposition from low temperature, rather than from high temperature, solutions would make no difference to his calculations and conclusions.

In spite of the formal success of his fluid transport calculations, *Feather* [1978] suggested it couldn't be accorded very great credulity. Obviously the fleeting existence of the Po isotopes and the rapid transit times required for their transport under ideal conditions drew this response from him. However, he did not indicate whether it was the chemistry of Po and its geochemical behavior that put severe limits on his model calculations. Understandably, little is known of the chemistry of Po and its geochemical behavior because of the fleeting existence of its isotopes, yet because of the increasing technical ability to study it, some data are now available in the literature, primarily with respect to ^{210}Po because of its relatively long half-life (138 days).

7.5 Po Geochemical Behavior—Volcanic Gases and Volcanic/Hydrothermal Fluids

We have already noted with respect to the ^{210}Po halos in coalified wood in Colorado Plateau samples that Po has a geochemical affinity with Pb and Se. Like Pb, Po has a 4+ valency, so it would appear that Po could substitute for Pb in combination with other elements with which Pb combines.

Because Po is a decay product of U it is expected that Po would be found in association with U, where U and its other decay products are found. Thus *Sheng et al.* [1986] observed large enrichments of ^{210}Po in the volatiles extracted when a sample of pitchblende was heated at 450°C, and then also at higher temperatures. They noted that a large quantity of ^{210}Po is known to be released into the earth's atmosphere during volcanic eruptions, such as the 1980 Mount St. Helens eruption [*Kuroda et al.*, 1984; *Sheng and Kuroda*, 1985]. Indeed, volcanic ash from the Mount

St. Helens eruption was found to be enriched in ^{210}Po relative to ^{210}Pb , suggesting enrichment of Po compounds in the volcanic gases from the hot magma relative to less volatile Pb compounds [Nevissi, 1984]. In their pitchblende heating experiment, Sheng *et al.* [1986] found the extracted volatiles several orders of magnitude enriched in ^{210}Po relative to the ^{210}Po content of the pitchblende, and they concluded that these results can best be explained as due to the volatile properties of ^{210}Po , which in turn provides strong support for the idea that a large excess of “parentless” ^{210}Po is injected into the earth’s atmosphere during major volcanic eruptions. In fact, ^{210}Po is now used to evaluate the extent of degassing of moderately volatile elements during magmatic eruptions, and also the residence time of magma in shallow magma chambers [Gill *et al.*, 1992]. Both ^{210}Po and ^{210}Bi are highly enriched relative to ^{210}Pb in the gaseous plumes above erupting volcanoes, enrichment factors, normalized to the parent ^{210}Pb in the plume, reaching 120. That this Po comes from magma from which volatiles are being expelled is confirmed by the virtual absence of ^{210}Po in day-old magma.

Rubin [1997] has reported that ^{210}Po is essentially completely (>95%) degassed from erupting magmas of basaltic to andesitic composition in all locales, and that the extent of Po degassing and therefore Po volatility during submarine eruptions is very similar to that at subaerial volcanoes. In volcanic emissions Po is completely gaseous at temperatures above 400°C , and it has been suggested that Po volatilizes as halogen species, which is reasonable considering that the di and tetra halogen compounds of Po boil or sublime at temperatures of $110\text{--}390^\circ\text{C}$ [Bagnall, 1957]. Rubin [1997] also reported large ^{210}Po enrichments have been found in seawater over erupting seamounts, and that the Po is scavenged from the water by Mn oxyhydroxide particulates, for which it has a great affinity.

Polonium-210 has also been reported in volcanic fluids emitted via fumarole activity. In their study of fumarolic fluids at Vulcano (Italy), Le Cloarec *et al.* [1994] found that the ^{210}Po concentration in these volcanic fluids rose by six orders of magnitude as the water temperature increased up to about 400°C and then plateaued beyond 450°C , because the ^{210}Po is completely volatilized at that temperature and so its activity

remains unchanged with increasing temperature beyond that. The ^{210}Po then concentrated in the gases. They also found that a significant majority of the ^{210}Po was probably in sublimates deposited in the volcanic edifice, presumably as its halide and sulfide salts. *Voltaggio et al.* [1998] subsequently studied these sulfur incrustations and found that it is highly improbable that Po can form sublimates with Po as the main cation because the formation of Po minerals or pure Po chemical phases at a scale of even 1 nm (nanometer), likely the lowest physical limit which allows a trace element to form pure phases, requires at least a time comparable with its half-life.

However, in a study of hydrothermal vent fluids and chimney deposits from the Juan de Fuca Ridge on the East Pacific Rise, *Hussain et al.* [1995] found that, whereas the hydrothermal fluids were significantly deficient in ^{210}Po relative to its precursor ^{210}Pb , very high excess ^{210}Po concentrations were found in sulfides and sulfidic material deposited as a chimney around the hydrothermal vent. Although it was not known exactly how much time the hot fluids spent within the chimney before emerging out, *Hussain et al.* [1995] concluded that such time could not be more than a few minutes, for otherwise there would be a significant temperature drop of the fluids as the hydrothermal fluids would rapidly cool in the vicinity of the cool ocean bottom waters. This suggested to them that the residence time of ^{210}Po with respect to its removal from the aqueous phase could be of the order of only a few minutes. They went further to use the observed $^{210}\text{Po}/^{210}\text{Pb}$ activity ratio to estimate a model dependent residence time for the Po in the hydrothermal fluids of the order of a few minutes. Furthermore, they concluded that if much of the observed ^{210}Po in the fluids was the result of *in situ* growth from dissolved ^{210}Pb in the fluids, then the residence time of the hot fluids in the hydrothermal system may not be more than 30 days. They added that this estimate of the residence time was an upper limit, as other sources of ^{210}Po in the fluids, for example, initial activity of ^{210}Po mobilized in basalt weathering and subsequent sediment leaching by the hot fluids during their ascent, would tend to reduce the net component of ^{210}Po produced from *in situ* decay of ^{210}Pb and thus lower the residence time estimate. In other words, transit time for fluid transport of the ^{210}Po

from source to rapid precipitation in the chimney and sulfide deposits would be less than 30 days, a figure which compares favorably with the estimated 20 days or more transit time suggested by *Feather* [1978], which would favor the development of ^{210}Po halos. Not only then was the Po demonstrated to have an affinity for S, it was concluded that Po behaves like Pb in hydrothermal fluids.

Two further comments are warranted. First, not only are these transportation rates for ^{210}Po very rapid, but the distances involved concurrently are enormous. In the case of ^{210}Po released in volcanic gases during magmatic eruptions, even shallow magma chambers are still at depths of 2–4 km. Thus the ^{210}Po is generated at such depths from the massive volume of magma involved, which is known to then degas within a day as the eruption transports magma and volatiles to the earth's surface. Similarly, volcanic and hydrothermal fluids are estimated to circulate through rock volumes of several cubic kilometers from magmas at 2–4 km depth over distances of several kilometers, as determined from investigations of geothermal and mid-ocean ridge hydrothermal vent systems [*Nicholson*, 1994; *Lowell et al.*, 1995]. Thus depending on the source of the ^{210}Po and/or its precursors, in the 20–30 days transit time the hydrothermal fluids may be transporting the ^{210}Po over distances of up to several kilometers.

Second, because volcanic and hydrothermal fluids significantly concentrate ^{210}Po with increasing temperatures up to 400°C [*Le Cloarec et al.*, 1994], any such fluids which become trapped as inclusions within crystallizing minerals will initially retain those high ^{210}Po concentrations. Fluid inclusion data from hydrothermal systems [*Kelley and Gillis*, 1993; *Moore and Gunderson*, 1995] indicate common fluid temperatures of 300–400°C and a brine chemistry dominated by Na and Cl, which would make such fluids capable of retaining ^{210}Po given the latter's affinity for halogens [*Bagnall*, 1957]. Such fluid inclusions in minerals have no connections with the outside crystal surfaces, being isolated within minerals with little or no evidence of being associated with crystal defects, cleavages or fractures. Thus it is conceivable that “parentless” ^{210}Po might have been trapped in such fluid inclusions, which then became radiocenters. However, this is only conjectural until direct

evidence is found. Furthermore, this timescale for fluid transport of ^{210}Po is completely inadequate to account for similar transport of ^{218}Po and ^{214}Po , because of their fleeting half-lives.

7.6 Po Geochemical Behavior—Ground Waters

In contrast, ^{210}Po is normally only present in most ground waters at very low concentrations, usually even lower than its insoluble precursor ^{210}Pb . However, *Harada et al.* [1989] have discovered that ^{210}Po exists at very high concentrations in the ground waters of some shallow aquifers in west-central Florida. These ground waters were found to be fairly acidic ($\text{pH} < 5$), sulfide-bearing, and relatively high in ^{222}Rn . The detailed study by *Harada et al.* [1989] found extraordinary levels of ^{210}Po almost completely unsupported and almost “parentless;” that is, ^{210}Po concentrations were approximately three orders of magnitude higher than its direct parents ^{210}Pb and ^{210}Bi . They also found that most of the Po in the water existed in a form which did not co-precipitate with an iron hydroxide scavenge, and that the conversion of soluble to particulate Po occurred over a timescale of a few days during sulfide oxidation and bacterial growth. Furthermore, although they hadn’t established what the release mechanism for ^{210}Po was, they concluded that the circumstantial evidence implied that it was probably related to the same mechanism that liberated sulfide, that is, microbial activity, and that therefore Po cycling in this groundwater environment was related to the sulfur cycle influenced by sulfur bacteria. Though they were not measured alongside of the ^{210}Po , it can be implied that because ^{222}Rn was also relatively high in these ground waters, then ^{218}Po and ^{214}Po would also have been present even if only fleetingly.

In a follow-up study, *LaRock et al.* [1996] sought to determine whether bacteria, particularly whether those species active in sulfur cycling, could account for the selective solubilization and mobilization of Po into these ground waters of central Florida at such extraordinary concentration levels in the absence of its radiogenic parents. It is known that Po has a chemical similarity to S, both occupying the same column in the periodic table, and that in fact Po (with 2+ and 4+ oxidation states) reacts with

sulfide to form PoS_2 [Bagnall, 1957]. LaRock *et al.* [1996] found that the sources of Po were the U-rich phosphate rock (phosphorite) mined and processed as a raw material for the manufacture of fertilizers and phosphoric acid, obtained by treating the phosphate rock with sulfuric acid. The by-product of the process is phosphogypsum, which is stockpiled because of the relatively high content of radionuclides, including ^{210}Po . Their series of experiments involved the interaction of sulfate-reducing bacteria with the phosphogypsum. They found that the bacteria were capable of releasing Po from the gypsum matrix in which it was bound, and that the sulfate-reducing bacteria enhanced the Po release into solution provided the sulfide levels resulting from their metabolism did not become excessive. Thus, Po can be selectively mobilized into groundwater systems over its radiogenic parent by bacterial action and enabled to migrate through the aquifer system. However, since the sulfate-reducing bacteria metabolize sulfate and release sulfide into solution, as the sulfide levels increase in the ground water the Po reacts with it to form PoS_2 and co-precipitates with metal sulfides, so that the presence of elevated sulfides actually serves to prevent Po mobilization.

These data may be significant in understanding Po transport in fluids and the formation of secondary radiohalos. It has been established that both hydrothermal and supergene fluids can rapidly mobilize Po within the time framework regarded as necessary [Feather, 1978], at least as far as ^{210}Po is concerned. Both hydrothermal and supergene fluids are known to affect granitic and other rocks in which Po halos are now found, and of course there is evidence that radioactive fluids have migrated through fractures, cracks and defects in these granitic rocks to produce Po bands and Po halos. Clearly, S is an important element for precipitating Po, but it may also be scavenged by Mn oxyhydroxides and even by bacteria, which we now know can live at great depths even in granitic rocks and in warm S-rich environments. Acidic and S-rich ground waters are known to be capable of leaching U and will thus also mobilize ^{222}Rn and the Po isotopes. Thus it would seem that the fluid transport secondary Po halo models of Henderson and Sparks [1939] and Meier and Hecker [1976] could be remotely feasible.

However, Gentry has quite correctly pointed out [*Gentry et al.*, 1976; *Gentry*, 1998; for example] that in the case of the secondary Po halos in the coalified wood where the conditions for fluid transport and diffusion appear to be far more amenable to the secondary Po halo formation process, only ^{210}Po halos have formed, whereas in biotite crystals in granites all three Po halos are found. *Gentry* [1998] explains this disparity as a result of the 138-day half-life of ^{210}Po enabling a sufficient number of these atoms to survive long enough in the permeable wood to be collected at the claustralite sites where they decay and form ^{210}Po halos, whereas in contrast the far more rapidly decaying atoms of ^{214}Po and ^{218}Po have largely decayed away before they could be collected at these same sites. His point is though, that if the ^{214}Po and ^{218}Po halos fail to form naturally under the good conditions of high U-daughter concentrations, rapid fluid transport and ideal collecting sites, then this effectively removes fluid transport as a basis for forming these Po halos in granitic rocks.

7.7 Po Halo Proportions, Cleavage Variations and Fluid Transport

Gentry [1998] points out that if the Po halos formed secondarily from U-decay products, then because of the different Po-isotope half-lives there would be greatly different quantities of each isotope co-existing. In particular, since the expected amounts would be directly proportional to the different half-lives, this would mean that at any given time the atomic ratio $^{210}\text{Po}:^{218}\text{Po}$ should be 67,000:1. Thus if Po halos in biotites were from secondarily-derived Po from U-decay there presumably should be about 67,000 ^{210}Po halos for each ^{218}Po halo. However, such proportions are not found, and in some biotite specimens the number of ^{218}Po or ^{214}Po halos is far greater than the number of ^{210}Po halos. In fact, the proportions of the different Po halos can vary from sample to sample. *Meier and Hecker* [1976] found a distribution in the Norwegian biotite they studied of more than 1,000 ^{210}Po halos, 90 ^{218}Po halos and only one ^{214}Po halo, yet *Gentry* reported to *Feather* [1978] that abundance ratios for other samples of biotite were $^{218}\text{Po} > ^{210}\text{Po} > ^{214}\text{Po}$, and even $^{214}\text{Po} > ^{218}\text{Po}$ or ^{210}Po .

However, based on a complete review of the literature it is possible to conclude that so far only ^{210}Po halos have been found in cordierite, and only ^{210}Po and ^{218}Po halos have been found in fluorite, whereas all three Po halos are present in biotites. Nevertheless, *Gentry* [1999] has estimated that there are more than one billion U and Po halos in the Wölsendorf fluorite, and even though he has examined several hundred large thin sections of this fluorite he has probably only seen about 10,000 halos, so any statement about the proportions of the different Po halos and what Po halos have been found in which minerals could be a matter of sampling statistics. *Gentry* [1999] also stated that when he first started examining biotite specimens he at first only found ^{210}Po and ^{218}Po halos, and it was not until he did more scanning of thin sections that he found the ^{214}Po halos.

Nevertheless, the observation based on current data of all three Po halos in biotites, only ^{210}Po and ^{218}Po halos in fluorites, and only ^{210}Po halos in cordierite may still be significant as a pattern that could be providing a clue about the formation of these halos. For example, the cleavage in biotite is more pronounced than the cleavage in fluorite, while it is even less pronounced and irregular in cordierite. Thus, could it be that fluid transport is therefore more rapid in biotite? And if the Po isotopes were able to be transported by fluids into these minerals, then the flow being more rapid in biotite could mean that all three isotopes had time to form their respective halos before they decayed away, whereas in cordierite the tighter structure and imperfect cleavage didn't allow the fluid to flow fast enough to deposit any Po for halos other than the ^{210}Po halos? Another consideration is not just the speed of transport, but the distance from the source to the deposition sites. Could it also be that the reason why only ^{210}Po halos are found in the coalified wood is that it was a long distance from the granitic and other basement rocks for the ground waters to carry the U and its decay products including Po through the sandstone aquifer system, whereas in the case of the biotites and fluorite the source U minerals from which the U, Ra, Rn, Po, etc. were leached and mobilized into solution were actually in the granitic and pegmatitic rocks themselves only a short distance away from the minerals now hosting the Po halos?

7.8 Combination Halos

Two other observations that Gentry has made are worth noting. First, he has reported, as have others, that it is possible to find combined U and Th halos. These are halos in which both U and Th have been in the radiocenters and thus the resulting halos are a combination of rings representing the decay products of both U and Th. Similarly, *Gentry et al.* [1974] reported that

other investigations have shown varying mixtures of U-derived and Po-derived Pb may occur in the same radiocenter, for there exists an almost continuous halo spectrum stretching from “pure” U to “pure” Po haloes.

Gentry [1999] has explained that he has seen in particular a halo with an inner ring from just ^{238}U , without a ring for the combined effects of ^{234}U , ^{230}Th and ^{226}Ra , surrounded by the rings for ^{210}Po , ^{214}Po and ^{218}Po . So in this case the halo center must clearly have had a small amount of U along with a sizeable amount of Po. In other cases, he says, it is evident from fission-track analyses of U halo centers that some Po was also present, because the outer rings from Po were too dark to be accounted for just by the decay of ^{238}U . Thus “pure” U halos and “pure” Po halos are those which only have rings from U or Po respectively, and these are actually in the great majority.

Second, *Gentry* [1971] reported a new type of composite radiohalo had been found with rings attributable both to the ^{218}Po decay sequence and to ^{212}Po and possibly ^{212}Bi . Then *Gentry* [1973] reported a combination ^{212}Bi - ^{212}Po halo which also had a ^{210}Po ring (see Figure 5). As *Gentry* [1999] explained, this latter combination halo is the product of both ^{212}Bi , which β -decays to ^{212}Po , and ^{210}Po in the halo center. The significance of these combination halos is that the ^{218}Po , ^{214}Po and ^{210}Po belong to the ^{238}U decay chain, whereas the ^{212}Bi and ^{212}Po belong to the ^{232}Th decay chain (see Figure 2), yet in each case the rings for isotopes higher in the respective decay chains are absent and so the ^{218}Po , ^{210}Po and ^{212}Bi respectively seem to be “parentless,” or “primordial” in *Gentry*’s terms.

Nevertheless, could it be that these composite radiohalos are evidence of mixing and separation of different U and Th decay-chain isotopes

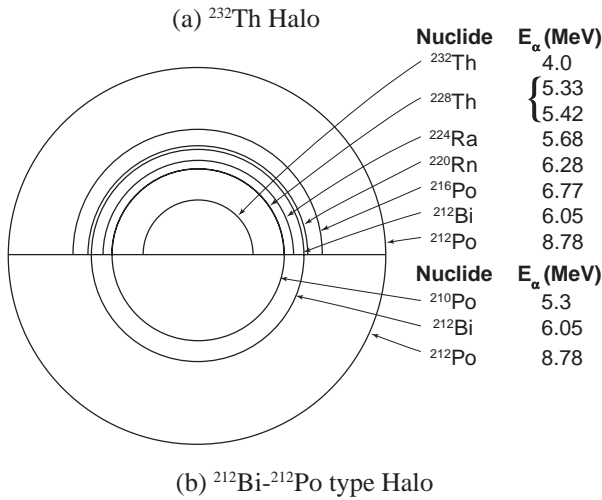


Figure 5. Schematic drawing of a (a) ^{232}Th halo and a (b) ^{212}Bi - ^{212}Po type halo with radii proportional to the ranges of α -particles in air. The nuclides responsible for the α -particles and their energies are listed for the different halo rings [after Gentry, 1973].

during fluid transport? It would seem enigmatic to recognize combination U-Th halos as forming from U-Th mixtures in radiocenters derived by natural processes, but then to regard “parentless” mixtures of U and Th decay products in combination halos as forming via “primordial” (supernatural) processes. Yet we have seen that in both hydrothermal fluids and ground waters (supergene fluids) “parentless” ^{210}Po has been separated from its precursors by natural processes. And how is it that there could be “primordial” Po and naturally-accumulated U in the same halo centers? These are intriguing issues that would seem to have a bearing on the origin and formation of the Po halos.

One last intriguing occurrence is the “spectacle” array of ^{210}Po halo radiocenters in one biotite sample [Gentry *et al.*, 1974]. This is composed of a “spectacle” coloration pattern which exhibits two almost circular rings of inclusions joined by a linear array of inclusions. The coloration was found to be identical to that of normal halos nearby in the same biotite flake, and the radii of the coloration bands around these unusually shaped linear inclusions signify a ^{210}Po origin for the α -decay responsible

for them. IMMA and SEMXRF results convinced *Gentry et al.* [1974] that not only was ^{210}Po α -decay responsible for these coloration bands and thus the “spectacle” halo, but this was “parentless” (“primordial”) ^{210}Po . However, while this “spectacle” array of ^{210}Po halos is unique, it is in fact a member of the class of halos described by *Gentry et al.* [1974] as forming around genuine single inclusions which are long compared with their width. Of course, an explanation for the “spectacle” shape of these long inclusions still has not been forthcoming, but it is clear that this inclusion array surrounded by its ^{210}Po coloration bands is centered on a cleavage plane within the biotite flake, because *Gentry et al.* [1974] describe cleaving the specimen through the inclusion array to reveal the matching “spectacle” coloration patterns on both halves.

7.9 Geological Occurrence and Distribution

This leads to one final important consideration—the geological occurrence and distribution of the Po halos. Gentry has maintained that the Po halos are found in granitic, pegmatitic and related rocks that are Precambrian in age, and therefore since the Po is primordial then these Precambrian granitic, pegmatitic and related rocks are likewise primordial [*Gentry*, 1988]. These claims have been challenged by *Wakefield* [1988a, c], *Wilkerson* [1989] and *Wise* [1989, 1998]. *Wakefield* [1988a, c] conducted field research and produced documentation of a number of the Canadian occurrences of Po halos, showing that at the Fission Mine the Po halos were found in biotite in a calcite-fluorite vein, while at the nearby Silver Crater Mine the Po halos are found in biotite in a calcite-biotite vein. In both instances these veins have intrusive relationships cross-cutting the foliation of gneisses. Similarly, at the Faraday Mine the Po halos in biotite are found in a granitic pegmatite which intrudes and cross-cuts metasediments and metagabbro. These host rocks can be shown to have been pre-existent to the formation of these vein and pegmatite intrusives, and the geological setting in each case points to a long apparent geological history in uniformitarian terms. Of course, it is entirely reasonable to conclude from Genesis 1 that fiat creation involved an appearance of age and a particular sequence

involving creative processes. From a geological perspective, this implies that the created rocks if inspected soon after would have looked in uniformitarian terms to have had a long apparent history, making them appear very old when in fact they had just recently been created. Nevertheless, in these Precambrian host rocks is found evidence of biological activity in the form of stromatolites in metamorphosed carbonate rocks, and thus the earliest these rocks could have formed and then been intruded by these veins and pegmatite dikes is on day 3 of the Creation week, after Creation of the plants (cyanobacteria are responsible for the stromatolites). Thus Gentry's contention that these Po halo occurrences are in created rocks could be still valid, although he is incorrect in describing the Fission Mine and Silver Crater Mine veins as being composed of "granites."

However, *Wise* [1989] made a list of the localities where Po halos have been reported, and also geological details of these localities. These and additional details have been tabulated here as Tables 4 and 5. Three observations can immediately be made from Table 5. First, apart from two locations, all the Po halos occur in biotite. The exceptions are the cordierite from South India which was reported by *Mahadevan* [1927], and the Wölsendorf fluorite first reported by *Schilling* [1926]. Second, while the majority of the rocks which host the Po halos are granitic pegmatites or granites, many of these designations are difficult to establish from the literature and some of these host rocks could in fact be from the granitic veins and segregations in gneisses and schists. As we have already seen, some of the host rocks are definitely veins that are not granitic, while the South Indian cordierite is actually hosted by a gneiss. Third, not all the host rocks have been designated as Precambrian, six of the 22 localities actually being designated as Phanerozoic. Such rocks would be regarded by most creationists as related to the Flood event, and therefore having formed subsequent to the Creation week are not created rocks.

In the case of the Conway Granite of New Hampshire which has been dated radioisotopically as Jurassic [*Foland et al.*, 1971; *Foland and Faul*, 1977; *Foland and Allen*, 1991], the host granite to the Po halo-bearing biotite intrudes Paleozoic or older Flood schists and gneisses with a

Table 4. A list of localities from which polonium halos have been reported

Locality	Reference(s)
1. South India	<i>Mahadevan, 1927; Gentry, 1971</i>
2. Ireland	<i>Gentry, 1968a</i>
3. County Carlow, Leinster Province, Ireland	<i>Joly, 1917b; Joly, 1923</i>
4. Ishigure District, Japan	<i>Iimori and Yoshimura, 1926;</i>
5. Wölsendorf, Bavaria, West Germany	<i>Gentry, 1973</i>
6. Scandinavia	<i>Schilling, 1926; Gentry, 1973</i>
7. Norway	<i>Gentry et al., 1973</i>
8. Norway	<i>Gentry, 1968a</i>
9. Iveland District, Aust-Agder County, Norway	<i>Gentry, 1971; Gentry, et al., 1974</i>
10. Froland, Aust-Agder County, Norway	<i>Meier and Hecker, 1976</i>
11. Moss, Ostfold County, Norway	<i>Meier and Hecker, 1976</i>
12. Kragero, Telemarck County, Norway	<i>Meier and Hecker, 1976</i>
13. Ytterby, Sweden	<i>Gentry, 1966; Gentry, 1973</i>
14. Mount Apatite, Androscoggin County, Maine	<i>Henderson and Sparks, 1939</i>
15. Portland, Middlesex County, Connecticut	<i>Henderson and Sparks, 1939</i>
16. Cottman Street Quarry, Philadelphia, Philadelphia County, Pennsylvania	<i>Henderson and Sparks, 1939</i>
17. La Malbaie (Murray Bay), Gaspé County, Quebec, Canada	<i>Henderson and Sparks, 1939</i>
18. Dingwall, Victoria County, Cape Breton Island, Nova Scotia, Canada	<i>Henderson and Sparks, 1939</i>
19. Huron Claim, Manitoba, Canada	<i>Henderson and Sparks, 1939</i>
20. Star Lake, Manitoba, Canada	<i>Henderson and Sparks, 1939</i>
21. Wilberforce, Haliburton County, Ontario, Canada	<i>Henderson and Sparks, 1939</i>
22. Weissman Mine, Dill Township, Sudbury District, Ontario, Canada	<i>Henderson and Sparks, 1939</i>
23. Cheddar, Hastings County, Ontario, Canada	<i>Henderson and Sparks, 1939</i>
24. Faraday Mine, Faraday Township, Hastings County, Ontario, Canada	<i>Gentry, 1971</i>
25. Silver Crater Mine, Faraday Township, Hastings County, Ontario, Canada	<i>Gentry et al., 1974</i>
26. Conway Granite, New Hampshire	<i>Gentry, personal communication, 1986</i>

and references to the geology of the areas [after *Wise*, 1989].

Reference(s) to Geology	Notes
<i>Krishnan</i> , 1968	“emanation halo” (^{210}Po)
---	possibly locality #3
<i>Stillman and Holland</i> , 1981	“emanation halo” (^{210}Po);
---	probably at Ballyellen
---	Z_1 halo
<i>Wakefield</i> , 1988b	on river near Wölsendorf
---	possibly one or more of localities
---	8 through 12
---	possibly one or more localities
---	8 through 11
<i>Bjorlykke</i> , 1935	---
<i>Barth and Dons</i> , 1960	---
<i>Barth and Dons</i> , 1960	---
<i>Kofseth</i> , 1942	---
---	type G halo; may be ^{210}Po halo
<i>Fisher and Barrell</i> , 1934	type A halo
<i>Stugard</i> , 1958	type C halo
<i>Rose</i> , 1970	type B and type C halos
<i>Alcock</i> , 1935	type A and type C halos
<i>Neale</i> , 1955	type A halo
<i>DeLury and Ellsworth</i> , 1931	type A halo
<i>Davies</i> , 1952; <i>Lang</i> , 1952	type C halo
<i>Rowe</i> , 1952; <i>Wakefield</i> , 1988a,c; <i>Wilkerson</i> , 1989	type A and type B halos—
---	probably the Fission Mine, since
---	Fission bought out Wilberforce
---	in 1947.
<i>Ellsworth</i> , 1932	type A and type C halos
<i>Slack</i> , 1949; <i>Hewitt</i> , 1957	type C halo
<i>Lang</i> , <i>Griffith and Steacy</i> , 1962; <i>Wakefield</i> 1988a, c;	---
<i>Wilkerson</i> , 1989	---
<i>Satterly and Hewitt</i> , 1955; <i>Wakefield</i> , 1988a, c;	---
<i>Wilkerson</i> , 1989	---
<i>Billings</i> , 1956	samples from <i>Foland et al.</i> , 1971;
---	<i>Foland and Faul</i> , 1977;
---	<i>Foland and Allen</i> , 1991

Table 5. Geology of localities from which polonium halos have been

Locality	Mineral	Rock
South India	cordierite	gneiss
Carlow	biotite*	granite
Ishigure	biotite*	---
Wölsendorf	fluorite*	vein
Iveland	biotite*	granitic pegmatite
Froland	biotite*	granitic pegmatite! (granite, gneiss)
Moss	biotite*	granitic pegmatite! (granite, gneiss)
Kragero	biotite*	granitic pegmatite! (granite, gneiss)
Ytterby	biotite*	granitic pegmatite
Mt Apatite	biotite*	granitic pegmatite! (schist, gneiss)
Portland	biotite	granitic pegmatite? (granite, gneiss, schist)
Cottman	biotite	granitic pegmatite? (granite, gneiss, schist)
Malbaie	biotite	granite?
Dingwall	biotite	granitic pegmatite? (gneiss, granite)
Huron Claim	biotite*	granitic pegmatite (granite, schist)
Star Lake	biotite*	granitic pegmatite? (granite, gneiss, schist)
Fission Mine	biotite*	calcite-fluorite vein
Weissman Mine	biotite*	granitic pegmatite (gneiss)
Cheddar	biotite*	granite
Faraday Mine	biotite*	granitic pegmatite
Silver Crater Mine	biotite*	calcite-biotite vein
Conway	biotite*	granite

Symbols: * uranium is reported from the locality, in the rock or mineral, or in an orebody

--- no data found (thus far)

distinct contact metamorphic zone, indicating that the host granite was hot when it intruded into the schists and gneisses. Furthermore, *Boucot et al.* [1958] found metamorphosed fossils in the schists and gneisses which the granite intruded, so these rocks clearly were originally Flood-deposited sediments. However, *Gentry* [1989] has responded by suggesting that in this case the granite is still a created rock dating back to the Creation week, and instead was tectonically intruded as a solid body into the schists and gneisses, the contact metamorphic zone (which

reported [after *Wise*, 1989].

Accepted Age	Older Rocks
Precambrian: Archean (Early Precambrian)!	---
Phanerozoic: Devonian	Phanerozoic sedimentary rock
---	---
Phanerozoic	granite/gneiss
Precambrian: Proterozoic (Late Precambrian)	granite/gneiss
Precambrian: Proterozoic (Late Precambrian)	granite/gneiss
Precambrian: Proterozoic (Late Precambrian)	granite/gneiss
Precambrian: Proterozoic (Late Precambrian)	granite/gneiss
Precambrian: Archean (Early Precambrian)	---
Phanerozoic: Devonian/Carboniferous!	gneiss and schist
Phanerozoic: Devonian/Carboniferous?	gneiss/granite/gneiss/schist
Precambrian	schist, granite and gneiss
Phanerozoic	Phanerozoic sedimentary rock
Precambrian!	granite/gneiss
Precambrian: Archean	schist
Precambrian	schist and gneiss
Precambrian: Proterozoic	gneiss
Precambrian: Proterozoic	gneiss
Precambrian: Proterozoic	gneiss
Precambrian: Proterozoic	metasediments and metagabbro
Precambrian: Proterozoic	gneiss
Phanerozoic: Jurassic	schist, gneiss

/ means "which is older than"
 ! possible, though somewhat uncertain, that this designation is correct
 ? very uncertain that this designation is correct

in this instance rarely outcrops) being produced by the heat and pressure generated by this tectonic movement, plus hot fluids from depth. In this way, even though Po halos are found in biotite in this granite which intrudes fossil-bearing sedimentary rocks, Gentry would still claim the granite and the Po were primordial (created).

To support his claim, Gentry has challenged the geological community to synthesize granite in the laboratory containing biotite with Po halos, all of which should be identical to the halos, biotites and granites found

at these localities in the field [Gentry, 1979, 1983, 1984, 1986, 1988, 1989]. Gentry maintains that man cannot duplicate what God has created, and that the apparent silence produced by this challenge proves that the “parentless” Po halos and the granites containing them did not form by natural processes. Nevertheless, Wakefield [1988c] Wilkerson [1989] and Wise [1989] have all responded with details of the experimental work that has been done to produce large crystals of the minerals found in granites, and also granitic textures. It is now clear that it previously was a misconception that large crystals required slow cooling rates [Wampler and Wallace, 1998], and it doesn’t necessarily take long periods of time to form and cool large bodies of granitic rock [Snelling and Woodmorappe, 1998]. Thus while a granite identical to those found in the field has so far not been made in the laboratory many features of granites have been, and it could be only a matter of time before a granite is simulated in the laboratory.

However, as Brown *et al.* [1988] have pointed out, the ability to synthesize granite in the laboratory may have little to do with Creation, the argument basically being a *non sequitur*. Whether certain rocks or minerals can or cannot be synthesized in the laboratory may just reflect how sophisticated or not are laboratory procedures, equipment, etc. In any case, minerals which could not be produced artificially in the past can now be synthesized—for example, diamonds and opals. Because all the basic minerals found in granite have already been synthesized in the laboratory [Jahns and Burnham, 1958; Winkler and von Platen, 1958; Mustart, 1969; Swanson *et al.*, 1972], it seems unwise to pose a challenge to geological uniformitarians on the basis of whether or not a hand-sized piece of granite is synthesized, since future developments in science are unpredictable. Furthermore, in a number of instances it appears that granite has clearly formed as a result of natural intrusive and magma cooling processes, such as where granite has intruded fossil-bearing rocks, as in the example of the Conway Granite of New Hampshire already cited. Even more convincing is the granite found in the central Urals which contained a number of fossil species of brachiopods [Malakhova and Ovchinnikov, 1970].

Finally, one occurrence of possible Po halos not listed in Table 5 is

that in a diamond, reported by *Armitage* [1995]. However, the full significance of this occurrence is difficult to ascertain, given that no information is available as to where the diamond itself was found, and the difficulty of identifying and explaining the structures associated with the halos. Nevertheless, *Armitage* [1995] noted that diamonds are believed to have formed in the earth's upper mantle, perhaps 1–3 billion years ago (conventionally speaking), and were then transported rapidly by kimberlite and lamproite magmas via propagating cracks to the earth's surface. If these possible Po halos in the diamond are indeed of primary origin, then as maintained by *Armitage* [1995] they potentially provide constraints on the processes and circumstances of diamond formation. However, *Armitage* [1995] admits that diamonds residing in the upper mantle are believed to have experienced temperatures of 800–1400°C subsequent to their formation, which could preclude a primary origin for these observed internal radiohalos given the lower temperatures at which halos are annealed [*Poole*, 1928a, b; *Armitage and Back*, 1994].

7.10 Proximity to U Sources

Wakefield [1988a, c] and *Wilkerson* [1989] reported that the calcite-fluorite vein hosting the Po halo-bearing biotite also contained cubic crystals and irregular masses of uraninite (primarily UO_2), which was the reason for the mining activity at that location (the Fission Mine). Indeed, the depth of color of the fluorite was an indicator of the proximity of uraninite. The postulated origin for the vein was the passage of hydrothermal fluids along bedding planes, joints and fractures in the host gneiss, probably containing volatiles such as fluorine, the biotite growing outward from the altered wall rock and replacing the calcite as a result of reactions between the wall rock, calcite and volatile fluids [*Wakefield*, 1988c]. The uraninite was found in cavities with biotite or calcite-fluorite intergrowths. It is in such biotite crystals in such close proximity to uraninite that the Po halos were found.

It should also be kept in mind that hydrothermal fluids containing volatiles such as fluorine are known to transport “parentless” Po [*Hussain et al.*, 1995]. As suggested previously, it may well be that the presence

of all three Po halos in such biotites compared with only ^{210}Po halos in the Colorado Plateau coalified wood may correlate with the distance of fluid transport and therefore proximity of the U source. In the case of the Fission Mine calcite-fluorite vein, the uraninite source is immediately adjacent to the biotite which has formed while hydrothermal fluids were carrying U and F, and possibly Po. Similarly, the pegmatite hosting the Po halo-bearing biotite at the Faraday Mine also hosts uraninite and other U minerals, which again were the target of the mining activity. The mineralogy of the pegmatite also indicates a flux of hydrothermal fluids carrying U and volatiles. And finally, at the Silver Crater Mine the calcite-biotite vein with the Po halo-bearing biotite also contains betafite (a complex U, rare earth element and F-bearing oxide mineral), often found as small crystals in close association with clusters of books of biotite and even within the books themselves (*Wakefield, 1988c*). Thus it would appear that at these three localities a strong case can be made for hydrothermal transport of Po over extremely short distances from U minerals directly associated with the biotite hosting the Po halos. In other words, these Po halos could be secondary and not primordial, the parent U source being right next to the host biotite crystals.

Wise [1989, 1998] has endeavored to take this argument a step further by suggesting that the majority of Po-bearing biotites have a U source in close proximity to them suggesting the Po halos may be secondary, possibly forming by fluid transport of Po over very short distances. To support his argument he included an indication on his list of Po halo localities of which ones had U reported from the locality, either in the rock or mineral, or in an orebody, and these details are therefore also indicated on Table 5 here. Five of the 22 localities have no reported indication of a nearby U source, and details of other localities are somewhat sketchy, so if the hydrothermal fluid transport of Po from immediately adjacent U sources could explain some of the Po halo occurrences it might not be able to explain them all. Since it seems more likely that there should be one unifying explanation, these five exceptions therefore question the secondary fluid transport hypothesis. However, it may well be that upon further investigation these five localities do in fact contain above average concentrations of U in close

proximity to the Po halo-bearing minerals.

Gentry [1989] has disputed the inclusion of the Conway Granite of New Hampshire in the list made by *Wise* [1989] of localities where U has been reported in the rock or mineral, or in an orebody (see Table 5), claiming that the Conway Granite is distinctly U-poor. He correctly states that typical U concentrations in granites are in the ppm range [*Gentry*, 1998], but is obviously unaware that the Conway Granite contains an average U concentration of 16 ppm that is considered abnormally high as far as granites are concerned, which is why this granite was drilled [*Rogers et al.*, 1965]. This is also why *Wise* [1989] was justified in including this locality in his list of those from where U has been reported in the rock or mineral. In those provinces known for their economic U deposits, granites with similar U concentrations to that found in the Conway Granite of New Hampshire contain accessory uraninite and other U-bearing minerals [*McAndrew and Finlay*, 1980], which have been regarded as at a sufficiently high enough level for the U to be leached from the granites to form large quantities of significant U ores [*Binns et al.*, 1980; *Ferguson et al.*, 1980]. And as has been suggested in the cases of the Fission, Silver Crater and Faraday Mines, it may be all that is required for the Po halos to form is uraninite or U-bearing minerals to exist in association with the host biotite so that there is only a very short distance for fluid transport from the U source to the Po halo radiocenters.

7.11 Significance of U and Th Halos?

Most attention has been focused on the Po halos, primarily because their origin has been enigmatic due to the fleeting existence of ^{218}Po and ^{214}Po , and so controversy has raged. However, the U and Th halos should not be overlooked in case their geological occurrence and distribution also has some potential significance for our understanding of the history of radioactive decay in the earth's crustal rocks.

Earlier (Section 4) it was concluded that the observed probable constancy of radiohalo radii does not necessarily imply constant radioactive decay rates, and thus the possibility of accelerated decay

rates cannot be precluded. However, *Gentry* [1968b] has highlighted another line of evidence that potentially is consistent with past accelerated decay rates. *Ramdohr* [1957, 1960] had reported observing radioactive halos due to U and/or Th in polished mineral sections (of ore samples) which exhibit an unusual appearance. Apart from the expected halos of discoloration, extensive lattice destructions occur in the immediate neighborhood of strongly radioactive minerals such as uraninite, pitchblende, brannerite and thorianite, which pave the way for dissolution or replacement of the affected areas [*Ramdohr*, 1969]. Grains of other minerals that are in the immediate neighborhood or enclosed in these above-mentioned radioactive minerals thus may have the appearance of having been “nibbled on”.

The continual bombardment of minerals by radioactivity can also cause what *Ramdohr* [1960] called “radioactive cracking,” or what is sometimes referred to as “radiation blasting.” The α -particles produced by radioactive decay of U and/or Th within a mineral such as zircon progressively disorders its atomic and lattice structures, and so it is essentially destroyed from within by its own U and/or Th content. As this disordering process (called metamictization) increases with time the mineral’s specific gravity (or density) and hardness decrease as its volume progressively increases, so the mineral eventually becomes isotropic. The volume increase can be considerable and the swelling can thus exert substantial forces on the surrounding minerals. If the latter are brittle, they often fracture in random patterns and are broken up, as illustrated by *Ramdohr* [1960, 1969]. The numerous examples of such “destruction halos” from locations scattered around the world include uraninite and zircon each destroying pyroxene and feldspars, and zircon breaking up uraninite, magnetite and even itself.

As reported by *Gentry* [1968b], *Ramdohr* has explained that the minerals surrounding the central radioactive mineral undergoing metamictization should also expand slowly over time as the swelling exerts substantial forces on them. Then individual cracks should appear as soon as the elastic limit is reached, these “expansion cracks” being expected to occur first along grain boundaries and cohesion minima (for example, cleavage planes). However, instead the individual cracks

are randomly distributed. The resultant pattern of cracks has the appearance of explosive fracturing, which thus could only have occurred quite suddenly and not by slow expansion. *Gentry* [1968b] therefore has suggested that one possible explanation would be accelerated radioactive decay at some time in the past, which would be expected to have caused very rapid metamictization of radioactive minerals and hence explosive fracturing of the surrounding minerals.

Whether this explanation can be verified or not by further investigation, these data do emphasize the importance of not just focusing on the Po halos. There is obviously a need for careful examination of all the effects of U- and Th-derived radiation both on host and surrounding minerals. It may well be that there is further significance to be found in the occurrence and distribution of these radiation effects, including the U and Th halos, particularly if these data potentially reveal if accelerated radioactive decay has occurred, when it occurred, and how much occurred. For example, it is evident from the examples documented by *Ramdohr* [1957, 1960, 1969] that these “destruction halos” showing explosive fracturing occur primarily in Precambrian rocks and ores. And like the Po halos, it appears that most occurrences of U and Th halos are in Precambrian granitic rocks, though this needs to be confirmed. If confirmed, these “destruction halos” and mature (fully-formed) U halos in Precambrian rocks would seem to be tangible, physical evidence consistent with a significant amount of radioactive decay having occurred in these rocks, probably at least 100 million years of decay at today’s observed rates, but back then at accelerated rates.

Furthermore, Baumgardner in Chapter 3 (Section 12) has suggested that there appears to be an “almost complete *non-occurrence*” of fully-formed U and Th halos in Phanerozoic rocks. In fact, the only unquestionable Phanerozoic U halos clearly documented in the literature appear to be those reported by *Gentry et al.* [1976] in coalified wood of Triassic and Cretaceous “age” from the Colorado Plateau and of Devonian “age” from the Chattanooga shale near Nashville, Tennessee. *Gentry* [1973, 1988, 1999] reported U halos in the Wölsendorf fluorite which according to *Wise* [1989] based on *Schilling* [1926] is of Phanerozoic “age” (see Tables 4 and 5), but further investigation is needed

to confirm this “age” and whether this is an exceptional occurrence. Nevertheless, the U halos found in the coalified wood from the Colorado Plateau and the Chattanooga shale are all embryonic in their stage of development (there are embryonic U halos in the Wölsendorf fluorite also [Gentry, 1973, 1988]), and even that degree of development has resulted from the large total amounts of U in their radiocenters. Furthermore, as reported already in Section 6, the $^{238}\text{U}/^{206}\text{Pb}$ ratios measured by ion microprobe mass spectrometry (IMMA) in several of these embryonic U halo radiocenters are surprisingly large [Gentry *et al.*, 1976] and thus suggest very little nuclear decay had occurred in the formation of these halos. Indeed, the highest and probably most reliable of these $^{238}\text{U}/^{206}\text{Pb}$ ratios was 27,300, which corresponds to an “age” of only about 240,000 years assuming constant decay rates at today’s observed values.

As Baumgardner (Chapter 3, Section 12) has explained, U-rich zircons in Paleozoic or Mesozoic aged biotite crystals should produce distinct, mature (fully-formed) U halos in 100 million years or less at present rates of nuclear decay, and because such zircons are common in granitic rocks of those “ages” there should be abundant mature U halos in them, if indeed 100–500 million years have truly elapsed since the biotites in the granites crystallized (assuming no intervening high temperatures that could have annealed the halos). Therefore, there is a pressing need to rigorously confirm whether the apparent absence of mature U halos in Phanerozoic granitic rocks is in fact real, or simply due to sampling bias or lack of reporting (the occurrences of U halos perhaps were not considered significant enough to routinely report). Since radiohalos provide a tangible, visible, physical record of nuclear decay, a well-documented case for the lack of mature U halos in Phanerozoic granitic rocks would seriously challenge the radioisotopic dating methods that rely on whole-rock and mineral isotopic ratios measured in those rocks, and which are vulnerable to inheritance and mixing of parent/daughter correlations (as elaborated by Snelling in Chapter 5). On the other hand, if mature U halos were systematically present in Phanerozoic granitic rocks, then that would seem to indicate a significant amount of radioactive decay has also occurred in those rocks, which would then need to be

accounted for during the Flood, possibly by accelerated decay (see Humphreys, Chapter 7).

7.12 Required Further Investigations

Though the evidence of Po halos associated with nearby U sources is suggestive, it is by no means yet conclusive. While it can be said that there appears to be a correlation between Po halos and elevated U concentrations, much more investigative work needs to be done to establish whether this correlation is merely fortuitous due to the current sampling bias, or whether it is in fact universal. Likewise, the majority of Po halo occurrences are in Precambrian granitic and pegmatitic rocks, and so those Phanerozoic examples and non-granitic/pegmatitic occurrences appear to be just minor exceptions to the rule. Thus there is a need for further field and laboratory studies to identify more localities where Po halos occur and to document the characteristics of those localities, as well as to further document those localities where we already know Po halos occur. Prime targets will be Phanerozoic granites which can be demonstrated to intrude fossil-bearing sediments, and any granite, pegmatite or biotite-bearing vein not associated with high U concentrations. It would be important also to document which Po halos occur at each locality and the approximate proportions of the different Po halos if more than one type occurs at any locality. For example, it may even be that ^{218}Po and ^{214}Po halos are rare or virtually absent from Phanerozoic granitic rocks. These data could provide patterns which may be significant in resolving the “tiny mystery” of the Po radiohalos. Additionally, further isotopic analyses of Po halo radiocenters might be useful to establish again that the Po originally there to form the halos was definitely “parentless.”

Furthermore, it should not be ignored that the Po halos are not the only unexplained variants from the normal U and Th halos. Thus far dwarf, giant, X and other intermediate-sized halo varieties remain unexplained, and it may well be that clues as to the formation of these halos may provide evidence for the origin of the Po halos. Dwarf and X halos are found with Po halos in biotite in the Ytterby (Sweden)

Precambrian granitic pegmatite (?), but these X halos have also been found at Arendal (Norway) and near Cape Town (South Africa), presumably without accompanying dwarf halos or Po halos. Nevertheless, *Gentry* [1973] has not been able to confirm the existence of these X halos. *Mahadevan* [1927] reported dwarf halos also in cordierite, but it is unclear whether it was the same cordierite in which he found the ^{210}Po halos. Most of the giant halos are found in a Madagascan biotite, though *Gentry et al.* [1978] also found giant halos in biotites at Arnö and Rickaby (Sweden), and in each instance the giant halos had no Po halos associated with them. *Krishnan and Mahadevan* [1930] reported and photographed giant halos in cordierite, but again it is unclear whether this was the same cordierite where the ^{210}Po halos were found. Thus these variant halos remain a mystery like the Po halos, and thus their formation may or may not be related to the process of formation of the Po halos. Further investigation of these other variant halos is also warranted.

Finally, the geological occurrence and distribution of U and Th halos, and of “destruction halos”, need to be likewise thoroughly documented. Specifically, it will be crucial to know if mature U (and Th) halos, plus “destruction halos”, are confined to Precambrian granitic rocks, and thus whether the tentatively proposed, apparent absence of mature U halos in Phanerozoic rocks is real. Such data will have significant bearing on our understanding of the history of radioactive decay in the earth’s crustal rocks, as already discussed.

Such research has already been initiated among the RATE group’s proposed projects (see Appendix). Relevant mineral samples from known U, Th, Po and other variant halo occurrences are being assembled for quantitative assessment of all halos, and more detailed information on the geology of these localities is being sought. Additionally, suitable samples are being collected from new localities where such halos might be found and where the geology is well documented. Such localities include more Precambrian granites and related rocks, but also some Phanerozoic granitic rocks clearly intrusive to Flood-deposited strata. Sample localities associated with U sources will be tested for Po halos, as will sample localities well removed from elevated U concentrations.

The relevance to the RATE project of the data, which it is hoped will be obtained, is that the halos provide physical evidence of a large dose (or doses) of radioactive decay having actually occurred during the young-earth creationist timeframe. Where these halos occur in the geologic record may indicate when accelerated radiodecay may have happened, and perhaps even how much, given that to form a typical halo probably requires 500 million–1 billion α -decays. Of course, it still may be claimed that God may have created rocks with the appearance of much radioactive decay in them, in which case the Po halos in particular may be regarded as characteristic of primordial rocks. However, God's character (His absolute integrity and trustworthiness) would rule out any interpretation of the halos that would suggest they are evidence of radioactive decay which really did not occur. Such a position would be tantamount to accusing God of deliberately confusing (and even deceiving) us! On the other hand, Po halos in Phanerozoic granitic rocks intruding fossiliferous Flood strata may help confirm their secondary origin. And even if a feasible model for a secondary origin of some or all Po halos (via fluid transport?) was established, the occurrence of Po halos may still be indicative of unique past processes, unless it can be demonstrated Po halos still form naturally today or can be formed experimentally in laboratory-prepared minerals. Furthermore, the presence of mature U halos in both Precambrian *and* Phanerozoic granitic rocks may suggest bursts of substantial accelerated radiodecay not only early during Creation, but additionally during the Flood. Alternately, confirmation of the tentatively proposed, apparent absence of mature U halos in Phanerozoic granitic rocks would severely limit the amount of accelerated decay during the Flood and provide unequivocal physical evidence contrary to the interpreted vast radioisotopic "ages" derived from such rocks. Thus a detailed knowledge of the geological occurrence and distribution of all types of halos is of significance to the RATE objective of grappling with the radioisotopic dating of rocks within a young-earth timeframe. It may well be that these halo data also help to resolve where the Creation and Flood boundaries are in the geologic record.

8. Conclusions

It has been clearly established that radiohalos are due to α -particles emitted as a result of the radioactive decay of unstable isotopes in the U and Th decay series, and as such they represent unequivocal physical evidence of large amounts of radioactive decay during earth history. It has also been established that the distances traveled by the α -particles are proportional to the energies of those α -particles, which are different for each of the α -emitting isotopes. Thus the radii of the darkened rings of the halos enable identification of which isotopes are responsible. The halo radii of the isotopes in the U and Th decay chains appear to have remained constant through earth history, but this neither confirms constancy of radioactive decay rates nor precludes the possibility of accelerated decay. Nevertheless, large amounts of radioactive decay in a young-earth timeframe seems to imply that there has been a period (or periods) of accelerated decay. Indeed, further research is needed to adequately document the occurrence and distribution in the geologic record of mature (fully-formed) U halos. Their presence in Precambrian granitic rocks seems to be consistent with a significant burst of accelerated decay early in Creation, whereas their apparent absence in Phanerozoic granitic rocks (tentatively proposed) would indicate very limited accelerated decay during the Flood.

Not all radiohalos match the standard U and Th halos. A number of variant halos exist—dwarf, X, intermediate-sized varieties and giant halos—but these have restricted occurrences and are rare. Only the Po halos have received considerable attention in the last two decades, primarily because analyses of the radiocenters in these halos indicate that only “parentless” Po isotopes were present to produce the respective ^{218}Po , ^{214}Po and ^{210}Po halos. Because the half-lives of these isotopes are three minutes, 164 microseconds and 138 days respectively, the data suggest an extremely rapid formation of these halos. It has therefore been suggested that the Po is primordial and the rocks containing them also products of fiat creation. Nevertheless, tiny inclusions capable of scavenging Po from hydrothermal fluids with a constant prolonged

supply of Po in them, to progressively replenish the Po in those radiocenters as the Po halos formed, would seem to largely circumvent these time constraints. Furthermore, God would not confuse or deceive us with evidence of radioactive decay which really did not occur.

When first discovered Po halos were postulated as having formed by fluid transport of U-decay products along fractures, defects and cleavage planes, but transport and diffusion rates seemed too slow to move the Po isotopes into the radiocenters before decaying. The occurrence and proportions of the different Po halos does not appear to match those predicted by fluid transport modeling, and it is claimed that many Po halos do not occur near fractures or defects. However, secondary Po halos are known in coalified wood and along fractures and defects in some host minerals, the passage of the radioactive fluids sometimes being marked by discoloration bands with widths matching ^{210}Po in particular. Furthermore, it can be established that many Po halos do occur along cleavage planes. While the apparent absence of α -recoil tracks from the passage of radioactive fluids and the uniform background distribution of fission-tracks seem to be evidence against a secondary origin for many Po halos, the fact that “parentless” ^{210}Po can be rapidly transported in volcanic gases and fluid emissions, hydrothermal fluids and in ground waters as halides and sulfides, and then precipitated in sulfides all in timescales matching fluid transport modeling, plus the association of many Po halo-bearing minerals with immediately adjacent U minerals and U sources, and the few combination halos, seem to support a secondary origin for at least some of the Po halos.

Nevertheless, a case for a secondary origin of all Po halos is far from fully established, given the fleeting half-lives of ^{218}Po and ^{214}Po . There are some unresolved difficulties with the primordial hypothesis, such as the occurrence of Po halos in non-granitic rocks and in Phanerozoic granitic rocks that intrude fossil-bearing and therefore Flood-related strata. Thus what is needed now is better geological documentation of the known localities of Po halos and new field studies to find further Po-halo localities and thoroughly document them so as to fully ascertain the geological distribution of Po halos in particular, but U, Th and all variant halos as well, and their proportions, particularly to test whether

proximity or association with high U concentrations or U-bearing minerals is crucial to halo occurrence and therefore potentially their formation. Further isotopic analyses of Po halo radiocenters would also be useful, as such currently available data seem to be consistent with the primordial hypothesis.

All of this required further research is now being undertaken as relevant to the RATE objective of grappling with radioisotopic dating and the history of nuclear decay in a young-earth timeframe, because the halo evidence may be indicative of accelerated radioactive decay at Creation and/or during the Flood, and may help to define those boundaries in the geologic record.

References

- Adler, H. H., Concepts of uranium-ore formation in reducing environments in sandstones and other sediments, in *Formation of Uranium Ore Deposits*, pp. 141–168, International Atomic Energy Agency, Vienna, 1974.
- Alcock, F. J., Geology of Chaleur Bay Region, *Geological Survey of Canada Memoir 183*, 1–146, map, 1935.
- Armitage, M., Internal radiohalos in a diamond, *Creation Ex Nihilo Technical Journal*, 9, 93–101, 1995.
- Armitage, M., Radiohalos in diamonds, *Creation Ex Nihilo Technical Journal*, 12, 286–287, 1998.
- Armitage, M., and E. Back, The thermal erasure of radiohalos in biotite, *Creation Ex Nihilo Technical Journal*, 8, 212–222, 1994.
- Bagnall, K. W., *Chemistry of the Rare Radioelements*, Butterworths, London, 1957.
- Barth, T. F. W., and J. A. Dons, Precambrian of southern Norway, in *Geology of Norway*, edited by O. Holtedahl, pp. 6–67, Ashekoug, Oslo, 1960.
- Bates, R. L., and J. A. Jackson, editors, *Glossary of Geology*, 751pp., American Geological Institute, Falls Church, Virginia, 1980.
- Billings, M. P., *The Geology of New Hampshire, Part 2—Bedrock Geology*, 203pp., The New Hampshire State Planning and Development Commission, Concord, New Hampshire, 1956.
- Binns, R. A., J. McAndrew, and S.-S. Sun, Origin of uranium mineralization at Jabiluka, in *Proceedings of International Uranium Symposium on the Pine Creek Geosyncline*, edited by J. Ferguson and A. B. Goleby,

- pp. 543–562, International Atomic Energy Agency, Vienna, 1980.
- Bjorlykke, H., The mineral paragenesis and classification of the granite pegmatites of Iveland, Setesdal, southern Norway, *Norsk Geologisk Tidsskrift*, 14 (3–4), 211–311, 1935.
- Boucot, A. J., G. J. F. MacDonald, C. Milton, and J. B. Thompson, Jr, Metamorphosed Middle Paleozoic fossils from central Massachusetts, eastern Vermont, and western New Hampshire, *Bulletin of the Geological Society of America*, 69, 855–870, 1958.
- Breger, I. A., The role of organic matter in the accumulation of uranium: the organic geochemistry of the coal-uranium association, in *Formation of Uranium Ore Deposits*, pp. 99–124, International Atomic Energy Agency, Vienna, 1974.
- Brown, R. H., Radiohalo evidence regarding change in natural process rates, *Creation Research Society Quarterly*, 27, 100–102, 1990.
- Brown, R. H., Reply to Gentry, *Creation Research Society Quarterly*, 28, 40–41, 1991.
- Brown, R. H., The nature of evidence for the activity of supernatural intelligence, as illustrated by polonium radiohalos, *Origins*, 24, 65–80, 1997.
- Brown, R. H., H. G. Coffin, L. J. Gibson, A. A. Roth, and C. L. Webster, Examining radiohalos, *Origins*, 15, 32–38, 1988.
- Brukl, A., F. Hernegger, and H. Hilbert, *Oesterr. Akad. Wiss. Math. Naturwiss. Kl. Sitzungsber. Abt. IIA*, 160, 129–146, 1951.
- Chaffin, E. F., Are the fundamental “constants” of physics really variables?, in *Proceedings of the Third International Conference on Creationism*, edited by R. E. Walsh, pp. 143–149, Creation Science Fellowship, Pittsburgh, Pennsylvania, 1994.
- Chaudhuri, N. K., and R. H. Iyer, Origin of unusual radioactive haloes, *Radiation Effects*, 53, 1–6, 1980.
- Collins, L. G., Polonium halos and myrmekite in pegmatite and granite, in *Expanding Geospheres*, edited by C. W. Hunt, pp. 128–140, Polar Publishing Calgary, Canada, 1992.
- Damon, P. E., Time: measured responses, *EOS, Transactions of the American Geophysical Union*, 60(22), 474, 1979.
- Davies, J. F., Geology of the West Hawk Lake—Falcon Lake Area, Lac du Bonnet Mining Division, Manitoba, *Province of Manitoba, Department of Mines and Natural Resources Mines Branch Publication 53–4*, 1952.
- DuLury, J. S., and H. V. Ellsworth, Uraninite from the Huron Claim, Winnipeg River area, S. E. Manitoba, *American Mineralogist*, 16, 569–575, 1931.

- Dutch, S., Creationism still again, *Physics Today*, 36(4), 12–13, 1983.
- Ellsworth, H. V., Rare-element minerals of Canada, *Geological Survey of Canada, Economic Geology Series*, 11, 1–272, 1932.
- Feather, N., The unsolved problem of the Po-haloes in Precambrian biotite and other old minerals, *Communications to the Royal Society of Edinburgh*, 11, 147–158, 1978.
- Ferguson, J., G. R. Ewers, and T. H. Donnelly, Model for the development of economic uranium mineralization in the Alligator Rivers Uranium Field, in *Proceedings of International Uranium Symposium on the Pine Creek Geosyncline*, edited by J. Ferguson and A. B. Goleby, pp. 563–574, International Atomic Energy Agency, Vienna, 1980.
- Fisher, L. W., and R. Barrell, Mount Apatite, Maine: a famous mineral locality, *Rocks and Minerals*, 9(2), 13–16, 1934.
- Fleischer, R. L., P. B. Price, and R. M. Walker, Tracks of charged particles in solids, *Science*, 149, 383–393, 1965.
- Foland, K. A., and J. C. Allen, Magma sources for Mesozoic anorogenic granites of the White Mountain magma series, New England, USA, *Contributions to Mineralogy and Petrology*, 99, 195–211, 1991.
- Foland, K. A., and H. Faul, Ages of the White Mountain intrusives—New Hampshire, Vermont and Maine, USA, *American Journal of Science*, 277, 888–904, 1977.
- Foland, K. A., A. W. Quinn, and B. J. Giletti, K-Ar and Rb-Sr Jurassic and Cretaceous ages for the intrusives of the White Mountain magma series, northern New England, *American Journal of Science*, 270, 321–330, 1971.
- Fowler, P. H., and A. R. Lang, Giant haloes in mica, *Nature*, 270, 163–164, 1977.
- Fremlin, J. H., Spectacle haloes, *Nature*, 258, 269, 1975.
- Gentry, D., Polonium halos: a closer view, *Bible-Science News*, 34(4), 1–6, 1996.
- Gentry, R. V., Abnormally long α -particle tracks in biotite (mica), *Applied Physics Letters*, 8(3), 65–67, 1966a.
- Gentry, R. V., Alpha radioactivity of unknown origin and the discovery of a new pleochroic halo, *Earth and Planetary Science Letters*, 1, 453–454, 1966b.
- Gentry, R. V., Extinct radioactivity and discovery of a new pleochroic halo, *Nature*, 213, 487–489, 1967.
- Gentry, R. V., Fossil alpha-recoil analysis of certain variant radioactive halos, *Science*, 160, 1228–1230, 1968a.
- Gentry, R. V., On the invariance of the decay constant over geological time,

- Creation Research Society Quarterly*, 5, 83–85, 1968b.
- Gentry, R. V., Giant radioactive halos: indicators of unknown radioactivity, *Science*, 169, 670–673, 1970.
- Gentry, R. V., Radiohalos: some unique lead isotopic ratios and unknown alpha activity, *Science*, 173, 727–731, 1971.
- Gentry, R. V., Radioactive halos, *Annual Review of Nuclear Science*, 23, 347–362, 1973.
- Gentry, R. V., Radiohalos in a radiochronological and cosmological perspective, *Science*, 184, 62–66, 1974.
- Gentry, R. V., Spectacle haloes, *Nature*, 258, 269–270, 1975.
- Gentry, R. V., Time: measured responses, *EOS, Transactions of the American Geophysical Union*, 60(22), 474, 1979.
- Gentry, R. V., Polonium halos, *EOS, Transactions of the American Geophysical Union*, 61(27), 514, 1980.
- Gentry, R. V., Creationism again, *Physics Today*, 35(10), 13, 1982.
- Gentry, R. V., Creationism still again, *Physics Today*, 36(14), 13–15, 1983.
- Gentry, R. V., Radioactive halos in a radiochronological and cosmological perspective, *Proceedings of the 63rd Annual Meeting, Pacific Division, American Association for the Advancement of Science*, 1(3), 38–65, 1984.
- Gentry, R. V., Radioactive halos: implications for creation, in *Proceedings of the First International Conference on Creationism*, edited by R. E. Walsh, C. L. Brooks, and R. S. Crowell, vol. 2, pp. 89–100, Creation Science Fellowship, Pittsburgh, Pennsylvania, 1986.
- Gentry, R. V., *Creation's Tiny Mystery*, 347pp., Earth Science Associates, Knoxville, Tennessee, 1988.
- Gentry, R. V., Response to Wise, *Creation Research Society Quarterly*, 25, 176–180, 1989.
- Gentry, R. V., Critique of “Radiohalo evidence regarding change in natural process rates,” *Creation Research Society Quarterly*, 27, 103–105, 1990.
- Gentry, R. V., Radiohalos in diamonds, *Creation Ex Nihilo Technical Journal*, 12, 287–290, 1998.
- Gentry, R. V., personal correspondence, email dated July 27, 1999.
- Gentry, R. V., T. A. Cahill, N. R. Fletcher, H. C. Kaufmann, L. R. Medsker, J. W. Nelson, and R. G. Flocchini, Evidence for primordial superheavy elements, *Physical Review Letters*, 37(1), 11–15, 1976.
- Gentry, R. V., W. H. Christie, D. H. Smith, J. F. Emery, S. A. Reynolds, R. Walker, S. S. Cristy, and P. A. Gentry, Radiohalos in coalified wood: new evidence relating to the time of uranium introduction and coalification,

- Science*, 194, 315–318, 1976.
- Gentry, R. V., W. H. Christie, D. H. Smith, J. W. Boyle, S. S. Cristy, and J. F. McLaughlin, Implications on unknown radioactivity of giant and dwarf haloes in Scandinavian rocks, *Nature*, 274, 457–459, 1978.
- Gentry, R. V., S. S. Cristy, J. F. McLaughlin, and J. A. McHugh, Ion microprobe confirmation of Pb isotope ratios and search for isomer precursors in polonium radiohalos, *Nature*, 244, 282–283, 1973.
- Gentry, R. V., L. D. Hulett, S. S. Cristy, J. F. McLaughlin, J. A. McHugh, and M. Bayard, “Spectacle” array of ^{210}Po halo radiocentres in biotite: a nuclear geophysical enigma, *Nature*, 252, 564–566, 1974.
- Gill, J. B., D. M. Pyle, and R. W. Williams, Igneous rocks, in *Uranium-Series Disequilibrium: Applications to Earth, Marine, and Environmental Sciences*, edited by M. Ivanovich and R. S. Harmon, pp. 207–258, Clarendon Press, Oxford, England, second edition, 1992.
- Granger, H. C., and C. G. Warren, Zoning in the altered tongue associated with roll-type uranium deposits, in *Formation of Uranium Ore Deposits*, pp. 185–200, International Atomic Energy Agency, Vienna, 1974.
- Gudden, B., The ranges of α -rays from U_I and U_{II} and the validity of the Geiger-Nutall relation, *Zeitschrift Physik*, 26, 110–116, 1924.
- Hallbauer, D. K., Radioactive haloes in microcline from a biotite-garnet-sillimanite gneiss of the Northern Southpansberg area, South Africa, *Neues Jahrbuch für Mineralogie Monatshefte*, 79–84, 1969.
- Harada, K., W. C. Burnett, P. A. LaRock, and J. B. Cowart, Polonium in Florida groundwater and its possible relationship to the sulfur cycle and bacteria, *Geochimica et Cosmochimica Acta*, 53, 143–150, 1989.
- Harshman, E. N., Distribution of elements in some roll-type uranium deposits, in *Formation of Uranium Ore Deposits*, pp. 169–183, International Atomic Energy Agency, Vienna, 1974.
- Hashemi-Nezhad, S. R., J. H. Fremlin, and S. A. Durrani, Polonium haloes in mica, *Nature*, 278, 333–335, 1979.
- Henderson, G. H., A quantitative study of pleochroic haloes—V. The genesis of haloes, *Proceedings of the Royal Society of London, Series A*, 173, 250–264, 1939.
- Henderson, G. H., and S. Bateson, A quantitative study of pleochroic haloes—I, *Proceedings of the Royal Society of London, Series A*, 145, 563–581, 1934.
- Henderson, G. H., and F. W. Sparks, A quantitative study of pleochroic haloes—IV. New types of haloes, *Proceedings of the Royal Society of London, Series A*, 173, 238–249, 1939.

- Henderson, G. H., and L. G. Turnbull, A quantitative study of pleochroic haloes—II, *Proceedings of the Royal Society of London, Series A*, 145, 582–598, 1934.
- Henderson G. H., C. M. Mushkat, and D. P. Crawford, A quantitative study of pleochroic halos—III. Thorium, *Proceedings of the Royal Society of London, Series A*, 158, 199–211, 1934.
- Hewitt, D. F., Geology of Cardiff and Faraday Townships, *66th Annual Report of the Ontario Department of Mines*, 66(3), 1–82, 1957.
- Hirschi, H., Radioaktivität einiger Schweizergesteine, *Vierteljahresschr. Naturforsch. Ges. Zürich*, 65, 209–247, 1920.
- Hirschi, H., Zuschriften und vorläufige Mitteilungen, *Naturwissenschaften*, 12, 939–940, 1924.
- Holbrow, C. H., Haloes from plutonium minerals and fission alphas?, *Nature*, 265, 504–508, 1977.
- Holmes, A., Radioactivity and geological time, *Bulletin of the National Research Council*, 80, 124–460, 1931.
- Höppe, G., Zur Frage des Auftretens übergrosser radioaktiver Höfe im Arnögranit, *Geologiska Föreningen Stockholm Förhandlingar*, 81, 485–494, 1959.
- Huang, W. H., and R. M. Walker, Fossil alpha-recoil tracks: a new method of age determination, *Science*, 155, 1103–1106, 1967.
- Hussain, N., T. M. Church, G. W. Luther III, and W. S. Moore, ^{210}Po and ^{210}Pb disequilibrium in the hydrothermal vent fluids and chimney deposits from Juan de Fuca Ridge, *Geophysical Research Letters*, 22, 3175–3178, 1995.
- Hutton, C. O., The nuclei of pleochroic halos, *American Journal of Science*, 245, 154–157, 1947.
- Iimori, S., and J. Yoshimura, Pleochroic halos in biotite: probable existence of the independent origin of the actinium series, *Scientific Papers of the Institute of Physical and Chemical Research*, 5(66), 11–24, 1926.
- Ilton, E. S., and D. R. Veblen, Copper inclusions in sheet silicates from porphyry Cu deposits, *Nature*, 334, 516–518, 1988.
- Jahns, R. H., and C. W. Burnham, Experimental studies of pegmatite genesis: melting and crystallization of granite and pegmatite, *U.S. Geological Survey Bulletin* 69, 1592–1593, 1958.
- Jedwab, J., *Advances in Chemistry Series*, 55, 119–130, 1966.
- Joly, J., Pleochroic halos, *Philosophical Magazine*, 13, 381–383, 1907.
- Joly, J., Radio-active halos, *Philosophical Transactions of the Royal Society of London, Series A*, 217, 51–79, 1917a.

- Joly, J., Radio-active halos, *Nature*, 99, 456–458, 476–478, 1917b.
- Joly, J., Radio-active halos, *Proceedings of the Royal Society of London, Series A*, 102, 682–705, 1923.
- Joly, J., The radioactivity of the rocks, *Nature*, 114, 160–164, 1924.
- Joly, J., and E. Rutherford, The age of pleochroic haloes, *Philosophical Magazine*, 25, 644–657, 1913.
- Kelley, D. S., and K. M. Gillis, Fluid evolution in submarine magma-hydrothermal systems at the Mid-Atlantic Ridge, *Journal of Geophysical Research*, 98B, 19,579–19,596, 1993.
- Kerr-Lawson, D. E., Pleochroic haloes in biotite from near Murray Bay, *University of Toronto Studies in Geology Series*, 24, 54–71, 1927.
- Kerr-Lawson, D. E., Pleochroic haloes in biotite, *University of Toronto Studies in Geology Series*, 27, 15–27, 1928.
- Kofseth, B., Petrography of the Levang Peninsula (Kragero, Norway), *Norges Geologiske Undersokelse*, 157, 1–42, 2 plates, 1942.
- Krishnan, M. S., *Geology of India and Burma*, fifth edition, Sankar, Madras, 1968.
- Krishnan, M. S., and C. Mahadevan, *Indian Journal of Science*, 5, 669–680, 1930.
- Kuroda, P. K., J. C. H. Liou, A. D. Banavali, J. D. Akridge, and L. A. Burchfield, Polonium-210 fallout from the 1980 eruption of Mount St Helens and the mystery cloud of 1982, *Geochemical Journal*, 18, 55–60, 1984.
- Laemmlein, G. G., Coloured haloes surrounding inclusions of monazite in quartz, *Nature*, 155, 724–725, 1945.
- Lang, A. H., Canadian deposits of uranium and thorium (interim account), *Geological Survey of Canada, Economic Geology Series*, 16, 142–145, 1952.
- Lang, A. H., J. W. Griffith, and H. R. Steacy, Canadian deposits of uranium and thorium, *Geological Survey of Canada, Economic Geology Series*, 16, 182–184, 1962.
- LaRock, P., J.-H. Hyun, S. Boutelle, W. C. Burnett, and C. D. Hull, Bacterial mobilization of polonium, *Geochimica et Cosmochimica Acta*, 60, 4321–4328, 1996.
- LeCloarec, M. F., M. Pennisi, E. Corazza, and G. Lambert, Origin of fumarolic fluids emitted from a nonerupting volcano: radionuclide constraints at Vulcano (Aeolian Islands, Italy), *Geochimica et Cosmochimica Acta*, 58, 4401–4410, 1994.
- Lingen, J. S. van der, Ueber pleochroitische höfe, *Zentralel. Mineral. Geol. Abt. A.*, 177–183, 1926.

- Lowell, R. P., P. A. Rona, and R. P. Von Herzen, Seafloor hydrothermal systems, *Journal of Geophysical Research*, 100, 327–352, 1995.
- McAndrew, J., and C. J. Finlay, The nature and significance of the occurrence of uranium in the Nanambu Complex of the Pine Creek Geosyncline, in *Proceedings of International Uranium Symposium in the Pine Creek Geosyncline*, edited by J. Ferguson and A. B. Goleby, pp. 357–362, International Atomic Energy Agency, Vienna, 1980.
- Mahadevan, C., Pleochroic haloes in cordierite, *Indian Journal of Physics*, 1, 445–455, 1927.
- Malakhova, N. P., and L. N. Ovchinnikov, A find of fossils in granite of the central Urals, *USSR Academy of Science, Doklady, Earth Science Section*, 188, 33–35, 1970.
- Meier, H., and W. Hecker, Radioactive halos as possible indicators for geochemical processes in magmatites, *Geochemical Journal*, 10, 185–195, 1976.
- Moazed, C., R. M. Spector, and R. F. Ward, Polonium radiohalos: an alternate interpretation, *Science*, 180, 1272–1275, 1973.
- Moore, J. N., and R. P. Gunderson, Fluid inclusion and isotopic systematics of an evolving magmatic-hydrothermal system, *Geochimica et Cosmochimica Acta*, 59, 3887–3907, 1995.
- Mügge, O., Radioaktivität als ursache der pleochroitischen höfe des cordierit, *Zentralbl. Mineral. Geol.*, 1907, 397–399, 1907.
- Mustart, D. A., Hydrothermal synthesis of large single crystals of albite and potassium feldspar, *EOS, Transactions of the American Geophysical Union*, 50, 675, 1969.
- Neale, E. R. W., Ringwall, Victoria County, Cape Breton Island, Nova Scotia (map with marginal notes), *Geological Survey of Canada, Paper 55-13*, map, 1955.
- Nevissi, A. E., Lead 210 and polonium 210 in Mount St. Helens ash, *Journal of Geophysical Research*, 89B, 6326–6328, 1984.
- Nicholson, K., Fluid chemistry and hydrological regimes in geothermal systems: a possible link between gold-depositing and hydrocarbon-bearing aqueous systems, in *Geofluids: Origin, Migration and Evolution of Fluids in Sedimentary Basins*, edited by J. Parnell, *Geological Society of London, Special Publication No. 78*, 221–232, 1994.
- Odom, A. L., and W. J. Rink, Giant radioactive-induced color halos in quartz: solution to a riddle, *Science*, 246, 107–109, 1989.
- Owen, M. R., Radiation-damaged halos in quartz, *Geology*, 16,

- 529–532, 1988.
- Picciotto, E. E., and S. Deutsch, *Pleochroic Halos*, Comitato Nazionale per l'Energia Nucleare, Rome, 1960.
- Pitcher, W. S., *The Nature and Origin of Granite*, Blackie Academic, Glasgow, pp. 73–74, 1993.
- Poole, J. H. J., The action of heat on pleochroic halos, *Philosophical Magazine, Seventh Series*, 5, 132–141, 1928a.
- Poole, J. H. J., Note on the formation of pleochroic halos in biotite, *Philosophical Magazine, Seventh Series*, 5, 444, 1928b.
- Ramdohr, P., *Neues Jahrbuch für Mineralogie Beilageband Abteilung A*, 67, 53–65, 1933.
- Ramdohr, P., *Abh. Deut. Akad. Wiss. Berlin. Kl. Chem. Geol. Biol.*, 2, 1–17, 1957.
- Ramdohr, P., Neue beobachtungen an Radioaktiven Höfen in verschiedenen Mineralien mit kritischen bemerkungen zur auswertung der Höfe zur Altersbestimmung, *Geologische Rundschau*, 49, 253–263, 1960.
- Ramdohr, P., *The Ore Minerals and Their Intergrowths*, Pergamon, Oxford, England, pp. 235–239, 1969.
- Rimsaite, J., Natural alteration of mica and reactions between ions in mineral deposits, *Clay and Clay Minerals*, 23, 247–255, 1975.
- Rink, W. J., and A. L. Odom, Giant radiation-damage halos in quartz, *Geology*, 17, 54, 1989.
- Rogers, J. J. W., J. A. S. Adams, and B. Gatlin, Distribution of thorium, uranium and potassium concentrations in three cores from the Conway Granite, New Hampshire, U.S.A., *American Journal of Science*, 263, 817–822, 1965.
- Rose, A. W., *Metal Mines and Occurrences in Pennsylvania. Atlas of Pennsylvania's Mineral Resources. Part 3*, Pennsylvania Geological Survey, Harrisburg, Pennsylvania, 1970.
- Rosholt, J. N., Radioactive disequilibrium studies as an aid in understanding the natural migration of uranium and its daughter products, *Proceedings of the Second UN International Conference on the Peaceful Uses of Atomic Energy*, 2, 230–236, 1958.
- Rowe, R. B., Petrology of the Richardson radioactive deposit, Wilberforce, Ontario, *Geological Survey of Canada, Bulletin* 25, 1–22, 1952.
- Rubin, K., Degassing of metals and metalloids from erupting seamount and mid-ocean ridge volcanoes: observations and predictions, *Geochimica et Cosmochimica Acta*, 61, 3525–3542, 1997.
- Rutherford, E., Action of the α rays on glass, *Philosophical Magazine*, 19,

- 192–194, 1910.
- Satterly, J., and D. F. Hewitt, Some radioactive mineral occurrences in the Bancroft area, *Geological Circular of the Ontario Department of Mines*, 2, 53–55, 1955.
- Schilling, A., Die radioaktiven Höfe im flusspat von Wölsendorf, *Neues Jahrbuch für Mineralogie, Geologie und Palaeontology, Abteilung A*, 53, 241–265, 1926.
- Schintlmeister, J., *Ger. Rep. G-111*, part III, 1941.
- Schintlmeister, J., *Ger. Rep. G-186*, 1942.
- Schintlmeister, J., and F. Hernegger, *Ger. Rep. G-55*, part I, 1940.
- Schintlmeister, J., and F. Hernegger, *Ger. Rep. G-112*, part II, 1941.
- Sheng, Z. Z., R. K. Guimon, and P. K. Kuroda, Volatile behaviors of polonium and protactinium in the heating experiments on pitchblende, *Geochemical Journal*, 20, 137–141, 1986.
- Sheng, Z. Z., and P. K. Kuroda, Atmospheric injections of polonium-210 from the recent volcanic eruptions, *Geochemical Journal*, 19, 1–10, 1985.
- Slack, H. A., Radioactivity measurements in the Kirkland Lake area, northern Ontario, *EOS, Transactions of the American Geophysical Union*, 30(6), 867–874, 1949.
- Snelling, A. A., and J. Woodmorappe, The cooling of thick igneous bodies on a young Earth, in *Proceedings of the Fourth International Conference on Creationism*, edited by R. E. Walsh, pp. 527–545, Creation Science Fellowship, Pittsburgh, Pennsylvania, 1998.
- Snetsinger, K. G., Nuclei of pleochroic halos in biotites of some Sierra Nevada granitic rocks, *American Mineralogist*, 52, 1901–1903, 1967.
- Spector, R. M., Pleochroic halos and the constancy of nature: a reexamination, *Physical Review A*, 5, 1323–1327, 1972.
- Stark, M., Pleochroitische (Radioaktive) Höfe, ihre Verbreitung in den Gesteinen und Veränderlichkeit, *Chemie der Erde*, 10, 566–630, 1936.
- Stern, T. W. and Stieff, L. R., Radium-uranium equilibrium and radium-uranium ages of some secondary minerals, *US Geological Survey, Professional Paper 320*, 151–156, 1959.
- Stillman, C. J., and C. H. Holland, *A Geology of Ireland*, Wiley, New York, 1981.
- Stugard, F., Pegmatites of the Middletown area, Connecticut, *United States Geological Survey, Bulletin 1042-Q*, 683, 1958.
- Swanson, S. E., J. A. Whitney, and W. C. Luth, Growth of large quartz and feldspar crystals from synthetic granitic liquids, *EOS, Transactions of the*

- American Geophysical Union*, 53, 1127, 1972.
- Voltaggio, M., P. Tuccimei, M. Branca, and L. Romoli, U-series disequilibrium radionuclides in sulphur incrustations from the fumarolic field of Vulcano Island, *Geochimica et Cosmochimica Acta*, 62, 2111–2127, 1998.
- Wakefield, J. R., Gentry's tiny mystery—unsupported by geology, *Creation/Evolution*, XXII, 13–33, 1988a.
- Wakefield, J. R., Personal communication to Kurt P. Wise, May 5, 1988b.
- Wakefield, J. R., The geology of Gentry's "tiny mystery", *Journal of Geological Education*, 36, 161–175, 1988c.
- Wampler, J. M., and P. Wallace, Misconceptions of crystal growth and cooling rates in the formation of igneous rocks: the case of pegmatites and aplites, *Journal of Geological Education*, 46, 497–499, 1998.
- Wilkerson, G., Polonium radio-halos do not prove fiat creation, *Origins Research*, 12, 1989.
- Wiman, E., Studies of some Archaean rocks in the neighbourhood of Uppsala, Sweden, and of their geological position, *Bulletin of the Geological Institute, University of Uppsala*, 23, 1–170, 1930.
- Winkler, H. G. F., and H. von Platen, Experimentelle Gesteinsmetamorphose—II. Bildung von anatektischen granitischen Schmelzen bei der Metamorphose von NaCl—führenden kalkfreien Tonen, *Geochimica et Cosmochimica Acta*, 15, 91–112, 1958.
- Wise, K. P., Radioactive halos: geological concerns, *Creation Research Society Quarterly*, 25, 171–176, 1989.
- Wise, K. P., Radiohalos in diamonds, *Creation Ex Nihilo Technical Journal*, 12, 285–286, 1998.
- York, D., Polonium halos and geochronology, *EOS, Transactions of the American Geophysical Union*, 60(33), 617–618, 1979.

Glossary

This glossary is a composite of definitions developed by the seven authors of this book. It is possible to tell which author wrote each definition by looking at the superscript following the word. The superscripts are coded to each author as follows:

- a—Steven A. Austin
- b—John R. Baumgardner
- c—Eugene F. Chaffin
- d—Don DeYoung
- h—D. Russell Humphreys
- s—Andrew A. Snelling
- v—Larry Vardiman

Italicized words in the definitions are defined elsewhere in the glossary.

A halo^s The designation given by some early investigators to what are now identified as ²¹⁰Po *radiohalos*.

abundance ratios^c The ratios of the average percents of occurrence. Sometimes this term refers to *isotopes* and sometimes the elemental abundances are meant, depending on the context.

accelerated nuclear decay^v A *young-earth* creationist hypothesis that *radioactivity* was sped up at some period or periods in earth history. The preferred periods are during the *Creation* events, during the judgment in the Garden of Eden, and during the *Genesis Flood*.

accretion^v The hypothetical process in conventional planetology whereby small particles and gases in the *solar nebula* came together over millions of years to form larger bodies, eventually of planetary size. The alternative *young-earth* creationist model would suggest that the Earth and the other planets and moons were formed almost instantaneously during the six days of *Creation*. If accretion occurred, it would have been extremely rapid.

achondrites^v A *stony meteorite* that lacks *chondrules*. Achondrites are

commonly more coarsely crystallized than *chondrites*, and nickel-iron (Ni-Fe) is almost completely lacking in most of them; they represent *meteorites* that are most like terrestrial *rocks*, with sizable fragments of various *minerals* visible to the naked eye.

acid rocks^s A descriptive term for those *igneous rocks* that contain more than 60% SiO₂ in their bulk *chemical* composition. It also refers loosely to any *igneous rock* composed predominantly of light-colored *minerals*, which invariably means these *rocks* are dominated by *quartz* and *feldspars*, which have a high silica content. While not synonymous, the term felsic is sometimes also applied to these rocks because of the predominance of *feldspars* in them.

actinium series^s An alternative name for the *radioactive decay* series beginning with ²³⁵U, the uranium (U) *isotope* which constitutes approximately 0.7% of all naturally-occurring U.

adsorption^s Adherence of gas *molecules*, or of ions or *molecules* in solution, to the surface of solids with which they are in contact.

aggregate^v A mass or body of *rock* particles, *mineral grains*, or a mixture of both.

albite^s A colorless or milky-white *mineral* of the *feldspar* group with the *chemical* formula of NaAlSi₃O₈. It is a variety of *plagioclase*, being an end-member in a series of *plagioclase* compositions ranging to the calcium *feldspar*, anorthite. Otherwise known as sodium *feldspar*.

alkali metals^s The metallic *elements* which constitute the first column or group IA of the periodic table. These *elements* include H, Li, Na, K, Rb, and Cs. These metallic *elements* have many *chemical* properties in common because of some similarities in their atomic structures.

alkaline earths^s The group of metallic *elements* in the second column of the periodic table which are called group IIA *elements*, having similar properties because of similarities in their atomic structures. These *elements* include Be, Mg, Ca, Sr, Ba and Ra.

allanite^s A cerium-bearing *mineral* of the epidote group of *minerals* with a *chemical* formula of (Ce, Ca, Y) (Al, Fe)₃ (SiO₄)₃ (OH). Most typically found as an accessory *mineral* of *igneous rocks* such as *granites* and *pegmatites*, and their metamorphic equivalents.

alpha daughter (α-daughter) products^v The *decay* products in a

radioactive process involving alpha-decay (α -decay).

alpha-decay (α -decay)^h The emission of a rapidly-moving *helium* (He) *nucleus* (two *protons* and two *neutrons*) by a large *atomic nucleus*.

alpha-particle (α -particle)^s A particle emitted from an *atomic nucleus* during one type of *radioactive decay*. It is positively charged and has two *protons* and two *neutrons*, being physically identical with the *nucleus* of a helium-4 (⁴He) *atom*.

alpha-recoil (α -recoil)^s When an *alpha-particle* (α -particle) is emitted from a uranium (U) or thorium (Th) radionuclide during *radioactive decay*, the *nucleus* from which the α -particle has been emitted moves slightly in the opposite direction to the α -particle being emitted from it. This slight backwards motion is called recoil.

alpha-recoil (α -recoil) tracks^s The paths of *radiation damage* in a solid substance caused by the recoil or backwards movement of the uranium (U) and thorium (Th) *decay series nuclei* as *alpha-particles* (α -particles) are emitted from those nuclei during *radioactive decay*. The tracks are similar to *fission tracks*, but are much smaller and more numerous.

amphibolite^s A *metamorphic rock* consisting mainly of *amphibole*, usually *hornblende*, and *plagioclase*, with little or no *quartz*. It is usually the result of *metamorphism* of a basalt occurring at moderate pressures and temperatures, and is characteristic of middle levels or grades of *metamorphism*.

amphibolite-facies^s The set of *metamorphic mineral groups* in which the *mafic rocks* are represented by *amphibolites* containing *hornblende* (*amphibole*) and *plagioclase*. In other *rocks* formed under these *metamorphic conditions* the *mineral groupings* present depend on the compositions of the original unmetamorphosed *rocks*. These *metamorphic conditions* are typical of regional-scale *metamorphism* under moderate to high pressures (in excess of 3000 bars) with temperatures in the range 450°–700°C.

anatexis^s Melting of pre-existing *rock*. This term is commonly modified by descriptors, such as *intergranular*, *partial*, *differential*, *selective*, or *complete*, depending on the scale and magnitude of the melting process.

andesite flows^s *Volcanic rock* formed from *lava flows* made up of *andesite*, a dark-colored, fine-grained *igneous rock* which often contains *phenocrysts* composed of *plagioclase* and one or more dark *minerals* such as *hornblende*,

biotite or *pyroxene*, the *phenocrysts* being set in a groundmass composed generally of the same *minerals* as the *phenocrysts* (*plagioclase*, *pyroxene*, *hornblende*, and often an iron oxide *mineral*).

andesitic composition^s The physical and *chemical* composition of a *rock* or material that pertains to, is composed of, contains or resembles andesite, which is a dark-colored, fine-grained *volcanic rock* composed primarily of the *minerals plagioclase* and one or more of *biotite*, *hornblende* or *pyroxene*, some of the crystals being larger and set within a fine-grained groundmass. Chemically such a composition usually has a bulk silica (SiO_2) content by weight of around 53–55%.

angstrom^d (Å) A unit of small length equal to 10^{-10} meters.

anhydrous lherzolites^s *Intrusive igneous rocks* composed chiefly of *olivine*, *orthopyroxene*, and *clinopyroxene*, in which *olivine* is generally most abundant and in which there is completely or essentially no water in *chemical* combination with any of its *minerals* or in the *rock* structure itself.

anisotropic^s A term used to describe crystals having some physical property that varies with the direction across the crystals. In normal usage this refers to the optical properties of the crystals of different *minerals*. Thus all crystal shapes apart from perfect cubes have different dimensions in each direction and can therefore be described as *anisotropic*. These differences can mean, for example, that when light passes through different directions in a crystal different colors can result.

annealing^c A process of heating followed by slow cooling to change physical attributes of a *mineral*.

annealing^s In the context of *radiohalos* it is the process of repairing the *crystal lattice* of the *mineral* hosting a *radiohalo* so that the damage caused by the penetration of the *alpha-particles* (α -*particles*) is removed, which thus removes the discoloration and the *halo* itself. This process is usually caused by heat, which in effect causes solid-state crystal growth or *recrystallization*, but fluids may also be involved. The net result is the recovery of the original undamaged *crystal lattice* and thus the *radiohalo* is obliterated.

annealing temperature^c The temperature reached during the *annealing* process.

anorthoclase phenocryst^s Large crystals of the *feldspar mineral* with the

formula $(\text{Na, K})\text{AlSi}_3\text{O}_8$. It is a sodium-rich *feldspar* that is a mixture of the sodium *plagioclase* end-member *albite* and the potassium *feldspar orthoclase*.

antediluvian^h Dating from before the *Genesis Flood*.

antineutrino^v An elementary particle of very small mass and magnetic moment and no electric charge emitted in company with an *electron* during *beta-decay* (β -*decay*) and in the disintegration of various types of *mesons*.

antiquark^h An antiparticle form of a *quark*. All fundamental particles of matter, say *electrons* and *protons*, have antiparticle counterparts, say positrons and antiprotons. When a particle meets its antiparticle, they annihilate each other, leaving only pure energy behind.

apatite^s A group of variously colored hexagonal *minerals* consisting primarily of calcium phosphate, but can also contain some fluorine or chlorine. It has the general *chemical* formula: $\text{Ca}_5(\text{PO}_4, \text{CO}_3)_3(\text{F, OH, Cl})$. Apatite occurs as an accessory *mineral* in almost all *igneous* rocks and *metamorphic* rocks. It is the *mineral* which makes up the bones and teeth of animals and humans.

apparent age^s A *radioisotopic* “age” of a *rock* or *mineral* based on the measured isotopic concentrations and ratios in it, but which is not the *rock* or *mineral*’s true age.

appearance of age^s The characteristics and qualities of an object which, though very young, may actually make it look old. This concept is best understood in terms of the description in Genesis chapter 1 of God creating fruit trees already bearing fruit (verse 11). However, in our normal experience trees bearing fruit must be at least some years old, having grown from a seed into a tree, which then flowers and fruits, yet these trees already were yielding fruit the instant God created them, meaning that these trees looked as if they were several years old when in fact they only came into existence moments previously.

Archean rocks^a The oldest *rocks* composing the basement and shield structures of the cores of the continents. Popular *radioisotope* techniques estimate *Archean rocks* to be more than 2.5 billion years old. Most *Archean rocks* are *gneiss* or *granite*, but some are stratified *sedimentary rocks*.

arc-related magma^s Any *magma* associated with island or volcanic arcs, which are chains of islands or island volcanoes rising from the deep-sea

floor near the continents in a curved belt. Such *magma* is generated as a result of *subduction* of the ocean floor underneath the island arc on its seaward side.

asphaltized wood^s Wood that has been impregnated with asphalt, which is a dark brown to black solid bitumen, consisting almost entirely of carbon and hydrogen. It is formed naturally in oil-bearing *rocks* by the evaporation of the volatiles in the oil, which leaves behind this residue.

assimilation and fractional crystallization (AFC)^s Two processes which may occur separately, but which usually take place simultaneously, resulting in the contamination of a *magma*. Assimilation is the incorporation and digestion of solid or fluid foreign material, that is, wall *rock* (usually *crustal rock*), in a *magma*. The term implies no specific mechanisms or results. Such a *magma*, or the *rock* it produces, may thus be called hybrid or contaminated. Fractional *crystallization* is *crystallization* in which the early-formed crystals are prevented from being in equilibrium with the liquid from which they grew, resulting in a series of residual liquids of more extreme compositions than would have resulted from *crystallization* at equilibrium. This term is synonymous with *fractionation*. One way that the early-formed crystals may be prevented from being in equilibrium with the liquid from which they grew is when these early-formed crystals fall to the bottom of the *magma chamber* under the influence of gravity.

asthenosphere^s The layer or shell of the earth's internal structure below the *lithosphere*. It is a relatively weak and hot region (at or near the melting point of *rocks*) in the upper part of the *mantle*. Its thickness is variable but typically on the order of 100 km. It is the region in which isostatic adjustments take place (vertical movements in the *lithosphere* above resulting from differences in thicknesses and densities), *magmas* may be generated, and seismic waves are strongly attenuated (reduced energy or amplitude).

asymmetric fission^c A *fission* in which the two fragment nuclei have different sizes.

atmophile^v Pertaining to *elements* that are most typical in the earth's atmosphere: H, C, N, O, I, Hg, and *inert gases*. An *element* that occurs in the uncombined state, or that "will concentrate in the gaseous *primordial* atmosphere."

atmospheric argon^s Argon (Ar) in the atmosphere and Ar absorbed on

the surfaces of *rocks* and *minerals* that have been exposed to the atmosphere.

atom^v The smallest particles of an *element* that combine with similar particles of other *elements* to produce *compounds*: *atoms* combine to form *molecules*, and consist of a complex arrangement of *electrons* revolving about a positively charged *nucleus* containing *protons* and *neutrons*.

atomic mass^v The mass of an *atom*. It is most often measured in atomic mass units (a.m.u.), one-sixteenth of the mass of an *atom* of ¹⁶O (oxygen-16).

atomic number^s The number of *protons* in the *nucleus* of the *atom* which determines the *element* to which that *atom* belongs. All *atoms* of the same *element* have the same number of *protons* in their nuclei and hence the same atomic number.

atomic weight^h Often simply the number of *protons* and *neutrons* in an atomic *nucleus*. More exactly, the mass of an *atom* or *nucleus* expressed in a system of units wherein the mass of a particular type of carbon *atom* (¹²C) is exactly 12. See *atomic mass*.

B halo^s The designation given by early investigators to what are now known as ²¹⁴Po *radiohalos*.

background dose^h The amount of damage done to a living organism by naturally-occurring *radioactivity* in a normal environment.

baddeleyite^s A colorless, yellow, brown or black *mineral* consisting of zirconium oxide, with a *chemical* formula of ZrO₂. It may contain some trace amounts of hafnium (Hf), titanium (Ti), iron (Fe), thorium (Th) and uranium (U), and therefore it is an important *mineral* in the uranium-thorium-lead (U-Th-Pb) radioisotopic dating of the *mafic rocks* which contain it, such as *diabase* or *carbonatite*.

basalt flows^s These are surface flows of basalt *lava*, having been molten when extruded from a volcano, the *lava* cooling to form basalt, which is a general term for a dark-colored, fine-grained *igneous rock*, composed chiefly of the *minerals* *plagioclase* and *clinopyroxene*.

basaltic achondrite best initial (BABI)^s Taken to be the starting point for the development of strontium (Sr) *isotopes* with time, and is said to be the ⁸⁷Sr/⁸⁶Sr ratio at the formation of the earth. It has been determined by isotopic analyses of *basaltic achondrite meteorites*, which are thought to have a composition approximating that of the *solar nebula* at the time of planetary

formation, because they show evidence of having crystallized from *silicate* liquids due to their resemblance to terrestrial basalts. Because their Rb/Sr ratios are very low, this is taken to mean that their $^{87}\text{Sr}/^{86}\text{Sr}$ ratios have changed little since their *crystallization*, which is believed to have occurred at the same time as the formation of the earth, and thus their $^{87}\text{Sr}/^{86}\text{Sr}$ ratios are believed to represent the $^{87}\text{Sr}/^{86}\text{Sr}$ ratio of the earth's initial *rocks*.

basaltic achondrite meteorites^s *Stony meteorites* that lack *chondrules* and are of *basaltic composition* and *mineralogy*. These *meteorites* are commonly more coarsely crystallized than the *stony meteorites* with *chondrules*, and metallic nickel-iron mixtures are almost completely lacking in most of them. They represent *meteorites* that are the most like terrestrial *rocks*, with sizeable fragments of various *minerals* visible to the naked eye.

basaltic composition^s The composition of a *rock* or material that pertains to, is composed of, contains or resembles basalt, which is a dark-colored *volcanic rock* composed chiefly of the *minerals plagioclase* and *clinopyroxene*, with a bulk silica (SiO_2) content by weight of around 46–49%.

basaltic glasses^s Black glassy material of *basaltic composition* produced by very rapid cooling of basalt *lavas*, usually by contact with water. The *lava* cools so quickly that crystals don't have time to grow and instead a glass is formed.

basaltic lava^v A general term for dark-colored *mafic igneous rocks*, extruded onto the surface of the earth and solidified.

bastnaesite^s A greasy, wax-yellow to reddish-brown *mineral* which is essentially a rare earth carbonate with a *chemical* formula: $(\text{Ce}, \text{La})\text{CO}_3(\text{F}, \text{OH})$. It may also contain yttrium (Y). It primarily occurs in rare *igneous rocks* that are carbonate-rich, such as *carbonatite*.

batholith^s A large *intrusive* igneous mass that has more than 40 square miles (100 square kilometers) of surface exposure and descends at depth without any known bottom to it. Its formation is generally believed to involve *intrusion of magma*, and the mass cools cross-cutting the orientation of the strata being intruded, said to be therefore *discordant*.

beryl^s A *mineral* with the *chemical* formula of $\text{Be}_3\text{Al}_2\text{Si}_6\text{O}_{18}$. It usually occurs in green or bluish-green long hexagonal crystals. Transparent and colored gem varieties include emerald and aquamarine.

beta-daughter (β -daughter) products^v The *decay* products in a radioactive process involving *beta-decay* (β -decay).

beta-decay (β -decay)^c A type of *decay* originally associated with the emission of positrons, *electrons*, and *neutrinos* from the *nucleus*, but which now is known to originate from emission of *W particles* or *Z particles*, which then *decay* to produce the familiar results.

betafite^s A yellow, brown, greenish, or black *mineral* of the pyrochlore group, with a *chemical* formula of $(\text{Ca}, \text{Na}, \text{U})_2(\text{Nb}, \text{Ta})_2\text{O}_6(\text{O}, \text{OH})$. It is thus a uranium(U)-rich oxide of niobium (Nb) and tantalum (Ta). It is found in granitic *pegmatites* and probably forms a continuous compositional series with pyrochlore (another oxide of Nb and Ta), the name being assigned to members of the series with U greater than 15%.

big bang origin^d The idea that the universe began as a point-like concentration of energy that has been expanding ever since.

biostratigraphic^s Pertaining to stratigraphy based on the paleontological or contained fossil aspects of *rock* strata, whereby the *rock* units are separated and differentiated on the basis of the description and study of the fossils they contain.

biotite^s A widely distributed and important *rock-forming mineral* of the *mica* group, with a *chemical* formula: $\text{K}(\text{Mg}, \text{Fe}^{2+})_3(\text{Al}, \text{Fe}^{3+})\text{Si}_3\text{O}_{10}(\text{OH})_2$. It is generally black, dark brown, or dark green, and is an important constituent of many *crystalline rocks*. Like all *micas*, it occurs as thin flakes due to the sheet structure of its *molecules*.

blocking temperature^s In a crystallizing *mineral*, this is the temperature at which a crystal structure has formed sufficiently to block the inclusion in its structure of any further *elements* or *isotopes*. The term is synonymous with *closure temperature*. Below this temperature an isotopic and *chemical* composition is said to be fixed. This is important in the case of the inclusion of argon (Ar) gas in *minerals*, because the Ar stops being included in the *mineral* structure at this temperature and thus becomes fixed below that temperature. If a *mineral* is heated again above that temperature the Ar gas can escape, and so this effects any resultant Ar-Ar radioisotopic dating of that *mineral* or the *rock* containing it.

boson^c Tiny particles that have an integer unit of *spin* (0,1,2, . . .). Particles with half a unit of *spin* are called fermions. More specifically, in particle

physics bosons (gluons, *W particles*, *Z particles*, pions and *photons*) are the quanta of the fields that bind other particles together.

bound particle^h A particle constrained by forces to remain in a particular region.

Bragg ionization curves^s When *alpha-particles* (α -particles) pass through a *mineral*, interactions occur between the positively charged α -particles and the negatively charged *electrons* orbiting the *atoms* making up the *mineral* structure. If the α -particles approach fairly close to *electrons*, or if *electrons* are far from their nuclei and, therefore, held loosely, they may be completely separated from their *atom* or *molecule*. This results in an ion pair, consisting of an *electron* and its “parent” *atom*, which is now a positive ion. This process is called ionization. As the moving α -particles, now of lesser energy, leave the field of the newly created ion pairs, the *electrons* and the positive ions may recombine. The decrease in velocity of the α -particles during their trajectory permits them to spend more time in the vicinity of orbital *electrons*, thereby increasing the probability of them creating more ion pairs. Therefore, as the α -particles slow down in their trajectory through the *mineral*, they will gradually increase the numbers of ion pairs formed until a maximum is reached at the end of the trajectory. This can be plotted on a diagram in which the number of ionizations per unit path length is compared with the distance traveled by the α -particles, and the result is a curve which reaches its maximum at the end of the α -particles’ paths. Such ionization curves can be experimentally determined for the α -particles emitted from the relevant *radionuclides* in the ^{238}U decay series, and in minerals such as *biotite* in which *radiohalos* occur. These ionization curves are named after Bragg, who is famous for his work on the passage of light through crystals. The significance of these ionization curves is that the ring structures in *radiohalos* result from the damage caused to the host *mineral* structures by α -particles as they slow down and reach the end of their trajectories, which is also where the maximum ionization occurs. This allows for experimentally comparing the ionization curves with the *radiohalo* rings to confirm which α -particle-emitting *radionuclides* were responsible for the rings in the *radiohalos*.

bulk earth^s Synonymous with *bulk silicate earth* (BSE), which is that *mantle geochemical reservoir* with the chemistry of the earth without the

core, that is, a *chemical* composition represented by a mixture of all *mantle* and *crustal rocks*. This composition is said to be equivalent to that of a conjectured homogeneous primitive *mantle* which formed during the postulated degassing of the planet and during *core* formation, prior to the formation of the continents. Even though some oceanic basalts have isotopic compositions which closely approximate to this *bulk earth* composition, at the present there are no *geochemical* data which require that such a *mantle* reservoir still survives. Thus this is a conjectural isotopic *reservoir* with no volume of *rock* in the *mantle* from which *magmas* and *volcanic rocks* are currently derived, but it is a logical concept which the unraveling of all the mixing in the *mantle*, and the separation of the earth's *crust* from the *mantle* via melting and production of *magmas*, both point back to as an initial uniform composition for the *silicate* portion of the earth as distinct from the *metallic core*. This has thus been regarded as the primary (or initial) uniform *reservoir*.

bulk silicate earth (BSE)^s See *bulk earth*, with which this term is synonymous.

buoyancy^h The tendency of a low-density material to rise when it is immersed in a high-density material.

C halo^s The designation given by early investigators to what have now been identified as ^{218}Po *radiohalos*.

calcite^s A common *rock-forming mineral* which is calcium carbonate with a *chemical* formula of CaCO_3 . It is usually white, colorless, or pale shades of gray, yellow and blue. It is characterized by perfect *rhombohedral cleavage* and a vitreous (glassy) luster. It readily effervesces in cold dilute hydrochloric acid. It is the principal constituent of limestone, and occurs in its *crystalline* form in *marble*. Its earthy form is chalk, and it also makes up the various forms of spectacular cave deposits.

calc-silicate rocks^s *Metamorphic rocks* consisting mainly of calcium-bearing (Ca-bearing) *silicate minerals* and formed by *metamorphism* of impure *limestone* or *dolomite*. This may be via *metamorphism* on a regional scale, or due to contact *metamorphism*, where the heat and fluids from a cooling igneous *intrusion* have metamorphosed the *limestones*.

Cambrian^s The earliest period of the *geological* timescale in the so-called Paleozoic (or "ancient life") era, conventionally thought to have covered

the span of time between 570 and 500 million years ago. The term also refers to the corresponding system of *rocks*, which are the lowermost *rock* strata in the *geological* column to contain a profusion of marine invertebrate fossils, multicellular creatures without backbones that lived in marine environments.

carbonaceous chondrite (CI)^v A *stony meteorite* characterized by abundant *chondrules* embedded in a dark, friable matrix of carbon-rich (C-rich) *compounds*, phyllosilicates and mafic *silicates*, nickel-iron (Ni-Fe) metal, and glass.

carbonaceous phases^c Different phases which carbon (C) may assume.

carbonado diamonds^s Impure opaque-dark *aggregates* composed of minute *diamond* particles, forming unusually rounded masses with granular to compact structure, and displaying a superior toughness as a result of their cryptocrystalline character and lack of *cleavage planes*. Sometimes called black *diamonds*, they are often used in industrial applications.

carbonatites^s Carbonate *rocks* of apparent magmatic origin, generally associated with *kimberlites*. The origin of these *rocks* is controversial, being variously explained as derived from magmatic melts, solid flow, hydrothermal solution and gaseous transfer of calcium (Ca) and magnesium (Mg) carbonate separated from *upper mantle* material.

cataclysmic^h Globally destructive, on the scale of the *Genesis Flood*.

catastrophic plate tectonics^v A *young-earth* creationist model of the movement of the *plates* composing the *lithosphere* of the earth. This model says the *plates* moved very rapidly during and immediately following the *Genesis Flood* and are now moving slowly, if at all. The conventional view is that the movement of the *plates* is extremely slow and has been occurring over millions of years.

catastrophism^v The principle that sudden, violent, short-lived, more or less worldwide events outside our present experience have greatly modified the earth's *crust*.

cation^s An electro-positive *element* produced at the cathode in electrolysis. It is a positively charged ion, which is an *atom* or *molecule* having a different number of *electrons* than *protons* making it electrically charged, in this case more *protons* than *electrons*. The opposite is an anion, a negatively charged ion.

cementation^v The process by which coarse *clastic sediments* become lithified or consolidated into hard, compact rocks.

cerite^s A mineral with the *chemical* formula: $(\text{Ce}, \text{Ca})_9(\text{Mg}, \text{Fe})\text{Si}_7(\text{O}, \text{OH}, \text{F})_{28}$. It is a primary source of the *rare earth element* cerium (Ce) and is essentially a calcium cerium *silicate*.

chalcophile^b *Elements* that have an affinity for sulfur and therefore tend to concentrate in the sulfide phase of molten material.

change of decay^s Alteration or change of the rate at which *radioactive decay* occurs, that is, the spontaneous disintegration of the *atoms* of certain *elements* into new *elements*.

chemical^v Any substance used in or obtained by a *chemical* process or processes.

chemical weathering^s The process of *weathering* by which *chemical* reactions (such as hydrolysis, hydration, oxidation, carbonation, ion exchange, and solution) transform *rocks* and *minerals* into new *chemical* combinations (of *rocks* and *minerals*) that are stable under conditions prevailing at or near the earth's surface. These processes primarily involve oxygen in the air and water reacting with the *rocks* and *minerals*. An example of this process is the alteration of *orthoclase* (potassium or alkali *feldspar*) to the *clay mineral*, kaolinite. In this instance the *orthoclase* is said to have decomposed to kaolinite.

chert^a A *sedimentary rock* formed from very finely *crystalline quartz*.

chimney deposits^s Accumulations of *minerals*, including metal sulfides, in chimney-shaped columns rising above their surroundings through which *hydrothermal fluids* are being discharged. These deposits are primarily associated with hydrothermal vents on the ocean floor, and have been built by the precipitation of the *minerals* from the hot waters upon their discharge into the cold ocean waters, these *minerals* building up around the vents to produce the characteristic chimney shape.

chondrite^v A *meteorite* containing *chondrules*.

chondritic meteorite^v A *stony* or *silicate-rich meteorite* with spherical granules (*chondrules*). The finely *crystalline chondrules* are composed of *orthopyroxene*, *olivine*, nickel-iron, and glass. Over 80% of the observed falls of *meteorites* are chondritic.

chondritic reservoir^s The presumed repository or particular volumes of

rock in the earth's *mantle* with *trace element* and isotopic compositions identical to that of *chondritic meteorites*, that is, *stony meteorites* characterized by *chondrules*.

CHondritic Uniform Reservoir (CHUR)^s A conceptual repository in the earth's *mantle* with a uniform chondritic *trace element* and isotopic composition, based on evidence that the earth's initial composition was similar to that of *chondrites*, *stony meteorites* characterized by *chondrules* embedded in a finely crystalline matrix consisting of *orthopyroxene*, *olivine* and nickel-iron, with or without glass. This model particularly applies to the samarium-neodymium (Sm-Nd) isotopic system and is used to describe the isotopic evolution of Nd in the earth beginning with an Sm/Nd ratio equal to that in the *chondritic meteorites*. This model thus supplies the presumed initial conditions in Sm-Nd *radioisotopic* "age" calculations.

chondrule^v A spheroidal granule or *aggregate*, often radially crystallized and usually about 1 mm in diameter, consisting chiefly of *olivine* and/or *orthopyroxene* and occurring embedded more or less abundantly in the fragmental bases of many *stony meteorites* (*chondrites*) and sometimes free in marine *sediments*.

circular halo^s A normal *radiohalo* which is circular in thin section, since in three dimensions the *halo* is spherical.

circulation^s The general term used for flow in a loop that is often closed, and generally refers to the flow of fluids, particularly water.

clastic^v A *rock* or *sediment* composed principally of broken fragments that are derived from preexisting *rocks* or *minerals* and that have been transported some distance from their places of origin.

clastic sedimentary rocks^s *Rocks* made up of *clastic sediments*, that is, those composed principally of broken fragments that are derived from pre-existing *rocks* or *minerals* and that have been transported some distance from their places of origin. This can include the solid products formed during *chemical weathering* of such *rocks*. Examples include sandstone, *conglomerate* and *shale*.

clausthalite sites^s Places or positions within the *radiocenters* of *halos* where the *mineral* clausthalite or lead selenide (PbSe) occurs as minute particles in the *aggregates* which make up the *radiocenters*.

clay^v A *soil* containing a high percentage of fine particles and *colloidal*

substances, becoming sticky and plastic when wet and forming hard lumps or clods when dry. Usually composed of characteristic *minerals* called clay *minerals*, such as kaolinite and montmorillonite.

cleavage^s The breaking of a *mineral* along its crystal planes, thus reflecting the *mineral's* crystal structure. In the case of *rocks*, it is the property or tendency of a *rock* to split along secondary, aligned fractures or other closely spaced, planar structures or textures, produced by deforming of the *rock* or *metamorphism*, and can be often governed by the alignment of the *minerals* in the *rock* and their crystal properties.

cleavage planes^s The surfaces along which *rocks* or *minerals* tend to split due to their structures. In the case of *minerals*, these surfaces are a result of the *minerals'* crystal structures, that is, the way the *atoms* connect to one another in repeating patterns. In the case of *rocks*, it is due to the alignment of the *minerals* in the *rocks* and these crystal properties of those *minerals*.

clinopyroxene^s A group name for *pyroxenes* crystallizing in the monoclinic system and sometimes containing considerable calcium (Ca), with or without aluminum (Al), and potassium (K) or sodium (Na). The term is also used to describe any *mineral* in this group.

closure temperature^s In a *mineral* that has crystallized but is still cooling, the temperature at which the *mineral's* crystal becomes closed to the loss or gain from its internal structure of gases or fluids. This is particularly relevant to the gas Ar (Ar) when measurements are made on *minerals* for Ar-Ar dating. Synonymous with *blocking temperature*.

coal^s A readily combustible (able to be burned) *rock* containing more than 50% by weight, and more than 70% by volume, of carbonaceous (carbon-rich) material including inherent moisture, formed by compaction and hardening of variously altered plant remains such as leaves, wood, pollen spores, and resins. It comes in two main varieties, black and brown, the latter being called lignite.

coalification^s The alteration or *metamorphism* of plant material into *coal*, including the biochemical processes of hardening and fossilizing of the plant material, and the *geochemical* processes of *metamorphism* to transform the plant material into *coal*.

coalified wood^s Wood that has been fossilized by being turned to *coal*, and yet is still recognizable as wood because of its inherent cellular structure,

etc. The biochemical processes and *geochemical* processes which occur in the formation of *coal* have changed the original wood, but kept its original structures.

cogenetic rock suites^s A set or group of *rocks* which have the same source, origin and mode of formation. Specifically, the term applies to a group of *igneous rocks* from the same area or region which have cooled and crystallized from the same *magma* source—for example, a series of basalt *lava* flows that were erupted from the same volcano and which thus came from the same *magma chamber*.

colloid^v Any fine-grained material in suspension, or any such material smaller than *clay* size that can be easily suspended.

colloidal gel^s A translucent or transparent, semi-solid, apparently homogeneous substance, generally elastic and jelly-like, offering little resistance to liquid *diffusion*, and containing a dispersion or network of fine particles <0.00024 mm in diameter in suspension but coalesced to some degree, yet not in a *crystalline* form.

combination halos^s *Radiohalos* which are a combination of ring structures indicating more than one original parent *radionuclide* has been present in the *radiocenters*—for example, *halos* with rings for both the ²³⁸U and ²³²Th *decay* series, thus being *halos* combining *radiohalos* produced by these two *decay* series, here combined in the same *halos*.

compactified^c Closely confined, not necessarily in technical senses defined in topology.

composite radiohalos^s Essentially synonymous with *combination halos*. They are *radiohalos* which are composites of other *halo* types, implying that they were parented by more than one original *radionuclide* in the *radiocenters*.

compound^v A substance containing two or more *elements* combined in fixed proportions.

compressional wave^v The component of a seismic wave which causes compressional motion in the direction of the motion of the wave, or P-wave. Its speed is about twice the speed of S-waves. P stands for primary because it arrives first, followed by the S (secondary)-wave.

concordance^d Agreement of a *rock* sample age using different techniques.

concordia diagram^s The graphed curve formed when the ²⁰⁶Pb/²³⁸U ratio

is plotted against the $^{207}\text{Pb}/^{235}\text{U}$ ratio as both increase in value due to *nuclear decay* of uranium to lead with the passage of time, assuming a closed U-Pb system (no additions or losses of U or Pb). The curve is called the concordia, and is the locus of all concordant U-Pb “ages”, so it is thus believed to be a time curve. In other words, all points along the curve represent “ages” that are in agreement with the relevant isotopic ratios representing those particular “ages”.

concordia interpretation^v The belief that the graphed curve formed when the $^{206}\text{Pb}/^{238}\text{U}$ ratio is plotted against the $^{207}\text{Pb}/^{235}\text{U}$ ratio is due to *nuclear decay* of uranium (U) to lead (Pb) with the passage of time assuming a closed uranium-lead (U-Pb) system. The curve (concordia) is the locus of all concordant U-Pb “ages” and is thus believed to be a time curve.

condensation^v The process by which a gas becomes a liquid, the opposite of evaporation.

conduits^s Tiny passages such as fractures that are filled with water under *hydrostatic pressure*. These therefore are passageways along which fluids can be transported within *rocks* or *minerals*.

conglomerate^v A coarse-grained *clastic sedimentary rock*, composed of rounded to subangular fragments larger than 2 mm in diameter (granules, pebbles, cobbles, boulders) typically containing fine-grained particles (sand, silt, *clay*) in the interstices, and commonly cemented by calcium carbonate, iron oxide, silica, or hardened *clay*.

contact metamorphic zone^s A zone or *halo* area surrounding a body of *igneous rock* where metamorphic changes have occurred in the *rocks* hosting the *intrusion* caused by the heat and fluids emanating from the *magma*. This is a local process of thermal *metamorphism* genetically related to the *intrusion* of the *magma*, and only takes place in *rocks* at or near the contact with the *intrusive igneous magma*. Thus this thermal *metamorphism* is called contact *metamorphism*, and the area of host *rock* surrounding the *intrusion* which has been effected by the heat and fluids is called the contact *metamorphic zone*, or *thermal aureole*.

contamination model^s Explanation for how the process of alteration of the *chemical* composition of a *magma* occurs as a result of incorporation in the *magma* of *inclusions* and pieces of *country* and wall *rocks*.

continental accretion^s The outbuilding or growth of the *continental crust*

at a *subduction zone* by the adding of ocean floor material and *sediments* scraped off a descending *plate* of *oceanic crust*, or by adding of newly deposited *sediments* from the slopes of the trench above the *subduction zone*, all these *sediments* and materials usually being deformed by being added to the upper *plate* in the *subduction zone* which consists of *continental crust*.

continental crust^b A layer of *rock* typically 30–35 km thick (frequently thicker in mountain belts) that is strongly enriched in *incompatible elements*, significantly enriched in silica, and depleted in iron and magnesium relative to typical *mantle rocks*. Its lower density (2700 kg/m^3) relative to *mantle rock* causes the continental surfaces to be some 4 km higher in elevation than the ocean basins that do not have such a thick crustal layer.

continental foundering^s The process of large volumes of continental *crustal rocks* giving way and sinking or collapsing along fault zones, due to extension or pulling apart and drifting of the *continental crust*. The result is a topographically depressed area on the earth's surface.

convective stirring^b A supposed mass movement of subcrustal or *mantle* material, either laterally or in upward- or downward-directed convection cells, mainly as a result of heat variations. This movement mixes the composition of the material into heterogeneous patterns.

convergent margin volcanism^b Volcanism that results from the localized melting of *sediments* and *oceanic crust* on the top side of a subducting oceanic *plate* at a depth of about 125 km. When the opposing *plate* is oceanic, this process generates an arc-like distribution of volcanic islands, such as the Aleutian Islands. When the opposing *plate* is continental, the process yields a chain of volcanic mountains, as in the Andes and Central America.

cordierite^s A light-blue to dark-blue or even violet-blue *crystalline mineral* with a *chemical* formula of $(\text{MgFe})_2\text{Al}_4\text{Si}_5\text{O}_{18}$. It exhibits strong color under the microscope, is easily altered by *weathering*, and is an accessory *mineral* in *granites* and a common constituent in *metamorphic rocks* formed under low pressure.

core^v The central zone or nucleus of the earth's interior, divided into an inner core which is solid, and an outer core which is liquid.

corona^v The bright, white aureole surrounding the Sun and extending

outward on the average to about four solar radii.

cosmic ray^c Fast-moving elementary particles in *space*, such as *protons*, *electrons*, light atomic nuclei, and *gamma rays*. *Protons* are the most common component of this radiation, which impinges on the earth from all directions, colliding with the *atoms* in the atmosphere to produce showers of secondary radiation.

cosmological constant^c A constant inserted in the field equations of General Relativity to allow control of the expansion rate of the universe, and thought to be related to the properties of the fields associated with the *vacuum*.

coulomb barrier^h The uppermost region, or rim, of the nuclear potential well, where the repulsive electrostatic, or coulomb force is about equal to the attractive nuclear force. This region acts as a barrier to *alpha-particles* (α -particles) trying to leave the *nucleus*.

coulomb repulsion^c The electric force pushing apart two particles which either both have positive charge or both have negative charge.

country rock^s The *rock* strata intruded by, and surrounding, an igneous *intrusion*, synonymous with the term *wall rock*.

coupling constant^h A number which specifies the strength with which a particle is coupled to the field it produces or responds to. For the electromagnetic field, the coupling constant is the electrical charge.

cratering^h The pattern of craters seen on planets and moons throughout the solar system.

cratons^s Parts of the earth's *crust* that have attained stability, and have been little deformed for prolonged periods of time. These are extensive central areas to most of the continents and include both shields and platforms, the areas surrounding the shields which are covered by flat-lying or gently tilted strata, mainly sedimentary strata, and which are underlain at varying depths by a basement of *rocks* that were consolidated during earlier episodes of folding.

Creation^v The process by which God brought forth mass, *space*, and time *ex nihilo* (from nothing) and formed them into the universe and world in which we live. Life was also created and placed upon the earth by God.

creative processes^s The means by which the various entities were created in a sequence of God-directed steps. These processes by which *Creation* took place, as described in Genesis 1, could be both the process of *fiat*

creation, or processes akin to those we observe today but speeded up incredibly to the point where the processes achieved their objectives virtually instantaneously, or in a matter of minutes or hours, under God's direct control and authority.

Cretaceous^s The final *geological* period of the *Mesozoic era* thought conventionally to have covered the span of time between 142 and 65 million years ago. The same term also applies to the *rock* strata in the *geological* record which were deposited or formed during this *geological* period. The name is derived from the Latin word for chalk (*creta*), because of the English chalk beds corresponding to this *geological* period.

Cretaceous-Tertiary boundary (also K/T boundary)^v The interface between the *Cretaceous* and the *Tertiary* layers in the geologic column. A strong demarcation in earth processes thought by many in the conventional geologic community to be caused by meteoritic bombardment of the earth, devastation, and extinction of most life on the earth some 65 million years ago. Frequently located by the widespread presence of iridium, a rare *element* found in *meteorites*. Thought by many *young-earth* creationists to be evidence for one of many catastrophic processes which occurred during the *Genesis Flood*.

crust^s The outermost layer or shell of the earth exposed at the earth's surface, defined according to various criteria including density and composition; lower in density than the *mantle*, with distinct differences in major *element* and *trace element* composition.

crustal anatexis^s Melting of pre-existing *rocks* in the *crust*. This melting may be between *grains*, partial, selective or complete.

crustal blocks^s Large volumes of *rocks* that form an integrated whole and which are stable within themselves, but which can move as a whole relative to adjoining large volumes of *crustal rocks* along faults.

crustal contamination^s Addition of continental *crustal rocks* to a mantle-derived *magma* after it has left its source region in the *mantle* so as to contaminate it. However, it can also refer to contamination with crustal material of a *mantle* source region from which *magmas* were derived at some time in the past by, for example, the incorporation of subducted *sediment* into the *mantle*. Fluids in the *crust* may also add to a *magma* specific *elements* and quantities characteristic of the *crust*, thus altering the

magma composition and contaminating it.

crustal-extraction ages^s This is said to be the times when melting occurred to form *magmas* which rose into the *crust* to then crystallize as new *crustal rocks*. These will be older than the *crystallization ages* of the *rocks* and refer to the times before when all the *elements* now making up the *rocks* were extracted from their source areas, usually in the *upper mantle*, but sometimes in the lower *crust*.

crustal fluids^s Any fluids consisting of liquids and/or gases found in the earth's crust.

crustal-residence ages^s Synonymous with “provenance ages”. They are said to be the average crustal residence times of all the components of *sedimentary rocks*. These will normally be older than the so-called *stratigraphic ages*, because they are based on the earlier times when the *minerals* in the pre-existing *rocks* crystallized before being weathered and eroded to form the *sediments*.

crustal rock^s Any *rock* in the earth's *crust*, which is the outermost layer or shell of the earth.

crust-formation ages^s Essentially synonymous with “*crustal-extraction ages*”, being the times of formation of a new segments of *continental crust* by *fractionation* (separation) of material from the *mantle*.

crystal lattice^h The geometric arrangement of *atoms* within a crystal, having spaces between them as in an ordinary *lattice* structure.

crystalline^v Having a crystal structure or a regular arrangement of *atoms* in a space *lattice*.

crystallization^a The process that causes *minerals* to form from semi-molten, molten, or fluid materials.

crystallization age^s The calculated *radioisotopic* “age” at the time of *crystallization* of a *mineral* or *rock*.

cubic diamonds^s Synonymous with *diamonds* because they belong to the cubic crystal system, even though they don't crystallize as cubes. Nevertheless, the axes of the octahedral crystals of *diamonds* are characteristic of the cubic or isometric system.

cyanobacteria^s Blue-green algae, that is, minute, plant-like organisms.

D halo^s The *halo* described by Henderson and Sparks in 1939 and given this designation. However, this ring structure seems to correspond to the

halo produced by ^{226}Ra , which is a member of the ^{238}U *radioactive decay chain*.

D layer^b The seismic region of the earth between 670 km and 2900 km, equivalent to the *lower mantle*. At a depth of 2700 km, there is a change from *chemical* homogeneity to inhomogeneity; the upper division is the D' layer, and the lower is the D'' layer. It is a part of a classification of the earth's interior made up of layers A to G.

dacite^s A fine-grained *igneous rock* with the same general composition as andesite, but having less *plagioclase* and instead some *quartz*, along with *pyroxene* and *hornblende*, or even *biotite*. Formed from a *lava flow*, it is a *volcanic rock* often regarded as the volcanic equivalent of one of the types of *granitic rocks*.

daughter elements^v The *decay* products in a radioactive process.

daughter isotope^d An *isotope* produced by the *radioactive decay* of a parent *isotope* (for example, ^{40}K changing into ^{40}Ar).

day-age theory^v The teaching that the days of *Creation* in the Bible are not 24-hour days but long periods of time lasting millions of years during which *evolution* could occur.

decay^v (a) The radioactive disintegration of a *parent element* into daughter products. (b) The general weathering or wasting away of *rock*.

decay chain^v A plot of sequential *radionuclides* through which *nuclear decay* converts a heavy *parent nuclide* to *daughter nuclides*, for example, the uranium-lead (U-Pb) *decay chain*.

decay constant^s A constant, characteristic of a nuclear species, which expresses the probability that an *atom* of the species will *decay* in a given time interval. For a large number of *atoms* of a species, the decay constant is the ratio between the number of decaying *atoms* per unit of time and the existing number of *atoms*. It is therefore a measure for any given radioactive *atom* of the rate at which it radioactively decays.

decay rate^h Applied to a group of atomic nuclei, the fraction of them which *decay* per unit time.

decompression melting^b Change of phase from solid to liquid due to the reduction in pressure during ascent of a *magma* body through the *mantle* or *crust*.

defects^s Departures from perfection in the *crystal lattice* structure of

minerals. This usually is the result of missing *atoms*, or it can be from physical dislocations having moved the *atoms* in the crystal structure relative to one another and so distorting the *lattice* structure.

Depleted Mantle (DM)^s The upper portion of the *mantle* that is strongly depleted in (has lost) *incompatible elements*, *chemical elements* that are excluded from the normal *crystalline lattice* structures of *upper mantle minerals*, having ionic radii that are too large to fit into the *lattice* structures (or high ionic charges that are incompatible), relative to what is conjectured to be the *mantle's primordial* (original) composition. These *incompatible elements* have been removed and lost from the *mantle* as a result of preferentially entering into melted *rocks* and then being carried up into the *crust* in *magmas*, thus leaving behind a large region of the *mantle*, perhaps a third or a half of its total volume, bereft (depleted) in these *elements*, which have with time become concentrated in the earth's *crust*.

depleted mantle model evolution curve^s The line on an *isotope* diagram which mathematically describes the supposed development with time of the isotopic compositions of *rocks*, based on those *rocks* being derived from a *depleted mantle*, that portion of the *upper mantle* which has been strongly depleted in the *incompatible elements*. The *rocks* normally under investigation would be basaltic and related *rocks* which have been derived from *magmas* that originated from melting in the *upper mantle* where this depletion has occurred with time.

depleted MORB mantle (DMM)^b A part of the earth's *mantle* which has been extruded at the *mid-ocean ridge* in which the concentrations of *incompatible elements* have been decreased, usually by partial melting.

depletion event^s A specific confined time period during which the process of loss of *elements* and *isotopes* from *rocks* and *minerals* occurred.

detritus^s A collective term for loose *rock* and *mineral* material that is worn off or removed by mechanical processes, as by disintegration or abrasion; especially fragmental material, such as sand, silt and *clay*, derived from older *rocks* and moved from its place of origin.

deuteron^c A *neutron* and *proton* bound together as a *nucleus*.

devitrified^s The description of volcanic glass in a *rock* when it is converted to *crystalline* material.

Devonian^s A *geological* period of the Paleozoic era conventionally thought

to have covered the span of time in the *geological* timescale between 417 and 354 million years ago. The term also is used to describe the *rock* strata in the *geological* record which were formed or deposited during this corresponding *geological* period. The name is derived from Devonshire in England where rocks of this *geological* period were first studied.

diabase^a *Igneous rock of basaltic composition* but coarser texture, formed underground when molten *rock* was injected into *dikes* or *sills*.

diagenesis^s All the *chemical*, physical and biologic changes undergone by a *sediment* after its initial deposition, and during and after its *lithification* (hardening), exclusive of surficial alteration (*weathering*) and *metamorphism*. It embraces processes such as compaction, *cementation*, reworking, *crystallization*, etc. that occur under conditions of pressure up to 1 kb and temperatures in the range 100° to 300°C that are normal to the surface or outer part of the earth's *crust*.

diametrical section^s That section which can be cut through a sphere or ball which passes through the very center of the sphere or ball. In two dimensions the section through the sphere is circular in shape and has a dimension measured through the center of that circle of the diameter of the original sphere or ball.

diamonds^s A naturally occurring *crystalline mineral* form of carbon which is the hardest natural substance known. They often occur in octahedrons with rounded edges or curved faces, being formed under extreme temperatures and pressures in the *upper mantle*. Pure *diamonds* are colorless or nearly so, colors being imparted by impurities.

dielectric constant^c A constant specifying the amount of polarization a material develops when an electric field is applied.

diffusion^h The spreading of one thing through another, from regions of higher to lower concentration, for example, the random spreading of *atoms* through the *crystal lattice* of a *mineral*, or the spreading of heat by conduction through solid materials.

diffusion radii^s The areas of influence from a central point or area from which gases or fluids have diffused or spread out. They are a measure of the distance that the gases or fluids have spread out from the central source point or area.

diffusion rates^s The speeds at which *diffusion* occurs, that is, the processes

of mass transfer in which *chemical* components move through a stationary material, such as the *crystal lattice* of a *mineral*. This process and the speed at which it occurs is influenced by the temperature and pressure conditions, by whether fluids are present in which the *chemical* components, *elements* or *isotopes* may be dissolved, and by the “packing” of *atoms* in *crystal lattices*.

dike^a A narrow *rock* body which has been formed from magma injected across or through stratification.

dimensionless ratios^c Dimensions are abstract quantities such as mass, length, time, charge, etc. without reference to specific units such as kilograms, meters, etc. A dimensionless ratio is a ratio in which all the dimensions divide out.

diopside^v A common *clinopyroxene mineral* having moderate amounts of calcium (Ca). As an iron-magnesium-calcium (Fe-Mg-Ca) *silicate mineral* it is similar to augite.

diorite^s A coarse-grained intrusive *igneous rock* with a *quartz* content between 0 and 5%, and the *plagioclase* to total *feldspar* (alkali *feldspar* or *orthoclase* plus *plagioclase*) >90%, the *plagioclase* being more sodic in composition than a 50% mixture of the sodic *plagioclase* and calcic *plagioclase* end members of the mixing series. This *rock* is intermediate in composition between felsic *granites* and mafic *gabbros*, characteristically composed of dark-colored amphibole (especially *hornblende*), sodic *plagioclase*, *pyroxene*, and a small amount of *quartz*. It is the approximate *intrusive* equivalent of andesite.

disconformable ore deposits^s An accumulation of *minerals* of economic value forming an ore body or *mineral* deposit whose contact with its host *rocks* is not essentially parallel to either its own internal structure or the structures of the host *rocks*.

discordance^d A substantial variation in ages measured for a *rock* sample using different methods.

discordant^v Said of isotopic ages, determined by more than one method for the same sample or coexisting *minerals*, that are in disagreement beyond experimental error.

discordant dates^a Two or more age estimates by *radioisotope* methods for a *rock* or *mineral* which do not agree within the limits of the error of the

radioisotope methods. *Discordant dates* can be divided into *discordant model ages* and *discordant isochron ages*. Four different categories of *discordant dates* allow critical evaluation of the assumptions of *radioisotope* dating.

dolomite^v A *sedimentary rock* composed of calcium-magnesium (Ca-Mg) carbonate.

drillcores^s Cylindrical sections of *rocks*, usually 5–10 cm in diameter and up to several meters in length, taken as samples as the subsurface *rocks* are penetrated by a drill bit on the end of a drill pipe, and brought to the surface inside the hollow drill pipe for geologic examination and/or laboratory analyses.

DSDP^s An acronym which stands for **Deep Sea Drilling Project**, an international project in which floating drill rigs have been used to drill holes into the ocean floor.

dual halo^s A *radiohalo* composed of two *halos* superimposed upon one another, one being circular in thin section and the other being elliptical, but both derived from the same parent radionuclide present in the central radiocenter. Those that have been described are ²¹⁰Po *halos*, the circular being the normal and the elliptical being an earlier-formed normal *halo* which has been subsequently squashed due to compression of the host material.

DUPAL signature^s This refers to a particular distinctive isotopic composition found in *oceanic island* and *mid-ocean ridge basalts* in the south Atlantic Ocean, the mid Indian Ocean and in the south-west Pacific Ocean basins. The descriptor DUPAL is derived from the names of the authors who first identified this characteristic isotopic composition in these *rocks*—DUPre and ALlegre. The characteristic isotopic composition represented by this term is a subset of the *enriched mantle geochemical* reservoir, and is highlighted by these particular geographical locations representing plumes of *rock* in the *mantle* which are the source areas for the *magmas* that produced these *volcanic rocks*.

earth accretion^s The process whereby small particles, dust and gases in the *solar nebula* came together to form the earth; an evolutionary view of the earth's origin, but the same term could be used to describe the initial formation of the earth instantly at *Creation*.

eclogite^s A granular *rock* composed essentially of *garnet* and sodium-rich *pyroxene*, with rutile (TiO_2), kyanite (Al_2SiO_5) and *quartz* (SiO_2) being typically present also.

edge dislocations^s A term used to describe those *atoms* marking the edges of crystal planes within a crystal, but only extending part way along the edge. These are a type of line defect, that is, a crystal defect occurring along certain lines in a crystal structure.

elastic wave^v A seismic wave including both compressional (P-wave) and shear (S-waves) components.

electromagnetic interactions^c Events involving charged particles and quanta called *photons*.

electron^h The smallest-mass stable particle in an *atom*. It has a negative electric charge and orbits around the *nucleus* in the outer part of the *atom*. The *electrons* control *chemical* reactions with other *atoms*.

electron charge^h (or elementary charge) The electrical charge, e , of a single *electron*, 1.6×10^{-19} of a Coulomb. See *fundamental charge*.

electron microprobe^s A sophisticated analytical instrument that uses a finely focused beam of *electrons* onto a spot on the surface of a *mineral* to cause x-rays to be emitted. These x-rays are characteristic of the composition of the sample at that spot. The x-rays are measured by detectors in the instrument and compared to the compositions of previously analyzed minerals, enabling the composition of the *mineral* being analyzed in the instrument to be determined. Spots on *mineral* surfaces as small as 1 *micron* (1 millionth of a meter) in diameter can be analyzed, with sensitivities around 50 parts per million (0.005%) or less for most *elements*. In this way, for example, zones of different compositions within a *mineral grain* can be analyzed.

electron microscope^s An *electron*-optical instrument in which a beam of *electrons*, focused by systems of electrical or magnetic lenses, is used to produce enlarged images of minute objects such as *mineral grains* on a fluorescent screen or photographic plate in a manner similar to that in which a beam of light is used in a normal light microscope. However, because of the very short wavelength of the *electrons*, the *electron microscope* is capable of resolving much finer structures than the optical instrument, and is capable of magnifications on the order of 100,000 times.

electrostatic repulsion^h The repulsive electric force between two particles

of the same electrical charge, such as the positive charge of an *alpha-particle* (α -particle) and its parent *nucleus*.

electroweak^c Having to do with combined *electromagnetic interactions* and *weak interactions*, in which the *photon* mediates the electromagnetic force and the *W* and *Z bosons* mediate the weak force.

elements^s The “building blocks” of all substances, composed of identical *atoms*.

elliptical halo^s This is a *radiohalo* which would have been a normal *circular halo* in thin section except that it has been squashed due to subsequent compression of the material hosting it. In three dimensions the *halo* would normally have been spherical, but with the squashing of the *halo* it is now elliptical in cross-section.

EM I^s Abbreviation for *Enriched Mantle* type I, which is the label for a *mantle geochemical reservoir*, a volume of *rock* that is the source of *magmas* which produce *lavas* and *volcanic rocks* with this distinctive *geochemical* and isotopic composition. This *enriched mantle* has variable $^{87}\text{Sr}/^{86}\text{Sr}$, low $^{143}\text{Nd}/^{144}\text{Nd}$ and high $^{207}\text{Pb}/^{204}\text{Pb}$ and $^{208}\text{Pb}/^{204}\text{Pb}$ at a given value of $^{206}\text{Pb}/^{204}\text{Pb}$. Type I *enriched mantle* has lower $^{87}\text{Sr}/^{86}\text{Sr}$ and the enrichment is regarded as being due to *subduction*, whereby crustal material has been injected into the mantle. In the case of *enriched mantle* type I, it has affinities with the lower *crust* and therefore may represent recycled lower crustal material, although an alternative hypothesis suggests that it is enriched by *mantle* metasomatism.

EM II^s An abbreviation for *Enriched Mantle* type II, being a *mantle geochemical reservoir*, a volume of *rock* in the *mantle* that is the source of *magmas* producing *lavas* and *rocks* with distinctive *geochemical* and isotopic compositions. *Enriched mantle* type II has a high $^{87}\text{Sr}/^{86}\text{Sr}$ distinguishing it from *enriched mantle type I*, but a low $^{143}\text{Nd}/^{144}\text{Nd}$ and high $^{207}\text{Pb}/^{204}\text{Pb}$ and $^{208}\text{Pb}/^{204}\text{Pb}$ at a given value of $^{206}\text{Pb}/^{207}\text{Pb}$ in common with *enriched mantle type I*. It is believed that the enrichment is related to *subduction*, whereby crustal material is injected into the *mantle*, but *enriched mantle type II* has affinities with the upper *continental crust*, and so may represent the recycling of continentally derived *sediment*, *continental crust*, altered *oceanic crust* or ocean-island *crust*.

emanation halos^s An early name for particular *radiohalos* or *pleochroic*

halos, so named because of the radiation emanating from the central tiny *mineral grains* producing the discoloration and spherical rings. They are now known as ^{210}Po *halos*.

energy density^c Energy per unit volume.

enriched mantle (EM)^s See *EM I* and *EM II*.

entrainment^s The process of picking up and carrying along, as with the collecting and movement of *sediments* by currents, or the incorporation of whatever is being picked up and carried along by the flow, such as *magmas* picking up *xenoliths*.

episodic lead loss model^s Mathematical and/or graphical description of the loss of lead (Pb) *isotopes* from a *mineral* or *rock* in an episodic manner, that is, loss concentrated into distinct episodes which from subsequent calculations and graphical representations can be assigned a specific time period or “age” when the host mineral lost the Pb isotopes.

epsilon parameter (ϵ)^s A mathematical notation assigned by comparing the neodymium (Nd) isotopic composition presently measured in a *rock* sample with the Nd isotopic composition of the *chondrite uniform reservoir (CHUR)* at the time the *rock* sample was presumed to have formed. This parameter allows the comparison of the initial Nd isotopic ratios of *igneous* and *metamorphic rocks* in the earth’s *crust* with the corresponding Nd isotopic ratios of *CHUR* at the time of *crystallization* of the *rocks* and magnifies the differences which are normally quite small.

errorchron^s An *isochron* (a straight line along which all points are consistent with the *rock* hosting the *radioisotopes* having formed at the same time) about which data (radioisotopic ratios measured in the *rock* under study) are scattered, not only because of analytical error, but also because of departures of the *rock* being investigated from the ideal (according to the underlying assumptions).

eruption^s The ejection of volcanic materials, particularly *lavas*, volcanic dust and volcanic gases onto the earth’s surface either from a central volcanic vent or from a gash in the ground called a fissure, or group of such fissures.

ether^h (also **aether**) In nineteenth-century physics, an imperceptible material which fills all *space*. It interacts with visible matter in subtle ways, but is otherwise invisible and undetectable by ordinary means. It was seen as the medium through which light waves and electromagnetic fields propagate.

Early twentieth-century physicists tried to do away with the *ether*, but the concept soon reappeared in more sophisticated forms under other names, such as “the *vacuum*,” “the *space-time continuum*,” etc. See *vacuum*, *fabric of space*, *space*, and *heavens*.

eucrite^v A *meteorite* with composition similar to terrestrial basalts. *Eucrites* are composed of calcium *plagioclase* and the *orthopyroxene* pigeonite.

euxenite^s A brownish-black *mineral* which is a complex oxide with the *chemical formula*: (Y, Ca, Ce, U, Th) (Nb, Ta, Ti)₂O₆. It also occurs in *granite pegmatites*, and because it contains uranium (U) and thorium (Th) it can also be used for uranium-thorium-lead (U-Th-Pb) radioisotopic dating of the *rocks* which contain it.

evolution^v An alternative hypothetical process to *Creation* by which life is believed to have spontaneously developed from the basic materials of the universe over millions of years by naturalistic (non-supernatural) means.

excess argon^s Argon-40 (⁴⁰Ar) that is incorporated into *rocks* and *minerals* by processes other than in situ *radioactive decay* of ⁴⁰K.

expans^h A Biblical word (Hebrew *raqia*) which, according to Humphreys, may include the modern concepts of the atmosphere and interstellar *space*.

exponential decay^v The functional change in *radioactive decay* whereby the number of nuclei decaying per unit time is high initially and decreases rapidly with time according to an exponential power function.

extra dimensions^c Hypothetical continua of values which are independent of the three *space* and one time dimensions ordinarily associated with reality and which for one reason or another are not noticeable in ordinary life, but which may have consequences in the ultra small realm of particle physics or in different moments or places in spacetime .

fabric of space^h A term used by popular science writers to graphically convey the idea of the *vacuum* in quantum *field theory*. See *vacuum*, *ether*, *space*, and *heavens*.

facies^s Metamorphic *rocks* of any original composition or mode of origin that have formed within certain pressure-temperature conditions of *metamorphism*. Thus it is a commonly-used term to describe particular metamorphic conditions, and is usually preceded with a descriptor such as *amphibolite* or *granulite*, which denotes the major type of *metamorphic rock* formed under those temperature and pressure conditions.

false vacuum^c The *vacuum* state associated with a zero value of the *Higgs field*. In inflationary cosmology the universe starts out in this *vacuum* state.

feldspar^s A group of abundant *rock-forming minerals* of the general *chemical* formula: $MAI(Al, Si)_3O_8$, where $M = K, Na, Ca, Ba, Rb, Sr,$ and Fe . Feldspars are the most widespread of any *mineral* group and constitute 60% of the earth's *crust*, occurring as components of all kinds of *crystalline rocks*. Feldspars are usually white or nearly white, and clear or translucent (they have no color of their own but are frequently colored by impurities). On decomposition, feldspars yield a large part of the *clay* in *soils*. The major varieties of feldspar include alkali feldspar or *orthoclase*, and *plagioclase* (a mixture of *albite* and *anorthite*).

felsic porphyry^s An *igneous rock* that contains conspicuous *phenocrysts* (large crystals) in a fine-grained groundmass, being dominated by the minerals *quartz* and *feldspars*, and to a lesser extent the white *mica*, *muscovite*. The descriptor is derived from *feldspar* + *silica* + *c*, which is descriptive of *quartz* and *feldspars*. Such a *rock* thus has these light-colored minerals in abundance. It is an *intrusive igneous rock* usually found in small *intrusive* bodies.

Fermi constant^h The *coupling constant* of the *weak nuclear force*.

Fermi^h One femtometer, or 1×10^{-15} of a meter. Used as the unit of distance around nuclei, named after the nuclear physicist Enrico Fermi.

fiat creation^s *Creation* by divine decree, as described in the Scriptures (Genesis 1), where God spoke and instantly plants, animals, etc. came into existence where no plants, animals, etc. were before, having been created either out of nothing, or formed from materials created earlier during Creation week. The term signifies God actively creating.

field theory^h A theory attributing the force on a particle to qualities of the *space* immediately in the vicinity of the particle. An example is classical electrodynamics, summed up in Maxwell's equations. A quantum field theory extends this concept to microscopic sizes, where quantum mechanical effects become important. The most successful quantum field theory is quantum electrodynamics. More recent ones are the Weinberg-Salaam *electroweak* theory, *quantum chromodynamics*, and *string theory*.

filar micrometer^s Finely-scaled markings within the optics of a microscope graduated into lengths of one *micron* between the thin linear markings, like

having a ruler under the microscope marked off in *microns*. This allows the dimensions of *grains*, crystals and other features to be accurately measured under the microscope. This measuring device is therefore used to measure the dimensions of *radiohalos*, such as the radii of the different rings.

fine-structure constant^c The ratio of the square of the *electron charge* divided by the product of the *speed of light* and *Planck's constant* h , having a value near $1/137$, and defining the fine structure of the hydrogen spectrum.

fissiogenic elements^c *Elements* derived from *fission*.

fission^c The breakup of a heavy *nucleus* into fragment nuclei, usually two, usually with the emission of *neutrons*. In a fission of uranium (U) the fragments have a total *kinetic energy* near 170 MeV , and the number of *neutrons* averages between two and three. There are more than thirty *elements* which have a large probability of being formed in fission.

fission track^c A narrow zone of damage in a solid caused by *fission* fragments moving rapidly away from the point where *fission* occurred. In the laboratory, etching with an acid then enlarges the track for observation.

fission track dating^c A method of age determination in which zones of damage caused by *fission* events are enlarged by etching with acid and the age determined by comparing the number of tracks to the concentration of uranium (U).

fluid inclusions^s In a *mineral*, these are tiny cavities, 1–100 *microns* (millionths of a meter) in diameter, containing liquid and/or gas, formed by the entrapment in crystal irregularities of fluids, commonly that from which the *rock* crystallized.

fluorite^s A transparent to translucent *mineral* with the *chemical* formula of CaF_2 . It is found in many different colors, but most often as blue or purple, and is commonly found in *crystalline* cubes with perfect octahedral *cleavage*.

focus zone^v A source for mantle-derived *magmas* (abbreviated as FOZO from focus zone), produced by mixing of the *EM*, *DM* and *HIMU* end-member *mantle reservoir* sources.

fossil fission tracks^s These are *fission tracks*, the paths of *radiation damage* made by nuclear particles in *minerals* by the *spontaneous fission* of ^{238}U impurities in the *minerals*, already etched into *minerals* and thus in a sense fossilized, without the need for laboratory etching before microscopic examination.

- fossiliferous Flood strata**^s *Rock layers containing fossils which were deposited during the Genesis Flood.*
- fractionation**^b Change in bulk *chemical* composition due to physical separation of crystals from *magma* or physical separation of liquid from a *rock* undergoing partial melting.
- fractions**^s A small piece or amount of original *rock*, or sample of *rock*. *Fractions* can also be the portions divided from an original *rock* sample so that each contain only one *mineral* constituent of the *rock*.
- free particle**^h A particle moving freely, unaffected by forces.
- friability**^v The condition of a *rock* or *mineral* that crumbles naturally or is easily broken, pulverized, or reduced to powder, such as a soft or poorly cemented sandstone.
- fumarole**^s A vent, usually volcanic, from which gases and vapors are emitted. Such is characteristic of a late stage of volcanic activity, that is, after volcanic *eruptions* when a volcano is said to be dying or becoming dormant. Fumaroles may also occur along a fissure or in apparently chaotic clusters or fields, but always associated with nearby volcanoes.
- fundamental charge**^c The smallest unit of charge. See *elementary charge*.
- G halo**^s The designation given to a *halo* found in *biotite* in a *pegmatite* in Norway which could not be matched with any other *halo* whose identity was known at the time of that investigation. In all probability it may be a ²¹⁰Po *radiohalo*.
- Ga**^s The abbreviation for the Latin words, *giga* (billion), *annum* (years), and so this abbreviation is short for “billion years.”
- gabbro**^s A group of dark-colored *intrusive igneous rocks*, which are coarse-grained and composed principally of *plagioclase* and *clinopyroxene*, with or without *olivine* and *orthopyroxene*, but often with magnetite (an iron (Fe) oxide *mineral*) as an accessory. It is the approximate *intrusive* equivalent of a basalt.
- galena**^s A bluish-gray to lead-gray *mineral* which is essentially lead (Pb) sulfide with a chemical formula of PbS. It frequently contains microscopic *inclusions* of silver *minerals* and occurs in cubic blocks, crystals and masses. It has a shiny metallic luster, exhibits highly perfect cubic *cleavage*, and is relatively soft and very heavy. It is the most important ore of lead (Pb) and one of the most important sources of silver (Ag). Being a Pb *mineral* it

often contains Pb *isotopes* derived from *radioactive decay* of uranium (U) and thorium (Th), and therefore it is an important *mineral* in Pb-Pb isotopic and dating studies. For example, the Pb *isotopes* in *galena* may help to determine the source of the Pb in the ore deposit containing the *galena*, and therefore the mode of origin and formation of that ore deposit.

gamma ray^v A *photon* from an atomic *nucleus*.

gap theory^v The teaching made popular by the Scofield Reference Bible that a hiatus occurred between Genesis 1:1 and Genesis 1:2 in which long periods of time transpired.

garnet^s A group of *minerals* with the *chemical* formula: $A_3B_2(SiO_4)_3$, where A = Ca, Mg, Fe^{2+} and Mn^{2+} , and B = Al, Fe^{3+} , Mn^{3+} , V^{3+} and Cr. The different *minerals* of the group are named according to the different compositions derived from this general formula. It is a brittle and transparent to sub-transparent *mineral* with a variety of colors, dark red being the most common. It occurs as an accessory *mineral* in a wide range of *igneous rocks*, but is most commonly found as distinctive crystals in some *metamorphic rocks*.

gauge boson^h *Bosons* involved in transmitting forces, such as the *photon*, π (*pi*) *meson*, and W *boson*.

gauge coupling^c A constant in a *gauge field theory* which specifies the strength of a form appearing in the fundamental equations of the theory. See *coupling constant*.

gedanken experiment^h Thought experiment, a phrase derived from Einstein's German name for his procedure of reducing complex questions to imaginary experiments simple enough to analyze unambiguously.

general theory of relativity^c A theory of gravity which originated with Albert Einstein in which gravitational mass and inertial mass are equivalent and mass and energy cause a curvature of *space*.

Genesis Flood^v The global catastrophic flood event described in the Bible which catastrophically killed all terrestrial life on earth and is believed to have dramatically changed the *crust*. A large part of the sedimentary "geologic column" is believed to be a result of the Flood rather than millions of years of slow-and-gradual *geological* processes.

geochemical^v Having to do with the chemistry of the earth.

geochemical reservoirs^s Subsurface volumes of *rock* with particular

uniform *chemical* characteristics. This will include characteristic proportions of *radioactive isotopes* and their *daughter isotopes*.

geochemistry^s The study of the distribution and amounts of the *chemical elements* in *minerals*, *ores*, *rocks*, *soils*, water, and the atmosphere, and the study of the circulation of the *elements* in nature on the basis of the properties of their *atoms* and ions, including the study of the distribution and abundance of *isotopes*.

geochron^s The *isochron* on a lead-lead (Pb-Pb) *isotope* diagram believed to correspond to the age of the earth because a suite of three *stony meteorites* and two *iron meteorites* plot on it. It also represents all leads having time $t = 0$, because all modern leads in the earth lie on it, such as those in terrestrial *sediments* on the ocean floor. The Pb-Pb isotopic composition at the starting point of this *isochron* was derived from the *troilite* in the Canyon Diablo *iron meteorite*, and is said to represent the *primordial* Pb isotopic composition of the solar system, that is, at time zero.

geochronology^a The study of the time relationships between different *rocks* as evidence from the earth's history. "Absolute age" determinations use *radioisotopes*, whereas "relative age" determinations use *stratigraphic* or crosscutting relationships.

geochronometer^s A physical feature, material, or *element* whose formation, alteration, or destruction can be calibrated or related to a known interval of time.

geodynamic models^s Working hypotheses to describe the physical processes at work inside the earth as they affect the features of the earth's *crust*. In the present context, they are derived from isotopic analyses of the earth's *crustal rocks* and seek to visualize the interaction of the source areas inside the earth's *crust* and *mantle* from which the *magmas* that produced those *crustal rocks* came.

geodynamics^s That branch of science which deals with the forces and processes of the interior of the earth.

geological^v Having to do with the *rock* units of the earth.

geophysical^v Having to do with the physics of the earth.

ghost rings^s Visible outlines of what look to be *radiohalo* rings. The normal dark rings have in fact been obliterated by total "bleaching" of the host crystal, and different diffuse dark rings are left where there should be normal

light areas. It is these diffuse, abnormal dark rings which are called “ghost rings”.

giant halos^s These are *radiohalos* which are very much larger than the standard *radiohalos* that can be shown to have been produced by *radioactive decay* of uranium (U) and/or thorium (Th) in the central mineral *inclusions*.

glassy mesostasis/groundmass^s The last-formed interstitial material between the *phenocrysts* of an *igneous rock* that then forms a mass, often glassy, in which the *phenocrysts* sit.

gluons^h In *quantum chromodynamics*, the *gauge bosons* which mediate forces between *quarks*.

gneiss^s A *rock* formed by *metamorphism* on a regional scale, in which bands of granular *minerals* alternate with bands in which *minerals* having flaky or elongate habits predominate. Generally less than 50% of the *minerals* show preferred parallel orientation. Although a *gneiss* is commonly *feldspar* and *quartz*-rich, the *mineral* composition is not an essential factor in its definition. Varieties are distinguished by their textures, characteristic *minerals* or general compositions.

grain^v A *mineral* or *rock* particle having a diameter of less than a few millimeters and generally lacking well-developed crystal faces.

grain boundary^s In a *rock*, this is the boundary between two crystals or the edges of the *grains* making up the *rock*.

granite^s A common *intrusive*, coarse-grained *igneous rock* in which *quartz* makes up between 10 and 50% of the *rock*, and which also contains alkali *feldspar* or *orthoclase*, predominating over *plagioclase* in a ratio of *orthoclase* to total *feldspar* (*orthoclase* plus *plagioclase*) that is generally restricted to the range of 65–90%. Broadly applied, the term refers to any *quartz*-bearing, coarse-grained *intrusive igneous rock*.

granitic rocks^s A general term to describe *rocks* pertaining to, or composed of, *granite* and its close relatives. A *granite* in the strictest sense of the term is a coarse-grained *intrusive igneous rock* with a *quartz* content of between 10 and 50% of the *rock*, and which also contains alkali *feldspar* or *orthoclase*, predominating over *plagioclase* in a ratio of *orthoclase* to total *feldspar* (*orthoclase* plus *plagioclase*) that is generally restricted to the range 65–90%. More broadly applied, the term refers to any coarse-grained, *quartz*-bearing *intrusive igneous rock*, and therefore includes *rocks* designated as

adamellite, *quartz monzonite*, tonalite and *granodiorite*.

granitoid plutons^s Bodies of coarse-grained igneous *intrusive rock* containing between 10 and 60% *quartz*. Synonymous with *granitic plutons*.

granoblastic^v A type of texture in a nonschistose *metamorphic rock* upon which *recrystallization* formed essentially equidimensional crystals with normally well *sutured* boundaries.

granodiorite^s A coarse-grained *intrusive igneous rock* with a *quartz* content between 20 and 60% and with a *plagioclase* content relative to the total *feldspar* (alkali *feldspar* or *orthoclase* plus *plagioclase*) content between 65 and 90%. As well as containing *quartz*, *plagioclase* and alkali (potassium) *feldspar*, the *rock* has minor amounts of *biotite*, *hornblende* or more rarely, *pyroxene*. Because this *rock* has affinities to a true *granite*, it is often referred to as one of the *granitic rocks*.

granulite^s A *metamorphic rock* consisting of even-sized, interlocking *mineral grains*, with less than 10% having any obvious preferred orientation. It is a relatively coarse, granular *rock* formed at the high pressures and temperatures of *high-grade metamorphism*.

granulite facies^s The set of metamorphic *mineral* groupings resulting from high temperatures and pressures of *metamorphism* on a regional basis deep within the earth's *crust*, the temperatures usually being in excess of 650°C. These characteristic *mineral* groupings are produced by these particular metamorphic conditions according to the compositions of the original *rocks* that have undergone the *metamorphism* at these high temperatures and pressures. The *metamorphic* rocks produced with these *mineral* groupings are *granulites*.

granulite-facies metamorphism^s Mineralogical, *chemical* and structural adjustment of *rocks* due to pressure and temperature conditions of deep-seated regional processes, the temperatures being in excess of 650°C, to produce sets of metamorphic *mineral* groupings according to the *chemical* and mineralogical compositions of the original *rocks*. The *rocks* produced by these high temperature and pressure metamorphic conditions consist of even-sized, interlocking *grains* less than 10% of which have any obvious preferred orientation.

gravitational coupling^s The constant specifying the amount of gravitational field developed when a specified amount of mass is

present. See *coupling constant*.

ground water^s All subsurface water, including underground streams, usually at the prevailing background temperatures in the *rocks* where the water resides or flows.

half-life^c The time required for half of the *atoms* of a radioactive sample to *decay*.

halide salt^s A *mineral compound* characterized by a halogen such as fluorine (F), chlorine (Cl), iodine (I), or bromine (Br) as the anion, that is, in combination with a metallic *element*, such as sodium chloride or common salt. The term derives from the name for naturally-occurring sodium chloride—halite.

halo photometer^s A photometer is an instrument for measuring the intensity of light. When such an instrument is attached to an *optical microscope*, it can measure the intensity of light passing through a *mineral* in thin section and can thus be applied to measuring the intensity of light passing through *radiohalos*, not only the darkened and discolored areas, but also the *radiohalo* rings.

halogen species^s Kind, sort or group of *chemicals* consisting of the halogens, which are the group VIIB *elements* on the periodic table, that is, fluorine (F), chlorine (Cl), bromine (Br) and iodine (I), the first two being gases at ambient temperatures, while bromine is a liquid and iodine a solid.

halos^s Used synonymously, and as an abbreviation, for *radiohalos*.

Hamiltonian^c A function defined in mechanics or in *field theory* which can be used to work out the dynamics or progress of a system.

heavens^h English translation of a Biblical word (Hebrew *shamayim*) which, according to Humphreys, may include the quantum field theoretical concept of the *vacuum*, and the nineteenth-century concept of the *ether*. See *vacuum*, *fabric of space*, *space*, and *ether*.

heavy liquid separation^a A laboratory technique using the density of a very heavy liquid to isolate the different *mineral phases* of a *rock*. *Minerals* have different densities which allow isolation in different heavy liquids.

Hebridean mantle^s This is a specific reference to the composition of the *upper mantle* below the Inner and Outer Hebrides, islands off the north-west coast of Scotland. This term specifically applies to the *trace elements* and isotopic ratios in the *lavas* on these islands, which reflect the chemistry

of the *mantle* source area from which the *lavas* came.

helium^h A gaseous *chemical element*, symbol He, *atomic number* 2 and *atomic weight* 4.0026; one of the *noble gases* in group 0 of the periodic table.

helium atom^h An *atom* having two *electrons* orbiting a *nucleus* consisting of two *protons* and two *neutrons*.

helium diffusion^v The random movement of *helium* (He) *atoms* from a region of high concentration to a region of lower concentration through a porous medium like *biotite* crystals within *granite*.

helium nucleus^h A cluster of two *protons* and two *neutrons* tightly bound to each other.

Higgs bosons^c Quanta of the *Higgs fields*, which may be detected in future particle accelerators.

Higgs fields^c Quantized functions of position and time proposed by Peter W. Higgs which generate particle masses and solve other theoretical problems. In general, the fields allow for the possibility of the presence of one or more particles at each position in *space*.

Higgs mechanism^c A process of changing the vacuum properties due to a change of the *Higgs field*, and leading to the production of the masses of some particles.

high-grade metamorphism^s The mineralogical, *chemical* and structural adjustment of solid *rocks* to high pressure and temperature physical conditions and the *chemical* affects of combined *crustal fluids* at considerable depths within the *continental crust*. Thus, this is a description of *metamorphism* which has occurred at high temperatures and pressures.

HIMU^s Abbreviation for a mantle *geochemical reservoir* with **HIgh MU** (μ), referring to the ratio $^{238}\text{U}/^{204}\text{Pb}$. This *geochemical reservoir* is a physical volume of *rock* in the *mantle* that is believed to be the source of some *magmas* that then give the *lavas* and resultant *rocks* a distinctive *isotope* chemistry with very high $^{206}\text{Pb}/^{204}\text{Pb}$ and $^{208}\text{Pb}/^{204}\text{Pb}$ ratios, low $^{87}\text{Sr}/^{86}\text{Sr}$ and intermediate $^{143}\text{Nd}/^{144}\text{Nd}$. This suggests that this *mantle* source is enriched in uranium (U) and thorium (Th) relative to lead (Pb) without an associated increase in rubidium/strontium (Rb/Sr). One explanation for this *mantle reservoir* is the mixing into the *mantle* of altered *oceanic crust* (possibly contaminated with seawater).

Holmes-Houtermans model^s The mathematical description (named after its proponents, Holmes and Houtermans) for the postulated evolution of lead (Pb) *isotopes* from the formation of the earth up to the present day, from which the age of the earth and the age of common Pb *minerals* can supposedly be determined. The model assumes that *radiogenic* Pb is produced by *decay* of uranium (U) and thorium (Th) in the source regions, and that the resulting Pb (*primeval* + *radiogenic*) is then separated from its parents and incorporated into ore deposits as *galena*, the Pb isotopic composition of which does not change from then on because the *galena* contains no U or Th.

holocrystalline^v Said of the texture of an *igneous rock* composed entirely of crystals, that is, having no glassy part.

holocrystalline basalts^s The texture of basalts composed entirely of crystals, and containing no *basaltic glasses* as part of their make-up or texture.

horizon problem^c The problem in standard big-bang cosmology of explaining uniformities between different regions of the universe, such as that of the 2.7 K cosmic background radiation, using a finite *speed of light* and a fixed time of origin of the universe.

hornblende^s The commonest *mineral* of the amphibole group, which is usually black, dark green, or brown, occurring in distinctive crystals. While having a variable composition, its general *chemical* formula is $\text{Ca}_2\text{Na}(\text{Mg}, \text{Fe}^{2+})_4(\text{Al}, \text{Fe}^{3+}, \text{Ti})(\text{Al}, \text{Si})_8\text{O}_{22}(\text{OH}, \text{F})_2$.

hotspot^b A locus of volcanism that remains mostly stationary relative to the moving lithospheric *plates*. Such a feature can form a long chain of volcanoes (such as the Hawaiian-Emperor chain) that become progressively older as one moves farther away from the site of active volcanism. Because these features appear to be mostly stationary relative to the motion of the surface *plates*, they are believed to be expressions of *mantle plumes* of hot *rock* originating somewhere in the more viscous *lower mantle*, probably near the *core-mantle* boundary in most cases.

hybrid crust^s *Rocks* whose *chemical* composition is the result of contamination and mixing. The name normally applies to *igneous rocks* that have resulted from where blocks of *rocks* adjacent to the *magma chamber* have been engulfed in the *magma* and mixed into it to change the *chemical* composition of the resultant crystallized *rock*.

- hydrogeochemical halo**^s A circular or crescent-shaped distribution pattern of *elements* that have been dispersed by ground and surface waters dissolving those *elements* (or *isotopes*) from the *rocks*, ores or *minerals* at the center of the *halo*.
- hydrostatic pressure**^v Pressure that is uniform in all directions, for example, beneath a homogeneous fluid, and causes dilation rather than distortion in *isotropic* materials.
- hydrothermal fluids**^s Primarily liquids, but also containing gases as well as dissolved metals and other *element compounds*, derived from hot waters often of magmatic or volcanic origin.
- hydrothermal process**^a The action of *chemical* agents which distinctively alter previously existing *rocks* in combination with hot water.
- hydrothermal transport**^s Movement of *elements*, *isotopes* or *compounds* by the action of hot water carrying them in solution. Strictly speaking, the term has been used for water of magmatic origin, but it is now generally applied to hot water of any source.
- hydrothermal vent fluids**^s Hot waters, primarily of volcanic origin, that are being discharged through vents or openings in the ground often, but not exclusively, on the ocean floor. These hot waters or fluids contain dissolved metals and *compounds* that have been derived from *magmas* deeper below the earth's surface, or by being leached and dissolved from the *rocks* through which the fluids have passed before being expelled through the vents.
- hydrothermal water**^s Subsurface water whose temperature is high enough to make it *geologically* or hydrologically significant, whether or not it is hotter than the *rock* containing it. It may include magmatic and metamorphic water, water heated by *radioactive decay* or by energy release associated with faulting, rain water that descends slowly enough to acquire the temperature of the *rocks* in accordance with the normal geothermal gradient but then rises more quickly so as to retain a distinctly above-normal temperature as it approaches the surface, and rain water that descends to and is heated by cooling *intrusive igneous rocks*.
- hydrothermally altered**^s *Rocks* or *minerals* that have been altered by the reaction of *hydrothermal water*, that is, hot water usually derived from a *magma* at depth flowing outwards and upwards through cracks and pores in crustal *rocks*, altering them by their reactions with the *rocks* and their

minerals, usually producing *minerals* with changed compositions and new *minerals* as a result.

hypabyssal drusy syenites^s A type of fine-grained *granitic rock* that has been intruded at a shallow depth in an irregular cavity or opening, the walls of which it has lined, its crystals being encrusted on the surfaces of the cavity or opening and infilling the space.

igneous rock^s *Rock* that has solidified from molten or partly molten material, that is, from a *magma* inside the earth or a *lava* that has flowed onto the earth's surface. Igneous rocks constitute one of the three main classes into which *rocks* are divided, and the term is derived from the Latin for fire, *ignis*.

ilmenite^s An iron-black, opaque, *mineral* with a *chemical* formula of FeTiO_3 . It occurs in characteristic crystal shapes, and is a common accessory *mineral* in *mafic igneous rocks*, that is, *igneous rocks* rich in iron (Fe) and magnesium (Mg), such as *gabbros*. An iron titanium oxide, it is the principal ore of titanium.

inclusions^s A tiny *grain* or crystal fragment within another larger *mineral grain* or crystal. This is usually within *igneous rocks*, and the tiny *grain* or fragment is usually crystallized from the *magma* before the enclosing larger *mineral grain* or crystal.

incompatible element^b A *chemical element* that is excluded from the normal *crystalline* lattice structure of *upper mantle minerals* and therefore preferentially enters an available melt phase. Common reasons for incompatibility are large ionic radius and high ionic charge. Such *elements* are also known as “*lithophile*,” or *rock-loving elements*. Examples include *radiogenic elements* such as K, Rb, U, and Th as well as Ti, Ba, Sr, and Nb.

indurated^v Said of a *rock* or *soil* hardened or consolidated by pressure, *cementation*, or heat.

inert gas^s Any of the six *elements* that have no tendency to react with any of the other *elements*: *helium* (He), neon (Ne), argon (Ar), krypton (Kr), xenon (Xe), and radon (Rn). They are all gases under usual conditions, and are sometimes called *noble gases*.

infiltration^s The flow of a fluid into a solid substance through pores or small openings; specifically, the movement of water into *soil* or porous

rock, but the same term can be applied to fluids moving into *mineral grains* and crystals.

infinite range^h The *range* of a force whose strength decreases with distance no more rapidly than the inverse-square law. Examples are gravitational and electromagnetic forces. See *range*.

inflationary big bang cosmology^c A model in which the universe begins as a tiny dense gas of particles, goes through a stage of very rapid expansion, called “inflation,” and then the expansion rate slows.

inheritance^s The process by which a geologic feature owes its character to conditions or events of a former period in time or condition of the *rocks*. In the context of radioisotopic dating, it is the process by which *isotopes*, gases or fluids from a former state of a *rock* or *mineral*, or in an area of the earth’s *crust* or *mantle*, are received from those *rocks*, *minerals* or areas and added to another *rock* or *mineral*. Thus, for example, argon (Ar) gas can be added to a *rock* or *mineral* from elsewhere in the earth’s *crust* or *mantle*, and this is the term used for that process.

inorganic^v Pertaining or relating to a *compound* that contains no carbon.

insulator^c A material which does not conduct electricity.

intermediate vector boson^h A *meson* mediating the *weak nuclear force*, either the *Z particle* or one of the two *W particles*.

intracrustal fractionation^s Separation of *chemical elements* and *isotopes* by natural processes within the *crust*, such as preferential concentration of an *element* in a *mineral* during *magmatic crystallization*, or differential solubility during fluid movement within the *crust*.

intrusion^s The process of emplacement of *magma* in pre-existing *rock*, and the term used for the *igneous rock* mass so formed within the surrounding *rocks*.

intrusive^s Of or pertaining to an *intrusion*, both the processes and the *igneous rocks* they formed. It is where molten *rock* is forced between and into pre-existing strata.

ion microprobe^a An instrument used to measure the *chemical* or isotopic composition on a very small spot on a *mineral*.

ion microprobe mass spectrometer^s This is the instrument used in *ion microprobe mass spectrometry* (IMMA).

Ion Microprobe MAAss spectrometry (IMMA)^s A sophisticated research

instrument in which a focused beam of ions is made to strike the surface of a sample, with the resultant emission of ions from the impact area. The emitted ions are characteristic of the *isotopes* of the *elements* present in the area of impact. These emitted ions are then analyzed by a mass spectrometer attached to the *ion microprobe*. A mass spectrometer is an instrument for producing and measuring, usually by electrical means, a mass spectrum, that is, for determining the spectrum of molecular weights and relative abundances of *isotopes* in the sample. Because *isotopes* have different weights they can be accelerated so that their paths diverge and the detectors can then measure the *isotopes* present and their relative abundances.

ionium^s An old but still-used name for ^{230}Th , a member of the uranium-238 (^{238}U) *decay* series and daughter of ^{234}U .

ionizing radiation^v Any electromagnetic or particulate radiation that displaces *electrons* within a medium.

ion-spike model^c The model of *fission track* formation in which the fragments from *fission*, traveling at high speed, cause the *electrons* to be stripped away along their path, and the positive ions thus formed repel outward into the material.

Irish halos^s Radiohalos found in *biotite* in *granites* in several parts of Ireland.

iron meteorite^v A *meteorite* composed dominantly of sulfide of iron (Fe) or nickel (Ni). *Troilite*, a *mineral* composed of iron sulfide (FeS) is dominant in *iron meteorites*.

irons^v *Meteorites* composed predominantly of iron-nickel metal.

island arc volcanics^s *Volcanic rocks* that can be of different composition, but which have all been extruded from volcanoes making up an island arc, which is a chain of islands rising from the ocean floor near continents, being produced as a result of a nearby *subduction* zone where the subducting *plate* is melting, producing *magmas* which rise to form the volcanoes and the volcanic islands with their volcanic *rocks*.

isochron^d A line of equal time on an *isotope* correlation diagram.

isochron age^a An estimate of the absolute age of a suite of several *rocks* or *minerals*. The method assumes that the initial abundances or ratios of stable daughter throughout the suite of several *rocks* or *minerals* was uniformly mixed or homogeneous. The method estimates the time it would take the suite of *rocks* or *minerals* to evolve from the uniformly mixed condition. A

linear array plot of daughter versus parent is believed to confirm the initially mixed condition. The slope of the linear array (*isochron*) is thought to indicate the absolute age assuming constancy of *decay* of radioactive parent. “*Whole-rock isochron ages*” come from a suite of *rocks* from a single *cogenetic* unit. “*Mineral isochron ages*” come from different *minerals* within a single *rock*.

isochronous^s Equal in duration or uniform in time. A term frequently applied in the sense of synchronous, having everywhere the same age or time value within a body of strata. It also refers to, for example, two or more *rock* units having formed at the same time.

isomers^s These are structurally different arrangements of *atoms* of the same *isotope* or *molecule* that have the same number and type of *atoms* but differ in the arrangement of those *atoms*.

isostasy^v The condition of equilibrium, comparable to floating, of the units of the *lithosphere* above the *asthenosphere*. Crustal loading, as by ice, water, *sediments*, or volcanic flows, leads to isostatic depression or downwarping; removal of load, to isostatic uplift or upwarping.

isotope pairs^s Any pair of *isotopes* related to one another by *radioactive decay* or which are compared to one another for the purpose of measuring the passage of time or *geochemical* processes. An *isotope* is one of two or more species of the same *chemical element*, that is, having the same number of *protons* in the *nucleus*, but differing from one another by having a different number of *neutrons*. In the case of an *isotope* pair related by *radioactive decay*, an example would be ⁴⁰K and ⁴⁰Ar.

isotopes^c Different forms of an *element* having different numbers of *neutrons*, leading to different *atomic weights*.

isotopic reservoirs^s These are volumes of *rock* in the *crust* and *mantle* of the earth which have particular distinctive isotopic characteristics that are identifiable and distinguishable from adjacent volumes of *rocks*. They have been recognized as a result of Nd, Sr and Pb isotopic analyses of *volcanic rocks*, but also *granitic rocks*, which represent the end result of melting in the *crust* and *mantle* to form *magmas* which are either intruded or extruded to produce these *rocks* accordingly. Since the *magmas* take on the isotopic characters of their source areas, which are then maintained during *intrusion* and extrusion, it is clear that the isotopic characteristics in the resultant *rocks*

reflect the volumes of *rock* in the *crust* and *mantle* from which the *magmas* came.

isotopic re-setting^s After some heating and/or fluid flow event disturbs the isotopic composition of a *mineral* or *rock*, the isotopic ratios in a *rock* or *mineral* settle into new values under stable conditions, having thus been “re-set”.

isotropic^s Said of a crystal or *mineral* whose properties are the same in all directions. That is, its physical properties do not vary according to variations in orientation so that light travels through it identically in any direction. Cubic crystals are typical examples.

I-type granites^s *Granites* which have been classified as being derived from predominantly igneous source materials on the basis of Sr *isotopes* and other *geochemical* criteria. An igneous source would be characterized by low initial $^{87}\text{Sr}/^{86}\text{Sr}$ ratios and a relatively high sodium (Na_2O) content.

Jurassic^s The second *geological* period of the *Mesozoic era*, after the *Triassic* and before the *Cretaceous*, conventionally thought to have covered the span of geologic time between 105 and 142 million years ago. The term also corresponds to the *rock* layers in the *geological* record which were deposited or formed during this *geological* period. The name is derived from the Jura Mountains between France and Switzerland, in which *rocks* of this period were first studied.

kimberlite^b A *rock* assemblage formed by an explosive *eruption* from within the *mantle*, in some cases from several hundred kilometer depths, through a narrow *conduit* and probably at near supersonic velocity to the earth’s surface. *Diamonds* are commonly found in such *rock* assemblages.

kimberlite magmas^s Those *magmas* responsible for producing a *rock* called *kimberlite*. *Mineral* assemblages in this *rock* indicate that these *magmas* formed at high pressures and temperatures within the *mantle*, in some cases up to several hundred kilometers below the earth’s surface. These *magmas* were explosively erupted through narrow *conduits* probably at near supersonic velocity to the earth’s surface, so that the abundant *phenocrysts* of *olivine* and *phlogopite* (a magnesium-rich *mica*), and sometimes *garnet*, in the resultant *rocks* tend to be fragmentary in nature and set in a fine-grained groundmass which also tends to be made up of fragments of a large number of *minerals*, all due to this explosive intrusion of the *rock*

material. These *magmas* also commonly carry *diamonds*, formed in the *mantle*, to the earth's surface where they are included in this resultant *kimberlite rock*.

kinetic energy^h The energy due solely to a particle's motion, not its *potential energy* or *rest mass energy*.

komatiites^s Specifically, this is the name for an *ultramafic lava* and the *rock* that cools from it, which has an unusual texture composed of needle-like crystals, called a spinifex texture, named after an Australian desert grass. These *rocks* have compositions which are low in titanium (Ti), but high in magnesium (Mg), nickel (Ni) and chromium (Cr). These *lavas* have a high *olivine* content and are believed to have crystallized from *magmas* which were erupted at higher than usual temperatures, up to 1800°C. More generally, the name is applied to a suite of *igneous rocks* ranging in composition from *peridotite* with a composition of approximately 30% MgO and 44% SiO₂, to basalt with a composition of 8% MgO and 52% SiO₂. To be given this name, such a suite of *igneous rocks* must contain some of these *ultramafic lavas* which have been given this specific name.

laminated^v Consisting of very thin compositional layers.

lamproite^s A group of dark-colored extrusive or shallow *intrusive igneous rocks* which are rich in potassium (K) and magnesium (Mg), and which can also be erupted explosively from great depths within the *mantle* through a narrow *conduit* and probably at near supersonic velocity to the earth's surface. *Diamonds* are sometimes found in this *rock* also, indicating its formation at high pressures and temperatures.

lamproite magmas^s Those *magmas* responsible for producing a group of dark-colored extrusive or shallow *intrusive igneous rocks* which are rich in potassium (K) and magnesium (Mg), and which can also be erupted explosively from great depths within the *mantle* through a narrow *conduit*, probably at near supersonic velocity, to the earth's surface. *Diamonds* are sometimes carried from the *mantle* by these *magmas* also, which are then hosted by the resultant *lamproites*, indicating that these *magmas* formed at high pressures and temperatures deep in the *mantle*.

lanthanides^s A sub-group of the *rare earth elements* in which lanthanum (La) is the chief member and the one whose properties are largely shared by other members of the group. These *elements* range from La (*atomic*

number 57) to lutetium (Lu) (71).

large hadron collider^c The high energy collider of *protons* and/or antiprotons being planned near Geneva on the French/Swiss border. The planned completion date is circa 2006.

large ion lithophile elements^s *Chemical elements* whose electrically charged *atoms* (ions) have large radii, making these *elements* difficult to fit into certain *mineral* structures. These *elements* are more readily concentrated in silicate *minerals* of the earth's *crust* and so are said to be *rock-loving* (*lithophile*). Examples include potassium (K), rubidium (Rb), barium (Ba), thorium (Th), uranium (U), strontium (Sr), titanium (Ti), and niobium (Nb).

laser “spot” argon-argon (Ar-Ar) “ages”^s *Radioisotopic “ages”* calculated from analyses of the argon (Ar) *isotopes* in a *mineral* by focusing a laser beam on a spot on the surface of a *mineral*. The Ar *isotopes* measured and used to calculate the “ages” are ⁴⁰Ar, derived from the *radioactive decay* of ⁴⁰K, and ³⁹Ar, present in normal Ar.

laths^s Crystals that are long and thin, and of moderate to narrow width.

lattice^v The three-dimensional regularly repeating set of points that represent the translational periodicity of a crystal structure.

lattice vacancies^s Vacant sites in a crystal structure due to the absence of an *atom* or ion from its normal structural position. These are in effect holes within the crystal structure, which is like a *lattice* of *atoms* connected to one another, a three-dimensional regularly repeating set of *atoms* giving the crystal its rigidity and structure.

lava^s The general term for a molten extrusive flowing mass which comes from a volcano, and which was originally called a *magma* at depth inside the volcano. The term is also used for the *rock* that is solidified from the molten material.

lava dome^s A dome-shaped mountain of solidified *lava* in the form of many individual flows, formed by the extrusion of highly fluid *lava*. A lava dome can also be a smaller dome-shaped mound made of *lava* flows within the crater of a volcano.

lead (Pb) paradox^s The unsolved, unexpected behavior in the distribution of Pb *isotopes* in *crustal rocks*, which by definition should on the Pb-Pb isotopic diagram lie to the left of the *geochron*, when the Pb isotopic compositions of *ocean island basalts* in fact lie to the right of the *geochron*,

implying that the *depleted mantle* which was the source of these *magmas* has an average composition more *radiogenic* than the *geochron*, or *bulk earth*. To explain this behavior there is supposed to be a complimentary *reservoir* with unradiogenic Pb to balance this *radiogenic depleted mantle*, but this other *reservoir* has not been located, thus leaving an unresolved mystery, that is, if this interpretation is correct, which is clearly based on assumptions regarding the age of the earth and the behavior of Pb *isotopes* with time.

leakage^s The process of losing gases or fluids from the structure of a *mineral grain* or crystal and then ultimately from a *rock*. This is usually a gradual process of steady loss of gases or fluids.

leptons^c A class of particles defined as fermions with spin $\frac{1}{2}$ which do not interact via *gluons*. The known leptons include the *electron*, the *muon*, the *tau*, and their associated *neutrinos*.

limestone^v A *sedimentary rock* composed of more than 50% calcium carbonate. Limestones are formed by either organic or *inorganic* processes. Many are highly fossiliferous and clearly represent the remains of ancient shell banks or coral reefs.

liquid drop model^h A theoretical model of the atomic *nucleus* which emphasizes its similarities to a drop of liquid, such as surface tension.

lithification^v The conversion of newly deposited, unconsolidated *sediment* into a coherent, solid *rock*, involving processes such as *cementation*, compaction, dessication, and *crystallization*.

lithologies^s The descriptions of *rocks*, especially in hand specimens and in *outcrops*, on the basis of such characteristics as color, mineralogical composition and grain size. In other words, the physical character of *rocks* and the descriptions of them.

lithophile^b Pertaining to *elements* that tend to become concentrated in the *silicate* phase of *meteorites* or the *crustal rocks* of the earth.

lithosphere^b The relatively cold and mechanically strong layer comprising the uppermost *mantle* and its overlying *crust*. The *lithosphere* is on the order of 50–100 km thick in oceanic regions and 100–300 km thick in continental regions. The moving *plates* at the earth's surface consist of *lithosphere*.

lower mantle^b The solid *silicate* region of the earth between the 660 km

seismic discontinuity and the 2890 km deep boundary with the mostly iron (Fe) liquid outer *core*.

Ma^s This is an abbreviation for the Latin words, *mega* (million), *annum* (years), and therefore this abbreviation stands for “million years”.

mafic granulites^s *Metamorphic rocks* consisting of even-sized, interlocking *mineral grains*, less than 10% of which have any obvious preferred orientation, the *mineral* composition of the *rocks* being composed chiefly of one or more dark-colored ferromagnesian (Fe-Mg) minerals. These *rocks* are relatively coarse and granular, being formed at the high pressures and temperatures of the *granulite facies*. The term mafic is derived from *magnesium + ferric + ic*.

mafic igneous rocks^s Any *igneous rock*, derived from *magmas*, composed chiefly of one or more of the dark-colored, ferromagnesian *minerals* such as *pyroxenes*. These *minerals* and therefore the *rocks* contain large amounts of magnesium (Mg) and iron (Fe), which has led to this terminology derived from *magnesium + ferric + ic*.

mafic magmas^s Any *magma* with a composition that will produce when it cools and crystallizes *igneous rocks* which are chiefly composed of one or more of the dark-colored, ferromagnesian *minerals*, such as the *pyroxenes*, *minerals* rich in iron and magnesium (*magnesium + ferric + ic*).

mafic rocks^s Specifically, *igneous rocks* composed chiefly of one or more dark-colored ferromagnesian minerals such as *pyroxenes*. The term mafic is derived from *magnesium + ferric + ic*, and indicates that these *rocks* have high concentrations of magnesium (Mg) and iron (Fe).

magma^s A naturally-occurring mobile *rock* material, generated by heat within the earth and therefore capable of *intrusion* and extrusion. This is the molten *rock* material from which *igneous rocks* are thought to have been derived through solidification, *crystallization* and related processes. It may or may not contain suspended solids (such as crystals and *rock* fragments) and/or gas or fluid phases.

magma chamber^s A reservoir of *magma* at a shallow depth in the earth’s *crust* (down a few kilometers, or tens of kilometers at most) from which volcanic materials are derived. The *magma* has usually ascended into the *crust* from a deeper crustal level or even the *mantle*, and resides in such a *reservoir* for some time before cooling there or eventual *intrusion* at a higher

level in the *crust* or extrusion/eruption.

magma cooling processes^s The means by which molten *rock* cools and crystallizes to form *igneous rocks*. For example, steam released from the *magma* can fracture those portions of the body of *magma* that have begun to crystallize, particularly around the perimeter of the *magma* body in contact with the surrounding *rocks* being intruded, and then fracture the surrounding *rocks*, thus allowing the water to carry away some of the heat from the *magma*, and allowing colder *ground water* to penetrate into the *magma* to cool it further and cause further *crystallization*.

magmatic argon (Ar)^s Argon in the gases either dissolved in a *magma* or released from a *magma*. This Ar will be distinct from atmospheric Ar and may be excess Ar inherited by the *magma* during its formation and transport in the earth's *crust*, rather than having come from in situ *radioactive decay* of ⁴⁰K.

magmatic crystallization^s The formation of *mineral* crystals or *crystallization* of a *rock* from the cooling of a *magma*, a naturally-occurring molten *rock* material which is mobile within the earth's *crust*.

magmatic rocks^v *Igneous rocks* formed from the solidification and cooling of *magma*.

magnetic separation^a A laboratory technique using a magnetic field to isolate different *mineral phases* of a *rock*. *Minerals* have different magnetic properties which allow isolation in magnetic fields.

main zone^s During the formation and cooling of some *igneous intrusions* *minerals* which crystallize first can sometimes settle due to gravity to the bottom of the *magma chamber*, so that the end result is an *intrusion* which is layered, that is, there are horizontal layers of *igneous rocks* with slightly different mineralogical and *chemical* compositions. The *main zone* in such layered *intrusions* is the principal central part of the *intrusion*, which may correspond to a single thick layer or a series of layers similar to one another in mineralogical and *chemical* composition.

mantle^s The internal zone of the earth below the *crust* and above the *core*, consisting of particular characteristic *minerals* and *rocks* due to the temperatures and pressures at those depths. It is divided into the *upper mantle* and the *lower mantle*, with a *transition zone* between.

mantle plume^b A narrow upwelling current of hot (but nevertheless solid)

mantle rock with a diameter on the order of 30–100 km that originates in the *lower mantle*, probably in most cases at the *core-mantle* boundary.

mantle separation ages^s Essentially synonymous with “*crustal-extraction ages*,” supposedly being the time when the melt separated from the *mantle* to become a *magma* and ascend into the *crust* to eventually crystallize and form new *crustal rocks*.

mantle wedge^s The wedge-shaped body of *mantle rock* between a subducting *plate* of *oceanic crust* and the overriding *plate* of *continental crust* above it. The subducting *plate* is pushed underneath the continental *plate* at an oblique angle and the *mantle wedge* is within that acute angle.

marble^v A *metamorphic rock* consisting predominantly of fine- to coarse-grained recrystallized *calcite* and/or *dolomite*, usually with a *granoblastic*, *saccharoidal* texture.

mass fractionation^s Separation of the different *isotopes* of a *chemical element* according to the *atomic mass* of each *isotope*, by processes such as the preferential concentration of one *isotope* over another in nature. This separation can also be done artificially in the laboratory because the different masses of the *isotopes* give them slightly different weights.

mass number^v The number of *nucleons* in the *nucleus* of an *atom*. See *atomic number*.

mass scans^s Graphical or photographic depictions of the distribution of *atomic masses* of the *isotopes* or *elements* in a sample produced by a mass spectrometer.

mass spectrograph^v A recording mass spectrometer that records on a photographic plate. It measures molecular weights and relative abundances of *isotopes* within a *compound*.

massif^v A massive topographic and structural feature, especially in an orogenic belt, commonly formed of *rocks* more rigid than those of its surroundings. These *rocks* may be protruding bodies of basement *rocks*, consolidated during earlier *orogenies*, or younger *plutons*.

matrices^c Rectangular arrays of quantities subject to mathematical operations.

melting temperature^v The temperature at which a particular *compound* or *element* liquifies from the solid. The melting temperature is a function of pressure.

meson^h A short-lived particle intermediate in mass between *electrons* and *protons*.

Mesozoic era^s Those sedimentary rock strata in the *crust* of the earth which contain fossils of multi-cellular creatures and which occur above the Paleozoic and below the Cenozoic. In conventional thinking these *rocks* were formed between 248 and 65 *Ma*.

metagabbro^s A *gabbro* which shows evidence of having been subjected to *metamorphism*. Alternately, it is a *metamorphic rock* that has clearly been derived by the *metamorphism* of a *gabbro*. A *gabbro* is a group of dark-colored *intrusive igneous rocks*, which are coarse-grained and composed principally of *plagioclase* and *clinopyroxene*, with or without *olivine* and *orthopyroxene*, but often with magnetite (an iron oxide *mineral*) as an accessory. When metamorphosed the *rock* will still be dark-colored and coarse-grained, but the *pyroxenes* will have been replaced by the amphibole *hornblende*. This term is an amalgamation of the words *metamorphism* and *gabbro*.

metallic core^v The central zone or nucleus of the earth's interior thought to be composed primarily of a mixture of metallic iron and nickel, with a few other minor *elements*. It is divided into a solid inner *core* and a fluid outer *core*.

metalliferous^v Metal-bearing; specifically, pertaining to a *mineral* deposit from which a metal or metals can be extracted by metallurgical processes. Also used as a modifier for brines rich in base metals.

metamict^s Said of a *mineral* containing *radioactive elements* in which various degrees of damage and changes have been caused to the crystal lattice, having taken place as a result of radiation, while the *mineral's* original external shape has been retained. Examples of such *minerals* in which this occurs are *zircon* and *thorite*, and not all *minerals* containing *radioactive elements* become metamict (for example, *apatite*).

metamorphic rock^s Any *rock* derived from pre-existing *rocks* by mineralogical, *chemical*, and/or structural changes, essentially in the solid state, in response to marked changes in temperature, pressure, shearing stress, and *chemical* environment, generally at depth in the earth's *crust*.

metamorphism^s The mineralogical, *chemical* and structural adjustment of solid *rocks* to physical and *chemical* conditions which have generally

been imposed at depth below the surface zones of weathering and *cementation*, and which differ from conditions under which the *rocks* in question originated. The primary agents which change *rocks* during *metamorphism* are temperature and pressure, which increase with depth, and fluids.

metamorphosed carbonate rocks^s *Sedimentary rocks* consisting primarily of carbonate *minerals*, such as *limestones*, *dolomites* and *chalks*, which have been metamorphosed, that is, changed by elevated temperatures and pressures, with or without fluids, inside the earth's *crust* into new *rocks* with new groups of *minerals*, though still dominated by *recrystallized* carbonate *minerals*. An example would be *marble*.

metasediments^s *Sediments* or *sedimentary rocks* that show evidence of having been subjected to *metamorphism*. In reverse, they are *metamorphic rocks* which were clearly derived from the *metamorphism* of *sediments* or *sedimentary rocks*. Examples would include *slate*, derived from the *metamorphism* of *shale*, and *marble*, derived from the *metamorphism* of *limestone*. Hence the term is an amalgamation of the words *metamorphism* and *sediments*.

metasomatise^s To replace *minerals* in a *rock* by a process of practically simultaneous capillary solution and deposition by which a new *mineral* of partly or wholly different *chemical* composition may grow in the body of an old *mineral* or *mineral aggregate*. Essential to the replacement process is the presence of interstitial, chemically active pore liquids or gases contained within the *rock* body or introduced from external sources, the process thus often, though not necessarily, occurring at constant volume with little disturbance of textural or structural features.

metavolcanics^s *Volcanic rocks* that show evidence of having been subjected to *metamorphism*. Hence the word is an amalgamation of *metamorphism* and *volcanics*.

meteor^c A bright trail or streak caused by a foreign body heated to incandescence as it enters the earth's atmosphere.

meteorite^c A stony or metallic mass of matter that has fallen to the earth's surface.

metric tensor^c A doubly subscripted quantity which specifies a length scale in terms of the infinitesimal variations of the coordinates.

MeV^h A million *electron* volts, the energy which an *electron* would acquire after being accelerated between electrodes with one million volts of electrical potential across them.

mica^s A group of *minerals* having the general *chemical* formula of (K, Na, Ca)(Mg, Fe, Li, Al)₂₋₃(AlSi)₄O₁₀(OH, F)₂. It is a complex *silicate mineral* that crystallizes with a perfect basal *cleavage*, which means that it can be readily split into thin, tough, and somewhat elastic laminae sheets or plates with a splendid pearly luster. Colors for the different members of the group include colorless, silvery white (*muscovite*), pale brown, or yellow to green or black (*biotite*). Micas are prominent, rock-forming constituents of *igneous* and *metamorphic rocks*, and commonly occur as flakes, scales, or shreds.

microbial activity^s Pertaining to living microbes, which are minute plants or animals, especially bacteria and algae. The term is used to describe the results of their living processes on their surroundings, including within *rocks* and contained *ground waters*.

microcline^s A clear, white to gray, brick-red or green *mineral* of the alkali *feldspar* group, with a *chemical* formula of KAlSi₃O₈. It is the fully-ordered, triclinic variety of potassium *feldspar*, being stable at lower temperatures, and usually containing some sodium (Na) in minor amounts. It is a common *rock-forming mineral* of *granitic rocks* and *pegmatites*, and is often secondary after *orthoclase*.

micro-inclusions^s Small to tiny fragments of older *rock* within an *igneous rock* to which they may or may not be genetically related.

micron^s A unit of length representing one-millionth of a meter. It is an abbreviation of micrometer and is referred to with the symbol μm .

Mid-Atlantic Ridge^v A continuous, median mountain range extending through the North and South Atlantic oceans. It is a broad, fractured swell with a central rift valley and usually extremely rugged topography; it is 1–3 km in height, about 1500 km in width, and extends from Iceland to the tip of South America. According to the theory of *sea-floor spreading*, the mid-Atlantic ridge is a source of new crustal material.

mid-ocean ridge^b A zone between diverging oceanic *plates* in which new *oceanic lithosphere* is being formed. The *buoyancy* of the hotter than average *rock* beneath such a zone produces an elevated ridge-like topography.

Mid-Ocean Ridge Basalt (MORB)^b MORB forms by partial melting of typically 2–10% of the *rock* in a localized volume in the *asthenosphere* beneath a *mid-ocean ridge* and becomes new *oceanic crust*. Density of MORB is about 2900 kg/m³ (2.9 g/cm³).

migmatite^s A composite *rock* composed of igneous, or igneous-appearing, and/or metamorphic materials, which are generally distinguishable with the naked eye. It is generally regarded as a *metamorphic rock* produced at reasonably high temperatures and pressures, such that some of the *minerals* in the original *rock* material began to melt, separate from the other *minerals* and then recrystallize.

migration^s The movement of *elements* and *isotopes* in fluids from source areas of *rocks* and *minerals* into other *rocks* and *minerals*, the scale of the movement measured by the distance the *elements* or *isotopes* have moved.

millirem^h One-thousandth of a *rem*.

milliSievert^h One thousandth of a *Sievert*, or one-tenth of a *rem*.

mineral^s A naturally-occurring *inorganic element* or *compound* having an orderly internal structure and characteristic *chemical* composition, crystal form, and physical properties.

mineral isochron^s An *isochron* derived from the radioisotopic analyses of the individual *minerals* in a *rock*, in contrast to the radioisotopic analysis of the entire *rock*.

mineral phase^v A part of a chemical system for a *mineral* that is homogeneous and physically distinct and at least hypothetically separable, and which has continuously variable *chemical* and mechanical properties. Frequently a *mineral* will change from one phase to another at distinct pressure-temperature boundaries forming different states and/or crystal structures which in turn affect the density.

mineralogy^s The study of *minerals*, their formation, occurrence, properties, composition and classification.

Miocene^s An epoch of the upper *Tertiary* period of the *geological* timescale and corresponding worldwide to a series of *rocks* in the *geological* column which are conventionally said to have been deposited and formed during that time interval between 23.8 *Ma* and 5.3 *Ma*.

mobilities^s The freedom of *elements*, *isotopes* or *compounds* to move and migrate, usually in fluids, and usually beyond the limits of a single *mineral*

grain or crystal. Referring to the ability to be easily moved from location to location within a *rock* or *mineral*.

mobilization^s Any process that redistributes and concentrates the valuable constituents of a *rock* into an actual or potential ore deposit. This can also be any process that renders a solid *rock* sufficiently plastic to permit it to flow, or to permit *geochemical migration* of its mobile components.

model age^a An estimate of the absolute age of a *rock* or *mineral* based on the measured abundances of a radioactive parent *isotope* and a stable *daughter isotope*. The method assumes that the initial abundance of stable daughter is known at the time the *rock* or *mineral* formed, that the *decay rate* of the parent *isotope* has been constant throughout the history of the *rock* or *mineral*, and that the *rock* or *mineral* remained closed to gain or loss of the *daughter isotope*.

Mohorovicic discontinuity^v The boundary surface or sharp seismic-velocity discontinuity that separates the earth's *crust* from the subjacent *mantle*.

molecule^v The smallest particle of an *element* or *compound* that can exist in the free state and still retain the characteristics of the *element* or *compound*: the *molecules* of *elements* consist of one *atom* or two or more similar *atoms*; those of *compounds* consist of two or more different *atoms*.

monazite^s A yellow-brown or reddish-brown *mineral* which is a rare-earth phosphate, with the *chemical* formula: (Ce, La, Nd, Th) (PO₄, SiO₄). It is a *mineral* that is widely disseminated as an accessory in *granites*, *pegmatites* and *metamorphic rocks*, and because it is hard and resistant to *weathering* and erosion, it is often naturally concentrated in sand deposits. The appreciable substitution of thorium (Th) for rare earths makes this *mineral* important in the uranium-thorium-lead (U-Th-Pb) radioisotopic dating of those *rocks* containing it.

monzonite^s A coarse-grained *intrusive igneous rock* with a *quartz* content of between 0 and 5%, and a *plagioclase* to total *feldspar* (alkali *feldspar* or *orthoclase* plus *plagioclase*) of between 35 and 65%. Commonly the main mafic *mineral* is a *clinopyroxene*. Often regarded as one of the *granitic rocks*.

MORB^s Acronym for *mid-ocean ridge basalt*.

muon^c A particle like the *electron* except its mass which is 207 times larger.

muscovite^s A *mineral* of the mica group with the *chemical* formula $\text{KAl}_2(\text{AlSi}_3)\text{O}_{10}(\text{OH})_2$. It is a colorless or silvery white to yellowish or pale brown *mineral* which is very flaky and breaks off easily into very thin sheets. It is a common *rock-forming mineral*, often found in *granites*.

neutrino^h A neutral particle of zero (or very small) mass which travels at (or nearly at) the *speed of light*. It is very penetrating and is involved with the *weak nuclear force*.

neutron^h A neutrally-charged heavy particle in an atomic *nucleus*. It has about the same mass as a *proton*. Its attractive *strong nuclear force* helps hold a *nucleus* together. In a *nucleus* it is stable, but outside the *nucleus* it *decays* with roughly a fifteen-minute *half-life*.

noble gas^c A normally inactive or *inert gas* consisting of *atoms* with a closed *electron shell*, for example, *helium* (He), neon (Ne), argon (Ar), krypton (Kr), xenon (Xe), and radon (Rn).

non-relativistic particle^h A particle traveling slowly enough, compared to the *speed of light*, to not require the equations of relativity to describe its motion.

nuclear decay^h See *radioactivity*.

nuclear fission^h The violent splitting of a *nucleus* into several smaller nuclei called *fission* fragments, which move rapidly away from one another. Accompanied by emission of several fast-moving *neutrons* and several energetic *gamma rays*. The total energy released by one *fissioning* uranium (U) *nucleus* is nearly 170 *MeV*. See *fission*.

nuclear fusion^h The joining of two lighter atomic nuclei to make one heavier *nucleus*, with a subsequent release of energy. An important process in the cores of stars.

nuclear physics^s Study of the make-up of the *nucleus* of the *atom* and of how its internal constituents behave.

nuclear unit radius^h The ratio between the radius of a *nucleus* and the cube root of its *atomic weight*, averaged for all nuclei.

nucleon^c Either a *neutron* or a *proton*.

nucleosynthesis^c The production of nuclei from *neutrons* and *protons*.

nucleus^h The tiny center of an *atom* containing most of its mass, consisting of *protons* and *neutrons*.

nuclide^c A specific *nucleus* with a fixed number of *neutrons* and *protons*.

obsidian^c A glassy, usually black, *volcanic rock*, which has congealed and cooled so rapidly that individual *mineral grains* have not had time to crystallize.

occluded^s Used to describe when gases are absorbed, retained or otherwise enclosed in crystals or solid materials such as *minerals*.

Ocean Island Basalt (OIB)^b OIB is restricted to islands produced by *hotspot* volcanism such as Hawaii, Iceland, and the Azores. Note this type of basaltic volcanism is to be clearly distinguished from that at a typical *mid-ocean ridge* as well as near a convergent margin (that is, near a *subduction zone*).

ocean islands^b Islands either composed of basalt or of biogenic origin (coral reef, etc.) as distinguished from islands having *rocks* characteristic of continents.

oceanic crust^b A layer typically about 6 km thick of *MORB rock* that comprises the upper, crustal part of an oceanic lithospheric *plate*.

oceanic lithosphere^s Composed of the *oceanic crust*, that is, the *rocky* outer layer of the earth's surface under the ocean basins which consists largely of basaltic *rocks* and which therefore has an average density of 3000 kg/m³. It thus is denser than the *continental crust* and so "sinks" making for a topographic low which is infilled by the ocean water. The *oceanic crust* is much thinner than the *continental crust*, being only about 5–10 km thick. Added to the *oceanic crust* to make up the oceanic lithosphere is the uppermost part of the *mantle*, the suboceanic *lithosphere*, making the total thickness 50–100 km. It is separated from the *mantle* below by the *asthenosphere*.

oceanic volcanics^s *Volcanic rocks* found in the ocean basins, either on the ocean floor, or on the ridges and mountain systems beneath the ocean, including volcanic islands.

ocular micrometer^s The ocular or eyepiece is the upper lens of an *optical microscope* on which the eye is placed to view the sample being studied. A micrometer is a graduated scale for measuring the size of *grains* and other objects under the microscope. This term thus refers to the situation where this graduated scale is marked on the eye-piece of the *optical microscope*.

Oklo reactor^v A natural nuclear reactor in uranium ore in *rock* strata at Oklo, Gabon, Africa, which appears to have reached critical mass and

generated *neutrons* and heat at some point during earth history. The conditions under which this reactor functioned may be important in establishing nuclear boundary conditions, particularly if accelerated *decay* has occurred.

old earth^v The belief that the earth is billions of years old, as opposed to *young earth*.

olivine^a A *mineral* composed of iron-magnesium *silicate* which is common in basaltic *igneous rocks*. *Olivine* has very low potassium (K) content and so allows any excess *radiogenic* ⁴⁰Ar to be detected in olivine-bearing basaltic *igneous rocks*.

opaque central inclusions^s The tiny *mineral grains* at the centers of *radiohalos* which contain the *radioisotopes* whose *decay* has been responsible for producing the *halos* and their discoloration. These tiny *mineral grains* are included in host *minerals* and in this instance are opaque, meaning that light cannot be passed through them as it does through the surrounding host *minerals* in the *thin sections* being examined under the microscope. See *radiocenters*.

open system mixing^s A *chemical system* in which material is either added or removed due to the processes of mixing. In other words, the mixing in the *chemical system* is open to external influences.

ophiolite^b A *rock mass* that represents a piece of *oceanic lithosphere* that has been emplaced by *tectonic processes* at the earth's surface, usually near a *plate margin* in a continental environment.

optical microscope^s An optical instrument that is used to produce an enlarged image of a small object, in this case so that *rocks* and *minerals* can be enlarged for study. It consists of two sets of lenses, the objective and the eye piece set into a tube and held by an adjustable arm over a stage in which the glass slides containing the *thin sections* of *rocks* and *minerals* are placed. Most such *geological* microscopes use light from a lamp beneath this stage, which then shines up through the sample and the lenses to the observer's eyes.

ore leads^s The isotopic composition of the lead (Pb) in the *minerals* making up the ore of an economic *mineral* deposit. The term primarily refers to the Pb isotopic composition of sulfide *minerals* such as *galena* (PbS) and pyrite (FeS₂).

orogenes^s This term is synonymous with orogenic belts, which are linear

or arcuate regions that have been subjected to folding, faulting and other deformation. They are mobile belts during their formative stages, and most of them later become mountain belts, that is, they result in mountainous regions of the earth's topography, consisting of folded and distorted *rocks*.

orogeny^s The process of the formation of mountains. Orogeny is the process by which deforming structures within blocks of *rocks* in mountainous areas were formed, including thrusting, folding and faulting in the outer and higher layers, and plastic folding, *metamorphism* and *intrusion* of *igneous rocks* in the inner and deep *rock* layers. *Rock* layers are buckled and crumpled so that the earth's *crust* is thickened and the earth's surface pushed upwards to form mountain ranges.

orphan halo^h *Radiohalo* with no evidence of rings produced by parent nuclei. See *parentless*.

orthoclase^s A colorless, white, cream-yellow, flesh-pink, or gray *mineral* of the alkali *feldspar* group, with a *chemical* formula of KAlSi_3O_8 . It is the partly ordered, monoclinic variety of potassium *feldspar*, being stable at higher temperatures, and usually containing some sodium (Na) in minor amounts. It is a common *rock-forming mineral*, occurring especially in *granites*, *acid igneous rocks* and *crystalline schists*.

orthopyroxene^s A group name for *pyroxenes* crystallizing in the orthorhombic crystal system, and usually containing no calcium (Ca) and little or no aluminum (Al). The term also applies to any of the *minerals* in this group.

outcrop^s That part of a geologic formation or structure that appears at the surface of the earth as bare *rock*, which can be sampled and studied, as opposed to other parts of the earth's surface covered in *soil*, alluvium, vegetation, etc.

oxyhydroxides^s *Compounds* or *minerals* which are oxides containing hydroxyl ions (hydroxides). An oxide is a *mineral compound* characterized by the linkage of oxygen with one or more metallic *elements*, while the hydroxyl ion is the combination of an oxygen *atom* and a hydrogen *atom* with a residual negative charge, by which it is linked to *cations* to form *compounds*, in this instance linking up with oxide *compounds* to form these *compounds* called oxyhydroxides.

parent element^v The original *radioactive element* from which *decay*

products are derived.

parent nucleus^h The original *nucleus* which produces another *nucleus* (the daughter *nucleus*) by *nuclear decay*.

parentless^s The term used to describe the occurrence of a daughter *radionuclide*, normally produced by *radioactive decay* from a parent *radionuclide*, but in this instance the parent *radionuclide* is no longer present and the evidence indicates that it might never have been present to have produced the daughter *radionuclide*. See *orphan halo*.

partial pressure^s In a mixture of gases that behaves ideally, each gas in the mixture exerts its own pressure independently of the other gases in the mixture, and thus this term describes the individual pressure of the gas in the mixture. If the gas is a constituent of a fluid, that is, mixed in a liquid, then it is the pressure of the gas as opposed to the pressure of the liquid, being a part of the total pressure of the fluid.

pegmatite^s An exceptionally coarse-grained *igneous rock*, with interlocking crystals, usually found as irregular elongated masses called *dikes*, lenses, or *veins*, especially at the margins of huge masses of *granite*. Most crystals it contains are 1 cm or more in diameter. The gross composition of *pegmatites* is generally that of *granite*, but may be complicated by the presence of rare *minerals* rich in such *elements* as lithium (Li), boron (B), fluorine (F), niobium (Nb), tantalum (Ta), uranium (U), and rare earths. A *pegmatite* represents the last and most water-rich portion of a *magma* to crystallize and hence contains high concentrations of *minerals* present in only trace amounts in *granitic rocks*.

pegmatitic rocks^s See *pegmatites*.

pelagic sediment^s Marine *sediment* in which the fraction derived from the continents indicates deposition from a dilute *mineral* suspension distributed throughout deep-ocean water.

penetration distance^s The distance traveled by α -*particles* in a *mineral* as they penetrate the *crystal lattice* of the host *mineral* around the central tiny inclusion or *radiocenter* and damage the host *mineral*, and the *crystal lattice* of the host *mineral*, discoloring it.

peridotite^b A rock type characteristic of the earth's *upper mantle* composed mostly of the *minerals olivine*, for example, Mg_2SiO_4 , and *pyroxene*, for example, $\text{Ca}(\text{MgFe})\text{Si}_2\text{O}_6$.

- permeability of the vacuum (μ_0)^v** The ratio of magnetic induction to magnetic field intensity, measured in free *space*. Its value is defined to be unity in the electromagnetic system and 1.257×10^{-6} henry per meter in the M.K.S system.
- permeable^s** The property or capacity of a porous *rock, mineral, sediment* or *soil* for transporting fluid. It is a measure of the relative ease of fluid flow through the material.
- permittivity^c** A constant defined via Coulomb's law of electrostatics and specifying how much electric force originates from a given amount of charge.
- permittivity of space^h** A constant appearing in Coulomb's law which has the value of 8.854 picofarads per meter.
- perovskite^v** A yellow, brown, or grayish-black cubic *mineral*: $\text{Ca}(\text{TiO}_3)$. It sometimes contains cerium (Ce) and other rare earth *elements*.
- petrogenesis^s** That branch of the study of *rocks* which deals with the origin and formation of all the different *rock* types.
- petrographic^s** That branch of geology dealing with the description and systematic classification of *rocks*, especially *igneous* and *metamorphic rocks*, and especially by microscopic examination of *rocks* in *thin sections*.
- petrological^s** That branch of geology which deals with the origin, occurrence, structure and history of *rocks*, especially of *igneous* and *metamorphic rocks*.
- Phanerozoic^s** That part of the *geological* timescale represented by *rocks* in which the evidence of multi-cellular life is abundant, that is, from the *Cambrian* period (conventionally thought to have begun 545 million years ago) until the present day, and all the *rocks* deposited and formed in the *geological* record in that period of time.
- phase transition^c** A process with a change of symmetry which before (or after) the phase transition is spontaneously broken.
- phengite^s** A variety of the white *mica muscovite*, but with a high silica content. *Muscovite* has the *chemical* formula $\text{K}_2\text{Al}_4(\text{Si}_6\text{Al}_2\text{O}_{20})(\text{OH}, \text{F})_4$ and *phengite* is a *muscovite* in which the Si/Al ratio is >3:1, the increase in Si being accompanied by substitution of Mg or Fe^{2+} for Al.
- phenocrysts^s** Relatively large, conspicuous crystals in an *igneous rock*, set in a general mass of smaller crystals.
- photoelectric formula^h** The equation relating the energy of a *photon* with

the frequency or wavelength of the light waves associated with it.

photon^c The particle that makes up light and transmits the electromagnetic force.

photosphere^v That region of the Sun which emits the main part of the flux of radiant energy escaping to the outside and appears to the eye as the Sun's visible surface.

pi meson^h (also **π -meson** or **pion**) A *gauge boson* which appears to mediate the *strong nuclear force*. Its mass is about 270 times that of an *electron*.

pillow lava^s A general term for those *lavas* displaying pillow structure and considered to have formed in a watery environment. A pillow structure is characterized by discontinuous pillow-shaped masses ranging in size from a few centimeters to a meter or more in greatest dimension (commonly between 30 and 60 cm). The pillows are close-fitting, the concavities of one matching the convexities of another. The spaces between the pillows are few and are usually filled with material of the same composition as the pillows. The pillows result from the hot *lava* being quickly cooled on contact with the water.

pipe eruptions^s Volcanic *eruptions* through narrow vertical *conduits* through the earth's *crust* and through which magmatic materials have passed, often explosively, so that the resulting "pipe" is usually filled with broken fragments of the resulting *volcanic rocks*.

pitchblende^s A massive brown to black variety of the *mineral*, *uraninite*, that is essentially uranium oxide, but a mixture of UO_2 and UO_3 . It is fine-grained, lacking crystal structure, or microcrystalline, and has a distinctive dull luster resembling pitch. It contains a slight amount of thorium and is highly radioactive. It can therefore be "dated" using the uranium-thorium-lead (U-Th-Pb) radioisotopic method.

plagioclase^s A *mineral* belonging to the *feldspar* group which has the general *chemical* formula: $(\text{Na}, \text{Ca}) \text{Al} (\text{Si}, \text{Al}) \text{Si}_2 \text{O}_8$. Formed at high temperatures, its composition can be variable from the $\text{NaAlSi}_3\text{O}_8$ end-member (*albite*) through mixtures to the $\text{CaAl}_2\text{Si}_2\text{O}_8$ end-member (*anorthite*). *Plagioclase* is among the commonest of the *rock-forming minerals*.

Planck's constant^h A basic constant, *h*, in quantum theory, atomic physics, *nuclear physics*, optics, and chemistry. It is the ratio between the energy of a *photon* and its frequency, having a value of

6.626×10^{-34} of a Joule-second.

planetismal^v Minute bodies in *space* that move in planetary orbits. A conventional explanation for the formation of the planets is that they were formed by the uniting of planetismals created by tidal eruptions caused on the Sun by the passage of a star close to it.

plastic deformation^s Permanent deformation of the shape or volume of a substance without rupture or breakdown of that substance.

plate^v A torsionally rigid segment of the earth's thin *lithosphere*, which shows evidence of having moved horizontally and adjoins other plates along zones of seismic activity.

plate tectonics^b A theory of global *tectonics* in which the *lithosphere* is divided into a number of *plates* whose pattern of horizontal movement is that of torsionally rigid bodies that interact with one another at their boundaries, causing seismic and *tectonic* activity along these boundaries. The conventional view is that the movement of the *plates* is extremely slow and has been occurring over millions of years. A young-earth creationist model, called *catastrophic plate tectonics*, says the *plates* moved very rapidly during and immediately following the *Genesis Flood* and are now moving slowly, if at all.

plate tectonic processes^s The processes which result from plate tectonics, that is, processes that result from the interaction of the earth's lithospheric *plates* as they are rifted apart, collide with one another, or one is pushed under another (subducted). This interaction causes seismic and *tectonic* activity along the *plate* boundaries and produces the structural and deformational features of the earth's *crust*.

Pleistocene^s A *geological* epoch of the latest period of *geological* history corresponding to a worldwide series of *rocks* which was supposedly deposited in the period from 1.8 million years ago up until about 10,000 years ago. The Pleistocene epoch is considered to be the time period in which the Ice Age occurred, and from a Biblical perspective corresponds to the *geological* deposits of the post-Flood Ice Age.

pleochroic halos^s Synonymous with *radiohalos*. The term pleochroic refers to the discoloration or darkening of the host *mineral*. The *radiation damage* causes the crystal structure to differentially absorb various wavelengths of transmitted light and thus to show different colors to that normally displayed

by the host *mineral*.

plumbotectonics models^s Constructed models for the development and distribution of lead (plumbum in Latin) *isotopes* in the earth's *crustal rocks* recognizing the broad architecture of the outer part of the earth with its regional assemblies of structural and deformational features.

plume/hotspot basalts^s Basalts formed from *lavas* at a *hotspot* volcanic center, 100 to 200 km across and persistent for supposedly at least a few tens of millions of years, that has been established as the surface expression of a persistent rising plume of hot *mantle* material.

plutonic rock^v An *igneous rock* formed at considerable depth; it is characteristically medium- to coarse-grained and of granitoid texture.

plutons^s A general term for igneous *intrusions*, originally signifying only deep-seated igneous bodies of granitoid texture. As a general term the igneous *intrusions* described can be of any size.

polonium halos^s *Radiohalos* which have discoloration and ring structures which can be shown experimentally to have been produced exclusively from *isotopes* of the *element* polonium (Po) in the central *mineral inclusions*. These Po *isotopes* are normally found in the uranium (U) *radioactive decay chain*. These *radiohalos* are therefore a puzzle because they indicate that only Po has been present in the central *mineral inclusions*, which implies that the Po must somehow have been separated from its parent U before coming to reside in the central *mineral inclusions*.

post-crystallization isotopic re-equilibrium^s The state of the isotopic systems plus the isotopic composition of a *rock* or a *mineral* said to be in equilibrium when there is no change in the isotopic systems or the composition with the passage of time. When a *rock* or *mineral* crystallizes it usually features such a state of isotopic equilibrium. An event or process which occurs after the *rock* or *mineral* has crystallized is said to be a *post-crystallization* event or process. This full descriptive term therefore applies to the situation when a process or event occurs after the *crystallization* of a *rock* or *mineral* which disturbs the isotopic equilibrium and eventually brings it into a new stable state of equilibrium concentration and composition. This can be the result of ground or *hydrothermal* waters dissolving *isotopes* and moving them out of the *rock* or *mineral*, or moving *isotopes* from other *rocks* and *minerals* into the *rocks* or *minerals* in view, so that the isotopic

composition is back into an equilibrium state.

potassic magmas^s *Magmas* containing a significant amount of potassium (K) that cool to form distinctive high K *igneous rocks*.

potential energy^h As applied to an *alpha-particle* (α -particle) the energy required to remove a motionless α -particle from a point within an atomic *nucleus* to a point far outside it. One can think of the potential energy-versus-radius curve as a deep hole, or potential well, out of which one must lift the particle to remove it from the *nucleus*.

Precambrian^s All of the *geological* timescale, and the corresponding *rocks* of the *geological* column, before the beginning of the *Cambrian* period of the Paleozoic era, thought conventionally to be about 545 million years ago. According to evolutionary estimates this era is equivalent to about 90% of all *geological* time. The *rocks* to which this label is applied are in the lowest part of the *geological* record and represent those *rocks* which were formed before the fossilization of complex, multi-cellular invertebrates, and then vertebrates. These *rocks* also go back to the time of the earth's formation.

Precambrian shields^s Large areas of exposed basement *rocks* or stable areas of the earth's *crust*, commonly with a very gentle convex surface and surrounded by *sediment*-covered platforms. These shield areas virtually all consist of *Precambrian* rocks, which are rocks belonging to that part of the *geological* timescale older than supposedly 545 million years ago (the beginning of the *Cambrian* period).

PREMA^s An abbreviation for **PRE**valent **MA**ntle, referring to a *mantle geochemical reservoir* which is prevalent, being a volume of *rock* in the *mantle* which yields *magmas* producing *lavas* and *volcanic rocks* with a distinctive *geochemical* and isotopic composition. The great frequency of basalts from oceanic islands, intra-oceanic island arcs and continental basalt suites with $^{143}\text{Nd}/^{144}\text{Nd} = 0.5130$ and $^{87}\text{Sr}/^{86}\text{Sr} = 0.7033$ indicates that this is a prevalent identifiable *mantle* component with this isotopic character. It also has $^{206}\text{Pb}/^{204}\text{Pb} = 18.2$ to 18.5.

prevalent mantle^s See **PREMA**.

primeval^s The earliest ages of the earth; for example, said of lead (Pb) which is associated with so little uranium (U) (as in some *meteorites*) that the Pb-isotopic composition has not changed appreciably in the supposed

4.57 billion years of earth history.

primordial^s Original, first in development, earliest or existing from the beginning. For example, *primordial rocks* would be *rocks* that have presumably existed from the earliest development, and the beginning, of the earth at its formation.

primordial argon (Ar)^v Argon which was originally present at *Creation*, rather than generated as a daughter product of *radioactive decay* of ⁴⁰K.

progressive creationism^v The teaching that God created life over millions of years by intervening at critical steps in *evolution*.

propagation speed^v The rate at which a seismic wave moves through the *crust* of the earth. S-waves and P-waves move at different speeds through the earth, revealing information about the composition and structure of the *lithosphere, mantle* and *core*.

Proterozoic^s The more recent of the two great divisions of the *Precambrian* in the *geological* timescale, and also is the term applied to *rocks* within that division of the *Precambrian* timescale, *rocks* which are conventionally said to be between 570 and 2500 million years old.

Proterozoic metamorphic basement^s A large area of *metamorphic rocks* of *Proterozoic* “age” upon which other younger *rock* strata have been deposited.

Proterozoic mobile belts^s Long, relatively narrow crustal regions of *tectonic* activity (processes resulting in the folding and faulting of *rocks, metamorphism* and generation of *igneous rocks*), measured in terms of multiples of 50 km. In this instance these are regions where the *tectonic* activity is believed to have occurred during the *Proterozoic*, that portion of the *Precambrian* era of the *geological* timescale conventionally between 570 and 2500 million years ago. The activity in these regions also involves sedimentation. What specific activities have taken place can be identified by the types of *rocks* formed in these regions.

proto-earth^v The original or primitive form of the earth. The conventional model of the earth’s formation suggests that it was formed from the *accretion* of *planetismals* over billions of years and after outgassing of volatile *elements* like water eventually formed the ocean and atmosphere. The Biblical description says that God created the earth much faster, but there was still a process. At the end of the first day of *Creation* it was “unformed” and

“void”, meaning it was fairly homogeneous and was not inhabited. On the second day the atmosphere was formed and on the third day oceans and continents.

protolith^a The original *rock* before temperature and pressure caused metamorphic processes which altered the *rock*.

protolith age^s The calculated *radioisotopic* “age” of the original unmetamorphosed *rock* from which a given *metamorphic rock* was formed by *metamorphism*. In other words, the presumed “age” of the parent *rock*.

proton^h Positively-charged stable heavy particle in an atomic *nucleus*. Its mass is 1836 times that of an *electron*. The number of *protons* determines the number of *electrons* in a normal, electrically-neutral, *atom*.

proton decay^c The proposed, but not yet seen, disintegration of the *proton* into other particles. In at least one theory the dominant *decay* mode is to a positron and pion.

pseudoisochron (or **fictitious isochron**)^v A line on an *isotope* correlation diagram which has no relationship with sample age, but rather, is simply due to the mixing of two material components. Such lines may even have a downward slope, implying a negative sample age.

pseudotachylyte^s A dense *rock* produced in the compression and sheer associated with intense fault movements, involving extreme crushing of the *rock* to flour-sized particles, and/or partial melting of the *rock*. It can also be a dark gray or black *rock* that externally resembles tachylyte, a type of volcanic glass formed from *magma* with a *basaltic composition*, and that typically occurs in irregularly branching *veins*. This *rock*, however, carries fragmented material enclosed within it and shows evidence of having been at high temperatures.

pyrolite^v A model for the material of the upper mantle, suggested by Ringwood, composed of one part basalt to three parts dunite and consisting mainly of *pyroxenes* (pyr) and *olivine* (ol), hence pyr+ol+ite. It is so designed that a partial melt will yield a basaltic *magma*.

pyroxene^s A group of dark *rock*-forming *silicate minerals*, closely related in crystal form and composition and having the general formula $ABSi_2O_6$, where A = Ca, Na, Mg, or Fe^{2+} , and B = Mg, Fe^{2+} , Fe^{3+} , Cr, Mn, or Al, with Si sometimes replaced in part by Al. Pyroxene crystals are usually dark green or black, and have distinctive crystal faces intersecting at regular

angles. Pyroxenes are a common constituent of *igneous rocks*.

quantum chromodynamics^h “*Quark* theory,” whereby nuclear particles and *mesons* are explained in terms of fractionally-charged *quark* constituents, and the *gluons* holding them together. Though complex, the theory does seem to explain much about elementary particles.

quantum fluctuations^h The unpredictable motion of elementary particles due to their being jostled by the invisible particles in the “*vacuum*” around them, analogous to the erratic Brownian motion of a dust particle being bumped by invisible air *molecules* around it.

quark^h A particle thought to be a constituent of *protons*, *neutrons*, and *mesons*. *Quarks* would have either $\frac{1}{3}$ or $\frac{2}{3}$ the electric charge of *protons* or *electrons*, and they come in a variety of “colors,” “flavors,” and other characteristics.

quartzofeldspathic rocks^s Synonymous with “*felsic rocks*.” These are *rocks* which are largely made up of *quartz* and *feldspars*, primarily *igneous rocks* having these abundant light-colored *minerals*.

quartz^s *Crystalline* silica, one of the most important *rock-forming minerals* with a *chemical* formula of SiO_2 . It occurs either in transparent hexagonal crystals which are colorless or colored by impurities, or in *crystalline* or cryptocrystalline masses. Quartz forms the major proportion of most sands and is one of the commonest *minerals* in all types of *rocks*. It is of the same composition as window glass.

quasar spectra^c The distribution of the intensity of quasar light over different wavelengths. Quasars are the sources of intense light supposedly emanating from distant points in the universe.

Quaternary^s That period in the *geological* timetable following the *Tertiary* period, and also the corresponding system of *rocks*. The Quaternary and *Tertiary* periods make up the Cenozoic era. The Quaternary period includes the *Pleistocene* epoch during which the Ice Age occurred, followed by the Holocene epoch that includes the very latest *geological* deposits up until the present. The Quaternary thus supposedly begins 1.8 million years ago according to conventional thinking and extends up to the present. However, in the Biblical timeframe these *rocks* are all post-Flood, the Ice Age deposits being produced during the post-Flood Ice Age.

quench^s In the experimental study of the formation of *rocks*, this describes

the very rapid cooling of a heated mixture in order to preserve certain physical-chemical characteristics of the high temperature state which would be changed by slow cooling.

radiation damage^v The damage done to a *crystal lattice* (or glass) by passage of *fission* particles or *alpha-particles* (α -particles) from the *nuclear decay* of a *radioactive element* residing in the *lattice*.

radioactive decay^d The spontaneous process by which a *nucleus* emits excess *neutrons*, *protons*, or energy.

radioactive elements^v Those *elements* which spontaneously emit energetic particles or radiation from their nuclei during *radioactive decay*.

radioactive halos^c Spherical regions of discoloration caused by *alpha-particle* (α -particle) tracks emanating from a speck of concentrated *radioactivity*. (See *radiohalos*).

radioactive isotopes^v Species of *chemical elements* which spontaneously emit energetic particles or radiation from their nuclei during *radioactive decay*. Some *isotopes* of a given *element* are radioactive and others are not.

radioactivity^h The emission of particles such as *electrons*, *positrons*, *alpha-particles* (α -particles), *fission* fragments, or *gamma rays*, from atomic nuclei.

radiocarbon inventory^h The total mass of radioactive carbon (^{14}C) on or in the earth and its atmosphere. Presently estimated to be about 62 metric tons.

radiocenters^s The abbreviated term for the tiny *mineral* crystals or *grains* central to *radiohalos*, that is, the central tiny *mineral inclusions* which evidently contain the radioactive uranium (U) and/or thorium (Th) responsible for producing the *radiohalos*. See *opaque central inclusions*.

radiogenic^s A descriptive term applied to the product of a radioactive process. For example, the lead (Pb) *isotopes* produced or derived from the *radioactive decay* of uranium (U) are described as *radiogenic* Pb.

radiohalos^s Minute zones of discoloration or darkening surrounding tiny central *mineral* crystals or *inclusions* in certain *minerals* in some *rocks*. The discoloration or darkening often has a concentric ring structure that has been produced by damage from *alpha-particle* (α -particle) radiation emitted from the central tiny *mineral grain* or crystal, which contains uranium (U) and/or thorium (Th) that has *radioactively decayed*. The emitted α -particles are like bullets, leaving a trail of damage in the *crystal lattice* through which

they pass, the damage causing discoloration or darkening of the *mineral* hosting the central radioactive inclusion. See *radioactive halos*.

radioisotope^v A radioactive *isotope* of an *element*.

radioisotopic ages^s “Ages” calculated from measurements of radioactive parent and *daughter isotopes* in *rocks*, based on the assumption that the rates of *radioactive decay* measured today have remained constant in the past.

radioisotopic signatures^s A characteristic or combination of characteristics in *rocks* provided by *radioactive isotopes* and their *daughter isotopes*.

radionuclides^s Radioactive *nuclides*, a term which is not synonymous with *radioisotopes*. *Nuclides* are species of *atoms* characterized by the numbers of *neutrons* and *protons* in their nuclei, whereas *isotopes* are species of the same *chemical element*, having the same numbers of *protons* in their nuclei, but differing from one another by having different numbers of *neutrons*.

range^h In *meson* theories, the distance at which the strength of a force starts decreasing significantly faster than the inverse-square law.

rare earth elements (REE)^v A series of fifteen metallic *elements*, from lanthanum (La) (*atomic number 57*) to lutetium (Lu) (71), and of three other *elements*: yttrium (Y), thorium (Th), and scandium (Sc). These *elements* are not especially rare in the earth’s *crust*, but concentrations are. The rare earth *elements* are constituents of certain *minerals*, especially, *monazite*, *bastnaesite*, and *xenotime*.

RATE^v An acronym which stands for **R**adioisotopes and the **A**ge of the **E**arth, a 5-year *young-earth* creationist research initiative to better understand how *radioisotopes* fit into the Biblical *Creation* model.

recrystallization^s The formation, essentially in the solid state, of new *crystalline mineral grains* in a *rock*. The new *grains* are generally larger than the original *grains*, and may have the same or a different mineralogical composition. Specifically, it is the way in which the crystal *aggregate* which has been deformed releases the stored strain energy due to that deforming process. *Defects* in the original crystal structures are eliminated and the *atoms* and *molecules* rearranged into stable crystal forms so that new *grains* and crystals grow, with the average *grain size* increasing. The net result is in a sense a renewal of the original crystals and *grains*.

red shift^v The generally greater displacement towards the red end of the

spectrum for light that comes from galaxies which are the farthest from earth. There are exceptions to these observations which are yet unexplained. In terms of the “Doppler effect” the proportionality factor is on the order of 50 km/sec per light year.

redox interface^s The boundary or interface between oxidized *rock* on one side and reduced *rock* on the other. Oxidized *rock* typically contains iron oxides, whereas reduced *rock* typically contains iron sulfides and organic matter. The oxidation process destroys the organic matter and changes the iron sulfides into iron oxides (hence the term oxidized).

refraction^v The deflection of a ray of light or of an energy wave (such as a seismic wave) due to its passage from one medium to another of differing density, which changes its velocity.

refractory^v An ore from which it is difficult or expensive to recover its valuable constituents. Said of an ore or *mineral* that is exceptionally resistant to heat.

refractory/volatile ratios^s The ratios of *elements* that readily vaporize and/or which are difficult to recover or isolate.

relict magmatic zoning^s Groupings of *minerals* into areas or zones within an *intrusive igneous rock* which have formed as part of the original cooling process of the *intrusive magma* and which have persisted in being preserved in a later *rock* after processes which have tended to destroy that zoning in the original *rock* cooled from the *magma*.

rem^h A unit of *ionizing* radiation equal to the amount that produces the same damage to human beings as 1 roentgen of high-voltage x-rays. Derived from roentgen equivalent man.

remobilized^s Having become mobile again, as a once-molten *rock* that was remelted. In this context it refers to *isotopes* and *trace elements* which have become mobile again, moving from the *rocks* and *minerals* (in which they were once held) via solution in fluids into other *minerals* and *rocks* where they are now found.

replacement ore deposits^s An accumulation of economic *minerals* to form an ore body or *mineral* deposit via a process whereby the metals and other elements involved are transported by solutions into the host *rock* where they are deposited. They gradually transform the host *rock* being permeated by the incoming solutions so that *rocks* of wholly differing *chemical* and

mineral composition may grow in the overall shape and volume of the original host *rocks* and their constituent *minerals*. Thus the eventual ore deposit replaces the original *rock*.

reservoirs^s Subsurface volumes of *rock*, either in the *crust* or the *mantle*, which are the sources of particular *elements* or *isotopes*, in this context via melting to form *magmas* which rise into the upper *crust* to form new *intrusive igneous rocks*, or to the surface to form new extrusive *igneous rocks*. These are repositories for *rocks* with particular elemental and isotopic compositions.

reset^s To start all over again from zero, in the context of changing the radioactive “clock” back to zero again.

rest mass^h The mass of a particle at rest. Some particles, such as the *photon*, cannot be at rest (having to travel at the *speed of light*) and so have zero rest mass.

retentivity^s The capacity to retain or hold on to, or keep in place, as in the ability of a *mineral* to retain its gas or water content.

retrograde metamorphism^a A type of *metamorphism* where *minerals* in lower temperature conditions are formed from *minerals* stable in higher temperature (or *metamorphic*) conditions. The net result is that the *metamorphism* appears to have gone backwards; hence the descriptor retrograde.

rhombohedral^v The class of crystal symmetry in the trigonal system in which the unit cell is a rhombohedron.

rhyolites^s A group of extrusive *igneous rocks*, cooled from *lavas*, and commonly exhibiting flow texture, with *phenocrysts* (large crystals) of *quartz* and alkali *feldspar* (*orthoclase*) in a glassy to very fine *crystalline* groundmass. These *rocks* are the extrusive equivalents of *granites*.

rocks^s *Aggregates* of one or more *minerals*, for example, *granite*, *shale*; or a body of undifferentiated *mineral* matter, for example, volcanic glass or *obsidian*, or of solid organic material, for example, *coal*.

roll front uranium (U) deposits^s Accumulations of economic uranium mineralization associated with a “*roll front*” (the boundary area between oxidized altered *rock* and relatively reduced altered *rock* due to *ground water* flow in a *sedimentary rock* unit) that form ore bodies.

roll front^s An area in a porous *sedimentary rock* layer where *ground water*

is flowing, such that the area is bounded on the concave side by oxidized altered *rock* typically containing iron (Fe) oxides such as hematite or limonite, and on the convex side by relatively reduced altered *rock* typically containing pyrite (iron sulfide) and organic matter. This area moves forward in the direction of *ground water* flow like an advancing front.

r-process^c A hypothetical process of nuclear transmutation by rapid absorption of *neutrons* during a *supernova* explosion.

saccharoidal^v A granular or *crystalline* texture resembling that of loaf sugar.

samarskite^s A velvet-black to brown, commonly *metamict mineral* with the *chemical* formula: (Y,Ce, U,Ca, Fe, Pb, Th) (Nb, Ta, Ti, Sn)₂O₆. It has a prominent glassy or resinous luster and is found in *granite pegmatites*. Because it can contain uranium (U) and thorium (Th) it is radioactive and can be useful in uranium-thorium-lead (U-Th-Pb) radioisotopic dating.

sapphire^s Any pure, gem-quality variety of the *mineral* corundum, which has the *chemical* formula of Al₂O₃, other than ruby. The most common variety is a transparent blue color whose crystals are of great value as gems. The color is due to small amounts of cobalt (Co), chromium (Cr) and titanium (Ti), and other colored varieties include pink, purple, yellow, green and orange. It is the second hardest *mineral* known, and occurs as shapeless *grains* and masses, or variously as distinctive crystals such as tapering hexagonal pyramids.

scalar^c A quantity remaining the same under symmetry transformations.

scanning electron microscope (SEM)^s A sophisticated research instrument in which a finely focused beam of *electrons* is electrically or magnetically moved across the specimen to be examined, from point to point, again and again, and the reflected and emitted *electron* intensity measured and displayed, sequentially building up a three-dimensional image of the specimen being examined.

scanning electron microscope x-ray fluorescence (SEM-XRF)^s A sophisticated research instrument in which a finely focused beam of *electrons* is electrically or magnetically moved across the specimen to be examined, from point to point, again and again, and the reflected and emitted *electron* intensity measured and displayed, sequentially building up a three-dimensional image of the specimen being examined. If x-ray detectors are also mounted around the specimen within the instrument the x-rays which

are emitted from the sample surface as the *electron* beam strikes the sample can be detected and measured, allowing the sample to be analyzed. The x-rays are characteristic of the composition of the sample, and the x-rays measured by the detectors are thus compared to the compositions of previously analyzed *minerals*, enabling the composition of the *mineral* sample in the area the *electron* beam is moving over to be determined.

schist^s A *crystalline rock* with a strong planar arrangement of its constituent *minerals* formed by *metamorphism* where pressure is the dominant condition. The *rock* can be readily split into thin flakes or slabs due to this well developed parallelism of more than 50% of the *minerals* present, particularly those *minerals* with an elongate habit, such as the *micas* which form sheet-like flakes. While the *mineral* composition is not an essential factor in the *rock's* definition, varieties are named according to their *mineral* constituents.

schistose^v A *rock* displaying foliation in *schist* or other coarse-grained, *crystalline rock* due to the parallel alignment of platy *mineral grains* (which also include *mica*).

sea-floor spreading^b The creation of new *oceanic lithosphere* at a *mid-ocean ridge* by the process of upwelling of solid *mantle* material, consequent partial melting, extrusion and freezing of the resulting *basaltic lava (MORB)* to form *crust* at the surface, and lateral movement of the new *lithosphere* away from the ridge.

seamount^s An elevated area of the ocean floor, 1000 m or higher above the surrounding sea floor, either flat topped or peaked. Seamounts may be either discrete, arranged in a linear or random grouping, or connected at their bases and aligned along a ridge or rise.

sediment^v Solid fragmental material that originates from *weathering of rocks* and is transported or deposited by air, water, or ice.

sedimentary rock^s Any *rock* resulting from the consolidation of loose *sediment* that has accumulated in layers, such as sandstone and *conglomerate*, which consist of mechanically formed fragments of older *rock* transported from their source and deposited in water; or a *rock* such as *limestone* where the lime has been precipitated from solution and engulfed the remains of seashells and other marine creatures. In a less restricted sense it is a general term for any material composed of *sediments* that are either consolidated or

unconsolidated, that is, hardened to *rock* or not.

seismic tomography^s A technique which uses the recording of vibrations within the earth produced by earthquakes, or artificially induced by detonation of nuclear bombs, to produce visual representations of the earth's three-dimensional internal structure. It involves computer processing of all the records of the passage of these seismic waves through the earth in order to build up such a three-dimensional picture of the internal layers of the earth characterized by their different physical and *chemical* properties.

seismology^v The study of earthquakes, and of the structure of the earth, by both natural and artificially generated seismic waves.

shale^v A *laminated, indurated rock* with more than 67% *clay-sized minerals*.

shape isomers^s *Isomers* are *molecules* that have the same number and type of *atoms* but differ in the arrangement of these *atoms*. In the case of *isotopes*, *isomers* are structurally different arrangements of *atoms* of the same *isotope*. Another way these structural differences can arise is by different ways of bonding for the same *atoms*, including bonding in different positions, which leads to different shapes.

shear wave^v The component of a seismic wave which causes motion in a direction perpendicular to the direction of motion, S-wave. Its speed is often about half of P-waves. S stands for secondary because it arrives later than the P-wave (primary wave). S-waves do not travel through liquids, or through the outer *core* of the earth.

shock metamorphism^s The totality of observed permanent physical, *chemical*, mineralogic and morphologic changes produced in *rocks* and *minerals* by the passage of high-pressure shock waves acting over time intervals ranging from a few microseconds to a fraction of a minute. The only known natural mechanism for producing such shock-metamorphic effects is the hypervelocity impact of large *meteorites*.

SHRIMP^v An acronym for sensitive **high resolution ion microprobe**.

siderophile^b *Elements* that have a weak affinity for oxygen and sulfur but are readily soluble in molten iron and therefore have a tendency to partition into the earth's *core*.

Sievert^h A unit of radiation dose, equal to 100 *rem*.

silicate (SiO₄)^s A compound whose crystal structure contains SiO₄ tetrahedra, either isolated or joined through one or more of the oxygen

atoms to form groups, chains, sheets, or three-dimensional structures with metallic *elements*. Most of the common rock-forming *minerals* are silicates, including *quartz*, *feldspars*, *pyroxenes*, *amphiboles*, and *micas*.

silicic magma^v Silica-rich molten *rock*.

sill^a A narrow *rock* body which has been injected between stratification.

slate^v A *metamorphic rock* which can be easily split into slabs and thin plates. Most *slate* was formed from *shale* by *metamorphism*.

sodic-granite^s *Granite* which has a bulk *chemical* composition high in sodium (Na), which results in it containing Na-rich *minerals*, such as Na-rich *pyroxenes* and *amphiboles*.

soil^v The unconsolidated *mineral* or organic material on the immediate surface of the earth that serves as a natural medium for the growth of land plants.

solar energetic particles^v High-energy particles (mainly *protons*, *electrons*, and *alpha-particles* [α -*particles*]) emitted by the Sun. The particles have velocities of hundreds of kilometers per second and the number are greatest during periods of maximum solar activity.

solar nebula^s The cloud of gas and/or dust which by rotating is conventionally thought to have led to the flattening of the mass and, as centrifugal forces exceeded gravity, matter was ejected to form the planets, while the gas and dust continued to coalesce to form the Sun.

solar spectroscopy^v The analysis of solar radiation using a spectroscope, an instrument whose main features are a slit and collimator, prism, telescope, and counter. A parallel beam of radiation is passed through the prism, dispersing different wavelengths through different angles of deviation, which can then be measured.

solar wind^v The stream of solar particles which is emitted by the Sun and travels outward through *space*. In the neighborhood of the Earth the solar wind has velocities in the range of 300–500 km/sec and an average density of 10^7 ions/m³.

solubilization^s The process of making a solid *compound* soluble, that is, preparing a solid to be dissolved in fluids (liquids and/or gases).

space^b The three-dimensional volume we can see directly. In relativity, a space-like slice of the four-dimensional space-time continuum. Often used as short form of the *fabric of space*, the *vacuum of quantum field theory*.

See *vacuum*, *fabric of space*, *ether*, and *heavens*.

spallation^c A nuclear reaction in which many particles are emitted from a *nucleus* by bombardment with particles of high enough energy.

specific heat capacity^v The amount of heat required to raise the temperature of a unit mass of material 1 °C.

specific ionization^s The number of ionizations per unit path length for *alpha-particles* (α -particles) with the same energy, as a result of *radioactive decay* of the same *radionuclide*. For a fuller explanation, see *Bragg ionization curves*.

speed of light^h The velocity, *c*, of *photons* in *vacuum*, 299,792 km/s, a number which pervades physics.

sphene^s See *titanite*.

spin^h The intrinsic angular momentum of an elementary particle or *nucleus*, which exists even when the particle is at rest, as distinguished from orbital angular momentum.

spin isomers^s *Molecules* that have the same number and type of *atoms* but differ in the arrangement of the *atoms*. When applied to *isotopes*, they are structurally different arrangements of *atoms* of the same *isotope*. One way this structural difference can occur is due to the *spin* of the *electrons* in their orbits which affects the way the *atoms* bond.

spinel^s A *mineral*: $\text{Al}_2(\text{MgO}_4)$. The magnesium (Mg) may be replaced in part by ferrous iron (Fe^{2+}), and the aluminum (Al) by ferric iron (Fe^{3+}). Spinel has great hardness, usually forms octahedral crystals (cubic system), varies widely in color, and is used as a gemstone. The name is also given to a group of oxide *minerals* with the general *chemical* formula: AB_2O_4 , where A=Mg, Fe, Zn, or Mn (or combinations), and B=Al, Fe^{3+} , Fe^{2+} , or Cr. The group includes magnetite (Fe_3O_4) and chromite (Fe, Mg) ($\text{Cr, Al}_2\text{O}_4$).

spinel-lherzolites^s *Intrusive igneous rocks* composed chiefly of the *minerals olivine*, *orthopyroxene* and *clinopyroxene*, in which *olivine* is generally the most abundant, but the *mineral spinel* is also present. *Spinel* has the general formula MgAl_2O_4 , but the magnesium (Mg) can be replaced by Fe^{2+} and the aluminum by Fe^{3+} . This *mineral* has great hardness and usually forms octahedral crystals which vary widely in color from colorless to purple-red, green, and yellow to black.

splits^s A term used to describe portions of a sample that have been broken

from, or separated/split from, the original larger sample.

spodumene^s A *mineral* of the *clinopyroxene* group with the *chemical* formula of $\text{LiAlSi}_2\text{O}_6$. It occurs in white to green elongated crystals, often of great size, especially in *pegmatites*.

spontaneous fission^c The splitting of a *nucleus* into two or more fragment nuclei without any external inducement by *neutrons* or other particles.

spontaneous symmetry breaking^c Under certain conditions a system obeying certain equations may transition to a solution which does not possess as much symmetry as the equations. The transition is said to “break” the symmetry. An example would be a magnetic field pointing in a certain preferred direction. The equations allow the field to point in any direction, but when the system magnetizes, it chooses a certain direction for the north-south axis of the magnetism.

sputtered^s Describes *atoms* or *molecules* ejected from the surface of a *mineral*, usually induced by an *electron* beam in a sophisticated research instrument. The word derives from an emitting process with a spitting sound, but at the atomic level on a *mineral* surface the ejection process need not be accompanied by sound.

stock^s An igneous *intrusion* that is less than 40 square miles (100 square kilometers) in surface exposure, and is usually (but not always) *discordant* (not parallel to the *rock* strata being intruded).

stony meteorites^s A general name for *meteorites* consisting largely or entirely of *silicate minerals* (chiefly *olivine*, *pyroxene* and *plagioclase*). They resemble *ultramafic rocks* in composition, and they constitute more than 90% of all *meteorites* seen to fall to the earth’s surface.

stony-irons^v A general name for relatively rare *meteorites* containing large (at least 25%) and approximately equal amounts (by weight) of both nickel-iron and heavy basic *silicates* (such as *pyroxene* and *olivine*).

stratigraphic^s The arrangement of *rock* strata, especially their geographic positions, the chronologic order of the strata sequence, interpretation of the strata in terms of environments or modes of origin, and their geologic history.

stratigraphic record^v *Geological*, *geochemical*, and *geophysical* information found in the layers of *rock* in the earth.

stretching-out of the heavens^h A Biblical concept which, according to Humphreys, may include the cosmological idea of the expansion of *space*.

- string theory^c** A theory in which the fundamental entities are not point particles but lines or curves which can vibrate and stretch in multidimensional spacetime.
- stromatolites^s** Organo-sedimentary structures produced by *sediment* trapping, binding, and/or precipitation as a result of the growth and metabolic activity of micro-organisms, principally *cyanobacteria* (blue-green algae). They occur in a variety of growth forms, from nearly horizontal to markedly columnar, domal, or subspherical.
- strong interactions^c** Events involving the quanta called *gluons* or of composite *bosons* such as the pion. The *strong interactions* provide the forces that hold the *nucleus* together. The *proton*, *neutron*, and other composite particles are also thought to be held together by *gluons*.
- strong nuclear coupling^c** A constant in the *field theory* of *strong interactions* which specifies the strength of the forms appearing in the fundamental equations of the theory. See *coupling constant*.
- strong nuclear force^h** The short-range force which holds an atomic *nucleus* together against the repulsive electrostatic force which would otherwise tear it apart.
- S-type granites^s** *Granites* which are defined as having been derived from predominantly sedimentary source materials based on using *Sr isotopes* and other *geochemical* criteria. This particular sedimentary source would be characterized by high initial $^{87}\text{Sr}/^{86}\text{Sr}$ ratios and a peraluminous composition [when the molecular proportion of aluminium (Al) oxides is greater than that of sodium (Na) and potassium (K) oxides combined].
- subaerial lava flows^s** Lateral outpourings of molten *rock* from a volcanic vent or fissure which flows over the land surface in the open air, where they cool and solidify to form *volcanic rocks*.
- subaerial volcanoes^s** Vents through which molten *rock* has come from the earth's interior about which a hill or mountain has been built, often of conical shape, from the ejected molten *rock*, called volcanoes, in this instance having occurred in the open air on a land surface.
- subcontinental lithosphere^s** That portion of the uppermost *mantle* beneath the *continental crust* which is cooler and mechanically stronger than the *mantle* below it and thus moves with the *continental crust* as part of the corresponding *plates* that are moving across the earth's surface

relative to one another.

subduction^b The recycling of *lithosphere* from the earth's surface into the *mantle*, usually at an oblique angle, and often adjacent to a continental margin.

subduction zone^b A long, narrow belt where one crustal *plate* has descended beneath another, for example, along the Peru-Chile Trench or in the volcanic arc belts of the western Pacific Ocean.

sublimates^s Solids that have been deposited by a gas or vapor, especially referring to a deposit made by a volcanic gas around the mouth of a volcanic vent or especially a *fumarole*. Usually such deposits are of metals or metal sulfides.

submarine basalts^s A general term for dark-colored, fine-grained *volcanic rocks* derived from *lava* flows under water on the ocean floor. They are chiefly composed of *plagioclase* and *clinopyroxene*, and different varieties are distinguished by the presence of other *minerals* such as *olivine*.

submarine eruptions^s Volcanic ejections or *eruptions* of molten *rock* and/or fluids and gases underwater on the ocean floor.

suites of rocks^s Sets or groups of *rocks*, usually of the same kind—*igneous*, *sedimentary* or *metamorphic rocks*—from the same area or region. In other words, they are a set or group of *rocks* that are usually related to one another.

sulfide salt^s A *mineral compound* characterized by the linkage of sulfur with a metal or semi-metal, such as lead sulfide (*galena*) or iron sulfide (pyrite).

sunburst effect^s The description for radiation being given off in all directions in three dimensional space from a centrally-placed particle, *grain* or object. It is derived from the analogy of the light being given off in all directions from the Sun.

supergene^s A *mineral* deposit or enrichment formed near the earth's surface, commonly by descending solutions, primarily *ground water*.

supergene hypothesis^s The idea or postulated theory that the subject in question is of *supergene origin*, that is, it has formed as a result of solutions, primarily *ground waters*, near the earth's surface having mobilized *elements*, *isotopes* or *compounds* in solution, taking them or leaching them from the source areas and transporting them downwards to enrich other *rocks* and *minerals*.

- supergene origin^s** The term used to describe the formation of a *mineral*, or a description of a process, that is related to the action of descending solutions, primarily *ground water*, near the earth's surface, usually to enrich or concentrate *elements*, *compounds* or residual materials that result from these processes.
- supergene solutions^s** The fluids responsible for enrichment and oxidation processes near the earth's surface, such solutions commonly being *ground waters* carrying dissolved *elements* and *compounds* leached from near the surface and carried downwards as part of the enrichment or *supergene* process.
- superheavy nuclei^c** Nuclei of mass beyond the mass range of the naturally occurring *elements*.
- supernova^c** A massive star which explodes when it has used all of its available nuclear fuel.
- superstring theory^c** *String theory* which incorporates supersymmetry, a symmetry relating *bosons* to fermion partners.
- sutured^v** The texture found in *rocks* in which *mineral grains* or irregularly shaped crystals interfere with their neighbors, producing interlocking, irregular contacts without interstitial *spaces*, resembling the sutural structures in bones.
- synthesize^s** To artificially produce *compounds* or *minerals* from their basic constituents, arriving at the true composition of the naturally-formed *mineral* or *compound*.
- tau^c** A *lepton* which is like an *electron* but about 3490 times as massive.
- tectonic^b** The earth's near surface structural features such as mountains, basins, arches, faults, and volcano chains and the large-scale dynamical processes that give rise to such features.
- tectonic province^v** A large area or region, all parts of which are characterized by a similar history of structural or deformational features differing significantly from those of adjacent areas.
- tensor^c** A quantity with subscripts transforming in a certain way defined by symmetry transformations of a problem.
- terrane^s** A term applied to blocks, or groups of *rocks*, and to the areas in which they crop out. The term is used in a general sense and does not imply specific *rock* units.

Tertiary^s The first period of the Cenozoic era of the *geological* timescale, conventionally thought to have covered the span of time between 65 and 1.8 million years ago. It is divided into five epochs—the Paleocene, Eocene, Oligocene, *Miocene*, and Pliocene. The term also applies to all the *rock* layers in the *geological* record which are believed to have been deposited or formed during that time period.

thermal aureole^s A zone surrounding an igneous *intrusion* in which the surrounding host *rock* (or *country rock*) shows the effects of the heat from the *magma* which has intruded it. It is often referred to as the zone of contact *metamorphism*, where the intruded host *rock* has been altered by the heat of the igneous *intrusion*.

thermal conductivity^v A measure of the ability of a material to conduct heat. A basic property of *rocks* that changes dependent on composition and geometry of *rock* matrix, porosity, and the pore medium.

thermal diffusivity^v The *thermal conductivity* of a substance divided by the product of its density and *specific heat capacity*. In *rock*, the common range of values is from 0.005 to 0.025 cm²/sec.

thin sections^s The fragments of *rocks* or *minerals* mechanically ground to a thickness of approximately 0.03 mm, and mounted on a glass microscope slide, with or without a glass cover slip. This reduction in thickness renders most *rocks* and *minerals* transparent or translucent, thus making it possible for light to be passed through so that their optical properties can be studied.

thorite^s A brown, black or sometimes orange-yellow *mineral* which is essentially thorium *silicate*, with a *chemical* formula of ThSiO₄. It is therefore highly radioactive and may contain as much as 10% uranium (U). It resembles *zircon* and occurs as a minor accessory *mineral* in *granites*, *pegmatites* and some related *granitic rocks*. It is therefore also another important *mineral* in the uranium-thorium-lead (U-Th-Pb) radioisotopic dating of those *rocks* containing it.

titanite^s A usually yellow or brown *mineral*, which can also be called *sphene*, with a *chemical* formula of CaTiSiO₅. It often contains other elements in trace amounts, such as niobium (Nb), chromium (Cr), fluorine (F), sodium (Na), iron (Fe), manganese (Mn) and yttrium (Y). It occurs in wedge-shaped or lozenge-shaped crystals as an accessory *mineral* in *granitic rocks* and in calcium-rich *metamorphic rocks*.

tonalitic gneisses^s Rocks formed by regional-scale *metamorphism* in which bands and layers of granular *minerals* alternate with bands and layers in which *minerals* having flaky or elongate habits predominate, with the *mineral* content being dominated by *quartz* (between 20 and 60%) and the *plagioclase* to total *feldspar* (alkali *feldspar* or *orthoclase* plus *plagioclase*) >90%. The descriptor is an essential factor in the definition of this *rock*, because it indicates the predominance of *quartz* and *plagioclase* in the *rock*. The other *minerals* in this *rock* would be *hornblende* and *biotite*, which would exhibit the preferred parallel orientation in contrast to the granular nature of the *quartz* and *plagioclase*.

tourmaline^s A group of *minerals* with the general *chemical* formula: $(\text{NaCa})(\text{Mg}, \text{Fe}^{2+}, \text{Fe}^{3+}, \text{Al}, \text{Li})_3\text{Al}_6(\text{BO}_3)_3\text{Si}_6\text{O}_{18}(\text{OH})_4$. It sometimes contains fluorine in small amounts. Tourmaline occurs in three-, six- and nine-sided elongated crystals, or in compact or columnar masses, its color varying greatly which provides the basis for naming its different varieties.

trace element^v An *element* that is not essential in a *mineral* but that is found in small quantities in its structure or adsorbed on its surfaces.

track density^c The number of *fission tracks* per unit area.

transition zone^b The solid *silicate* region of the earth between the 410-km *seismic discontinuity* and the 660-km *seismic discontinuity*. Several *mineral phase* changes occur in this region causing it to have a strong gradient in seismic velocity.

transitional element^v Any of the elements scandium (Sc), titanium (Ti), vanadium (V), chromium (Cr), manganese (Mn), iron (Fe), cobalt (Co), nickel (Ni), and copper (Cu), which have a partially filled subshell of *electrons* in their atomic structure. They commonly give color to *minerals*, exhibit a variable oxidation state, and may give rise to magnetism.

transmute^h To change one kind of *nucleus* into another.

Triassic^s The first *geological* period of the *Mesozoic era* in the *geological* timescale which is conventionally thought to have covered the span of time between 248 and 205 million years ago. The term is also applied to the *rock* strata of the *geological* record which were deposited or formed during this *geological* period. The name is derived from the three-fold division of these *rocks* in Germany.

troilite^s A hexagonal *mineral* present in small amounts in almost all

meteorites. It is an iron sulfide *mineral* with a *chemical* formula of FeS. It is a variety of the iron sulfide *mineral* called pyrrhotite, with almost no ferrous-iron (Fe^{2+}) deficiency.

true vacuum^c The *vacuum* state associated with a nonzero, equilibrium value of the *Higgs field*.

tunneling^h In nuclear and quantum theory, the process by which a particle can occasionally go through a *potential energy* barrier which would be classically impenetrable.

ultramafic^s Any variety of *igneous rock* composed chiefly of mafic *minerals* such as *pyroxenes* and *olivine*. Such *rocks* have a silica (SiO_2) content of <45%, and thus can sometimes just consist of one of the mafic *minerals*, as is the case with pyroxenite (solely *pyroxene*) and dunite (solely *olivine*).

ultramafic xenolith^s A foreign inclusion in an *igneous rock* of fragments of another *igneous rock* composed chiefly of mafic *minerals* such as a *pyroxene* and *olivine*, which usually have come from the earth's *mantle*.

ultraviolet laser ablation microprobe^s A sophisticated research instrument which uses ultraviolet light amplified by stimulated emission of radiation (laser), very finely focused as a beam onto the surface of a *mineral* to melt and remove *atoms* and *molecules* from the surface so that the *mineral* and its constituent *atoms* and *molecules* can be analyzed. The *atoms* and *molecules* removed from the surface of the *mineral* under the ultraviolet laser give off characteristic radiation which can be picked up by detectors as part of the instrument, which by comparison with previously analyzed materials with known compositions can then be used to calculate the composition or the level of constituents in the *mineral* being focused on by the laser beam.

unified theory^c A sought-after theory which explains all the known forces within the same framework and contains no artificially specified constants but instead derives all results from basic principles.

uniformitarianism^v The principle that the *geological* processes of the past differ neither in kind nor in intensity from those now in operation. (The present is the key to the past.) By its emphasis on the cumulative effect of slow actions over protracted periods of time, *uniformitarianism* implies a vast extension of geologic time.

upper mantle^b The mostly solid *silicate* region of the earth between the crust and the *410-km seismic discontinuity*.

uraninite^s A black, brown or steel gray *mineral* that consists of uranium (U) oxide, with a *chemical* formula of UO_2 . It is strongly radioactive and is the chief ore of U. It is a very dense and heavy *mineral*, and usually contains impurities such as thorium (Th) and lead (Pb), so that it can be very important in uranium-thorium-lead (U-Th-Pb) radioisotopic dating of those *rocks* and ores which contain it. It can be a trace *mineral* in some *granites* and *pegmatites*.

vacuum^h In modern quantum *field theory*, an imperceptible material which fills all *space*. It interacts with visible matter in subtle ways, but is otherwise invisible and undetectable by ordinary means. It is seen as the medium through which all fields propagate. It is supposed to be extremely dense, but it seems to be without direct gravitational effect, a major mystery in present-day physics. See *ether*, *fabric of space*, *space*, and *heavens*.

vaporized^s Synonymous with evaporated. This refers to when a substance has passed from the liquid or solid state to the vapor state, as in the example of the boiling of water which produces steam, water in the vapor or gaseous state.

variant dwarf halos^s These are *radiohalos* which are smaller in size than the standard *radiohalos* produced by *radioactive decay* of uranium (U) and/or thorium (Th) in the central *mineral inclusions*. They thus vary in size from the norm, and are a puzzle that still requires explanation.

vector^c A *tensor* requiring only one subscript. In three-dimensional *space*, a quantity having both direction and magnitude, often pictured as an arrow whose length is proportional to the magnitude being represented.

vein^s A thin, sheet-like igneous *intrusion* into a fracture or fissure. It can also be the infilling of a fault or other fracture in a host *rock* in tabular or sheet-like form, with introduced *minerals* deposited from solutions which flowed into the fracture or fault.

vesicles^s Cavities of variable shapes in a *lava*, formed by the entrapment of gas bubbles during solidification of the *lava*.

viscosity^v The property of a substance to offer internal resistance to flow.

volatility^v A measure of the tendency for materials in a *magma* to give off gases and vapors such as water or carbon dioxide when the temperature is

increased and the pressure is reduced.

volatilized^s To be made volatile, that is, readily converted to a vapor or gas, usually by heating.

volcanic rock^s A generally finely *crystalline* or glassy *igneous rock* resulting from volcanic action at or near the earth's surface, either ejected explosively or extruded as *lava*; for example, basalt. The term includes near-surface *intrusions* that form a part of the structure of a volcano.

volumetric cooling^v The reduction in temperature by the removal of energy throughout a three-dimensional volume by a process which does not depend on the *diffusion* of heat out of the body. Examples of such processes are adiabatic expansion, piezoelectric, and piezomagnetic effects.

W particle^h Either of two electrically charged *intermediate vector bosons*, either positive or negative, with a mass about 85 times that of a *proton*.

weak interactions^c Events now understood to involve the quanta of the W and Z *bosons*. The processes involved in *beta-decay* (β -decay) were the first *weak interactions* to be discovered.

weak mixing angle^h A constant appearing in the *Weinberg-Salam electroweak theory*.

weak nuclear force^h The extremely short-range force involved with *beta-decay* (β -decay) of *neutrons* and nuclei.

weathering^s The destructive process or group of processes by which earthy and *rocky* materials on exposure to atmospheric agents at or near the earth's surface are changed in color, texture, composition, firmness or form, with little or no transport of the loosened or altered material; specifically, the physical disintegration and *chemical* decomposition of *rocks* that produce an *in situ* mantle of loose particles that are thus prepared as *sediments* for subsequent transportation. Most *weathering* occurs at the earth's surface, but it may take place down to considerable depths, particularly where there are cracks in the *rocks* that permit easy penetration of atmospheric oxygen and circulating surface waters.

Weinberg-Salam electroweak theory^h A quantum *field theory* unifying the electromagnetic field and the *weak nuclear force*.

whitlockite^a A *mineral* found in some *meteorites*. The *mineral* is calcium-magnesium-iron (Ca-Mg-Fe) phosphate. Uranium (U) sometimes substitutes in this phosphate *mineral* making the uranium-lead (U-Pb) *model age*

method a possibility using this *mineral*.

whole-rock isochron^s An *isochron* derived from the radioisotopic analyses of a suite of samples from a *rock* unit where each entire *rock* sample is analyzed, in contrast to the radioisotopic analyses of each of the *minerals* in a single *rock*.

whole-rock ages^s *Radioisotopic “ages”* determined by totally crushing all of the *rock* sample, thus homogenizing all the contained individual *minerals*.

Wölsendorf halos^s *Radiohalos* found in a *fluorite vein* in *granite* at Wölsendorf, Bavaria, Germany.

xenocrysts^s Crystals that resemble *phenocrysts* in an *igneous rock*, that is, large crystals amongst many very fine crystals, but which are foreign to the body of *rock* in which they occur.

xenolith^b A *rock* fragment, usually within a larger *magmatic rock* body, whose origin is distinct or foreign from that of the larger *rock* body. Such *rocks* frequently represent pieces of wall *rock* stripped away as *magma* flows through a narrow *conduit*.

xenotime^s A brown, yellow or reddish *mineral* which is essentially yttrium phosphate, with a *chemical* formula of YPO_4 . It has an identical crystal structure to *zircon* and often contains *rare earth elements*, as well as thorium (Th), uranium (U) and zirconium (Zr), or other *elements*. It can thus be used for uranium-thorium-lead (U-Th-Pb) radioisotopic dating. It can occur as an accessory *mineral* in *granites* and *pegmatites*.

X-halos^s *Halos* of unknown origin of size intermediate between dwarf and *giant halos* only reported from three locations by early investigators between 1917 and 1926, but not found since even in many samples from the same locations. These *halos* have some similarities to thorium (Th) *halos*, but the ring structure does not seem to correlate with any known *alpha-decay* (α -*decay*) sequence corresponding to the energies represented. Some of the rings are diffuse, bleached or wide.

x-ray emission^s Non-nuclear electromagnetic radiation of very short wavelength, in the interval of 0.1–100 *angstroms* (Å) (10^{-11} – 10^{-8} m), issuing from a source.

x-ray fluorescence^s The type of *x-ray emission* in which the characteristic x-rays of a substance are produced by using x-rays of short wavelengths to induce the substance to emit x-rays of a longer wavelength.

young earth^v The belief that the earth is thousands of years old, as opposed to an *old earth*.

Z halo^s The designation given to *radiohalos* found in *biotite* in *rocks* in Japan by Japanese investigators in 1926 because they could not match these *halos* with other known *halo* types. This identification problem was probably due to the *thin sections* being too thick to permit accurate *halo* radii measurements, and it is quite probable that these *halos* were either uranium (U) *halos*, or a combination of (U) and thorium (Th) *halos*.

Z particle^h The electrically neutral *intermediate vector boson*, with a mass about 95 times that of the *proton*.

zircon^s A mineral which consists of zirconium *silicate* with a *chemical* formula of $ZrSiO_4$. It has a distinctive crystal structure, occurs in various colors, and is a common accessory *mineral* in *granites* and related *granitic rocks*, as well as in some *metamorphic* and *sedimentary rocks*. Because it is a hard *mineral* which is resistant to *weathering* and erosion, it is often present in sand deposits on beaches and along rivers. It contains trace amounts of uranium (U) and thorium (Th), and therefore is radioactive and an important *mineral* for uranium-thorium-lead (U-Th-Pb) radioisotopic dating.

zoned crystals^s The term used to describe crystals or *mineral grains* in which there are zones or areas varying in composition. For example, the margin of a crystal may have a different composition than the *core*, and this will have resulted from the *elements* available to the crystallizing *mineral* during its formation having changed as the crystal grew in size. The zones may sometimes result in physical differences within the crystals, reflecting the slight differences in *chemical* composition of the *mineral* and therefore of its resultant physical properties.

410-km seismic discontinuity^b Surface of moderate increase in seismic wave speed at approximately 410 km depth in the *mantle*. The increase in seismic wave speed is a consequence of *mineral phase transitions* from *upper mantle* phases to denser *transition zone* phases due to increasing *hydrostatic pressure*.

660-km seismic discontinuity^b Surface of abrupt increase in seismic wave speed at approximately 660 km depth in the *mantle*. The increase in seismic wave speed is a consequence of *mineral phase transitions* from *transition*

zone phases to denser *lower mantle* phases due to increasing *hydrostatic pressure*.

Appendix

July 2000

Research Proposals for RATE

Contents

Introduction	563
Research Proposals	
Helium (He) Diffusion	566
Isochron Discordance	569
Nuclear Decay Theory	576
Radiohalos	580
Fission Tracks	587
Uranium (U) and Thorium (Th) Halos	597
Case Studies in Isotope Decay	601
Biblical Word Studies	611
Plutonium (Pu) in Oklo Reactor	612
Allende Meteorite Origin	616
Diffusion of Argon (Ar) in Biotite	619
Origin of Chemical Elements	622
Cosmology and Nuclear Decay	626

Introduction

The RATE initiative (**R**adioisotopes and the **A**ge of the **E**arth) is a research program started in 1997 to develop and communicate an understanding of radioisotope data from a young-earth perspective. The group of six research scientists composing RATE have met four times so far to organize the research and publishing. The six scientists are: Dr. Steven A. Austin, Institute for Creation Research, Dr. John R. Baumgardner, Los Alamos National Laboratory, Dr. Eugene F. Chaffin, Bob Jones University, Dr. Don DeYoung, Grace College, Dr. D. Russell Humphreys, Sandia National Laboratory, and Dr. Andrew A. Snelling, Institute for Creation Research. Dr. Larry Vardiman of the Institute for Creation Research serves as senior editor and facilitator of the RATE group.

The RATE group is publishing this Status Report in 2000 to be followed by five years of research and a Final Report in 2005. At the 1999 meeting in Albuquerque, New Mexico a full day was devoted to the discussion of suggested research projects. Thirteen research projects were offered to the RATE group which are designed to resolve various issues or answer questions about how nuclear decay has occurred. The basic question which is addressed in most of these research projects is how do we explain the evidence for large amounts of daughter products.

It appears that much larger quantities of nuclear decay have occurred than would be expected for less than 10,000 years of radioactivity at the currently-observed rate. The evidence for this concern stems from (1) the presence of daughter isotopes along the entire decay chain in proximity to parent isotopes, (2) visible scars (halos) from α -decay, (3) the presence of the α -particles themselves (He nuclei) still within the rock where they were apparently formed by nuclear decay, (4) visible tracks from decay by fission, and (5) residual heat produced by nuclear decay in proximity to high U concentrations.

One of the models hypothesized by the RATE group is that at some time in the past a much higher rate of radioisotope decay has occurred leading to the production of large quantities of daughter products in a short period of time. It has been suggested that this increased decay rate could have been part of the Creation process and/or results of God's judgments upon man following the curse or during the Flood. A second model suggests that primordial daughter elements like Pb, Sr, He, and Ar were mixed together with parent elements like U, Rb, and K during catastrophic processes of Creation and the Flood. Both the

accelerated decay model and the mixing/inheritance model are beginning to show real promise in explaining why there seems to be an apparent conflict between the age of the earth stated in Scripture and simplistic calculations based on measurements of radioisotopic concentrations.

The rates differ between the conventional old-earth model and the young-earth creationist model in some cases by over five orders of magnitude (that is, 100,000 times). The RATE group believes this large difference may make it possible to validate a true model of earth history. For example, the expected rate of escape of He from rocks which have undergone a large degree of nuclear decay only a few thousand years ago would seem to indicate that much of the He should still be trapped in the rocks. The observation of missing He in the atmosphere and abundant He in the rocks would seem to validate this model. The amount of He diffusion for the Creation and evolution models are estimated to differ by about five orders of magnitude. This difference should be capable of confirmation in the laboratory. The exciting part of this effort is that the evolution model will be on the defensive if these differences are confirmed.

High Priority Research

Of the thirteen research projects suggested to the RATE group, five were selected for their value in addressing some of the most important questions in distinguishing the Creation and evolution models. These five projects will be emphasized in fundraising and rapid accomplishment. Estimated costs and timetables are approximate at this point. It is the intent of the RATE group to contract most of the studies to commercial, university, or government laboratories with oversight by members of the RATE group. Analysis, interpretation, and reporting of the results would be conducted by a principal RATE investigator. It is recognized that establishment of laboratories to specifically conduct this type of work may be extremely expensive and the results would tend to be disbelieved by critics. Consequently, cost and time estimates will need refinement after contract negotiations with selected laboratories have been completed. Estimated costs for each project are shown on the last page of each proposal including salaries and overhead.

Although all thirteen projects will contribute to the solution of the radioisotope dating problem, it is believed that priority should be given to the five projects identified with a “**High Priority**” flag on the first page of the proposal. Attempts will be made to advance the solution to these research projects rapidly during the first few years. If some of the first five projects are completed quickly or

sufficient amounts of funding and expertise are received to address the others, then the group will advance the timetable to address them as well.

Financial Support

Donors have already contributed about \$150,000 toward this effort. Another \$350,000 will be needed over the next five years to complete the entire research plan. Interested potential donors may contribute to either of the young-earth creationist organizations participating in RATE—the Institute for Creation Research or the Creation Research Society. Addresses and phone numbers for these organizations are shown below. Please refer to RATE when you call or write.

Institute for Creation Research
P.O. Box 2667
El Cajon, CA 92021
Telephone: (619) 448-0900

Creation Research Society
c/o Robert Gentet
305 Cloudmont Dr.
San Antonio, TX 78239

HIGH PRIORITY

Helium (He) Diffusion Experiments Can Test Accelerated Nuclear Decay Theory

D. Russell Humphreys, Ph.D.*

Introduction

Experimental measurements on the rate of diffusion of He through a naturally-occurring mineral, biotite, could provide a crucial test of a theory which explains “old” radiometric ages in a young world. The theory proposes that nuclear decay rates were millions of times faster during several episodes in the earth’s history, such as the third day of Creation and the year of the Genesis Flood. This “accelerated decay” theory would then explain the large variety of evidence for “billions of years” worth of nuclear decay in a world which other evidence and Scripture says is much younger than that.

One important evidence for accelerated-decay episodes is the *experimentally observed* large retention of radiogenic (nuclear-decay-generated) He in tiny crystals of zirconium silicate (zircons) in ancient granite in the Jemez volcanic caldera near Los Alamos, New Mexico. Uranium-238 trapped in the zircons has decayed through many steps to become ^{206}Pb , emitting eight α -particles per U atom in doing so. The α -particles are nuclei of ^4He , and as they come to a stop in the zircon, they grab electrons and become He atoms. Helium atoms are small and slippery, and they diffuse (spread out, “wobble”) through the crystal lattice of zircon fairly quickly.

At the He diffusion rates experimentally observed in zircon [Magomedov, 1970], the microscopic Jemez zircons should, even at room temperature, lose essentially all their He within just a few centuries. At the higher temperatures (100–200°C) at which the zircons existed deep within the formation, the loss rate should have been even faster. According to conventional nuclear dating, the zircons have existed for about “1.3 billion years.” Yet, as reported in a

* Sandia National Laboratories, Albuquerque, New Mexico

respected geoscience journal [*Gentry et al.*, 1982], the zircons still retain up to 58% of the He which would normally have been generated during that alleged time. It is hard to imagine how, unassisted, the zircons could retain that much He for even thousands of years, much less billions of years!

The Jemez zircons are embedded in larger crystals of a black mica called biotite, which in turn are sandwiched in between crystals of feldspar and quartz, all of which compose the fined-grained granite-like rock (granodiorite) of the formation. My hypothesis is that He diffuses much more slowly through biotite than through zircon. Thus the biotite would keep the He “bottled up” in the zircons for the necessary thousands of years elapsing from an episode of rapid nuclear decay until now.

To check this hypothesis, we need experimental measurements of the diffusion of He through biotite. There is extensive literature on various gases diffusing through a large variety of materials, but I have not found any experiments on He through biotite. However, there have been diffusion measurements of another noble gas, Ar, in biotite. Since He atoms are lighter and smaller than Ar atoms, He should diffuse faster. From the Ar-in-biotite data we can make very crude estimates of the He diffusion rates in biotite. The results turn out to be in just the right ballpark for an episode of rapid decay between 4000 and 6000 years ago—good news for creationists!

The same crudely-estimated diffusion rates for He in biotite are about 100,000 times too fast for the conventional geologic-age scenario, namely steady production and diffusion of the He over 1.3 billion years. That is, those rates would not allow the Jemez zircons to retain, after such a long time, anywhere near the amounts of He actually observed. That’s bad news for evolutionists!

One can always argue about the method of estimating the rates. But experiments could settle the matter decisively. Thus I propose that such experiments be done—radiogenic He diffusion in actual biotites from the Jemez. I think granodiorite samples from the same borehole are still available. For example, we could isolate the biotites containing zircons, heat them in a mass spectrometer under vacuum, and measure how much He emerges from the biotite at each temperature. We could also do the same thing for larger pieces of the granodiorite, perhaps crushing them under vacuum, to see how much He is retained in the other materials of the formation. It would also be good to repeat measurements on the zircons themselves.

Such experiments are not to be entered into lightly! The literature reports many subtle pitfalls in diffusion observations, so we require first of all a *highly-qualified experimenter* who is very experienced in such measurements. I am

not such a person! However, I would be happy to act as an advisor and sounding-board for such experiments, and to help analyze the data. Second, we need good laboratory equipment, such as a quantitative mass spectrometer with a vacuum-tight and clean oven attached. Possibly we could install such equipment either at the Institute for Creation Research in San Diego, or at the Creation Research Society's Van Andel Creation Research Laboratory near Prescott, Arizona.

I also propose some field measurements at Jemez caldera on how much He is actually leaving the ground surface and how much is emerging from the borehole in question. I'd like to find out if the He flow is in steady state, that is, if the rate leaving the ground is equal to the production rate estimated from the radioactivity of the formation. That could tell us whether there are any "sinks" of He between the zircons and the surface.

These experiments might be difficult, but the payoff could be great. The predictions of the Creation model and the evolution model differ by many orders of magnitude, and we already have a crude estimate which strongly favors the Creation model. If the experiment agrees with the Creation model, we could say with confidence that "over a billion years' worth of nuclear decay took place within thousands of years ago!"

At one stroke these experiments could both undermine conventional nuclear decay dating and also strongly support an alternative creationist explanation, accelerated nuclear decay.

References

- Magomedov, Sh. A., Migration of radiogenic products in zircon, *Geokhimiya*, 2, 263–267, 1970. In Russian. English abstract in *Geochemistry International*, 7, 203, 1970. English translation available from D. R. Humphreys.
- Gentry, R. V., G. L. Gish, and E. H. McBay, Differential helium retention in zircons: implications for nuclear waste containment, *Geophysical Research Letters*, 9, 1129, 1982.

TOTAL ESTIMATED COST \$100,000

HIGH PRIORITY

Mineral Isochron Method Applied as a Test of the Assumptions of Radioisotope Dating

Steven A. Austin, Ph.D.*

Introduction

The isochron dating method has been widely applied to indicate great ages of rocks. The most frequently cited “age of the earth” (4.54 ± 0.2 billion years) comes from a whole rock Pb-Pb isochron of selected meteorites. This age-of-the-earth calculation assumes that both the earth and the meteorites began billions of years ago with a common Pb isotope ratio. The “age of the earth” is thus based on (1) a cosmological assumption of homogeneous Pb, (2) constant radioactive decay of U to Pb, and (3) a closed isotopic system within the rocks being dated.

The whole-rock isochron dating method supposes a “cogenetic suite of rocks.” In the case of the chondritic meteorites, it is supposed that they all formed about the same time as the rest of the solar system from a mixture of pre-solar material that was isotopically homogeneous with respect to Pb. This assumption is elegant in its simplicity, but it has not gone unchallenged. One of the problems with whole-rock isochron dating is that different radioisotopes often give different ages for the same “cogenetic suite” of rocks [see *Austin and Snelling*, 1998]. The “cogenetic suite” must have significant variation in the concentration of the parent isotope in order to allow the various concentrations of the daughter isotope to exist. For Grand Canyon, the deeply buried Cardenas Basalt gives discordant Rb-Sr and K-Ar whole-rock isochron ages [*Austin and Snelling*, 1998]. The discordance between the two radioisotope systems indicates a fundamental problem with the assumptions of the whole-rock isochron method [*Austin*, 1994]. Alternatives to the conventional dating assumptions need to be explored.

* *Chairman, Geology Department, Institute for Creation Research, Santee, California*

Because the results of the “whole-rock isochron method” are tied to the debatable notion of a “cogenetic suite,” a better method of dating rocks needs to be devised. The “mineral isochron method” involves assumptions that are less speculative. The minerals within a single rock could be argued by the geologic character of a rock to have been in an isotopically homogeneous condition when the rock formed. Three examples are provided here.

First, a lava flow involves a mixing condition that should produce homogeneous isotopes within a single rock cooled from the lava flow. The crystallization process that forms minerals as a lava flow cooled is recognized to have little ability to concentrate selectively daughter isotopes within certain minerals.

Second, a diabase sill or dike that formed from magma injected rapidly into sedimentary strata should be well mixed isotopically. A rock extracted from such a sill or dike should have also been isotopically homogeneous in the beginning.

Third, a metamorphic event which heated a rock to above 400°C would cause recrystallization to occur throughout the rock, and that event would be expected to cause local homogenization of isotopes within mineral phases as recrystallization occurred.

Therefore, the concept of a “mineral isochron” within a rock may be geologically defensible and not as debatable as the notion of a “cogenetic suite” of rocks. This is why the “mineral isochron method” is superior to the “whole-rock isochron method.”

How the Mineral Isochron Method Works

Because different mineral phases of a rock each have different chemical affinities for parent and daughter elements, each mineral phase should have its own characteristic parent-daughter isotopic ratio at the time of crystallization. However, each mineral phase is likely to have been isotopically homogeneous with respect to the daughter isotope in the beginning because of the geologic condition of mixing. Crystallization cannot selectively isolate just the radiogenic isotope within the various isotopes of the daughter element. This is a geologically more-believable initial condition established for isochron dating.

Over time, the minerals within the rock will deviate from their assumed initial homogeneous values of the daughter isotope as significant radioisotope decay of parent occurs. Over time the mineral phase within a single rock that has the largest quantity of parent will acquire the largest quantity of daughter. According

to this theory, the degree of deviation within different mineral phases from the assumed initial value will be proportional to “age” of the rock. Furthermore, “mineral isochron ages” for different parent-daughter radioisotope pairs should give concordant “ages” if the two other assumptions of radioisotope dating apply (constancy of decay rates, closed-system requirement).

The “mineral isochron method” requires extraction and separation of significant quantities of different mineral phases of a single rock. This is a very tedious process involving significant skill in the laboratory. Heavy liquids and magnetism are the preferred techniques for separating minerals.

Once different mineral phases of a single rock are isolated, they need to be analyzed isotopically on a mass spectrograph. These multiple isotope analyses required are very costly. It is no wonder that geologists rarely perform mineral isochrons on rocks! Much more common are the abundant whole-rock “model ages” and the occasional whole-rock “isochron ages” published in the geologic literature.

Applications

Mineral isochron techniques find significant applications in testing two assertions made by the millions-of-years chronology of conventional geology. The technique allows a test of (1) “model ages” and “whole-rock isochron ages” published in the geologic literature, and a test of (2) concordance of different radioisotope pairs that, it might be supposed, all concordantly date the rock to one age. Ultimately, the mineral isochron method can be used as a partial test of the assumption of constant decay rate of radioisotopes in rocks. If the homogenization and closed system are assumed, then discordant mineral isochrons could argue for different decay rates between the various parent isotopes. Could α -emitting radioisotopes (U, Th, and Sm) have been accelerated to faster decay rates in the past than β -emitting radioisotopes (Rb and K)? This hypothesis could be testable by the mineral isochron method. If this hypothesis is correct, there should be systematic discordance within mineral isochrons.

In 1998, I extracted pure olivine from a basalt flow of the Toroweap lava dam in western Grand Canyon. That basalt had been dated by the whole rock K-Ar model age technique at 1.1 million years [*Rugg and Austin, 1998*]. However, the olivine contained a significant quantity of radiogenic Ar, even though the olivine has virtually no radioactive K. The simple measurement of “excess Ar” in the olivine of the basalt disproved the zero Ar initial condition assumption of the conventional K-Ar dating method. How many more published K-Ar model

ages await this simple challenge? *Snelling* [1999] summarized the “excess Ar” problem in volcanic rocks.

In 1998, I measured Rb-Sr, Sm-Nd, and Pb-Pb within three different mineral phases of a single diabase rock sample from the Precambrian sill in the Grand Canyon. The three mineral isochron “ages” appear to be strongly discordant with the Pb-Pb “age” being oldest and the Rb-Sr “age” being youngest. The cause of the discordance of “ages” from a single rock is very mysterious because logic dictates that a single rock should have a single age.

The implications need to be explored as to their impact on the assumptions of radioisotope dating. Mineral isochron analyses published in the literature usually involve only one radioisotope parent and daughter. These published analyses rarely contain the “complete” condition of various radioisotopes within the mineral phases of a single rock. The peer-review process within the evolutionary literature rarely allows discordant mineral isochrons to be published. That is why creationists need to do this work.

Proposal

My proposal is to continue to do mineral isochron dating of rocks which, because of their geologic context, had a high probability of being isotopically homogeneous when they crystallized (for example, ancient lava flows, ancient diabase sills, and ancient metamorphic crystallization events). Three mineral isochron applications are suggested:

- **The Beartooth Andesitic Amphibolite, Wyoming**—This rock of the Beartooth Mountains of northwestern Wyoming is widely claimed to be one of the oldest rocks of the United States. An impressive Rb-Sr whole-rock isochron age of 2.790 ± 0.035 Ga [*Wooden et al.*, 1982] is believed to date the metamorphic event that recrystallized this rock. The precursor rock is suggested to be over 3.2 billion years old. The minerals quartz, plagioclase, biotite, hornblende, titanite and magnetite have been separated from a sample of the rock. A mineral isochron analysis should be performed to test for concordance of the different radioisotopic clocks. Will the various mineral isochron ages agree with the Rb-Sr whole-rock isochron?
- **Diabase Sill from the Precambrian of Grand Canyon**—The diabase of western Grand Canyon is an excellent target for mineral isochron analysis. Olivine, diopside and plagioclase are abundant minerals within the diabase. Whole-rock isochron ages need to be constructed from ten samples collected from the sill at Bass Rapids. Will Pb-Pb, Sm-Nd and Rb-Sr mineral and whole-

rock isochrons be concordant? Study of the diabase is enhanced because the geochemistry is well understood and problems are evident in the K-Ar dating method.

• **Chert and Dolomite of the Redwall Limestone, Grand Canyon**—Interbedded chert and dolomite of the Thunder Springs Member of the Redwall Limestone have been demonstrated to have a significant variation in their Rb-Sr ratios. Hydrothermal sedimentary process appears to have homogenized Sr isotopes very early in the history of these rocks. The hydrothermal process transformed the original lime sediment either to dolomite or chert according to the texture of the original lime sediment. Today, because of the differences in abundances of Rb between chert and dolomite, a significant variation in Sr isotopes should be expected to exist between the chert and dolomite. Thus, a Rb-Sr isochron should be easily constructed. Whole-rock Rb-Sr, Sm-Nd and Pb-Pb isochrons should be attempted. Mineral concentrates from chert and dolomite could be made by acid treatment of the rock. Would any of these dates agree with the formation's conventional Mississippian assignment?

• **Lava Dams in Western Grand Canyon**—*G. Brent Dalrymple and W. K. Hamblin* [1998] have concluded recently that most of more than 60 published K-Ar model ages on Pleistocene basalts in western Grand Canyon are in error. What is the cause of this widespread error when the conventional K-Ar model age is produced? Could it be a mineral phase of these basaltic flows is retaining excess ^{40}Ar making them appear excessively old? Recently, *Rugg and Austin* [1998] concentrated olivine from a Pleistocene lava dam in western Grand Canyon and found it to yield an K-Ar "age" of 20.7 ± 1.3 million years. Could olivine be the mineral phase that is giving unacceptably old K-Ar model ages? This hypothesis needs to be tested by Ar isotopic analysis of individual mineral phases of Grand Canyon lava dams. The simple measurement of "excess Ar" in the olivine of the basalt disproves the zero Ar initial condition assumption of the conventional K-Ar dating method. How many more published K-Ar model ages await this simple yet profound challenge? *Snelling* [1999] summarized the "excess Ar" problem in volcanic rocks.

Cost and Hour Analysis for a Mineral Isochron

In this section I summarize the cost of materials and contracted measurements that are needed to generate a five point mineral isochron using six isotopic pairs. I also estimate the researcher's time requirement. This analysis assumes a "complete" analysis. The isotopic pairs are U-Pb, Th-Pb, Pb-Pb, Sm-Nd, Rb-

Sr, and K-Ar. This is the cost analysis for the “Beartooth Andesitic Amphibolite” that I am currently conducting at the ICR Geology Lab. For the Beartooth project there are five mineral phases and one whole rock.

Heavy liquids used to separate minerals	\$100
X-ray diffraction analysis of mineral phases (to prove identity and purity of mineral phases)	\$700
Postage, supplies, and telephone	\$50
Multi-element chemical analysis (6 x \$151) (68 elements on whole rock and mineral phases)	\$906
K-Ar analysis (6 x \$350)	\$2100
Rb-Sr, Sm-Nd, and Pb-Pb isotopes (6 x \$800)	\$4800
U (ppm) and Th (ppm) by ID (6 x \$300)	\$1800
Total	\$10,456

This cost estimate of \$10,500 for a “complete” mineral isochron analysis of a rock does not include the salary of the primary scientist or the cost of sample collection in the field. Sampling costs differ by collection location.

The primary research is expected to require about 500 hours of time to perform a “complete” mineral isochron analysis and prepare a document ready for publication. The hourly allotment of the single scientist is as follows:

Sample selection and collection	40 hours
Sample preparation and mineral separations	150 hours
Administrative Time (working with vendors)	60 hours
Analysis Time (data analysis and computations)	150 hours
Report Writing (writing and review for publication)	100 hours
Total	500 hours

Summary

Mineral isochron analysis, a tedious procedure that is performed on a single rock, has significant applications to testing the “ages” of rocks assumed by evolutionists. The process of generating a “complete” mineral isochron (see Beartooth example described above) potentially generates 36 model “ages” and six “mineral isochron ages” for a single rock. These ages should be concordant if evolutionary assumptions are true. Thus, the mineral isochron provides a significant test of the evolutionary model. If there are significantly discordant “ages” within a single rock, creationists may be able to propose an alternate model. These research challenges await creationists of the future who seek to reinterpret “ages” assigned by radioisotopes to rocks.

References

- Austin, S. A., (editor), *Grand Canyon: Monument to Catastrophe*, Institute for Creation Research, Santee, California, pp. 111–131, 1994.
- Austin, S. A., and A. A. Snelling, Discordant potassium-argon and model and isochron “ages” for Cardenas Basalt (Middle Proterozoic) and associated diabase of Eastern Grand Canyon, Arizona, in *Proceedings of the Fourth International Conference on Creationism*, edited by R. E. Walsh, pp. 35–51, Creation Science Fellowship, Pittsburgh, Pennsylvania, 1998.
- McKee, E. D., W. K. Hamblin, and P. E. Damon, K-Ar age of lava dam in Grand Canyon, *Geological Society of America Bulletin*, 79, 133–136, 1968.
- Rugg, S. H., and S. A. Austin, Evidences for rapid formation and failure of Pleistocene “lava dams” of the Western Grand Canyon, Arizona, in *Proceedings of the Fourth International Conference on Creationism*, edited by R. E. Walsh, pp. 475–486, Creation Science Fellowship, Pittsburgh, Pennsylvania, 1998.
- Snelling, A. A., “Excess argon”: the “Achilles’ Heel” of potassium-argon and argon-argon “dating” of volcanic rocks, *Institute for Creation Research Impact #307*, 4 p., 1999.
- Wooden, J. L., P. A. Mueller, D. K. Hunt, and D. R. Bowes, Geochemistry and Rb-Sr geochronology of the Archean rocks from the interior of the southeastern Beartooth Mountains, Montana and Wyoming, *Montana Bureau of Mines and Geology Special Publication 84*, pp. 45–55, 1982.

TOTAL ESTIMATED COST \$50,000

HIGH PRIORITY

Theoretical Mechanisms of Accelerated α (Alpha) and β (Beta) Decay

Eugene F. Chaffin, Ph.D.*

Introduction

Within physics research today, there are various theoretical models being considered which involve variable “constants,” and hence could lead to accelerated nuclear decay. The models include variable fine-structure constant, cosmological constant, dielectric permittivity, speed of light, gravitational coupling G , strong nuclear coupling g , etc. [*Damour and Dyson*, 1996; *Okun*, 1996; *Wyss*, 1997; *Barrow and Mageuijo*, 1998a, b; *Li and Gott*, 1998; *Ivanchik et al.*, 1999].

On the one hand, experimental and observational limits on possible recent variation of these so-called “constants” keep getting tighter, while on the other hand new bodies of theory keep appearing which may indicate that accelerated decay is possible. Usually, conventional science restricts these variations to the time of the early universe, soon after the big bang. As has been noted [*Chaffin*, 1990, 1994], episodic or transient variations are more difficult to rule out, and may be needed as mechanisms of the variable decay useful to explain isotopic abundances found in rocks.

Why the Research Project is Needed

Study of fission track dating, isochrons using various isotopes, etc. keep turning up data which appears to be convergent upon an old age for a rock, contrary to what a young-earth creationist might at first expect. We also find that various data which give old ages for recent rocks, that is, the Kilauea lava flows measured in the 1970s, the Austin data for Grand Canyon rocks, etc. indicate that apparent

* *Professor of Physics, Bob Jones University, Greenville, South Carolina*

“age” can be inherited from parent magmas.

What we need is a creationist theory of the isotopic abundances in the earth, including the source regions for these magmas. Where physics enters the picture is in explaining or attempting to explain the isotopic abundance variations with time. If there has been accelerated decay at some points in earth history, it will be impossible to successfully explain the data without recognizing and modeling this fact.

Description of the Research Project

Various models of accelerated decay exist already in the conventional literature, but have not been adapted to the creationist worldview. For example, *Olson and Jordan* [1987] considered the effect of a variation in the cosmological constant on the age of the universe, but ruled out *a priori any ages less than several billion years*. The reason they did that was not due to any inherent difficulties within their model, but due to their assumption that this would be inconsistent with other bodies of knowledge about earth history. What we propose to do in this project is to examine various theoretical models without allowing this bias to color the results.

We examine the theories which exist already in the physics literature, examine the extent to which they can be useful to a young-earth viewpoint, and develop where necessary the equations and theory needed to extend these results to the parts of parameter space appropriate to the young-earth viewpoint. If new theories suggest themselves which have not already been developed, we pursue those theories until it becomes apparent whether they work.

Estimates of Manpower and Costs

Manpower would consist of the man-hours needed to reach the goals outlined above; finding the best theories. Since the best theories may not turn out to be the first ones examined, the needed number of man-hours is only speculation at present. A secondary problem is computer resources and availability of literature resources.

Estimates of Timeframe

Each theory which is taken seriously is its own problem. To examine a theory involves reading the background papers, gathering new papers when needed,

working on the derivations and understanding of the equations, and adaptation to the values of the parameters appropriate to a young-earth model. In some cases papers may need to be translated out of foreign languages such as German or French, in order to extract the information.

To properly evaluate a theory involves the problem of how much familiarity the physicist already has with the background subject matter. For a person with a Ph.D. in theoretical physics, we may typically be talking about a timeframe of several months to a few years, depending on the extra duties which the physicist may be responsible for at his place of employment. Theories may turn out to be dead-end streets. For example, *Georgi and Glashow* [1974], proposed the SU(5) group as the basis for unifying strong, weak, and electromagnetic forces. It predicted that the same coupling strength, the fine-structure constant, characterizes all three kinds of interaction. The theory was very successful, and is still accepted as a good approximation to the real world of particle physics. However, it predicted decay of the proton, a prediction which is still not verified. Consequently, theorists look for alternatives to this theory to represent the real world.

What is Expected to Be Learned from the Research Project

I expect to find out if there are any good theories which can be successfully applied within a young-earth framework, to explain isotopic data with accelerated decay.

What Follow-up Research is Needed

After a successful theory is found, follow-up research might involve applying the theory to various data, to see what the limits of the method might be. For example, Rb-Sr data might be examined to see if there is any signal present in the noisy data present in the literature.

References

- Barrow, J. D., and J. Magueijo, Varying-alpha theories and solutions to the cosmological problems, *Physics Letters*, *B443*, 104–110, 1998a. Also available on the Los Alamos preprint server (xxx.lanl.gov) as paper astro-ph/9811072.
- Barrow, J. D., and J. Magueijo, Solutions to the quasi-flatness and quasi-lambda problems, *Physics Letters*, *B447*, 246–250, 1998b. Also available on the Los

- Alamos preprint server (xxx.lanl.gov) as paper astro-ph/9811073.
- Chaffin, E. F., The difficulty in obtaining realistic conclusions about variable “constants”, *Creation Research Society Quarterly*, 27, 6–9, 1990.
- Chaffin, E. F., Are the fundamental “constants” of physics really variables? in *Proceedings of the Third International Conference on Creationism*, edited by R. E. Walsh, pp. 143–150, Creation Science Fellowship, Pittsburgh, Pennsylvania, 1994.
- Damour, T., and F. Dyson, The Oklo bound on the time variation of the fine-structure constant, *Nuclear Physics*, B480, 37–54, 1996. Also available on the Los Alamos preprint server (xxx.lanl.gov) as paper hep-ph/96066486.
- Georgi, H., and S. L. Glashow, Unity of all elementary-particle forces, *Physical Review Letters*, 32, 438–441, 1974.
- Ivanchik, A. V., A. Y. Potekhin, and D. A. Varshalovich, The fine-structure constant: a new limit on its cosmological variation and some theoretical consequences, *Astronomy and Astrophysics*, 343, 439 1999. Also available on the Los Alamos preprint server (xxx.lanl.gov) as paper astro-ph/9810166.
- Li, L.-X., and J. R. Gott, III, Inflation in Kaluza-Klein theory: relation between the fine-structure constant and the cosmological constant, *Physical Review*, D58, 102513, 1998. Also available on the Los Alamos preprint server (xxx.lanl.gov) as astro-ph/9804311.
- Okun, L. B., Fundamental constants of nature, invited paper to appear in the *Proceedings of the Fifteenth International Conference on Atomic Physics: Zeeman-effect centenary*, held at the Wan der Waals-Zeeman Laboratory, University of Amsterdam, August 5–9, 1996. Also available on the Los Alamos preprint server (xxx.lanl.gov) as paper astro-ph/9612249.
- Olson, T. S., and T. F. Jordan, Ages of the universe for decreasing cosmological constants, *Physical Review*, D35, 3258, 1987.
- Wyss, W., The speed of light as a dilaton field. Available on the Los Alamos preprint server (xxx.lanl.gov) as paper gr-qc/9711065, 1997.

TOTAL ESTIMATED COST \$30,000

HIGH PRIORITY

The Geological Distribution of Polonium (Po) Radiohalos

Andrew A. Snelling, Ph.D.*

Introduction

For three decades creationist Robert Gentry has been at the forefront of research on radiohalos, identifying and characterizing them [*Gentry*, 1966; 1973; 1974; 1986]. These halos are minute spheres of discoloration around microscopic inclusions within grains of minerals such as biotite. The microscopic inclusions (often the mineral zircon) contain significant quantities of radioactive elements such as U and Th. At various steps in the decay chains of these radioactive elements α -particles are released. These are energetic and fly off in all directions surrounding the inclusion, and like little bullets they damage the crystal lattice of the host mineral, discoloring it. However, the particles only have a finite amount of energy, so as they pass through the crystal lattice of the host mineral their energy is dissipated and they quickly stop.

Since all α -particles at a particular step in the decay chains have the same amount of energy, they will all travel the same distance and stop at the surface of a sphere whose center is the microscopic inclusion. Since the most damage is done to the host mineral's crystal lattice at the point where the particles stop, that will be where there is the greatest discoloration. In cross-section there will be a dark ring equidistant from the minute inclusion. Furthermore, because those steps in the decay chains responsible release α -particles of different energies characteristic of each step, the resultant damage to the host mineral's crystal lattice appears as concentric spheres, or in cross-section, as concentric rings. Knowing the energies of the different α -particles it is possible to identify each of the rings corresponding to the steps responsible in the decay chains.

It is therefore possible, by measuring in a thin section that passes through the

* *Geology Department, Institute for Creation Research, Santee, California*

central inclusion the radii of the different rings, to identify which radionuclides were responsible for each ring and therefore which radionuclide was the original parent. In this way Gentry (and others) have identified copious numbers of U and Th radiohalos in biotites and other minerals in various rocks from different parts of the world. However, Gentry has also found radiohalos, whose rings indicate that the parent radionuclides responsible for them were the three isotopes of Po which are found in the lower half of the ^{238}U decay chain.

There are three types of Po radiohalos— ^{218}Po radiohalos (in which the ^{218}Po ring represents the highest radionuclide from the ^{238}U decay chain present); ^{214}Po radiohalos (in which the ^{214}Po ring represents the highest radionuclide in the ^{238}U decay chain present); and ^{210}Po radiohalos (in which the ^{210}Po ring represents the highest radionuclide in the ^{238}U decay chain present.) In each case all the higher radionuclides in the ^{238}U decay chain are absent, which implies that there has been no U but only Po in the central inclusions. However, herein lies the “tiny mystery” of these Po radiohalos. Since the half-lives of these radionuclides are three minutes (^{218}Po), 164 microseconds (^{214}Po) and 138.4 days (^{210}Po), there were only brief intervals of time during which the Po could be separated from its parent U, incorporated in its inclusion host, and then emit the 100–500 million α -decays necessary to produce the radiohalo rings before all the Po radionuclides had decayed away.

Gentry has interpreted these occurrences to imply that the host rocks were instantaneously formed and therefore represent created rocks. This is because he interprets the parent Po radionuclides as themselves being parentless, that is, they were not formed by radioactive decay from U but are primordial or created Po. Gentry has thus called the Po radiohalos, God’s fingerprints on Creation.

Needless to say, establishment scientists have reacted against this interpretation, and thus all manner of efforts have been made to present counter explanations for these Po radiohalos that do not require supernatural intervention. However, in the words of G. Brent Dalrymple (at the 1981 Arkansas “trial”), these Po radiohalos remain a “very tiny mystery” [Gentry, 1986, p. 122], simply because none of the alternate interpretations satisfactorily explain the occurrence of these radiohalos (or so it would appear.)

Of course, the major objection by the scientific establishment community to Gentry’s interpretation of the Po radiohalos is based on what they believe the age of the earth to be. Nevertheless, some young-earth creationists have also been critical of Gentry’s interpretation of the evidence, or they have suggested alternative explanations.

Why the Research Project is Needed

Gentry has maintained that the rocks in which the Po radiohalos are found (apart from the secondary ^{210}Po radiohalos found in coalified wood) are granites, or granitic rocks, but opponents dispute that. Being a physicist, it is understandable that Gentry did not have the full geological background, and did not do all the field work necessary, to identify the rocks in which the Po radiohalos occur or to understand their geological settings.

Where the Po radiohalos are found in biotite in Mesozoic granite of the White Mountains of New Hampshire, which intrudes metamorphosed fossiliferous Paleozoic sediments which would be accepted as Flood-deposited rocks, Gentry still insists that the granite is a created rock. Interestingly, this Conway Granite of New Hampshire contains above average U concentrations, while a number of other rocks containing these Po radiohalos are either associated with, or occur close to, known U deposits (for example, in Canada).

This has led to the tentative suggestion that the Po may have somehow been separated from its parent U in hydrothermal solutions, that then penetrated the cleavage planes in the crystal lattices of biotite grains where it was quickly concentrated within the microscopic inclusions, there to subsequently form the radiohalos. But this would seemingly all have to happen in a very short timespan because of the half-lives of these Po isotopes. This problem might be overcome if the concentrations of U, and therefore Po, were high, which is why there may be an association with U-rich rocks or U deposits, and if the flow of the hydrothermal fluids was prolonged while the microscopic inclusions continually "scavenged" the Po from them to replenish the Po which was rapidly decaying.

Gentry has responded to the criticisms hurled against his interpretation and to alternate explanations [for example, *Gentry*, 1986; 1989], yet the geological distribution of these Po and other radiohalos has never been fully determined. Gentry has said that there is some evidence in one instance that is consistent with enhanced radioactive decay (perhaps faster decay rates), and from the evidence we have already, all three Po radiohalos are not always present in the samples so far studied and documented, nor are U and Th halos.

Gentry usually obtained his samples of biotite, fluorite and other minerals in which the radiohalos occur from various museums, or in the case of the New Hampshire granite, samples of biotite separates that had been made at the University of Ohio for K-Ar dating of the biotites. *Wise* [1989] has endeavored to tabulate all that we know about the geological occurrences of the rocks in which Gentry found Po radiohalos (uniformitarian age, rock type, intrusive

relationships, host mineral, etc.), but details are incomplete. Not all the Po radiohalos are in granites of uniformitarian Precambrian age, and some are in “vein-dikes” of unusual mineralogical composition. Some are in pegmatites.

This is why we need to find out exactly what is the geological distribution of these Po radiohalos—the types of rocks they are in, any correlations to U deposits or elevated U contents, what spread of uniformitarian ages, what host minerals, which Po radiohalos, whether U and/or Th halos are also present, and any other pertinent details. From these data it should be possible to test the interpretations of, and explanations for, these Po radiohalos, including whether there has been an episode of rapid radioactive decay rates in the past. There may be also other clues as to the geochemical behavior of the radionuclides in the U and Th decay chains, which are needed in our quest for alternative explanations to the long-age radioactive dating methods.

Description of the Research Project

Given the widespread occurrence of granitic rocks, and other potential host rocks, it would first of all be necessary to narrow down the enormity of the task by selecting geological provinces or geographical areas of Phanerozoic (Flood) age for investigation and sampling according to their accessibility and their likelihood of containing Po radiohalo-bearing rocks. Since we already know that Po radiohalos have been found in granites with elevated U concentrations, and in rocks associated with, or in proximity to, U deposits, then these criteria could be used for sampling site selections.

Pegmatites and pegmatitic veins containing minerals known to host Po radiohalos could be another sampling target. Areas from where Gentry’s Po radiohalo-bearing samples came would also be worth further investigation and sampling if accessible. For example, a suite of granite samples from the White Mountains of New Hampshire has already been collected from the outcrops where Gentry’s biotite samples were selected, so they now need to be searched for halos.

Once prospective areas have been selected then the field work could commence, with suites of samples being collected from respective rock types, particularly if they contain large biotite grains. Attention needs to be paid to recording the field relationships of the rocks sampled. Back in the laboratory the painstaking search for Po radiohalos begins with liberating biotite grains from the samples. It is best if the biotite flakes and grains can be handpicked, but if required the rocks can be coarsely crushed so that the biotite grains can be

separated.

Following Gentry's procedure, the next stage is to use clear durex or "sticky" tape to lift thin flakes from the separated biotite grains and to stick them onto glass microscope slides for examination under the microscope. There the flakes can be scanned visually to see if they contain inclusions with radiohalos around them. The process often has to be repeated for a given sample, because in order to identify the radiohalos one has to have a cross-section that cuts centrally through the minute inclusions and gives the proper dimensions of the rings. Thus it can be a process of repeatedly peeling off flakes of biotite and examining them under the microscope, discarding many until success is achieved.

Even when Po radiohalos are found in a sample, it could well be necessary to continue studying the biotite flakes in those samples to get a statistical estimate of the numbers of the Po radiohalos and to guarantee their correct identification, plus to be sure all three types of Po radiohalos are present or whether one or more are absent, and to determine whether U and/or Th halos are also present and how many. Such data could prove significant when it comes to compiling the results of the study and drawing conclusions.

There will obviously be some trial and error in the course of the project, as not all areas selected for sampling will yield samples containing Po radiohalos. Also, extra samples may have to be collected from some areas, and enough areas need to be sampled to guarantee a good statistical coverage so as to have enough data from which to draw significant conclusions. Thus, the project could end up being quite large, with large suites of samples collected and processed from quite a few field areas.

Estimates of Manpower and Costs

Clearly this is a project where competent and trained people can be enlisted to assist with the field work, sample collection, and sample processing. Obviously, the more of such people that can be enlisted, the more areas that can be sampled and the more samples that can be processed to give the largest possible database within the timeframe of the project. Several people have already been approached and are keen to help.

The major costs would be incurred in doing the field work and sample collection, and will depend on the mode of travel and length of stay in field areas. There would also be costs sometimes incurred in transporting samples to the processing laboratory (laboratories). Laboratory costs would be minimal. Manpower costs could be minimized if those collaborating had their salaries

already covered by their institutions or if they were volunteering their time. Whilst it is difficult to provide a specific estimate of the overall costs when there are so many unknowns, it would be hoped that the project could be accomplished for \$50,000.

Estimates of Timeframe

The extensiveness of this project would require a full five-year period to accomplish, even with several collaborators. There would be 3–6 months of literature search to select the target areas, followed by three years of field work and sample collection overlapping with sample processing, but aiming to have all samples processed and the database generated by the end of the fourth year. This would allow the last year for data interpretation and preparing a paper or papers reporting the results.

What We Expect to Learn from the Research Project

We would expect the project initially to teach us a lot more about the distribution in the Phanerozoic (Flood) geological record of Po radiohalos and to test the various explanations that have been proposed for the production of these radiohalos. There may even be evidence for accelerated radioactive decay, but we would definitely learn whether there is a correlation between the occurrence of radiohalos and granitic rocks with elevated U contents and/or U deposits. This could then have implications, particularly if the Po radiohalos were repeatedly found in the Phanerozoic (Flood) section of the geological record. The project would certainly be a test of Gentry's interpretation. We are agreed that the radiohalos as a physical record of radioactive decay are significant, and therefore this project would further the objectives of the RATE initiative.

What Follow-up Research would be Needed

A lot will depend on how much is achieved during the five-year period the project is in progress, and in particular how large a database is gathered. It may well be that further time is needed to gather and process more rock samples to build the database large enough so that significant correlations, trends and implications can be drawn from it.

Alternately, the data gathered may indicate certain correlations, trends or peculiarities that need follow-up work, sample collection and sample processing.

A lot will depend on what comes out of the project as it proceeds, but we would still hope that some closure could be brought to the project sufficient for the immediate needs of the RATE initiative. Further investigations would then continue beyond the RATE initiative, including an inventory of Po, U and Th halos in Precambrian (pre-Flood) rocks following the same procedures.

References

- Gentry, R. V., Alpha radioactivity of unknown origin and the discovery of a new pleochroic halo, *Earth and Planetary Science Letters*, 1, 453–454, 1966.
- Gentry, R. V., Radioactive halos, *Annual Review of Nuclear Science*, 23, 347–362, 1973.
- Gentry, R. V., Radiohalos in a radiochronological and cosmological perspective, *Science*, 184, 62–66, 1974.
- Gentry, R. V., *Creation's Tiny Mystery*, Earth Science Associates, Knoxville, Tennessee, 1986.
- Gentry, R. V., Response to Wise, *Creation Research Society Quarterly*, 25, 176–180, 1989.
- Wise, K. P., Radioactive halos: geological concerns, *Creation Research Society Quarterly*, 25, 171–176, 1989.

TOTAL ESTIMATED COST \$50,000

HIGH PRIORITY

A Research Proposal to Survey Fission Track Densities of Holocene Volcanic Tephra

Joseph W. Bielecki, M.S.*

Introduction

Although this proposal was originally written at the request of the RATE group to study Holocene rock strata, it has been determined that the same method could also be applied to rock strata which were formed during the Flood. Therefore, the references to Holocene strata or Flood/post-Flood boundary should be revised to include the Paleozoic and Mesozoic strata which are considered to be Flood layers. (editors)

Subject and Purpose

The Flood/Post-Flood boundary in the geologic column is highly debated by supporters of the recent Creation model of the universe. This boundary marks the end of a global Flood event described in Scripture. It is speculated that other fundamental universal effects (that is, increases in radioactive decay rates) are connected to this global event. Taking into account these speculations, the following proposal gives a plan for research to analyze Holocene tephras for such radioactivity effects to help locate the Flood/post-Flood boundary.

Statement of the Problem

The recent-Creation model of the universe places Creation about ten thousand years ago. This earth history model includes a global catastrophic Flood described in Scripture (Genesis 6–8). One geological effect of the Flood is that massive tectonic changes brought about an event of volcanism sometime during and

* Clinton Township, Michigan

immediately after the waters subsided. One sub-theory suggests that the Flood may be connected to or be a result of a more universal episode, namely a change in universal physical constants.

A growing group of recent-creationists recognize that attempts to date archaeological and geological artifacts by way of radioactivity are in principle legitimate methods. Though, they would caution that the assumptions intrinsic to the methods must be made appropriately. This same group faces a difficulty. In situations where old ($>10,000$ yr) radioactive derived ages, or in other terms, high amounts of radioactivity (large amounts of radiogenic daughter or higher spontaneous fission track densities than expected) are observed in specimens some scientists may be inclined to propose episodes of accelerated nuclear decay in universe history. The claim is that one such episode occurred during the Flood. To date, no clear scientific experimental evidence has identified any such event.

Proposed Solution

This study will provide data points to judge when in geologic time an accelerated nuclear decay event occurred. An attempt was made to find a signature related to accelerated nuclear decay brought about during the Flood based on fission track densities in glass from tephros of the Miocene to Pleistocene [Bielecki, 1994, 1998]. Samples analyzed in this previous study show evidence of amounts of radioactivity greater than post-Flood expected amounts. A plausible explanation for this result is that these strata, from which the specimens were taken, experienced an accelerated nuclear decay even though these strata tend to be considered the later effects of the Flood event or even post-Flood. This proposed study will focus on strata after the Pleistocene. These results have direct implication to the location of the Flood/post-Flood boundary. Discovering a strong physical signature for an abrupt change in radioactive decay rates is desired to bring the recent-creationist community to consensus over assigning this boundary.

Why is the spontaneous fission track density of ^{238}U in natural rocks an appropriate radioactive effect to apply to this issue? The spontaneous fission of ^{238}U is a unique radioactive phenomenon which occurs in terrestrial materials possessing trace amounts of the element. For those materials that are glassy or crystal-like, a fission event is recorded in the structure as a visible microscopic pit also referred to as a fission track. Other characteristics of this decay mode are that it occurs at a very slow rate (that is, about 10^7 times slower than α -

decay of the same isotope) and that only isotopes of mass number near 100 and higher are able to spontaneously fission.

Details that make the spontaneous fission of ^{238}U a unique tool for the search for a change in radioactive decay rates can be summarized as follows. This radioisotope method does not require the user to assume what portion of daughter isotope in the specimen is radiogenic. This is because the density of fission tracks from ^{238}U is the signature that an amount of radioactivity has occurred since solidification. Fission tracks cannot be present in the rock before it solidifies. Finding considerable amounts of isotopes of about 100 or higher mass number naturally on earth and that also spontaneously fission comparable to ^{238}U is very rare [Fleischer *et al.*, 1975]. Spurious tracks (fission track-like objects in the specimen) can be clearly ruled out given the fission track observer/counter knows the unique characteristics of fission tracks [Bigazzi *et al.*, 1988].

The spontaneous fission of ^{238}U is governed by the radioactive decay relationship discovered and verified at the beginning of the twentieth century by Rutherford. Concisely stated, the number of decaying isotope atoms at time t is directly proportional to the change (or decrease) in that number with respect to time. In equation form,

$$\frac{dN}{dT} = -\lambda N \quad (1)$$

where λ is the decay constant. Starting with the established radioisotope age equation for ^{238}U α -decay which can be derived from the above equation and here stated,

$$D = {}^{238}\text{U} \left(e^{\lambda_{\alpha} t} - 1 \right) \quad (2)$$

where D is the total number of radiogenic daughter atoms, ${}^{238}\text{U}$ is the number of parent isotope atoms at time t , and λ_{α} is the decay constant for ^{238}U α -decay.

It is reasonable to represent the slower fission count as a fraction of the dominant decay mode as

$$F_s = \left(\frac{\lambda_f}{\lambda_{\alpha}} \right) {}^{238}\text{U} \left(e^{\lambda_{\alpha} t} - 1 \right) \quad (3)$$

where λ_f is the fission constant of ^{238}U . This constant is a measured quantity. An accepted value may be taken, otherwise a value may be determined via an independent experiment on a “known age” fission track specimen [Faure, 1986].

An approximation is introduced for ages less than 500,000,000 yr (500 Ma)

because for $t < 500$ Ma,

$$e^{\lambda_{\alpha} t} - 1 \sim \lambda_{\alpha} t \quad (4)$$

so the equation can be written as

$$F_s = \lambda_f \left(\frac{U \rho N_A}{U_{aw}} \right) 1 - I^{\lambda_{\alpha} t} \quad (5)$$

where N_A is Avogadro's number, U_{aw} is the atomic weight of U, U is the amount of U in ppm, I is the ratio of U isotopes, ρ is the density of the specimen, and

$$^{238}\text{U} = \left(\frac{U \rho N_A}{U_{aw}} \right) 1 - I \quad (6)$$

Some fission track methods utilize a similar equation with a ratio of induced to spontaneous fission tracks where the induced track density replaces the measurement of U in the sample.

It is the last equation presented above that can be utilized to determine how much nuclear decay has taken place in a rock sample of a certain age based on the amount of U in the sample. Any sample bearing the appropriate amount of U can be fission track analyzed to check against this relationship. Samples originating in the post-Flood era should have fission track data that comply with the above relation. Given an event of accelerated rates of radioactivity at the time of the Flood, spontaneous fission track densities of samples from Flood strata should be underestimated from the equation above. It is the uniqueness of the fission track phenomenon in nature that provides the tool to locate this signature in the geologic column.

Scope

Locating an episode of accelerated nuclear decay in the geologic column will refine the location of the Flood era and the Flood/post-Flood boundary. The proposed plan which follows will list the required steps to achieve this goal, support, facilities, costs, and estimated time for results.

Methods

The methods detailed below can be completed in less than two years. This is based on the author working between 5–10 hours per week. Two weeks per

year the author plans to take time off his full-time job for travel and high volume work requirements related to complete this study. Compensation for these two weeks from work is included in this estimate (\$1000 gross per week).

Processing a sample for fission track analysis requires separating the fission track bearing component from the whole rock, mounting the aliquot on a micro slide, polishing the sample to a smooth surface, and etching the specimen to enlarge the width of the tracks. Fission track analysis in this paper refers to observing the distribution from shard to shard and counting the fission tracks, using a point-counting technique, for a surface density.

1. Select, obtain and analyze a fission track calibrated glass sample for laboratory calibration and for verifying the present day spontaneous fission rate of ^{238}U .

The reason for taking this step to determine the spontaneous fission rate of ^{238}U is because at least two fission rate values differing by 17% are commonly used in the fission track community. The author has confidence that the higher fission rate value (near $8.5 \times 10^{-17}\text{sec}$) is more accurate [*Galliker et al.*, 1970].

Option A. The author has contacted Dr. R. H. Brill of the Corning Museum of Glass and discussed the possibility of acquiring an experimental U-containing glass prepared by Alan Werner in December of 1943 [*Brill et al.*, 1964]. Because of the known age of glass and high U content (near 4.4%), it is a prime candidate for use in demonstrating the presence of fission rate ^{238}U using the last equation stated above. Dr. Brill offered to look for this specimen in his archives and provide a sample free of charge. As of May 29, 1999, the author has had no response from the Corning Museum of Glass. Processing and fission track analysis cost on this sample is \$1000.

Option B. The author has contacted NIST to obtain a quotation and specification of a likely U-containing glass for the ^{238}U fission rate verification. A possible candidate glass is SRM 1874 that contains about 0.25% of U. This specimen is definitely a second choice to a well preserved sample of option A, but this option is very plausible given that this sample is well over 10 years old [*Marinenko et al.*, 1990]. The cost of the sample is about \$500. Processing and fission track analysis on this sample is \$1000. This includes performing the work with the help of a research nuclear engineer and facilities and independent analysis quoted from Geotrack International Pty Ltd.

Obtaining and analyzing either of the samples mentioned above will take approximately 10 to 12 weeks.

2. Strategically select and retrieve tephra samples in the late Cenozoic era for fission track analysis.

The plan is to obtain tephra samples from at least 5 locations globally, if possible, in what is called the Holocene geologic time period for fission track analysis. The likely locations in North America at this time are listed below followed by prime candidates to obtain worldwide if finances or creationist contacts are available in these distant places. Information related to these Holocene locations was found using GEOREF.

Rhyolitic obsidian flow from Little Glass Mountain, Medicine Lake Highland, northern California conventionally dated to be between 300–100 years old [*Fink, 1983*].

Glacier Peak ash, Trinity Mine, Washington (also from sites in western Montana) conventionally dated to be between 9000–11,200 years old [*Friedman et al., 1992*].

Mount St. Helens ash, Swift Creek and Vantage, Washington conventionally dated to be between 8500–13,650 years old [*Friedman et al., 1992*].

Mazama ash, Crater Lake, Oregon conventionally dated to be about 6800 years old [*Powers and Wilcox, 1964, Berger and Huntley, 1994*].

Hayes ash (Jarvis Creek, Tangle Lakes, and Cantwell ash), Hayes Volcano, south-central Alaska radiocarbon conventionally dated to be between 3500 and 3800 years old [*Riehle, 1994*].

Tephra near Managua, Nicaragua conventionally dated to be Holocene [*Bice, 1979*].

Mono-Inyo Tephra, Nevada conventionally dated to be Holocene [*Davis et al., 1991*].

Sunwapta Pass, Jasper National Park, Alberta radiocarbon conventionally dated to be Holocene [*Beaudoin and King, 1994*].

Locations other than North American

Tephra of the South Rift Zone, Mauna Kea Volcano, Hawaii of which the youngest layer inferred to be about 3600 years old [*Porter, 1973*].

Waimihia, Stent, and Hinemaiaia tephra from Taupo Volcanic Centre, New Zealand ¹⁴C conventionally dated to about 4000 years old [*Alloway et al., 1994*].

The five North American tephtras could be gathered in one outing. At least five of the above samples could be gathered in a month's time with a one to two week field trip. Estimated costs for travel (by car) and lodging for two persons on a two week sample retrieval trip is \$1500. Miscellaneous costs like geological survey maps for locating sites and equipment for removal of specimen are

estimated at \$500.

3. Determine the U content and fission track analyze these chosen samples for comparison to the spontaneous fission track equation predictions assuming a constant fission rate.

The U content of the sample is critical in determining if the sample is a good specimen to fission track analyze. In general, a sample containing 10 ppm or more of U is a good sample. Samples will be separated for both glass and zircon aliquots, because these components of the rock best retain fission tracks. Zircon is more commonly fission track analyzed by commercial laboratories. It also provides a check for U homogeneity within the sample. To analyze both glass and zircon the cost will be \$1000 per sample. The estimate of time to finish analysis of the five samples is 40 weeks. The author will plan two weeks of leave from his full-time job during this step of the study.

4. Incorporate these radioisotopic data and results into the recent-Creation model of the universe for refinement of the model.

The results of this study can only be an asset to the recent-creationist community. Thus, the rest of the time will be spent on preparing the study for publication. At this time, further research avenues related to or to build on this study will be addressed.

Summary of Estimated Costs and Timing

Cost	Time
Acquire and fission track analyze a calibrated glass.	\$1500 12 weeks
Select and retrieve Holocene samples for analysis.	\$4000 2 weeks
Process and analyze Holocene samples for U content.	\$500 6 weeks
Process and analyze Holocene samples for fission tracks.	\$7000 40 weeks
Prepare study for publication in the recent-creationist community.	12 weeks
Total	\$13,000 72 weeks

*Notice that values are rounded up to the nearest \$100.

Personnel and Facilities

Support on this project will be available at the University of Michigan in the

form of technical labor from a chemistry graduate student (Arnold Guikema), nuclear engineering research professor (Dr. Douglas McGregor), and the author. Professor McGregor will also make available his nuclear detector development laboratory. Many of the steps for processing the glass or zircon aliquots can be completed in this laboratory setting. The university also has a clean room, which the author has previously utilized for fission track analysis, and a research nuclear reactor (2 Megawatt) for neutron activation or irradiation. Mr. Guikema published an article for the International Conference on Creationism (ICC4) on the issue of the fission rate of ^{238}U and the implications to calibrating fission track dating to K-Ar dating [Guikema, 1998]. The author has written a Master's thesis and an article in the ICC4 using fission track analysis and data to locate the Flood/post-Flood boundary.

Steps are being taken to establish a tax-exempt scientific organization to assure that the funds obtained for this study will be used efficiently and legally. The author plans to submit information to the IRS as required by Publication 557 Section 501(c)(3) for Scientific Organizations. Any advice the RATE group can provide in this issue is appreciated.

Conclusion

Obtaining experimental evidence for the Flood/post-Flood boundary is a long awaited marker for the recent-creationist community. Without it, harmonizing earth and Biblical chronology is at a standstill. If accelerated nuclear decay occurred during the Flood, a detailed fission track analysis of Holocene tephra as this proposal outlines will find a signature in the rocks. With the RATE group's support this study can be completed.

References

- Alloway, B., D. J. Lowe, R. P. K. Chan, D. Eden, and P. Froggatt, Stratigraphy and chronology of the Stent tephra, a.c. 4000 year old distal silicic tephra from Taupo Volcanic Centre, New Zealand, *New Zealand Journal of Geology and Geophysics*, 37, 37–47, 1994.
- Beaudoin, A. B., and R. H. Roger, Holocene palaeoenvironmental record preserved in a paraglacial alluvial fan, Sunwapta Pass, Jasper National Park, Alberta, Canada, *Catena (Giessen)*, 22, 227–248, 1994.
- Berger, G. W., and D. J. Huntley, Tests for optically stimulated luminescence from tephra glass, *Quaternary Geochronology (Quaternary Science Reviews)*,

- 13, 509–511, 1994.
- Bice, D. C., Tephra correlation and the age of human footprints near Managua, Nicaragua, *Abstracts with Programs—Geological Society of America*, 11, 388, 1979.
- Bielecki, J. W., *A Study of Spontaneous Fission Track Densities in Resting Spring Range Obsidian (Miocene) near Shoshone, California*, Institute for Creation Research Master Thesis, Santee, California, 77 pp., 1994.
- Bielecki, J. W., Search for accelerated nuclear decay with spontaneous fission of ^{238}U , in *Proceedings of the International Conference on Creationism*, edited by R. E. Walsh, pp. 79–88, Creation Science Fellowship, Pittsburgh, Pennsylvania, 1998.
- Bigazzi, G., J. C. Hadler Neto, P. Norelli, A. M. Osorio Araya, R. Paulino, G. Poupeau, and L. Stellade Navia, Dating of glass: the importance of correctly identifying fission tracks, *International Journal of Radiation Applications and Instrumentation., Part D*, 15, 711–714, 1988.
- Brill, R. H., R. L. Fleischer, P. B. Price, and R. M. Walker, The fission-track dating of man-made glasses: preliminary results, *Journal of Glass Studies*, 7, 151–156, 1964.
- Davis, J. O., N. L. Ingraham, R. L. Jacobson, and Anonymous, The use of D/H ratios from hydrated tephra glass from the Great Basin to reconstruct Pleistocene and Holocene climates, *Abstracts with Programs—Geological Society of America*, 23, 98, 1991.
- Faure, G., *Principles of Isotope Geology*, John Wiley & Sons, Inc., New York, 589 pp, 1986.
- Fink, J. H., Structure and emplacement of a rhyolitic obsidian flow; Little Glass Mountain, Medicine Lake Highland, Northern California, *Geological Society of America Bulletin*, 94, 362–380, 1983.
- Fleischer, R. L., P. B. Price, and R. M. Walker, *Nuclear Tracks in Solids: Principles and Applications*, University of California, Los Angeles, California, University of California, 605 pp., 1975.
- Friedman, I., J. Gleason, R. Wilcox, and A. Warden, Modeling of ancient climate from deuterium content of water in volcanic glass, *Quaternary International*, 13/14, 201–203, 1992.
- Galliker, D., E. Hugentobler, and B. Hahn, Spontane kernspaltung von ^{238}U und ^{241}Am , *Helvetica Physica Acta*, 43, 593–606, 1970.
- Guikema, A. J., Potassium/argon derived ^{238}U fission decay constants and consequences for the recent-creation theory, in *Proceedings of the International Conference on Creationism*, edited by R. E. Walsh, pp. 271–282, Creation

- Science Fellowship, Pittsburgh, Pennsylvania, 1998.
- Marinenko, R. B., D. H. Blackburn, and J. B. Bodkin, Glasses for microanalysis: SRM's 1871–1875, *NIST Special Publication 260–112*, 49 pp, 1990.
- Porter, S. C., Stratigraphy and chronology of Late Quaternary tephra along the South Rift Zone of Mauna Kea Volcano, Hawaii, *Geological Society of America Bulletin*, 84, 1923–1940, 1973.
- Powers, H. A., and R. E. Wilcox, Volcanic ash from Mount Mazama (Crater Lake) and from Glacier Peak, *Science*, 144, 1334–1336, 1964.
- Riehle, J. R., Heterogeneity, correlatives, and proposed stratigraphic nomenclature of Hayes Tephra Set H, Alaska, *Quaternary Research*, 41, 285–288, 1994.
- Wan, E., C. E. Meyer, A. M. Sarna-Wojcicki, D. P. Adam, J. P. Bradbury, W. E. Dean, and J. V. Gardner, Correlations of latest Pleistocene and Holocene tephra layers in sediments of the Pacific Margin and adjacent land areas, Western Conterminous U. S., *Open-File Report—U. S. Geological Survey*, pp. 60–61, 1995.

TOTAL ESTIMATED COST \$50,000

Occurrence of U and Th Radiohalos in Phanerozoic Crystalline Rocks

Andrew A. Snelling Ph.D.*

John R. Baumgardner, Ph.D.**

Objective

The goal of this project is to evaluate the frequency of occurrence and state of development of ^{238}U and ^{232}Th radiohalos in Phanerozoic crystalline rocks. In particular, the focus is to establish whether or not it is likely there is a systematic absence of mature U and Th radiohalos in rocks crystallized since the first evidence of multi-cellular life in the geological record. The non-existence of such radiohalos would represent a compelling argument that dramatically less nuclear decay has occurred during this interval of earth history than the approximately 540 million years claimed by evolutionary science.

Background

The paucity of reports in the scientific literature of U and Th radiohalos in crystalline rocks of Phanerozoic age is puzzling since mature ^{238}U halos should form around mineral inclusions of zircon with commonly observed concentrations of ^{238}U in 100 million years or less, assuming current rates of nuclear decay. This is especially puzzling since mature U and Th radiohalos are common in crystalline rocks of Archean and Proterozoic age. That there may be a complete absence of mature U and Th halos in Phanerozoic rocks is at least suggested by observations of *Gentry et al.* [1976] who found U halos only very weakly developed in coalified wood from the Devonian Chattanooga shale and from Jurassic/Cretaceous localities in the Colorado Plateau. Ion microprobe measurement of the $^{238}\text{U}/^{206}\text{Pb}$ ratio of the radiocenters of some of these halos gave ratios that imply very little decay of U to Pb has occurred since coalification. The best estimate of *Gentry et al.* [1976] was 240,000 years' worth of decay at present rates. Even the embryonic stage of development of the observed U

* *Geology Department, Institute for Creation Research, Santee, California*

** *Los Alamos National Laboratories, Los Alamos, New Mexico*

halos was due to the extremely high concentrations of ^{238}U in their radiocenters. The fact that radiohalos represent a visible, physical record of nuclear decay that is wiped away when a rock recrystallizes means that the problem of inheritance of parent/daughter correlations that complicates standard isochron methods is avoided. A careful documentation of an absence of mature U and Th radiohalos in Phanerozoic crystalline rocks would therefore represent a powerful argument that very little nuclear decay has taken place since multicelled life has existed on earth and that ages in the range of hundreds of millions of years commonly given by standard isochron methods are primarily a consequence of inheritance of parent/daughter correlations from Archean and Proterozoic surfaces.

Technical Approach

This project is fairly straightforward, involving two steps:

- Field work to collect samples of Phanerozoic crystalline rocks.

The most likely rocks to contain ^{238}U and ^{232}Th halos would be granitic rocks in which biotite is the major ferromagnesian mineral, and in which minor zircon is also present. Such Phanerozoic granitic rocks outcrop throughout southeastern Australia in the Lachlan and New England Orogens and are accessible from the highways linking Brisbane, Sydney and Melbourne. The conventional ages of these granitic rocks are Silurian to Triassic, so to supplement the conventional timespan covered by sampling them, Cretaceous granitic rocks are readily accessible just to the east of San Diego in the Peninsular Ranges Batholith. Thus in order to have a statistically acceptable sample set, it is proposed to sample the suitable granitic rocks in 40–50 different plutons from these localities representing the conventional timespan of 100–400 Ma. Other granitic rocks with other relevant conventional ages from other appropriate locations may also be sampled to supplement the sample set. Since mature ^{238}U halos should form in 100 million years or less, assuming current rates of nuclear decay, if the conventional ages for these granitic rocks containing zircon and biotite are valid, then it would be expected that the biotites would have mature ^{238}U halos in them.

- Laboratory processing of the collected samples to search for mature ^{238}U and ^{232}Th halos.

Given that there may be 2–3 samples collected from 40–50 plutons, there could be as many as 100–150 granitic rock samples requiring laboratory processing. Each sample only needs to be crushed sufficiently to liberate the biotite as

intact flakes, which can then be handpicked and peeled apart so as to be thin enough with clear scotch or “sticky” tape, which is then used to stick the thin flakes onto glass microscope slides. The flakes are then scanned visually under a petrological microscope to see if they contain tiny zircon inclusions with mature ^{238}U and/or ^{232}Th halos around them. The process often has to be repeated for a given sample, because in order to identify the radiohalos one has to be a cross-section that cuts centrally through the minute inclusions and so gives the proper dimensions of the rings. Thus numerous flakes of biotite may have to be repeatedly peeled for microscope examination, many being discarded until success is achieved. In any case, it will be necessary to scan dozens of biotite flakes in every sample to ensure that it is then valid to conclude mature ^{238}U and ^{232}Th halos are absent from these Phanerozoic rocks.

Estimates of Manpower, Costs and Timeframe

Because of overlapping with the Po radiohalos research project, there will be some savings in manpower needs and costs, as well as making accomplishment of this research project feasible within the 4–5 year timeframe available. Some samples have already been collected, and a field trip already planned for September 2000 will enable further outcrops to be sampled. Thus there are already sufficient suitable rock samples available for laboratory processing to commence immediately. One or two subsequent field trips will probably then be necessary to build up the sample set to the required size.

Two research assistants have already been contracted to help with the processing of samples in the search for Po radiohalos, so they would be available to look for mature ^{238}U and ^{232}Th radiohalos also in the same samples, and in those samples for this project which are additional to them. One of the principal investigators (Dr Andrew Snelling) would also be involved in sample processing, as well as in recording and collating the data generated.

Some costs would be incurred in doing the field work and sample collection, as well as in the transporting of samples to the processing laboratories. Laboratory costs would be minimal. Thus the major cost would be the manpower, since many hours will need to be spent visually scanning biotite flakes under microscopes. So while it is difficult to provide a fully itemized cost estimate, it is expected the project's objective could be achieved for \$50,000.

Reference

Gentry, R. V., W. H. Christie, D. H. Smith, J. F. Emery, S. A. Reynolds, R. Walker, S. S. Christy, and P. A. Gentry, Radiohalos in coalified wood: new evidence relating to the time of uranium introduction and coalification, *Science*, 194, 315–318, 1976.

TOTAL ESTIMATED COST \$50,000

Selected Case Studies in Rock Dating (Model “Age”, Whole-Rock Isochron and Mineral Isochron) to Understand How the Radioisotopic Systems Behave Geochemically

Andrew A. Snelling, Ph.D.*

Introduction

Regardless of whether there has or has not been accelerated radioactive decay in the past, we already know that open-system behavior in most of the radioactive decay systems of interest produces anomalous results (as far as the established scientific community is concerned). In our quest to comprehensively deal with radiodating we have recognized that it is not sufficient just to point out that there are departures from the closed-system behavior required for a standard radioisotopic dating determination.

We need to produce an alternative explanation for the behavior of the radioactive decay systems that is reflective of processes other than those involved in the standard interpretation of the resultant isotopic ratios. Thus, it may well be that it is the anomalous results that will provide us with the clues as to what alternate processes might be in operation (additional to, or in place of, accelerated radioactive decay in the past).

It has been known for a long time that excess Ar in minerals and rocks is responsible for anomalous K-Ar and Ar-Ar “dates.” This is primarily because Ar is a gas, and even though Ar is an inert element, as a gas it is mobile, able to be dispersed along fractures, dislocations and cleavage in rocks and minerals.

The other factor which has been discovered is that the mantle is a geochemical reservoir of primordial Ar, including ^{40}Ar which is identical to, and indistinguishable from, radiogenic ^{40}Ar . Because mafic magmas are derived by melting of mantle rocks, then such magmas also carry with them up into the crust this primordial ^{40}Ar , which is then inherited as excess ^{40}Ar in the resultant basalt flows, and diabase and gabbro intrusions.

Open-system behavior is also well documented for the Rb-Sr and

* *Geology Department, Institute for Creation Research, Santee, California*

U-Th-Pb decay systems. For example, the Rb-Sr system can easily be perturbed by the heat released from a granitic intrusion, and hydrothermal fluids and ground waters are capable of redistributing the radionuclides in the U-Th-Pb decay system, including Rn which like Ar is a gas.

The mantle is also regarded as a geochemical reservoir for Nd, Sr and Pb isotopes, and it is now common practice in the established geological community to use these isotopes measured in recent basalt lava flows to determine the source areas in the mantle from which they came. It is also known that the geochemical behavior is different for different elements, so that in mafic intrusives, for example, there can be fractionation of elements between the crystal and melt phases that leads to adjacent rocks having different geochemical fingerprints.

It is thus also possible for parent and daughter elements to have different geochemical behavior, and this could well affect the resultant isotopic ratios that are normally interpreted as “ages” but perhaps can be better explained by various geochemical processes.

Why the Research is Needed

A large amount of information on the geochemical behavior of these radioisotopes of interest can certainly be gleaned from the voluminous literature. However, while anomalous results are sometimes published many are often ignored within the scientific establishment, particularly if the results do not give the desired “ages.” However, as already indicated above, results are really only anomalous in the eyes of the establishment scientific community because they do not give the desired “ages,” whereas it is the anomalous results which are departures from the expected behavior which are likely to give us the best clues as to the geochemical behavior of these isotopes and the geochemical processes that affect them.

Thus, to ensure all radioisotopic results are available for interpretation from a given suite of rock samples, it would seem necessary to supplement data from the literature with data from reputable laboratories on parallel suites of rock samples collected by ourselves. Hence, the need for case studies carefully selected to gain maximum coverage of possible geochemical behavior and to test specific hypotheses.

Another reason for the need for this research project is that if accelerated radioactive decay has occurred in the past, then the different radioactive decay systems would have been accelerated by different amounts. This is because in

some systems the radioactive decay is via β -decay, and in others via α -decay, or a combination. Another factor is the different atomic weights of the radionuclides involved. Thus there should be a pattern in the “ages” derived from different decay systems in the same rock.

For example, the K-Ar “age” should be younger than the Rb-Sr “age,” which should be younger than the Sm-Nd “age,” etc. These case studies could potentially confirm such a pattern and thus potentially confirm the occurrence of accelerated decay in the past. But if geochemical processes have perturbed the decay systems, then the pattern could be blurred, so by identifying such geochemical processes the patterns (if there) could be unraveled.

Description of the Research Project

The selections that have been made include areas that are already well studied by creationists, or are extensions to them. This makes good sense because it will maximize the consequent benefits. For example, since the rock sequence in the Grand Canyon and surrounding areas is well studied by creationists and offers a good geological cross-section through the Flood and into pre-Flood rocks, then it makes sense to continue radioisotopic dating studies already begun there and to extend them to surrounding areas.

It is equally important to make sure that the rocks studied span the scope of conventional geological time. Furthermore, since there are a wide range of rock types that could be studied it is important to narrow down the selections to a narrow band of rock types/compositions so as to make the project more achievable in the short term and to contain costs. This also has the additional advantage of removing the bulk chemistry of the rocks as a variable, simplifying the interpretation of results. The choice to focus on mafic rock units has also been made because they are derived from the mantle which is regarded as a geochemical reservoir. The selected case studies are:

Case Study 1—Cardenas Basalt and associated diabases, Grand Canyon.

These are Middle Proterozoic and thus within the basement complex at the bottom of the Canyon. A paper has already been published at the ICC on the K-Ar dating results that are discordant with the more constrained published Rb-Sr isochron [Austin and Snelling, 1998]. Publication of Rb-Sr, Sm-Nd and Pb-Pb analyses on our own collected samples is pending subject to the completion of all analytical work, including that on more diabase samples from one of the thick sills collected in March 1999, that is now in progress. This sill

was chosen for further systematic sampling from top to bottom because it is highly differentiated, with an olivine diabase at the base and a granophyre at the top, so this will be a good test of whether these radioisotopes have been fractionated with the minerals that contain them during magmatic differentiation. As well as producing whole-rock isochrons for this sample suite, one sample has also been chosen for mineral separations in order to generate mineral isochrons from radioisotopic analyses of its constituent minerals.

It will also be important in this case study to compare the radioisotopic ratios and trace element geochemistry of the diabases with those of the basalts, given their spatial separation and their different mode of occurrence (intrusive versus extrusive).

Case Study 2—Vishnu Complex amphibolites, Grand Canyon.

Amphibolites are metamorphosed basalts and the Vishnu Complex in the inner gorge of Grand Canyon is a metamorphosed sequence of sediments and interbedded volcanics, including basalts. Thus it makes good sense to analyze these rocks also, to see if they have the same sample source signature as the Cardenas Basalt and associated diabases, which would imply not only the same mantle source area, but the 500 million years that is supposed to be between these two rock units may never have happened. Also, it is important to see how metamorphism of these original basalts affected the radioisotopes, since we know that heat can perturb these systems.

Thus far, five samples have been collected and K-Ar, Rb-Sr, Sm-Nd and Pb-Pb analyses of them have been obtained. Another seven samples were collected in March 1999 and analytical work on them is soon to commence. The results on the first batch of five samples indicate that the K-Ar model “ages” are considerably less than the published results for other metamorphic rocks in the Vishnu Complex. Furthermore, all the whole-rock isochron “ages” are also considerably less than the “expected” 1.75 Ga “age”, the Rb-Sr isochron “age” of 1.25 Ga being the worst, and discordant with the K-Ar isochron “age” of 1.52 Ga. The radioisotopic analyses of the further seven samples are needed to better constrain these isochrons statistically.

Case Study 3—Pahrump Group diabases, Kingston Range, California

The Pahrump Group sedimentary rocks in this area near Death Valley are the equivalent to the Grand Canyon Supergroup rocks found on top of the Vishnu Complex and associated crystalline basement rocks in Grand Canyon. Drs. Austin and Wise have correlated the Kingston Peak Formation in this area with

the Sixtymile Formation and Great Unconformity in Grand Canyon as the onset of the Flood [*Austin and Wise, 1994*]. In the Pahrump Group are diabase sills which have been reported in the literature as yielding a Rb-Sr isochron “age” identical to the Cardenas Basalt and the associated diabases in Grand Canyon.

Already 34 samples have been collected and these would be submitted for whole-rock geochemical analyses (major, minor, trace and rare earth elements). Then from their number a suite of 8–10 samples would be sent for K-Ar, Rb-Sr, Sm-Nd and Pb-Pb analyses. Further field work will be necessary to complete the sampling of the lower section of the sills, due to the fact that the traverse already sampled did not contain the lower section of the sills. Infill sampling may also be necessary. Thus the number of samples analyzed for radioisotopes will only be finalized once all field work and sampling have been completed.

Case Study 4—Apache Group diabases and basalts, Globe Area, Arizona

In the Globe Area of Central Arizona, east of Phoenix, are the diabase sills and basalt flows of the Apache Group which are also claimed to be Middle Proterozoic with an approximate Rb-Sr isochron “age” identical to the Cardenas Basalt and associated diabases in Grand Canyon and to the Pahrump Group diabases in the Kingston Range of California. If it can be shown that the diabases and basalts in each area are related to one another geochemically, radioisotopically and from the same source area in the mantle, then this would have implications for the extent of contemporaneous mafic magmatism over a huge area in the South-West, which may potentially be related to the breaking open of the fountains of the great deep at the commencement of the Flood. Unlike the Cardenas Basalt and associated diabases in Grand Canyon, there is field evidence to connect these Apache Group diabases directly to associated basalts. In fact, it is claimed that some of the diabase was intruding less than 100 meters below the seafloor at the same time as basalt was flowing out onto the ocean floor from the same magma chamber and conduit.

Thus, in this case study it would be possible to determine if there were any geochemical and radioisotopic differences between the diabases and the basalts as a guide to more firmly establishing the relationship between the Cardenas and its associated diabases. Field work has already been undertaken, and it was observed that not only are the diabase sills intruded at different stratigraphic levels within the Apache Group, but there were closely related multiple pulses of magma intrusion resulting in diabase sills being intruded into existing diabase sills such that the boundaries are very hard to discern. It would be interesting to

see if there are any geochemical and isotopic differences to distinguish these different pulses.

Forty-two (42) samples have been collected in all, and whole-rock geochemical analyses already undertaken. Perhaps as many as 15 of these samples will be chosen for K-Ar, Rb-Sr, Sm-Nd and Pb-Pb analyses. Whether any further field work and sampling will be necessary can only be decided after all this analytical work has been completed.

Case Study 5—Somerset Dam Layered Gabbro Intrusion, near Brisbane, Australia

This field area is about 70 miles west of Brisbane and is therefore very accessible. The rationale behind this case study is that in this intrusion (gabbro is the coarse-grained intrusive equivalent of basalt) there are five repeated cycles of layering which are supposed to represent a sequence of pulses that gradually filled the magma chamber at depth in the crust. However, within each cycle there is also layering, where there has been magmatic differentiation and crystal settling so that there are now five varieties of gabbro.

The objective is to test not only the mineralogical and geochemical differences between these pulses and the layers within them, but also to see whether there are any radioisotopic differences which would then indicate that fractionation of radioisotopes has occurred in conjunction with the mineralogy and geochemistry. Very little radioisotopic work has been done on this intrusion, which is regarded as Triassic in age based on two K-Ar analyses more than 30 years ago, and on recent Ar-Ar spectral analyses of the ubiquitous plagioclases, coupled with Rb-Sr and Sm-Nd whole-rock analyses, by a creationist geology student as part of a thesis project on the intrusion at a local university.

So far nineteen (19) samples have been collected for this RATE case study, including a suite of six samples systematically through one of the gabbro layers. Fifteen (15) samples from this set have now been analyzed for major, minor and trace elements. It is intended that a smaller number of samples from this set will soon be sent out for K-Ar, Rb-Sr, Sm-Nd and Pb-Pb analyses to complement the data already available. Additionally, one gabbro sample has been chosen for mineral separations so that the mineral isochrons generated from the radioisotopic analyses of its mineral constituents can be compared to the whole-rock isochrons and model “ages” derived from it and the other gabbro samples.

Case Study 6—Late Tertiary Maars (dry volcanoes), near Camperdown, Victoria, Australia

The basalts associated with these volcanoes contain mantle xenoliths that are reported to contain elevated levels of rare gases such as Ar brought up from the mantle. This case study therefore is a good test of inheritance from the mantle, because not only has the basalt magma been formed in the mantle, but portions of mantle rock have been brought up with it. So far six samples have been collected from two volcanoes, and all six have had whole-rock geochemical and K-Ar, Rb-Sr, Sm-Nd and Pb-Pb analyses performed on them.

As expected, the samples all have excess radiogenic ^{40}Ar in them, and the K-Ar model “ages” range from 3.9 Ma to 7.3 Ma for one volcano and from 2.9 Ma to 5.8 Ma for the other. No meaningful isochrons can so far be generated, but the radioisotopic data do distinguish between the two volcanoes, which is indicative of different source areas in the mantle for these lavas. It is expected that another 6–10 samples incorporating at least another one of these volcanoes will still need to be collected from another field trip to effectively complete this case study. This particular case study allows us to directly test what comes up from the mantle and thus what mantle conditions are like, which is obviously critical to our understanding of the radioisotope data generally.

Case Study 7—Recent andesite flows, Mt. Ngauruhoe, New Zealand.

This is an active volcano on New Zealand’s North Island. Its most recent eruptions were in 1949, 1954 and 1975. Samples have been collected from five of these flows and whole-rock geochemical and K-Ar analyses have been completed, with the latter being the subject of an ICC98 paper [*Snelling, 1998*]. The samples produced results up to 3.5 Ma because of excess radiogenic ^{40}Ar inherited from the mantle source area from which the magma came. Rb-Sr, Sm-Nd and Pb-Pb results have now also been received, and interpretation and publishing of them is pending. It is unlikely that there will be the need for any further field work or sampling in this project, as these analytical results should be sufficient for the purpose of this project.

Case Study 8—Elves Chasm Gneiss (granodiorite), Grand Canyon.

This is currently the oldest “dated” rock in the Grand Canyon at around 1.8 Ga. Over a number of years, samples of this rock unit have been collected during ICR raft trips through the Canyon, and already a lot of analytical data have been amassed. The purpose for working on this rock unit is that it ties in with investigations of the crystalline basement complex to the Flood-deposited rocks

in the walls of the Canyon, which makes these rocks definitely pre-Flood and potentially related to the Creation week.

It is therefore useful to look at radioisotopic data from that period in earth history to see if there are differences with the radioisotope data in later rocks, as we not only seek to determine whether there has been a period of enhanced radioactive decay rates in the past, but exactly when that might have been. Also, the major element chemistry of these rocks is in marked contrast to that of all the rocks in the other case studies, so here we can determine whether variation in major element chemistry in the rocks has a marked effect on the radioisotopes.

Once all analytical work on the samples is completed, the present data set will be reviewed and a decision made as to whether any further sampling and radioisotopic analyses are necessary.

Estimates of Manpower and Costs

The outlay of manpower has largely been made, and any necessary extra field trips can easily be incorporated into existing plans. The costs, however, are enormous because of all the laboratory analytical work involved. It is difficult to give an exact figure because of a number of variables, including the final number of samples to be analyzed, but a reasonable estimate would be around \$100,000 over the next 4–5 years.

Estimates of Timeframe

It is expected that these case studies can all be completed in the 2000–2005 period, with the field work and sampling completed by 2002 and the laboratory work completed by 2004, so that data assessment, interpretation and writing can be done for the second RATE monograph to be published in 2005.

What We Expect to Learn from the Research Project

In conjunction with continuing literature research, these case studies should enable us to acquire a broad understanding of the nature and contribution of the mantle geochemical reservoir to the radioisotopic ratios found in crustal rocks. The data provided by these case studies should tell us just how real this mantle contribution is, and whether some of that contribution is in fact merely based

on assumptions made by the establishment geological community to produce the desired “dates.” The case studies should also teach us whether the geochemical behavior of different elements during magma ascent, intrusion and/or extrusion, and cooling have had any effects on the radioisotopic systems that might be either systematic, and therefore be an alternate explanation for the resultant “dates,” or need to be superimposed on a period of enhanced radioactive decay in the past.

We will have data from these case studies that can be trusted in the sense that they have not been through an interpretative filter between laboratories and us, and will therefore be able to be compared with data in the literature and explained in conjunction with them. We would hope to learn a lot more about the behavior of radioisotopic decay schemes, and also if there are patterns of results on each of the samples which fit predictions about the effects of any accelerated radiodecay in the past on the different radioactive decay systems.

What Follow-up Research Will be Needed

It is unclear what follow-up research might be needed, except that even if the results and outcomes are as hoped for, there will always be the possibility of another case study, and then perhaps another case study, to give us even more confidence in the conclusions we draw from these existing case studies. What of course would be ideal would be to use the results of these case studies to make predictions which could then be tested in follow-up research.

References

- Austin, S. A., and A. A. Snelling, A.A., Discordant potassium-argon model and isochron “ages” for Cardenas Basalt (Middle Proterozoic) and associated diabase of Eastern Grand Canyon, Arizona, in *Proceedings of the Fourth International Conference on Creationism*, edited by R. E. Walsh, pp. 35–51, Creation Science Fellowship, Pittsburgh, Pennsylvania, 1998.
- Austin, S.A., and K. P. Wise, The pre-Flood/Flood boundary: as defined in Grand Canyon, Arizona and eastern Mojave Desert, California, in *Proceedings of the Third International Conference on Creationism*, edited by R. E. Walsh, pp. 37–47, Creation Science Fellowship, Pittsburgh, Pennsylvania, 1994.
- Snelling, A. A., The cause of anomalous potassium-argon “ages” for recent andesite flows at Mt. Ngauruhoe, New Zealand and the implications for potassium-argon “dating”, in *Proceedings of the Fourth International*

Conference on Creationism, edited by R. E. Walsh, pp. 503–525, Creation Science Fellowship, Pittsburgh, Pennsylvania, 1998.

TOTAL ESTIMATED COST \$100,000

Biblical Word Studies on Critical Issues Related to the Age of the Earth

David M. Fouts, Ph.D.*

Introduction

Dr. Fouts was requested to offer a proposal to the RATE group which would assist in understanding Biblical statements which relate to the research being attempted. He was asked to indicate the effort, cost, and timeframe to conduct a full study on the word “fire” which seems to occur in relation to mountains and earth processes. This may offer some help with Dr. Humphrey’s views on nuclear decay processes and the release of heat. There will likely be several other words which could be studied in a similar manner. Dr. Fout’s proposal for one word follows and the estimate for the total research cost is shown for up to four possible words. (editors)

Proposal

I propose to do a thorough study of the Hebrew term for fire (*‘esh*), particularly as demonstrated in Deuteronomy 32:22, illustrated by Psalm 18:7–8 (II Samuel 22:11) and II Peter 3:7–12, as potentially applicable to the issue of an increased rate of radioactive decay. I estimate preliminarily that the project will take from 60–80 hours in order to produce a result of publishable quality. The work is to be completed prior to July 1, 2001 (sooner as time permits).

TOTAL ESTIMATED COST \$10,000

* Bryan College, Dayton, Tennessee

Plutonium (Pu) in Oklo Reactor

Eugene F. Chaffin, Ph.D.*

Introduction

In a nuclear reactor, the U fuel is made up of a mixture of ^{235}U and ^{238}U . Instead of fissioning, the ^{238}U often absorbs a neutron and then undergoes two β -decays to produce ^{239}Pu . This is what a breeder reactor does: it generates ^{239}Pu , which then can be used as a reactor fuel itself. ^{239}Pu has a half-life of 24,100 years. In the 1970s a body of U ore was discovered in Gabon, Africa, which had undergone chain reactions in the ancient past [Chaffin, 1982, 1985, 1990, 1994]. If no accelerated decay has occurred since these reactions, and if the earth is only several thousand years old, then there should be appreciable amounts of Pu present in the Oklo ore.

If Oklo samples can be obtained, then this project would be to measure the ^{239}Pu and ^{238}U so that we can decide if accelerated decay is needed to explain the data. Even if no chain reactions are occurring, stray neutrons from spontaneous fissions of ^{235}U and ^{238}U will be absorbed by the ^{238}U , and extremely small amounts of ^{239}Pu will be produced. However, the amount produced in this way is much smaller than if, say, the Oklo ore had been experiencing chain reactions some few thousands of years ago. The amount expected can be calculated for the two cases, and compared with the measurements. The other isotopes of Pu are either short-lived or, for ^{244}Pu , are not produced in great quantities in a reactor. Hence, this project would concentrate on measuring ^{239}Pu and ^{238}U concentrations.

Why the Research Project is Needed

Since the Oklo reactors are in Precambrian ores (conventional age of 1.9 gigayears), they provide important constraints, and we need to be prepared to explain these data. More than that, attempting to explain these data should lead us to realistic models, consistent with the young-earth timeframe.

If the Pu turns out to be of negligible concentration, then accelerated decay

* Professor of Physics, Bob Jones University, Greenville, South Carolina

had to occur after the deposit of the Oklo ores. The Precambrian, steeply-dipping sandstone/mudstone deposits at Oklo are quite near the Chaillu pluton (Massif du Chaillu) to the west. They should be either pre-Flood or early Flood deposits. They should be old rocks even in the young-earth worldview, but not billions of years old.

The evidence seems to be in favor of very little migration of the bulk of the Pu at Oklo. However, limited amounts of Pu may have migrated over distances on the order of a meter or so [*Naudet, 1978*]. Some samples from the periphery of reactor zone 9 were analyzed by some Australians, with the result that only about 10^{-12} grams of ^{239}Pu per gram of U were found [*Fabrika-Martin and Curtis, 1992, Table 4.5; Curtis et al., 1989*]. Since these data were from the periphery of the reactor zone, a second look at other data seems warranted. We may find the same order of magnitude of plutonium or perhaps more? That is what we want to know.

Description of the Research Project

We hope to work with more than a small, isolated amount of Pu. Actually, we expect to receive about a couple of ccs of eluate from a Dowex X1 ion exchange column which had passed just the Pu fraction. The Pu fraction would then be extracted from the solution by solvent extraction and evaporated to dryness on a stainless steel disk for α -spectroscopy. Limits on detection get better the longer you count the specimen. Even the small amount (in the case of no accelerated decay after the chain reactions were finished) could be detected in a reasonable time.

Alternatively, it might be possible to get other Oklo samples from Australian or American labs that still have them in storage. Dr. Steve Austin has worked with a lab that uses isotope dilution techniques to measure U and Pu in the ore samples. If there has been no accelerated decay since the reactor shut down, a few thousand years ago, then the ^{239}Pu should have a concentration of the order of the ^{235}U concentration, ^{235}U being about 0.72% of the U. That would be easily detectable by that technique. If there was accelerated decay, then the lab would tell us that no Pu was found (the actual amount would be below their limits of detection). We would need a sample of the Oklo ore of about 5 to 10 grams.

The ChemPet Laboratory of Santa Barbara has previously measured the ^{238}U in some of Austin's Grand Canyon rocks using isotope dilution. They do routine Pb measurements and their mass spectrometry machine did U and Th

measurements. They charged US\$75 for each isotope dilution measurement. Errors were less than 5%. The price may now have increased to about US\$150. We could contract with ChemPet to measure ^{232}Th , ^{238}U and ^{239}Pu in a split of the rock sample. Then we could check their U and Th measurements by “neutron activation” from XRAL Lab of Ontario. The NA measurements would be less than US\$20 each with errors of about 20%. If they repeated the ^{232}Th and ^{238}U measurement, then we could believe the ^{239}Pu measurement.

Estimates of Manpower and Costs

We would need to have resources on the order of US\$450 to US\$600 available to pay for sample analysis.

Estimates of Timeframe

Once samples are in hand, the project would take a few months.

What is Expected to be Learned from the Research Project

We would learn whether there is evidence for accelerated nuclear decay since the occurrence of the Oklo chain reactions. If expected results are obtained, there is a need to repeat them again to make sure no mistakes have been made.

References

- Chaffin, E. F., The Oklo natural uranium reactor examined from a creationist’s viewpoint, *Creation Research Society Quarterly*, 19, 32–35, 1982.
- Chaffin, E. F., The Oklo natural uranium reactor: evidence for a young earth, *Creation Research Society Quarterly*, 22, 10–16, 1985.
- Chaffin, E. F., The difficulty in obtaining realistic conclusions about variable “constants”, *Creation Research Society Quarterly*, 27, 6–9, 1990.
- Chaffin, E. F., Are the fundamental “constants” of physics really variables? in *Proceedings of the Third International Conference on Creationism*, edited by R. E. Walsh, Creation Science Fellowship, Pittsburgh, Pennsylvania, pp. 143–150, 1994.
- Curtis, D., T. Benjamin, A. Gancarz, R. Loss, K. Rosman, J. DeLaeter, J. E. Demore, and W. J. Maeck, Fission product retention in the Oklo natural fission reactors, *Applied Geochemistry*, 4, 49–62, 1989.

- Damour, T. and F. Dyson, The Oklo bound on the time variation of the fine-structure constant, *Nuclear Physics*, B480, 37–54, 1996. Also available on the Los Alamos preprint server (xxx.lanl.gov) as paper hep-ph/96066486.
- Fabrika-Martin, J. T. and D. B. Curtis, Geochemistry of ^{239}Pu , ^{129}I , ^{99}Tc , and ^{36}Cl , *Alligator Rivers Analogue Project*, Final Report, Volume 15, 1992.
- Naudet, R., Summary of the data on the stability and the remobilization of the rare earths, *Natural Fission Reactors*, International Atomic Energy Agency, Vienna, paper IAEA-TC-119/25, pp. 643–673, 1978.

TOTAL ESTIMATED COST \$25,000

Allende Meteorite Origin

Don DeYoung, Ph.D.*

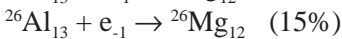
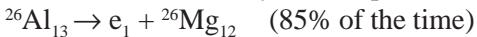
Introduction

Meteorites are placed in one of three categories based on both their content and appearance. They are commonly called irons (31.5% of falls), stones (65%), and stony-iron mixtures (3.5%). One type of stone meteorites, called carbonaceous chondrites, are commonly thought to be the most primitive available objects in the solar system. They contain volatile elements, 1–4% carbon usually in the form of graphite, and as much as 1% amino acids.

These amino acids once caused excitement regarding an extraterrestrial origin of life on earth, but the idea is now largely discounted since the molecules are racemic and abiotic in nature. Chondrules within the samples are small spherical nodules, about 1 mm in size, and are embedded in a fine-grained matrix. This matrix typically consists of olivine, hydrous silicate, and sulfide minerals.

The chondrules typically contain an anomalously high abundance of the stable isotope ^{26}Mg . This Mg is thought to have formed from the decay of radioactive Al, ^{26}Al .

There are two Al decay modes, positron emission and electron capture:



The combined half-life of ^{26}Al from these decay processes is 0.716 million years, a very short lifetime in evolutionary terms. It is thought that complete decay of the ^{26}Al long ago occurred within primordial solar system planetesimals, perhaps asteroids. This decay process furthermore melted the interiors of the planetesimal objects. The result was then a slow differentiation between metallic and non-metallic regions. Much later, the planetesimals were fractured by catastrophic space collisions, with the three categories of meteorites finally resulting as isolated solar system debris.

The carbonaceous chondrite (cc) meteorites typically give radiometric ages of about a billion years, mainly from Ar-Ar dating. The evolutionary age of the earth is largely based on this particular type of meteorite. As a beginning

* Professor of Physics, Grace College, Winona Lake, Indiana

challenge to meteorite age assumptions, this research project explores the possibility of a rapid decay of the ^{26}Al isotope. It is here proposed that the ^{26}Al decay occurred *after* formation of the cc meteorites. The Al atoms were concentrated in small regions of the meteorite. Heat generated by the rapid Al decay then resulted in the melting and formation of the chondrules themselves within the matrix. This suggestion challenges the early history assumptions for these meteorites.

Project

In 1969, over two tons of cc meteorite material fell near the town of Allende, Mexico. These samples have been radiometrically dated at 4.55 billion years. Allende fragments are commercially available for study. This research proposal includes two measurements of an Allende sample.

First, one could look for microscopic evidence that heating of the chondrules *within* the meteorite sample caused melting or metamorphism of the bordering matrix material. Such evidence would completely overthrow accepted cc meteorite origins. It should be noted that there is no obvious evidence of any complete melting of cc meteorites.

Second, the majority of ^{26}Al decays result in the emission of a positron with an energy of 3.3 MeV. One could look for defect trails in the surrounding matrix, resulting from these energetic positrons.

Detailed Description

Allende samples are not expensive; I presently have a 20 gram sample, and have access to additional material. Electron microscopy would probably be the best way to explore the chondrule environment within the cc meteorite. This could be done commercially, or with the help of RATE consultants. The results may or may not reveal evidence of Al decay *within* the formed cc meteorites. Regardless, measurements on cc meteorites, considered the oldest objects in the solar system, should provide good insight into their history from a recent Creation perspective.

Cost Estimates

Literature search.....	\$400
Obtain Allende meteorite samples	\$1000

Electron microscopy search for heat evidence around chondrules. including sample preparation.	\$2000
Electron microscopy search for positron tracks in samples, including sample preparation.	\$2000
Total	\$5400

Time Estimates

A suitable electron microscope laboratory must be identified. The analysis could be completed within six months, leaving one month for data analysis.

References

A literature search is needed regarding the Allende meteorite since its discovery in 1969. There are many Allende references in:
Faure, G., *Principles of Isotope Geology*, John Wiley and Sons, New York, 1986

TOTAL ESTIMATED COST \$25,000

Diffusion of Argon (Ar) in Biotite

Don DeYoung, Ph.D.*

Introduction

Potassium-argon ($^{40}\text{K}/^{40}\text{Ar}$) remains the most popular radiometric rock dating method. One major selling point is the statement that Ar is trapped within the crystal structure of the particular mineral like a “bird in a cage” [Dalrymple, 1991, p. 91]. Thus the daughter Ar atoms, although a gas, are assumed to totally accumulate in the crystal over time, available for later measurement. This assumption is well known and has been used in Creation-evolution debates to support the reliability of K-Ar dating. This “bird in a cage” assumption needs to be challenged, to illustrate just one serious weakness of this particular radiometric method.

Project

It is proposed that controlled temperature studies be done on the diffusion or migration of Ar atoms out of a biotite mica sample. Biotite is suggested because it is one of the most common minerals used in K-Ar dating. It is a sheet silicate containing K, Fe, Mg, and Al atoms. The expected goal is to find that Ar readily moves through heated biotite. In nature, this Ar migration into or out of rock samples would invalidate age assumptions. That is, the quantitative isotope data may have a diffusion interpretation completely different from sample age [Giletti, 1974, p. 353].

Detailed Description

Twelve similar biotite samples could be separated from the same host specimen. This specimen will naturally contain Ar, or else Ar can be added by holding the sample in an Ar-enriched atmosphere. Great care is needed to exclude any effects from atmospheric Ar absorption by sample surfaces [Faure, 1986,

* Professor of Physics, Grace College, Winona Lake, Indiana

p. 74, *Armstrong*, 1978, p. 325]. The twelve samples are then heated for ten hours at 100°C in a vacuum, after which one sample is removed and sealed. The remaining samples are then heated at 150°C for ten additional hours, and another sample is removed. These 50°C increments are continued until all samples have been removed at a final, maximum temperature of 700°C. Previous studies have shown that this temperature range may lead to positive results without melting or altering the biotite samples [*Plummer*, 1998, p. 100].

The samples, protected from atmospheric Ar contamination, are now analyzed for remaining Ar content. There are several precise spectroscopic methods available. A commercial laboratory that can provide the analysis must be identified. Another possibility is the Creation Research Society Van Andel Research Lab in Arizona, which has some spectroscopic capabilities.

Analysis

A plot of temperature against Ar content for the twelve samples should indicate the amount of diffusion that has occurred within samples. The results may or may not validate large-scale movement of Ar in biotite.

Additional Ideas

Crystal x-ray diffraction could show the amount of expansion of the biotite tetrahedral lattice structure with temperature increase. That is, the “bars on the bird cage” widen with temperature by a measureable amount. This data could be compared with the known size of Ar atoms. The presence of bound water molecules within the biotite may be an additional factor in atomic diffusion. Thus, water content is another variable which could be studied with Ar diffusion.

Qualifier

A literature search needs to be done on this proposed experiment. This particular research may or may not have already been carried out.

Cost Estimates

Literature search	\$400
Obtain biotite sample	\$100
Preparation of 12 samples (\$50 each)	\$600

Vacuum heating of samples (\$100 each)	\$1200
Spectroscopic sample analysis for Ar	\$2400
Total	\$4700

Time Estimate

Once a suitable laboratory is located, the project could be completed within six months. The data analysis would require one month.

References

- Armstrong, R. L., Removal of atmospheric argon contamination and the use and misuse of the K-Ar isochron method: Discussion, *Canadian Journal of Earth Sciences*, 15, 325–326, 1978.
- Dalrymple, G. Brent, *The Age of the Earth*, Stanford University Press, Stanford, California, 1991.
- Faure, G., *Principles of Isotope Geology*, John Wiley and Sons, New York, 1986.
- Giletti, B. J., Diffusion related to geochronology, in *Geochemical Transport and Kinetics*, edited by A. W. Hofmann, B. J. Giletti, H. S. Yoder, Jr., and R. A. Young, Carnegie Institution of Washington, Publication 634, pp. 61–76, 1974.
- Plummer, C. C., and D. McGeary, *Physical Geology*, Wm. C. Brown Publishers, New York, 1998.

TOTAL ESTIMATED COST \$40,000

Origin of Chemical Elements

Edward A. Boudreaux, Ph.D.*

Basis and Mechanism

At the onset of Creation the mass of all components of the universe is attributed solely to H₂O. Upon considering the formation of the earth alone, the total effective mass would be 6.026×10^{24} kg. This would provide 3.345×10^{26} gram moles of H₂O or 2.014×10^{50} H₂O molecules. Upon dissociation, each water molecule produces 2.014×10^{50} oxygen atoms and 4.029×10^{50} hydrogen atoms. The breaking of two O-H bonds involved 9.64 eV of energy per mole of H₂O. Thus a total of 3.22×10^{27} eV of energy is associated with this process alone. Furthermore, each hydrogen atom ionizes with 13.5 eV and the ionization of all eight electrons from each oxygen atom involves 871.4 eV. Hence, the total energy of ionization for all hydrogen and oxygen atoms is 1.809×10^{53} eV, or 1.809×10^{47} MeV.

Of course, a sizeable number of protons (H⁺) and electrons (e⁻) will fuse (0.78 MeV each) to neutrons (n⁰). The production of all elements (except hydrogen and oxygen) are derived from oxygen atoms. It is noted that oxygen is by far the most abundant element on earth. This reinforces the basis of oxygen being the starting material for elemental production.

From the reaction scheme produced in this study, it is notable that the elements lithium (Li), beryllium (Be) and boron (B) are readily produced with no special assumptions being required, as in the evolutionary scenario. In fact, Henderson has blatantly stated, "There is no theory for this production that has been generally accepted" [Henderson, 1982]. The two requirements for this study are:

- Only the most energetically efficient mechanisms for established nuclear processes be incorporated.
- Only stable nuclides be involved.

The production of deuterium (²H) alone releases more energy (3.90×10^{50} MeV) than the sum total energies of all other nuclear processes

* Professor Emeritus, University of New Orleans, New Orleans, Louisiana.

considered in this study. The 2.014×10^{50} oxygen atoms available from the initial H_2O is reduced to 9.72×10^{49} , thus leaving 1.042×10^{50} oxygen atoms for reactions. There are no elements formed subsequent to oxygen which exceed the number of atoms available for those reactions.

Rate of Production

While the pertinent reactions for producing specific elements can be deduced, it is equally important to know the time required for the production of these elements. The evolutionary model requires some 700,000 years for the production of atomic nuclei, from the moment of the big bang, and 15 billion years to produce all known chemical elements. But if the earth is young (that is, 6000–7000 years) as we presume, then the evolutionary scheme of elemental nucleosynthesis is seriously flawed.

The major difference in this present model versus that of evolution, is that elemental production begins with two atoms, hydrogen and oxygen, whereas the evolution model requires the formation of subatomic particles first, which in turn condense into atomic nuclei and then atoms. This model requires collisions between atomic nuclei under thermonuclear conditions.

According to standard collision theory of hard spheres, the collision rate between pairs of unlike particles is given by:

$$R_{(1,2)} = \pi N_{(1)} N_{(2)} d_{(1,2)} \left(v_{(1)} + v_{(2)} \right)^2 \quad (1)$$

where the collision rate is $R_{(1,2)}$ for particles $m^{-3}s^{-1}$; N = number of particles m^{-3} ; d = average diameter (m) of colliding particles; v^2 = the root mean square velocities of colliding particles. The average collision diameter, $d_{(1,2)}$, is equal to $\sqrt{\pi}(r_1+r_2)$, where r are nuclear radii. Also, $v^2 = 3 kT/M$, where $k = 1.381 \times 10^{-23}$ J/K, T = temperature in K degrees, and M = mass in kilograms. The magnitude of the temperature in these processes is deduced as follows. The average energy transferred in a two-body hard sphere collision between particles (1), the *projectile*, and (2), the target, is $E_{(1,2)}$ given by the equation:

$$E_{(1,2)} = \frac{1}{2} KE_{(\max)}(1,2) = \frac{2KE_{(\min)}(1) \times M_{(1)}M_{(2)}}{(M_{(1)} + M_{(2)})^2} \quad (2)$$

where $KE_{(\max)}$ is the maximum kinetic energy for collision, $KE_{(\min)}$ (1), the minimum kinetic energy for the projectile is given by

$$KE_{(\min)} = \left[\frac{1 + M_{(1)}}{M_{(2)}} \right] |Q| \quad (3)$$

where Q is the energy excess of a given nuclear reaction. In both equations (2) and (3), M is the particle mass in kilograms. The critical energy for reaction is $E_{(1,2)}$, for which the temperature equivalent of the energy is $1 \text{ MeV} = 1.161 \times 10^{10} \text{ K}$. Upon substituting the appropriate data for evaluating equations (2) and (3) for all reactions, it is found that T ranges from 7.68×10^9 to $3.57 \times 10^{10} \text{ K}$ with the average value $T = 2.17 \pm 0.80 \times 10^{10} \text{ K}$. This is the temperature used to evaluate v^2 for equation (1).

If every collision is effective in promoting a new element product (as energy conditions require), then the number of product atoms divided by the collision rate for their production, gives the *time* required for element production.

It is noted that the time required to produce 10^{50} atoms of all elements considered here, ranges from about 12,000 to 63,000 seconds (that is, $3\frac{1}{3}$ to $17\frac{1}{2}$ hours). By contrast, the times to produce each element in its current number of atoms, spans the range of some 6×10^{-7} to 5.8×10^3 seconds.

If, however, the activation energy is the primary controlling factor in these processes, the reaction rate will be given by:

$$\text{Rate} = d_{(1,2)} \left[\frac{8kT}{\pi\mu} \right]^{\frac{1}{2}} e^{-\frac{E^*}{kT}} N_{(1)} N_{(2)} \quad (4)$$

where

$$\mu = \frac{(M_{(1)}M_{(2)})}{(M_{(1)} + M_{(2)})} \quad (5)$$

the reduced mass and E^* is the activation energy. If this energy of activation is taken to be the average kinetic energy for the collision process, then

$$E^* = \frac{3kT}{2} \quad (6)$$

All other quantities in equation (4) are the same as before. Upon inclusion of the appropriate data in equation (4), the rates determined range from 5.44×10^{54} to $2.80 \times 10^{58} \text{ s}^{-1}$, which correspond to production times of 14 to 36 microseconds.

Conclusion

It is obvious that given the conditions specified for these nucleosynthesis reactions, the product elements can all be produced almost instantaneously. No matter what approach is taken for the reaction rate, this model certainly fits well within a timeframe of much less than even one day of Creation.

On the basis of these findings, it is strongly recommended that this project be continued, to investigate the rest of the elements in the Periodic Table. The next phase of this study will be devoted to completing the fourth and fifth periods of elements (that is, Sc through Xe). Various isotopes, including the major radioactive ones, and their decay processes, will be considered subsequently.

Bibliography

Henderson, P., *Inorganic Geochemistry*, Pergamon Press, New York, p. 40, 1982.
Hutchinson, R., *Nature*, 250, 556–568, 1974.

Linde, D. R., editor-in-chief, *C.R.C. Handbook of Chemistry and Physics*, Chemical Rubber Company, Boca Raton, Florida, 71st edition, pp. 11–33 to 11-140, 1990–1991.

Mason, B., *Principles of Geochemistry*, third edition, Wiley, Inc., New York, 1966.

Ringwood, A. E., The chemical composition and origin of the earth, in *Advances in Earth Sciences*, edited by P. M. Hurley, pp. 287–356, MIT Press, Boston, 1966.

Wapstra, A. H. and K. Bos, *Atomic Data and Nuclear Data Tables*, 19, 215–275, 1977.

TOTAL ESTIMATED COST \$10,000

Cosmology and Accelerated Nuclear Decay

D. Russell Humphreys, Ph.D.*

Most people, when they hear of physical evidence that God accelerated nuclear decay rates during early Creation week and the Genesis Flood, ask, “But how did He do it?” I want to answer that question. There are several strong Biblical hints that the periods of decay acceleration coincided with the times when God “stretched out the heavens.” In my book, *Starlight and Time*, I point out Biblical evidence that the heavens are the fabric of space itself, and that the “stretching” is the cosmological expansion of space. Since the fabric of space communicates forces between particles, it is quite possible that this rapid stretching of space could affect the forces themselves.

Nuclear forces, both the strong force and the weak force, are different from the other two forces we know about, gravity and electromagnetism. The latter are long-range forces, while the nuclear forces operate only over very short ranges. There appears to be a theoretical connection between the “tension” of space (often expressed as the “cosmological constant”) and the range of the two nuclear forces. I intend to explore this connection, first by understanding the weak force more deeply than I now do, second by delving into quantum field theory and quantum chromodynamics (quark theory) at a more basic level than I have before. Dr. Eugene Chaffin has been working on this field theory aspect of the problem also, and I expect our efforts will fit together well. Eventually I would try to work such knowledge of the force-space connection into the cosmological models I have been working on.

Another connection to explore is a little publicized but moderately well understood relation in general relativity between the expansion of space and heat. Rapid expansion of space would cause the large amounts of heat generated by rapid nuclear decay to *disappear* from rocks deep within the earth. I plan to write a technical article explaining this effect and applying it to the catastrophic geologic phenomena of the Genesis Flood. This work would be of benefit to *all* scientific models of the Flood, since all models have a serious heat disposal problem.

Thus it appears that God’s stretching out the heavens could be a unifying

* Sandia National Laboratories, Albuquerque, New Mexico

theoretical concept, at one stroke causing three major effects:

- rapid nuclear decay,
- the Genesis Flood, and
- rapid cooling of the earth after the Flood.

I intend to pursue these theoretical clues on my own, but at present I am only able to do so in my off hours, as I have done for several decades. With sufficient levels of funding, however, I could retire immediately and work full-time on these and other theoretical problems of vital interest to Creation science. Even with such funding and time, I have at least ten years worth of work to do simply developing these and other ideas already in my file cabinets.

TOTAL ESTIMATED COST \$100,000

Index

A

a priori statements, 23

a bird in a cage, 38

A halo, 443

α -activity, 399, 401, 411, 413

α -decay, 11, 13, 14, 15, 16, 33, 34, 35, 166, 308, 313, 315, 316, 317, 318, 319, 320, 322, 323, 335, 336, 337, 357, 359, 360, 361, 362, 363, 365, 374, 382, 384, 387, 389, 392, 395, 396, 397, 398, 399, 400, 401, 403, 405, 408, 425, 439, 440, 455

α -damage trails, 382

α -dose, 395, 409, 418

α -emission, 14, 29, 106, 115, 165, 382, 383, 386, 387, 388, 401, 402, 403, 404, 408, 409, 419, 456

α -energy, 307, 392, 395, 399

α -particles, 14, 15, 32, 307, 314, 324, 335, 336, 337, 357, 358, 359, 361, 374, 382, 383, 386, 387, 388, 394, 396, 397, 398, 400, 402, 403, 404, 405, 406, 407, 408, 416, 418, 439, 450, 456

α -radioactivity, 392, 403, 408, 411

α -recoil, 23, 322, 323, 381, 407, 411, 423, 424, 457

Abitibi Belt, 216

Abranches, M. C., 103

absolute abundances, 69, 73

abundance, 73, 74, 78, 97, 100, 101, 116, 140, 201, 211, 239,

268, 306, 406, 414, 436

abundance of elements, 61

abundance ratios, 311

Ac, 384, 385

accelerated decay, 3, 6, 7, 8, 9, 11, 12, 13, 16, 18, 19, 20, 21, 22, 27, 28, 42, 43, 44, 50, 83, 84, 85, 86, 89, 90, 106, 108, 115, 125, 275, 282, 305, 306, 307, 311, 312, 316, 317, 323, 324, 325, 333, 334, 339, 340, 341, 343, 344, 345, 349, 350, 351, 352, 356, 357, 358, 362, 364, 366, 367, 368, 369, 373, 374, 397, 398, 449, 450, 451, 453, 455, 456, 458

accelerated geological processes, 276, 277, 278, 279

acceleration factor, 339, 340

accretion, 124, 278, 281

achondritic meteorites, 30, 63, 64

actinium, 401

actinium series, 34

Adam, 9, 89, 338, 356

Adler, H. H., 413

adsorption, 143

AFC processes, 262, 263

Africa, 142

Ag, 55, 62, 70, 72

age, 101, 129, 186, 223

age of the earth, 2, 7, 19, 23, 80, 102, 103, 318

age of the solar system, 113

Ahrens, L.H., 164, 165

air, 350, 373, 386, 393, 395, 408

- akal*, 352
 Akka Water Fall, 128
 Al, 55, 60, 62, 68, 69, 70, 71, 72
 Albarede, F., 266, 268
 albite, 144, 203, 210
 Albrecht, A., 311
 Albuquerque, 14, 15, 20, 333
 Alcock, F. J., 443
 Alexander, E. C., 321
 algae, 140
 alkali, 127, 128, 192, 212, 225, 227
 allanite, 220, 391
 Allègre, C. J., 101, 192, 244, 245, 246, 257, 266, 267
 Allen, J. C., 441
 Allende meteorite, 17, 112, 113
 allogenic minerals, 204, 206
 Alps, 147
 alteration stage, 55
 ambient fluids, 425
 Amitsoq gneisses, 261
 Amos, 352
 amphibole, 38
 amphibolite, 110, 111, 127, 144, 145, 149, 154, 182, 199, 200, 211, 216, 217, 249
 anatexis, 144, 233
 Anders, E., 61, 62, 65, 321
 Anderson, D.L., 54
 andesite, 129, 431
 Androscoggin County, 442
 anhydrous lherzolites, 139
 animal predation, 89
 annealing, 318, 423, 424, 447, 452
 anomalous isochrons, 188, 210
 anorthoclase phenocryst, 135
 anorthoclase volcanic bomb, 128
 Answers in Genesis, 10, 11
 Antarctic gneiss, 168
 Antarctica, 128, 220
 antediluvian world, 354, 374
 anti-Biblical worldview, 305
 antineutrino, 29
 antiquark, 367, 368
 Antoniadis, I., 312
 apatite, 30, 161, 198, 209, 211, 391, 427
 Apollo 14 mission, 316
 Appalachian, 236
 apparent age, 132, 136, 145, 155, 155, 193, 199, 203, 206, 207, 216, 219, 306, 335, 441
 apparent isochron, 193, 198, 203, 214
 appearance of age, 440
 aquifers, 434
 Ar, 13, 30, 37, 38, 39, 42, 55, 65, 96, 117, 123, 126, 127, 129, 130, 131, 132, 133, 134, 135, 136, 137, 138, 139, 140, 141, 142, 143, 144, 146, 147, 148, 149, 150, 151, 153, 154, 155, 156, 158, 159, 187, 199, 200, 206, 221, 237, 266, 267, 268, 272, 274, 276, 277, 280, 344, 346, 348, 349, 350
 Ar-Ar method, 11, 12, 21, 39, 95, 113, 114, 137, 140, 141, 142, 144, 146, 147, 148, 152, 153, 154, 159, 220, 237, 276,
 Ar diffusion, 346, 348
 Ar in biotite, 346, 349
 Ar inheritance, 157
 Ar in magma, 136
 Ar isotopes, 39
 Ar leakage, 157
 Ar loss, 157, 200
 Ar mixing, 157
 Ar reset, 157

- Archean, 87, 88, 95, 109, 139, 165, 182, 203, 214, 215, 222, 225, 227, 231, 234, 240, 250, 253, 261, 264, 445
- Arendal, 400, 454
- Arizona, 127, 133, 134, 156, 157
- ark, 8, 340, 373, 374
- Armitage, M., 390, 424, 428, 447
- Armstrong, R., 6
- Armstrong, R. L., 128
- Arnaud, A. O., 148
- Arndt, N. T., 230, 231, 234
- Arno, 405, 454
- Arshavskaya, N. I., 82
- As, 55, 70, 72
- Ascension Island, 179, 180
- Ashwal, L. D., 82, 167
- asphaltized wood, 390
- assimilation, 143, 197
- asteroid, 32, 144
- asthenosphere, 52, 247, 271
- asymmetric fission, 321
- Atlantic Ocean, 179, 181, 233
- atmosphere, 127, 135, 136, 137, 142, 143, 148, 159, 210, 247, 266, 268, 350, 374, 430, 431
- atmospheric Ar, 37, 39, 136, 138
- atmospheric O, 264
- atmosphile elements, 55
- atomic mass, 29, 360, 363
- atomic nucleus, 29, 333
- atomic number, 29, 211, 359, 385
- atomic weight, 29, 359
- atoms, 336, 355, 371
- Au, 55, 62, 70, 72, 74, 425
- Auckland, 128
- Aust-Agder County, 442
- Austin, S. A., 7, 10, 14, 21, 42, 45, 52, 95, 107, 108, 117, 129, 133, 134, 156, 157, 158, 267, 271, 273, 274, 306, 339, 343, 344
- Australia, 139, 146, 174, 184, 185, 193, 194, 195, 196, 215, 229, 234, 259
- Australian granodiorite, 168
- authigenic minerals, 204, 206
- average chondritic meteorite, 278
- axial vector, 308
- axial asymmetry, 320
- Azores, 180
- ## B
- B halo, 443
- β -decay, 11, 16, 31, 33, 34, 35, 106, 115, 308, 309, 313, 316, 362, 363, 364, 365, 375, 384, 403, 410, 411, 416, 417, 418, 419, 438
- B, 55, 62, 70, 72
- Ba, 54, 55, 60, 62, 68, 70, 73, 75, 224
- BABI, 251, 252
- Back, E., 424, 447
- bacteria, 140, 435
- baddeleyite, 161, 163, 170, 171
- Bagnall, K. W., 425, 426, 431, 433
- Bailin, D., 309
- Baksi, A. K., 146, 152
- Ballentine, C. J., 142
- Balling, N., 82
- Ballyellen, 443
- Barrell, R., 443
- Barrow, J. D., 305, 308, 309, 311
- Bartel, A. J., 160, 163, 169, 175
- Barth, T. F. W., 443
- basalt, 30, 52, 56, 57, 58, 59, 60, 66, 67, 73, 74, 76, 117, 127, 130, 131, 132, 133, 135, 136, 137, 138, 142, 151, 158, 179, 181,

- 186, 188, 190, 191, 215, 216,
227, 230, 237, 251, 252, 258,
263, 271, 344, 431, 432
- basement age, 232, 233
- basement granite, 186
- basement rocks, 166, 413, 437
- Bass Rapids, 116
- bastnaesite, 211
- Bates, R. L., 382, 383
- Bateson, S., 388, 390, 391, 393,
395, 399
- Baumgardner, J. R., 7, 11, 14, 19,
21, 49, 52, 103, 273, 278, 356,
370, 373, 451, 452
- Bavaria, 442
- Be, 55, 62, 70
- Beartooth andesitic amphibolite,
116
- Beartooth Mountains, 116, 199
- Beckinsale, R. D., 107
- Becquerel, H., 28
- bedding planes, 447
- beginning, 338
- Bell, K., 189 251, 252
- Ben Othman, D., 251, 252, 257
- Bencubbin meteorite, 64
- Bennett, V. C., 233
- Benue, 128
- Berridale Batholith, 195
- beryl, 144, 276, 277
- betafite, 448
- Bi, 55, 70, 72, 336, 384, 385, 386,
396, 401, 421, 425, 429, 431,
434, 438, 439
- bias, 186, 191, 280, 306, 452, 453
- Bi-Po halo, 438, 439
- Bible, 2, 17, 23, 87, 90, 276, 367
- Bielecki, J.W., 315, 336
- big bang, 306, 309, 310, 323
- bilinear covariants, 308
- Billings, M. P., 443
- Bingie Bingie Point, 197
- Binns, R. A., 449
- biogenic carbon, 140
- biological activity, 441
- biosphere, 374
- biostratigraphy, 123, 192, 202, 272,
281, 341, 344
- biotite, 13, 16, 30, 109, 111, 116,
144, 145, 154, 155, 156, 160,
187, 199, 200, 208, 209, 211,
345, 346, 347, 346, 347, 348,
349, 350, 382, 387, 388, 389,
390, 391, 392, 393, 394, 395,
397, 399, 400, 401, 402, 403,
405, 406, 407, 408, 409, 410,
411, 412, 413, 414, 416, 418,
419, 421, 423, 424, 425, 426,
427, 428, 429, 436, 437, 439,
440, 441, 444, 445, 447, 448,
449, 452, 453, 454
- Birunga, 189
- Bjorlykke, H., 443
- Black Bluff, 147
- black mica, 345
- Black, L. P., 252
- bleaching, 388, 399, 400, 405, 406,
407
- blocking temperatures, 198, 199,
219
- Bob Jones University, 12, 305
- boiling, 431
- Bonhomme, M. G., 206
- boreholes, 82, 345
- Born, H. J., 333
- boson, 309, 360, 363, 364, 366,
369
- Botswana, 141
- Bottino, M. L., 208
- Boucot, A. J., 444

Bouvet, 180
 Bowring, S. A., 98
 Boylan, D., 14
 Br, 55, 70, 72
 brachiopods, 446
 Bragg ionization curves, 393
 brannerite, 450
 Breger, I. A., 413
 Brevart, O., 258
 Briggs, C. A., 368
 Brink, D. M., 359
 Broadhurst, C. L., 130
 Broken Hill, 146, 147
 Brooks, C., 108, 188, 189, 193, 209
 Bros, R., 232
 Brown, F., 368
 Brown, R.H., 396, 397, 426, 446
 Brown, W., 339
 Brukl, A., 399
 bulk assimilation, 260
 bulk composition, 278
 bulk earth (BE), 222, 241, 242, 243, 248, 251, 252, 253, 255, 266, 280
 bulk earth geochemical reservoir, 149
 bulk mantle, 58
 bulk refractory element composition, 67
 bulk rock, 56
 bulk silicate earth (BSE), 66, 71, 75, 76, 239, 242, 244, 245, 248, 266
 Bullen, K. E., 53
 buoyancy, 52, 56
 burial, 202, 204
 Burnard, P., 138, 142
 Burnham, C. W., 446
 burning, 351, 352, 353, 355
 Burton, K. W., 109, 111, 112
 Bushveld intrusion, 260, 261

C

C, 30, 55, 65, 66, 70, 72, 139, 211, 373, 374
 C halo, 443
 c-variation, 308
 Ca, 30, 35, 37, 55, 60, 62, 68, 69, 70, 71, 72, 161, 173, 208, 209, 211, 227, 229, 400, 406, 407
 Ca-Al-rich inclusions (CAI), 112, 113
 Cajon Pass, 82
 calc-silicate rocks, 229, 230
 calcite, 209, 390, 440, 444, 447, 448
 California, 95, 123, 127, 128, 194, 213, 315, 320, 381
 California State University, 13
 Cambrian, 157, 196, 197, 342
 Cameron, M., 202
 Canada, 98, 142, 216, 251, 252, 440, 442
 Canary Islands, 180, 248
 Canyon Diablo, 103, 112, 176, 179, 257
 Cape Breton Island, 442
 Cape Town, 400, 454
 Cape Verde, 180
 carbon-14 dating, 9, 44
 carbon dioxide, 141, 142, 144
 carbonaceous chondrites, 63, 64, 65, 66, 73, 79, 321
 carbonaceous phases, 321
 carbonado diamonds, 144
 carbonate rock, 441
 carbonates, 30, 141
 carbonatites, 139
 Carboniferous, 445
 Cardenas Basalt, 107, 133, 134, 156, 158, 159, 274
 Carlow, 444

- Carlson, R. W., 59, 113
 Carrol, M. R., 346, 348
 Carslaw, H. S., 84, 347
 cataclysmic events, 89, 353, 354, 356
 catastrophic, 5, 52, 89, 124, 278, 356
 catastrophic judgment, 89
 catastrophic plate tectonics, 52, 267, 271, 273, 277, 278, 281, 369
 catastrophic mantle-crust geodynamics model, 278
 category one discordance, 106, 107
 category two discordance, 106, 108
 category three discordance, 107, 109
 category four discordance, 21, 95, 107, 109, 112
 Cattell, A., 216
 Cawthorn, R. G., 191
 Cd, 55, 62, 70, 72
 Ce, 31, 54, 60, 62, 70, 75, 161, 211
 cerite, 211
 Cf, 318, 319, 321, 322, 323, 324
 Chadwick, J., 29
 Chaffin, E. F., 7, 12, 13, 14, 22, 305, 306, 311, 312, 314, 315, 320, 362, 365, 374, 397
 chalcophile elements, 55, 72
 change of decay, 157
 channels of water, 353
 Chappell, B. W., 194, 195, 196, 259
 chart of the nuclides, 318, 385, 386
 Chattanooga, 415, 451
 Chattanooga shale, 88
 Chaudhuri, N. K., 407, 422, 424
 Chauvel, C. A., 60, 107, 214, 215
 Cheddar, 442, 444
 chemistry, 124, 160, 174, 179, 193, 194, 196, 200, 212, 219, 238, 248, 259, 260, 266, 365, 385, 419, 430
 Chen, Y. D., 168, 194, 213
 chert, 116
 childbirth, 357
 chimney, 432
 chimney deposits, 432
 China, 95, 112
 Chivas, A. R., 262
 chondrite, 63, 64, 67, 68, 69, 72, 74, 101, 102, 112, 113, 114, 115, 223, 225
 chondrite abundances, 72
 chondrite reservoir, 223, 224, 225, 255
 chondritic abundance, 69, 71
 chondritic composition, 72
 chondritic inclusion, 64
 chondritic meteorites, 19, 21, 95, 103, 114, 115, 222, 253, 280
 chondritic model, 67, 249
 chondritic spherules, 64
 chondritic uniform reservoir (CHUR), 222, 223, 224, 225, 226, 227, 228, 229, 230, 231, 233, 242, 243, 249, 253, 254, 255, 257, 259
 chondrules, 63, 113
 Christ, 2, 337, 338, 366, 367
 Christians, 3
 chronology, 197, 220
 CHUR evolution line, 225, 227, 242
 Church, F. E., 182
 Church, T. M., 432, 447
 Churchill, 236
 circular halo, 416
 circulating water, 160
 circulation, 142, 149, 152, 267, 415, 433

- Cl, 55, 62, 70, 72, 135, 141, 142, 433
 Claoue-Long, J. C., 215
 clastic dikes, 339
 clastic sedimentary rocks, 232
 Clauer, N., 205, 206, 207, 232, 262
 Clauser, C. P., 82
 clauthalite, 415, 416, 417, 418, 436
 clay, 32, 35, 38, 169, 204, 205, 206, 207, 208, 232
 clay layer, 32
 clay minerals, 38, 204
 cleavage planes, 199, 381, 403, 418, 422, 423, 425, 427, 428, 429, 433, 436, 437, 440, 450, 457
 cleave the earth, 353
 climatic change, 32
 clinopyroxene, 65, 130, 218, 219
 clocks, 204
 closed system, 12, 40, 45, 103, 105, 106, 149, 151, 156, 161, 164, 165, 174, 177, 182, 188, 198, 204, 205, 217, 219
 closure temperature, 109, 156, 198, 219, 220
 Cm, 318, 319
 Co, 55, 62, 70, 72
 co-magmatic rock suites, 222
 coal, 390
 coalification, 415, 416, 417, 418
 coalified wood, 88, 89, 275, 381, 390, 413, 414, 415, 416, 417, 418, 430, 436, 437, 448, 451, 452, 457
 Cocherie, A., 172
 cogenetic suite of rocks, 21, 95, 99, 101, 103, 104, 105, 106, 107, 108, 188, 190, 210, 212, 213, 280
 Collerson, K. D., 257
 Collins, L. G., 425
 colloidal gel, 131
 Colorado, 154, 155, 167, 199, 227
 Colorado Plateau, 88, 89, 275, 413, 415, 430, 448, 451, 452
 Colossians, 366
 comagmatic suite, 193
 combination halos, 438, 439
 common denominator effect, 263
 compactified, 311, 361
 compaction, 275
 components, 61
 composite radiohalos, 438
 composition, 49, 51, 53, 54, 59, 60, 61, 65, 66, 71, 73, 74, 75, 76, 78, 79, 86, 89, 101, 103, 136, 140, 141, 150, 151, 156, 161, 163, 168, 174, 175, 176, 178, 179, 181, 182, 183, 184, 186, 187, 188, 191, 194, 195, 196, 197, 205, 206, 209, 210, 214, 218, 221, 222, 224, 225, 227, 228, 230, 234, 239, 242, 246, 248, 249, 250, 251, 252, 253, 254, 257, 258, 259, 261, 262, 263, 266, 277, 278, 280, 281, 321, 431
 compressional wave speed, 51
 Compston, W., 170, 172, 192, 194, 202, 205, 215, 216, 237
 concordance, 36, 88, 95, 98, 105, 106, 110, 111, 112, 113, 114, 115, 116, 117, 123, 167, 168, 169, 170, 200, 216, 272, 273, 277, 281,
 concordia diagram, 98, 164, 165, 170, 171, 172, 257
 condensation, 55, 112
 condensation temperature, 71, 72
 conduits, 74, 322, 410, 411, 418, 419, 426, 427, 428, 429
 conglomerate, 36

- Congo Republic, 189
 Connecticut, 442
 consuming, 351, 352
 contact metamorphism, 199, 200
 contamination, 108, 127, 137, 138, 142, 148, 178, 179, 182, 189, 190, 197, 205, 210, 211, 215, 216, 218, 228, 237, 246, 258, 260, 261, 262, 263, 280
 continent, 270, 271
 continental accretion, 178
 continental basalt, 149, 150, 237, 248,
 continental crust, 38, 49, 50, 52, 54, 55, 57, 58, 59, 60, 73, 74, 75, 76, 77, 78, 79, 80, 82, 86, 87, 89, 90, 142, 149, 150, 151, 152, 195, 213, 227, 230, 231, 234, 237, 238, 239, 240, 243, 244, 247, 248, 249, 250, 253, 254, 255, 257, 260, 261, 262, 266, 268, 269, 270, 352
 Continental Deep Drilling Project, 148
 continental granite bodies, 83, 85, 373, 374
 continental igneous rocks, 188, 224, 227
 continental lithosphere, 151, 179
 continental magmatic rocks, 109
 continental mantle, 149, 150, 152
 continental metamorphic rocks, 95
 continental Precambrian shields, 139
 continental rocks, 190
 continental sediments, 232, 247, 271
 continental volcanic rocks, 210
 continents, 182, 248, 264
 continuous Pb diffusion, 165
 convecting mantle, 150, 151, 267
 convection, 49, 74, 87, 151, 149, 179, 188, 221, 266, 270, 271, 281
 convergent margin volcanism, 57
 Conway Granite, 441, 442, 446, 449
 Cook, M. A., 350
 cooling, 9, 87, 131, 135, 156, 159, 178, 198, 199, 219, 220, 410, 432, 446
 Copeland, P., 169
 copper sulfide, 31
 cordierite, 144, 387, 388, 389, 390, 391, 392, 395, 399, 403, 409, 411, 413, 418, 423, 437, 441, 444, 454
 core, 5, 49, 51, 52, 53, 55, 66, 71, 72, 73, 74, 78, 79, 104, 177, 203, 248, 267, 268, 269, 374
 core formation, 72
 core reservoirs, 269
 core-mantle boundary, 58, 61, 73, 79
 I Corinthians, 356
 corona, 61
 correlation diagram, 259
 corruption, 357
 Cortini, M., 191
 cosmic expansion, 364
 cosmic rays, 135, 314, 315, 340, 356, 374,
 cosmological assumption, 103
 cosmological constant, 16, 305, 306, 312
 cosmological model, 251, 313, 320
 cosmological term, 310
 cosmology, 9, 17, 86, 321, 366, 367, 420
 cosmos, 338, 356, 367, 370
 Cottman, 444

- Cottman Street Quarry, 442
 coulomb barrier, 358, 359, 361
 coulomb repulsion, 313
 country rock, 177, 178, 185, 186,
 221, 233
 County Carlow, 442
 coupling constants, 307, 308, 309,
 310, 312, 313, 361, 363
 Cr, 55, 62, 70, 72
 cracks, 172, 322, 418, 419, 427,
 428, 429, 435, 450, 451
 cratering, 356
 cratons, 139
 Crawford, D. P., 388
 created rocks, 441, 445
 Creation, 1, 2, 4, 5, 6, 7, 9, 15, 17,
 19, 22, 43, 89, 91, 275, 276, 277,
 278, 281, 282, 316, 333, 338,
 340, 341, 349, 357, 362, 420,
 422, 441, 446, 455, 456, 458
 creation event, 413
 Creation model, 32, 310, 321, 323,
 346, 348, 349, 369, 375
 Creation Research Society, 10, 12
 Creation Research Society
 Quarterly, 12
 Creation week, 8, 21, 49, 89, 276,
 307, 333, 341, 346, 357, 362,
 365, 368, 373, 398, 441, 444
 creationist, 3, 314, 339, 341, 349,
 441, 455
 creationist communities, 18
 creationist framework, 82
 creationist worldview, 16, 306
 creative processes, 441
 Creator, 5, 9, 356, 366
 Cretaceous, 262, 414, 451
 Cretaceous-Tertiary boundary, 32
 Crocker, C. H., 107
 cross-cutting, 440
 Crowley, J. L., 172
 Crozaz, G., 313, 314, 315, 316
 crust, 5, 8, 11, 21, 37, 52, 53, 76,
 78, 79, 82, 123, 125, 136, 139,
 142, 143, 144, 149, 150, 151,
 152, 159, 177, 178, 182, 183,
 190, 191, 194, 196, 197, 210,
 212, 221, 224, 225, 227, 230,
 231, 234, 237, 238, 239, 240,
 243, 247, 248, 249, 250, 251,
 253, 254, 257, 258, 259, 260,
 263, 264, 265, 266, 267, 268,
 269, 272, 273, 276, 277, 278,
 279, 281, 340, 350, 352, 356, 373
 crust formation ages, 212, 213, 232
 crust generation, 255
 crust reservoirs, 258
 crust-mantle differentiation
 processes, 73
 crust-mantle geodynamics models,
 272
 crustal Ar, 148
 crustal basement, 235, 236
 crustal component, 195, 196
 crustal contamination, 215, 260,
 262
 crustal evolution curves, 253
 crustal extraction ages, 228, 232,
 234, 235
 crustal fluids, 123, 143, 149, 279
 crustal formation age, 227, 233
 crustal fusion, 196
 crustal growth, 57, 267, 273, 276,
 277, 278, 281
 crustal magma chamber, 143
 crustal material 75, 197, 248, 260,
 263, 278
 crustal Nd, 215
 crustal processes, 239
 crustal sources, 22, 123, 124, 194,

230, 231, 232, 273, 280
 crustal radioactivity, 76
 crustal residence age, 232
 crustal reservoirs, 234, 238, 239,
 249, 263, 264
 crustal rocks, 11, 21, 32, 74, 79, 83,
 97, 98, 109, 123, 142, 144, 148,
 149, 152, 159, 175, 187, 197,
 212, 216, 224, 225, 234, 237,
 243, 251, 267, 268, 273, 274,
 275, 276, 279, 280, 281, 282,
 369, 381, 449, 454
 crystal matrix, 38, 153, 164, 165,
 199, 336, 345, 372
 crystalline rocks, 86, 159, 310
 crystalline silicates, 63
 crystallization, 56, 96, 97, 104, 105,
 109, 116, 131, 135, 163, 164,
 166, 191, 198, 201, 211, 212,
 219, 221, 224, 411, 413, 425,
 427, 433, 452
 crystallization age, 214, 230, 231,
 234
 crystals, 166, 168, 169, 170, 172,
 179, 198, 211, 215, 237, 276,
 336, 355, 425, 428, 433, 436,
 446, 447, 448, 452
 Cs, 54, 55, 70, 72,
 Cu, 55, 62, 70, 72, 425, 426
 Cumming, G. L., 177, 257
 Cumming, K., 7, 10
 Curie, M., 29
 Curie, P., 29
 curse, 4, 43, 356
 curvature, 371, 372
 Cwiok, S., 320
 cyanobacteria, 441
 cycling, 86, 90, 434

D

D halo, 401, 419
 D'' layer, 76, 78
 dacite, 129
 Dalrymple, G. B., 37, 38, 45, 108,
 117, 126, 128, 130, 131, 135,
 136, 144, 158
 Damon, P. E., 130, 144, 276, 420
 Damour, T., 305
 Dasch, E. J., 208
 dating, 21, 27, 123, 186
 daughter-daughter model age, 98
 daughter isotopes, 1, 3, 4, 5, 8, 10,
 12, 15, 24, 30, 32, 37, 39, 41, 44,
 45, 96, 99, 100, 101, 104, 105,
 106, 108, 123, 126, 160, 161,
 166, 199, 214, 219, 221, 222,
 238, 239, 246, 250, 251, 253,
 319, 335, 336, 337, 344, 383,
 392, 401, 404, 407, 410, 419, 424
 David, 24, 25, 353
 Davidson, B., 368
 Davies, G. F., 267
 Davies, J. F., 443
 Davis, G. L., 166, 167, 168
 day three, 87, 88, 89, 277, 278,
 338, 340, 357, 441
 day-age theory, 2
 decay, 99, 151, 153, 175, 176, 184,
 189, 190, 192, 195, 198, 220,
 239, 246, 257, 305, 307, 312,
 316, 317, 322, 333, 335, 337,
 340, 352, 357, 387, 401, 408,
 412, 413, 414, 416, 422, 423,
 424, 436, 451, 457
 decay chains, 323, 337, 385, 386,
 404, 419
 decay constant, 28, 97, 99, 102,
 113, 114, 115, 307, 309, 312,

- 315, 317, 392, 397
 decay episode, 12, 84, 85
 decay heat, 317
 decay mode, 319
 decay model, 316
 decay probability, 14
 decay products, 4, 165, 343, 344, 430, 437, 438
 decay rate, 4, 16, 17, 44, 88, 96, 105, 106, 275, 311, 340, 341, 343, 356, 358, 369, 374, 392, 396, 397, 398, 452
 decay speedup, 352
 decompression melting, 56
 deep, 354
 Deep Sea Drilling Project (DSDP), 131
 deeper mantle, 59
 defects, 381, 428, 429, 433, 435, 457
 deformation, 418
 degassing, 136, 144, 148, 149, 159, 248, 276, 431, 433
 dehydration, 143
 DeLury, J. S., 433
 density, 450
 DePaolo, D.J., 197, 213, 214, 222, 224, 225, 227, 228, 233, 234, 242, 243, 255, 259, 262
 depleted mantle (DM), 59, 73, 76, 77, 78, 181, 195, 196, 216, 222, 223, 224, 225, 226, 227, 228, 229, 230, 231, 238, 241, 242, 243, 244, 245, 246, 247, 248, 250, 251, 252, 253, 254, 255, 257, 258, 259, 270
 depletion, 69, 71, 72, 216, 255, 264, 266, 270
 deposition, 178, 204, 205, 275, 426, 429, 432, 437
 destruction halos, 450, 451, 454
 determined age, 214
 Deuteronomy, 351
 deuterons, 314
 Deutsch, S., 166, 399
 devitrification, 158
 Devonian, 88, 415, 445, 451
 DeWolf, C. P., 220
 DeYoung, D., 7, 12, 14, 20, 27, 42, 45, 307, 344
 diabase, 104, 116, 199, 146
 diagenesis, 187, 204, 205, 232
 diamonds, 65, 66, 139, 140, 141, 142, 144, 390, 428, 429, 446, 447
 Dickin, A., 31, 36, 45, 97, 98, 108, 154, 160, 161, 169, 174, 181, 188, 190, 198, 201, 202, 204, 205, 216, 234, 235
 Dickmann, F., 320
 Dickson, B. L., 184, 185
 dielectric permittivity, 305
 Dienes, K. R., 312
 differential erosion, 80
 differentiation, 21, 49, 54, 55, 57, 65, 78, 86, 87, 90, 177, 179, 181, 182, 189, 190, 191, 192, 212, 218, 246, 254, 262, 270
 diffusion, 135, 136, 143, 144, 154, 155, 158, 164, 165, 166, 167, 172, 191, 199, 203, 219, 220, 221, 345, 347, 348, 410, 422, 423, 424, 425, 436
 diffusion coefficients, 155, 156, 220, 347, 348, 407, 416, 422, 423
 diffusion depth, 83
 diffusion radii, 156
 diffusion rate, 13, 17, 18, 19, 166, 346, 422, 424, 457
 diffusivity, 156
 dike, 104, 146, 200

- Dill Township, 442
 dimensionless ratios, 311
 Dingwall, 442, 444
 dinosaurs, 32
 diopside, 116
 diorites, 262
 discontinuities, 53, 150, 266
 discordance, 10, 11, 16, 21, 36, 95, 97, 98, 106, 107, 108, 109, 110, 111, 113, 114, 115, 118, 123, 164, 165, 172, 173, 274
 Discovery Tablemount, 180
 dislocations, 426
 distribution of radioactive elements, 11, 16, 21, 49, 56, 61, 74, 90
 Dobrzhinetskaya, L. F., 144
 Dodson, M. H., 198, 199, 219, 263
 Doe, B. R., 178, 239, 263
 dolomite, 116, 205
 Dons, J. A., 443
 Doppler red shift, 370
 Dora Maira, 147
 dose, 455
 downpour of waters, 353
 Draine, B. T., 321
 Drescher, J., 148, 149, 152, 159
 drillcores, 124, 131, 160, 164
 Driver, S. R., 368
 Drozd, R., 321
 dry land, 87, 277, 278
 dual halo, 416, 417, 418, 399
 Duluth, 199, 200
 Duluth Gabbro, 199, 200
 dunites, 190
 DUPAL anomaly, 246
 Dupre-Allègre (DUPAL), 244, 246
 Dupre, B., 246
 Dutch, S., 420, 422
 dwarf halos, 381, 399, 400, 405, 407, 453, 454, 456
 Dy, 60, 62, 70
 Dymond, J., 128, 131
 Dyson, F., 305
 Dziewonski, A. M., 53
- E**
 early stage volatility trend, 72
 earth accretion, 268, 281
 earth rocks, 305
 earth structure, 51
 earthquakes, 51
 earth's magnetic field, 339
 East Africa, 142, 189
 East Pacific Rise, 127, 128, 131, 138, 262, 432
 Easter Island, 180
 Eckelmann, W. R., 173, 174
 eclogite, 58, 139, 141, 219
 economy of action, 364
 edge dislocations, 146
 Egyptians, 338
 Einstein, A., 311, 370
 elastic waves, 51
 Eldora stock, 154, 155, 167, 199
 Eldridge, C. S., 140
 electric fields, 309, 311
 electrical, 312
 electricity, 311
 electromagnetic forces, 307, 362, 363, 365
 electromagnetic interactions, 307, 309, 310, 397
 electromagnetism, 363, 365
 electron, 29, 32, 309, 313, 314, 360, 362, 363, 366, 369
 electron capture, 37, 316
 electron charge, 359, 363
 electron emission, 38

- electron microprobe, 172, 406
 electronic structure, 365
 electrostatic repulsion, 357, 359
 electroweak theory, 310
 element, 61, 62, 67, 76, 90, 150, 159, 161, 179, 187, 190, 201, 211, 216, 224, 238, 239, 260, 272, 323, 355, 416, 425, 430, 432, 435
 elementary particles, 312, 355
 elements will melt, 354
 Ellam, R. M., 259
 Elliott, T., 264
 elliptical halo, 416
 Ellsworth, H. V., 433
 emanation halos, 401, 410, 443
 embryonic halos, 394, 395, 397, 414, 415, 419, 452
 emission, 396, 431
 EMXRF, 414, 415
 end members, 60, 174, 183, 195, 242, 246, 249, 259, 408
 end-product isotopes, 389
 energy, 311, 318, 322, 355, 372
 energy density, 310
 England, 192, 201
 enriched mantle (EM), 59, 60, 67, 76, 77, 223, 241, 242, 243, 244, 245, 246, 247, 248, 249, 250, 251, 252, 255, 259
 enrichment, 69, 142, 246, 248, 249, 250, 253, 254, 266, 270, 431
 entrainment, 140, 150
 epidote, 160
 episode of nuclear decay, 83
 episodic Pb loss model, 165
 ϵ , 195, 197, 224, 226, 228, 231, 242, 243, 245, 249, 257, 259
 Er, 60, 62, 70
 erosion, 31, 143, 166, 178, 184, 225, 232, 269
 error bars, 101
 errorchron, 108, 163
 erupted isochrons, 190
 eruption, 138, 143, 216
 Esser, R.P., 128, 135, 137
 ether, 367
 Eu, 60, 62, 70
 eucrite, 101
 Europe, 109, 312
 euxenite, 173
 Evans, R. D., 359, 360, 361, 363
 Eve, 9, 89
 Evernden, J. F., 158
 evolution, 1, 2, 17, 176, 413
 evolution model, 4, 15, 117, 267, 346, 348, 349
 evolutionary assumptions, 152
 evolutionary origin, 268
 evolutionary timescale, 153, 154, 156, 158, 187, 274
 evolutionary view, 338
 evolutionist, 321, 341, 349, 345, 350
 evolutionist communities, 18
 evolutionist interpretation, 337
ex nihilo (from nothing), 5
 excess Ar, 123, 126, 127, 128, 129, 130, 131, 132, 135, 136, 137, 139, 140, 141, 142, 146, 147, 148, 149, 151, 152, 153, 154, 155, 156, 157, 158, 159, 267, 276, 277, 280
 excess Pb, 169, 177, 179
 excessive grinding, 153
 excessive heat, 44
 exchange, 31
 executive committee, 20
 expanding universe, 310, 371
 expanse, 368

expansion, 367, 369, 370, 371, 372
 expansion cracks, 450
 expansion of the universe, 312
 explosive fracturing, 451
 exponential decay, 28
 extinction of the dinosaurs, 32
 extra dimensions, 311, 312, 371
 extraction, 225, 278, 279
 extraneous Ar, 127
 extraterrestrial origin, 32
 extrusion, 202

F

F, 55, 62, 70, 72, 211, 447, 448
 fabric, 367, 371, 372
 Fall, 7, 8, 9, 307, 333, 340
 false isochrons, 184, 185, 210
 false vacuum, 310
 Faraday Mine, 440, 442, 444, 448, 449
 Faraday Township, 442
 fast decay, 339, 341, 344
 fast deposition, 339
 Faul, H., 441, 443
 Faure, G., 38, 44, 45, 96, 98, 101, 108, 153, 161, 169, 178, 181, 182, 183, 190, 204, 223
 Fe, 49, 50, 51, 52, 53, 55, 60, 62, 63, 69, 70, 71, 72, 74, 156, 166, 413
 Fe-Ni mixture, 66
 Fe-poor continental crust, 55
 Fe-Ti oxides, 129
 Feather, N., 421, 422, 429, 430, 433, 435, 436
 Fechtig, H., 156
 feldspar, 38, 144, 155, 161, 162, 163, 198, 205, 209, 211, 239, 422, 450
 felsic rocks, 215, 217, 252, 253
 Fenton Lake, 345
 FeO, 69
 Ferguson, J., 449
 Fermi constant, 363
 Fermi, E., 358, 363
 Fernando de Noronha, 180
 ferroselite, 413
 fiat Creation, 4, 23, 381
 fictitious isochrons, 42
 field theory, 367
 Field, D., 201
 final report, 14, 23, 24
 fine-structure constant, 305, 307, 308, 311, 362
 fingerprinting, 123, 237, 273
 Finlay, C. J., 449
 Finsch, 141
 fire, 351, 352, 353, 354
 first RATE meeting, 6
 Fisher, D. E., 127, 128
 Fisher, L. W., 443
 fissiogenic elements, 321
 fissiogenic Xe, 320
 fission, 15, 312, 313, 314, 315, 316, 318, 320, 321, 322, 336, 403, 411
 Fission Mine, 440, 441, 443, 444, 447, 448, 449
 fission tracks, 4, 8, 16, 22, 23, 275, 281, 282, 305, 306, 313, 314, 315, 316, 317, 318, 319, 320, 321, 322, 323, 324, 336, 337, 381, 387, 401, 411, 412, 419, 423, 438, 457
 fissioning nuclides, 22, 305
 Fitz Gerald, J. D., 66
 five dimensions, 311
 Fleischer, R. L., 313, 387
 Flood, 2, 4, 6, 7, 8, 9, 16, 91, 275,

- 276, 277, 278, 279, 281, 307,
 333, 340, 341, 344, 349, 368,
 373, 374, 392, 398, 453, 455,
 456, 457, 458
 Flood basalts, 228
 Flood boundaries, 8
 Flood event, 441
 Flood gneisses, 441
 Flood model, 369
 Flood rocks, 16, 369
 Flood schists, 441
 Flood-deposited, 444
 Flood-deposited strata, 454
 Florida, 434
 flows, 273
 fluid emissions, 457
 fluid transport, 422
 fluoride ions, 425
 fluorine oxide, 448
 fluorite, 387, 388, 389, 390, 391,
 392, 394, 395, 397, 409, 410,
 411, 412, 414, 418, 422, 428,
 437, 440, 444, 447, 448
 flux, 149, 159, 269
 focus zone (FOZO), 61
 Foland, K.A., 441, 443
 forearc, 143
 formation, 55, 90
 Fortier, S. M., 346
 fossil-bearing, 337, 341, 445, 446,
 453, 457
 fossil dating, 152
 fossil-determined, 341
 fossil graveyards, 339
 fossil record, 89
 fossil strata, 344
 fossiliferous Flood strata, 455
 fossils, 52
 foundation of the world, 338
 foundations of the mountains, 351,
 352, 353, 354
 foundering, 178
 Fountain, D. M., 75
 Fournier, R. O., 153
 fourth RATE meeting, 18
 Fowler, W. A., 323
 Fowler, P. H., 407
 FOZO basalt, 61
 Fra Mauro, 316
 fractional crystallization, 191, 193,
 197, 212
 fractionation, 12, 30, 32, 44, 45, 55,
 57, 69, 123, 135, 136, 175, 178,
 179, 190, 191, 192, 210, 213,
 221, 224, 225, 229, 230, 232,
 233, 235, 237, 238, 239, 255,
 257, 258, 263, 267, 269, 278,
 279, 280
 fractures, 57, 218, 381, 422, 425,
 426, 433, 435, 447, 457
 Fraser Range, 146
 Fremlin, J. H., 411, 412
 Frey, F.A., 213
 friability, 63
 Froland, 442, 444
 Front Range, 154, 199, 227
 Froude, D. O., 168
 Fullagar, P. D., 208
 fully-formed halos, 452, 456
 fumaroles, 431
 fundamental charge, 311
 Funkhauser, J. G., 128, 136, 144
 fusion, 194
 futility, 357
- ## G
- G halo, 443
 gabbro, 16, 144, 146, 152, 425
 Gaebelein, A. C., 353

- gain, 161
 Galapagos Islands, 127
 galaxies, 370, 371
 Gale, N. H., 103, 262
 galena, 174, 175, 176, 177, 184
 Galer, S. J. G., 109, 266
 Ganguly, J., 220
 Gap theory, 2
 Garden of Eden, 6
 garnet, 30, 53, 65, 109, 146, 161, 203, 211, 218, 220
 gas condition, 308
 gaseous diffusion, 424
 gaseous transport, 424
 Gaspé County, 442
 Gast, P. W., 179, 187, 199, 200, 208
 gauge, 309
 gauge bosons, 360, 362, 364, 366, 369
 gauge coupling, 308
 gauge coupling constants, 309
 gauge field theory, 309
 gauge theories, 310
 Gd, 60, 62, 70, 211
 Ge, 55, 62, 70, 72
 gedanken experiment, 372
 Genesis, 2, 5, 43
 general theory of relativity, 311, 370, 371
 Genesis Flood, 2, 5, 12, 19, 21, 32, 43, 50, 52, 78, 82, 85, 87, 89, 90, 277, 307, 323, 333, 337, 338, 340, 341, 343, 344, 352, 353, 354, 355, 356, 357, 368, 369, 373, 374, 413, 440
 Gentry, R. V., 88, 89, 275, 322, 323, 335, 336, 339, 344, 345, 346, 350, 351, 382, 383, 387, 389, 390, 391, 392, 393, 394, 395, 396, 397, 399, 400, 401, 402, 404, 405, 406, 407, 408, 409, 410, 411, 412, 413, 414, 415, 416, 417, 418, 419, 420, 421, 422, 423, 424, 428, 435, 436, 437, 438, 439, 440, 441, 442, 444, 445, 446, 449, 450, 451, 452, 454
 geochemical affinity, 430
 geochemical data, 61, 78
 geochemical fingerprinting, 22
 geochemical mixing, 282
 geochemical models, 73, 78, 266, 269, 273
 geochemical processes, 18, 21, 123, 125
 geochemical reservoirs, 22, 152, 266, 268, 277, 281
 geochemical signatures, 22, 281
 geochemistry, 49, 51, 54, 58, 73, 74, 77, 89, 116, 124, 125, 149, 151, 177, 179, 181, 191, 192, 193, 196, 200, 213, 224, 225, 237, 247, 248, 267, 268, 269, 270, 271, 272, 273, 278, 416, 430, 434
 geochemists, 54, 66
 geochron, 102, 179, 181, 244, 244, 256, 257
 geochronology, 21, 29, 44, 95, 101, 112, 137, 146, 148, 160, 187, 234, 235, 392, 420
 geochronometer, 9, 10, 21, 123, 163, 205, 210
 geodynamic models, 263, 266, 267, 282
 geodynamics, 77, 123, 124, 237, 260, 263, 266, 272, 273, 277, 278
 geologic ages, 337, 338, 414, 415
 geologic column, 315

- geologic histories, 175
 geologic process, 87, 99, 151
 geologic record, 274, 275, 276, 277, 278, 281, 282, 455, 456, 458
 geologic time, 165, 182, 224, 392, 395, 398, 425
 geological formations, 397
 geological history, 440
 geological model, 370
 geological occurrence, 440
 geological periods, 392, 393
 geological perspective, 441
 geological uniformitarians, 446
 geological work, 370
 geology, 106, 125, 155, 172, 173, 177, 186, 187, 188, 192, 193, 203, 211, 374, 381, 420, 440, 443, 445, 449, 454, 455, 457
 geometric decay, 28
 geophysicists, 54
 geophysics, 266, 267, 270, 271, 278
 Georgi, H., 307
 geoscience, 333, 334, 335, 339
 geoscientists, 337, 342, 352
 geothermal systems, 433
 German graphites, 209
 German volcanics, 192
 Germany, 82, 148, 320
 Geyh, M. A., 126
 Ghent, E. D., 172
 ghost rings, 388, 393, 394, 400
 giant halos, 381, 402, 403, 405, 406, 407, 453, 454, 456
 Giblin, A. M., 184
 Giem, P. A. L., 136
 Giletti, B. J., 165, 346
 Gill, J. B., 431
 Gillis, K. M., 433
 Girifalco, L. A., 349
 Glashow, S. L., 307, 309
 Glass Mountains, 128
 glassy spherules, 63
 glauconite, 206, 207
 global Flood, 124, 273, 281, 337
 gluons, 367
 gneiss, 36, 98, 146, 148, 168, 169, 201, 208, 216, 217, 229, 235, 249, 261, 390, 440, 441, 444, 445, 447
 gneiss terrane, 235
 God, 2, 8, 9, 21, 22, 24, 25, 49, 50, 78, 79, 86, 87, 88, 89, 90, 91, 333, 335, 337, 338, 340, 351, 352, 353, 354, 355, 356, 357, 360, 364, 365, 366, 367, 368, 369, 373, 397, 398, 446, 455, 457
 Goldrich, S. S., 166, 208
 Goldstein, S. L., 222, 228, 230, 231, 234, 255
 Goliath, 24, 25
 Göpel, C., 114
 Gorda Ridges and Seamounts, 180
 Gott, J. R., 305
 Gough Island, 179, 180
 Grace College, 12, 27
 Gran Canaria, 248
 Grand Canyon, 10, 16, 107, 116, 117, 133, 134, 156, 157, 159, 274, 306, 344
 Grand, S. P., 54, 58
 Granger, H. C., 413
 granite, 13, 18, 19, 33, 83, 85, 88, 146, 160, 164, 168, 169, 175, 182, 183, 186, 191, 193, 194, 194, 195, 196, 199, 208, 209, 210, 212, 215, 217, 218, 221, 230, 231, 233, 234, 249, 250, 254, 400, 402, 405, 406, 410, 413, 414, 425, 426, 435, 436,

- 437, 440, 441, 444, 445, 446,
449, 451, 452, 453, 454, 455,
456, 457
- Granite Mountains, 160, 161, 163,
164, 169, 175
- granitic rocks, 166, 168, 345, 381,
413
- granitoids, 160, 194, 196, 227, 230
- granodiorite, 262, 345
- granules, 112
- granulite, 144, 145, 146, 167, 216,
217, 229, 232, 250
- graphite, 209
- gravitation, 311, 312, 362, 365
- gravitational collapse, 71
- gravitational coupling, 305
- gravitational mass of atoms, 366
- gravitational mass of planets, 366
- gravitational mass of stars, 366
- Greek, 354, 355, 357, 366
- Green, J., 351
- Greenland, 261
- Green's function, 14
- Greenstein, J.L., 323
- greenstones, 196, 197, 228
- Greenville, 305
- Grenville, 236
- Grevasse, N., 61, 62, 65
- Griffith, J. W., 443
- ground water, 123, 160, 172, 184,
208, 209, 279, 381, 413, 414,
417, 434, 435, 437, 439, 457
- Grove, M., 156, 346, 348
- growth curve, 256, 257
- Gruinard Bay, 110, 111
- Guadalupe, 180
- Gudden, B., 391, 395
- Guidong granodiorite, 95, 112
- Gunderson, R. P., 433
- Gurney, J. J., 139, 140
- gypsum, 435
- ## H
- H, 55, 65, 66, 211
- Haack, U., 192
- Habakkuk 3:8–10, 15, 353
- Haelen, R., 82
- Hahn, H. P., 333
- Haines, S. M., 264, 265
- half-life, 12, 28, 30, 31, 35, 36, 37,
38, 39, 42, 44, 213, 307, 313,
315, 316, 317, 318, 319, 320,
322, 335, 358, 360, 361, 362,
363, 364, 381, 385, 386, 396,
397, 398, 399, 408, 410, 411,
416, 417, 420, 422, 423, 425,
430, 432, 434, 436, 456, 457
- half-space surface, 83
- Haliburton County, 442
- halide, 432, 457
- Hall, A., 191
- Hallbauer, D. K., 390
- Halliday, A., 250
- halogen, 431, 433
- halos, 4, 15, 16, 23, 88, 89, 184,
307, 322, 324, 335, 337, 381,
382, 383, 386, 387, 388, 389,
390, 391, 392, 393, 394, 397,
399, 400, 401, 402, 404, 405,
407, 408, 409, 411, 412, 413,
415, 419, 421, 424, 427, 428,
429, 431, 437, 438, 439, 440,
445, 447, 450, 452, 454, 455,
456, 457, 458
- Halzen, F., 363, 364, 369
- Hamblin, W. K., 117
- Hamilton, P. J., 216
- Hamiltonian, 308
- hanging-wall basalts, 215, 216

- Hansen, G. N., 187, 188, 199, 200
Hanyu, T., 138
Harada, K., 434
hardness, 450
Harrison, D., 138
Harrison, E. R., 370
Harrison, T. M., 144, 146, 147, 152, 155, 156, 346, 348
Harshman, E. N., 413
Hart, S. R., 59, 60, 61, 67, 104, 131, 154, 155, 199, 241, 242, 244, 245, 246, 247, 248, 249, 251, 252, 266
Harte, B., 140, 149, 150
Hashemi-Nezhad, S. R., 422, 423, 424
Hastings County, 442
Hawaii, 60, 127, 128, 136, 137, 139, 149, 258
Hawaiian Islands, 180
Hawaiian volcanoes, 127
Hawkesworth, C. J., 140, 149, 150, 237, 259, 260
He, 13, 21, 32, 55, 61, 65, 137, 140, 143, 150, 336, 337, 344, 345, 346, 347, 348, 349, 350, 388, 394, 395
He diffusion, 13, 16, 18, 20, 339, 346, 347, 348, 349, 350,
He escape, 350
He-in-biotite, 346, 348, 349, 375
He nuclei, 15, 32, 335, 337, 345, 357, 387, 388, 394, 395,
He production, 346
He retention, 344, 346, 347, 348, 350, 351,
heat, 3, 8, 9, 11, 12, 21, 49, 74, 75, 76, 77, 80, 81, 82, 83, 84, 85, 86, 87, 90, 337, 352, 354, 356, 370, 372
heating, 31, 109, 146, 147, 155, 172, 336, 337, 369, 373
heavens, 87, 91, 356
heavens and earth, 355
heavy liquids, 105
heavy nuclei, 320
Hebrew, 354, 368
Hebrew words, 352
Hebrews 11:3, 323
Hebridean mantle, 183
Hecker, W., 419, 421, 427, 430, 435, 436, 442
Hedge, C. E., 190, 192
Henderson, G. H., 388, 390, 391, 393, 395, 399, 401, 409, 410, 416, 418, 419, 420, 421, 422, 427, 428, 435, 442
Hensen, B. J., 220
Hermes, O. D., 191
Hernegger, F., 400
Hewitt, D. F., 443
Hf, 30, 38, 54, 55, 60, 62, 68, 70, 73, 267
Hg, 55, 70, 72
Higgs bosons, 310
Higgs fields, 309, 310
Higgs mechanism, 309, 310, 311
Higgs, P.W., 309
high μ (HIMU), 59, 60, 76, 77, 241, 242, 244, 245, 246, 247, 248
HIMU basalts, 59
highly volatile elements, 55
Hills, J. H., 174, 184
Himalayan granite, 168, 172
Hirschi, H., 391, 402
history of nuclear decay, 458
history of the solar system, 316
history of the earth, 49, 51, 61, 73, 78, 86, 87, 89, 116, 178, 232, 239, 257, 264, 267, 270, 276,

- 278, 279, 306, 315, 318, 323,
 324, 338, 339, 340, 381, 392,
 398, 449, 456,
 history of the Sun, 323
 history of the universe, 308, 309,
 338
 Ho, 62, 70
 Hoernle, K., 248
 Hofmann, A. W., 57, 58, 60, 76, 77,
 251, 252
 Hofmann, S., 320
 Holbrow, C. H., 403
 hold together, 366
 holes, 146
 Holladay, W. L., 368
 Holland, C. H., 443
 Holmes-Houtermans model, 176
 Holmes, A., 164, 176, 343, 391
 Holocene, 206, 207
 holocrystalline basalts, 131
 Holy Spirit, 6
 homogenization, 202
 Honda, M. I., 127, 137
 Hoppe, G., 402
 horizon problem, 310
 hornblende, 30, 110, 116, 129, 144,
 146, 154, 155, 156, 199, 200,
 219, 220
 host, 161, 168, 184, 217, 388, 392,
 394, 411, 421, 422, 424, 440,
 441, 444, 448, 457
 hot, 355
 hot plume, 59
 hotspot, 59, 138, 139, 269, 270
 Hough, R. M., 144
 Houtermans, F. G., 176
 Hower, J., 206
 Hoyle, F., 323
 Hualalai, 127, 128, 136
 Huang, W. H., 322, 411
 Huey, J. M., 102, 113, 114
 Huh, C. A., 333
 Huizenga, J. R., 319, 320, 321
 human bloodshed, 338
 human population, 339
 Humbert, F., 127
 Humphreys, D. R., 7, 13, 14, 22,
 86, 108, 275, 324, 333, 339, 351,
 352, 367, 368, 371, 373, 397, 453
 Hurley, T. M., 205, 235, 236
 Huron Claim, 442, 444
 Huss, G. R., 321
 Hussain, N., 432, 447
 Hutcheon, I. D., 313, 315
 Hutton, C. O., 391
 hybrid crust, 234
 hydrated oceanic crust, 143
 hydrostatic pressure, 53, 56
 hydrothermal, 31, 57, 116, 123,
 155, 156, 175, 178, 192, 202,
 203, 212, 217, 218, 221, 225,
 229, 238, 239, 272, 276, 279,
 381, 419, 421, 422, 424, 425,
 426, 429, 430, 432, 433, 435,
 439, 447, 448, 456, 457
 hydrous, 143
 hydroxyl ions, 425
 hypabyssal drusy syenites, 127
- ## I
- I-type granite, 194, 195, 196, 197,
 259
 I, 55, 70, 72, 151, 323
 IBM, 320
 Iceland, 138, 180
 Iceland plume, 138
 igneous, 30, 36, 38, 51, 80, 95, 163,
 168, 182, 183, 188, 189, 191,
 194, 195, 201, 202, 208, 212,

- 214, 216, 219, 222, 223, 224, 227, 234, 260, 351, 390
- Imori, S., 390, 391, 392, 393, 401, 442
- illite, 205, 206
- ilmenite, 390
- Ilton, E.S., 426
- IMMA, 389, 411, 414, 417, 440, 452
- immobility, 219, 222, 238
- immutability, 90, 91
- impact event, 32
- In, 55, 62, 70, 72
- Incarnation, 2
- inclusions, 65, 66 139, 140, 141, 142, 146, 161, 172, 211, 220, 307, 324, 382, 383, 387, 389, 390, 391, 394, 395, 399, 400, 401, 403, 404, 405, 406, 407, 409, 411, 412, 413, 415, 416, 417, 419, 421, 425, 426, 427, 428, 429, 433, 439, 440, 456
- incompatibility, 60, 238, 239, 263
- incompatible elements, 21, 49, 50, 54, 55, 56, 57, 58, 59, 60, 74, 75, 77, 78, 86, 90, 141, 142, 190, 239, 249, 270, 271
- India, 390
- Indian Ocean, 127, 138
- induced spallation, 314
- inert gas, 37, 123, 126, 276
- infiltration, 415
- infinite half-space, 83, 84
- infinite range, 365
- inflationary big bang cosmology, 309, 310
- inheritance, 89, 140, 153, 159, 164, 168, 169, 172, 186, 191, 193, 194, 196, 198, 204, 205, 207, 210, 211, 221, 232, 234, 246, 254, 272, 274, 276, 277, 278, 279, 280, 281, 282, 306, 452
- initial daughter composition, 42
- initial report, 20, 23
- inner core, 51, 52
- Institute for Creation Research (ICR), 1, 6, 10, 11, 14, 95, 123, 315, 381
- intense heat, 354
- intermediate vector boson, 363, 364
- internal clocks, 36
- interstellar cloud, 71
- intracontinental extension, 234
- intracrustal fractionation zone, 269
- intracrustal reworking, 233
- intraoceanic island arcs, 248
- Introduction, 1
- intrusions, 200, 214, 260
- intrusives, 155, 440, 446
- inventory of elements, 61
- ion-explosion spike model, 313, 314
- ion microprobe, 98, 170, 336, 406, 409, 412, 421
- ion microprobe mass spectrometer, 88
- ionic bonds, 212
- ionic charge, 56
- ionic potential, 212
- ionic size, 56
- ionium, 385
- ionizing radiation, 8
- ions, 191, 208, 211, 313, 372
- Ir, 32, 55, 62, 70, 72, 74
- Irber, W., 209, 210
- Ireland, 442
- Irifune, T., 58
- Irish halos, 427
- iron hydroxide, 434

- iron meteorites, 31, 51, 63, 66, 101, 102, 103, 176
 irradiated sample, 39
 Isaiah, 367
 Ishigure, 444
 Ishigure District, 442
 island arc volcanics, 150, 152, 227
 Isle of Skye, 182, 183
 isochrons, 3, 10, 16, 21, 31, 36, 39, 40, 41, 42, 99, 100, 101, 102, 103, 104, 105, 106, 108, 109, 113, 115, 116, 124, 140, 141, 148, 152, 156, 157, 159, 160, 161, 162, 178, 181, 183, 184, 185, 186, 188, 189, 191, 192, 193, 194, 198, 201, 202, 204, 205, 208, 209, 210, 212, 213, 214, 215, 217, 221, 222, 232, 235, 251, 256, 257, 258, 274, 277, 280, 305, 306, 325
 isomers, 411, 421
 isostasy, 50
 isotopes, 16, 27, 38, 39, 44, 45, 51, 54, 59, 61, 88, 98, 99, 101, 103, 104, 107, 108, 109, 116, 117, 123, 136, 139, 143, 156, 159, 169, 170, 174, 175, 176, 177, 179, 182, 183, 186, 188, 191, 193, 195, 196, 204, 206, 208, 209, 210, 216, 217, 219, 221, 222, 224, 227, 228, 229, 230, 232, 234, 235, 237, 238, 239, 240, 242, 243, 244, 245, 246, 247, 248, 249, 250, 251, 255, 257, 258, 259, 260, 261, 262, 263, 266, 267, 268, 269, 272, 274, 277, 278, 279, 280, 281, 306, 311, 313, 315, 316, 321, 336, 352, 373, 381, 392, 403, 407, 411, 412, 429, 430, 435, 436, 437, 438, 456, 457
 Israel, 351
 Israelites, 338
 Italian Alps, 145
 Italy, 128, 147, 431
 Ivanchik, A. V., 305
 Iveland, 444
 Iveland District, 442
 Iyer, R. H., 407, 422, 424
- ## J
- Jackson, J. A., 382, 383
 Jacobsen, S. B., 114
 Jaeger, J. C., 84, 347
 Jahn, B. M., 252, 253
 Jahns, R. H., 446
 Japan, 442
 Jedwab, J., 390
 Jeffreys, H., 53
 Jemez, 346, 348, 349
 Jemez biotite, 375
 Jemez Caldera, 345
 Jemez zircons, 346, 347, 348, 350
 Jesus Christ, 353, 367
 John, 323, 338
 Johnson, L. H., 142
 joints, 447
 Joly-Mugge hypothesis, 383
 Joly, J., 382, 383, 387, 390, 391, 392, 393, 399, 400, 401, 410, 427, 442
 Jones, T. A., 42, 45
 Jordan River, 351
 Jordan, T. F., 306
 Jorgensen, U. G., 321
 Juan de Fuca, 180
 Juan de Fuca Ridge, 432
 judgment, 4, 6, 357
 Jurassic, 88, 275, 415, 417, 441, 445

K

- K, 8, 30, 35, 37, 38, 39, 44, 50, 54, 55, 62, 67, 70, 72, 73, 74, 75, 76, 96, 106, 115, 123, 126, 129, 131, 133, 135, 136, 140, 142, 144, 148, 150, 151, 152, 153, 155, 156, 157, 159, 183, 190, 203, 206, 207, 208, 209, 210, 211, 221, 224, 237, 266, 267, 268, 272, 274, 276, 280, 344, 373, 400, 403, 406, 407
 K-Ar, 10, 11, 12, 37, 38, 39, 42, 96, 97, 107, 116, 117, 123, 125, 126, 128, 129, 130, 131, 133, 134, 135, 136, 137, 140, 144, 146, 147, 152, 153, 154, 155, 156, 157, 158, 159, 199, 200, 208, 209, 214, 221, 237, 272, 274, 276, 280
 K-Ca, 27, 44, 407
 K-decay, 267
 K-feldspar, 154, 161, 168, 198, 199, 203, 204, 209, 210, 211
 Kalbitzer, S., 156
 Kaluza-Klien approach, 311
 Kaluza, T., 311
 Kambalda, 215
 Kambalda lavas, 215
 Karason, H., 77
 Karpinskaya, T. B., 130, 131
 Keay, S., 196, 197
 Kelley, D. S., 433
 Kelley, S. P., 148
 Kellogg, L. H., 61, 77
 Kerguelen, 180
 Kerguelen Archipelago, 138
 Kerr, R. A., 333
 Kerr-Lawson, D. E., 388, 390, 391, 392, 393, 395
 Kesson, S. E., 66, 139
 Kilaeua, 127, 128, 131, 137, 306
 Kim, J. I., 333
 Kimberley, 141
 kimberlites, 65, 139, 141, 150, 259, 447
 kindled, 351, 352, 353, 354, 368
 kinetic energy, 322, 357, 358, 359, 371, 372
 Kirkley, M. B., 139, 140, 141
 Klein, O., 311
 Knolls Atomic Power Company, 318
 Kofseth, B., 443
 Kohler, H., 107, 192
 Kohman, T. P., 102, 113, 114
 Kola project, 82, 139
 komatiites, 87, 215, 216, 252, 258
 Koongarra, 174, 184, 185
 Kosciusko Batholith, 195
 Kr, 55
 Kragero, 442, 444
 Kramers, J. D., 177, 257, 268, 269
 Kremenetsky, A. A., 82
 Krishnan, M. S., 403, 443, 454
 Krogh, T. E., 169
 Kroner, A. P., 166, 168
 Kruger, F. J., 109, 203
 Krummenacher, D., 128, 136
 KTB drill-hole, 148
 KTB project, 82
 Kulp, J. L., 144, 165, 173, 174, 208, 276
 Kuroda, P. K., 321, 430

L

- La, 29, 54, 60, 62, 70, 75, 161
 La Malbaie, 442
 La-Ba, 27

- La-Ce, 27
 Lachenbruch, A.H., 80, 82, 337
 Lachlan Fold Belt, 193, 196, 197
 Laemmlein, G.G., 390
lahat, 352
 Lake District, 192, 201
 Lake Tanganyika, 189
 Lake Victoria, 189
 Lambert, D. D., 214
 lamproites, 139, 141, 150, 259, 447
 Landau, L. D., 371, 372
 Lang, A. R., 407, 443
 Langmuir, C. H., 258, 263
 Lankin Dome, 160, 164
 Lanphere, M. A., 126, 136, 144
 lanthanides, 29, 221
 Laramie Mountains, 200
 Large Hadron Collider, 312
 LaRock, P., 434
 Larson, E. E., 107, 133, 157
 laser probe, 141
 late stage accretion event, 72
 lattice, 54, 56, 130, 146, 198, 313,
 324, 336, 367, 368, 369, 425,
 426, 450
 Laughlin, A. E., 130
 Laughlin, A. W., 144, 152
 lava, 104, 116, 117, 126, 128, 129,
 130, 131, 133, 135, 136, 149,
 156, 158, 159, 179, 181, 182,
 183, 189, 191, 202, 213, 249,
 251, 272, 273, 280, 281, 306,
 343, 344
 Lazerev, Y. A., 320
 Le Cloarec, M. F., 431
 leaching, 160, 165, 172, 209, 210,
 218, 340, 413, 414, 419, 432,
 435, 437, 449
 leakage, 165
 Lee, J. K. W., 166
 Lee, T. D., 308, 309
 Leinster Province, 442
 leptons, 309, 310
 Lewis, R. S., 321
 Lewisian Metamorphic Complex,
 95, 109, 110, 111, 182, 216
 Li, 55, 70, 71, 72, 208
 Li, L.-X., 305
 Li, S., 109
 Li, X., 108, 112
 Liew, T.C., 255
 life, 365
 Lifshitz, E. M., 371, 372
 light emission, 365
 light reception, 365
 lime, 116
 limestones, 36
 Linde, A. D., 310
 Lingen, J. S., 390, 400
 Lippolt, H. J., 348, 349
 liquid, 51, 310, 355
 literal interpretation of the Bible, 3,
 9
 lithology, 82, 213, 215
 lithophile elements, 54, 55, 66, 71,
 72, 73, 103, 192, 224
 lithosphere, 52, 57, 58, 66, 149,
 189, 250, 266, 267, 270, 271
 Loihi, 127, 139
 Loihi Seamount, 127, 137
 long-age isotopes, 9
 long-range force, 397
 LORD, 25, 353
 Los Alamos, 345
 Los Alamos National Laboratories,
 11, 49
 loss, 149, 153, 154, 156, 159, 161,
 164, 165, 167, 169
 Love, A., 309
 Loveland, W. D., 320

- Lovering, J. F., 64
 Lowell, R. P., 433
 Lu, 30, 38, 54, 60, 62, 70, 73
 Ludwig, K.R., 101, 161, 168
 Lu-Hf, 38, 258
 Luke, 338
 lunar rocks, 31, 39, 305, 316, 318, 319, 320
- M**
- μ value, 177, 178, 181, 182, 256, 257
 Macdougall, J. D., 313
 Madagascar, 402, 403, 405, 454
 mafic, 76, 147, 150, 163, 179, 182, 188, 189, 196, 212, 215, 217, 229, 230, 235, 252, 253
 magma, 36, 49, 56, 57, 65, 74, 87, 90, 104, 109, 112, 114, 127, 129, 135, 136, 137, 138, 143, 146, 149, 151, 152, 159, 166, 168, 169, 175, 178, 179, 181, 182, 189, 191, 196, 211, 212, 214, 215, 216, 218, 223, 224, 234, 235, 237, 238, 239, 242, 253, 258, 259, 260, 261, 262, 263, 276, 279, 306, 352, 425, 427, 431, 433, 446, 447,
 magmatism, 189, 196, 227, 234
 magnetism, 105, 309, 311, 312
 magnetite, 116, 450
 Magomedov, S. A., 346, 347
 Magueijo, J., 305, 311
 Mahadevan, C., 388, 390, 391, 395, 399, 401, 403, 209, 441, 442, 454
 Main Zone, 260
 Maine, 442
 major element, 65, 66, 67, 79, 263
 Malakhova, N. P., 446
 Malbaie, 444
 Manitoba, 442
 Mankinen, E. A., 158
 mantle, 5, 11, 21, 49, 51, 52, 53, 55, 57, 58, 59, 60, 61, 65, 66, 67, 72, 73, 74, 75, 76, 77, 78, 79, 86, 87, 90, 104, 123, 125, 136, 137, 138, 139, 140, 141, 142, 143, 144, 149, 150, 151, 152, 159, 177, 178, 179, 181, 182, 188, 189, 190, 194, 195, 196, 197, 210, 212, 213, 214, 215, 221, 222, 223, 225, 226, 227, 228, 229, 230, 234, 235, 237, 238, 239, 240, 242, 246, 247, 248, 249, 250, 251, 253, 254, 255, 257, 258, 259, 260, 261, 262, 263, 264, 265, 266, 267, 268, 269, 270, 271, 272, 273, 276, 277, 278, 279, 280, 281, 447
 mantle chemistry, 69, 141, 195, 230, 234, 252, 260, 271
 mantle dynamics, 61, 87, 138, 140, 226, 227, 252, 253, 266, 269, 270, 272, 273, 277, 278, 281
 mantle isochrons, 188, 189, 190
 mantle lithosphere, 143, 152
 mantle reservoir, 139, 140, 222, 225, 238, 240, 243, 244, 245, 246, 248, 250, 251, 258, 263, 272, 273, 281
 mantle rock, 55, 56, 58, 65, 78, 86, 90, 159, 175
 mantle sources, 22, 123, 124, 137, 177, 186, 188, 190, 194, 197, 221, 222, 229, 232, 234, 250, 253, 264, 266, 280,
 Manus Basin, 127
 many waters, 353, 354
 marine, 206

- Mark, 338
 Mars, 8, 356
 Martin, A. D., 363, 364, 369
 Marty, B., 127, 138, 139, 268
 mass flow, 267
 mass number, 321, 322
 mass spectrometry, 30, 39, 98, 105, 170, 187, 406
 massifs, 65, 67, 68
 matrices, 270, 309
 Matsumoto, T., 138, 152
 Matthew, 338
 mature halos, 452, 455, 456
 Mauger, R. L., 153
 Mauna Loa, 60, 127
 Maxwell, J. C., 311
 Mazor, E., 153
 McAndrew, J., 449
 McCarthy, T. S., 191
 McCulloch, M. T., 109, 195, 196, 215, 219, 229, 230, 234, 252, 255, 259
 McDonald Seamount, 127
 McDonough, W. F., 55, 63, 67, 68, 69, 71, 72, 73, 74
 McDougall, I., 127, 128, 144, 146, 147, 152, 155
 McGeary, D., 38, 45
 McKee, E. H., 107, 157
 mechanical breakdown, 153
 Medicine Lake Highland obsidian, 128
 Meier, H., 419, 421, 427, 430, 435, 436, 442
 Melby, E. L., 355
 Meldrum, A. L., 166
 melt, 56, 57, 65, 67, 69, 261, 271, 277, 354, 355
 melting, 56, 57, 65, 144, 153, 168, 178, 190, 194, 198, 223, 230, 232, 233, 258, 260, 269, 270, 271, 279, 356, 369
 melting point, 356
 Mensing, T. M., 263
 Menzies, M. A., 250
 Merensky Reef, 261
 mesons, 359, 360, 361, 362, 359, 360, 369,
 Mesozoic, 32, 452
 metabolism, 435
 metagabbro, 110, 440, 445
 metallic core, 51
 metallic meteorites, 30
 metamictization, 166, 169, 450, 451
 metamorphic, 30, 31, 36, 38, 104, 109, 112, 116, 144, 145, 146, 148, 152, 154, 165, 166, 168, 172, 175, 198, 199, 200, 201, 207, 208, 216, 217, 219, 220, 224, 227, 238, 444
 metamorphism, 31, 108, 133, 144, 153, 154, 160, 166, 167, 168, 178, 187, 193, 198, 199, 200, 201, 202, 204, 205, 207, 212, 214, 216, 217, 218, 219, 225, 232, 239, 250, 279
 metamorphosed, 166, 167, 441, 444
 metasediments, 440, 445
 metasomatism, 143, 191, 246, 248, 253, 425
 meteoric water, 210
 meteorite composition, 90
 meteorite impact, 144
 meteorite material, 78
 meteorites, 19, 32, 39, 49, 61, 62, 63, 64, 65, 66, 80, 88, 90, 101, 102, 103, 104, 112, 113, 114, 115, 176, 179, 186, 251, 252,

- 256, 257, 280, 313, 314, 320, 321
 meteoroids, 321
 metric tensor, 311
 Mezgar, K., 220
 Mg, 50, 55, 60, 62, 67, 69, 70, 71, 74, 156, 208, 211
 Mg-poor continental crust, 55
 MgO, 69
 mica, 35, 38, 198, 200, 204, 205, 383, 391, 421, 423
 microbial activity, 434
 microcapillary networks, 166
 microcline, 390
 microfissures, 165
 mid-Atlantic ridge, 52, 127, 138, 183
 mid-ocean ridge, 52, 54, 56, 57, 138, 139, 149, 151, 433
 mid-ocean ridge basalt (MORB), 54, 56, 59, 60, 61, 77, 137, 138, 142, 143, 149, 150, 151, 179, 180, 181, 212, 225, 242, 244, 245, 246, 247, 252, 259, 262, 264, 269, 270, 271
 mid-ocean ridge sulfide, 262
 mid-ocean ridge volcanism, 138
 Middle Proterozoic Musgrave Block, 146
 Middlesex County, 442
 migmatite, 146
 migration, 31, 36, 45, 142, 143, 149, 152, 169, 186, 190, 200, 203, 221, 279, 324, 416, 423, 424, 435
 millirem, 340
 milliSieverts, 340
 mineral ages, 187, 199, 200, 221, 277
 mineral component, 56
 mineral grains, 123, 164
 mineral inclusions, 36
 mineral isochrons, 10, 11, 16, 18, 21, 95, 96, 104, 105, 107, 108, 109, 110, 111, 112, 113, 114, 115, 116, 117, 163, 198, 202, 214, 218, 219, 221
 mineral isotope ratios, 452
 mineral lattice, 153
 mineral lattices, 126, 165
 mineral U-Th-Pb dating, 161
 mineralization, 184, 185, 215, 218, 413, 383, 390
 mineralogy, 53, 79, 125, 133, 154, 160, 191, 194, 201, 209, 232, 266, 406, 448
 minerals, 36, 56, 57, 88, 95, 96, 97, 98, 104, 105, 106, 108, 109, 111, 113, 116, 117, 124, 125, 126, 129, 130, 131, 133, 142, 144, 146, 147, 148, 153, 154, 155, 159, 160, 161, 164, 165, 166, 168, 169, 172, 173, 174, 175, 176, 178, 179, 186, 187, 190, 198, 199, 200, 202, 204, 205, 206, 207, 208, 211, 212, 213, 214, 215, 218, 219, 221, 232, 239, 272, 276, 280, 324, 346, 348, 381, 382, 383, 390, 391, 392, 393, 394, 395, 399, 410, 413, 415, 416, 422, 423, 425, 427, 432, 433, 437, 444, 446, 448, 449, 450, 451, 454, 457, 458
 Minnesota, 169, 199, 208
 minor elements, 65, 67
 Minster, J. F., 113, 114, 115
 Miocene, 249, 315, 336
 miracles, 10
 Mississippian, 117
 mixed reservoir, 264
 mixed source, 231

- mixing, 19, 32, 61, 99, 103, 104, 105, 108, 123, 124, 129, 138, 142, 149, 168, 169, 175, 176, 178, 179, 181, 182, 183, 184, 186, 189, 191, 193, 194, 195, 196, 197, 210, 211, 230, 231, 232, 234, 235, 237, 238, 242, 246, 247, 248, 258, 259, 260, 261, 262, 263, 264, 268, 269, 270, 271, 273, 274, 277, 278, 279, 280, 281, 282, 412, 438, 452
- mixing angle, 309
- mixing diagrams, 263
- mixing equation, 258
- mixing isochron, 198
- mixing lines, 42, 178, 182, 184, 189, 195, 196, 197, 258, 259, 262
- mixing model, 19, 196, 234
- mixing processes, 6, 19
- mixture of minerals, 56
- mixtures, 60
- Mn, 55, 62, 70, 72, 431, 435
- Mo, 55, 62, 70, 72
- Moab, 351
- Moazed, C., 420
- mobile belts, 250
- mobile fluid, 143
- mobility, 160, 161, 169, 175, 186, 187, 198, 199, 200, 201, 206, 207, 210, 216, 217, 219, 220, 232, 253, 272, 276, 279, 280, 324, 415, 423, 432, 434, 435, 437
- model age, 95, 96, 97, 98, 99, 106, 112, 113, 114, 117, 129, 152, 174, 206, 222, 224, 225, 226, 227, 228, 229, 230, 231, 232, 233, 234, 235, 277
- moderately volatile elements, 55
- Mohorovicic discontinuity, 53
- Mojavia terrane, 233, 234
- molecular structure, 365
- molecule, 372
- molten material, 37
- molybdenite, 30
- momentum, 311, 371
- monazite, 30, 97, 161, 164, 172, 173, 211, 220, 391, 403, 405, 427
- Montana, 214
- monzonite, 154, 199
- Moon, 8, 316, 321
- moon rocks, 313
- Moorbath, S., 182
- Moore, J. G., 128, 131, 132, 136
- Moore, J. N., 433
- Moreira, M., 137, 142
- Morgan, W. J., 269, 270, 271
- Morris II, H. M., 7, 337, 339
- Morris, J. D., 7, 10, 14, 339
- Moses, 351, 352
- Moss, 442, 444
- Mount St. Helens, 129, 430
- Mt. Apatite, 442, 444
- Mt. Erebus, 128, 135
- Mt. Etna, 128
- Mt. Etna basalt, 127
- Mt. Lassen, 127, 135
- Mt. Ngauruhoe, 11, 129
- Mt. Stromboli, 128
- Mudrey, M. J., 166
- Mugge, O., 382, 383
- Muir, R. J., 168
- Mukasa, S. B., 107
- Muller-Sohnius, D., 192
- multi-celled life, 88
- multi-celled organisms, 52
- muon, 309
- murder, 338
- Murray Bay, 442
- muscovite, 30, 130, 131, 187, 199, 200, 203, 205, 209, 349, 423

- Mushkat, C. M., 388
 Mustart, D. A., 446
 myrmekite, 425
 mythologies, 338
- N**
- N, 30, 55, 65, 70, 144, 268
 Na, 35, 55, 62, 70, 72, 190, 208, 339, 433
 Nagler, T. F., 268, 269
 Nanivak, 180
 Nashville, 88, 451
natah, 368
 Nathan Hills, 128
 natural gas, 142, 152
 natural reactor, 12, 13
 naturalistic explanations, 367
 nature, 367
 Naughton, J. J., 128, 131, 136
 Navon, O., 141
 Nd, 29, 30, 31, 54, 55, 60, 62, 68, 70, 71, 73, 75, 107, 109, 110, 111, 195, 200, 203, 211, 212, 213, 214, 215, 216, 217, 218, 219, 220, 221, 222, 223, 224, 225, 226, 227, 228, 229, 230, 232, 233, 234, 235, 237, 238, 240, 241, 242, 243, 245, 246, 248, 249, 250, 253, 254, 255, 257, 259, 262, 266, 267, 268, 272, 277, 279, 280
 Nd-Sr, 258, 259, 262, 266
 Ne, 55, 65, 137, 143
 Neale, E. R. W., 443
 negative ages, 135, 172
 Nelson, B. K., 227, 233, 255
 neptunium series, 33
 neutrino, 29, 362
 neutron, 29, 39, 135, 308, 310, 316, 323, 336, 357, 360, 362, 366, 369, 385, 403
 neutron bombardment, 39
 neutron numbers, 320
 Nevada, 130
 Nevissi, A. E., 431
 New England, 81
 New Hampshire, 441, 442, 446, 449
 New Mexico, 14, 15, 20, 130, 333, 345
 New South Wales, 146
 New Testament, 354
 New Zealand, 128, 129, 130, 168
 NHRL, 244, 246, 258
 Ni, 51, 55, 62, 63, 70, 72
 Nicholson, K., 433
 Nickel, K. G., 67
 Nicolaysen, L. O., 40, 165
 Nier, A. O., 176
 Nigam, B. P., 355
 Nigeria, 128
 Nishio, Y., 138
 Nix, J. R., 320
 Nkomo, I. T., 160, 161, 164
 Noah, 8, 9, 89, 373
 Noah's Flood, 52, 356
 Noble, C. S., 128, 131
 Noble, D. C., 107, 157
 Nobel prize, 309
 noble gas, 126
 noble gases, 137, 140, 142, 143, 144, 153, 321, 346
 Noerdlinger, P. D., 371
 non-mafic rocks, 217
 nonradiogenic, 40, 41, 78, 250, 280
 Noonan, T. W., 371
 normal halos, 439
 North America, 81, 235, 236
 North Atlantic Ocean, 137

North Broken Hill Mine, 147
 North Island, 129
 Northern Territory, 184, 185
 Norway, 201, 400, 436, 442, 454
 Nova Scotia, 442
 novas, 374
 Noyes, R. W., 374
 nuclear decay, 3, 4, 12, 14, 15, 16, 22, 28, 82, 83, 84, 85, 86, 87, 88, 89, 90, 108, 324, 333, 335, 336, 337, 339, 341, 350, 351, 352, 355, 369, 373, 374, 381, 452, 458
 nuclear fire, 351, 352, 353, 354, 368
 nuclear forces, 356, 359, 360, 365, 366, 367, 368, 369, 397
 nuclear particles, 313, 359, 360
 nuclear physics, 28, 124, 125, 358, 396
 nuclear potential well, 306, 358
 nuclear reactions, 39, 124, 135, 323, 336, 354, 356, 374
 nuclear shape, 320
 nuclear theory, 334, 357
 nuclear transformations, 87, 89, 366, 367
 nuclei, 29, 306, 309, 310, 311, 312, 313, 314, 316, 318, 320, 322, 324, 335, 336, 355, 356, 357, 358, 359, 360, 361, 362, 363, 364, 366, 396
 nucleogenic Ne, 143
 nucleon, 314
 nucleosynthesis, 313, 323
 nuclides, 161, 165, 305, 315, 316, 317, 318, 319, 323, 324, 385, 386, 388, 408, 416, 439
 Nuk gneisses, 261
 Numbers, 352

O

O'Nions, R. K., 232, 266, 267
 O, 55, 65, 66, 161, 190, 194, 207, 211, 447
 obsidian, 315
 Occam's razor, 10
 ocean, 49, 50, 52, 54, 56, 57, 58, 59, 60, 65, 75, 76, 77, 78, 79, 103, 104, 123, 136, 138, 139, 140, 149, 150, 151, 179, 180, 182, 186, 190, 210, 237, 241, 242, 244, 246, 247, 248, 250, 254, 258, 259, 262, 264, 266, 268, 269, 272, 279, 280
 ocean island basalt (OIB), 59, 60, 61, 76, 138, 149, 150, 179, 180, 181, 188, 242, 246, 247, 248, 269, 270, 271
 Odom, A. L., 390
 Oklo natural reactor, 12, 13, 17
 Okun, L. B., 305
 old earth, 4, 7, 337, 338, 339
 old earthers, 338
 Old Testament, 354, 367
 olivine, 53, 65, 116, 117, 127, 128, 130, 136, 137, 142, 144, 211
 Olson, T. S., 306
 Ontario, 216, 442
 opals, 446
 open systems, 36, 129, 159, 160, 161, 164, 165, 198, 201, 202, 203, 204, 207, 209, 211, 232, 274, 277, 279, 281
 ophiolites, 65, 252
 Ordovician, 196, 197
 orebody, 448, 449
 ores, 451
 origin, 78, 420
 orogene, 265
 orogenes, 264

orphan radiohalos, 351
 orthoclase, 390
 orthopyroxene, 65, 219
 Os, 30, 31, 32, 55, 62, 70, 72, 73, 74
 Ostfold County, 442
 outer core, 52, 53, 66
 outer liquid layer, 51
 outer shell, 51
 outgassing, 276, 277
 Ovchinnikov, L. N., 446
 Oversby, V. M., 177
 Owen, M. R., 390, 391
 oxidation states, 434
 oxygen isotopes, 260, 262
 oxyhydroxide, 431, 435
 Ozima, M., 140, 141, 144

P

P, 55, 60, 62, 70, 72, 73, 161, 211
 Pa, 336, 384
 Pachner, J., 371
 Pacific Ocean, 103, 127, 131, 181, 233, 236
 Paleozoic, 194, 276, 452
 Palme, H., 66
 Pandey, B. K., 107
 parent-daughter, 89, 98, 105, 188, 279, 452
 parent isotopes, 1, 3, 5, 8, 12, 19, 30, 41, 45, 96, 99, 100, 101, 105, 106, 108, 126, 161, 168, 176, 190, 191, 214, 218, 221, 222, 238, 239, 242, 250, 251, 253, 254, 306, 321, 322, 335, 336, 351, 386, 392, 399, 407, 410, 411, 418, 424, 426
 parentless, 23, 142, 381, 421, 431, 433, 434, 439, 440, 446, 447, 453, 456, 457, 458
 parents, 421
 parity, 308
 Parrish, R. R., 168
 partial melting, 49, 50, 56, 57, 77, 78, 86, 90, 108, 143, 146, 147, 152, 153, 182, 191, 193, 212, 222, 223, 224, 237, 253, 260
 particle physics, 307, 308
 partition coefficients, 55, 69, 218
 Patel, S. C., 200
 Patterson, C. C., 101, 102, 103, 104, 113, 127, 130, 137, 142, 176, 179
 Patyk, Z., 320
 Pb, 30, 32, 33, 34, 35, 55, 57, 60, 61, 62, 70, 72, 75, 88, 89, 97, 98, 99, 101, 102, 103, 104, 111, 113, 114, 140, 150, 160, 161, 162, 163, 164, 165, 166, 167, 168, 170, 171, 172, 173, 174, 175, 176, 177, 178, 179, 180, 181, 182, 183, 184, 185, 186, 203, 212, 215, 216, 217, 237, 238, 239, 240, 241, 242, 244, 245, 246, 248, 250, 256, 257, 258, 260, 261, 264, 265, 272, 275, 277, 280, 324, 336, 345, 350, 384, 385, 389, 405, 406, 411, 412, 413, 414, 415, 416, 417, 418, 422, 423, 425, 426, 429, 430, 431, 432, 433, 434, 452
 Pb atoms, 417
 Pb decay, 418
 Pb diffusion, 339, 350, 423, 424
 Pb evolution diagram, 181
 Pb isochrons, 34
 Pb isotopes, 178, 179, 186, 190, 239, 256, 257, 258, 260, 262, 263, 264, 265, 280

- Pb isotope ratios, 98
 Pb isotopic mixing, 182
 Pb loss, 161, 165, 166, 167, 169, 176, 246
 Pb migration, 186
 Pb paradox, 104, 181
 Pb-Pb, 10, 21, 95, 98, 101, 102, 107, 109, 110, 111, 112, 113, 114, 115, 116, 147, 163, 174, 175, 176, 177, 179, 180, 181, 182, 183, 184, 203, 212, 215, 217, 258, 280, 345
 Pb ratios, 184
 Pb signature, 186
 Pb-Sr-Nd-Hf, 258
 Pd, 55, 62, 70, 72, 74, 323
 pegmatite, 144, 152, 203, 276, 399, 405, 437, 440, 441, 444, 448, 453, 454
 pelitic sedimentary rocks, 194
 Peninsular Ranges, 213
 Pennsylvania, 442
 Penokean terrane, 234
 peridotite, 66, 67, 69, 71, 72, 73, 74, 76, 139, 190
 peridotitic diamonds, 141
 periodic table, 29, 318, 355, 434
 periodites, 68
 permeability of the vacuum, 311
 permittivity of space, 359
 perovskite, 53
 II Peter 9, 79, 91, 276, 338, 354, 355, 356, 366
 Peterman, Z. E., 190
 petrogenesis, 182, 196, 234
 petrogenetic provenance, 194, 196
 petrography, 130, 154
 petrology, 130, 238
 Petrosian, V., 371
 Phalaborwa carbonatite, 170
 Phanerozoic, 19, 88, 89, 250, 341, 381, 392, 441, 445, 451, 453, 454, 455, 456, 457
 phase contrast microscope, 322
 phase transition, 310
 phengite, 148
 phenocrysts, 130, 135, 159
 Philadelphia, 442
 Philadelphia County, 442
 Philistines, 24, 25
 Phillips, D., 141
 Phillips, M. J., 141
 Phipps Morgan, J., 267, 269, 270, 271
 phosphate, 30, 113, 435
 phosphoric acid, 435
 phosphorite, 435
 phosphogypsum, 435
 photoelectric formula, 370
 photomicrographs, 386
 photon, 309, 365, 370, 371
 photosphere, 61, 62
phthoras, 357
 phyllosilicates, 210
 physical law, 90, 91
 physicists, 305, 369, 370
 physics, 238, 305, 306, 307, 308, 309, 311, 312
 π meson, 360, 363, 364, 366, 368, 369
 Picciotto, E. E., 399
 Pickles, D. S., 144, 145
 Pidgeon, R. T., 166, 205
 pillow, 131, 132, 133
 Pioline, B., 312
 pion mass, 368
 pipe eruptions, 139
 pit, 322, 411
 pitchblende, 30, 34, 173, 430, 431, 450

- Pitcher, W. S., 425
 Piton des Niges volcano, 127
 plagioclase, 50, 56, 111, 116, 129, 130, 135, 136, 142, 144, 146, 147, 158, 187, 198, 209, 211, 214, 218, 239, 390, 425
 Planck's constant, 359, 370
 planetary formation, 251
 planetesimals, 71
 planets, 71, 371
 plants, 441
 plate, 57, 281
 plate tectonics, 49, 52, 123, 179, 260, 263, 266, 273, 278, 281
 Pleistocene, 117
 pleochroic halos, 382, 383
 Pliocene, 189
 plum-pudding, 271, 279
 plumbotectonics, 123, 178, 263, 265, 272, 277, 281
 plume, 61, 76, 137, 139, 149, 152, 267, 270, 271, 281, 431
 plume volcanism, 138
 Plummer, C. C., 38, 45
 plums, 270, 271, 277
 plutonic rocks, 80, 81, 82, 182, 188, 191, 210
 plutons, 178, 222, 225, 227, 233
 Po, 336, 351, 381, 384, 385, 386, 389, 391, 396, 401, 402, 403, 404, 408, 409, 410, 411, 412, 413, 414, 416, 417, 418, 419, 420, 421, 422, 423, 424, 425, 426, 428, 429, 430, 431, 432, 433, 434, 435, 436, 437, 438, 439, 440, 441, 443, 445, 448, 453, 454, 456, 457
 Po decay, 412, 417, 438, 440
 Po deposition, 430
 Po-derived Pb, 438
 Po diffusion, 424
 Po halos, 16, 19, 22, 23, 275, 322, 335, 351, 381, 389, 401, 408, 409, 410, 411, 412, 416, 417, 418, 419, 420, 421, 422, 423, 424, 425, 426, 427, 428, 429, 430, 433, 435, 436, 437, 438, 439
 Po inclusions, 411
 Po isotopes, 22, 381, 410, 411, 412, 416, 420, 422, 423, 424, 425, 426, 427, 428, 430, 436, 437, 440, 441, 442, 444, 445, 446, 447, 448, 449, 451, 453, 455, 456, 457, 458
 Po-savenging, 426
 Podosek, F.A., 140
 poisons, 13
 Poitrasson, F., 217, 218, 221, 225, 232
 polonide ions, 425
 polymetamorphic terranes, 202
 Polynesian, 138
 polystrate fossils, 339
 Poole, J. H. J., 424, 447
 Porcelli, D., 149
 porphyry Cu, 426
 Portland, 442, 444
 PoS, 434
 post-crystallization, 213
 post-Flood rocks, 315
 post-magmatic processes, 192
 potassic magmas, 141
 potassic lava flows, 189
 potassium feldspar, 30, 35, 38, 425
 potassium oxide, 134, 158
 potassium-argon clock, 126
 potential energy, 320, 357, 358, 359, 397
 potential well, 306, 307
 Poths, J., 130

- Powell, J. L., 189, 190
 Powell, R., 262
 Pr, 62, 70
 Precambrian, 31, 107, 116, 154, 161, 167, 168, 194, 196, 199, 205, 227, 233, 276, 323, 345, 381, 391, 392, 413, 414, 440, 441, 445, 451, 453, 454, 455, 456
 precipitation, 432, 457
 pre-Flood soil, 373
 Premier kimberlite, 141
 prevalent mantle (PREMA), 241, 242, 244, 245, 247, 248
 Pribilof Islands, 180
 Pribnow, D. F. C., 82
 Price, P. B., 313, 315
 primary ages, 203
 primary halos, 413
 primeval, 176, 256, 257, 323
 primitive mantle (PM), 60, 63, 75, 77, 103, 135, 136, 222, 247, 248, 251, 252, 271, 278
 primordial, 5, 11, 19, 23, 114, 123, 136, 137, 139, 140, 148, 149, 151, 152, 153, 159, 176, 177, 179, 186, 251, 280, 282, 381, 412, 413, 420, 421, 422, 426, 438, 439, 440, 445, 448, 455, 456, 457, 458
 pristine mantle, 67
 probable age, 174
 processes, 4, 5, 9, 21, 49, 50, 54, 56, 86, 87, 89, 90, 238
 progressive creationism, 2
 propagation speed, 51
 Proterozoic, 87, 146, 156, 157, 164, 172, 227, 228, 231, 233, 234, 240, 250, 445
 protocrust, 269
 protoearth, 72
 protolith, 110, 111, 200, 201, 203, 216, 217
 proton decay, 312
 protons, 29, 39, 307, 308, 310, 313, 316, 322, 323, 357, 360, 362, 366, 369, 403
 prototerrestrial material, 268, 269
 Proverbs, 367
 province, 233, 235
 Psalms, 338, 352, 353, 367, 368
 pseudo isochrons, 42, 189, 193, 216
 pseudoscalar, 308
 pseudotachylyte, 146
 Pt, 55, 62, 70, 71, 72, 74
 Pu, 151, 313, 315, 316, 319, 321, 322, 403
 Pu decay, 313
 Pu tracks, 322
 published age, 342
pur, 354
 pyrolite, 65
 pyrolite model, 66, 67, 71, 72
 pyroxene, 53, 129, 130, 136, 142, 144, 211, 214, 450
 pyroxenite, 261
- ## Q
- qadach*, 351
 quantum chromodynamics, 360, 369
 quantum field theory, 366, 367, 368, 369
 quantum fluctuations, 358
 quantum mechanical, 395, 397
 quark-antiquark pairs, 367, 368, 369
 quark theory, 360, 369
 quarks, 367, 368

quartz, 50, 56, 116, 144, 146, 154,
199, 390, 391
quartzofeldspathic rocks, 229, 230
quasar spectra, 311
Quaternary, 130
Quebec, 442
quenching, 131, 136

R

r-process, 321
Ra, 336, 360, 361, 381, 384, 385,
386, 396, 401, 408, 410, 419,
426, 429, 437, 438, 439
Ra halos, 419
radiation, 153, 165, 166, 172, 307,
347, 450
radioactive cracking, 450
radioactive dating, 124, 125, 314
radioactive daughters, 426
radioactive decay, 1, 2, 4, 5, 7, 8,
9, 19, 22, 43, 50, 101, 103, 123,
124, 126, 133, 135, 136, 142,
148, 152, 159, 163, 176, 201,
239, 274, 275, 278, 280, 281,
282, 346, 381, 383, 387, 392,
395, 396, 398, 399, 414, 449,
450, 451, 454, 455, 456, 457
radioactive elements, 3, 11, 18, 29,
30, 32, 49, 51, 54, 58, 73, 74, 75,
79, 80, 83, 90, 124, 173, 272,
281, 340, 373, 374, 399, 451
radioactive fluids, 435, 457
radioactive halos, 307, 322, 382,
383, 450
radioactive origin, 383, 405
radioactive processes, 4, 6, 12, 28,
80, 82, 173
radioactive Rn gas, 352
radioactivity, 1, 3, 11, 28, 29, 80,
82, 83, 86, 90, 151, 324, 333,
340, 356, 369, 373, 382, 383,
394, 399, 403, 404, 406, 407,
418, 419, 427, 450
radiocarbon inventory, 374
radiocenter, 22, 88, 275, 335, 336,
381, 383, 387, 390, 391, 403,
407, 411, 414, 415, 416, 417,
418, 420, 421, 422, 423, 424,
425, 426, 433, 438, 439, 449,
452, 453, 456, 457, 458
radiodecay, 275
radiodecay rates, 275
radioelements, 429
radiogenic, 108, 181, 235
radiogenic Ar, 123, 131, 136, 143,
144, 151, 208, 209
radiogenic daughter products, 36
radiogenic daughter element, 156,
175
radiogenic He, 143, 339, 344, 345,
346, 347, 350
radiogenic heat production, 77, 81,
82
radiogenic isotope, 105
radiogenic isotopes, 219, 235, 237,
238, 262, 272, 281
radiogenic lead, 97, 98
radiogenic Nd, 260
radiogenic nuclides, 149
radiogenic parents, 434, 435
radiogenic Pb, 160, 161, 163, 164,
166, 168, 169, 170, 172, 174,
175, 176, 177, 178, 179, 184,
185, 186, 187, 190, 191, 192,
193, 199, 201, 203, 204, 205,
207, 208, 264, 350, 412, 414, 417
radiogenic Sr, 208, 209, 250
radiohalos, 16, 18, 19, 22, 88, 89,
275, 282, 335, 336, 339, 374,

- 381, 382, 383, 386, 387, 390, 391, 392, 393, 394, 395, 396, 397, 398, 404, 412, 423, 424, 447, 449, 452, 453, 456
- radioisotope dating, 1, 3, 14, 18, 20, 20, 22, 23, 27, 29, 30, 31, 36, 39, 42, 43, 45, 73, 86, 87, 88, 90, 91, 95, 96, 99, 105, 115, 123, 152, 161, 163, 165, 237, 274, 275, 279, 280, 452, 455, 458
- radioisotope decay, 4, 16, 99, 105
- radioisotope methods, 3, 31
- radioisotope pairs, 106
- radioisotope plot, 99
- radioisotopes, 3, 6, 7, 8, 20, 27, 29, 59, 66, 95, 96, 106, 112, 118, 123, 124, 125, 159, 187, 192, 210, 211, 216, 272, 336, 381, 396, 397, 422, 426
- radioisotopic, 22, 50, 80, 98, 116, 124, 211, 237, 272, 273, 275, 276, 277, 278, 279, 281, 282, 341, 342, 343, 344, 345, 364, 375,
- radiometric dating, 12, 125, 140, 339, 343, 362
- radionuclide, 10, 383, 386, 387, 388, 390, 396, 398, 399, 402, 412, 416, 423, 429, 435
- Raheim, A., 201
- Ramdohr, P., 324, 390, 391, 394, 450, 451
- Randall, L., 312
- Rangitoto basalt, 128
- rapid burial, 339
- rapid decay, 318
- rapid expansion, 310, 368, 369, 370
- raqia*, 368
- rare earth elements (REE), 29, 54, 55, 68, 72, 173, 211, 212, 217, 218, 219, 225, 232, 249, 250, 255, 448
- rare gases, 77, 139, 141, 149, 151, 266, 267, 268, 270, 271
- RATE, 1, 7, 454, 455, 458
- RATE experiments, 16, 17, 18
- RATE group, 1, 3, 4, 5, 6, 7, 9, 10, 12, 13, 14, 15, 17, 18, 19, 20, 23, 24, 87
- RATE initiative, 24, 89
- RATE investigators, 17, 24
- RATE research, 9
- RATE Research Program, 23
- rate of decay, 3
- Rb decay, 199
- Rb-depleted, 216
- Rb loss, 198, 253
- Rb, 10, 11, 12, 21, 30, 35, 36, 40, 41, 42, 43, 54, 55, 60, 62, 67, 70, 72, 73, 75, 95, 106, 107, 109, 112, 113, 114, 115, 116, 123, 133, 147, 148, 154, 155, 157, 158, 159, 187, 188, 189, 190, 191, 192, 193, 197, 198, 199, 200, 201, 202, 203, 204, 205, 206, 207, 208, 209, 210, 211, 212, 214, 216, 217, 221, 222, 224, 225, 235, 236, 237, 238, 239, 240, 241, 243, 246, 249, 250, 251, 252, 254, 255, 257, 258, 272, 274, 277, 280
- Rb-Sr, 10, 11, 12, 21, 35, 36, 40, 43, 95, 107, 109, 112, 113, 114, 115, 116, 133, 187, 188, 193, 199, 200, 201, 202, 203, 204, 205, 207, 208, 209, 235, 236, 274, 123, 147, 148, 154, 155, 157, 158, 159, 192, 197, 198, 199, 200, 201, 202, 204, 205,

- 206, 208, 209, 210, 211, 212, 214, 217, 221, 222, 235, 237, 238, 239, 240, 241, 255, 258, 272, 274, 277, 280
- Rb/Sr ratios, 40
- Re, 30, 31, 55, 70, 72, 73, 74
- re-assimilation stage, 55
- re-equilibration, 202
- Re-Os method, 12, 31
- reaction textures, 220
- recoil, 322
- recoil energy, 165
- recrystallization, 104, 105, 116, 166, 191, 204
- recycling, 143, 238, 247, 248, 264, 267, 270, 271, 279
- Red Sea, 127, 138
- red shift, 370
- redeposition, 153, 225
- redistribution, 200
- redox interface, 413
- reducing conditions, 413
- Redwall Limestone, 116
- refraction seismology, 75
- refractory elements, 55, 66, 68, 69, 71, 72, 73, 79, 139, 194, 267
- Reifenschweiler, O., 334
- relativist, 371
- relativistic equations, 372
- remelting, 31, 234, 239
- remobilization, 108, 109, 184, 198, 214, 217, 232
- removal of heat, 87
- repository, 58
- research plan, 14
- research proposals, 18, 20
- reserved for fire, 354
- reservoirs, 5, 58, 76, 77, 104, 123, 149, 151, 177, 178, 179, 181, 223, 224, 227, 228, 237, 238, 239, 247, 249, 250, 251, 252, 253, 263, 264, 266, 267, 268, 269, 271, 272
- resetting, 36, 144, 166, 168, 200, 201, 202, 203, 204, 206, 214, 215, 216, 217, 220, 221, 232, 235, 280
- residence time, 431, 432
- residual heat, 4, 15
- residual solids, 56, 223, 224
- residue, 269, 270, 271
- rest mass energy, 363
- Resting Spring Range, 315
- retentivity, 154, 219, 346
- retrograde metamorphism, 109
- Reunion, 127, 180
- Reykjanes Ridge, 180
- Rh, 55, 62, 70, 72, 74
- Rhodesia, 164
- rhyolite, 192, 202, 217
- Richards, J. R., 174, 177, 184, 257
- Richardson, S. H., 139
- Rickaby, 405, 454
- ridge, 56, 57, 269, 270, 271
- rift, 189
- Rimsaite, J., 406
- Ringwood, A. E., 58, 65, 66, 139
- Rink, W. J., 390
- Rn, 165, 336, 352, 381, 384, 385, 386, 387, 396, 401, 407, 408, 409, 424, 425, 434, 435, 437, 439
- Robertson, H. P., 371
- rock chemistry, 260
- rock crystal, 336
- rock layers, 356
- rock suites, 188, 189
- Roentgen, W., 29
- Rogers, J. J. W., 449
- Rohlf, J. W., 33, 34, 35, 45
- roll front, 413

- Rollinson, H., 187, 213, 221, 222, 225, 226, 228, 235, 240, 244, 247, 252, 254, 255, 257
 Romans, 357, 338
 roots of the mountains, 352
 Rose, A. W., 443
 Rose, M. E., 308
 Rosholt, J. N., 160, 163, 164, 169, 175, 414, 415
 Ross Islands, 180
 rotation of the isochron, 192
 Rousseau, D., 257
 Rowe, R. B., 443
 Roy, R. F., 80, 81, 84, 85, 355
 Ru, 55, 62, 70, 72, 74
 Rubin, K., 431
 Rudnick, R. L., 75
 Rugg, S. H., 117
 runaway subduction, 89
 Russell, R. D., 165, 177
 Russia, 82, 139, 320
 Rutherford, E., 28, 29, 387
 Rwanda, 189
- S**
- S, 55, 62, 66, 70, 72, 425, 426, 432, 433, 434, 435
 Sagan, C., 2
 Salam, A., 309
 samarskite, 173
 Samoa, 251, 252
 sample age, 27, 42, 43, 45
 I Samuel, 25
 II Samuel, 353
 San Diego, 6, 10, 18
 Sandia National Laboratories, 13, 333
 sandstone, 186, 414, 437, 232, 413, 415, 417, 418
 Santee, 1, 95, 123, 381
 sapphirine, 146
 Sass, J. H., 82
 Satterly, J., 443
 Saunders, A. D., 249
 Sb, 55, 62, 70, 72
 Sc, 55, 62, 68, 70
 Scaillet, S., 148
 scalar, 308, 309
 scaling, 346, 350
 Scandinavia, 442
 scanning electron microscope, 145
 scars, 337
 scavenging, 431, 434
 Scharer, U., 169
 Schatsky, V. S., 144
 Schilling, A., 388, 391, 392, 394, 395, 410, 427, 441, 442, 451
 Schintlmeister, J., 400
 schist, 154, 185, 186, 199, 441, 444, 445
 Schleicher, H., 126, 192
 Schleien, B., 340
 Scotland, 95, 109, 110, 111, 182, 183, 216, 250
 Scripture, 2, 5, 6, 10, 19, 323, 334, 337, 351, 352, 353, 354, 356
 Se, 70, 72, 413, 414, 415, 416, 417, 418, 425, 426, 430
 Seaborg, G. T., 320
 seafloor, 49, 78, 90, 339
 seamounts, 127, 128, 431
 seas, 5, 339, 373
 seawater, 57, 143, 204, 206, 246, 262, 264, 431
 second RATE meeting, 10
 secondary decay products, 1
 secondary fluid transport hypothesis, 448
 secondary halos, 413, 418, 419,

- 426, 429, 435, 436, 448, 457
secondary melt enrichment, 67
secondary origin hypothesis, 381, 455, 457
sediment, 57, 59, 102, 116, 133, 143, 163, 168, 205, 206, 248, 260, 339, 432
sedimentary crustal component, 259
sedimentary marine carbonates, 140
sedimentary processes, 238
sedimentary reservoirs, 152
sedimentary rocks, 36, 37, 104, 140, 163, 178, 187, 194, 195, 202, 204, 206, 390, 445
sedimentation, 196, 205, 206, 232, 239
sediments, 140, 143, 151, 177, 193, 204, 222, 232, 444, 453
segregation, 49
Seidemann, D. E., 131, 133
seismology, 51, 52, 53, 54, 58, 61, 66, 76, 77, 79, 266
SEM-XRF, 145, 389, 411, 421, 440
sericite, 205
sericitization, 210
set on fire, 351, 352
shale, 36, 204, 205, 232, 260, 415, 451
shape isomers, 403
Sharpe, M. R., 260, 261
Shaw, D. M., 75, 107
shear, 51, 233, 425
Sheng, Z. Z., 430
Sheol, 351, 352
Sherlock, S. C., 148
Shirey, S. B., 259
shock, 53, 144, 153
short-lived fission track sources, 323
short-range force, 397
Shoshone, 315
SHRIMP, 98, 170
Si, 55, 60, 62, 66, 67, 69, 70, 71, 72, 161, 190, 194, 211
sialic material, 190
Sicily, 127, 128
siderophile elements, 55, 62, 71, 72, 73, 74, 78
Sierra Nevada, 81
Sievverts, 340
signature, 44, 123, 124, 184, 185, 186, 200, 206, 217, 264, 274
silicate, 30, 53, 55, 31, 49, 52, 54, 56, 62, 63, 66, 67, 69, 71, 72, 73, 74, 76, 77, 79, 86, 89, 126, 143, 194, 211, 212, 229, 239
Siljan, 82
sill, 104, 116
Silurian, 95
Silver, L. T., 161, 166, 168
Silver Crater Mine, 440, 441, 442, 444, 448, 449
sin, 357
SiO₂, 69
Slack, H. A., 443
slate, 36
Slave Province, 98
Sm-Nd, 10, 11, 12, 29, 31, 107, 109, 110, 111, 112, 113, 116, 123, 203, 211, 212, 213, 215, 216, 217, 218, 219, 220, 221, 227, 228, 230, 232, 234, 235, 237, 238, 240, 241, 258, 268, 269, 272, 277, 279, 280
Sm, 10, 11, 12, 29, 30, 31, 54, 60, 62, 70, 73, 75, 106, 107, 109, 110, 111, 112, 113, 115, 116, 123, 200, 203, 211, 212, 213, 214, 215, 216, 217, 218, 219,

- 220, 221, 223, 224, 225, 226, 227, 228, 229, 230, 232, 233, 234, 235, 237, 238, 240, 241, 243, 249, 250, 254, 255, 257, 258, 268, 269, 272, 277, 279, 280, 399
- Sn, 55, 62, 70, 72, 425
- Snelling, A. A., 7, 11, 14, 19, 21, 22, 107, 108, 117, 123, 128, 129, 133, 134, 156, 157, 158, 174, 184, 274, 306, 307, 324, 341, 343, 381, 446, 452
- Snetsinger, K. G., 391
- Sobiczewski, A., 320
- Sobolev, N. V., 144
- Soddy, F., 28
- soil, 184, 186, 373, 374
- solar abundances, 63, 65, 66, 79, 90
- solar flares, 323
- solar nebula, 124, 222, 251, 267, 278, 281
- solar particles, 61
- solar spectroscopy, 66
- solar system, 50, 65, 79, 101, 102, 103, 112, 176, 316, 321, 323, 356
- solar wind, 61
- solid state, 355
- solubility, 130, 153, 239, 264, 336, 434
- sources, 59, 76, 108, 151, 168, 176, 178, 181, 188, 190, 194, 196, 223, 224, 230, 232, 235, 237, 238, 239, 242, 246, 248, 249, 253, 254, 258, 260, 262, 263, 273, 281, 306
- South Africa, 141, 170, 203, 260, 261, 390, 400, 454
- South Carolina, 305
- South India, 441, 442, 444
- space, 143, 350, 367, 368, 370, 371, 372
- spallation, 314
- Sparks, F. W., 388, 401, 409, 410, 416, 418, 419, 421, 422, 427, 428, 435, 442
- specific gravity, 450
- specific heat, 84, 372
- specific ionization, 400
- spectacle array halo, 439, 440
- Spector, R. M., 395
- spectroscopic analysis, 61
- speed of light, 305, 308, 310, 311, 313, 357, 359, 360, 370
- Spencer, W. R., 356
- sphene, 391
- spherically symmetric, 310
- spin, 360
- spinel structure, 53
- spinel-lherzolites, 138
- split, 336
- spodumene, 144
- spontaneous fission, 308, 309, 312, 313, 315, 316, 317, 318, 319, 320, 322, 323, 336, 403
- Spooner, E. T. C., 262
- Sr, 30, 35, 36, 40, 41, 42, 43, 54, 55, 60, 62, 70, 73, 75, 107, 109, 115, 116, 187, 188, 189, 190, 191, 192, 193, 194, 195, 198, 199, 200, 201, 202, 203, 204, 205, 206, 207, 208, 209, 210, 211, 212, 216, 217, 221, 222, 225, 230, 235, 237, 238, 240, 241, 242, 243, 245, 246, 248, 249, 250, 252, 252, 253, 254, 257, 258, 260, 261, 262, 263, 266, 267, 272, 274, 277, 280
- Sr loss, 187, 198, 199, 200, 201, 203, 208, 210

- Sr isotope, 203, 205, 208, 209, 222, 239, 252, 253, 257, 260, 262
 Sr model ages, 235
 Sr-Nd, 196, 197
 Sr-Pb-Nd, 235, 258
 St. Helena, 180
 St. Severin meteorite, 113
 stable isotopes, 31, 260, 262
 Stacey, F. D., 64, 74, 76, 77, 83, 85, 177, 257
 standard evolutionary picture, 89
 Star Lake, 442, 444
 Stark, M., 390, 391
 stars, 356, 371, 374
 status report, 14
 Staudacher, T., 127, 137, 142, 152
 Steacy, H. R., 443
 Stein, C. A., 57
 Stein, S., 57
 Steinberg, E. P., 321
 Stern, T. W., 169, 414, 415
 Stieff, L. R., 414, 415
 Stille, P., 232, 258
 Stillman, C. J., 443
 Stillwater Complex, 214
 stirring, 278, 279, 281
 Stockdale rhyolite, 192, 201, 202
 Stockholm, 399
stoicheion, 355
 Stone, R., 320
 stone-age graves, 339
 stony meteorites, 31, 101, 102, 112, 176
 stony-irons, 63
 Strangeways Range, 146, 229
 stratigraphy, 123, 201, 206, 211, 270, 272, 281, 341, 342, 457
 Straumann, N., 367
 stretched out the heavens, 86, 367, 368
 string theory, 312, 361, 367, 368, 369
 stromatolites, 441
 strong nuclear coupling, 305, 307, 312, 313, 357, 359, 361, 362, 365, 366, 368, 397
 structural deformation, 204
 structure, 51, 54, 56, 86, 149
 Stuckless, J. S., 160, 161, 164
 Stugard, F., 443
 S-type granite, 194, 195, 197, 259
 SU groups, 307, 309
 subaerial volcanoes, 431
 subcontinental lithosphere, 189, 240, 247, 248, 250
 subducted, 57, 58, 60, 76, 77, 138, 143, 149
 subduction, 52, 54, 55, 78, 139, 140, 149, 152, 178, 182, 248, 259, 260, 267, 269, 270, 273, 281
 sublimating, 432
 subliming, 431
 submarine, 127, 131, 133, 137, 431
 suboceanic mantle, 138
 Sudbury District, 442
 suite of rocks, 40, 174, 253, 191
 sulfide, 57, 215, 262, 432, 457
 sulfur bacteria, 434
 sulfur cycling, 434
 Sun, 49, 61, 62, 71, 80, 140, 278, 323, 374
 Sun, S. S., 55, 63, 66, 67, 68, 69, 71, 72, 73, 74, 180, 181, 188
 sunburst effect, 382
 sunburst pattern, 382
 Sundrum, R., 312
sunistemi, 366
 Sunset Crater basalt, 127
 supergene, 430, 435, 439, 419, 421, 424

superheavy nuclei, 319, 320, 321, 322, 403
 Superior, 236
 Superior craton, 233
 Superior Province, 251, 252
 supernatural, 6, 9, 10, 43, 439
 supernova, 321, 323, 374
 superstring theory, 311, 312
 surface, 50, 59, 65, 75, 76, 77, 80, 81, 82, 83, 86, 90, 96, 149, 151, 160, 161, 164, 175, 184, 199, 207, 337, 340, 374, 433, 447
 Surtsey, 135
 Sustainer, 9, 366
 Swanson, S. E., 446
 Sweden, 82, 399, 400, 405, 406, 442, 453, 454
 swelling, 450
 symmetry, 309, 310

T

Ta, 54, 55, 70
 Tarney, J., 75
 Tatsumoto, M. R., 103, 179, 181
 tau, 309
 Tavsanlı Zone, 148
 Taylor, H. P., 242, 261, 262
 Tb, 62, 70
 Tc, 70
 Te, 55, 72, 403
 tectonic, 56, 65, 74, 75, 80, 87, 89, 149, 266, 277, 278, 356, 418, 444
teko, 355
 Telemarck County, 442
 temperature rise, 85
 Tennessee, 88, 451
 tension, 367, 368, 369
 tensor, 308, 309
 Tera, F., 113

terrane, 227
 terrestrial, 32, 63, 88, 95, 104, 112, 176, 211, 222, 268
 Tertiary, 166, 172, 182, 183, 199, 391
 tertiary diagram, 61
 Th, 13, 28, 30, 32, 33, 34, 35, 50, 54, 55, 60, 62, 68, 70, 73, 74, 75, 76, 106, 140, 150, 151, 160, 161, 163, 166, 167, 170, 171, 172, 173, 174, 175, 176, 178, 181, 184, 212, 224, 237, 238, 239, 240, 241, 244, 246, 249, 250, 264, 266, 272, 277, 336, 381, 383, 384, 385, 386, 387, 388, 389, 391, 392, 396, 398, 403, 404, 405, 406, 407, 408, 411, 412, 426, 438, 439, 450, 454, 456, 457
 Th decay, 388, 392, 398, 402, 404, 405, 406, 407, 438, 439, 456
 Th halos, 381, 386, 387, 389, 392, 398, 400, 401, 404, 405, 411, 419, 427, 438, 439, 449, 451, 453, 454, 456
 Th inclusions, 411
 Th nuclides, 427
 Th-Pb, 12, 160, 161, 163, 238, 239, 240, 241
 Th/Pb ratios, 175
 Th-radiation, 451
 Th-rich inclusions, 407
 Th-series, 385, 386, 387
 Th-U-Pb, 268
 Thayer, J. H., 355
 the fountains of the great deep, 277, 279
 the heavens, 367
 theoretical models, 22, 305, 306
 theories, 307, 309, 310, 311, 312,

323, 325
 thermal, 76, 83, 84, 86, 90, 154,
 165, 187, 198, 199, 318
 thermodynamics, 51, 355
 thermonuclear, 62, 374
 third RATE meeting, 14, 20
 tholeiites, 183
 Thompson, G. R., 206
 Thompson, J. J., 29
 Thompson, R. N., 182, 183
 't Hooft, G., 367, 368
 thorianite, 450
 thorite, 161, 173, 391
 thorium series, 35
 Thunder Springs Member, 116
 Ti, 54, 55, 60, 62, 68, 69, 70, 71,
 72, 73, 161, 173, 385
 tight folds, 339
 Tilton, G. R., 112, 113, 165
 time dependence, 310
 time dilation, 373
 timeframe, 398, 435, 455
 timescale, 201, 203, 237, 343, 368,
 375, 407, 433, 434, 457
 Tirrul, R., 168
 tissues, 373, 374
 titanite, 116, 161, 173, 220, 391
 Tl, 55, 62, 70, 72
 Tm, 62, 70
 to make liquid, 355
 to stretch out, 368
 Tolstikhin, I. N., 267, 268, 269
 tomography, 266
 tonalitic gneiss, 217
 Toro-Ankole, 189
 tourmaline, 144
 trace elements, 49, 51, 59, 60, 61,
 65, 66, 67, 79, 90, 211, 249, 262,
 263, 270
 tracks, 313, 322

transfer, 276
 transit times, 429, 430, 432, 433
 transition zone, 53, 59, 65
 transitional elements, 55, 69
 transport, 178, 203, 205, 218, 232,
 262, 268, 269, 280, 381, 417,
 422, 424, 426, 428, 429, 430,
 432, 433, 435, 436, 437, 439,
 448, 449, 455, 457
 transportation, 143
 Triassic, 88, 275, 414, 415, 417, 451
 tribulation, 338
 Trinidad, 180
 Tristan da Cunha, 60, 180
 troilite, 101, 103, 112, 176, 257
 trondhjemitites, 110
 true ages, 208
 true isochrons, 210
 true vacuum, 310
 Tubuai, 60
 tunneling, 13, 14, 358, 359
 turbidites, 196, 197
 Turkey, 148
 Turnbull, L. G., 388, 390, 391, 393,
 395, 399
 Turner, G., 141
 two-point isochrons, 218

U

U, 12, 28, 30, 34, 50, 54, 55, 60,
 69, 70, 71, 73, 74, 75, 76, 88, 89,
 97, 98, 99, 103, 106, 113, 114,
 115, 140, 150, 151, 159, 160,
 161, 162, 163, 164, 165, 166,
 167, 169, 170, 171, 172, 173,
 174, 175, 176, 177, 178, 181,
 184, 185, 186, 212, 215, 216,
 217, 220, 224, 237, 238, 239,
 240, 241, 242, 244, 246, 249,

- 250, 256, 257, 264, 266, 267, 268, 272, 275, 277, 313, 313, 315, 316, 318, 321, 322, 323, 324, 335, 336, 352, 381, 383, 384, 386, 387, 388, 389, 391, 392, 393, 395, 396, 398, 401, 403, 404, 405, 406, 407, 408, 410, 411, 412, 413, 414, 415, 416, 417, 418, 419, 421, 424, 425, 426, 429, 430, 435, 437, 438, 439, 444, 447, 448, 449, 450, 452, 453, 454, 456, 457, 458
- U daughter, 411
- U decay, 98, 165, 239, 335, 336, 352, 388, 392, 393, 398, 401, 403, 404, 405, 406, 407, 408, 409, 412, 414, 417, 419, 420, 436, 438, 439, 456, 457
- U deposits, 413
- U fission, 336
- U inclusions, 411
- U nuclides, 335, 386, 427, 457
- U radiohalos, 19, 21, 87, 88, 274, 275, 278, 323, 324, 335, 381, 386, 387, 388, 389, 392, 393, 395, 396, 397, 398, 399, 401, 404, 405, 406, 408, 409, 411, 414, 415, 427, 437, 438, 449, 451, 452, 456
- U sources, 423, 424, 447, 448, 449, 453, 454, 457
- U-bearing solutions, 410, 418
- U-daughter, 416, 436
- U-depleted, 216
- U-derived Pb, 438
- U-Pb, 12, 97, 98, 112, 160, 161, 163, 164, 165, 166, 167, 168, 169, 170, 172, 174, 175, 184, 215, 216, 217, 220, 234, 238, 239, 240, 241, 258, 268, 343
- U-radiation, 451
- U-rich inclusions, 407
- U-series, 385, 386, 387
- U-Th, 401, 439
- U-Th-Pb, 11, 123, 159, 161, 163, 169, 170, 172, 173, 174, 184, 186, 220, 237, 258, 272, 277
- U/Pb ratios, 174, 175, 176, 177
- U/Th-Pb method, 32
- Uganda, 189
- ultramafic, 136, 138, 142, 212, 215
- ultraviolet laser ablation probe, 145
- undegassed, 267
- undepleted material, 77, 270
- undifferentiated earth, 78
- unified theory, 312
- uniformitarian, 37, 83, 86, 123, 125, 148, 158, 200, 201, 204, 220, 221, 264, 267, 268, 271, 272, 273, 274, 276, 277, 281, 305, 313, 314, 315, 316, 318, 397, 429, 440, 441
- uniformitarianism, 49, 50, 315, 398
- United States, 82, 116, 233
- universe, 306, 308, 310, 313, 337, 355
- Unnikrishnan-Warrier, C., 109
- unradiogenic Pb, 264
- upper mantle, 52, 53, 59, 149, 150, 151, 264, 266, 267, 268, 269, 270, 271
- upwelling plume, 271
- UR, 248
- Urach, 82
- Urals, 446
- uraninite, 30, 33, 97, 164, 165, 173, 174, 184, 186, 391, 447, 448, 449, 450

V

V, 55, 62, 70, 72
 vacancies, 146
 vacuum, 310, 311, 312, 367, 368, 369, 370, 372
 Valbracht, P. J., 127, 137, 138, 139
 valid isochron, 203
 Valley of Elah, 25
 van der Hilst, R. D., 77
 van Calsteren, P. W. C., 237, 260
 Vance, D., 220
 Vandebosch, R., 319, 320, 321
 Vardiman, L., 1, 7, 10, 14, 339, 350
 variable constants, 305, 306, 311
 variable decay, 312, 313
 variable half-lives, 315
 variant halos, 381, 398, 457
 Veblen, D. R., 426
 vector, 308, 309
 veins, 270, 444
 Venus, 356
 vermicular quartz, 425
 vesicles, 137, 138
 Victoria County, 442
 Victoria Land, 128
 Vidal, P., 262
 Virginia, 208
 viscosity, 56, 356
 visible scars, 15
 visible tracks, 15
 volatile, 62, 63, 65, 67, 71, 73, 138, 139, 141, 144, 430, 431, 433, 447, 448
 volatility, 55, 71, 72, 276, 431
 volcanic, 30, 59, 61, 117, 123, 127, 128, 129, 130, 136, 139, 178, 181, 182, 184, 188, 189, 190, 201, 210, 215, 216, 244, 249, 280, 430, 431, 433, 457

volcanism, 57, 58, 59, 137
 volcanoes, 130, 137, 191, 210, 213, 249, 273, 280, 352, 356, 431
 Voltaggio, M., 432
 volume diffusion, 198, 199, 200, 203
 volumetric contraction, 57
 volumetric cooling, 86
 von Platen, H., 446

W

W, 55, 62, 70, 72, 73
 W bosons, 309
 Waenke, H. G., 66
 Wakefield, J. R., 422, 440, 443, 446, 447, 448
 Walker, R. M., 322, 411
 wall-rock, 190, 258
 Wallace, P., 446
 Walthall, F. G., 192
 Wampler, J. M., 446
 Wanser, K., 13
 Warren, C. G., 413
 Wasserburg, G. J., 114, 149, 165, 197, 214, 222, 224, 225, 242, 243, 259
 water, 5, 50, 52, 57, 63, 78, 86, 87, 90, 141, 142, 143, 151, 153, 154, 172, 206, 208, 210, 262, 374, 431, 432
 wavelength, 370
 weak forces, 307, 309, 310, 312, 313, 362, 363, 365, 366
 weather, 50
 weathering, 153, 160, 168, 169, 172, 175, 184, 186, 205, 207, 208, 209, 210, 211, 212, 264, 272, 279, 419, 432
 Weaver, B. L., 59, 75, 248, 249

- Webb, A. W., 146, 152
 Webb, J. K., 311
 Weber, B., 107
 Wedepohl, K. H., 75
 wedge, 143
 week, 338
 Weigel, E., 348, 349
 Weinberg angle, 363, 366
 Weinberg, S., 309
 Weinbert-Salam electroweak theory, 363
 Weingreen, J., 351
 Weissman Mine, 442, 444
 Welke, H., 182
 West Africa, 205
 West Germany, 442
 Wetherill, G. W., 98, 165
 Whitcomb, J. C., 337, 339
 white mica, 148
 White, A. J. R., 194
 White, W. M., 60, 251, 252
 Whitehouse, M. J., 108, 109, 110, 112, 217, 232
 whitlockite, 113, 316
 Whitney, P. R., 205
 whole rock, 10, 16, 21, 36, 42, 88, 95, 96, 99, 101, 102, 104, 105, 106, 107, 108, 109, 110, 111, 112, 113, 114, 115, 116, 124, 127, 128, 129, 148, 159, 160, 161, 162, 163, 169, 173, 174, 175, 181, 184, 186, 187, 192, 198, 200, 201, 202, 205, 212, 213, 214, 215, 216, 217, 221, 230, 268, 271, 267, 277, 452
 Wilberforce, 442, 443
 Wilczek, F., 367
 Wilkerson, G., 440, 443, 446, 447
 Wilkins, B. D., 321
 Williams, I. S., 98, 168, 194
 Wilson, A. F., 146, 152
 Wiman, E., 390, 391, 402, 406
 Windrim, D. P., 219, 229, 230
 Wingate, M. T. D., 170, 237
 Winkler, H. G. F., 446
 Winona Lake, IN, 27
 Winter, H. R., 82
 Wise, K. P., 390, 391, 409, 422, 426, 428, 429, 440, 441, 443, 445, 446, 448, 449, 451
 Wölsendorf, 410, 427, 437, 441, 442, 443, 444, 451, 452
 Wooden, J. L., 116
 Woodmorappe, J., 341, 342, 446
 Word of God, 6
 world, 338
 worldview, 305
 worldwide, 177, 338
 Wu, C. S., 308
 Wuest, K. S., 354
 Wyoming, 116, 160, 161, 163, 164, 169, 175, 199, 200, 214, 215
 Wyss, W., 305
- ## X
- X halos, 400, 453, 454, 456
 x-rays, 29, 205, 403, 405, 406
 Xe, 55, 320, 321
 xenocrysts, 137, 215
 xenoliths, 65, 68, 74, 75, 136, 137, 139, 142, 152, 195
 xenotime, 173, 391
- ## Y
- Y, 55, 60, 62, 70
 Yang, C. N., 308, 309
yaqad, 352
 Yates, K. M., 351

- Yb, 62, 68, 70
York, D., 42, 45, 101, 420, 422
Yoshimura, J., 390, 391, 392, 393, 401, 442
young earth, 1, 2, 3, 4, 7, 9, 13, 19, 20, 24, 124, 125, 267, 271, 273, 275, 276, 277, 281, 306, 307, 308, 311, 312, 315, 317, 318, 321, 334, 337, 338, 339, 374, 398, 455, 456, 458
Young, R., 351
Ytterby, 399, 400, 405, 407, 442, 444, 453

Z

- Z bosons, 309
Z halos, 401, 443
Zaire, 140, 141, 142, 189
Zartman, R. E., 178, 239, 263, 264, 265, 345
Zashu, S., 140, 141
zero age, 179
Zhang, L. S., 169
Zhao, J., 109
Zheng, Y. F., 188, 192, 193, 197, 201, 202, 203
Zhou, B., 220
Zimbabwe, 164
Zimmermann, J. L., 138
Zindler, A., 59, 60, 67, 88, 104, 165, 241, 242, 244, 245, 246, 247, 248, 249, 251, 252, 258, 266
zircon, 13, 30, 33, 97, 98, 112, 161, 163, 166, 167, 168, 169, 170, 172, 173, 186, 194, 196, 211, 215, 216, 217, 220, 234, 268, 335, 336, 344, 345, 346, 347, 349, 350, 391, 394, 406, 427, 450, 452
Zn, 55, 62, 70, 72

- Zoth, 82
Zr, 5, 62, 70, 71, 161
Zuni-Bandera volcanic field, 130

Atomic Weights of the Elements (Based on ¹²C)

Values in parentheses are used for radioactive elements whose atomic weights cannot be quoted precisely without knowledge of the origin of the elements; the value given is the atomic mass number of the isotope of longest known half-life.

Name	Symbol	Atomic Number	Atomic Weight	Footnotes	Name	Symbol	Atomic Number	Atomic Weight	Footnotes
Actinium	Ac	89	227.0278	z	Mendelevium	Md	101	(258)	
Aluminum	Al	13	26.98154		Mercury	Hg	80	200.59	
Americium	Am	95	(243)		Molybdenum	Mo	42	95.94	
Antimony	Sb	51	121.75		Neodymium	Nd	69	144.24	x
Argon	Ar	18	39.948	w,x	Neon	Ne	10	20.179	y
Arsenic	As	33	74.9216		Neptunium	Np	93	237.0482	z
Astatine	At	85	(210)		Nickel	Ni	28	58.69	
Barium	Ba	56	137.33	x	Niobium	Nb	41	92.9064	
Berkelium	Bk	97	(247)		Nitrogen	N	7	14.0067	
Beryllium	Be	4	9.01218		Nobelium	No	102	(259)	
Bismuth	Bi	83	208.9804		Oxniun	Os	76	190.2	x
Bohrium	Bh	107	(262)		Oxygen	O	8	15.9994	w
Boron	B	5	10.81	w,y	Palladium	Pd	46	106.42	x
Bromine	Br	35	79.904		Phosphorus	P	15	30.97376	
Cadmium	Cd	48	112.41	x	Platinum	Pt	78	195.08	
Calcium	Ca	20	40.08	x	Plutonium	Pu	94	(244)	
Californium	Cf	98	(251)		Polonium	Po	84	(209)	
Carbon	C	6	12.011	w	Potassium	K	19	39.0983	
Cerium	Ce	58	140.12	x	Praseodymium	Pr	59	140.9077	
Cesium	Cs	55	132.9054		Promethium	Pm	61	(145)	
Chlorine	Cl	17	34.453		Protactinium	Pa	91	231.0359	z
Chromium	Cr	24	51.996		Radium	Ra	88	226.0254	x,z
Cobalt	Co	27	58.9332		Radon	Rn	86	(222)	
Copper	Cu	29	63.546	w	Rhenium	Re	75	186.207	
Curium	Cm	97	(247)		Rhodium	Rh	45	102.9055	
Dubnium	Db	105	(262)		Rubidium	Rb	37	85.4678	x
Dysprosium	Dy	66	162.50		Ruthenium	Ru	44	101.07	x
Einsteinium	Es	99	(252)		Rutherfordium	Rf	104	(261)	
Erbium	Er	68	167.26		Samarium	Sm	62	150.36	x
Europium	Eu	63	151.96	x	Scandium	Sc	21	44.9559	
Fermium	Fm	100	(257)		Seaborgium	Sg	106	(263)	
Fluorine	F	9	18.998403		Selenium	Se	34	78.96	
Francium	Fr	87	(223)		Silicon	Si	14	28.0855	
Gadolinium	Gd	64	157.25	x	Silver	Ag	47	107.868	x
Gallium	Ga	31	69.72		Sodium	Na	11	22.98977	
Germanium	Ge	32	72.59		Strontium	Sr	38	87.62	x
Gold	Au	79	196.9665		Sulfur	S	16	32.06	w
Hafnium	Hf	72	178.49		Tantalum	Ta	73	180.9479	
Hassium	Hs	108	(265)		Technetium	Tc	43	(98)	
Helium	He	2	4.00260	x	Tellurium	Te	52	127.60	x
Holmium	Ho	67	164.9304		Terbium	Tb	65	158.9254	
Hydrogen	H	1	1.0079	w	Thallium	Tl	81	204.383	
Indium	In	49	114.82	x	Thorium	Th	90	232.0381	x,z
Iodine	I	53	126.9045		Thulium	Tm	69	168.9342	
Iridium	Ir	77	192.22		Tin	Sn	50	118.71	
Iron	Fe	26	55.847		Titanium	Tu	22	47.88	
Krypton	Kr	36	83.80	x,y	Tungsten	W	74	183.85	
Lanthanum	La	57	138.9055	x	Uranium	U	92	238.029	x,y
Lawrencium	Lr	103	(260)		Vanadium	V	23	50.9415	
Lead	Pb	82	207.2	w,x	Xenon	Xe	54	131.29	x,y
Lithium	Li	3	6.941	w,x,y	Ytterbium	Yb	70	173.04	
Lutetium	Lu	71	174.967		Yttrium	Y	39	88.9059	
Magnesium	Mg	12	24.305	x	Zinc	Zn	30	65.39	
Manganese	Mn	25	54.9380		Zirconium	Zr	40	91.224	x
Meitnerium	Mt	109	(266)						

w Element for which known variations in isotopic composition in normal terrestrial material prevent a more precise atomic weight being given; values should be applicable to any "normal" material.

x Element for which geological specimens are known in which the element has an anomalous isotopic composition, such that the difference between the atomic weight of the element in such specimens and that given in the table may exceed considerably the implied uncertainty.

y Element for which substantial variations from the value given can occur in commercially available material because of inadvertent of undisclosed change of isotopic composition.

z Element for which the value is that of the radioisotope of longest half-life.

From *Pure and Applied Chemistry*, 56, 653, 1983.